Reprogramming Alkaloid Biosynthesis in *Catharanthus roseus*: Synthetic Biology in Plants

by

Weerawat Runguphan

A.B., Chemistry and Physics
Harvard University, 2006

SUBMITTED TO THE DEPARTMENT OF CHEMISTRY IN PARTIAL FULFILLMENT OF THE REQUIREMENTS FOR THE DEGREE OF

DOCTOR OF PHILOSOPHY IN CHEMISTRY
AT THE
MASSACHUSETTS INSTITUTE OF TECHNOLOGY

JUNE 2011

Signature of Author: _____
Department of Chemistry
March 28, 2011

Certified by: _____
Sarah E. O'Connor
Associate Professor of Chemistry
Thesis Supervisor

Accepted by: _____
Robert W. Field
Professor of Chemistry
Chairman, Departmental Committee on Graduate Studies

This doctoral thesis has been examined by a committee of the Department of Chemistry as follows:

Professor Catherine L. Drennan

Chair_____

Professor Sarah E. O'Connor

Thesis Supervisor____ _____

Professor Gerald R. Fink

Committee Member_ _____

METABOLIC REPROGRAMMING OF ALKALOID BIOSYNTHESIS IN *CATHARANTHUS ROSEUS*: SYNTHETIC BIOLOGY IN PLANTS

By

Weerawat Runguphan

Submitted to the Department of Chemistry on March 28, 2011
in Partial Fulfillment of the Requirements for the
Degree of Doctor of Philosophy in Chemistry

ABSTRACT

The medicinal plant Madagascar periwinkle (*Catharanthus roseus*) produces over 130 monoterpene indole alkaloid (MIA) natural products. Many of these compounds have pharmaceutical value, such as the anticancer agents vinblastine and vincristine. Unnatural modifications can impart novel bioactivity to the parent natural product. Advances in synthetic biology and microbial engineering have allowed overproduction of natural products and their analogs in non-native organisms such as yeast and *E. coli*. However, re-engineering of plant pathways to yield "novel" products has been limited, particularly when compared to the successes achieved in prokaryotic systems. This thesis describes several strategies to re-engineer MIA biosynthesis in periwinkle to produce novel alkaloids. The first strategy involves the introduction of a biosynthetic enzyme with redesigned substrate specificity into periwinkle. The resulting transgenic plant culture produces a variety of unnatural alkaloid compounds when co-cultured with precursors that the re-engineered enzyme has been designed to accept. The second strategy improves upon this work by enabling periwinkle to autonomously synthesize precursor analogs *in situ*. Specifically, the prokaryotic halogenation machinery was introduced into the genome of periwinkle, which lacks the biosynthetic ability to produce halogenated compounds. These halogenases function within the context of the plant cell to generate halogenated precursor, which is then shuttled into MIA metabolism to yield halogenated alkaloids. Altogether, a new functional group—an organohalide—was introduced into plant secondary metabolism in a regioselective and predictable manner. The third strategy involves RNAi-mediated suppression of MIA biosynthesis in periwinkle. Alkaloid production was obliterated in the resulting transgenic plant culture. The silenced plant culture produces a variety of fluorinated alkaloids when co-cultured with fluorinated starting substrate. The yields of some unnatural alkaloids were improved since the natural precursor was absent. Finally, the fourth strategy describes chemical functionalization of halogenated MIAs. Postbiosynthetic chemical derivatizations of halogenated MIAs using palladium-catalyzed Suzuki-Miyaura cross-coupling reactions robustly afforded aryl and heteroaryl analogs of MIAs. Altogether, the work described in this thesis demonstrates the versatility of medicinal plants in the generation of unnatural alkaloids. Thus, despite their genetic complexity, plants are a viable platform for synthetic biology efforts.

Thesis Supervisor: Sarah E. O'Connor

Title: Associate Professor of Chemistry

Acknowledgements

This thesis would not have been possible without the support and guidance of these several individuals:

First and foremost, my advisor, Professor Sarah O'Connor, for your endless encouragement, insightful guidance and inexhaustible enthusiasm. It has truly been an honor working in your lab. You have shown me how exciting and impactful science can be. You have given me the freedom to explore unconventional ideas that have proven to be rewarding. I will always be eternally grateful to you.

Professor Catherine Drennan and Professor Gerald Fink, my thesis committee members, for your support and suggestions on my research and my graduate/postgraduate career. Professor Barbara Imperiali and Professor Kristala Jones Prather also for your steadfast encouragement and helpful advice.

Members of the O'Connor lab, for the most amazing time one could ever ask for. Special thanks to Peter Bernhardt, for letting me work on your re-engineered strictosidine synthase and for your support throughout my graduate career; Justin Maresh and Xudong Qu, for your vision and the hard work that you contributed in our collaborations; Nancy Yerkes, for giving me a crash course in plant molecular biology, and for always making the lab a fun environment to work in; Lesley-Ann Giddings, Dave Liscombe, Aimee Usera and Zeke Nims, for your encouragement and advice both in science and in life; Weslee Glenn for carrying on with the halogenase work and for your unfailing patience and understanding; Bettina Ruff and John Cheng, for your friendship and kindness. It is in large part because of you all that I am motivated and happy to spend countless hours in lab.

Professor Stuart Schreiber, Professor Yongyuth Yuthavong, Dr. Sumalee Kamchonwongpaisan, Ajarn Anchalee, P'Ked (Sirinya Matchacheep) and P'Nok (Supanee Taweechai), for your guidance and for inspiring me to become a scientist.

My friends in Boston and elsewhere in the US, for helping me feel at home. I am most grateful for Prae, Gob, Aam, Fang, O, P'Tape, Yui, Kob, Tao, P'Joe, Mike, Amp and Sam for being patient with me and for making me sane in trying times. Special thanks to Effendi Leonard and Jill Hagel for our fruitful collaborations and for your helpful advice. Thanks also to the Liu family, Jonathan, Chiu-Hui, Ken, Lucy, Kenneth and Omi for your support and advice, as well as for helping me maintain a good balance in life.

Most importantly, my family—especially my mother, father and grandmother—for the sacrifices that you have made to ensure my success and happiness in life, and for instilling into me the importance of knowledge. I am so proud to have you in my life. Although I only get to see you once a year, you give me enough love and warmth to last me the entire lifetime. Thanks also to Chris and P'Nammon, my American family, for loving me for who I am and for always being there for me.

Weerawat (Ricky) Runguphan

Table of Contents

List of Figures

Chapter 1

Chapter 2

Chapter 3

Chapter 4

Chapter 5

Appendix B

Appendix C

Appendix D

List of Tables

Conventions and Abbreviations

Compounds that are illustrated in Figures and Tables are numbered consecutively, starting from 1 in each chapter; NMR data are presented by the chemical shift (δ) in parts-per-million (ppm), multiplicity (singlet, s; doublet, d; triplet, t; etc.), and J-coupling constant in Hertz (Hz); NMR spectra are referenced to the NMR-solvents' residual proton (for ^{1}H NMR), most intense carbon (for ^{13}C NMR) or fluorine (for ^{19}F NMR) isotope signal.

16OMT	16-hydroxytabersonine 16-O-methyltransferase
4'-OMT	3'-hydroxy-N-methylcoclaurine-4'-O-methyltransferase
4HPAA	4-hydroxyphenylacetaldehyde
6OMT	norcoclaurine 6-O-methyltransferase
AVLBS	α-3′,4′-anhydrovinblastine synthase
AS	anthranilate synthase
AtANS	*Arabidopsis thaliana* anthocyanidine synthase
BBE	berberine bridge enzyme
BIA	benzylisoquinoline alkaloid
°C	temperature in the Celsius scale
cDNA	complementary deoxyribonucleic acid
CNMT	coclaurine-N-methyltransferase
CODM	codeine O-demethylase
COR	codeinone reductase
CrSTR	*Catharanthus roseus* strictosidine synthase
D4H	desacetoxyvindoline 4-hydroxylase
DAT	deacetylvindoline O-acetyltransferase
DMAPP	dimethyl allyl pyrophosphate
DMSO	dimethylsulfoxide
DNA	deoxyribonucleic acid
dNTP	deoxyribonucleotide triphosphate
DRR	1,2-dehydroreticulene reductase
DRS	1,2- dehydroreticuline synthase
DTT	dithiothreitol
DXPS	1-deoxy-D-xylulose synthase
EDTA	ethylenediaminetetraacetic acid
ESI-MS	electrospray ionization mass spectrometry
EtOAc	ethyl acetate
FAD	flavin adenine dinucleotide
G1OH	geraniol 10-hydroxylase
GI	GenBank index number
Glc	glucosė
HMBC	heteronuclear multiple bond coherence
HPLC	high-performance liquid chromatography
HPT	hygromycin phosphotransferase
HRMS	high-resolution mass spectrometry
HSQC	heteronuclear single quantum coherence

Hz	Hertz (s^{-1})
IPP	isopentenyl pyrophosphate
IPTG	isopropyl β-D-1-thiogalactopyranoside
KBr	potassium bromide
KCl	potassium chloride
KI	potassium iodide
K_M	Michaelis constant; the substrate concentration at a half of the maximal reaction velocity (V_{max})
kDa	kilo Dalton (one thousand Dalton)
K_3PO_4	potassium phosphate
LB	Luria-Bertani media
LC	liquid chromatography
LC-MS	liquid chromatography coupled to mass spectrometry
LOMT	loganic acid methyltransferase
MAO	monoamine oxidase
MAT	minovincinine 19-O-acetyltransferase
Me	methyl
MeCN	acetonitrile
MeOD	tetradeuterated (d4) methanol
MeOH	methanol
MEP	methyl erythritol pathway
MIA	monoterpene indole alkaloid
mRNA	messenger RNA
MS	mass spectrometry
NAA	naphthyl acetic acid
NADPH	reduced nicotinamide adenine dinucleotide phosphate (hydride)
NCS	norcoclaurine synthase
NH_4OH	ammonium hydroxide
NMR	nuclear magnetic resonance
NMT	16- methoxy-2,3-dihydro-3-hydroxytabersonine N-methyltransferase
NPTII	neomycin phosphotransferase II
NSCLC	non small-cell lung cancer
ODn	optical density at n nm
OpSTR	*Ophiorrhiza pumila* strictosidine synthase
ORCA3	jasmonate-responsive APETALA2 (AP2)-domain transcription factor
PCR	polymerase chain reaction
PDA	photodiode array (detector)
PDK	pyruvate dehydrogenase kinase
$Pd(OAc)_2$	palladium acetate
PsCODM	*Papaver somniferum* codeine O-demethylase
PsT6ODM	*Papaver somniferum* thebaine 6-O-demethylase
ppm	parts per million
PVP	Polyvinylpyrrolidone
RNA	ribonucleic acid
RNAi	RNA interference
rpm	revolutions per minute

RsSTR	*Rauvolfia serpentina* strictosidine synthase
rt	retention time
SAR	structure-activity relationship
SDM	site-directed mutagenesis
SDS-PAGE	sodium dodecyl sulfate polyacrylamide gel electrophoresis
SGS	strictosidine glucosidase
SLS	secologanin synthase
SMT	scoulerine 9-O-methyltransferase
SPhos	2-dicyclohexylphosphino-2',6'-dimethoxybiphenyl
STR	strictosidine synthase
STRvm	strictosidine synthase V214M mutant (STRv214m)
T16H	tabersonine 16-hydroxylase
T6ODM	thebaine 6-O-demethylase
TDC	tryptophan decarboxylase
TFA	trifluoroacetic acid
THF	tetrahydrofuran
TLC	thin-layer chromatography
TOF	time-of-flight
UPLC	ultra-performance liquid chromatography
UV	ultraviolet light
UV-vis	ultraviolet and visible spectroscopy
Vmax	maximum reaction velocity as [S] approaches ∞

CHAPTER 1

BACKGROUND AND SIGNIFICANCE

Part of this chapter is published as a perspective in

Nature Chemical Biology **2009**, *5*, 292-300

1.1 Significance and Biosynthesis of Alkaloid Natural Products

Medicinal chemists are continually inspired by Nature, whose repertoire of biologically active compounds is a proven and rich source of disease-fighting drugs[1-3]. In fact, a report in 2007 estimated that about one-third of new pharmaceuticals from 1981-2006 originated from, or were inspired by, natural products[4]. Plant alkaloids are a structurally diverse class of nitrogen-containing secondary metabolites with over 10,000 structurally characterized members[5,6], many of which exhibit biological activities. While the physiological role of alkaloids in plants has not been fully elucidated, current evidence suggests that alkaloids are primarily involved in plant defense against pathogens, insects, and herbivores[7]. For example, the indolizidine, indolizine, and β-carbolines alkaloid backbone structures exhibit up to 25 biological properties, including dopamine reuptake inhibitor, glucosidase inhibitor and sodium channel blocker[8]. Throughout history, the bioactivities of plant alkaloids have been recognized and exploited: Socrates' death in 399 B.C. from consuming *Conium maculatum* (hemlock) extract containing the neurotoxin alkaloid coniine **1**; Cleopatra's use of *Hyoscyamus muticus* (Egyptian henbane) extract containing atropine **2** to make her eyes more alluring; and the more common use of caffeine **3** in coffee and tea as a mild stimulant (**Figure 1.1**)[9]. Modern examples of medicinally important alkaloids are shown in **Table 1.1**[10].

Despite their medicinal properties and commercial potential, the exploration of alkaloids as drug candidates remains a slow process, largely because of the inefficiency and high expense of their extraction and purification. To screen a particular alkaloid for biological activities, the compound must first be isolated and purified from crude plant extracts

often containing hundreds of contaminating metabolites. Extensive structural characterizations are also required to ensure the identity and purity of the compound. All of these steps—isolation, purification, and structural characterization—are time-consuming and expensive. Low accumulation levels of bioactive alkaloids and inconsistent yields, which depend heavily on the source organisms as well as geographical and climate conditions, also complicate. For example, the anticancer agent vincristine **5** (**Figure 1.1**), is isolated from *Catharanthus roseus* at concentrations that reach only 0.0003% by dry weight[11].

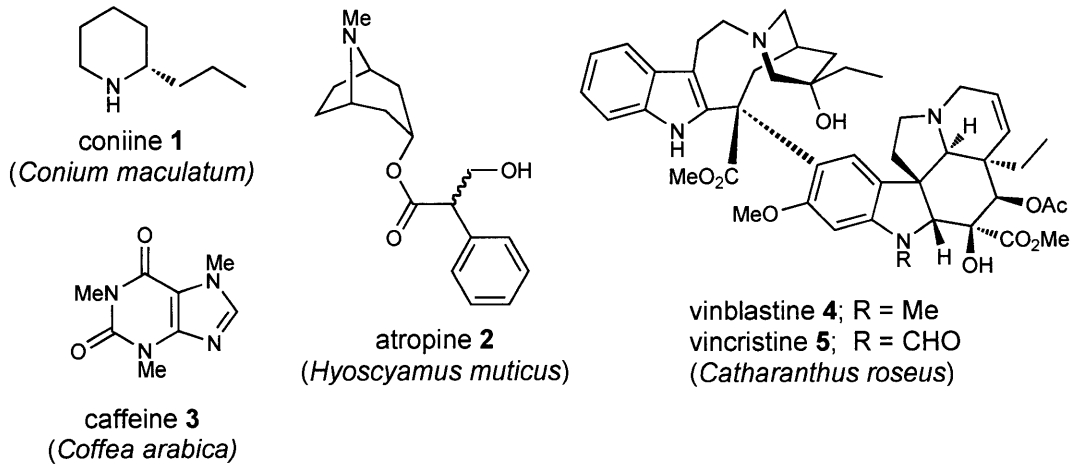

Figure 1.1. Examples of plant alkaloids and their sources.

Table 1.1. Examples of medicinally important alkaloids. *Yield represents % dry weight. MIA: monoterpene indole alkaloid; BIA benzylisoquinoline alkaloid. (Adapted from *Nature Chemical Biology* **2009**, *5*, 292-300)

Alkaloid	Type	Approximate yield* (organ)	Source plant	Pharmaceutical applications
Ajmaline	MIA	1 (root)	*Rauwolfia sellowii*	Antiarrhythmic
Berberine	BIA	1 (root)	*Berberis vulgaris*	Antimicrobial
Caffeine **3**	Purine	1 (bean)	*Coffea arabica*	Stimulant
Camptothecin	MIA	0.05 (bark)	*Camptotheca acuminata*	Chemotherapeutics
Cocaine	Tropane	0.8 (leave)	*Erythroxylon coca*	Stimulant
Codeine	BIA	0.5 (seed capsule)	*Papaver somniferum*	Antitussive, analgesic
Hyoscyamine	Tropane	0.4 (leave)	*Hyoscyamus muticus*	Anticholinergic, antimuscarinic
Morphine **45**	BIA	10 (seed capsule)	*Papaver somniverum*	Analgesic
Nicotine	Tropane	3 (leave)	*Nicotiana tabacum*	Stimulant
Noscapine	BIA	2 (seed capsule)	*Papaver somniverum*	Analgesic, antitussive
Papaverine	BIA	1 (seed capsule)	*Papaver somniverum*	Vasodilator
Quinidine	MIA	0.2 (bark)	*Cinchona ledgeriana*	Antiarrhythmic
Quinine	MIA	6 (bark)	*Cinchona ledgeriana*	Antimalarial, analgesic
Reserpine	MIA	0.03 (root)	*Rauwolfia nitida*	Antihypertensive
Sanguinarine	BIA	0.001 (root)	*Sanguinaria canadiensis*	Antibacterial (in dental products)
Scopolamine	Tropane	0.1 (leave)	*Hyoscyamus muticus*	Anticholinergic, antimuscarinic
Strychnine	MIA	2 (root)	*Strychnos nux-vomica*	Stimulant, pesticide
Vinblastine **4**	MIA	0.0001 (whole plant)	*Catharanthus roseus*	Chemotherapeutics
Vincristine **5**	MIA	0.0003(whole plant)	*Catharanthus roseus*	Chemotherapeutics
Yohimbine	MIA	1 (bark)	*Pausinystalia yohimbe*	Erectile dysfunction treatment

Advances in the field of organic synthesis over the last century have produced various methodologies suitable for constructing complex natural products with multiple stereocenters and functional groups[11-14]. Nevertheless, total or semi-synthesis of alkaloids remains a daunting task and is impractical at the industrial level. For example, the total synthesis of vinblastine **4** (**Figure 1.1**) from simple starting materials involves 44 steps, with an overall yield of less than 1%[14].

1.2 Halogenated Natural Products

Though once considered a rare occurrence in nature, halogenation has been observed in many natural products[15]. Approximately 4000 halogenated compounds have been identified from natural sources including marine organisms, bacteria, fungi, plants, insects and higher animals (**Figure 1.2**)[16]. Chlorination and bromination predominate, while iodination and fluorination are relatively rare. Many halogenated natural products have biological activities, and in many cases, the presence of the halogen groups has been demonstrated to play a vital role in establishing the bioactivity of a compound. For example, salinosporamide A **6**, a proteosome inhibitor currently in clinical trials for multiple myeloma treatment, contains a chlorine group that is required for bioactivity. A high-resolution crystal structure of the 20S proteosome bound to salinosporamide A **6** reveals that the hydroxyl group of the active site threonine opens up the β-lactone of **6** upon binding, which, consequently, releases a free hydroxyl group[17, 18]. This hydroxyl group then performs an irreversible intramolecular displacement of the primary chlorine substituent to form a tetrahydrofuran ring. Unsurprisingly, analogs of salinosporamide A **6** devoid of this chlorine group exhibit significantly lower proteosome inhibitory activity.

Similarly, rebeccamycin **7**, an antitumor antibiotic isolated from the soil bacterium *Lechevalieria aerocolonigenes*, also requires the presence of the two chlorine substituents for its biological activity. The deschloro analog of rebeccamycin **7** exhibits more than ten-fold lower cytotoxic activity against melanoma and leukemia cell lines[19]. The decrease in antitumor activity of the deschloro analog is proposed to be a result of the lack of cell membrane permeability in the absence of the chlorine moieties. Likewise, the non-halogenated analog of the antitumor sesterpenes neomangicol A **8** and B **9** also exhibits lower cytotoxic activity against breast and colon tumor cell lines[20].

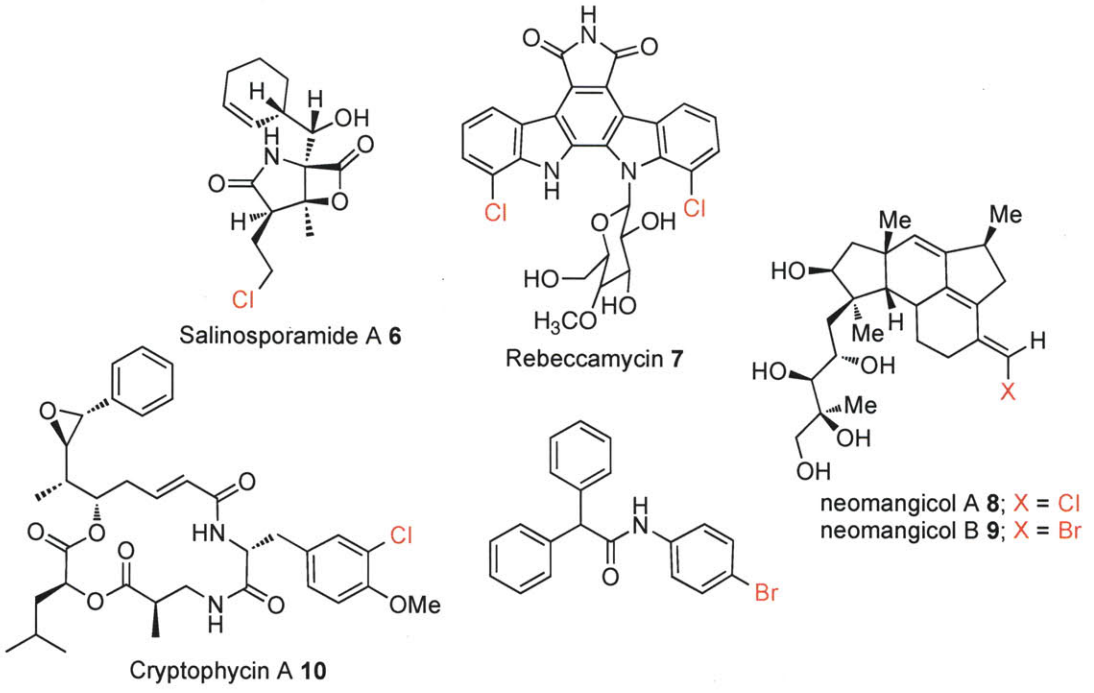

Figure 1.2. Examples of halogenated natural products. Salinosporamide A **6**, a proteosome inhibitor, is isolated from the marine bacterium *Salinospora tropica*; rebeccamycin **7**, an antitumor antibiotic, is isolated from the soil bacterium *Lechevalieria aerocolonigenes*; neomangicol A **8** and B **9**, antitumor agents, are isolated from the marine fungi *Fusarium* sp. strain CNC-477; cryptophycin A **10**, a cytotoxin, is found in cultures of the blue-green algae *Nostoc linckia*; the bromo-phenyl amide is found in the Thai plant *Arundo donax*.

Since the presence of a halogen moiety often has a profound impact on the biological activity of a compound, enzymatic halogenation has been studied in extensive detail over the past four decades[15, 21]. The current understanding of halogenating enzymes and their mechanisms of action suggest that halogenases can be divided into three groups[21]. The first group is the molecular oxygen (O_2)-dependent halogenases, which are further divided into flavin-dependent halogenases and non-heme iron-dependent halogenases. The second group is the hydrogen peroxide (H_2O_2)-dependent haloperoxidases, which are also divided into heme-dependent haloperoxidases and vanadium-dependent haloperoxidases. Finally, the last group is the nucleophilic halogenases.

The main focus of our studies is the flavin-dependent halogenases (**Figure 1.3**). Several members of this class of halogenases are well characterized and have been shown to carry out enzymatic halogenation using flavin as the redox cofactor and molecular oxygen as the oxidant[21]. Flavin-dependent halogenases can catalyze regioselective chlorination of free substrates (i.e. tryptophan **11** by PyrH, Thal, RebH or PrnA enzymes) as well as substrates that are covalently attached to a thiolation domain in a nonribosomal polypeptide synthetase (i.e. pyrrolyl-S-PltL by PltA enzyme) (**Figure 1.3**)[21]. Examples of known flavin-dependent halogenases are the following: PyrH, which converts free tryptophan **11** to 5-chlorotryptophan **11a** in pyrroindomycin biosynthesis[22]; Thal, which converts free tryptophan **11** to 6-chlorotryptophan **11b**, an intermediate in thienodolin biosynthesis[23, 24]; and finally, PrnA and RebH, both of which convert free tryptophan **11** to 7-chlorotryptophan **11c** during the biosynthesis of pyrrolnitrin[25] and rebeccamycin[26], respectively.

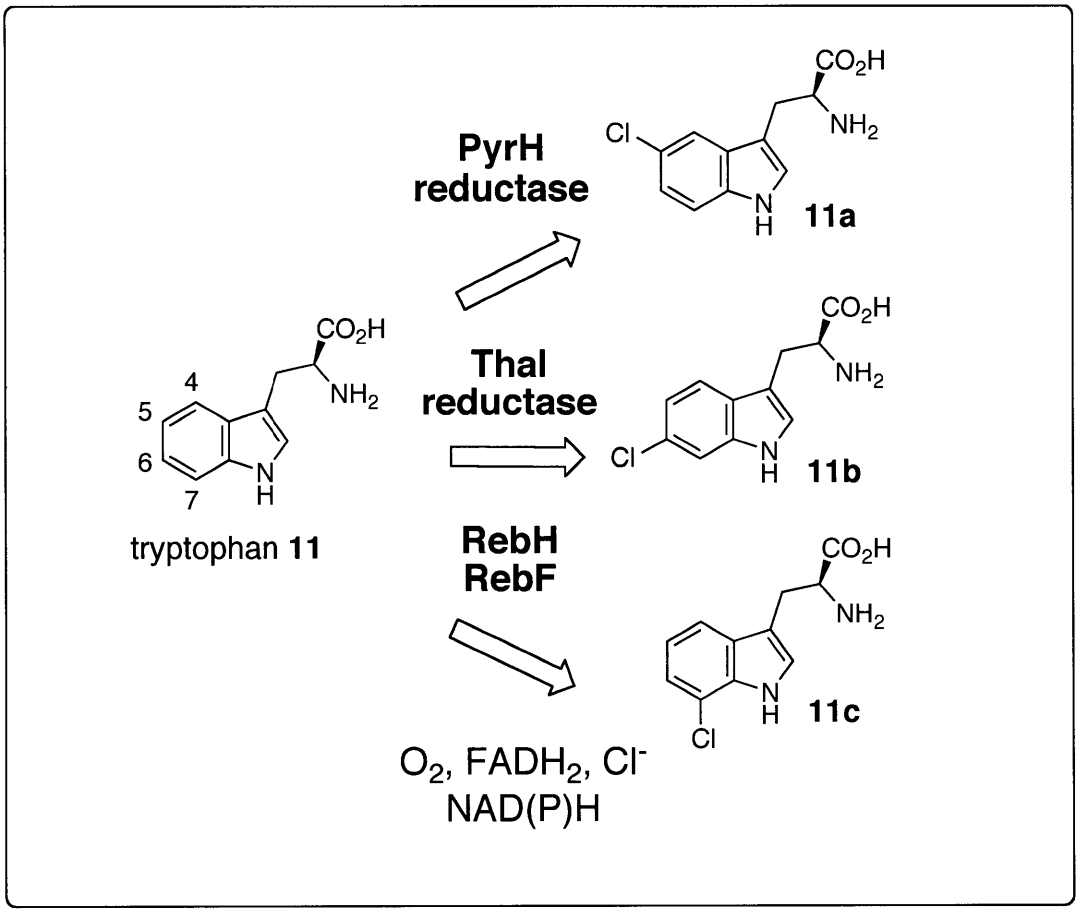

Figure 1.3. Enzymatic chlorination of tryptophan **11**. PyrH chlorinates tryptophan **11** at the 5-position; Thal chlorinates tryptophan at the 6-position; and RebH chlorinates tryptophan at the 7-position. All reactions require molecular oxygen, reduced flavin cofactor and chloride ion. The reduced flavin cofactor is reduced *in situ*, and therefore, PyrH, Thal and RebH also require an NAD(P)H-dependent partner reductase to regenerate the reduced flavin cofactor. Adapted from *Chem. Biol.* **2008,** *15*, 99-109.

Out of all known flavin-dependent halogenases, only PrnA and RebH have been structurally characterized by X-ray crystallography[27, 28]. The crystal structures of both enzymes revealed a binding module that is consistent with those in known flavin monooxygenases. Therefore, it was proposed that the reduced flavin would react with molecular oxygen (O_2) to form FAD-C_{4a}-OOH in a similar manner to that of known flavin monooxygenases (**step 1, Figure 1.4**)[29]. This proposed first step is also supported

by spectroscopic and kinetics studies, which indicate that the flavin redox chemistry could occur without tryptophan **11** present in the active site[30]. After the initial FAD-C_{4a}-OOH formation step, it is mechanistically plausible that the chloride ion could attack the proximal oxygen of FAD-C_{4a}-OOH to form FAD-C_{4a}-OCl, which would then function as the direct halogenating agent of tryptophan **11**. However, the crystal structures of PrnA and RebH showed that the tryptophan binding pocket and the flavin binding pocket are separated by over 10 angstroms[27, 28]. Moreover, the channel that connects the two binding pockets is too narrow to allow direct interaction between the tryptophan substrate and the oxidized flavin cofactor. Therefore, instead of forming FAD-C_{4a}-OCl, the next step is proposed to be an attack of the chloride ion on the distal oxygen of FAD-C_{4a}-OOH to yield the reactive oxidant hypochlorous acid (HOCl) (**step 2, Figure 1.4**)[30]. HOCl is a strong oxidant that is known to react indiscriminately with many biological molecules, including the side chains of many amino acids[31]. Therefore, the enzyme must come up with a strategy to ensure selective chlorination of tryptophan **11**. The crystal structures of both RebH and PrnA revealed a lysine residue (Lys79) in the channel that connects the tryptophan and flavin binding pockets[27, 28]. Moreover, Walsh and coworkers' ^{36}Cl radiolabeling studies indicated that chlorine forms a covalent adduct with the enzyme prior to incorporation in the product[28]. By evaluating these data in light of the known reactivity of lysine residues[31], Walsh and coworkers proposed that the trapped HOCl reacts with Lys79 to form Lys- εNH-Cl (**step 3, Figure 1.4**). While less reactive than HOCl, this lysine chloramine species is highly stable ($t_{1/2}$= 28 h at 25 °C and 63 h at 4 °C) and more discriminant towards the tryptophan **11** substrate. Therefore, in the final step of enzymatic chlorination tryptophan by RebH and PrnA, the lysine chloramine species is

proposed to deliver a Cl^+ equivalent for electrophilic aromatic substitution of tryptophan **11** at the 7-position to form 7-chlorotryptophan **11c**.

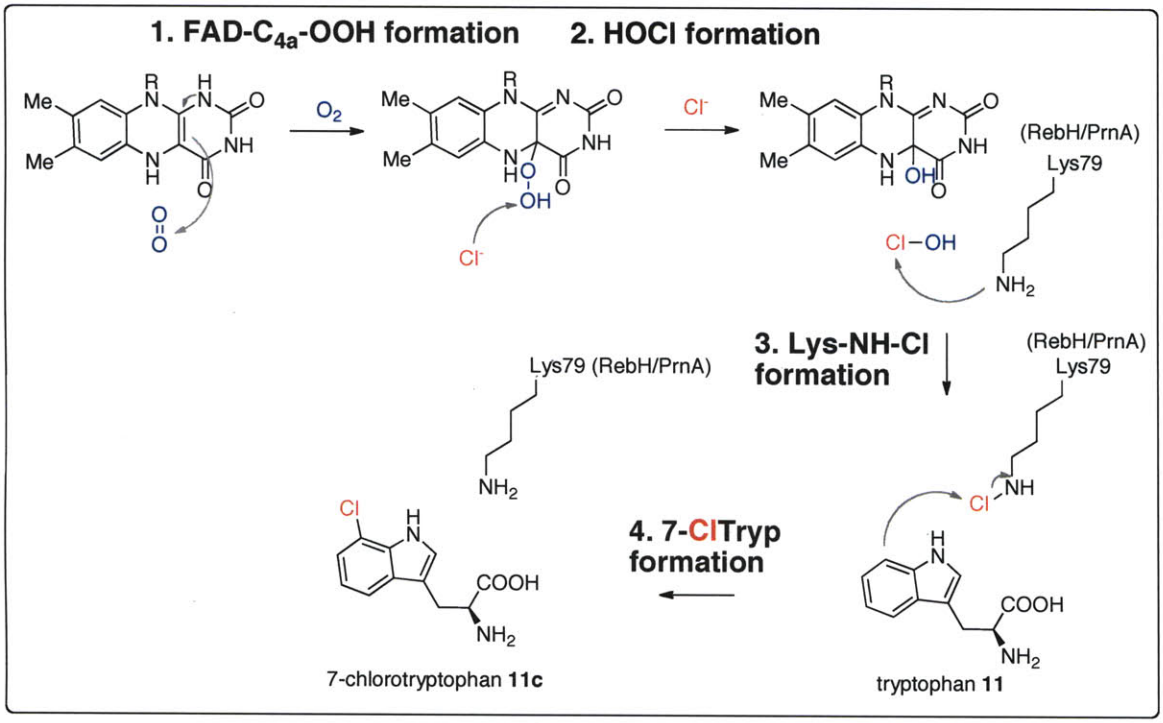

Figure 1.4. Proposed mechanism for the enzymatic chlorination of tryptophan by RebH and PrnA. Adapted from *Acc. Chem. Res.* **2009,** *42*, 147-155.

1.3 Monoterpene Indole Alkaloids from *Catharanthus roseus*

Monoterpene indole alkaloids (MIAs) comprise a structurally diverse class of natural products with over 2000 members[32]. The tropical flowering plant Madagascar periwinkle (*Catharanthus roseus*) produces over 130 MIA natural products, including the anticancer agents vinblastine **4** and vincristine **5** (**Figure 1.1**), all of which are derived from tryptophan **11**[33-35]. MIA biosynthesis begins with the stereo-selective Pictet-Spengler reaction of tryptamine **12** (derived from the decarboxylation of tryptophan **11**[33-35]) and

secologanin **13** (derived from terpene biosynthesis[36-38]) to form strictosidine **15** (**Figure 1.5**). This reaction is catalyzed by the enzyme strictosidine synthase (STR) and represents the first committed step of MIA biosynthesis[39-44]. Following the strictosidine glucosidase (SGD)-catalyzed deglucosylation of strictosidine, equilibrium of the unstable aglycon intermediates leads to the formation of 4, 21-dehydrogeissoschizine **16**, the branch-point precursor of MIAs, and cathenamine **17** (**Figure 1.5**)[45-49]. Two distinct NADPH-dependent reductases catalyze reduction of 4, 21-dehydrogeissoschizine **16** and cathenamine **17** to produce geissoschizine **18** and ajmalicine **19**, respectively[50-53].

The proposed biosynthetic pathways for catharanthine **22**, tabersonine **23** and dihydroakuammicine **25** begin with geissoschizine **18** (**Figure 1.6**)[54]. None of the enzymes responsible for the production of **22**, **23** and **25** has been cloned, and the proposed pathways are based mainly on studies that involve feeding isotopically labeled substrates to *C. roseus* seedlings[55-64]. Preakuammicine **19** is the common precursor to catharanthine **22**, tabersonine **23** and dihydroakuammicine **25**[60, 65]. The actual mechanism for the formation of preakuammicine **19** from geissoschizine **18** remains unclear. Elimination of one molecule of formaldehyde followed by reduction yields dihydroakuammicine **25** from preakuammicine **19**. Alternatively, reduction of the iminium of preakuammicine **19** leads to stemmadenine **20**, which rearranges to form the ester dehydrosecodine **21**[66, 67]. While it may be possible that both catharanthine **22** and tabersonine **23** are formed via a Diels-Alder cycloaddition from dehydrosecodine **21**, there is no precedent for this type of reaction in plant metabolism[68].

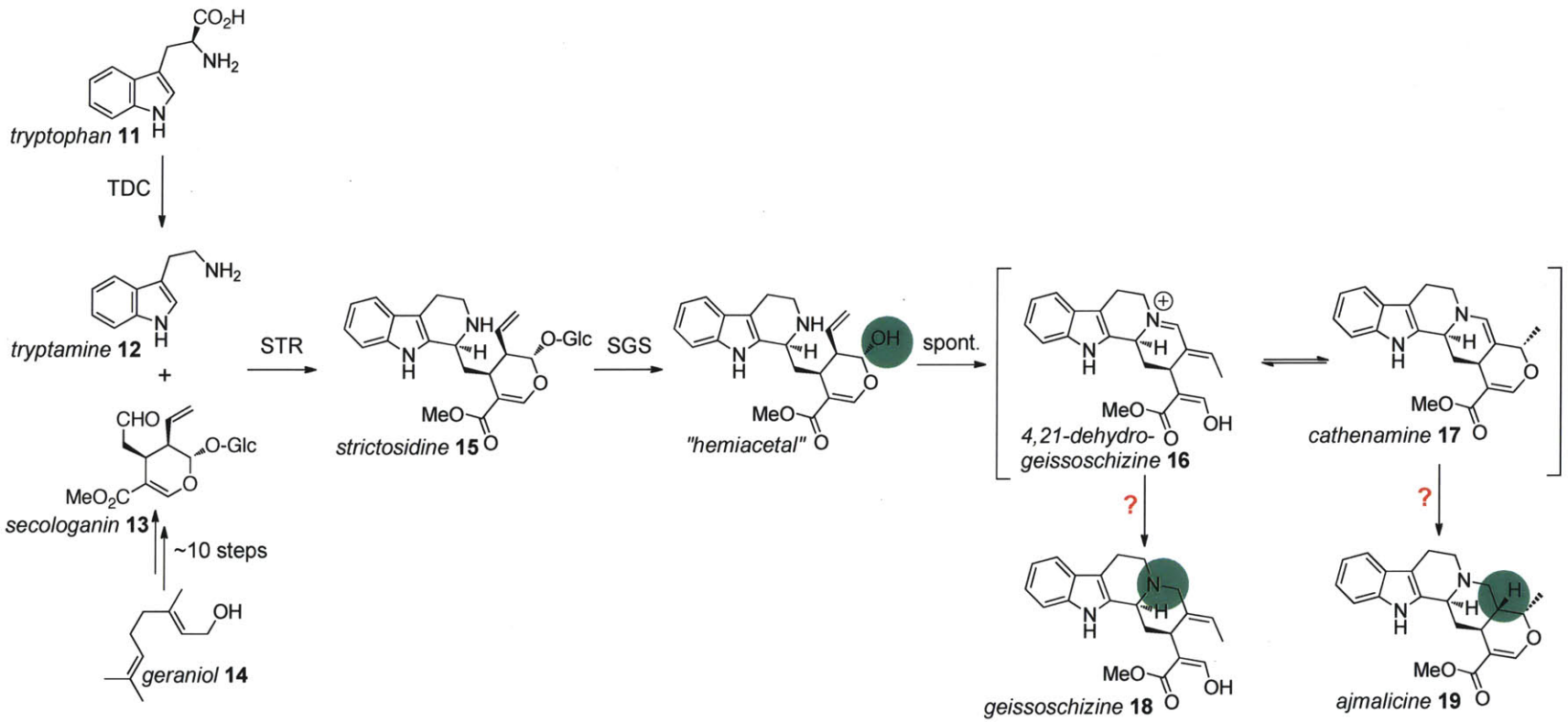

Figure 1.5. The early steps of MIA biosynthesis in *C. roseus*. TDC: tryptophan decarboxylase; STR: strictosidine synthase; SGS: strictosidine glucosidase; spont.: spontaneuous. Green circle designates the location where the enzymatic transformation has occurred. ? indicates that the biosynthetic enzyme has not been identified.

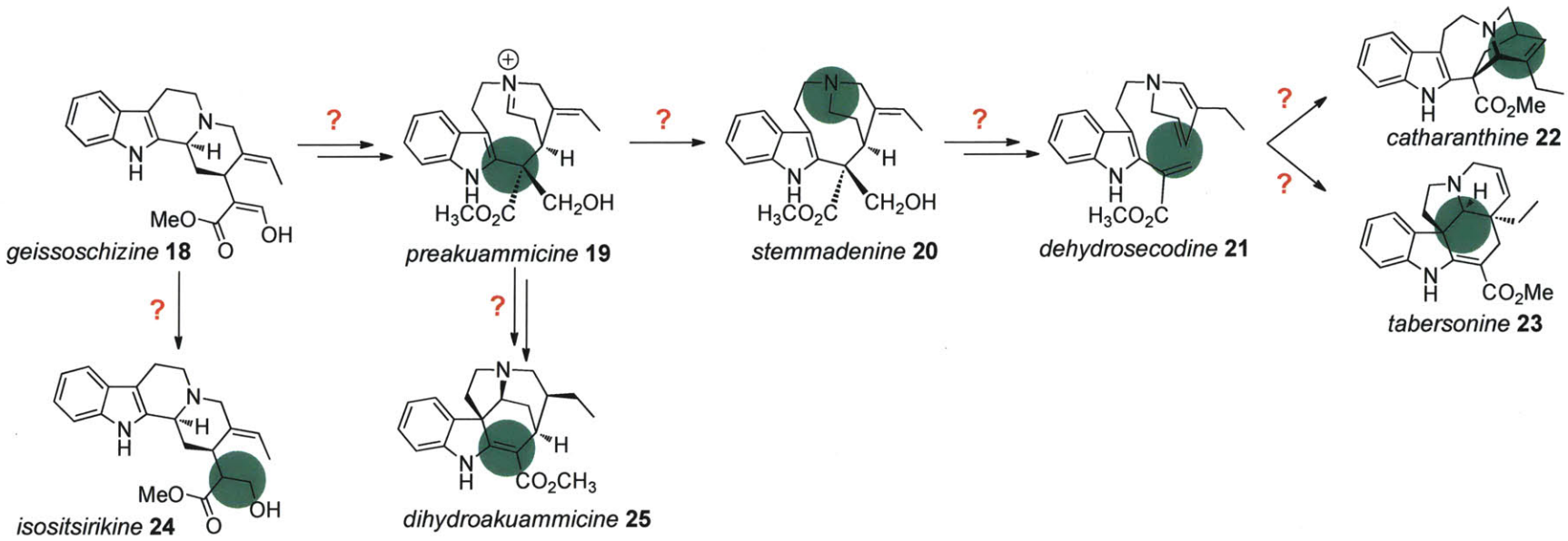

Figure 1.6. Biosynthesis of catharanthine **22**, tabersonine **23** and dihydroakuammicine **25** in *C. roseus*. Green circle designates the location where the enzymatic transformation has occurred. ? indicates that the biosynthetic enzyme has not been identified.

The six steps from tabersonine **23** to vindoline **31** have been fully elucidated at the genetic level, with the exception of the hydration step (**Figure 1.7**)[69, 70]. This pathway begins with the hydroxylation of tabersonine **23** by a cytochrome P450 monooxygenase (tabersonine 16-hydroxylase (T16H)) to form 16-hydroxytabersonine **26**[71, 72]. The hydroxyl group is subsequently methylated by a SAM-dependent O-methyltransferase (16-hydroxytabersonine 16-O-methyltransferase (16OMT)) to yield 16-methoxytabersonine **27**[73]. Following this step, a double bond in 16-methoxytabersonine **27** is hydrated by an uncharacterized enzyme to yield 16-methoxy-2,3-dihydro-3-hydroxytabersonine **28**. The recently discovered SAM-dependent N-methyltransferase then methylates the indole nitrogen of methoxy-2,3-dihydro-3-hydroxytabersonine **28** to form desacetoxyvindoline **29**[74]. The penultimate step in this sequence, the hydroxylation of desacetoxyvindoline **29**, is carried out by the 2-oxoglutarate-dependent dioxygenase desacetoxyvindoline 4-hydroxylase (D4H) to form deacetylvindoline **30**[75]. Finally, deacetylvindoline **30** is acetylated by deacetylvindoline O-acetyltransferase (DAT) to form vindoline **31**[76]. Notably, the enzymes that catalyze the last three steps of this sequence, namely NMT, D4H and DAT, are only present in the aerial parts of the plants and are absent altogether from plant cell cultures[74-76]. The dimerization of catharanthine **22** and vindoline **31** is proposed to proceed via an iminium intermediate, which is subsequently reduced to form anhydrovinblastine[77]. A peroxidase (AVLBS, α-3′,4′-anhydrovinblastine synthase) has been cloned from *C. roseus* leaves and shows robust activity in the dimerization of catharanthine **22** and vindoline **31** to anhydrovinblastine[78, 79]. Hydroxylation of anhydrovinblastine yields vinblastine **4**. Subsequent oxidation of the N-methyl group of vinblastine **4** yields vincristine **5**.

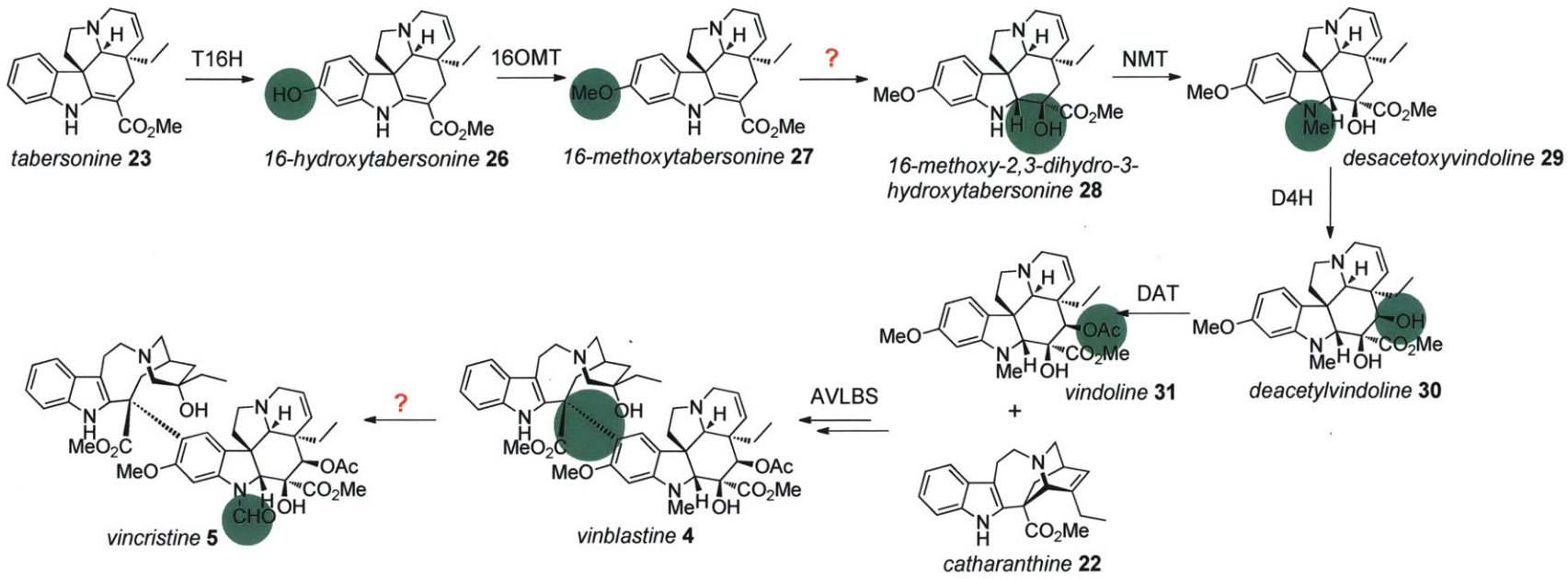

Figure 1.7. The late steps of MIA biosynthesis in *C roseus*. T16H: tabersonine 16-hydroxylase; 16OMT: 16-hydroxytabersonine 16-O-methyltransferase; NMT: 16- methoxy-2,3-dihydro-3-hydroxytabersonine N-methyltransferase; D4H: desacetoxyvindoline 4-hydroxylase; DAT: deacetylvindoline O-acetyltransferase; and AVLBS: α-3′,4′-anhydrovinblastine synthase. Green circle designates the location where the enzymatic transformation has occurred. ? indicates that the biosynthetic enzyme has not been identified.

1.4 Precursor-Directed Biosynthesis of Monoterpene Indole Alkaloids and Re-Engineering of Strictosidine Synthase

Modification of natural alkaloids can lead to the generation of compounds with improved or altered biological properties. For example, vinflunine **51**, a fluorinated analog of vinblastine, is currently in phase III clinical trials for treatment of bladder cancer[80,81]. The current supply of novel alkaloids, often generated through semi-synthesis, is limited because the requisite precursors are typically produced in low levels. Recently, however, precursor-directed biosynthesis has emerged as a powerful strategy to produce alkaloid derivatives[82]. It was discovered that supplementing *Datura stramonium* root cultures with fluorinated analogs of the phenyllactic acid substrate yielded several fluorinated tropane alkaloids[83]. In a similar effort, a wide variety of tryptamine **12** and secologanin **13** substrate analogs were fed into *C. roseus* root cultures and seedlings, affording many unnatural MIAs[84,85]. Notably, this study also identified the stringent substrate specificity of strictosidine synthase (STR) as a major bottleneck in precursor-directed biosynthesis efforts. The apparent flexibility of downstream alkaloid pathways suggested that STR could be reengineered to yield variants with improved or novel selectivity towards unnatural substrate analogs. The structural elucidation of *Rauvolfia serpentina* STR[86] has led to the development of several re-engineered STR variants with altered substrate specificity (**Figure 1.8**). The earliest re-engineering attempt of STR yielded a mutant (D177A) that was able to accept a secologanin analog harboring a pentynyl group[87]. In order to explore a larger mutational space, a medium-throughput colorimetric assay was developed to identify functional STR mutants that can accept tryptamine analogs not accepted by the wild type enzyme [88]. The assay relied on the formation of products

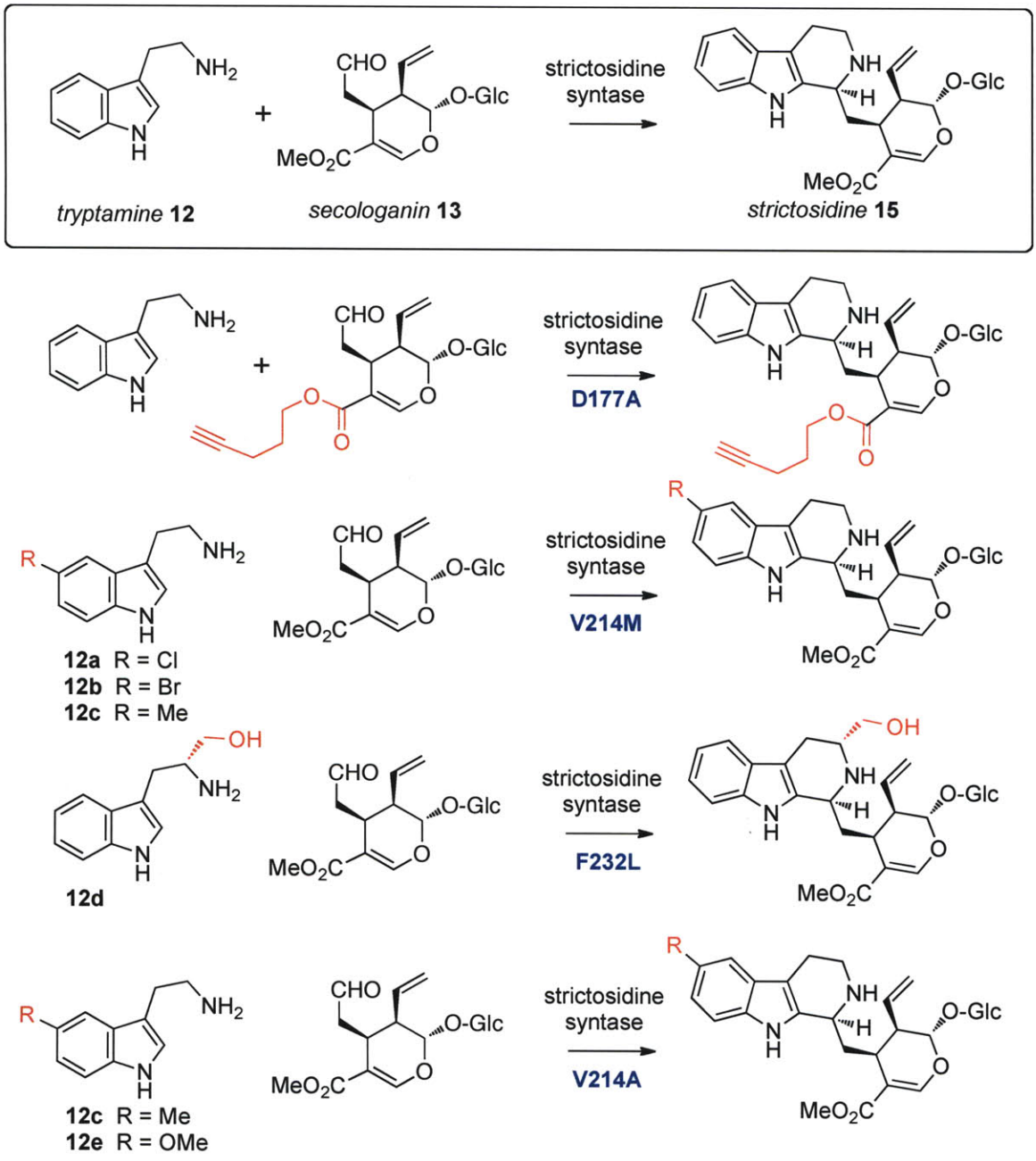

Figure 1.8. Re-engineering of strictosidine synthase (STR) to accept tryptamine **12** and secologanin **13** analogs not accepted by the wild type enzyme.

downstream of STR that can be visualized when metabolized by strictosidine glucosidase (SGD), the next enzyme in the biosynthetic pathway. By using saturation mutagenesis on several key residues that comprise the tryptamine binding pocket, two STR mutants that could turnover unnatural tryptamine compounds were identified [88]. Specifically, the V214M mutant was able to turn over 5-chloro-, 5-bromo- and 5-methyltryptamine analogs (**12a-c**), while the F232L mutant was able to turn over (*R*)-tryptaphanol **12d**. In a separate study, another STR mutant (V214A) was identified that is capable of turning over 5-methyl- and 5'methoxytryptamine (**12c, e**)[89].

1.5 Plant Cell and Tissue Cultures

In light of the difficulties involved in the total syntheses, semi-syntheses and isolation of many medicinally important alkaloids, tissue and cell cultures have been considered as alternative production platforms (**Figure 1.9**). The discovery in the 1950s[90] that undifferentiated plant cells have the necessary biosynthetic machinery to produce many of the same secondary metabolites as whole plants has led to the commercial use of plant tissue cultures for production of several important pharmaceuticals. For example, taxol, a widely used anticancer drug whose global sales have reached over one billion dollars annually, has been a subject of intense yield optimization research. After decades of studies involving various elicitation conditions and growth media formulations, concentrations of taxol as high as 0.5% of dry weight have been achieved in plant cell culture with methyl jasmonate elicitation[91]. This is a dramatic increase from levels observed in Pacific yew trees, which accumulate taxol at only 0.01 % of the dry weight[92]. More recently, cultures of undifferentiated meristematic cells from *Taxus cuspidata* have

been shown to be an environmentally friendly and cost-effective source for sustainable production of taxol[93]. Another example of a natural product that has been obtained from plant cell culture at commercial scales is shikonin, a naphthoquinone pigment. The compound has been successfully derived from *Lithospermum erythrorhizon* cell suspension cultures for use in the cosmetic industry[94].

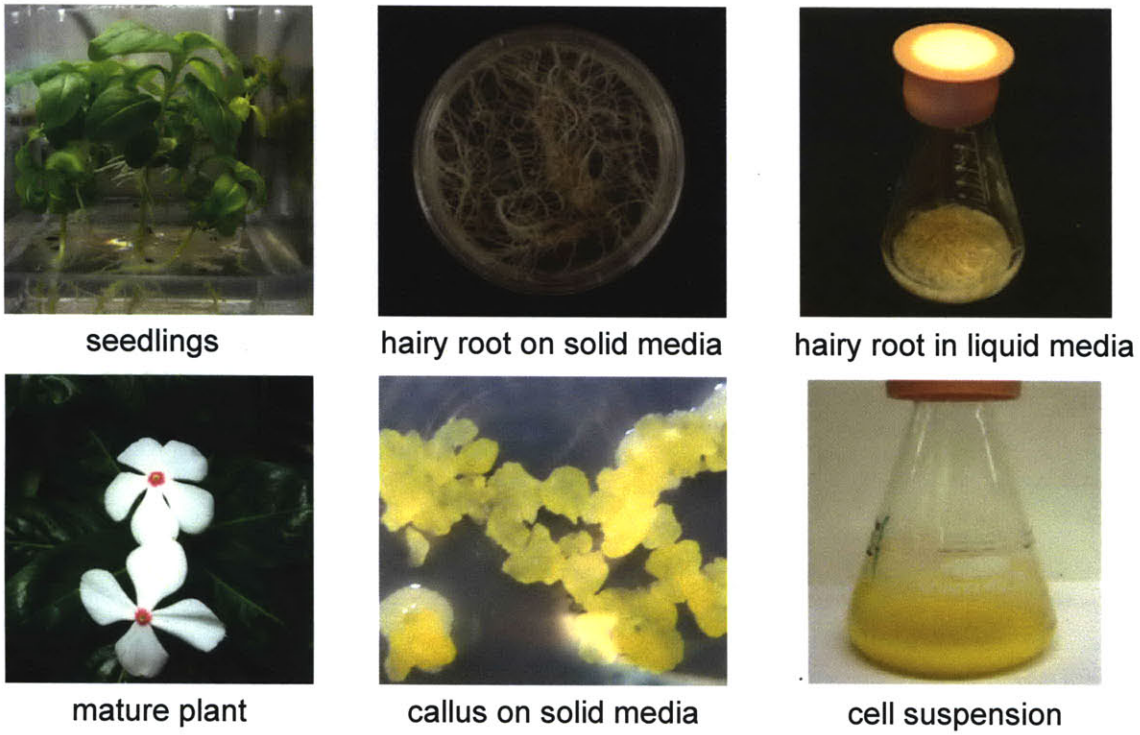

Figure 1.9. *C. roseus* whole plants, tissue and cell cultures.

The use of cell and hairy root cultures of *C. roseus* as a source for pharmaceutically important alkaloids began in the early 1960s[95]. Cell cultures can be generated by growing *C. roseus* stem explants in the presence of α-napthaleneacetic acid (an auxin) and kinetin (a cytokinin). Cultivation of *C. roseus* cell suspension cultures for alkaloid production is not feasible on an industrial scale because alkaloid levels are normally low and unstable. Extensive efforts have focused on optimizing undifferentiated plant cell suspension cultures to obtain better yield, controllability and reproducibility of several pharmaceutically important alkaloids[96]. However, because alkaloid biosynthesis appears to be tissue/organ specific and varies according to the developmental stages[97], differentiated plant tissue cultures have also been utilized as production platforms instead of cell suspension cultures[98]. Notably, *C. roseus* hairy root cultures offer more stable alkaloid profiles and yields, owing in part to their higher genetic and biochemical stability compared to cell suspension cultures[5]. Hairy root cultures can be obtained by infection of *C. roseus* stems with *Agrobacterium rhizogenes* (**Figure 1.10**)[98, 99]. While hairy root cultures of *C. roseus* have been studied extensively for their production of medicinal alkaloids, like cell suspension cultures, their commercial use has not been widespread. A key limitation of tissue cultures is that they do not make the bisindole alkaloids, vinblastine **4** and vincristine **5**, which only accumulate in the aerial parts of the plants, or the direct precursor vindoline **31**[5, 100].

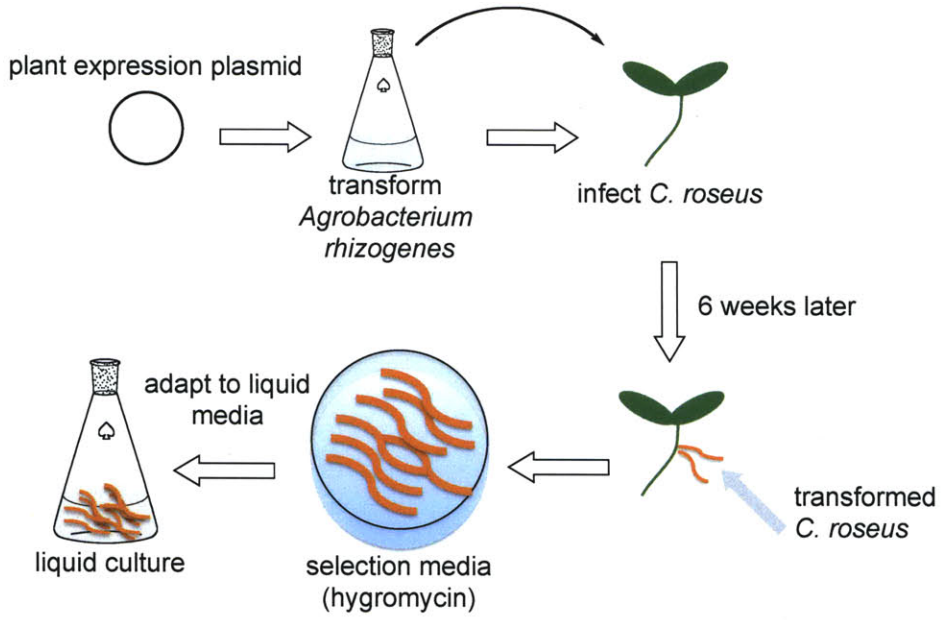

Figure 1.10. Procedure to generate transgenic *C.roseus* hairy root cultures. *C. roseus* seedlings are wounded, and transformed *A. rhizogenes* from a freshly grown liquid culture are inoculated on the wound. Hairy roots appeared at the wound site 2-3 weeks after infection. After hairy roots reached 1-4 cm in length (usually about six weeks after infection), they are excised and transferred to solid media containing hygromycin for the selections. After the solid media selection process, hairy roots are adapted to liquid culture.

1.6 Elicitation of Monoterpene Indole Alkaloid Biosynthesis and Metabolic Engineering in *C. roseus*

The biosynthesis of alkaloids can often be improved through various elicitation and culture manipulation strategies. Elicitation of MIA biosynthesis using biotic and abiotic elicitors has been successful at increasing the alkaloid yields in both tissue and cell culture systems[9]. When elicitors are present, a number of signal-transduction pathways are activated, which subsequently lead to transcriptional activation of many alkaloid biosynthetic genes and transcription factors[95]. For example, methyl jasmonate (MeJA), a plant hormone, has been shown to increase the expression of several biosynthetic genes, including TDC, STR, AVLBS and three other genes that are involved in the biosynthesis of secologanin and tryptophan[101]. Addition of jasmonic acid, another plant hormone, to *C. roseus* hairy root cultures led to increased accumulations of the majority of alkaloids typically found in root tissue including ajmalicine **19**, serpentine **32**, lochnericine **33** and horhammericine **34**[102-104]. Similarly, elicitation with extracts from the plant pathogen *Phytophthora cactorum* and the cell walls of the fungi *Pennicillium citrinum* stimulated alkaloid production in *C. roseus* cell suspension cultures[105]. Abiotic elicitors, such as light and heavy metals, also affect MIA biosynthesis in *C. roseus*. Visible[106, 107] and UV-lights[108, 109] have been demonstrated to increase alkaloid accumulations in cell and hairy root cultures. Treating *C. roseus* cell suspension cultures with cadmium[110] and rare-earth elements such as vanadium, cerium, yttrium and neodymium[111, 112] also improved the yield of total alkaloids.

In addition to elicitation and growth condition optimization, metabolic engineering strategies have also been utilized to improve alkaloid production in plant tissue and cell cultures (**Figure 1.11**). The increasing availability of systems biology datasets has led to more effective metabolic engineering efforts to expand the capacity for alkaloid biosynthesis in plant cultures. For example, overexpression of strictosidine synthase (STR) in *C. roseus* plant culture led to 10-fold higher STR activity compared to wild type lines and higher levels of the downstream alkaloids, ajmalicine **19**, serpentine **32**, catharanthine **22** and tabersonine **23** [116,117]. Interestingly, alkaloid levels in highly productive lines were unstable; after two years of subculture, the transgenic cell lines lost their ability to produce high levels of alkaloids. Constitutive overexpression of tryptophan decarboxylase (TDC) only enhanced tryptamine **12** production but not levels of downstream alkaloids[113]. Cell cultures overexpressing TDC also exhibited slow growth as high levels of tryptamine seemed to be detrimental to *C. roseus*. Tryptophan **11** biosynthesis has previously been shown to be feedback-inhibited; accumulation of tryptophan **11** can inhibit expression of anthranilate synthase (AS)[114]. Overexpression of both *Arabidopsis thaliana* feedback-resistant AS and tryptophan TDC in *C. roseus* did improve the yields of early precursors tryptophan **11** and tryptamine **12**, but failed to increase the yields of downstream alkaloids[114-116]. These studies suggest that the availability of tryptophan **11** and tryptamine **12** do not appear to be rate-limiting in MIA biosynthesis. Conversely, secologanin **13** availability has been shown to be rate-limiting as improvements in secologanin branch pathway successfully increased the alkaloid yields in cell and hairy root cultures[117-119]. Overexpression of geraniol 10-hydroxylase (G10H) in *C. roseus* hairy root cultures led to a three-fold increase in alkaloid

accumulations[120]. Similarly, overexpression of both 1-deoxy-D-xylulose synthase (DXS) and geraniol 10-hydroxylase (G10H) in *C. roseus* hairy roots led to increased accumulations of ajmalicine **19**, lochnericine **33** and tabersonine **23**[121].

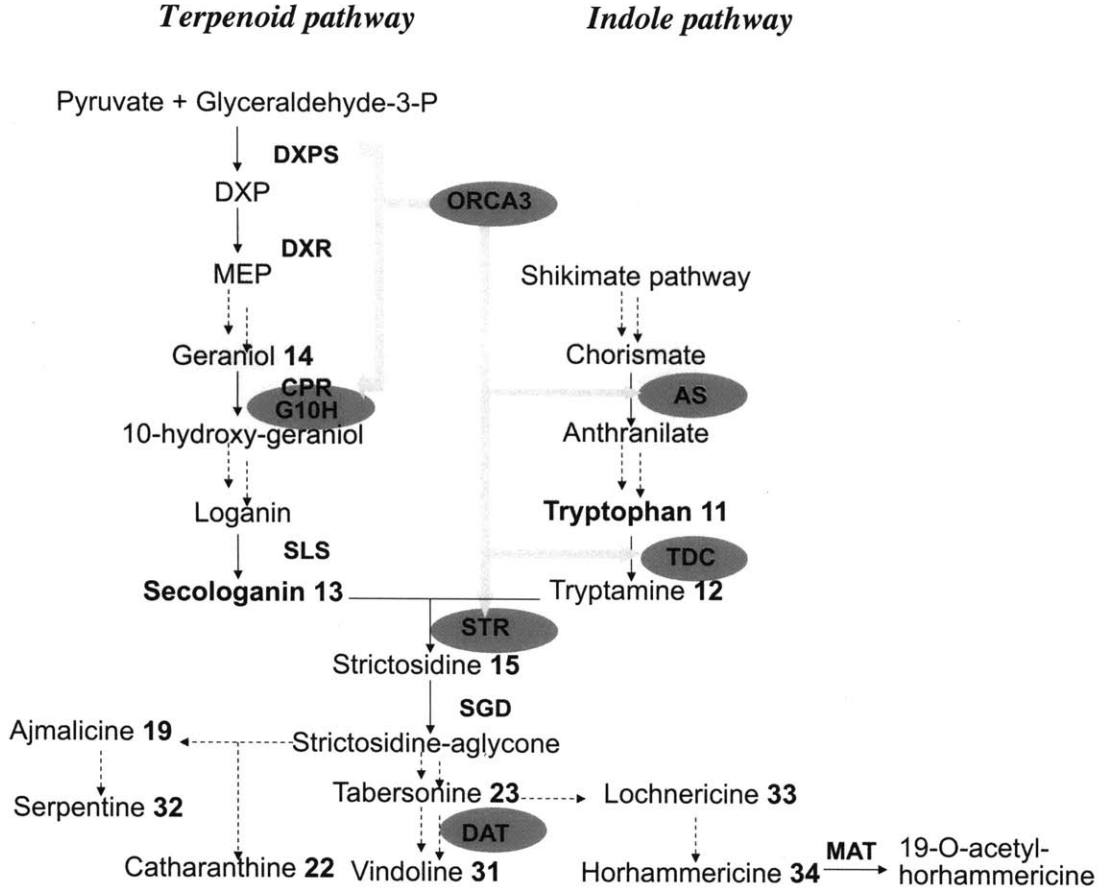

Figure 1.11. Summary of metabolic engineering efforts of monoterpene indole alkaloids in *C. roseus*. Enzymes that are highlighted in gray ovals have been targeted for overexpression in *C. roseus* cell suspension or hairy root cultures.

Downstream enzymes have also been targeted for metabolic engineering (**Figure 1.11**). Overexpression of deacetylvindoline 4-O-acetyltransferase (DAT), which catalyzes the acetylation of deacetylvindoline **30** to form vindoline **31**, led to a four-fold increase in the accumulation of horhammericine **34**, an alkaloid not in the vindoline pathway[122]. The authors concluded that there is crosstalk between vindoline biosynthesis and horhammericine pathway. Specifically, overexpression of DAT inhibited the activity of minovincinine 19-O-acetyltransferase (MAT), the enzyme that turns over horhammericine. Complex relationships between metabolic pathways such as these are among the many factors that often hamper the ability to target overproduction of a particular metabolite in plant cell and tissue cultures predictably.

Over the past decade, the alkaloid metabolic regulatory machinery, such as transcription factors, has emerged as another target for metabolic engineering efforts. Transcriptomic analysis of alkaloid biosynthetic genes has led to the identification of several transcription factors in MIA biosynthesis[101, 123]. Targeting transcription factors that upregulate the expression of multiple MIA biosynthetic genes simultaneously, as compared to overexpressing one or two biosynthetic genes at a time, was hypothesized to lead to higher overproduction of MIAs. For example, a metabolic engineering strategy was devised to exploit the utility of the ORCA3 transcription factor to upregulate the expression of many MIA biosynthetic genes simultaneously (**Figure 1.11**)[101]. Surprisingly, overexpression of ORCA3 in *C. roseus* cell cultures did not significantly improve MIA synthesis. While ORCA3 upregulates the expression of many alkaloid biosynthetic genes, it does not appear to regulate the expression of G10H, the enzyme in

the terpenoid pathway that leads to the synthesis of secologanin **13**[101]. A ~3-fold increase in MIA accumulation levels of ORCA3-overexpressing cell culture occurred only after the media was supplemented with loganin, the precursor of secologanin **13**. Therefore, there appears to be a bottleneck in the terpenoid pathway that can be overcome by loganin feeding. Altogether, these studies suggest that MIA biosynthesis is tightly regulated. Consequently, it is often hard to predict the outcome of metabolic engineering designs in the native plant host.

1.7 Reconstitution of Alkaloid Biosynthetic Pathways in Microbial Hosts

The past decade has witnessed an increasing interest in engineering of microorganisms, particularly *Escherichia coli* and *Saccharomyces cerevisiae,* for the synthesis of high-value natural products[124]. Because of their smaller genome size, the degree of complexity in microorganisms is significantly lower than that of plants. Notably, microbial genetics—with key features that include the coordinately regulated and clustering of genes that encode biosynthetic pathways—are significantly more tractable. Moreover, microorganisms have fewer intracellular organelles compared to plant cells; thus, transport of metabolites between enzymatic steps are likely negligible. The difficult genetic manipulation of plants coupled to the tractability of microorganisms has encouraged significant interest in microbial engineering for the synthesis of several plant-derived metabolites[125-129].

More recently, alkaloids joined the list of plant-derived natural products that have been successfully fermented in microbes[126, 128]. In one study, reconstitution of alkaloid

biosynthetic pathways in *E. coli* and *S. cerevisiae* has led to scalable productions of several benzylisoquinoline alkaloids (BIAs) (**Figure 1.12**)[128]. In BIA-producing plants, the first committed step of all BIAs begins with the condensation of dopamine **36** and 4-hydroxyphenyl-acetaldehyde **37** to form *(S)*-norcoclaurine **38** (**Figure 1.12, left panel**)[130, 131]. This reaction is catalyzed by the enzyme norcoclaurine synthase (NCS). *(S)*-norcoclaurine **38** is then sequentially methylated by norcoclaurine 6-O-methyltransferase (6-OMT) and coclaurine-N-methyltransferase (CNMT). The resulting dimethylated intermediate is hydroxylated by the cytochrome-P450 CYP80B3, and further methylated by 3'-hydroxy-N-methylcoclaurine-4'-O-methyltransferase (4'-OMT) to yield *(S)*-reticuline **39**. To reconstitute reticuline biosynthesis in *E. coli*, *Micrococcus luteus* monoamine oxidase (MAO) was introduced together with *Coptis japonica* NCS, 6-OMT, CNMT, and 4'-OMT in a plasmid-based expression systems (**Figure 1.12, center panel**)[128]. The utilization of the microbial MAO allowed the incorporation of the hydroxyl group early in the reticuline pathway through the synthesis of 3, 4-dihydroxyphenyl-acetaldehyde **47** from dopamine **36**, thereby precluding the need to express the plant P450 CYP80B3 in the bacterium, which is usually challenging. *(R, S)*-reticuline **40** (approximately 11mg/L) could be detected in the culture media of the engineered *E. coli* upon induction of enzyme expression and supplementation of the media with dopamine **36**. Interestingly, while *in vitro* studies of plant NCS indicated that the enzyme is stereoselective and produces the *(S)*-enantiomer exclusively, both enantiomers of reticulene **40** were observed in the growth media, suggesting the presence of a chemical non-stereoselective reaction. Nevertheless, the availability of *(R, S)*-reticuline **40** set the stage for the production of downstream BIAs. Co-culturing the

reticuline-producing *E. coli* with *S. cerevisiae* expressing the *C. japonica* berberine bridge enzyme (BBE) led to the production of *(S)*-scoulerine **42** (8.3 mg/L) after 2-3 days of incubation.

While the study highlighted above is a tremendous achievement in microbial engineering, its significance is hampered by the utilization of two microbial systems. The use of two microbial systems likely led to lower efficiency of alkaloid biosynthesis because of the need to transport metabolites between cells. Hawkins and Smolke overcame this problem by reconstituting part of the artificial BIA pathways entirely in *S. cerevisiae* (**Figure 1.12, right panel**)[126]. Instead of using the natural intermediate norcoclaurine **38**, Hawkins and Smolke used the commercially available norlaudanosoline **48** to produce *(R, S)*-reticuline **40** in engineered *S. cerevisiae* expressing 6-OMT, CNMT, and 4'-OMT from plants (*Thalictrum flavum* and *Papaver somniferum*). By choosing enzymes that had optimal catalytic efficiency and promoters that led to optimal expression levels, the authors successfully produce *(R, S)*-reticuline **40** in titres reaching 150 mg/mL. To produce alkaloids *(S)*-scoulerine **42**, *(S)*-tetrahydrocolumbamine and *(S)*-tetrahydroberberine, which are further downstream, three additional enzymes from *T. flavum*, *P. somniferum* and a reductase partner from *Arabidopsis thaliana* were introduced into the *(R, S)*-reticuline-producing strain. The authors showed that the introduction of a human cytochrome P450 enzyme (CYP2D6) and its reductase partner into *(R, S)*-reticuline-producing strain led to the production of *(S)*-salutaridine **41**, an intermediate in the morphine branch pathway.

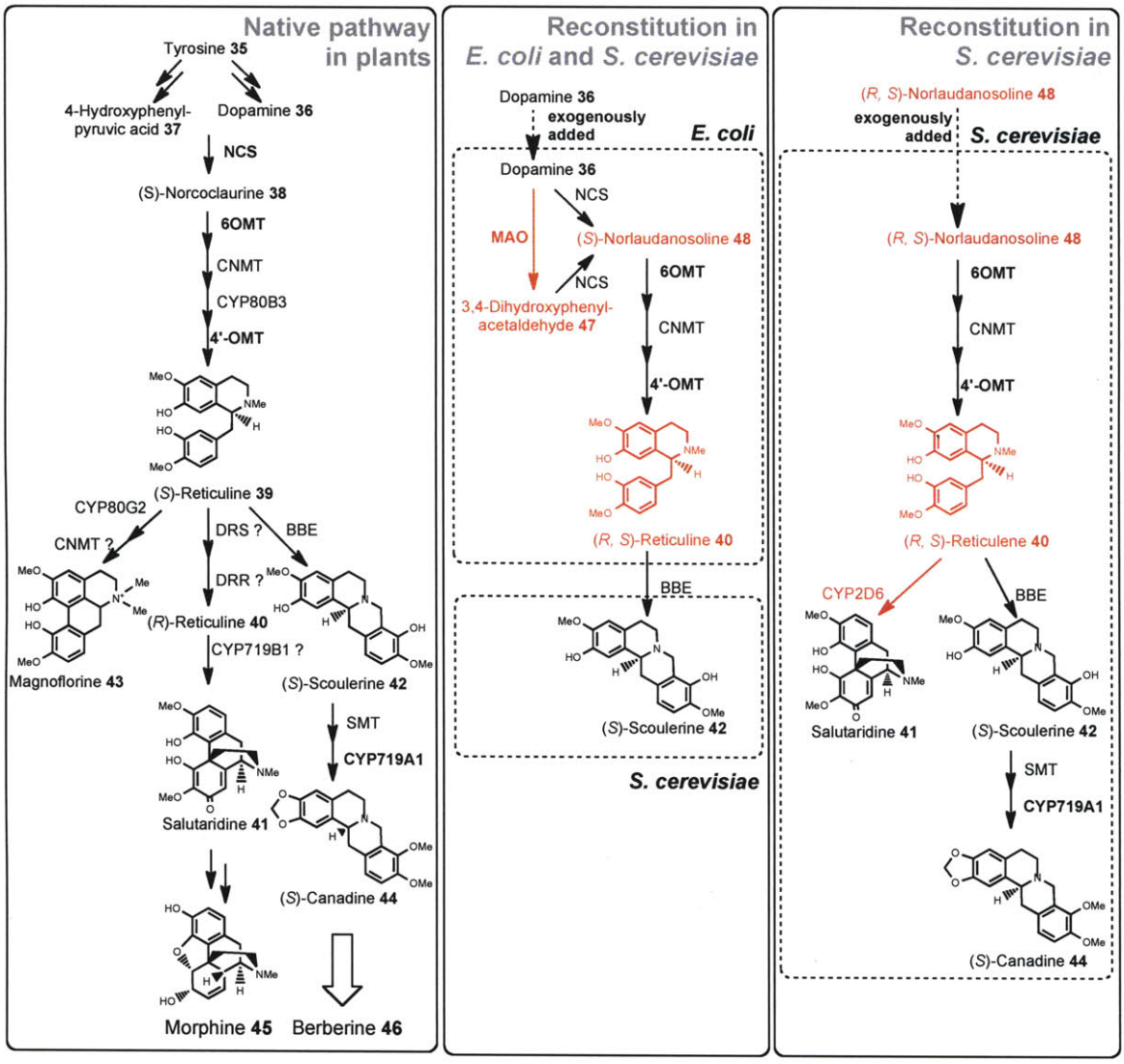

Figure 1.12. Reconstitution of benzylisoquinoline alkaloid pathway in microorganisms. Plant pathway (left). Reconstituion in both *E. coli* and *S. cerevisiae* (center). Reconstitution in *S. cerevisiae* only (right). Modified enzymatic steps and metabolites are highlighted in red. NCS, norcoclaurine synthase; 6-OMT, norcoclaurine 6-O-methyltransferase; CNMT, coclaurine-N-methyltransferase; 4′-OMT, 3′-hydroxy-N-methylcoclaurine-4′-O-methyltransferase; DRS, 1,2- dehydroreticuline synthase; DRR, 1,2-dehydroreticulene reductase; BBE, berberine bridge enzyme; SMT, scoulerine 9-O-methyltransferase; MAO, bacterial monoamine oxidase; CYP2D6, human cytochrome P450 enzyme; CYP80G2, CYP719B1 and CYP719A1, plant cytochrome P450 enzymes. Adapted from *Nature Chemical Biology* **2009**, *5*, 292-300.

Efforts to reconstitute monoterpene indole alkaloid (MIA) pathways in microbial systems have been hampered by the paucity of cloned biosynthetic genes. Consequently, the only MIAs that have been successfully produced through microbial fermentation at this time are pathway intermediates that are well upstream of the higher-value alkaloids vinblastine **4** and vincristine **5**. In one study, expression of *C. roseus* strictosidine synthase (STR) and strictosidine glucosidase (SGD) in *S. cerevisiae* led to the production of strictosidine **15** and cathenamine **17** when the precursors secologanin **13** and tryptamine **12** were supplemented to the media[132]. As was also the case in reconstitution of BIA pathways, supplementation of the yeast culture media with expensive intermediate metabolites was necessary for alkaloid production. Enzymes responsible for the multi-step conversion of geraniol **14** to secologanin **13** have not all been identified. Therefore reconstitution of secologanin pathway in yeast is not possible at this time. However, since a major goal of microbial fermentation is to produce complex molecules from inexpensive and commercially available starting substrates, it is imperative to identify these enzymes and express them in yeast or *E. coli* to make microbial fermentation of high-value alkaloids commercially feasible.

The studies highlighted above demonstrated the power of microbial engineering in producing structurally complex alkaloids. Interestingly, these studies also revealed that the plant enzymes involved in BIA synthesis appeared to have relatively flexible substrate specificity. Therefore, as this field, recently coined "synthetic biology", progresses, it may be advantageous to extend the goals of microbial engineering to encompass the production of unnatural alkaloids in the search for new medicines.

1.8 Chemical Derivatizations of Monoterpene Indole Alkaloids

Functional group modification of natural products can lead to the generation of compounds with improved or altered pharmacological properties[133]. Extensive efforts have focused on using synthetic strategies to produce alkaloid analogs. Beginning in the 1960s, several analogs of MIAs have been synthesized either via total synthesis or semi-synthesis (**Figure 1.13**)[138-142]. Notably, ring contraction and dehydration of vinblastine **4** afforded vinorelbine **49**, which was approved for the treatment of non small-cell lung cancer (NSCLC) in 1995[134-136]. Similarly, vindesine **50**, another vinblastine analog with modifications in the vindoline portion of the molecule, has been approved for treatment of melanoma in Europe[137]. Finally, vinflunine **51**, a fluorinated derivative of vinblastine, is currently in phase III clinical trials for treatment of bladder cancer[80,81].

Vinblastine **4** and vincristine **5** are the main targets for most of the chemical derivatization efforts reported mainly because of their established anticancer properties. The earliest attempts to diversify MIAs focused mostly on halogenation reactions. Bromination of vinblastine **4** and vincristine **5** with N-bromosuccinamide at room temperature afforded 10-bromovinblastine **4a** and 10-bromovincristine **5a** in moderate yields[138]. Similarly, iodination of vinblatine **4** and vincristine **5** can be achieved using N-iodosuccinamide to yield 10-iodovinblastine **4b** and 10-iodovincristine **5b** (**Figure 1.14**)[138]. The abundance and versatility of palladium-catalyzed cross-coupling reactions today allows further modification of halogenated alkaloids. **Figure 1.14** summarizes palladium-mediated coupling reactions of halogenated vinblastine **4** and vincristine **5**,

including the Suzuki-Miyaura, Negishi, Sonagashira and Stille coupling reactions as well as nitrillation, thioetherification, and carboxylation[138].

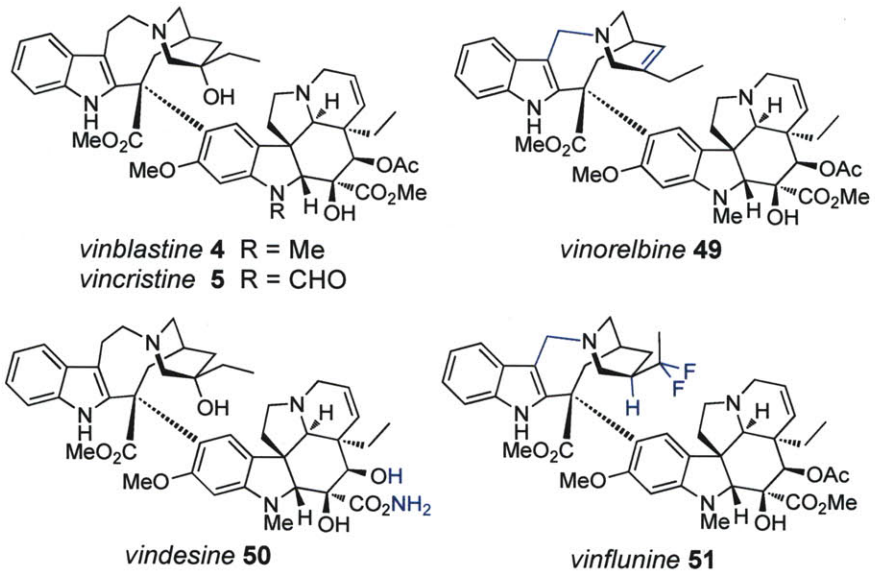

Figure 1.13. Examples of vinblastine analogs that have been approved for clinical use or are currently under clinical trials.

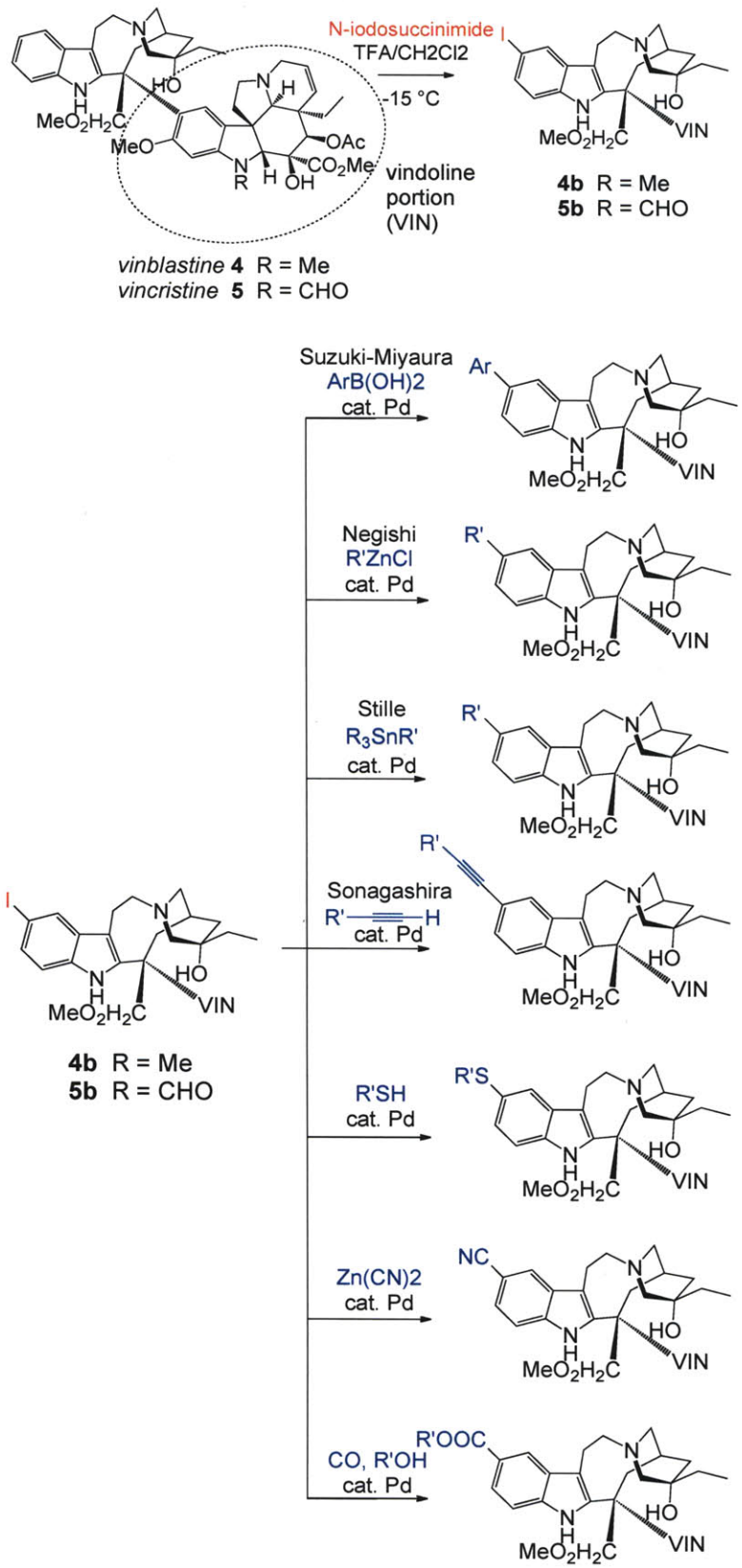

Figure 1.14. Synthetic diversification of MIAs via palladium-catalyzed cross-coupling reactions. Adapted from *Bioorg Med Chem Lett* **2009,** *19*, 1245-9.

1.9 Research Goals and Thesis Overview

The research goals that are addressed in this thesis are the following:

A: To Expand the Diversity of Plants' Natural Products

Medicinal plants have been a source and inspiration for medicinal chemists. *Catharanthus roseus* (Madagascar periwinkle) produces over 130 monoterpene indole alkaloids (MIAs), many of which have pharmaceutical properties, such as the antitumor agents vinblastine **4** and vincristine **5**. Expanding the diversity of plants' natural products via functional group modification can yield "unnatural" products with altered or improved biological activities. Chapter 2 describes the introduction of a biosynthetic enzyme with redesigned substrate specificity into periwinkle. The resulting transgenic plant hairy root culture was able to produce a variety of unnatural MIA compounds by incorporating tryptamine **12** analogs that the re-engineered enzyme was designed to accept. Chapter 3 describes the introduction of a new functional group– the organohalide– into periwinkle MIAs. Prokaryotic halogenase enzymes were transformed into the genome of periwinkle, which lacks the biosynthetic capability to produce halogenated compounds. These prokaryotic halogenases competently functioned in the plant cell to generate halogenated tryptophan **11** analogs, which were then incorporated into alkaloid metabolism to yield a variety of halogenated MIAs. A new functional group–the organohalide– was thereby integrated into the complex metabolism of periwinkle in a predictable and regioselective manner. Finally, chapter 4 describes the suppression of tryptamine **12** biosynthesis in periwinkle for the production of unnatural MIAs. Alkaloid production almost completely disappeared in silenced cultures, but could be rescued by the addition of exogenous tryptamine **12** to the culture media. A

representative unnatural tryptamine analog was also incorporated into the pathway to yield a variety of unnatural alkaloids.

B: To Explore Plant Cell Culture as a Platform for Synthetic Biology

The past decade has witnessed an increasing interest in engineering of microorganisms, particularly *Escherichia coli* and *Saccharomyces cerevisiae*, for the synthesis of high-value plant natural products. Up until now, this so-called 'synthetic biology' approach has been demonstrated exclusively in microbial systems. The organisimal complexity and genetic intractability of plants have prevented widespread interest in using plants as a platform for synthetic biology. Chapter 3 describes the successful engineering of plant cell culture to autonomously produce halogenated alkaloids. The yields of unnatural alkaloids in plant cultures are comparable to reconstitution of alkaloid pathways in microorganisms. In short, we demonstrated that plant cell cultures are indeed a viable platform for synthetic biology efforts.

C: To Complement Synthetic Biology with Organic Chemistry

While halogenation, in and of itself, often has profound effects on the bioactivity of natural products, halides could also serve as a useful handle for further chemical derivatization. Chapter 5 describes the post-biosynthetic chemical derivatizations of halogenated alkaloid analogs via palladium-catalyzed Suzuki-Miyaura cross-coupling reactions to yield aryl and heteroaryl analogs of MIAs. The complementation of synthetic biology and organic chemistry approaches provides an effective route to form a library of analogs in a synergistic fashion—a library not attainable using either approach alone.

Financial Support

The MIT/Dupont Presidential Fellowship, the Royal Thai Government, the Department of Chemistry, the MIT Graduate Student Council and via research grants from the Beckman Foundation, the NIH (GM074820), the US National Science Foundation (MCB0719120), and the American Cancer Society (RSG-07-025-01-CDD)

1.10 References

1. Koehn, F. E.; Carter, G. T., The evolving role of natural products in drug discovery. *Nat. Rev. Drug Discov.* **2005,** *4*, 206-220.
2. Maplestone, R. A.; Stone, M. J.; Williams, D. H., The evolutionary role of secondary metabolites-a review. *Gene* **1992,** *115*, 151-157.
3. Williams, D. H.; Stone, M. J.; Hauck, P. R.; Rahman, S. K., Why are secondary metabolites (natural products) biosynthesized? *J. Nat. Prod.* **1989,** *52*, 1189-1208.
4. Newman, D. J.; Cragg, G. M., Natural products as sources of new drugs over the last 25 years. *J. Nat. Prod.* **2007,** *70*, 461-477.
5. Facchini, P. J.; De Luca, V., Opium poppy and Madagascar periwinkle: model non-model systems to investigate alkaloid biosynthesis in plants. *Plant J.* **2008,** *54*, 763-784.
6. Verpoorte, R.; van der Heijden, R.; Memelink, J., Engineering the plant cell factory for secondary metabolite production. *Transgenic Res.* **2000,** *9*, 323-343.
7. Hartmann, T., Plant-derived secondary metabolites as defensive chemicals in herbivorous insects: a case study in chemical ecology. *Planta* **2004,** *219* (1), 1-4.
8. Beghyn, T.; Deprez-Poulain, R.; Willand, N.; Folleas, B.; Deprez, B., Natural compounds: leads or ideas? Bioinspired molecules for drug discovery. *Chem. Biol. Drug Des.* **2008,** *72*, 3-15.
9. Kutchan, T. M., Alkaloid biosynthesis[mdash]the basis for metabolic engineering of medicinal plants. *Plant Cell* **1995,** *7*, 1059-1070.
10. Leonard, E.; Runguphan, W.; O'Connor, S.; Prather, K. J., Opportunities in metabolic engineering to facilitate scalable alkaloid production. *Nat Chem Biol* **2009,** *5* (5), 292-300.
11. Kuboyama, T.; Yokoshima, S.; Tokuyama, H.; Fukuyama, T., Stereocontrolled total synthesis of (+)-vincristine. *Proc. Natl. Acad. Sci. USA* **2004,** *101*, 11966-11970.
12. Miyazaki, T., Synthesis of (+)-vinblastine and its analogues. *Org. Lett.* **2007,** *9*, 4737-4740.
13. Uchida, K.; Yokoshima, S.; Kan, T.; Fukuyama, T., Total synthesis of (+/-)-morphine. *Org. Lett.* **2006,** *8*, 5311-5313.

14. Yokoshima, S., Stereocontrolled total synthesis of (+)-vinblastine. *J. Am. Chem. Soc.* **2002,** *124*, 2137-2139.
15. Neumann, C. S.; Fujimori, D. G.; Walsh, C. T., Halogenation strategies in natural product biosynthesis. *Chem. Biol.* **2008,** *15*, 99-109.
16. Gribble, G. W., The diversity of naturally produced organohalogens. *Chemosphere* **2003,** *52*, 289-297.
17. Groll, M.; Huber, R.; Potts, B. C., Crystal structures of Salinosporamide A (NPI-0052) and B (NPI-0047) in complex with the 20S proteasome reveal important consequences of beta-lactone ring opening and a mechanism for irreversible binding. *J Am Chem Soc* **2006,** *128* (15), 5136-41.
18. Borissenko, L.; Groll, M., 20S proteasome and its inhibitors: crystallographic knowledge for drug development. *Chem Rev* **2007,** *107* (3), 687-717.
19. Rodrigues Pereira, E. t.; Belin, L.; Sancelme, M.; Prudhomme, M.; Ollier, M.; Rapp, M.; Severe, D. l.; Riou, J.-F. o.; Fabbro, D.; Meyer, T., Structure-Activity Relationships in a Series of Substituted Indolocarbazoles: Topoisomerase I and Protein Kinase C Inhibition and Antitumoral and Antimicrobial Properties. *Journal of Medicinal Chemistry* **1996,** *39* (22), 4471-4477.
20. Renner, M. K.; Jensen, P. R.; Fenical, W., Neomangicols: Structures and Absolute Stereochemistries of Unprecedented Halogenated Sesterterpenes from a Marine Fungus of the Genus Fusarium. *The Journal of Organic Chemistry* **1998,** *63* (23), 8346-8354.
21. Blasiak, L. C.; Drennan, C. L., Structural perspective on enzymatic halogenation. *Acc. Chem. Res.* **2009,** *42*, 147-155.
22. Zehner, S.; Kotzsch, A.; Bister, B.; Süssmuth, R. D.; Méndez, C.; Salas, J. A.; van Pée, K. H., A regioselective tryptophan 5-halogenase is involved in pyrroindomycin biosynthesis in Streptomyces rugosporus LL-42D005. *Chem. Biol.* **2005,** *12*, 445-452.
23. Seibold, C.; Schnerr, H.; Rumpf, J.; Kunzendorf, A.; Hatscher, C.; Wage, T.; Ernyei, A. J.; Dong, C.; Naismith, J. H.; Van Pee, K.-H., A flavin-dependent tryptophan 6-halogenase and its use in modification of pyrrolnitrin biosynthesis. *Biocatalysis and Biotransformation* **2006,** *24* (6), 401-408.
24. van Pee, K. H.; Dong, C.; Flecks, S.; Naismith, J.; Patallo, E. P.; Wage, T., Biological halogenation has moved far beyond haloperoxidases. *Adv Appl Microbiol* **2006,** *59*, 127-57.
25. Keller, S.; Wage, T.; Hohaus, K.; Holzer, M.; Eichhorn, E.; van Pee, K. H., Purification and Partial Characterization of Tryptophan 7-Halogenase (PrnA) from Pseudomonas fluorescens *Angew Chem Int Ed Engl* **2000,** *39* (13), 2300-2302.
26. Yeh, E.; Garneau, S.; Walsh, C. T., Robust in vitro activity of RebF and RebH, a two component reductase halogenase generating 7-chlorotryptophan during rebeccamycin biosynthesis. *Proc. Natl. Acad. Sci.* **2005,** *102*, 3960-3965.
27. Dong, C.; Flecks, S.; Unversucht, S.; Haupt, C.; van Pee, K. H.; Naismith, J. H., Tryptophan 7-halogenase (PrnA) structure suggests a mechanism for regioselective chlorination. *Science* **2005,** *309* (5744), 2216-9.
28. Yeh, E.; Blasiak, L. C.; Koglin, A.; Drennan, C. L.; Walsh, C. T., Chlorination by a long-lived intermediate in the mechanism of flavin-dependent halogenases. *Biochemistry* **2007,** *46*, 1284-1292.
29. Entsch, B.; Van Berkel, W. J. H., Structure and mechanism of para-hydroxybenzoate hydroxylase. *FASEB Journal* **1995,** *9* (7), 476-483.

30. Yeh, E.; Cole, L. J.; Barr, E. W.; Bollinger, J. M.; Ballou, D. P.; Walsh, C. T., Flavin redox chemistry precedes substrate chlorination during the reaction of the flavin-dependent halogenase RebH. *Biochemistry* **2006,** *45*, 7904-7912.
31. Nightingale, Z. D.; Lancha Jr, A. H.; Handelman, S. K.; Dolnikowski, G. G.; Busse, S. C.; Dratz, E. A.; Blumberg, J. B.; Handelman, G. J., Relative reactivity of lysine and other peptide-bound amino acids to oxidation by hypochlorite. *Free Radical Biology and Medicine* **2000,** *29* (5), 425-433.
32. O'Connor, S. E.; Maresh, J., Chemistry and biology of monoterpene indole alkaloid biosynthesis. *Nat. Prod. Rep.* **2006,** *23*, 532-547.
33. de Luca, V.; Marineau, C.; Brisson, N., Molecular cloning and analysis of a cDNA encoding a plant tryptophan decarboxylase. *Proc. Natl. Acad. Sci. USA* **1989,** *86*, 2582-2586.
34. Facchini, P. J.; Huber-Allanach, K. L.; Tari, L. W., Plant aromatic L-amino acid decarboxylases: evolution, biochemistry, regulation, and metabolic engineering applications. *Phytochemistry* **2000,** *54*, 121-138.
35. Hong, S.-B. P., Christie A. M.; Shanks, Jacqueline V.; San, Ka-Yiu; Gibson, Susan I., Terpenoid indole alkaloid production by Catharanthus roseus hairy roots induced by Agrobacterium tumefaciens harboring rol ABC genes. *Biotech. Bioengineer.* **2006,** *93*, 386-390.
36. Battersby, A. R.; Burnett, A. R.; Parsons, P. G., Preparation of secologanin: its conversion into ipecoside and its role in indole alkaloid biosynthesis. *Chem. Comm.* **1968**, 180-1281.
37. Battersby, A. R.; Burnett, A. R.; Parsons, P. G., Secologanin: Its conversion into ipecoside and its role as a biological precursor of the indole alkaoids. *J. Chem. Soc., C* **1969**, 1187-1192.
38. Battersby, A. R.; Byrne, J. C.; Kapil, R. S.; Martin, J. A.; Payne, T. G.; Arigoni, D.; Loew, P., The mechanism of indole alkaloid biosynthesis. *Chem. Comm.* **1968**, 951-953.
39. Battersby, A. R.; Lewis, N. G., The basic glucosdides related to the biosynthesis of indole and ipecac alkaloids. *Tetrahedron Lett.* **1978,** *48*, 4849-4852.
40. Brown, R. T.; Leonard, J.; Sleigh, S. K., The role of strictosidine in monoterpenoid indole alkaoid biosynthesis. *Phytochemistry* **1978,** *78*, 899-900.
41. Heckendorf, A. H.; Hutchinson, C. R., Biosynthesis of campothecin II. Confirmation that isovincoside is the penultimate biosynthetic precursor of indole alkaloids. *Tetrahedron Lett.* **1977,** *48*, 4153-4154.
42. Nagakura, N.; Ruffer, M.; Zenk, M. H., The biosynthesis of monoterpenoid indole alkaloids from strictosidine. *J. Chem. Soc. Perkin Trans. I* **1979**, 2308-2312.
43. Scott, A. I.; Lee, S. L.; de Capite, P.; Culver, M. G., The role of isovincoside in the biosynthesis of the indole alkaloids. *Heterocycles* **1977,** *7*, 979-984.
44. Stockigt, J.; Zenk, M. H., Strictosidine: The key intermediate in the biosynthesis of monoterpenoid indole alkaloids. *J. Chem. Soc. Chem. Comm.* **1977**, 646-648.
45. Geerlings, A., Strictosidine-b-D-glucosidase; and enzyme in the biosynthesis of pharmaceutically important indole alkaloids. *Ph.D. thesis, Leiden University, ISBN 90-74538-40-1* **1999**.
46. Geerlings, A.; Ibanez, M. M.-L.; Memelink, J.; Van der Heijden, R.; Verpoorte, R., Molecular cloning and analysis of strictosidine b-D-glucosidase, an enzyme in

terpenoid indole alkaloid biosynthesis in Catharanthus roseus. *J. Biol. Chem.* **2000,** *275*, 3051-3056.
47. Hemscheidt, T.; Zenk, M. H., Glucosidases involved in indole alkaloid biosynthesis of Catharanthus cell cultures. *FEBS Lett.* **1980,** *110*, 187-191.
48. Luijendijk, T. J. C.; Stevens, L. H.; Verpoorte, R., Purification and characterisation of strictosidine-b-glucosidase from Catharanthus roseus cell suspension cultures. *Plant Physiol. Biochem.* **1998,** *36*, 419-425.
49. Scott, A. I.; Lee, S. L.; Wan, W., Indole alkaloid biosyntheis: Partial purification of "ajmalicine synthetase" from Catharanthus roseus. *Biochem. Biophys. Res. Comm.* **1977,** *75*, 1004-1009.
50. Hemscheidt, T.; Zenk, M. H., Partial purification and characterization of a NADPH dependent tetrahydroalstonine synthase from Catharanthus rosues cell suspension cultures. *Plant Cell Rep.* **1985,** *4*, 216-219.
51. Stockigt, J., Indirect involvement of geissoschizine in the biosynthesis of ajmalicine and related alkaloids. *J. Chem. Soc. Chem. Comm.* **1978**, 1097-1099.
52. Stockigt, J.; Hemscheidt, T.; Hofle, G.; Heinstein, P.; Formacek, V., Steric course of hydrogen transfer during enzymatic formation of 3a-heteroyohimbine alkaloids. *Biochemistry* **1983,** *22*, 3448-3452.
53. Stoeckigt, J.; Hoefle, G.; Pfitzner, A., Mechanism of the biosynthetic conversion of geissoschizine to 19-epi-ajmalicine in Catharanthus roseus. *Tetrahedron Lett.* **1980,** *21*, 1925-1926.
54. Qureshi, A. A.; Scott, A. I., Biosynthesis of indole alkaloids: Sequential precursor formation and biological conversion in Vinca rosea. *Chem. Comm.* **1968**, 948-950.
55. Battersby, A. R.; Bhatnagar, A. K., Evidence from synthesis and isolation concerning the rearrangement process in indole biosynthesis. *Chem. Comm.* **1970**, 193-195.
56. Battersby, A. R.; Burnett, A. R.; Hall, E. S.; Parsons, P. G., The rearrangement process in indole alkaloid biosynthesis. *Chem. Comm.* **1968**, 1582-1583.
57. Battersby, A. R.; Burnett, A. R.; Parsons, P. G., Alkaloid biosynthesis. Partial synthesis and isolation of vincoside and isovincoside. Biosynthesis of the three major classes of indole alkaloids from vincoside. *J. Chem. Soc., C* **1969**, 1193-1200.
58. Battersby, A. R.; Gibson, K. H., Further studies on rearrangement during biosynthesis of indole alkaloids. *Chem. Comm.* **1971**, 902-903.
59. Battersby, A. R.; Hall, E. S., The intermediacy of geissoschizine in indole alkaloid biosynthesis: Rearrangement to the strychnos skeleton. *Chem. Comm.* **1969**, 793-794.
60. Scott, A. I.; Qureshi, A. A., Biogenesis of Strychnos, Aspidosperma and Iboga alkaloids. The structure and reactions of preakuammicine. *J. Amer. Chem. Soc.* **1969,** *91*, 5874-5876.
61. Scott, A. I.; Reichardt, P. B.; Slaytor, M. B.; Sweeny, J. G., Mechanisms of indole alkaloid biosynthesis. *Bioorg. Chem.* **1971,** *1*, 157-173.
62. Scott, A. I.; Wei, C. C., Regio and stereospecific models for the biosynthesis of the indole alkaloids. The corynanthe/strychnos/iboga relationship. *J. Am. Chem. Soc.* **1972,** *94*, 8263-8264.

63. Scott, A. I.; Wei, C. C., Regio and stereoslective models for the biosynthesis of the indole alkaloids. The corynanthe aspidosperma relationship. *J. Am. Chem. Soc.* **1972,** *94*, 8264-8265.
64. Scott, A. I.; Wei, C. C., Regio and stereoslective models for the biosynthesis of the indole alkaloids. The aspidosperma iboga relationship. *J. Am. Chem. Soc.* **1972,** *94*, 8266-8267.
65. Wenkert, E.; Wickberg, B., General methods of synthesis of indole alkaloids. IV. A synthesis of dl-eburnamonine. *J. Amer. Chem. Soc.* **1965,** *87*, 1580-1589.
66. Kutney, J. P.; Ehret, C.; Nelson, V. R.; Wigfield, D. C., Studies on indole alkaloid biosynthesis. *J. Amer. Chem. Soc.* **1968,** *90*, 5929-5930.
67. Qureshi, A. A.; Scott, A. I., Interconversion of corynanthe, aspidosperma and iboga alkaloids a model for indole alkaloid biosynthesis. *Chem. Comm.* **1968**, 945-946.
68. Laschat, S., Pericyclic Reactions in Biological Systems—Does Nature Know About the Diels—Alder Reaction? *Angewandte Chemie International Edition in English* **1996,** *35* (3), 289-291.
69. De Luca, V., Biochemistry and molecular biology of indole alkaloid biosynthesis: the implication of recent discoveries. *Rec. Adv. Phytochem.* **2003,** *37*, 181-202.
70. Hashimoto, T.; Yamada, Y., New genes in alkaloid metabolism and transport. *Curr. Opin. Biotech.* **2003,** *14*, 163-168.
71. Schroder, G.; Unterbusch, E.; Kaltenbach, M.; Schmidt, J.; Strack, D.; de Luca, V.; Schroder, J., Light induced cytochrome P450 dependent enzyme in indole alkaoid biosynthesis: tabersonine 16-hydroxylase. *FEBS Lett.* **1999,** *458*, 97-102.
72. St. Pierre, B.; De Luca, V., A cytochrome P-450 monooxygenase catalyzes the first step in the conversion of tabersonine to vindoline in Catharanthus roseus. *Plant Physiol.* **1995,** *109*, 131-139.
73. Cacace, S.; Schroder, G.; Wehinger, E.; Strack, D.; Schmidt, J.; Schroder, J., A flavonol O-methyltransferase from Catharanthus roseus performing two sequential methylations. *Phytochemistry* **2003,** *62*, 127-137.
74. Liscombe, D. K.; Usera, A. R.; O'Connor, S. E., Homolog of tocopherol C methyltransferases catalyzes N methylation in anticancer alkaloid biosynthesis. *Proc Natl Acad Sci U S A* **2010,** *107* (44), 18793-8.
75. Vazquez-Flota, F.; De Carolis, E.; Alarco, A.; De Luca, V., Molecular cloning and characterization of desacetoxyvindoline-4-hydroxylase, a 2-oxoglutarate dependent-dioxygenase involved in the biosynthesis of vindoline in Catharanthus roseus (L.) G. Don. *Plant Mol. Biol.* **1997,** *34*, 935-948.
76. St. Pierre, B.; Laflamme, P.; Alarco, A.; De Luca, V., The terminal O-acetyltransferase involved in vindoline biosynthesis defines a new class of proteins responsible for coenzyme A-dependent acyl transfer. *Plant J.* **1998,** *14*, 703-713.
77. Scott, A. I.; Gueritte, F.; Lee, S. L., Role of anhydrovinblastine in the biosynthesis of the antitumor dimeric indole alkaloids. *J. Am. Chem. Soc.* **1978,** *100*, 6253-6255.
78. Hillou, F.; Costa, M.; Almeida, I.; Lopes Cardoso, I.; Leech, M.; Ros Barcelo, A.; Sottomayor, M., Cloning of a peroxidase enzyme involved in the biosynthesis of pharmaceutically aciveterpenoid indole alkaloids in Catharanthus roseus. In *Proceedings of the VI International Plant Peroxidase Symposium.*, Acosta, M.; Rodriguez-Lopez, J. N.; Pedreno, M. A., Eds. 2002; pp 152-158.

79. Sottomayor, M.; Lopez-Serrano, M.; DiCosmo, F.; Ros Barcelo, A., Purification and characterization of anhydrovinblastine synthase (peroxidase like) from Catheranthus roseus. *FEBS Lett.* **1998,** *428*, 299-303.
80. Fumoleau, P.; Campone, M.; Vorobiof, D.; Casado, M.; Ruff, P.; Khoo Kei, S.; Cortes-Funes, H.; Khalfallah, S.; Caroff, I.; Colin, C., Phase II study of i.v. vinflunine as second line in patients with metastatic breast cancer after anthracycline-taxane failure. *J. Clin. Oncology* **2004,** *22*, 542.
81. Bellmunt, J.; Delgado, F. M.; George, C., Clinical Activity of Vinflunine in Transitional Cell Carcinoma of the Urothelium and Other Solid Tumors. *Seminars in Oncology* **2008,** *35* (SUPPL 3), S34-S43.
82. Chartrain, M.; Salmon, P. M.; Robinson, D. K.; Buckland, B. C., Metabolic engineering and directed evolution for the production of pharmaceuticals. *Curr. Opin. Biotech.* **2000,** *11*, 209-214.
83. O' Hagan, D.; Robins, R. J.; Wilson, M.; Wong, C. W.; Berry, M., Fluorinated tropane alkaloids generated by directed biosynthesis in transformed root cultures of Datura stramonium. *J. Chem. Soc. Perkin Trans. 1* **1999**, 2117-2120.
84. Galan, M. C.; McCoy, E.; O'Connor, S. E., Chemoselective derivatization of alkaloids in periwinkle. *Chem. Commun.* **2007**, 3249-3251.
85. McCoy, E.; O'Connor, S. E., Directed biosynthesis of alkaloid analogues in the medicinal plant periwinkle. *J. Am. Chem. Soc.* **2006,** *128*, 14276-14277.
86. Ma, X.; Panjikar, S.; Koepke, J.; Loris, E.; Stockigt, J., The structure of *Rauvolfia serpentina* strictosidine synthase is a novel six-bladed beta-propeller fold in plant proteins. *Plant Cell* **2006,** *18*, 907-920.
87. Chen, S.; Galan, M. C.; Coltharp, C.; O'Connor, S. E., Redesign of a central enzyme in alkaloid biosynthesis. *Chem. Biol.* **2006,** *13*, 1137-1141.
88. Bernhardt, P.; McCoy, E.; O'Connor, S. E., Rapid identification of enzyme variants for reengineered alkaloid biosynthesis in periwinkle. *Chem Biol* **2007,** *14* (8), 888-97.
89. Loris, E. A.; Panjikar, S.; Ruppert, M.; Barleben, L.; Unger, M.; Schubel, H.; Stockigt, J., Structure-based engineering of strictosidine synthase: Auxiliary for alkaloid libraries. *Chem. Biol.* **2007,** *14*, 979-985.
90. Stafford, A. M.; Pazoles, C. J.; Siegel, S.; Yeh, L. A., Plant Cell Culture: a Vehicle for Drug Delivery. Nature Publishing Group: 1998.
91. Yukimune, Y.; Tabata, H.; Higashi, Y.; Hara, Y., Methyl jasmonate-induced overproduction of paclitaxel and baccatin III in Taxus cell suspension cultures. *Nat. Biotechnol.* **1996,** *14*, 1129-1132.
92. Witherup, K. M., Taxus spp. needles contain amounts of taxol comparable to the bark of Taxus brevifolia: analysis and isolation. *J. Nat. Prod.* **1990,** *53*, 1249-1255.
93. Lee, E. K.; Jin, Y. W.; Park, J. H.; Yoo, Y. M.; Hong, S. M.; Amir, R.; Yan, Z.; Kwon, E.; Elfick, A.; Tomlinson, S.; Halbritter, F.; Waibel, T.; Yun, B. W.; Loake, G. J., Cultured cambial meristematic cells as a source of plant natural products. *Nat Biotechnol* **2010,** *28* (11), 1213-7.
94. Touno, K.; Tamaoka, J.; Ohashi, Y.; Shimomura, K., Ethylene induced shikonin biosynthesis in shoot culture of Lithospermum erythrorhizon. *Plant Physiol. Biochem.* **2005,** *43*, 101-105.

95. Zhou, M.-L.; Shao, J.-R.; Tang, Y.-X., Production and metabolic engineering of terpenoid indole alkaloids in cell cultures of the medicinal plant Catharanthus roseus (L.) G. Don (Madagascar periwinkle). *Biotechnology and applied Biochemistry* **2009,** (4), 313.
96. Gamborg, O. L., Plant tissue culture. Biotechnology. Milestones. *In Vitro Cell. Dev. Biol. Plant* **2002,** *38*, 84-92.
97. Filner, P.; Varner, J. E.; Wray, J. L., Environmental or developmental changes cause many enzyme activities of higher plants to rise or fall. *Science* **1969,** *165*, 358-367.
98. Shanks, J. V.; Morgan, J., Plant 'hairy root' culture. *Curr. Opin. Biotechnol.* **1999,** *10*, 151-155.
99. Bhadra, R.; Vani, S.; Shanks, J. V., Production of indole alkaloids by selected hairy root lines of Catharanthus roseus. *Biotechnol. Bioeng.* **1993,** *41*, 581-592.
100. O'Connor, S. E.; Maresh, J. J., Chemistry and biology of monoterpene indole alkaloid biosynthesis. *Nat. Prod. Rep.* **2006,** *23*, 532-547.
101. van der Fits, L.; Memelink, J., ORCA3, a jasmonate-responsive transcriptional regulator of plant primary and secondary metabolism. *Science* **2000,** *289* (5477), 295-7.
102. Rijhwani, S. K.; Ho, C. H.; Shanks, J. V., In vivo 31P and multilabel 13C NMR measurements for evaluation of plant metabolic pathways. *Metab Eng* **1999,** *1* (1), 12-25.
103. Rijhwani, S. K.; Shanks, J. V., Effect of elicitor dosage and exposure time on biosynthesis of indole alkaloids by Catharanthus roseus hairy root cultures. *Biotechnol Prog* **1998,** *14* (3), 442-9.
104. Shanks, J. V.; Bhadra, R.; Morgan, J.; Rijhwani, S.; Vani, S., Quantification of metabolites in the indole alkaloid pathways of Catharanthus roseus: implications for metabolic engineering. *Biotechnol. Bioeng.* **1998,** *58*, 333-338.
105. Asada, M.; Shuler, M. L., Stimulation of ajmalicine production and excretion from Catharanthus roseus: effects of adsorption in situ, elicitors and alginate immobilization. *Applied Microbiology and Biotechnology* **1989,** *30* (5), 475-481-481.
106. De Luca, V.; St Pierre, B., The cell and developmental biology of alkaloid biosynthesis. *Trends Plant Sci.* **2000,** *5*, 168-173.
107. Vazquez-Flota, F. A.; St-Pierre, B.; De Luca, V., Light activation of vindoline biosynthesis does not require cytomorphogenesis in Catharanthus roseus seedlings. *Phytochemistry* **2000,** *55*, 531-536.
108. Ouwerkerk, P. B.; Hallard, D.; Verpoorte, R.; Memelink, J., Identification of UV-B light-responsive regions in the promoter of the tryptophan decarboxylase gene from Catharanthus roseus. *Plant Mol Biol* **1999,** *41* (4), 491-503.
109. Ramani, S.; Chelliah, J., UV-B-induced signaling events leading to enhanced-production of catharanthine in Catharanthus roseus cell suspension cultures. *BMC Plant Biol* **2007,** *7*, 61.
110. Zheng, Z.; Wu, M., Cadmium treatment enhances the production of alkaloid secondary metabolites in Catharanthus roseus. *Plant Science* **2004,** *166* (2), 507-514.
111. Zhao, J.; Zhu, W.-H.; Hu, Q.; Guo, Y.-Q., Improvement of indole alkaloid production in Catharanthus roseus cell cultures by osmotic shock. *Biotechnology Letters* **2000,** *22* (15), 1227-1231-1231.
112. Smith, J. I.; Smart, N. J.; Misawa, M.; Kurz, W. G. W.; Tallevi, S. G.; DiCosmo, F., Increased accumulation of indole alkaloids by some cell lines of Catharanthus roseus in response to addition of vanadyl sulphate. *Plant Cell Reports* **1987,** *6* (2), 142-145.

113. Canel, C.; Lopes-Cardoso, M. I.; Whitmer, S.; van der Fits, L.; Pasquali, G.; van der Heijden, R.; Hoge, J. H.; Verpoorte, R., Effects of over-expression of strictosidine synthase and tryptophan decarboxylase on alkaloid production by cell cultures of Catharanthus roseus. *Planta* **1998,** *205* (3), 414-9.
114. Hong, S. B.; Peebles, C. A.; Shanks, J. V.; San, K. Y.; Gibson, S. I., Expression of the Arabidopsis feedback-insensitive anthranilate synthase holoenzyme and tryptophan decarboxylase genes in Catharanthus roseus hairy roots. *J. Biotechnol.* **2006,** *122*, 28-38.
115. Hughes, E. H.; Hong, S. B.; Gibson, S. I.; Shanks, J. V.; San, K. Y., Expression of a feedback-resistant anthranilate synthase in Catharanthus roseus hairy roots provides evidence for tight regulation of terpenoid indole alkaloid levels. *Biotechnol. Bioeng.* **2004,** *86*, 718-727.
116. Hughes, E. H.; Hong, S. B.; Gibson, S. I.; Shanks, J. V.; San, K. Y., Metabolic engineering of the indole pathway in Catharanthus roseus hairy roots and increased accumulation of tryptamine and serpentine. *Metab. Eng.* **2004,** *6*, 268-276.
117. Morgan, J. A.; Shanks, J. V., Determination of metabolic rate-limitations by precursor feeding in Catharanthus roseus hairy root cultures. *J. Biotechnol.* **2000,** *79*, 137-145.
118. Whitmer, S.; Canel, C.; Hallard, D.; Goncalves, C.; Verpoorte, R., Influence of precursor availability on alkaloid accumulation by transgenic cell line of Catharanthus roseus. *Plant Physiol.* **1998,** *116*, 853-857.
119. Whitmer, S.; van der Heijden, R.; Verpoorte, R., Effect of precursor feeding on alkaloid accumulation by a tryptophan decarboxylase over-expressing transgenic cell line T22 of Catharanthus roseus. *J. Biotechnol.* **2002,** *96*, 193-203.
120. Wang, C. T.; Liu, H.; Gao, X. S.; Zhang, H. X., Overexpression of G10H and ORCA3 in the hairy roots of Catharanthus roseus improves catharanthine production. *Plant Cell Rep* **2010,** *29* (8), 887-94.
121. Peebles, C. A.; Sander, G. W.; Hughes, E. H.; Peacock, R.; Shanks, J. V.; San, K. Y., The expression of 1-deoxy-d-xylulose synthase and geraniol-10-hydroxylase or anthranilate synthase increases terpenoid indole alkaloid accumulation in Catharanthus roseus hairy roots. *Metab Eng* **2011,** *13* (2), 234-40.
122. Magnotta, M.; Murata, J.; Chen, J.; De Luca, V., Expression of deacetylvindoline-4-O-acetyltransferase in Catharanthus roseus hairy roots. *Phytochemistry* **2007,** *68*, 1922-1931.
123. Menke, F. L.; Champion, A.; Kijne, J. W.; Memelink, J., A novel jasmonate- and elicitor-responsive element in the periwinkle secondary metabolite biosynthetic gene Str interacts with a jasmonate- and elicitor-inducible AP2-domain transcription factor, ORCA2. *EMBO J.* **1999,** *18*, 4455-4463.
124. Khosla, C.; Keasling, J. D., Metabolic engineering for drug discovery and development. *Nat. Rev. Drug Disc.* **2003,** *2* (1019-1025).
125. Ajikumar, P. K.; Xiao, W. H.; Tyo, K. E.; Wang, Y.; Simeon, F.; Leonard, E.; Mucha, O.; Phon, T. H.; Pfeifer, B.; Stephanopoulos, G., Isoprenoid pathway optimization for Taxol precursor overproduction in Escherichia coli. *Science* **2010,** *330* (6000), 70-4.
126. Hawkins, K. M.; Smolke, C. D., Production of benzylisoquinoline alkaloids in Saccharomyces cerevisiae. *Nat. Chem. Biol.* **2008,** *4*, 564-573.

127. Leonard, E.; Ajikumar, P. K.; Thayer, K.; Xiao, W. H.; Mo, J. D.; Tidor, B.; Stephanopoulos, G.; Prather, K. L., Combining metabolic and protein engineering of a terpenoid biosynthetic pathway for overproduction and selectivity control. *Proc Natl Acad Sci U S A* **2010,** *107* (31), 13654-9.
128. Minami, H.; Kim, J.-S.; Ikezawa, N.; Takemura, T.; Katayama, T.; Kumagai, H.; Sato, F., Microbial production of plant benzylisoquinoline alkaloids. *Proc. Natl. Acad. Sci. USA* **2008,** *105*, 7393-7398.
129. Ro, D. K.; Paradise, E. M.; Ouellet, M.; Fisher, K. J.; Newman, K. L.; Ndungu, J. M.; Ho, K. A.; Eachus, R. A.; Ham, T. S.; Kirby, J.; Chang, M. C.; Withers, S. T.; Shiba, Y.; Sarpong, R.; Keasling, J. D., Production of the antimalarial drug precursor artemisinic acid in engineered yeast. *Nature* **2006,** *440* (7086), 940-3.
130. Facchini, P. J., Alkaloid biosynthesis in plants: Biochemistry, cell biology, molecular regulation and metabolic engineering applications. *Annu. Rev. Plant Physiol. Plant Mol. Biol.* **2001,** *52*, 29-66.
131. Facchini, P. J.; Bird, D. A.; Bourgault, R.; Hagel, J. M.; Liscombe, D. K.; MacLeod, B. P.; Zulak, K. G., Opium poppy: a model system to investigate alkaloid biosynthesis in plants. *Can. J. Bot.* **2005,** *83*, 1189-1206.
132. Geerlings, A.; Redondo, F. J.; Contin, A.; Memelink, J.; van der Heijden, R.; Verpoorte, R., Biotransformation of tryptamine and secologanin into plant terpenoid indole alkaloids by transgenic yeast. *Appl. Microbiol. Biotechnol.* **2001,** *56*, 420-424.
133. Ganesan, A., The impact of natural products upon modern drug discovery. *Curr Opin Chem Biol* **2008,** *12* (3), 306-17.
134. Budman, D. R., Vinorelbine (Navelbine): A third-generation vinca alkaloid. *Cancer Investigation* **1997,** *15* (5), 475-490.
135. Gregory, R. K.; Smith, I. E., Vinorelbine - A clinical review. *British Journal of Cancer* **2000,** *82* (12), 1907-1913.
136. Potier, P., Synthesis of the antitumor dimeric indole alkaloids from catharanthus species (vinblastine group). *Journal of Natural Products (Lloydia)* **1980,** *43* (1), 72-86.
137. Barnett, C. J.; Cullinan, G. J.; Gerzon, K.; Hoying, R. C.; Jones, W. E.; Newlon, W. M.; Poore, G. A.; Robison, R. L.; Sweeney, M. J.; Todd, G. C.; Dyke, R. W.; Nelson, R. L., Structure-activity relationships of dimeric Catharanthus alkaloids. 1. Deacetylvinblastine amide (vindesine) sulfate. *Journal of Medicinal Chemistry* **1978,** *21* (1), 88-96.
138. Voss, M. E.; Ralph, J. M.; Xie, D.; Manning, D. D.; Chen, X.; Frank, A. J.; Leyhane, A. J.; Liu, L.; Stevens, J. M.; Budde, C.; Surman, M. D.; Friedrich, T.; Peace, D.; Scott, I. L.; Wolf, M.; Johnson, R., Synthesis and SAR of vinca alkaloid analogues. *Bioorg Med Chem Lett* **2009,** *19* (4), 1245-9.

CHAPTER 2

OVEREXPRESSING AN ENGINEERED GENE IN *C. ROSEUS* CELL CULTURE

Part of this chapter is published as a brief communication in

Nature Chemical Biology **2009**, *5*, 151-153

2.1 Introduction

Natural products are a rich source of medicinally and commercially important compounds such as drugs, fragrances, dyes, flavors and insecticides[1]. Functional group substitution of natural products can yield analogs of natural products, or "unnatural products", with improved or altered medicinal properties[2]. Incorporation of genes with re-engineered substrate specificity into existing natural product biosynthetic pathways has resulted in production of unnatural microbe-derived compounds from non-natural starting substrates[3]. Significant progress in plant metabolic engineering has enabled fine-tuning of production levels of natural products in plants[4] and heterologous expression of natural compounds in plants[5]. However, biosynthesis of unnatural plant-derived compounds has primarily focused on relatively short flavonoid[6] or carotenoid[7] pathways that can be heterologously expressed in microbial hosts. To the best of our knowledge, production of unnatural products in plants is unprecedented. It is important to explore the capacity, scope and limitations for metabolic engineering of unnatural products—or metabolic reprogramming—within the plant cell environment.

Monoterpene indole alkaloid biosynthesis in *C. roseus* is exceptionally complicated and only partially characterized[8]. This pathway produces a variety of alkaloids with diverse biological activities and complex molecular architecture from the iridoid terpene secologanin **1** and tryptamine **2** (**Figure 2.1** and **Chapter 1**). Some successes have been recently reported for heterologous expression of benzylisoquinoline type alkaloids in microbes[9, 10]. However, the scarcity of cloned biosynthetic genes makes heterologous expression of monoterpene indole alkaloids impossible at present. Furthermore, the

complexity of this pathway makes the prospects for monoterpene indole alkaloid expression in microbes a daunting undertaking. For example, biosynthesis of tabersonine **5**, an early precursor for the anti-cancer bis-indole alkaloids, requires an estimated 15 distinct enzymatic steps from the geraniol terpene and tryptamine precursors[8]. Moreover, the biosynthesis of these alkaloids is organelle and cell-type specific, requiring highly regulated inter- and intracellular trafficking of biosynthetic intermediates. In light of these difficuties, plant cell culture is therefore a more suitable system for exploring unnatural monoterpene indole alkaloid biosynthesis.

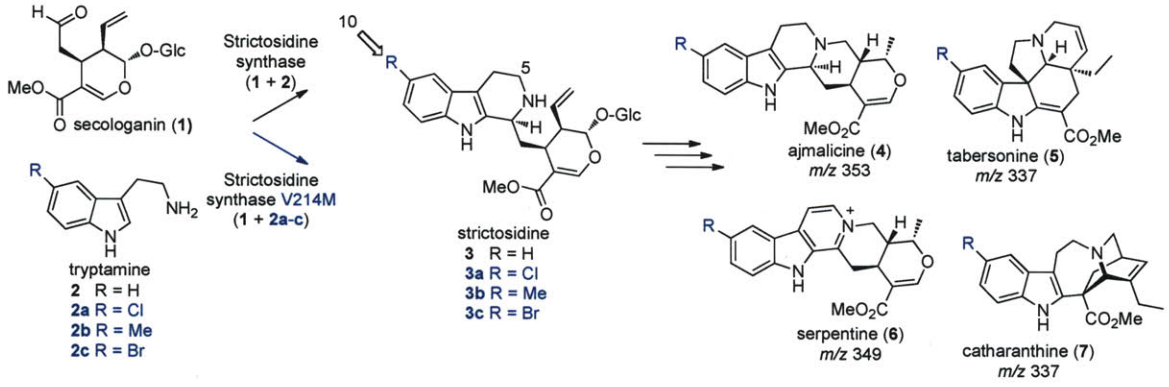

Figure 2.1. Biosynthesis of monoterpene indole alkaloids in *C. roseus*. Secologanin **1**, a complex terpenoid derived from geraniol, and tryptamine **2**, derived from tryptophan, form monoterpene indole alkaloids **4-7** via the biosynthetic intermediate strictosidine **3**. Strictosidine synthase, the enzyme that catalyzes formation of strictosidine **3**, has expanded substrate specificity enabling turnover of tryptamine analogs **2a-c** when the point mutation Val214Met (V214M) is incorporated into the protein sequence.

Previous precursor directed biosynthesis studies in *C. roseus* have revealed that one major bottleneck in the production of unnatural alkaloids is the narrow substrate specificity of strictosidine synthase, the enzyme that catalyzes formation of the strictosidine biosynthetic intermediate **3** from secologanin **1** and tryptamine **2** (**Figure 2.1**)[11, 12]. While some analogs of tryptamine and secologanin starting materials can be turned over by the strictosidine synthase enzyme, many substrates are not recognized by this enzyme, such as tryptamine analogs with substituents at the 5 and alpha positions. The reported crystal structure of strictosidine synthase[13] from *Rauvolfia serpentina* has enabled design of enzyme mutants with broadened substrate specificities, thereby allowing enzymatic production of a greater variety of strictosidine analogs as previously reported[11, 14, 15]. When fed to wild type *C. roseus* cultures, strictosidine analogs substituted at the ester and 5 positions were incorporated only into heteroyohimine type alkaloids (i.e. ajmalicine **4**)[11, 14]. However, a strictosidine analog substituted at the 10 position, **3c**, appeared to be incorporated into many branches of the pathway (**Figure 2.1**)[11]. The strictosidine synthase mutant (V214M) that is able to catalyze the formation of **3a-c** was therefore chosen for transformation into *C. roseus* to explore the prospects of metabolic reprogramming in this medicinal plant.

This chapter describes the introduction of a re-engineered alkaloid biosynthetic gene into *Catharanthus roseus* (Madagascar periwinkle) cell culture. The resulting transgenic cell culture produces a variety of unnatural alkaloid compounds when co-cultured with simple and commercially available precursors that the re-engineered enzyme has been designed

to accept. This work highlights the power of genetic engineering to retailor the structures of complex alkaloid natural products in plant culture.

2.2 Results and Discussion

2.2.1 Generation and Verification of Transgenic Hairy Root Cultures

We used *Agrobacterium rhizogenes* to generate hairy root culture of *C. roseus* transformed with the re-engineered strictosidine synthase. Transformed hairy root cell culture produces a range of alkaloids including ajmalicine **4**, tabersonine **5** and serpentine **6** (**Figure 2.1**)[16]. Using previously established transformation protocols[17], the strictosidine synthase mutant gene containing the point mutation V214M was transformed into hairy root culture under the control of the 35S CMV promoter (derived from pCAMBIA vector, **Figure 2.2**). In addition to this, we also transformed *C. roseus* with the strictosidine synthase mutant gene under the control of an inducible promoter (derived from a pTA7002 vector).

The constitutive system (derived from pCAMBIA vector) requires no inducer for expression and may therefore be simpler to work with. However, the effects of constitutive expression of strictosidine synthase through all developmental stages on hairy root growth and alkaloid production are not well understood. Detailed molecular and biochemical studies suggest that alkaloid biosynthesis is developmentally and temporally regulated[18]. Previous attempts to overexpress strictosidine synthase by Canel *et al* in *C. roseus* cell suspension culture were well tolerated by the cells[19]. Since cell suspension cultures are dedifferentiated cells with many strikingly different features from

hairy roots, it was unclear how findings pertaining to cell suspension system could be translated into the hairy root system. The inducible expression system (derived from pTA7002 vector) was therefore generated as an alternative to allow temporal control of gene expression and alkaloid production. We envisioned that if constitutive expression of the mutant strictosidine synthase gene has detrimental effects on hairy root growth, then inducing the expression at specific times in the culture would overcome this problem.

PCR analysis of genomic DNA confirmed incorporation of the strictosidine synthase sequence encoding the V214M point mutation, the 35S CMV promoter, and the hygromycin antibiotic selection marker (HPT), thereby indicating that the strictosidine synthase mutant was incorporated into the *C. roseus* genome (**Figure 2.3A-C**). Specifically, PCR amplification of genomic DNA from all of the selected transformed lines (pCAMV214M_31: lanes 4-6, pCAMV214M_37: lanes 7-9, and pCAMV214M_49: lanes 10-12) was successful for all three sets of primers (**Figure 2.3A**). PCR-amplification of genomic DNA from hairy root transformed with *A. rhizogenes* lacking the pCAMBIA vector (provided by Professor Jacqueline Shanks (Iowa State) and Professor Carolyn Lee-Parsons (Northeastern)) was successful only when STR specific primers were used (lanes 1-3). These results indicated that STR mutant was successfully incorporated into the *C. roseus* genome in all chosen lines. Similarly, in the inducible system, PCR amplification of genomic DNA from a representative transformed line (pTAV214M_26: lane 2-5) were successful was all set of primers (**Figure 2.3B**).

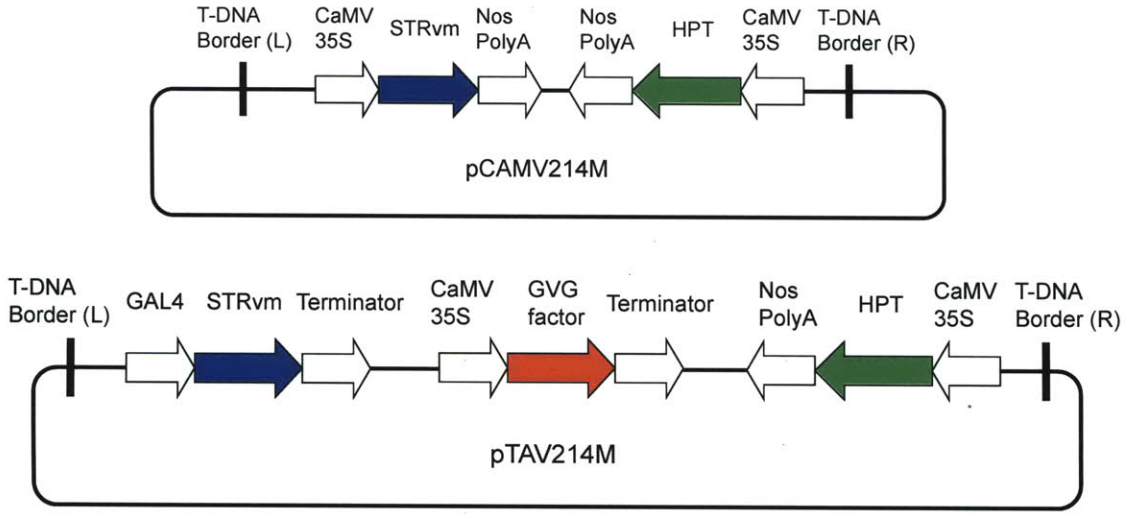

Figure 2.2. Schematic diagram of strictosidine synthase mutant (STRvm) constitutive expression system (pCAMV214M) and inducible expression system (pTAV214M) constructs.
CaMV35S: Cauliflower Mosaic Virus 35S promoter; STRvm: strictosidine synthase with the Val214Met mutation; Nos PolyA: poly(A) signal from nopaline synthase; HPT: hygromycin phosphotransferase; GVG factor: chimeric transcription factor containing GAL4 DNA-binding domain and VP16 transactivating domain and rat-glucocorticoid receptor hormone binding domain.

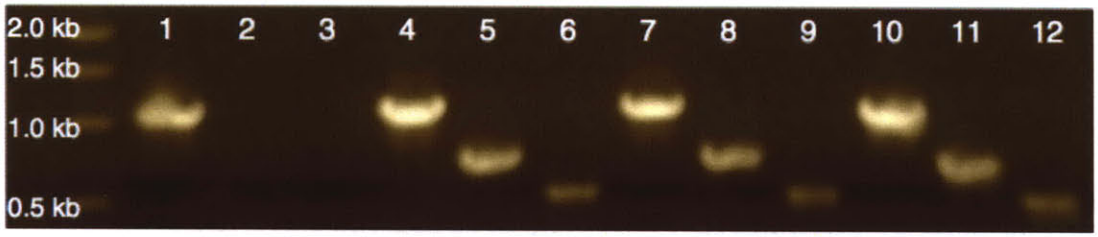

Figure 2.3A. 1% agarose gel of PCR amplification of pCAMV214M and wild-type hairy root genomic DNA.

Lane: template, primers.

1: wild-type, STR

2: wild-type, HPT

3: wild-type, CaMV35S

4: pCAMV214M cell line 31, STR

5: pCAMV214M cell line 31, HPT

6: pCAMV214M cell line 31, CaMV35S

7: pCAMV214M cell line 37, STR

8: pCAMV214M cell line 37, HPT

9: pCAMV214M cell line 37, CaMV35S

10: pCAMV214M cell line 49, STR

11: pCAMV214M cell line 49, HPT

12: pCAMV214M cell line 49, CaMV35S

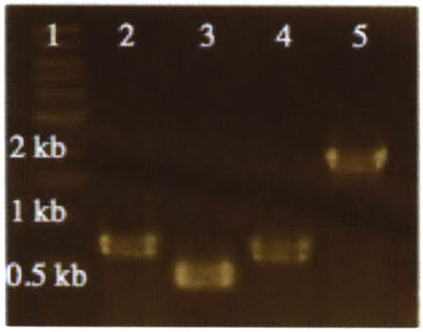

Figure 2.3B. 1% agarose gel of PCR amplification of pTAV214M hairy root genomic DNA.

Lane: template, primers.

1: DNA ladder

2: pTAV214M cell line 26, HPT

3: pTAV214M cell line 26, STRV214M (specific for V214M mutation)

4: pTAV214M cell line 26, STRV214M (specific for V214M mutation)

5: pTAV214M cell line 26, HPT-STR

Additionally, a primer pair was designed to match the point mutation corresponding to the V214M sequence change at the 3' end of the forward primer (STRV214M_for and STRV214M_rev) (**Figure 2.3C**). These primers readily amplified a 500bp region of the mutant gene. However, the mismatch at the 3' end prevented efficient amplification of the native STR gene in wild type hairy root cultures.

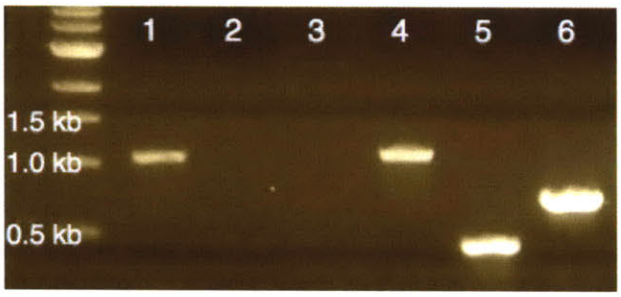

Figure 2.3C. 1% agarose gel of PCR amplification of pCAMV214M and wild-type hairy root genomic DNA demonstrating V214M point mutation

Lane: template, primers

1: wild-type, STR

2: wild-type, STRV214M (specific for V214M mutation)

3: wild-type, HPT

4: pCAMV214M cell line 31, STR

5: pCAMV214M cell line 31, STRV214M (specific for V214M mutation)

6: pCAMV214M cell line 31, HPT

2.2.2 Evaluation, Isolation and Characterization of Alkaloids from Engineered *C. roseus*

Transgenic hairy root lines that have been transformed with the pCAMV214M construct (constitutive system) were cultured in liquid Gamborg's B5 media in the presence of 0.5 mM 5-chlorotryptamine **2a**, 5-methyltryptamine **2b**, or 5-bromotryptamine **2c**. These substrate analogs are only turned over by the V214M mutant enzyme, and are not recognized by wild type strictosidine synthase[11]. The substrate analog concentration of 0.5 mM has been previously determined to be optimal for feeding studies (McCoy and O'Connor, unpublished). After one week of culture, the plant material was lysed and alkaloids were extracted into organic solvent. Liquid chromatography mass spectral (LC-MS) analysis of these extracts indicated appearance of novel compounds that appeared to be derived from the exogenous substrates **2a-c** (**Figure 2.4-2.8** and **Appendix A**). Unnatural alkaloids could be rapidly assigned by LC-MS as deriving from **2a** and **2c**, since chlorine and bromine exhibit a characteristic isotopic signature ($^{35}Cl/^{37}Cl$ ratio of 3:1 and $^{79}Br/^{81}Br$ ratio of 1:1), (**Figure 2.4** (iv, v), **Figure 2.5** (iii, iv) and **Appendix A**). Control experiments clearly indicated that these compounds were not present when the tryptamine analog was absent from the media (**Figure 2.4-2.5** (i)). Hairy root lines transformed with the wild type strictosidine synthase gene also failed to produce chlorinated alkaloids when cultivated with **2a** (**Figure 2.4**, (ii) and **Appendix A**). Hairy root cultures infected with *A. rhizogenes* lacking the V214M mutant did not produce these compounds when cultivated in the presence of tryptamine analogs **2a-c** (**Figure 2.4** (iii), **Figure 2.5** (ii), and **Appendix A**). High-resolution mass spectral (HRMS) analysis was performed on all unnatural alkaloids (**Table 2.1**).

For transgenic hairy root lines that have been transformed with the pTAV214M construct (inducible system), 10 or 30 μM dexamethasone (an artificial glucocorticoid receptor ligand for activation of gene expression) was added to two to three-week old liquid culture. Since previous reports suggest that mutant enzyme expression peaks approximately 72 hours after induction, 0.5 mM 5-chlorotryptamine **2a** was added to the liquid media at this point and processed in the same manner as in the constitutive system. Despite various induction conditions, we did not observe the formation of unnatural alkaloids after culturing these lines with 5-substituted tryptamine analogs **2a** (**Appendix A**).

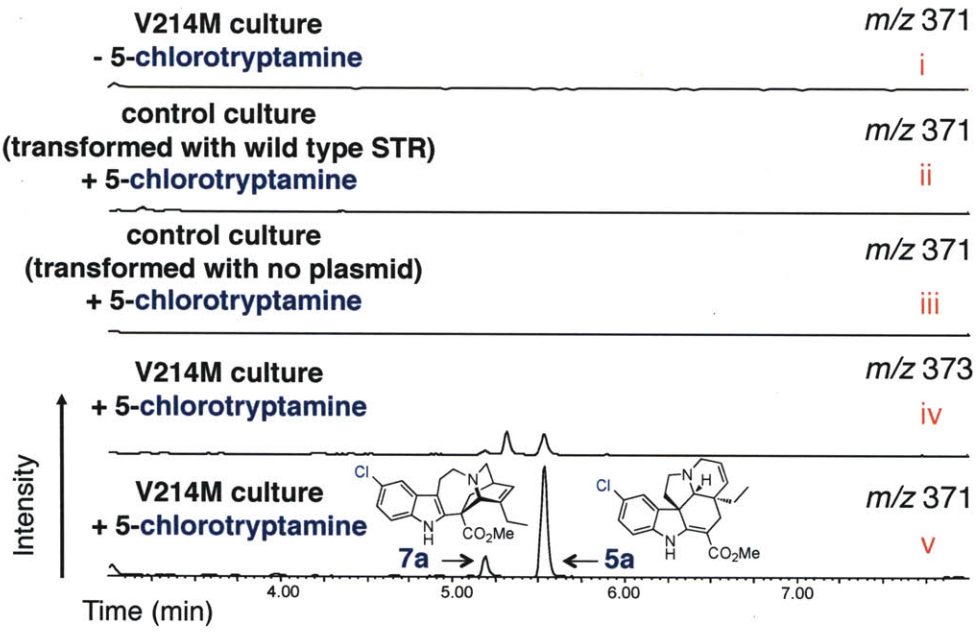

Figure 2.4. Unnatural alkaloid production in *C. roseus* hairy root culture expressing re-engineered strictosidine synthase V214M (I). Extracted LC-MS traces for a representative unnatural alkaloid (*m/z* 337+34) derived from 5-chlorotryptamine **2a**. This compound is not observed when **2a** is absent from the media (i), nor in control hairy root cultures transformed with wild type strictosidine synthase gene (ii), nor in control cultures transformed with no plasmid (iii). The compound displays the isotopic distribution expected for a chlorinated compound (iv, v). LC-MS spectra are normalized to the same y-axis scale.

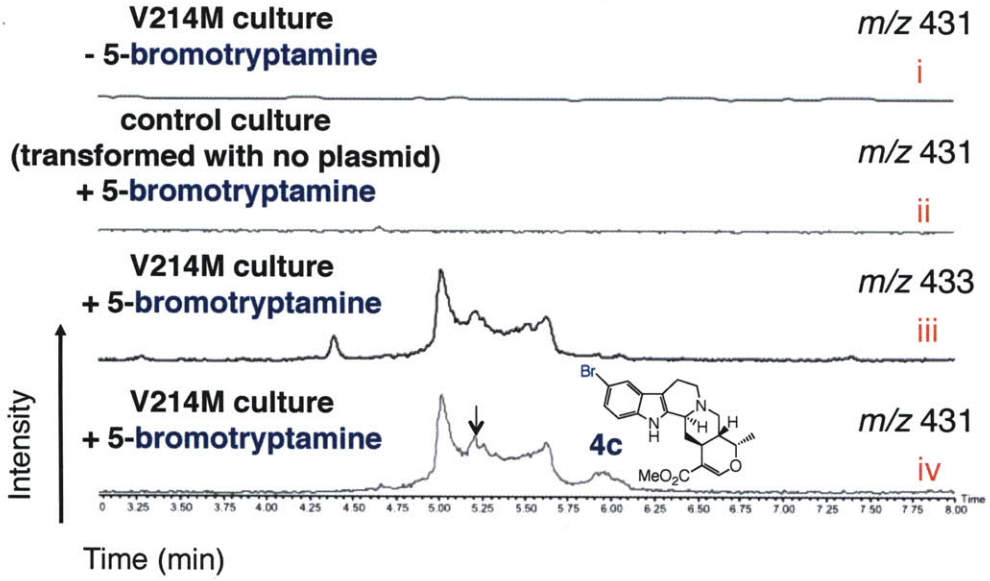

Figure 2.5. Unnatural alkaloid production in *Catharanthus roseus* hairy root culture expressing re-engineered strictosidine synthase V214M (II). Extracted LC-MS traces for a representative unnatural alkaloid (*m/z* 353+78) derived from 5-bromotryptamine **2c**. This compound is not observed when **2c** is absent from the media (i), nor in control cultures transformed with no plasmid (ii). The compound displays the isotopic distribution expected for a brominated compound (iii, iv). LC-MS spectra are normalized to the same y-axis scale.

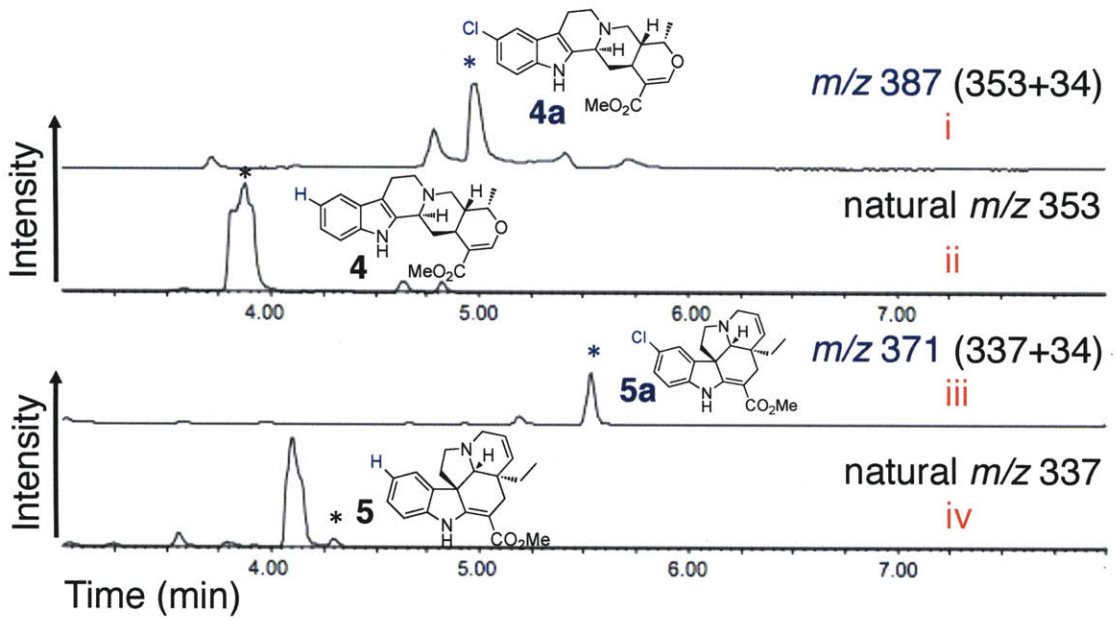

Figure 2.6. Unnatural alkaloid production in *Catharanthus roseus* hairy root culture expressing re-engineered strictosidine synthase V214M. Extracted LC-MS traces showing production of two unnatural alkaloids derived from **2a** (i, iii), along with the traces showing production of the parent natural alkaloids from the same cultures (ii, iv). Asterisked compounds **4a** (i) and **5a** (iii), were isolated and characterized by NMR. Asterisked compound **4** (ii) and **5** (iv) was assigned based on coelution with an authentic standard (Bestchemistry, Zhjiang, China). LC-MS spectra of i and ii are normalized to the same y-axis scale to allow comparison of the relative amounts of **4** relative to **4a**; iii and iv are normalized to allow comparison of the relative amounts of **5** and **5a**.

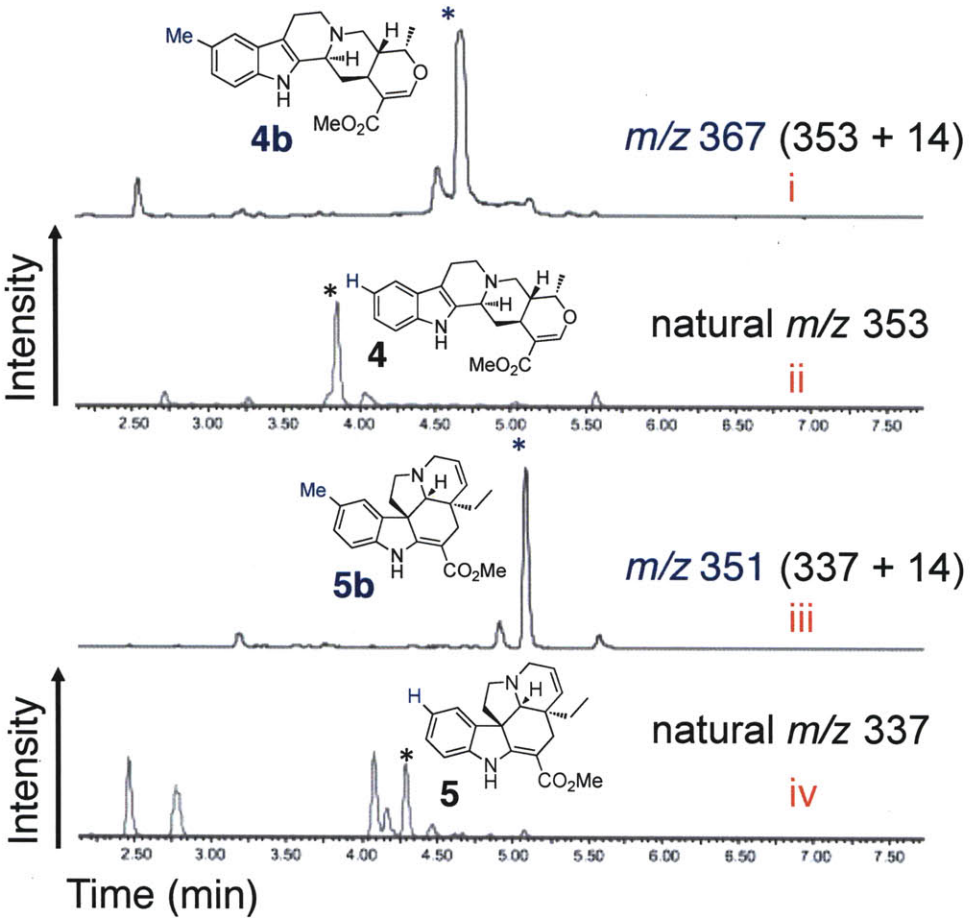

Figure 2.7. Unnatural alkaloid production in *Catharanthus roseus* hairy root culture expressing re-engineered strictosidine synthase V214M (IV). Extracted LC-MS traces showing production of two unnatural alkaloids derived from **2b** (i, iii), along with the traces showing production of the parent natural alkaloids from the same cultures (ii, iv). Asterisked compounds **4** (ii) and **5** (iv) were assigned based on coelution with an authentic standards (Bestchemistry, Zhjiang, China). LC-MS spectra of i and ii are normalized to the same y-axis scale to allow comparison of the relative amounts of **4** relative to **4b**; iii and iv are normalized to allow comparison of the relative amounts of **5** and **5b**.

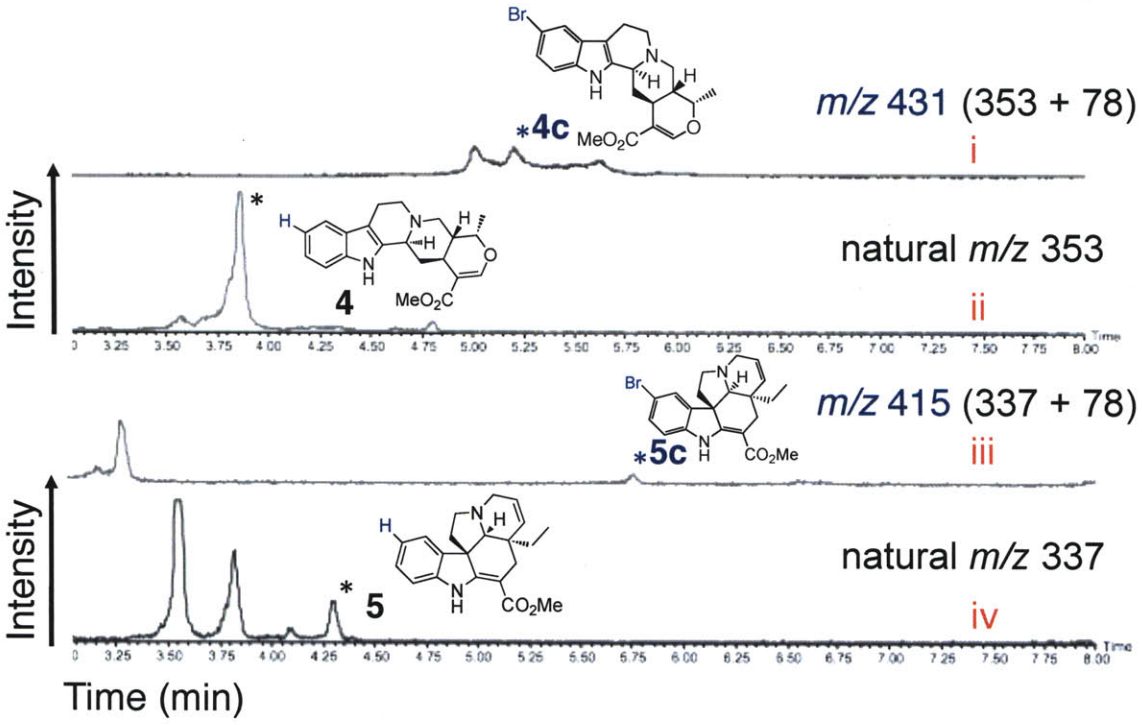

Figure 2.8. Unnatural alkaloid production in *Catharanthus roseus* hairy root culture expressing re-engineered strictosidine synthase V214M (V). Extracted LC-MS traces showing production of two unnatural alkaloids derived from **2c** (i, iii), along with the traces showing production of the parent natural alkaloids from the same cultures (ii, iv). Asterisked compounds **4** (ii) and **5** (iv) were assigned based on coelution with an authentic standards (Bestchemistry, Zhjiang, China). LC-MS spectra of i and ii are normalized to the same y-axis scale to allow comparison of the relative amounts of **4** relative to **4c**; iii and iv are normalized to allow comparison of the relative amounts of **5** and **5c**.

Table 2.1. Tabulated high-resolution mass spectral data of the major unnatural alkaloids produced from transgenic hairy root lines and **2a-c**.

			a	b	c
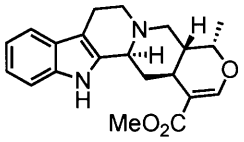	**Ajmalicine**	**4**	**4a***	**4b*****	**4c*****
	Expected [M+H]	353.1865	387.1490	367.2022	431.0970
	Observed [M+H]	353.1856	387.1483	367.2015	431.0983
	Accuracy (ppm)	-2.5	2.1	-1.9	3.0
	RT (min)	3.85	4.95	4.67	5.19
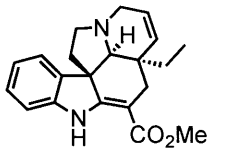	**Tabersonine**	**5**	**5a***	**5b*****	**5c**
	Expected [M+H]	337.1916	371.1526	351.2073	
	Observed [M+H]	337.1922	371.1528	351.2064	not obs.
	Accuracy (ppm)	1.8	0.5	-2.6	
	RT (min)	4.28	5.51	5.07	
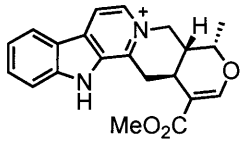	**Serpentine**	**6**	**6a*****	**6b*****	**6c*****
	Expected [M+H]	349.1552	383.1162	363.1709	427.0657
	Observed [M+H]	349.1548	383.1177	363.1699	427.0650
	Accuracy (ppm)	-1.1	3.9	-2.8	-1.6
	RT (min)	4.07	4.94	4.91	5.17
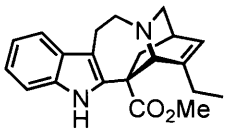	**Catharanthine**	**7**	**7a****	**7b*****	**7c**
	Expected [M+H]	337.1916	371.1526	351.2073	
	Observed [M+H]	337.1916	371.1531	351.2059	not obs.
	Accuracy (ppm)	0.0	1.3	-4.0	
	RT (min)	4.09	5.17	4.90	
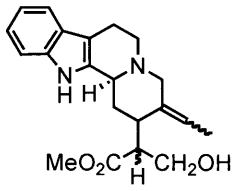	**Isositsirikine**		***	***	***
	Expected [M+H]	355.2022	389.1636	369.2178	433.1127
	Observed [M+H]	355.2020	389.1632	369.2182	433.1118
	Accuracy (ppm)	-0.6	1.0	1.1	-2.1
	RT (min)	2.99	4.13	3.82	4.38
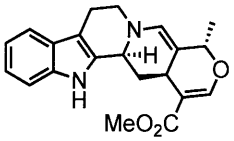	**Cathenamine**		***	***	
	Expected [M+H]	351.1709	385.1319	365.1865	
	Observed [M+H]	351.1724	385.1328	365.1860	not obs.
	Accuracy (ppm)	4.3	2.3	-1.4	
	RT (min)	4.52	5.70	5.32	

RT = retention time, LC gradient 10-60% acetonitrile/water (0.1% TFA) in 13 minutes
*Assigned based on exact mass, retention time, UV spectra, ^{1}H-NMR, and known alkaloid profile of *C. roseus*. ** Assigned based on exact mass, retention time, UV spectra, and alkaloid profile. *** Assigned based on exact mass, retention time and alkaloid profile.

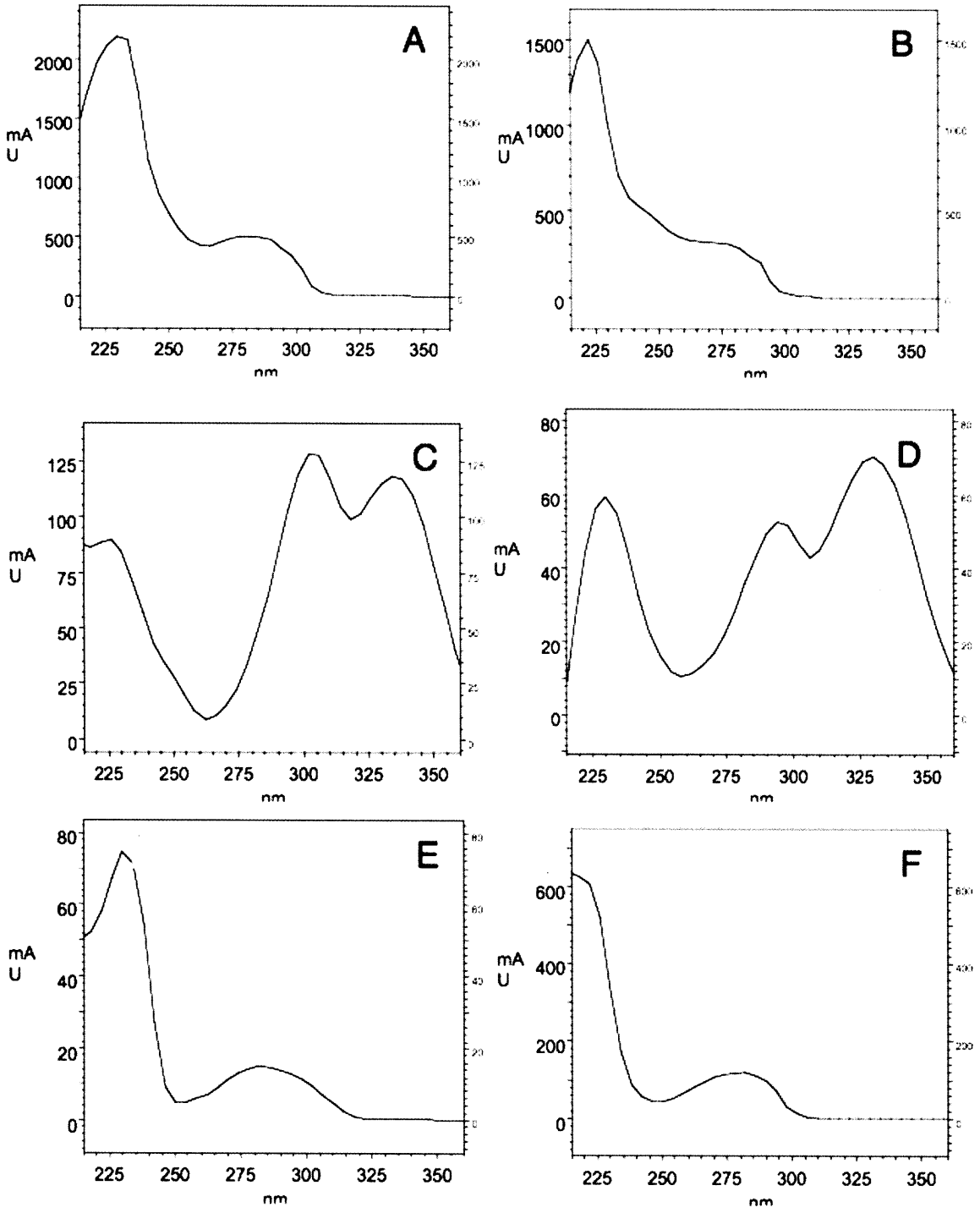

Figure 2.9. UV spectra of alkaloid standards and isolated alkaloids from pCAMV214M hairy root (cell line 31) fed with 5-chlorotryptamine (0.5 mM). **A.** 10-chloroajmalicine **4a**; **B.** ajmalicine standard; **C.**10-chlorotabersonine **5a**; **D.** tabersonine standard; **E.** Unknown chlorinated alkaloid with *m/z* 371 with UV spectra comparable to that of catharanthine **7**; **F.** catharanthine standard.

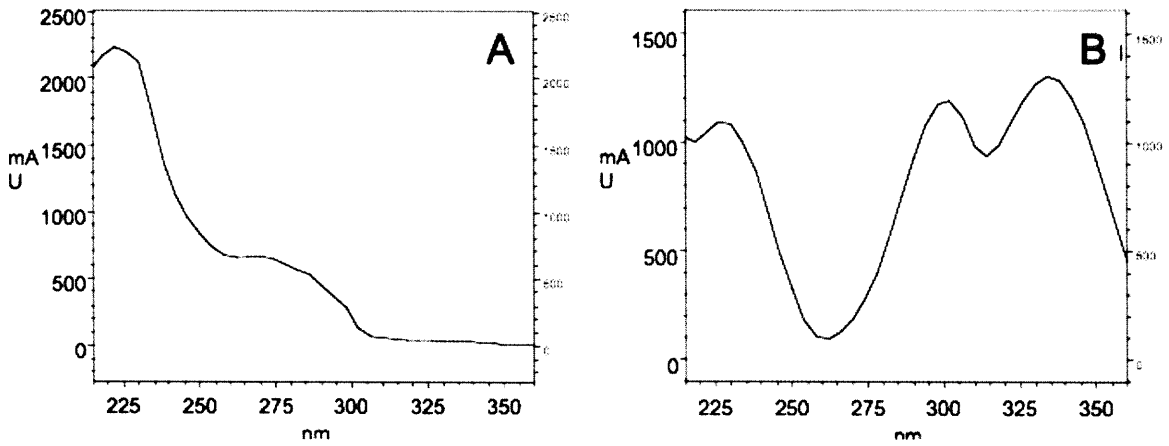

Figure 2.10. UV spectra of isolated alkaloids from pCAMV214M hairy root (cell line 31) fed with 5-methyltryptamine (0.5 mM). **A.** 10-methylajmalicine **4b**; **B.** 10-methyltabersonine **5b.**

Although a variety of unnatural alkaloids clearly appear to be formed from tryptamine analogs **2a-c** in these transgenic cultures (**Figure 2.4-2.8** and **Appendix A**), analysis of the flux of **2a-c** into downstream metabolites will require extensive characterization of all alkaloid products. Only a limited analysis is addressed in this chapter. When 5-chlorotryptamine **2a** (0.5 mM) was added to the culture media, approximately equal amounts of natural ajmalicine **4** and chlorinated ajmalicine **4a** were produced (**Figure 2.6**). Compound **4a** was purified and characterized by ^{1}H NMR, ^{1}H-^{13}C HSQC NMR, UV spectroscopy and high-resolution mass spectrometry (*m/z* 387.1483, isolated yield of approximately 1.5 mg/150 mL culture) (**Table 2.1**, **Figure 2.9**, and **Appendix A**). The aromatic region of ^{1}H NMR and ^{1}H-^{13}C HSQC spectra of **4a** supports the presence of the chlorine group at the 10-position (**Figure 2.11**).

Cultivation of transgenic hairy roots in the presence of 5-methyltryptamine **2b** (0.5 mM) resulted in production of methylated ajmalicine **4b** at levels greater than natural ajmalicine **4** (**Figure 2.7** and **Appendix A**). Compound **4b** could not be readily separated from a contaminating product, but ^{1}H NMR, UV spectroscopy and high-resolution mass spectrometry (*m/z* 367.2015) of the partially purified compound supported a structural assignment of **4b** (**Table 2.1**, **Figure 2.10**, and **Appendix A**).

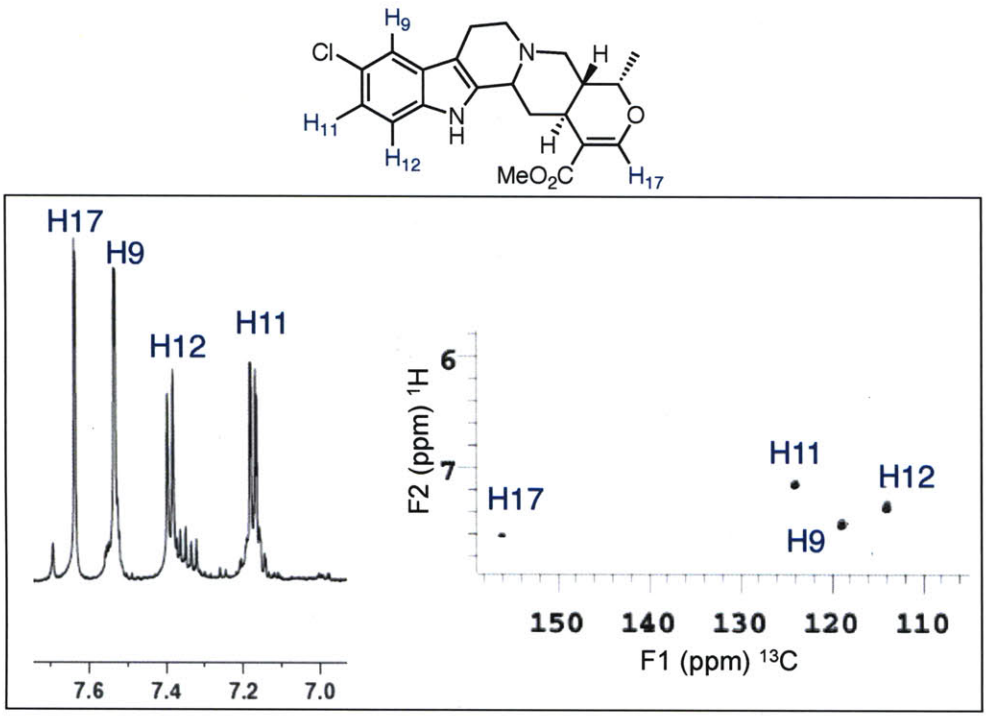

Figure 2.11. Aromatic region of ^{1}H NMR and ^{1}H-^{13}C HSQC spectra of **4a** isolated from transgenic *C. roseus* hairy root culture expressing V214M cultured with 500 mM **2a**.

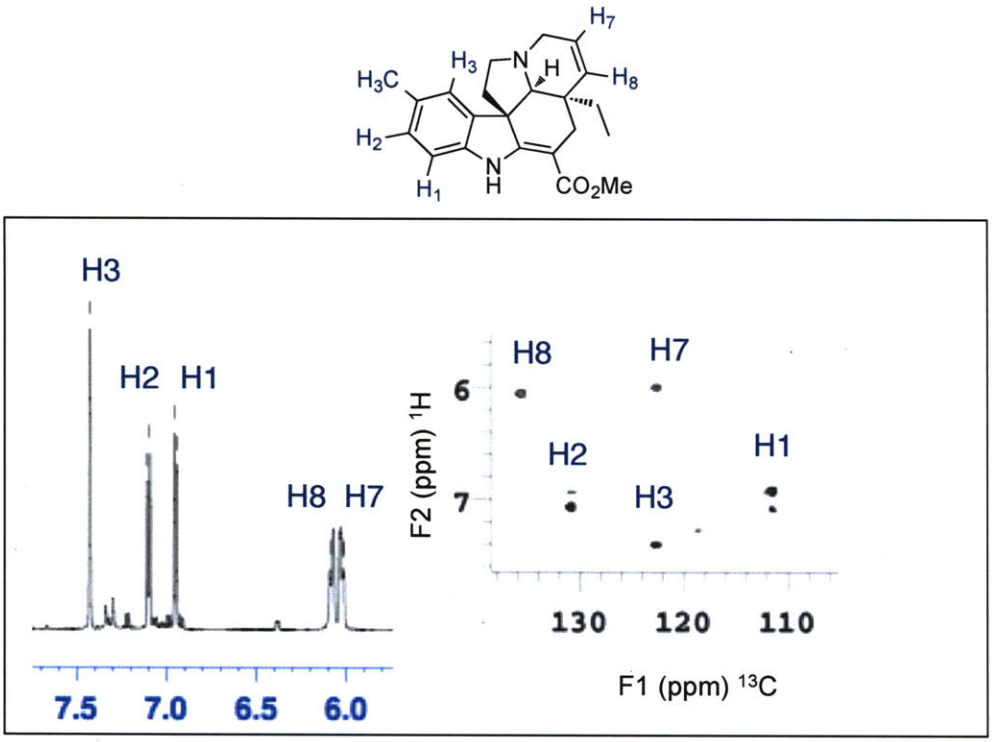

Figure 2.12. Aromatic region of ^{1}H NMR and ^{1}H-^{13}C HSQC spectra of **5b** isolated from transgenic *C. roseus* hairy root culture expressing V214M cultured with 500 mM **2b**.

When hairy root cultures were cultivated with 5-methyltryptamine **2b** (500 μM), higher levels of methylated tabersonine **5b** relative to natural tabersonine **5** were observed (**Figure 2.7** and **Appendix A**). Compound **5b** was isolated and characterized by ^{1}H NMR, ^{1}H-^{13}C HSQC, ^{1}H-^{13}C HMBC NMR, UV spectroscopy and high-resolution mass spectrometry (*m/z* 351.2064, isolated yield of approximately 2 mg/150 mL culture) (**Table 2.1**, **Figure 2.10**, **2.12** and **Appendix A**). Cultivation with 5-chlrotryptamine **2a** (500 μM) led to formation of chlorinated tabersonine **5a**, also produced at higher levels than natural tabersonine **5** (**Figure 2.6** and **Appendix A**). Although **5a** could not be readily purified from contaminating alkaloid products, characterization of the partially purified compound by ^{1}H NMR, UV spectroscopy and high-resolution mass spectrometry (*m/z* 371.1528) supported a structural assignment of **5a** (**Table 2.1**, **Figure 2.10**, and **Appendix A**).

While hairy roots that have been transformed with *A. rhizogenes* lacking the pCAMV214M plasmid produce only trace amounts of catharanthine **7**, for reasons that remain unclear, cultures transformed with *A. rhizogenes* harboring the pCAMV214M plasmid (and other pCAMBIA-derived plasmids) displayed enhanced production of **7**, though the yields vary significantly from line to line (**Figure 2.13**). Low levels of a compound with molecular weight and UV spectrum consistent with a chlorinated catharanthine analog derived from **2a** was also observed in transgenic lines expressing the V214M mutant (**Table 2.1**, **Figure 2.4, 2.9** and **Appendix A**).

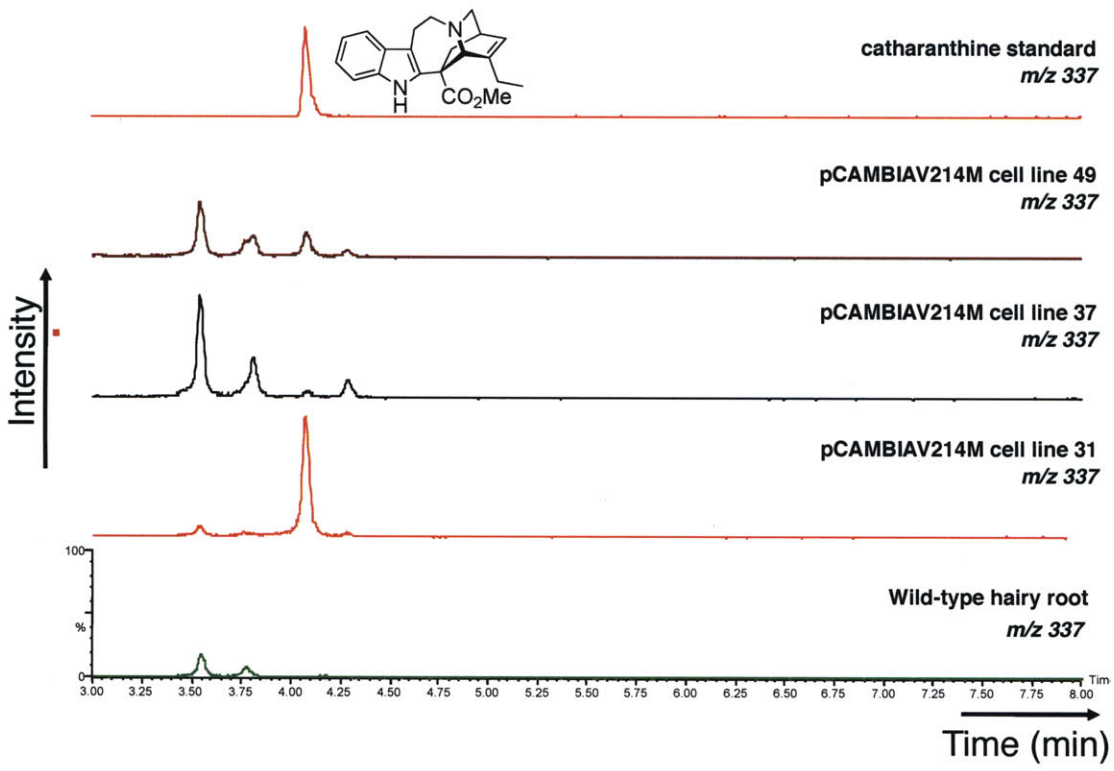

Figure 2.13. LC-MS trace of catharanthine production in transgenic hairy roots. Hairy roots that do not express the mutant STR produce only trace amounts of catharanthine **7**. All lines expressing the mutant STR displayed enhanced production of **7**.

2.2.3 Verification of Expression of Mutant STR Enzyme by Real Time RT-PCR

We quantified the total levels of strictosidine synthase mRNA (mRNA encoding wild type plus V214M mutant strictosidine synthase) in several hairy root lines. Three unnatural alkaloid producing hairy root lines showed robust production of strictosidine synthase mRNA at levels approximately 10 to 30 fold higher than what was observed in hairy root cultures not transformed with the pCAMBIA plasmid harboring the V214M mutant gene (**Figure 2.14**). RT-PCR of hairy root lines that were transformed with V214M under the control of an inducible promoter also showed low levels of strictosidine synthase mRNA in this particular system. The apparent negligible expression of the V214M mutant in these lines was consistent with the observation that no unnatural alkaloid production was produced in these lines after incubation with 5-substituted tryptamine analog **2a** (**Appendix A**).

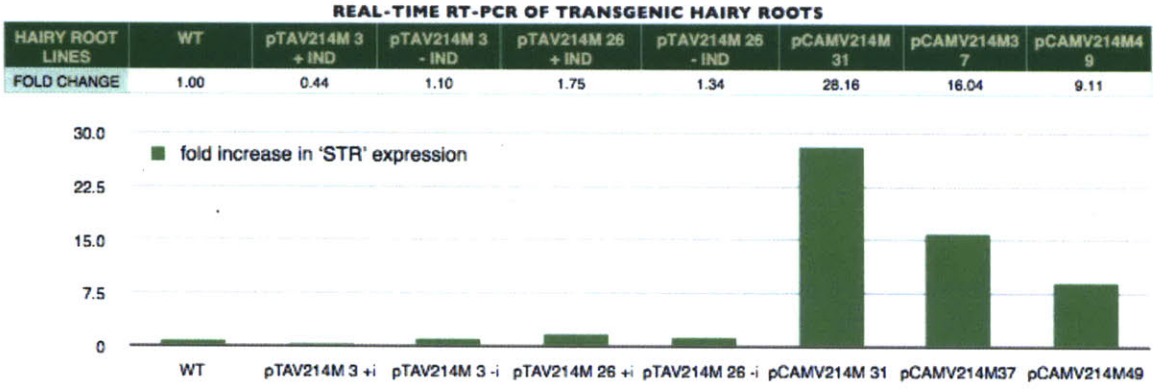

Figure 2.14. Real-time RT-PCR analysis shows relative expression levels of 'STR' (sum total of both wild-type and V214M mutant) in transgenic hairy roots. All chosen pCAMV214M hairy root lines (cell line 31, 37 and 49) produce STR mRNA at levels approximately 10 to 30 fold higher than the expression level of the endogenous STR observed in "wild type" culture transformed with *A. rhizogenes* lacking plasmid. pTAV214M hairy roots (cell line 3 and 26) do not show significant changes in mRNA expression levels of the enzyme either with (+ i) or without (- i) treatment with the glucocorticoid inducer, dexamethasone (10 μM).

2.2.4 In vitro Enzymatic Assay of Transformed Hairy Roots Expressing STR Mutant

Strictosidine synthase from crude plant tissue lysates has been shown to be catalytically active. Gratifyingly, lysates from cultures transformed with V214M converted **2a** and **2b** to strictosidine **3a** and **3b** *in vitro* (**Figure 2.15A-B**). LC-MS analysis indicated the formation of the corresponding 10-chloro and 10-methylstrictosidine analogs **3a** and **3b** in samples with crude lysate from pCAMV214M hairy roots in all chosen lines. The strictosidine analog peaks co-eluted with chemically synthesized standards[20]. Additionally, substantial levels of deglycosylated strictosidine (cathenamine) analogs were formed in these crude extracts (**Figure 2.16A-B**). Deglycosylated strictosidine, or cathenamine, is the next biosynthetic intermediate of the pathway, and is formed after strictosidine is deglycosylated by the enzyme strictosidine glucosidase (SGD) (**Chapter 1**). Cathenamine analogs were observed as evidenced by formation of a product with the correct molecular weight and retention time, indicating that the endogenous SGD of the hairy roots efficiently deglycosylated the strictosidine analogs **3a** and **3b** (**Figure 2.16A-B**). Interestingly, no downstream alkaloid biosynthesis (i.e. **4**, **5** or **6**) was observed in the hairy root lysates. These observations confirm Yerkes and O'Connor's findings that biosynthetic enzymes downstream of SGD are extremely labile and great care must be taken to preserve the activity of these enzymes in cell free lysates. Strictosidine and cathenamine analogs were not observed in negative controls. Samples with crude lysates from hairy roots transformed with wild-type *A. rhizogenes*, samples lacking hairy root extracts and samples without tryptamine analogs each failed to produce strictosidine analogs **2a** and **2b** and the corresponding deglycosylated strictosidine (cathenamine)

analogs. Some background reaction occurred in the absence of hairy root extract with substrate **2b**, as evidenced by formation of a small amount of **3b** in the control reaction that lacked hairy root lysate. However, formation of **3b** was significantly enhanced upon addition of lysate derived from transformed hairy root lines containing the V214M gene (**Figure 2.15B**). The corresponding strictosidine and cathenamine analogs were not formed when 5-bromotryptamine **2c** was used as the tryptamine analog substrate (data not shown). This was consistent with Bernhardt and O'Connor's findings that the catalytic efficiency of the Val124Met enzyme for 5-bromotryptamine is significantly lower than for 5-chloro and 5-methyltryptamine.

For the inducible system, 10 μM or 30 μM dexamethasone (an artificial glucocorticoid receptor ligand required for activation of gene expression in pTA7002) was added to two or three-week-old hairy roots in liquid culture. Since previous reports suggest that inducible protein expression peaks approximately 72 hours after induction, hairy roots were harvested at this point and processed in the same manner as described for the constitutive system. Despite various expression and induction conditions, we did not observe the formation of strictosidine analogs **3a** or **3b** when the crude lysates from two chosen lines (pTAV214M cell lines 3 and 26) were incubated with tryptamine analogs **2a** or **2b** (data not shown). These results were consistent with the real time reverse transcriptase PCR data that indicated negligible expression of the V214M mutant in these lines (**Figure 2.14**).

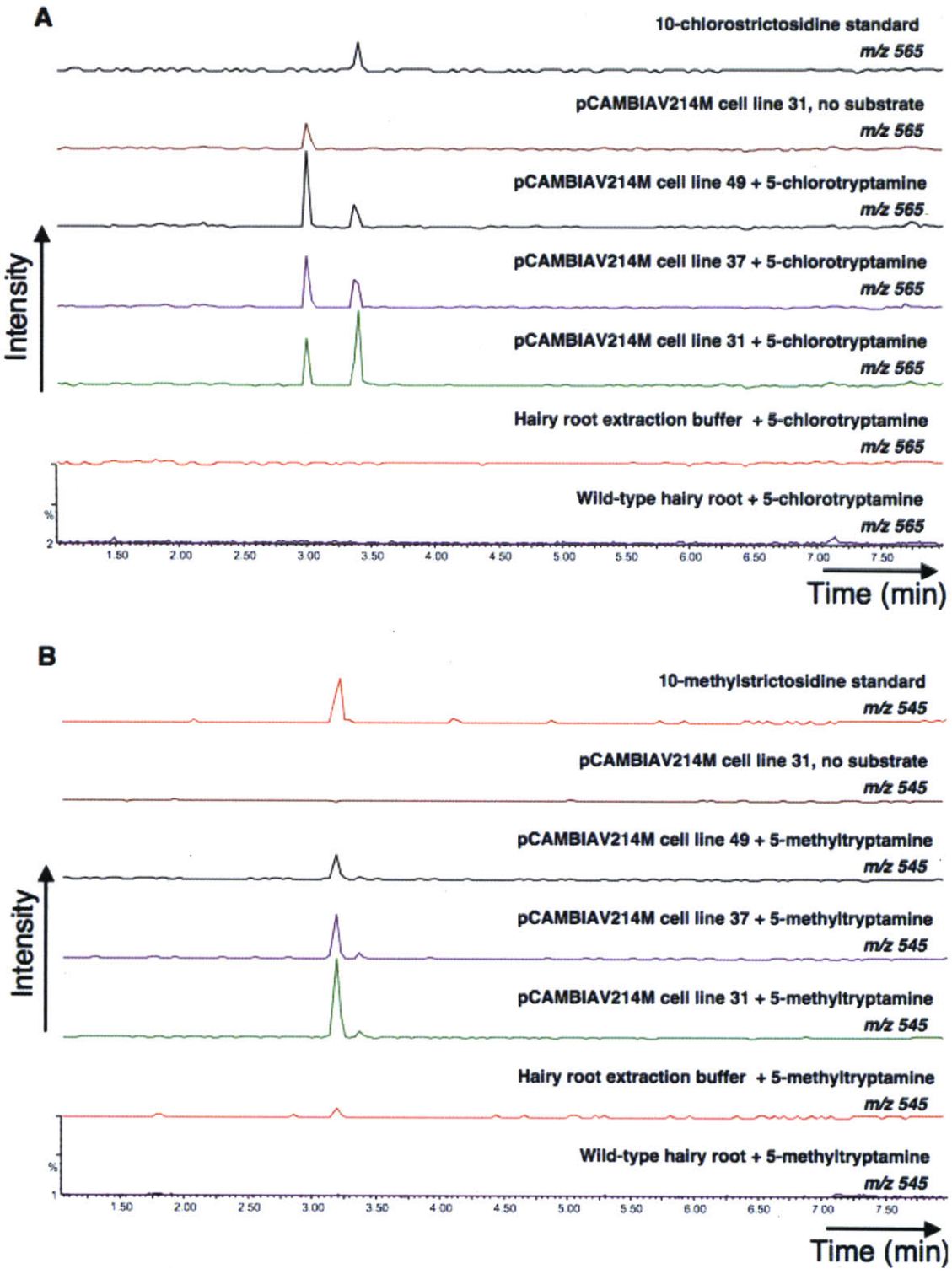

Figure 2.15A-B. LC-MS traces of an *in vitro* enzymatic assay of pCAMV214M hairy root (cell lines 31, 37 and 49) lysates with 1 mM secologanin and 1 mM 5-chlorotryptamine **1a** (**A**) or 5-methyltryptamine **1b** (**B**). *m/z* 565 corresponds to 10-chlorostrictosidine **3a** and *m/z* 545 corresponds to 10-methylstrictosidine **3b**.

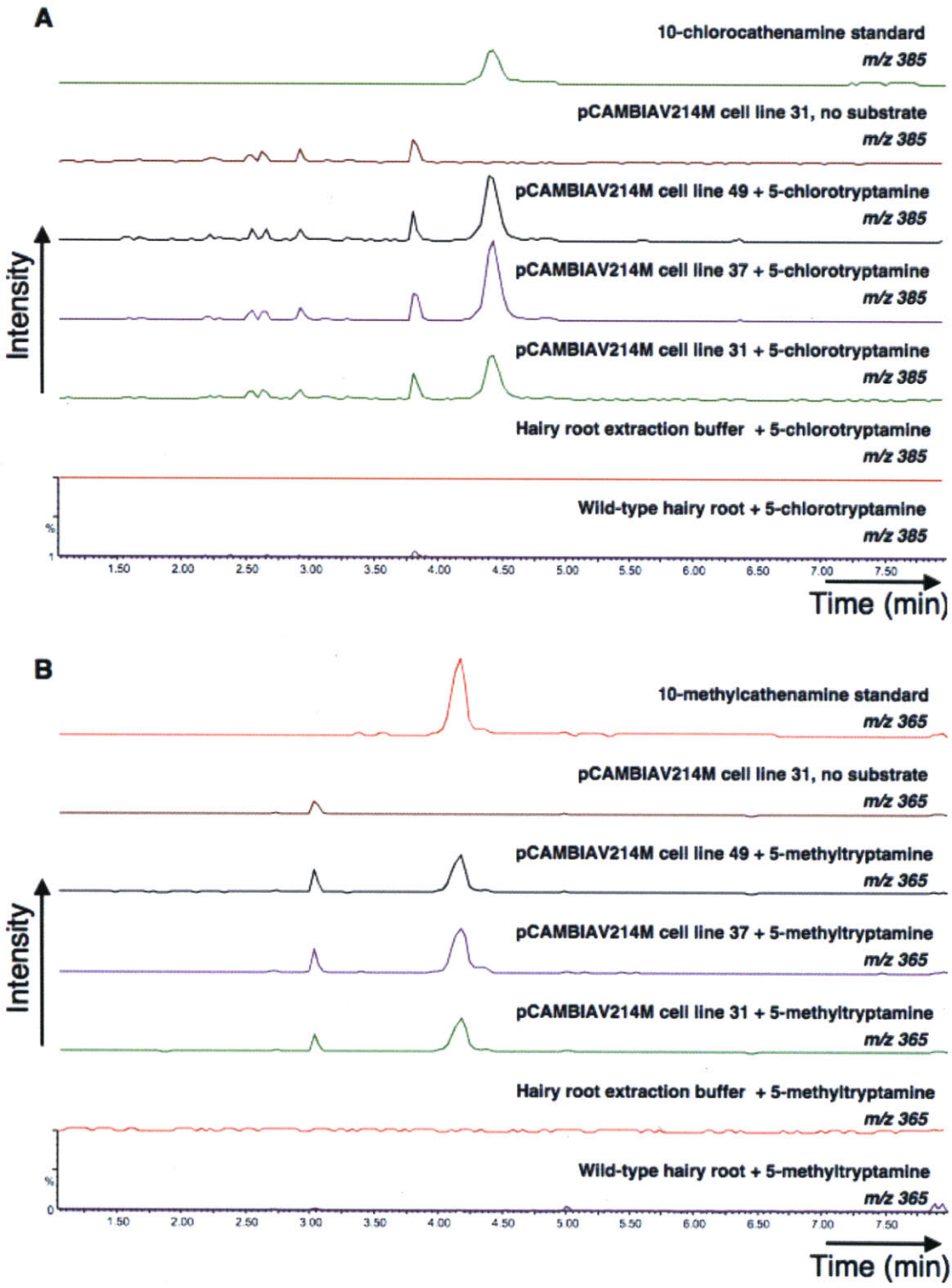

Figure 2.16A-B. LC-MS traces of an *in vitro* enzymatic assay of pCAMV214M hairy root (cell lines 31, 37 and 49) lysates with 1 mM secologanin and 1 mM 5-chlorotryptamine **2a** (top) or 5-methyltryptamine **2b** (bottom). *m/z* 385 corresponds to 10-chlorocathenamine (deglycosylated strictosidine **3a**) and *m/z* 365 corresponds to 10-methylcathenamine (deglycosylated strictosidine **3b**).

As an additional control, we verified that the production of unnatural strictosidine analogs was specifically due to overexpression of the STR V214M mutant and not a result of other genetic changes related to the *Agrobacterium*-mediated transformation. Lysate from hairy roots overexpressing *wild-type* strictosidine synthase ("pCAMWT") was incubated with either 5-chlorotryptamine **2a,** 5-methyltryptamine **2b** or tryptamine **2** using conditions described above. Formation of 10-chlorostrictosidine **3a** or 10-chlorocathenamine was not observed when lysates from pCAMWT control hairy roots were incubated with 5-chlrotryptamine **2a** (**Figure 2.17A** and **Figure 2.18A**). While the formation of 10-methylstrictosidine **3b** was not observed, a small amount of 10-methylcathenamine formed when lysates from pCAMWT control hairy roots were incubated with 5-methyltryptamine **2b** (**Figure 2.17B** and **Figure 2.18B**). This suggests that 10-methylstrictosidine **3b** could form from a chemical reaction (background, as was also observed in the no enzyme control (hairy root extraction buffer)) and was subsequently deglycosylated by strictosidine glusosidase. Formation of both strictosidine **3** and cathenamine was observed when lysates from pCAMWT control hairy roots were incubated with tryptamine **2** suggesting that enzymes remain active under the assay conditions (**Figure 2.17C** and **Figure 2.18C**). These results confirm that genetic changes that occur exclusively as a result of the plant transformation (i.e. changes that are unrelated to the expression of the engineered STR) do not give rise to the formation of unnatural strictosidine intermediates.

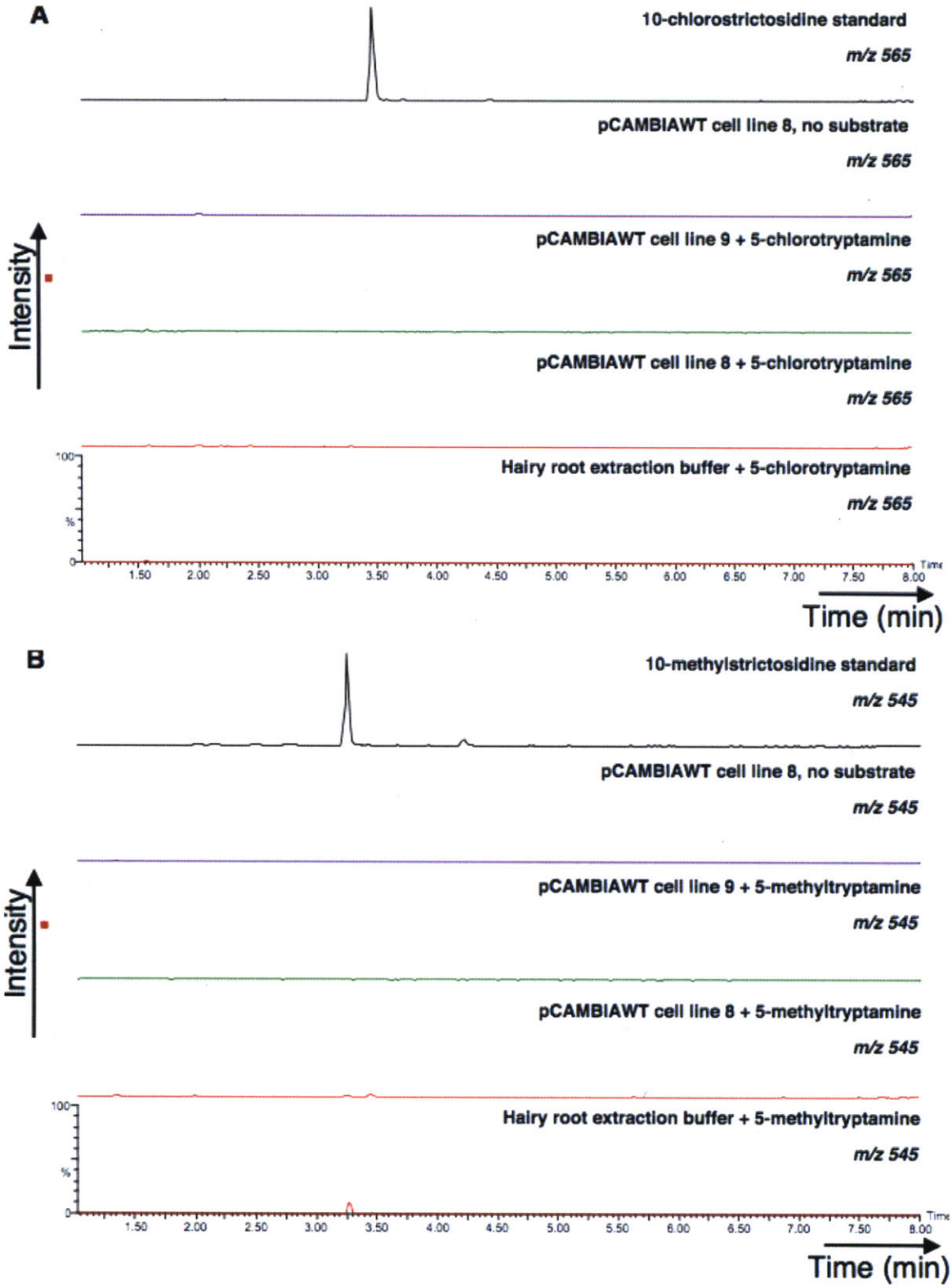

Figure 2.17 A-B. LC-MS traces of an *in vitro* enzymatic assay of pCAMWT hairy root (cell lines 8 and 9) lysates with 1 mM secologanin and 1 mM 5-chlorotryptamine **1a** (**A**) or 5-methyltryptamine **1b** (**B**). *m/z* 565 corresponds to 10-chlorostrictosidine **3a** and *m/z* 545 corresponds to 10-methylstrictosidine **3b**.

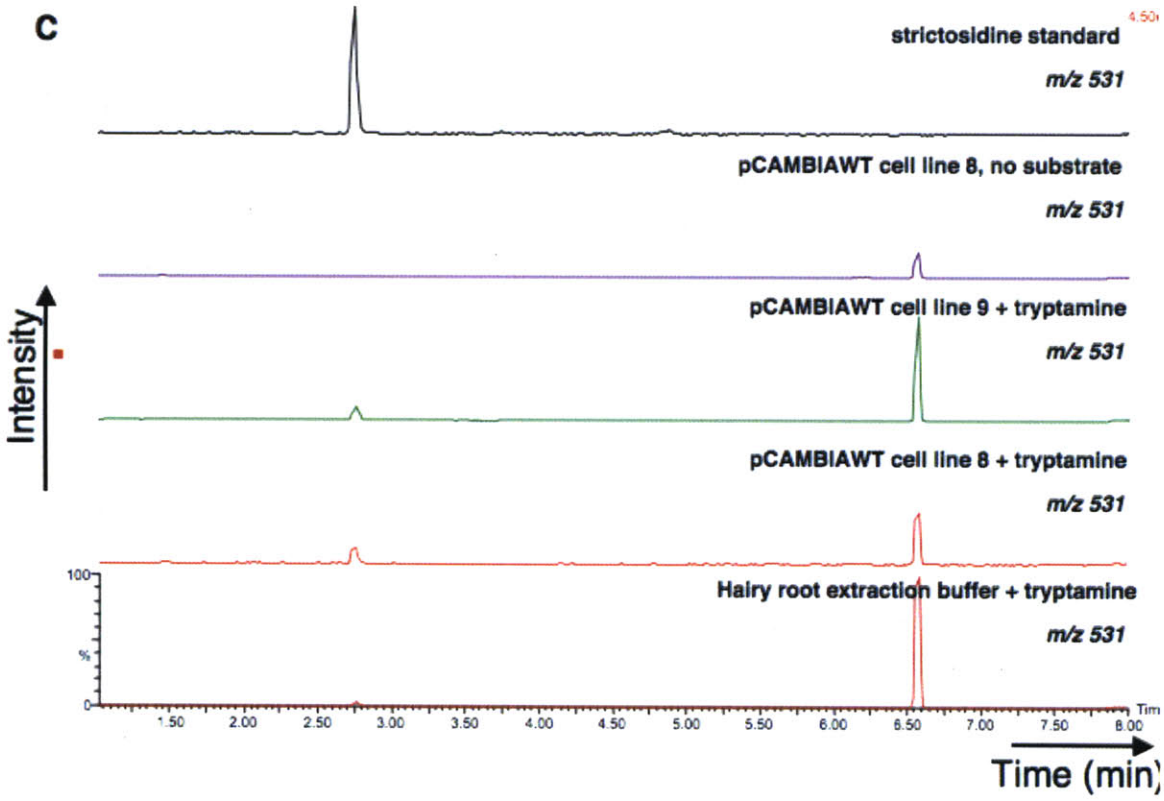

Figure 2.17 C. LC-MS traces of an *in vitro* enzymatic assay of pCAMWT hairy root (cell lines 8 and 9) lysates with 1 mM secologanin and tryptamine (**C**). *m/z* 531 corresponds to strictosidine.

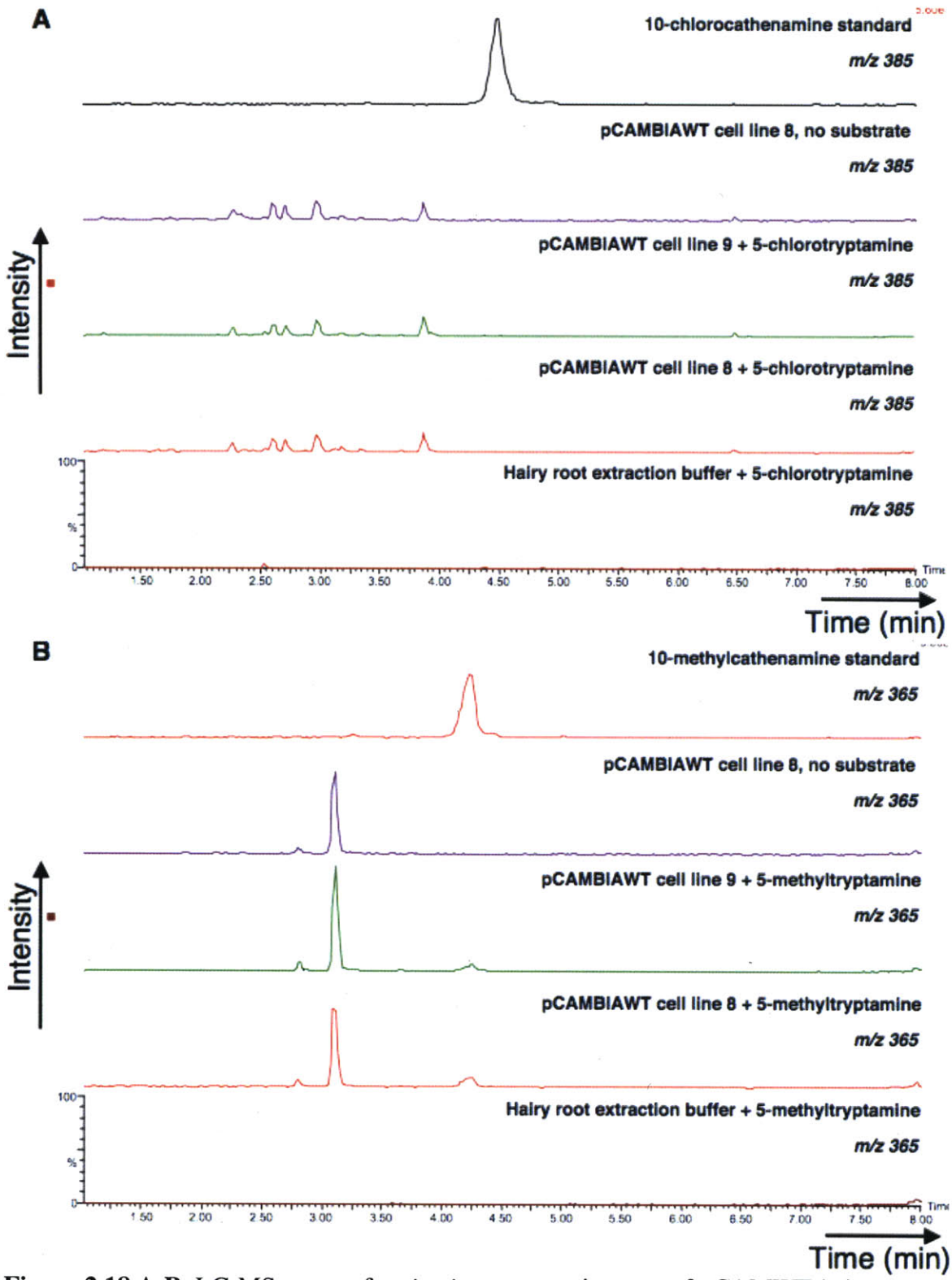

Figure 2.18 A-B. LC-MS traces of an *in vitro* enzymatic assay of pCAMWT hairy root (cell lines 8 and 9) lysates with 1 mM secologanin and 1 mM 5-chlorotryptamine **1a** (**A**) or 5-methyltryptamine **1b** (**B**). *m/z* 385 corresponds to 10-chlorocathenamine and *m/z* 365 corresponds to 10-methylcathenamine.

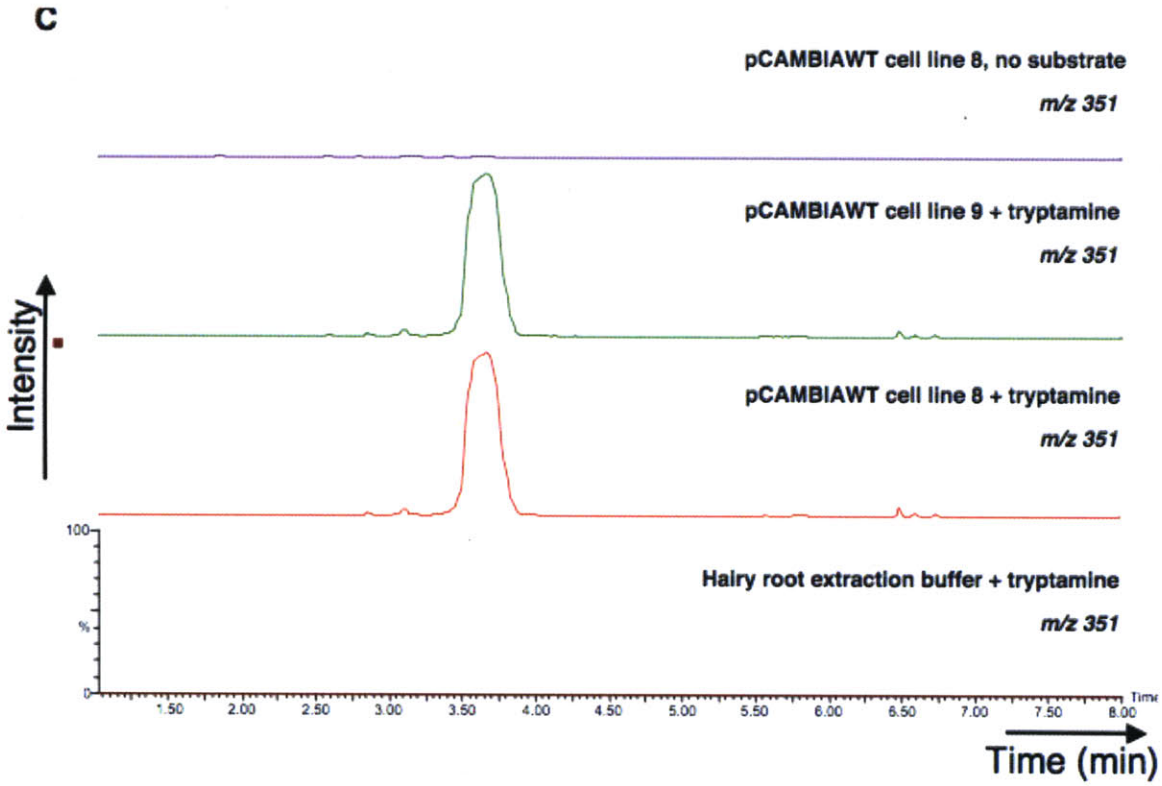

Figure 2.18 C. LC-MS traces of an *in vitro* enzymatic assay of pCAMWT hairy root (cell lines 8 and 9) lysates with 1 mM secologanin and tryptamine (**C**). *m/z* 351 corresponds to cathenamine.

To ensure that a large amount of *wild type* strictosidine synthase could not turn over 5-chlorotryptamine **2a** and 5-methyltryptamine **2b**, various concentrations (1 nM, 10 nM and 100 nM; wild type enzyme k_{cat}/K_m 208333 $M^{-1}s^{-1}$ for tryptamine; no detectable activity for **2a**, **2b** or **2c**) of recombinant wild-type strictosidine synthase (*Cr*STR) were added to lysates of control hairy root cultures lacking V214M expression. Assay conditions were identical to those used in the above section. Formation of 10-chlorostrictosidine **3a** or 10-methylstrictosidine **3b** was not observed when lysates of control hairy roots were incubated with 5-chlorotryptamine **2a** and 5-methyltryptamine **2b**, respectively, even in the presence of 100 nM recombinant *Cr*STR (**Figure 2.19 A-C**). Collectively, these data indicate that production of unnatural strictosidine biosynthetic intermediates and the downstream unnatural alkaloid products strictly correlates with overexpression of the engineered enzyme displaying the desired unnatural substrate specificity.

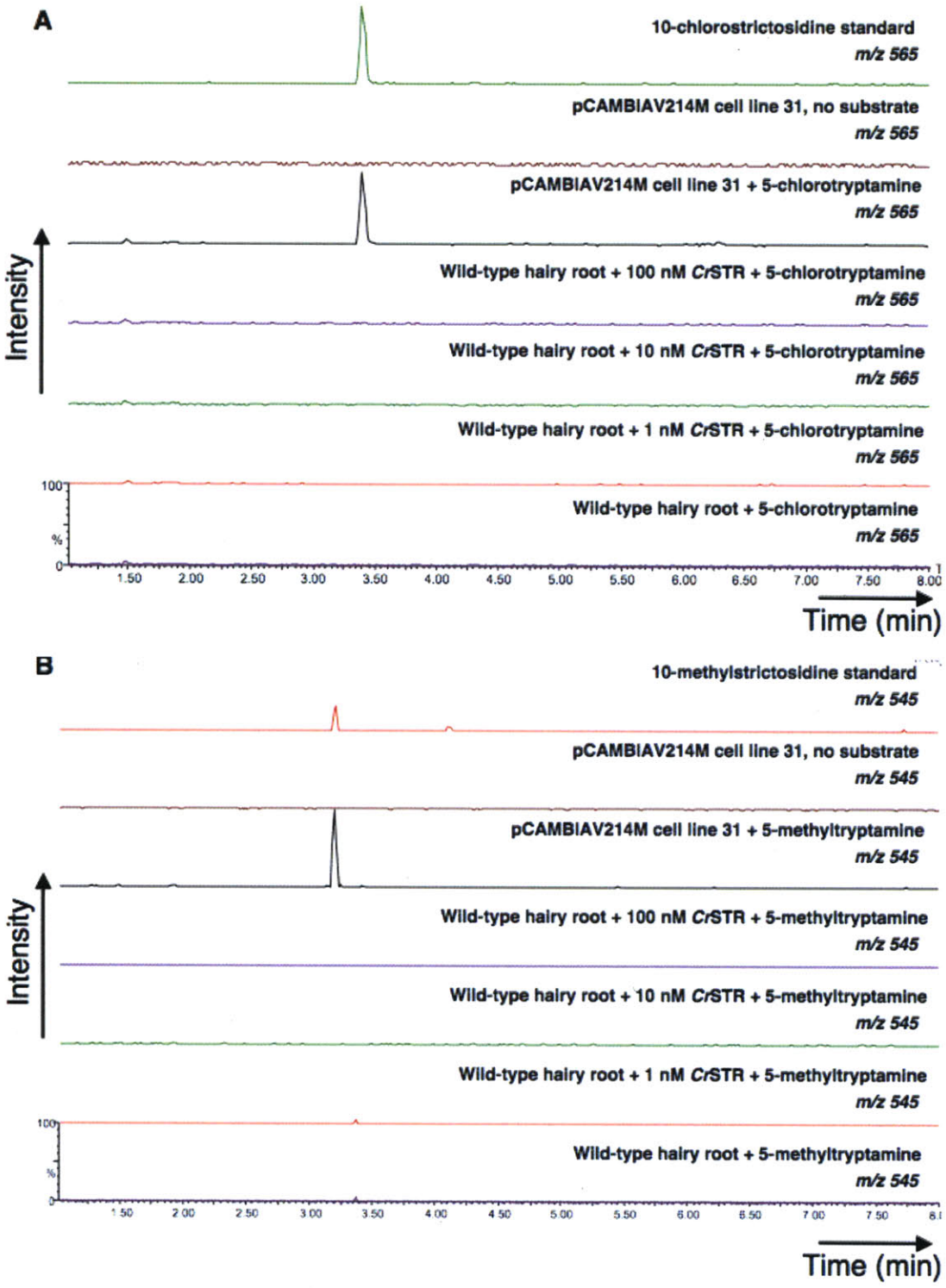

Figure 2.19 A-B. LC-MS traces of the *in vitro* enzymatic assay of wild-type hairy root lysates 'spiked' with 1 nM, 10 nM or 100 nM recombinant wild-type strictosidine synthase (CrSTR) in the presence of 1 mM secologanin and 1 mM 5-chlorotryptamine (**A**) and 5-methyltryptamine (**B**). *m/z* 565, 10-chlorostrictosidine **3a**; and *m/z* 545, 10-methylstrictosidine **3b**.

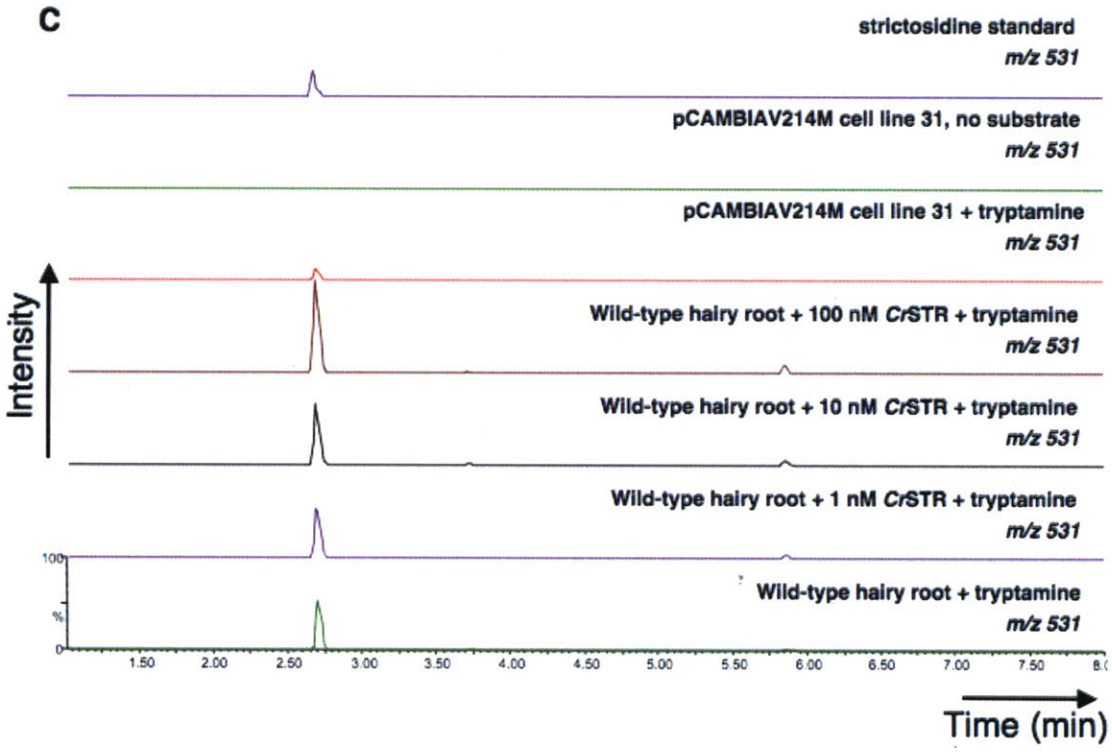

Figure 2.19 C. LC-MS traces of the *in vitro* enzymatic assay of wild-type hairy root lysates 'spiked' with 1 nM, 10 nM or 100 nM recombinant wild-type strictosidine synthase (CrSTR) in the presence of tryptamine (**C**). *m/z* 351, strictosidine **3**.

2.2.5 Regeneration of *C. roseus* Plants from Transformed Hairy Roots Expressing STR Mutant

Differentiated *C. roseus* plants exhibit several advantages over hairy roots and other cell cultures. In particular, *C. roseus* plants produce the alkaloids vindoline, vinblastine and vincristine, which are not observed in hairy root culture (**Chapter 1**). In order to obtain analogs of these more complex alkaloids, we developed a method to obtain transgenic *C. roseus* plants that express the V214M STR mutant. A regeneration process of *C. roseus plants* from hairy root culture has previously been reported[21]. We applied this strategy using the transgenic hairy roots containing the V214M STR gene to yield whole plants (**Figure 2.20**). The regenerated plants exhibit normal growth and flower regularly. While we have been able to "self" wild type plants (grown from commercial seeds, not regenerated from hairy roots), efforts to "self" regenerated plants have not been successful. Real time PCR analysis has shown that the leaves of the regenerated plant express the V214 strictosidine synthase mutant gene. Mass spectrometry analysis of leaf extracts indicate that the leaves of the transgenic plants have a very similar expression profile as wild type plant leaves (**Figure 2.21**).

Figure 2.20. Regeneration of *C. roseus* plants from root culture transformed with the V214M mutant of strictosidine synthase.

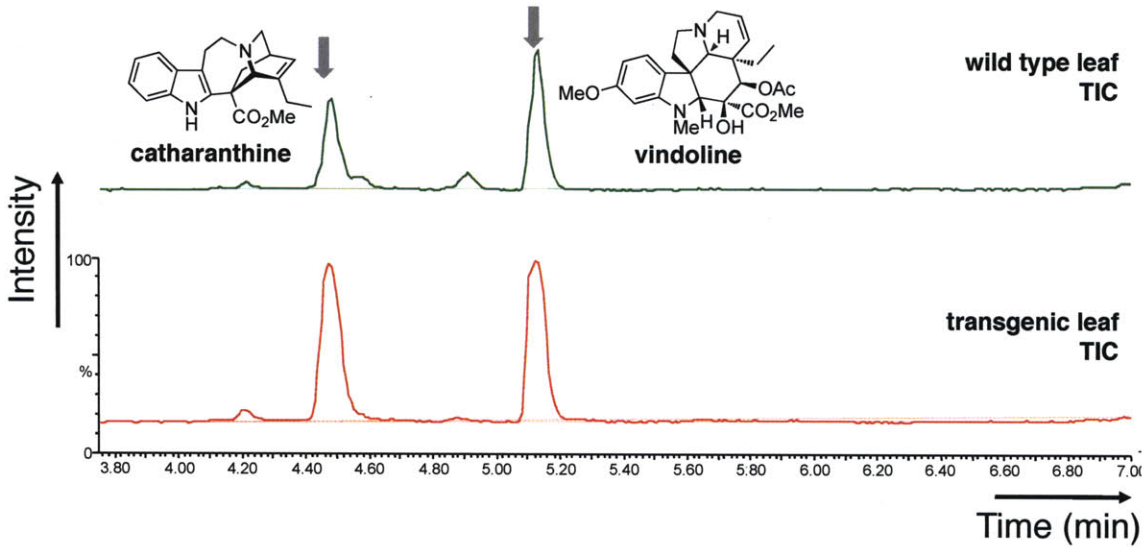

Figure 2.21. Accumulations of catharanthine **7** and vindoline, two representative alkaloids, in both wild type leaves from a plant grown from seed, and in leaves derived from the regenerated plant shown in **Figure 2.20.**

2.3 Conclusions

Fermentation is an attractive way to produce a diversity of natural product-inspired molecules. Although plants have been previously engineered to produce greater amounts of a known natural product or a known biosynthetic intermediate by metabolic engineering strategies, use of plants or plant cell culture as a reactor for unnatural product production has not been widely demonstrated. This chapter describes the introduction of a re-engineered alkaloid biosynthetic gene into *C. roseus* cell culture. The resulting transgenic cell culture produces a variety of unnatural alkaloid compounds when co-cultured with simple and commercially available precursors that the re-engineered enzyme has been designed to accept. The results highlighted in this chapter demonstrate that metabolic reprogramming of alkaloid metabolism can be achieved in medicinal plant cell culture, even though the genetic, biochemical and regulatory aspects of the pathway are still not fully understood. We envision that our work will demonstrate the potential

for reprogramming complex alkaloid pathways to improve the scope and practicality of unnatural product biosynthesis in plants.

2.4 Experimental Methods

2.4.1 Construction of Plant Expression Vectors Containing STR Mutant Gene

The native strictosidine synthase (STR) gene with the complete signal sequence for correct localization (accession number X61932) was obtained by reverse-transcription PCR amplification of mRNA isolated from *C. roseus* hairy root culture (Qiagen, Rneasy kit). Site-directed mutagenesis was then performed to introduce the Val214Met mutation using overlapping mutagenic primers (5' gaaagagctacatATGcccggcggtgcag 3' and 5' ctgcaccgccgggCATatgtagctctttc 3') (Stratagene, Quikchange). For constitutive STR mutant expression, the mutant STR gene was ligated into the NcoI/BstEII site downstream of the CaMV 35S promoter in the pCAMBIA 1305.1 vector[22] (**Figure 2.22**) to yield the construct pCAMV214M. A construct harbouring the *wild-type* STR under control of the constitutive promoter, pCAMWT, was also generated as a control. For inducible STR mutant expression, the mutant STR gene was ligated into the XhoI/SpeI site downstream of the GAL4-UAS promoter in the pTA7002 vector[23] (**Figure 2.22**) to yield the construct pTAV214M. Both pCAMBIA 1305.1 and pTA7002 also contain a hygromycin plant selection marker and a kanamycin bacterial selection marker. Complete constructs for both constitutive and inducible expression were sequenced to ensure plasmid integrity.

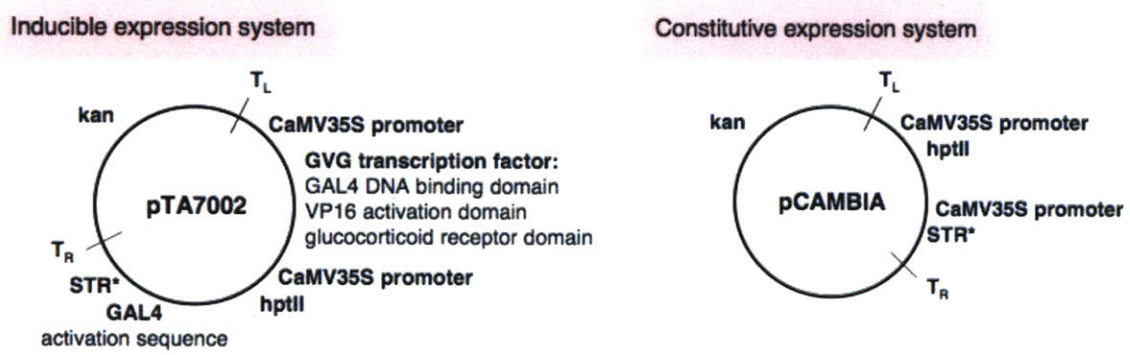

Figure 2.22. Schematic diagrams of strictosidine synthase (STR) mutant inducible expression system (left) and constitutive expression system (right) constructs.

2.4.2. Generation of Transgenic Hairy Root Cultures

The constructs containing the STR Val214Met mutant gene, as well as the construct containing the *wild type* STR gene, were each transformed into *Agrobacterium rhizogenes* ATCC 15834 via electroporation (1mm cuvette, 1.25 kV). Transformation of *C. roseus* seedlings with the generated *Agrobacterium* strains was performed as previously reported[17]. Briefly, 250-300 *C. roseus* seedlings (Vinca Little Bright Eyes, Nature Hills Nursery) were germinated aseptically on Gamborg's B5 media (full strength basal salts, full strength vitamins, 30 g/L sucrose, pH 5.7) and grown in a 16-hour light 8-hour dark cycle at 26 °C for three weeks. Seedlings were then wounded with extra-fine forceps at the stem tip, and transformed 3-5 μL of *A. rhizogenes* from a freshly grown liquid culture were inoculated on the wound.

Hairy roots appeared at the wound site 2-3 weeks after infection for about 80% of the seedlings infected. After hairy roots reached 1-4 cm in length (usually about six weeks after infection), they were excised and transferred to Gamborg's B5 solid media (half strength basal salts, full strength vitamins, 30 g/L sucrose, 6 g/L agar, pH 5.7) containing

hygromycin for selection (three weeks on 0.01 mg/mL in first selection and three weeks on 0.03 mg/mL in second selection) and the antibiotic cefotaxime (0.25 mg/mL in both selections) to remove remaining bacteria. All cultures were grown in the dark at 26°C. After the solid media selection process, hairy roots were subcultured at least once in media lacking both hygromycin and cefotaxime prior to adaptation to liquid culture.

To adapt the line to liquid culture, approximately 200 mg of hairy roots (typically five 3-4 cm long stem tips) from each line that grew successfully on solid media were transferred to 50 mL of half-strength Gamborg's B5 liquid media. The cultures were grown at 26°C in the dark at 125 rpm. All lines were maintained on a 21-28 day subculture cycle depending on the growth rate of each line.

Table 2.2 Hairy roots selection and adaptation processes.

Plasmid	# transformed hairy roots	# hairy roots after solid media selection	# hairy roots after liquid media adaptation
pCAMV214M	240	53	29
pCAMWT	280	74	5*
pTAV214M	270	44	15

* only 5 (out of 74) lines were selected for adaptation to liquid media

The solid media selection and liquid media adaptation processes are summarized in **Table 2.2**. Hairy root transformants were screened for survival in solid media supplemented with hygromycin and subsequently for fitness and fast growth in liquid media. The number of transformants decreased significantly after solid media selection for each of the constructs transformed. Adaptation to liquid media further eliminated

slow growing lines. After the selection and adaptation processes, four to eight hairy root lines from each STR mutant that grew the most rapidly in liquid media were chosen for alkaloid production and mutant enzyme expression assays.

2.4.3 Verification of Transferred DNA (T-DNA) Integration by Genomic DNA Analysis

To verify the integration of transferred DNA (T-DNA) into the plant genome, the genomic DNA from transformed hairy roots was isolated (Qiagen Dneasy kit) and then subjected to PCR amplification using T-DNA specific primers with STR primers serving as a positive control (see below). Specifically, primers for PCR amplification were designed to amplify the complete STR gene (STR_for and STR_rev), an 800bp region of the selection marker HPT gene (HPT_for and HPT_rev), and a 500bp region of the CaMV 35S promoter (CaMV 35S_for and CaMV 35S_rev). Additionally, a primer pair was designed to match the point mutation corresponding to the V214M sequence change at the 3' end of the forward primer (STRV214M_for and STRV214M_rev). These primers readily amplified a 500bp region of the mutant gene. However, the mismatch at the 3' end prevented efficient amplification of the native STR gene in wild type hairy root cultures

PCR primers for verification of T-DNA integration of transformed hairy roots.

	Primer Name	Primer Sequence ('5 → 3')
1	STR_for	CCATGGCAAACTTTTCTGAATCTAAATCC
2	STR_rev	GGTCACCCTAGCTAGAAACATAAGAATTTC
3	HPT_for	GCCTGAACTCACCGCGACGTC
4	HPT_rev	CCTCCAGAAGAAGATGTTGGC
5	CaMV 35S_for	TAGAGGACCTAACAGAAC

6	CaMV 35S_rev	CCGTGTTCTCTCCAAATG
7	STRV214M_for	CCTTATTATTGAAAGAGCTACATATG
8	STRV214M_rev	GCTAGAAACATAAGAATTTCCCTTG

2.4.4 Evaluation of Alkaloid Production in Engineered *C. roseus*

Transgenic hairy root lines were evaluated for alkaloid production after substrate analog feeding. Transformed hairy roots were initially grown in half-strength Gamborg's B5 liquid media supplemented with the corresponding tryptamine analog at 0.5 mM concentration. Co-cultivation with tryptamine analogs 5-chlorotryptamine **2a**, 5-methyltryptamine **2b** and 5-bromotryptamine **2c** at this relatively high concentration at the initial growth phase resulted in growth retardation. Hairy roots fragmented and became brown a few days after addition of the tryptamine analogs. To address this problem, tryptamine analogs (and 10 μM dexamethasone for the inducible expression system) were added to the liquid culture towards the end of the log phase and the beginning of the stationary phase (usually after three weeks). After one week of co-cultivation with the substrate, hairy roots were ground with a mortar, pestle and 106 μm acid washed glass beads in methanol (10 mL/g of fresh weight hairy roots) from the harvested tissue. The crude natural product mixtures were filtered and subsequently subjected to LC-MS analysis. In total, three hairy root lines transformed with *A. rhizogenes* harboring the pCAMV214M plasmid and two hairy root lines with pTAV214M plasmid were evaluated for alkaloid production. Additionally, hairy roots transformed with wild-type *A. rhizogenes* lacking the plasmid were also evaluated.

These crude alkaloid mixtures were diluted 1/100 with methanol for mass spectral analysis. Samples were ionized by ESI with a Micromass LCT Premier TOF Mass

Spectrometer. The LC was performed on Acquity Ultra Performance BEH C18, 1.7 μm, 2.1 x 100 mm column on a gradient of 10-60% acetonitrile/water (0.1% TFA) over 13 minutes at a flow rate of 0.6 mL/min. The capillary and sample cone voltages were 1300 and 60 V, respectively. The desolvation and source temperature were 300 and 100 °C. The cone and desolvation gas flow rates were 60 and 800 L/hour. Analysis was performed with MassLynx 4.1. Accurate mass measurements were obtained in W-mode. The spectra were processed using the Mass Lynx 4.1 mass measure, in which the mass spectrum of peaks of interest was smoothed and centered with TOF mass correction, locking on the reference infusion of reserpine.

2.4.5 Purification and Isolation of Alkaloids from Transformed Hairy Roots Supplemented with 5-chlorotryptamine 2a and 5-methyltryptamine 2b

Root tips (10-15) from transformed hairy roots (line 31) were subcultured in 150 mL Gamborg's B5 liquid media and grown at 26°C in the dark at 125 rpm for three weeks prior to supplementing the media with either 5-chlorotryptamine **2a** or 5-methyltryptamine **2b**. After one week of co-cultivation, hairy roots were extracted as described above in methanol (10 mL/g of fresh weight hairy roots). Alkaloid extracts were filtered, concentrated under vacuum and redissolved in 20% acetonitrile/water (0.1% TFA) (1 mL/g of fresh weight hairy roots).

For 5-chlorotryptamine **2a** feeding, the redissolved mixture was purified on a 10 x 20 mm Vydec reverse phase column using a gradient of 20-60% acetonitrile/water (0.1% TFA) over 35 minutes. Alkaloids were monitored at 228 nm and fractions containing the

alkaloid analogs of interest, as determined by the characteristic isotopic distribution expected for chlorinated molecules ($^{35}Cl/^{37}Cl$) from LC-MS analysis, were combined and concentrated under vacuum (**Figure 2.23**). Isolated alkaloids were analyzed by LC-MS (same parameters as above), analytical HPLC, and where possible, NMR (Bruker AVANCE-600 NMR spectrometer equipped with a 5mm 1H{13C,31P} cryo-probe).

Fractions a-d (**Figure 2.23**) were characterized by LC-MS, compared to characteristic UV spectra of known alkaloids and, when greater than 1 mg quantities were obtained in sufficient purity, also by ^{1}H NMR and ^{1}H-^{13}C HSQC. Chlorinated alkaloids generally displayed longer retention times than the natural alkaloids. Fraction **a** corresponded to ajmalicine **4**; fraction **b** corresponded to catharanthine **7**; fraction **c** corresponded to 10-chloroajmalicine **4a**; and fraction **d** appeared to be a mixture of 15-chlorotabersonine **5a** and another chlorinated alkaloid also with *m/z* 371.

For 5-methyltryptamine **2b** feeding, similar procedures were performed to feed and isolate alkaloids from transgenic hairy roots. One notable difference was in the purification step: since methylated alkaloids are generally more hydrophilic than chlorinated alkaloids, the redissolved alkaloid mixture was purified on a 10 x 20 mm Vydec reverse phase column using a gradient of 20-50% acetonitrile/water (0.1% TFA) over 35 minutes.

Alkaloids were monitored at 228 nm and fractions containing the alkaloid analogs of interest, as determined by LC-MS analysis, were combined and concentrated under

vacuum (**Figure 2.24**). All isolated alkaloids were characterized by LC-MS, compared to characteristic UV spectra of known alkaloids and, when greater than 1 mg quantities were obtained in sufficient purity, also by ^{1}H NMR and ^{1}H-^{13}C HSQC. Fraction **a** appeared to be a mixture of 10-methylajmalicine **4b** and another compound with *m/z* 379; fraction **b** contained a mixture of 15-methyltabersonine **5b** and a compound with *m/z* 353. Fraction b was further purified on a 10 x 20 mm Vydex reverse phase column using an isocrat 28% acetonitrile/water (0.1% TFA) to obtain 15-methyltabersonine **5b** in over 85% purity.

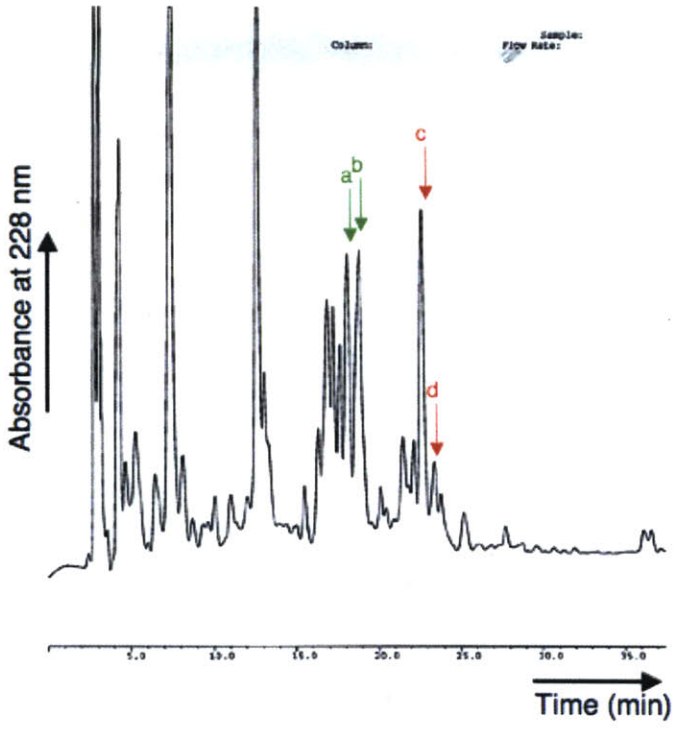

Figure 2.23. HPLC trace of alkaloids from pCAMV214M hairy root (cell line 31) fed with 5-chlorotryptamine **2a** (0.5 mM). Fractions a, b, c and d were collected and analyzed.

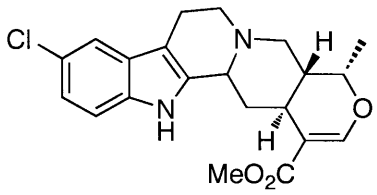

4a

Tabulated NMR data for 10-chloroajmalicine **4a** (Fraction c in **Figure 2.23**)

^{1}H NMR (600 MHz, CD_3OD): δ 7.64 (d, J = 1.8 Hz, 1H), 7.53 (d, J = 1.8 Hz, 1H), 7.39 (d, J = 9.0 Hz, 1H), 7.17 (dd, J = 1.8, 8.4 Hz, 1H), 4.87 (m, 1H), 4.59 (qd, J = 3.6, 6.6 Hz, 1H), 3.89 (dd, J = 5.7, 12.6 Hz, 1H), 3.79 (s, 3H), 3.70 (dd, J = 3.0, 12.0 Hz, 2H), 3.45 (dd, J = 1.2, 1.8 Hz, 1H), 3.25 (m, 1H), 3.22 (m, 1H), 3.15 (dd, J = 4.2, 16.2 Hz, 1H), 2.84 (br t, J = 11.4 Hz, 1H), 2.26 (m, 1H), 1.53 (m, 1H), 1.28 (d, J = 6.6 Hz, 3H); ^{13}C NMR (500 MHz, CD_3OD): δ 156.20, 124.05, 118.88, 114.07, 73.61, 63.03, 55.67, 54.54, 51.88, 40.94, 32.28, 30.29, 20.30, 14.74 (note that quaternary carbon peaks are not observed in ^{1}H-^{13}C HSQC ;ESI-MS (*m/z*): $[M]^+$ calcd. for $C_{21}H_{23}N_2O_3Cl$, 387.1490; found, 387.1483.

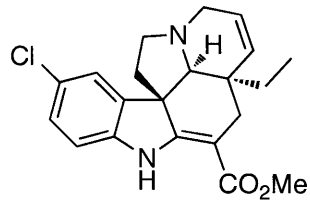

5a

NMR data for 15-chlorotabersonine **5a** (Fraction d in **Figure 2.23**)

^{1}H NMR (500 MHz, CD_3OD): δ 7.68 (d, J = 2.0 Hz, 1H), 7.26 (dd, J = 2.0, 8.0 Hz, 1H), 7.03 (d, J = 8.0 Hz, 1H), 6.06 (d, J = 10.5 Hz, 1H), 6.00 (dd, J = 4.0, 10.5 Hz, 1H), 4.21 (d, J = 10.0 Hz, 1H), 3.80 (s, 3H), 3.67 (m, 1H), 3.57 (m, 1H), 3.17 (m, 1H), 2.94 (m, 1H), 2.34 (d, J = 17.5 Hz, 1H), 1.83 (d, J = 7.0 Hz, 1H), 1.78 (dd, J = 2.5, 7.0 Hz, 2H), 1.67 (d, J = 6.50 Hz, 1H), 1.14 (t, J = 7.50, 1H), 0.73 (t, J = 7.5 Hz, 3H); ESI-MS (*m/z*):

$[M]^+$ calcd. for $C_{21}H_{23}N_2O_2Cl$, 371.1526; found, 371.1528.

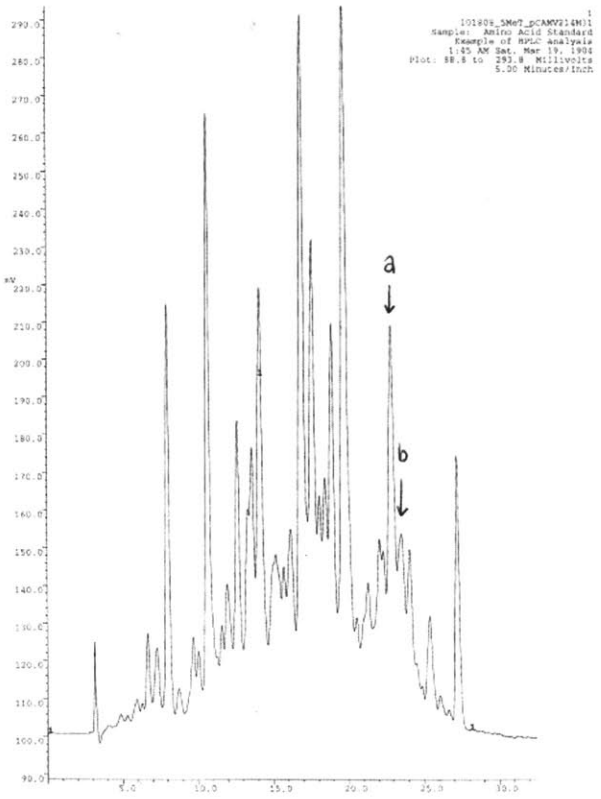

Figure 2.24. HPLC trace of alkaloids from pCAMV214M hairy root (cell line 31) fed with 5-methyltryptamine **2b** (0.5 mM). Fractions a and b were collected and analyzed.

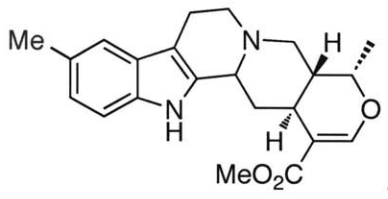

4b

Tabulated NMR data for 10-methylajmalicine **4b** (Fraction a in **Figure 2.24**)

^{1}H NMR (500 MHz, CD_3OD): δ 7.60 (d, J = 1.5 Hz, 1H), 7.01 (d, J = 9.0 Hz, 1H), 6.93 (dd, J = 4.5, 8.0 Hz, 1H), 4.81 (dd, J = 4.0, 11.0 Hz, 1H), 4.57 (dd, J = 4.0, 6.5 Hz, 1H), 3.89 (m, 1H), 3.77 (s, 3H), 3.66 (m, 2H), 3.45 (m, 1H), 3.25 (m, 1H), 3.22 (m, 1H), 3.13

(m, 1H), 2.84 (m, 1H), 2.41 (s, 3H), 2.25 (m, 1H), 1.52 (m, 1H), 1.26 (d, J = 6.5 Hz, 3H); ESI-MS (*m/z*): $[M]^+$ calcd. for $C_{22}H_{27}N_2O_3$, 367.2022; found, 367.2015.

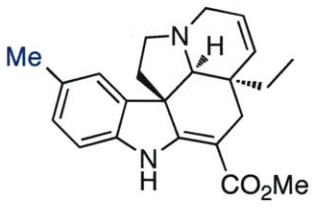

5b

NMR data for 10-methyltabersonine **5b** (Fraction b in **Figure 2.24**)

^{1}H NMR (600 MHz, CD_3OD): δ 7.40 (s, 1H), 7.08 (d, J = 8.0 Hz, 1H), 6.93 (d, J = 7.9 Hz, 1H), 6.06 (d, J = 10.0 Hz, 1H), 6.00 (dd, J = 4.4, 10.1 Hz, 1H), 4.22 (d, J = 15.4 Hz, 1H), 4.01 (d, J = 14.0 Hz, 1H), 3.93 (s, 1H), 3.80 (s, 3H), 3.67 (m, 1H), 3.57 (m, 1H), 2.92 (d, J = 16.6 Hz, 1H), 2.42 (m, 1H), 2.33 (s, 3H), 2.19 (br s, 2H), 1.29 (s, 1H), 1.19 (m, 2H), 0.71 (t, J = 7.0 Hz, 3H); ^{13}C NMR (500 MHz, CD_3OD): δ 135.49, 130.89, 122.80, 122.62, 111.49, 72.15, 54.30, 51.98, 51.78, 44.44, 30.96, 28.80, 21.25, 7.81 (note that quaternary carbon peaks are not observed in ^{1}H-^{13}C HSQC); ESI-MS (*m/z*): $[M]^+$ calcd. for $C_{22}H_{27}N_2O_2$, 351.2073; found, 351.2064.

2.4.6 Verification of Expression of Mutant STR Enzyme by Real Time RT-PCR

Real time RT-PCR was used to assess the expression levels of STR (sum total of both mutant V214M STR and native STR). Expression levels in hairy roots infected with *A. rhizogenes* lacking the pCAMV214M STR mutant construct were compared to expression levels in hairy roots harboring pCAMV214M. mRNA from transformed hairy roots was isolated and purified from contaminant DNA using Qiagen RNeasy Plant Mini Kit and Rnase-free DnaseI, respectively. The resulting mRNA was then reverse-

transcribed to cDNA using Qiagen QuantiTect Reverse transcription kit and then subjected to PCR with specific primers (see below), Qiagen SYBR Green PCR kit and a Biorad DNA Engine Opticon 2 system. The threshold-cycle (C_T) was determined as the cycle with a signal higher than that of the background plus 10 x standard deviation (SD). *C. roseus* 40S ribosomal protein S9 (Rps9), a house keeping gene, was used to adjust the amount of the total mRNA in all samples. Real time RT-PCR was performed in triplicate and the data are pictured as the relative expression levels of STR (sum total of both V214M mutant and native STR) mRNA in transgenic hairy roots as well as hairy roots lacking the pCAMBIA plasmid. Hairy root lines containing the pTAV214M construct also failed to show expression of the V214M mutant STR both in the presence and absence of dexamethasone, the inducer.

PCR primers for real-time RT-PCR of transformed hairy roots. Primers were designed using GenScript web tool (http://www.genscript.com/ssl-bin/app/primer)

Primer Name	Primer Sequence ('5 → 3')	Amplicon size
Homol_STR_for	GTCCAAGATGGCCGAGTTAT	140
Homol_STR_rev	TATGTCCTCCCACACAATGG	
STR_V214M_for	TATTATTGAAAGAGCTACATATG	134
STR_V214M_rev	CTCTGCACTGCCTTTCTTG	
Rbps9_for	TTGAGCCGTATCAGAAATGC	122
Rbps9_rev	CCCTCATCAAGCAGACCATA	

2.4.7 In vitro Enzymatic Assay of Transformed Hairy Roots Expressing STR Mutant

After at least three rounds of subculture in liquid media, transformed hairy roots were subjected to an enzymatic assay to evaluate the expression of the STR mutant *in vitro*. In the constitutive expression system (hairy roots transformed with pCAMV214M), hairy

roots subcultured for three weeks were harvested and ground with a mortar, pestle and 106 μm acid washed glass beads in extraction buffer (0.1 M phosphate buffer, 2 mM EDTA, 4 mM DTT, 0.1 μM pepstatin, 0.1 μM leupeptin, 1% PVP, pH 7.2) at 4 °C. The hairy root extracts were centrifuged for 10 min at 13000 rpm at 4 °C to remove cell debris, concentrated, and assayed for STR V214M enzymatic activity without further purification. Total protein concentration in the extracts was quantified using Biorad Protein Assay Solution.

A typical reaction mixture contained 0.1 M phosphate buffer pH 7, 2.5 mM DTT, 1 mM secologanin, and 1 mM tryptamine analog **2a-c**. Approximately 20 μg of crude enzyme was added to 100 μL reaction mixture and the reaction was incubated at 30 °C for 4 hours. To quench the reaction, 625 μL of methanol was added to 50 μL of the reaction mixture and the resulting solution was centrifuged, filtered through a 0.2 μm filter and then subjected to LC-MS analysis. Samples were ionized by ESI with a Micromass LCT Premier TOF Mass Spectrometer. The LC was performed on an Acquity Ultra Performance BEH C18, 1.7 μm, 2.1 x 100 mm column on a gradient of 10-60% acetonitrile/water (0.1% TFA) over 7 minutes at a flow rate of 0.6 mL/min. In total, three lines (pCAMV214M_31, pCAMV214M_37, and pCAMV214M_49) with constitutive mutant STR expression were assayed for enzymatic activity. Lysate from hairy roots overexpressing *wild-type* strictosidine synthase and hairy roots infected with *A. rhizogenes* lacking plasmid ("wild type hairy root") were used as negative controls. Additionally, any non-enzymatically catalyzed background reaction that occurred simply

in the presence of the hairy root extraction buffer was also measured (no enzyme control).

2.4.8 Regeneration of *C. roseus* Plants from Transformed Hairy Roots Expressing STR Mutant

Regeneration of transformed hairy roots expressing STR mutant to whole plants was performed as previously reported[21]. Briefly, one-centimeter-long root tips of two-week-old transformed hairy roots were excised and transferred to shoot regeneration media (full strength Murashige and Skoog basal salts and vitamins, 31 μM 6-benzyladenine, 5.4 μM α-naphthaleneacetic acid, 30 g/L sucrose, pH 5.7). After nine weeks on this media, explants were transferred to root regeneration media (half strength Murashige and Skoog basal, full strength Murashige and Skoog vitamins, 30 g/L sucrose, pH 5.7). After four weeks on this media, regenerated plants were transferred to full strength Gamborg's B5 media (full strength basal salts, full strength vitamins, 30 g/L sucrose, pH 5.7). After three weeks of acclimation, regenerated plants were transferred to Miracle gro soil and maintained in a culture room.

2.5 Acknowledgements

We gratefully acknowledge financial support from the NIH (GM074820), the US National Science Foundation (MCB0719120), and the American Cancer Society (RSG-07-025-01-CDD). We thank Professor Jacqueline V. Shanks (Iowa State University) and Dr. Christie Peebles (Colorado State University) for detailed advice in the transformation procedure. CAMBIA is acknowledged for providing the pCAMBIA vectors, and

Professor Nam-Hai Chua (Rockefeller University) is acknowledged for providing pTA7002. We thank Lisa Smeester (MIT) for assistance with rt-PCR, Dr. Justin J. Maresh (MIT) for helpful discussions regarding the *Agrobacterium* transformation and Dr. Nathan E. Nims (MIT) for helpful suggestions regarding primer design for rt-PCR experiments. Dr. Nancy Yerkes (MIT) generously provided strictosidine standards. We thank Professor Toni M. Kutchan (Danforth Plant Science Center) for suggesting the pCAMBIA vector system. We gratefully acknowledge Dr. Jeffrey H. Simpson's (MIT) assistance in obtaining two-dimensional NMR data.

2.6 References

1. Dewick, P. M., *Medicinal Natural Products: A Biosynthetic Approach, 2nd Edition* John Wiley and Sons, Ltd: New York, 2003.
2. Ganesan, A., The impact of natural products upon modern drug discovery. *Curr Opin Chem Biol* **2008,** *12* (3), 306-17.
3. Menzella, H. G.; Reeves, C. D., Combinatorial biosynthesis for drug development. *Curr Opin Microbiol* **2007,** *10* (3), 238-45.
4. Yun, D. J.; Hashimoto, T.; Yamada, Y., Metabolic engineering of medicinal plants: transgenic Atropa belladonna with an improved alkaloid composition. *Proc Natl Acad Sci U S A* **1992,** *89* (24), 11799-803.
5. Ye, X.; Al-Babili, S.; Kloti, A.; Zhang, J.; Lucca, P.; Beyer, P.; Potrykus, I., Engineering the provitamin A (beta-carotene) biosynthetic pathway into (carotenoid-free) rice endosperm. *Science* **2000,** *287* (5451), 303-5.
6. Katsuyama, Y.; Funa, N.; Miyahisa, I.; Horinouchi, S., Synthesis of unnatural flavonoids and stilbenes by exploiting the plant biosynthetic pathway in Escherichia coli. *Chem Biol* **2007,** *14* (6), 613-21.
7. Schmidt-Dannert, C.; Umeno, D.; Arnold, F. H., Molecular breeding of carotenoid biosynthetic pathways. *Nat Biotechnol* **2000,** *18* (7), 750-3.
8. O'Connor, S. E.; Maresh, J. J., Chemistry and biology of monoterpene indole alkaloid biosynthesis. *Nat Prod Rep* **2006,** *23* (4), 532-47.
9. Hawkins, K. M.; Smolke, C. D., Production of benzylisoquinoline alkaloids in Saccharomyces cerevisiae. *Nat Chem Biol* **2008,** *4* (9), 564-73.
10. Minami, H.; Kim, J. S.; Ikezawa, N.; Takemura, T.; Katayama, T.; Kumagai, H.; Sato, F., Microbial production of plant benzylisoquinoline alkaloids. *Proc Natl Acad Sci U S A* **2008,** *105* (21), 7393-8.

11. Bernhardt, P.; McCoy, E.; O'Connor, S. E., Rapid identification of enzyme variants for reengineered alkaloid biosynthesis in periwinkle. *Chem Biol* **2007,** *14* (8), 888-97.
12. McCoy, E.; O'Connor, S. E., Directed biosynthesis of alkaloid analogues in the medicinal plant periwinkle. *J. Am. Chem. Soc.* **2006,** *128*, 14276-14277.
13. Ma, X.; Panjikar, S.; Koepke, J.; Loris, E.; Stockigt, J., The structure of Rauvolfia serpentina strictosidine synthase is a novel six-bladed beta-propeller fold in plant proteins. *Plant Cell* **2006,** *18* (4), 907-20.
14. Chen, S.; Galan, M. C.; Coltharp, C.; O'Connor, S. E., Redesign of a central enzyme in alkaloid biosynthesis. *Chem Biol* **2006,** *13* (11), 1137-41.
15. Loris, E. A.; Panjikar, S.; Ruppert, M.; Barleben, L.; Unger, M.; Schubel, H.; Stockigt, J., Structure-based engineering of strictosidine synthase: auxiliary for alkaloid libraries. *Chem Biol* **2007,** *14* (9), 979-85.
16. Toivonen, L.; Balsevich, J.; Kurz, W. G. W., Indole alkaloid production by hairy root cultures of Catharanthus roseus. *Plant Cell Tissue Organ Culture* **1989,** *18*, 79-93.
17. Hughes, E. H.; Hong, S. B.; Shanks, J. V.; San, K. Y.; Gibson, S. I., Characterization of an inducible promoter system in Catharanthus roseus hairy roots. *Biotechnol Prog* **2002,** *18* (6), 1183-6.
18. St-Pierre, B.; Vazquez-Flota, F. A.; De Luca, V., Multicellular compartmentation of catharanthus roseus alkaloid biosynthesis predicts intercellular translocation of a pathway intermediate. *Plant Cell* **1999,** *11* (5), 887-900.
19. Canel, C.; Lopes-Cardoso, M. I.; Whitmer, S.; van der Fits, L.; Pasquali, G.; van der Heijden, R.; Hoge, J. H.; Verpoorte, R., Effects of over-expression of strictosidine synthase and tryptophan decarboxylase on alkaloid production by cell cultures of Catharanthus roseus. *Planta* **1998,** *205* (3), 414-9.
20. Yerkes, N.; Wu, J. X.; McCoy, E.; Galan, M. C.; Chen, S.; O'Connor, S. E., Substrate specificity and diastereoselectivity of strictosidine glucosidase, a key enzyme in monoterpene indole alkaloid biosynthesis. *Bioorg Med Chem Lett* **2008,** *18* (10), 3095-8.
21. Choi, P. S.; Kim, Y. D.; Choi, K. M.; Chung, H. J.; Choi, D. W.; Liu, J. R., Plant regeneration from hairy-root cultures transformed by infection with Agrobacterium rhizogenes in Catharanthus roseus. *Plant Cell Rep* **2004,** *22* (11), 828-31.
22. Broothaerts, W.; Mitchell, H. J.; Weir, B.; Kaines, S.; Smith, L. M.; Yang, W.; Mayer, J. E.; Roa-Rodriguez, C.; Jefferson, R. A., Gene transfer to plants by diverse species of bacteria. *Nature* **2005,** *433* (7026), 629-33.
23. Aoyama, T.; Chua, N. H., A glucocorticoid-mediated transcriptional induction system in transgenic plants. *Plant J* **1997,** *11* (3), 605-12.

CHAPTER 3

INTRODUCING PROKARYOTIC HALOGENASES

INTO *C. ROSEUS* CELL CULTURE

Part of this chapter is published as a letter in

Nature **2010**, *468*, 461-464

3.1 Introduction

Halogenated metabolites, once considered 'chance products of nature', have now been observed in many natural product biosynthetic pathways[1]. However, out of over 4000 halogenated natural products that have been reported in literatures, only a few are from terrestrial plants[2]. While halogenating enzymes are undoubtedly present in certain plant species, no plant-derived halogenase has been reported. Given the impact that halogenation can have on the biological activity of natural products[1], introduction of halides into medicinal plant metabolism would provide the opportunity to rationally engineer a broad variety of novel plant products with altered, and perhaps improved, pharmacological properties. Moreover, the halogen moiety can serve as a chemical handle for further chemical derivatization.

While none of the halogenase enzymes from plants have been identified, numerous halogenase enzymes from soil bacteria have been identified and characterized extensively[1,3-5]. One class of halogenase that chlorinates aromatic substrates utilizes a flavin cofactor, along with a partner flavin reductase, to catalyze transfer of the halide to the substrate. Two of these enzymes, PyrH[6,7] and RebH[8-11], chlorinate the indole ring of tryptophan in the 5 and 7 positions, respectively. We envisioned that the introduction of these enzymes into other natural product pathways would allow regioselective incorporation of halogens onto a range of tryptophan-derived alkaloid products[12], provided that the downstream enzymes could accommodate the chlorinated tryptophan precursor.

Previous work has shown that the downstream alkaloid biosynthetic enzymes of *Catharanthus roseus* are not particularly substrate specific[13-15] (**Chapter 2** and **Chapter 4**). For example, when *C. roseus* cell culture is supplemented with a variety of halogenated tryptamines, the corresponding halogenated alkaloid analogs are produced in isolable yields[13-15]. Therefore, we envisioned that if prokaryotic halogenases could function in the eukaryotic plant cell, and if tryptophan decarboxylase could convert halogenated tryptophan into halogenated tryptamine, then we could engineer *C. roseus* to produce halogenated alkaloids *de novo* by integrating these prokaryotic genes to the *C. roseus* genome (**Figure 3.1**).

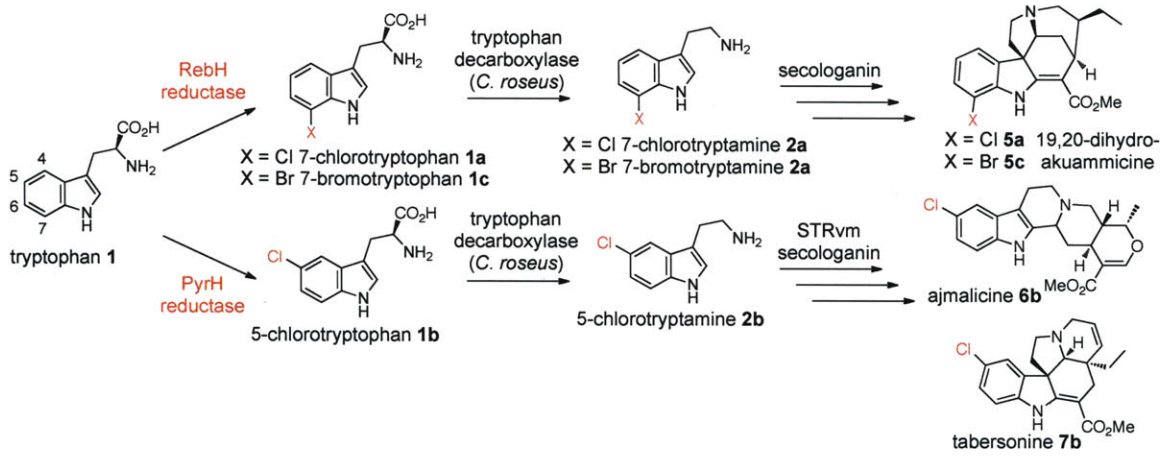

Figure 3.1. RebH and PyrH, along with a partner reductase, halogenate the indole ring of tryptophan **1** to yield chloro-tryptophan. After transformation of these enzymes into *C. roseus*, halogenated tryptophan **1a** and **1b** can be decarboxylated by tryptophan decarboxylase (*C. roseus*) to form chlorotryptamine **2a** and **2b**, and then converted into chlorinated monoterpene indole alkaloids.

This chapter describes the successful introduction of chlorination biosynthetic machinery from soil bacteria into the medicinal plant *C. roseus*, which lacks the biosynthetic capability to produce halogenated compounds. These prokaryotic halogenases function within the context of the eukaryotic plant cell to generate chlorinated tryptophan, which is then shuttled into monoterpene indole alkaloid metabolism to yield chlorinated alkaloids. Moreover, when the plant culture media was supplemented with bromide salts, accumulation of brominated alkaloids was observed in crude plant extracts. Altogether, we have introduced a new functional group—a halide—into complex plant metabolism to rationally alter product outcome.

3.2 Results and Discussion

3.2.1 Determining the Steady-State Kinetic Constants of TDC for Tryptophan Substrate Analogs, 5- and 7-chlorotryptophan 1a and 1b

Since RebH and PyrH do not turnover tryptamine, our strategy requires that tryptophan decarboxylase from *C. roseus* can competently decarboxylate halogenated tryptophan. We heterologously expressed tryptophan decarboxylase from *C. roseus* in *Escherichia coli* (**Figure 3.2**). Purified enzyme was assayed with tryptophan **1**, 7-chlorotryptophan **1a** and 5-chlorotryptophan **1b** .The steady state kinetics for *C. roseus* tryptophan decarboxylase and tryptamine substrates are summarized in **Table 3.1** and **Figure 3.3 A-C**. These steady state kinetic data indicated that the catalytic efficiency of the decarboxylase was approximately 30 folds lower with the halogenated substrates **1a** and **1b** than with tryptophan **1**. Nevertheless, the activity of the enzyme suggested that halogenated tryptophan **1a** and **1b** could be decarboxylated *in vivo*.

Table 3.1. Kinetic constants for *C. roseus* tryptophan decarboxylase and tryptamine substrates.

Tryptamine substrates	**K_m (mM)**	**k_{cat}(min^{-1})**	**k_{cat}/ K_m($mM^{-1}min^{-1}$)**
Tryptophan **1**	51.7 ± 9.2	5.1 ± 0.1	0.099
7-chlorotryptophan **1a**	499 ± 74	1.6 ± 0.04	0.00327
5-chlorotryptophan **1b**	538 ± 48	2.5 ± 0.08	0.00455

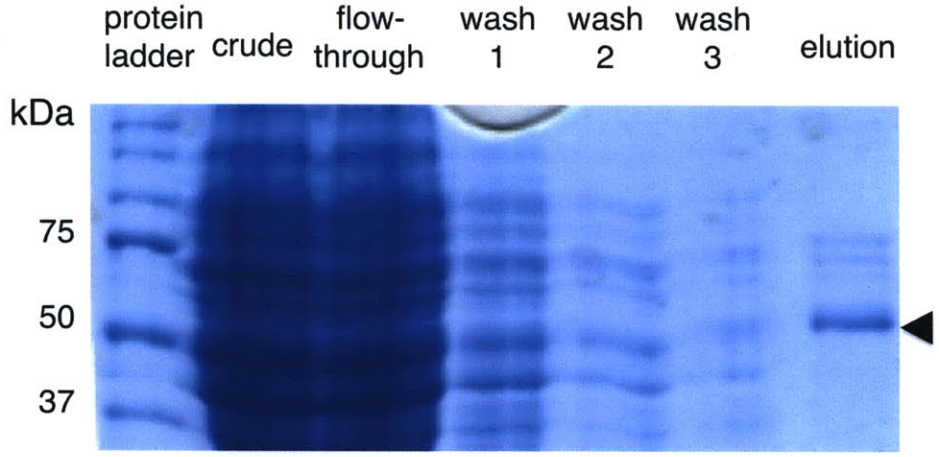

Figure 3.2. SDS-PAGE of *C.roseus* tryptophan decarboxylase (TDC) purification from Ni-NTA affinity resin (Qiagen Ni-NTA Spin Kit).

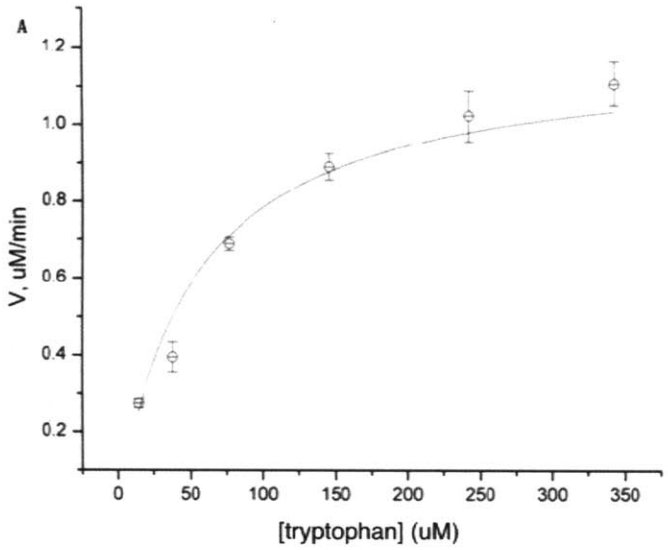

[tryptophan] (uM)	V (uM/min)
13.90	0.2748
37.69	0.3951
76.63	0.6885
145.87	0.8906
242.35	1.0230
342.79	1.1073

Equation	V=Vmax*S/(Km+S)	
Adj. Rsqr	0.9936	
	Value	Standard E
Km	52	9
Vmax	1.19	0.09
kcat	5.12	

Figure 3.3 A. Steady state kinetic data for *C. roseus* tryptophan decarboxylase (TDC) with tryptophan **1**.

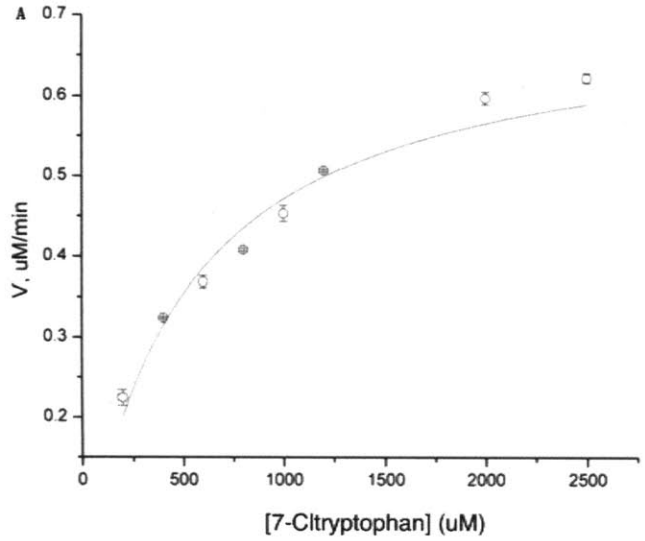

[7-Cltryptophan] (uM)	V (uM/ min)
199	0.2243
399	0.3239
599	0.3683
799	0.4080
998	0.4529
1198	0.5070
1997	0.5972
2496	0.6224

Equation	V=Vmax*S/(Km+S)	
Adj. Rsqr	0.9559	
	Value	Standard E
Km	499	74
Vmax	0.71	0.04
kcat	1.63	

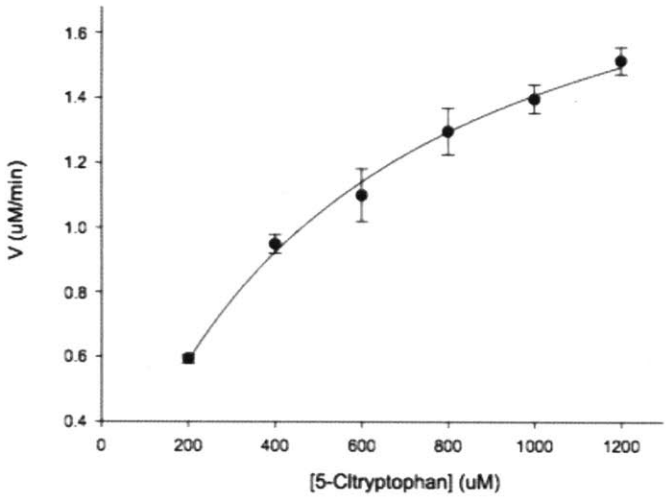

[5-Cltryptophan] (uM)	V (uM/ min)
200	0.5936
400	0.9489
600	1.1004
800	1.2967
1000	1.3972
1200	1.5150

Equation	V=Vmax*S/(Km+S)	
Adj. Rsqr	0.9936	
	Value	Standard E
Km	538	48
Vmax	2.16	0.08
kcat	2.45	

Figure 3.3 B (top) and C (bottom). Steady state kinetic data for *C. roseus* tryptophan decarboxylase (TDC) with 7-chlorotryptophan **1a (B)** and 5-chlorotryptophan **1b (C)**.

3.2.2 Construction of Halogenase Plant Expression Vectors pCAMPyrH/RebF/ STRvm and pCAMRebH/RebF

We considered two strategies for merging the prokaryotic chlorination machinery with the plant alkaloid pathway. The first strategy involves reconstitution of both the plant alkaloid biosynthetic pathway and the prokaryotic chlorination machinery in a microbial host, such as *Escherichia coli* or *Saccharomyces cerevisiae*. The second strategy involves introduction of the prokaryotic halogenase enzymes into *C. roseus*. We chose the latter strategy, which is transferring the halogenase enzymes into *C. roseus,* rather than moving the plant biosynthetic enzymes into a microbial host. Most of the monoterpene indole alkaloid biosynthetic genes have not been identified, and therefore heterologous expression of this pathway in a microbial host is not possible at present. Moreover, reconstitution of plant alkaloid pathways continues to be a challenging endeavour that requires sophisticated and time-consuming genetic manipulation and yield optimization[16, 17]. Additionally, many alkaloids use complex starting materials (such as secologanin for monoterpene indole alkaloids) that are only produced by a few specialized plants, so reconstitution of plant alkaloid pathways must also include biosynthesis of these precursors. For example, ajmalicine (**6**; **Figure 3.1**), one of the simplest of the monoterpene indole alkaloids, requires an estimated 14 discrete enzymes for biosynthesis from tryptophan and the terpene geraniol[18]; reconstitution of a pathway of this length (in tandem with the prokaryotic chlorination machinery) is a challenging engineering problem. Therefore, we believe that exploring alkaloid metabolic engineering in the host plant—rather than in a heterologous host—is a more appropriate strategy to achieve our goal of introducing halides into medicinal plant metabolism.

To produce 7-chlorotryptophan *in planta*, we generated an expression construct containing complementary DNA encoding the 7-tryptophan chlorinase RebH and its required partner flavin reductase, RebF, in a plant expression vector (pCAMBIA1300[19]), both under the control of constitutive Cauliflower Mosaic Virus (CaMV) 35S promoters (**Figure 3.4**). For production of 5-chlorotryptophan, an expression construct encoding the 5-chlorinating enzyme PyrH, along with RebF as the partner reductase, was generated. No signal sequence was added to the halogenase genes, to ensure that RebH, PyrH and RebF would produce chlorinated tryptophan in the cytosol, where it would most readily encounter the decarboxylase, which is also localized in the cytosol[20]. The halogenase genes, RebH, PyrH and RebF were codon-optimized to ensure efficient expression in plant cell culture. PCR analysis of genomic DNA indicated that the prokaryotic chlorination machinery and the hygromycin antibiotic selection marker (HPT) were incorporated into the *C. roseus* genome (**Figure 3.5-3.6**).

We used *Agrobacterium rhizogenes* to generate hairy root culture of *C. roseus* transformed with the halogenase genes[21]. One of the early biosynthetic enzymes, strictosidine synthase, cannot turn over 5-chlorotryptamine **2b**[15, 22]. Therefore, when transforming *C. roseus* with PyrH and RebF, we also introduced a mutant of strictosidine synthase (STRvm) that can convert 5-chlorotryptamine to 10-chlorostrictosidine **4b**[13, 23]. The construction of STRvm constitutive expression plasmid is described in **Chapter 2**. After a selection process, we cultivated the transformed root culture on standard Gamborg's B5 plant media and monitored chlorinated alkaloids using liquid chromatography-mass spectrometry (LC–MS).

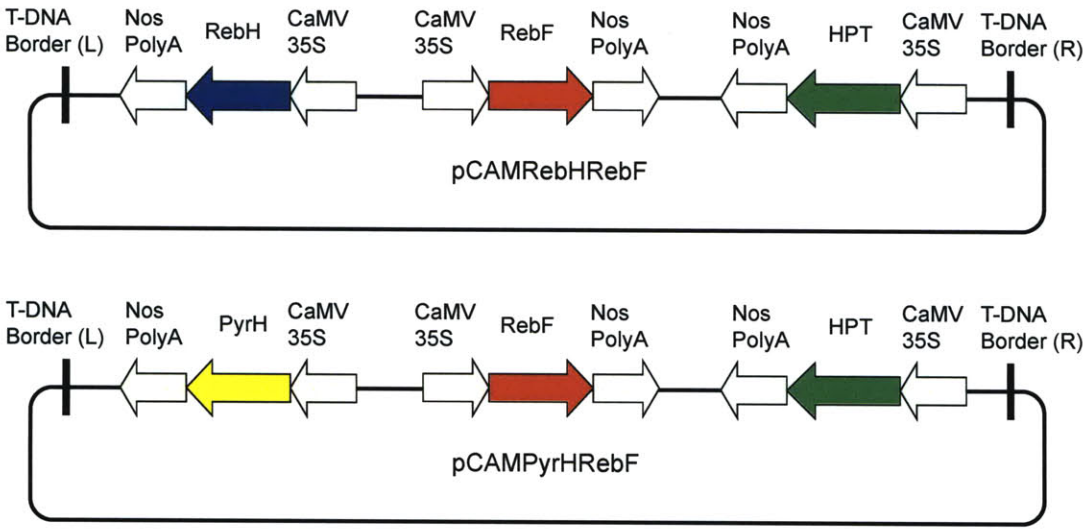

Figure 3.4. Schematic diagram of prokaryotic halogenase plant expression plamids pCAMRebHRebF and pCAMPyrHRebF.
CaMV35S: Cauliflower Mosaic Virus 35S promoter; Nos PolyA: poly(A) signal from nopaline synthase; RebH: codon-optimized RebH; PyrH: codon-optimized PyrH, RebF: codon-optimized RebF; and HPT: hygromycin phosphotransferase.

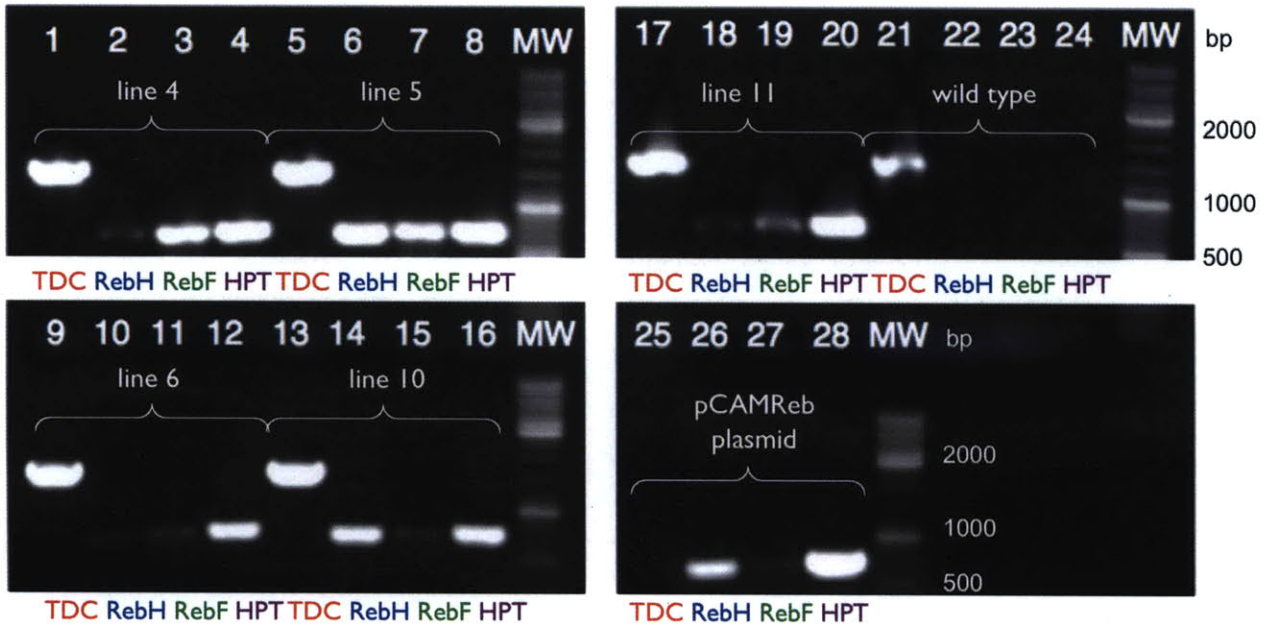

Figure 3.5. 1% agarose gel of PCR amplification of RebF/H and wild-type hairy root genomic DNA.

Lane: template, primers.

1: RebF/H cell line 4, TDC
2: RebF/H cell line 4, RebH
3: RebF/H cell line 4, RebF
4: RebF/H cell line 4, HPT
5: RebF/H cell line 5, TDC
6: RebF/H cell line 5, RebH
7: RebF/H cell line 5, RebF
8: RebF/H cell line 5, HPT
9: RebF/H cell line 6, TDC
10: RebF/H cell line 6, RebH
11: RebF/H cell line 6, RebF
12: RebF/H cell line 6, HPT
13: RebF/H cell line 10, TDC
14: RebF/H cell line 10, RebH
15: RebF/H cell line 10, RebF
16: RebF/H cell line 10, HPT
17: RebF/H cell line 11, TDC
18: RebF/H cell line 11, RebH
19: RebF/H cell line 11, RebF
20: RebF/H cell line 11, HPT
21: wild type, TDC
22: wild type, RebH
23: wild type, RebF
24: wild type, HPT
25: pCAMRebH/RebF plasmid, TDC
26: pCAMRebH/RebF plasmid, RebH
27: pCAMRebH/RebF plasmid, RebF
28: pCAMRebH/RebF plasmid, HPT

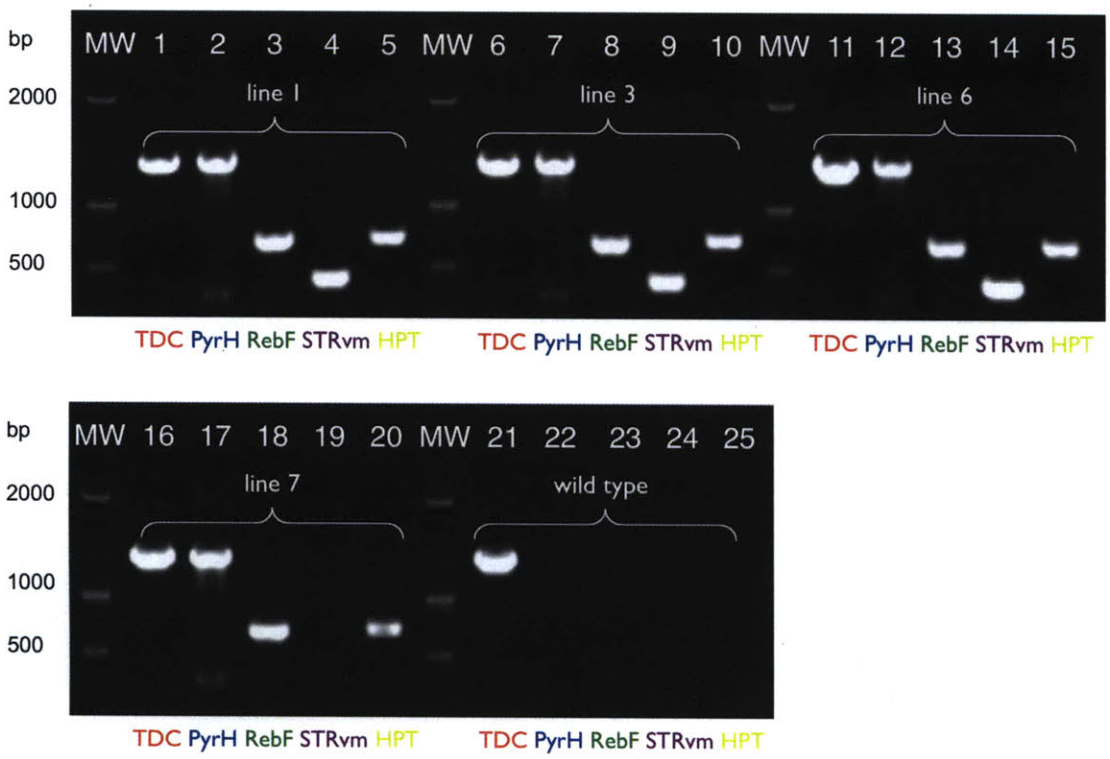

Figure 3.6. 1% agarose gel of PCR amplification of PyrH/RebF/STRvm and wild-type hairy root genomic DNA.

Lane: template, primers.

1: PyrH/RebF/STRvm cell line 1, TDC
2: PyrH/RebF/STRvm cell line 1, PyrH
3: PyrH/RebF/STRvm cell line 1, RebF
4: PyrH/RebF/STRvm cell line 1, STRvm
5: PyrH/RebF/STRvm cell line 1, HPT
6: PyrH/RebF/STRvm cell line 3, TDC
7: PyrH/RebF/STRvm cell line 3, PyrH
8: PyrH/RebF/STRvm cell line 3, RebF
9: PyrH/RebF/STRvm cell line 3, STRvm
10: PyrH/RebF/STRvm cell line 3, HPT
11: PyrH/RebF/STRvm cell line 6, TDC
12: PyrH/RebF/STRvm cell line 6, PyrH
13: PyrH/RebF/STRvm cell line 6, RebF
14: PyrH/RebF/STRvm cell line 6, STRvm
15: PyrH/RebF/STRvm cell line 6, HPT
16: PyrH/RebF/STRvm cell line 7, TDC
17: PyrH/RebF/STRvm cell line 7, PyrH
18: PyrH/RebF/STRvm cell line 7, RebF
19: PyrH/RebF/STRvm cell line 7, STRvm
20: PyrH/RebF/STRvm cell line 7, HPT
21: wild type, TDC
22: wild type, PyrH
23: wild type, RebF
24: wild type, STRvm
25: wild type, HPT

3.2.3 Evaluation of Alkaloid Production in Transgenic *C. roseus* Hairy Roots

Transformed hairy roots were cultured in solid Gamborg's B5 media for two to three weeks prior to alkaloid extractions. Gratifyingly, we observed formation of chlorinated tryptophans **1a** and **1b** and chlorinated alkaloids in both the RebF/H and PyrH/RebF/STRvm hairy root lines (**Figure 3.7-3.9**, **Table 3.2-3.3** and **Appendix B**). These results indicate that RebH, PyrH and the partner reductase function productively in the plant cell environment, demonstrating that the flavin halogenases are highly transportable among kingdoms. Since production of both chlorinated tryptamine and chlorinated alkaloids was observed in the transformed lines, we conclude that tryptophan decarboxylase can competently turn over halogenated tryptophan substrates *in vivo*.

Hairy roots transformed with RebH and RebF, which produce 7-chlorotryptophan **1a**, yielded a major chlorinated product at *m/z* 359 (**Figure 3.7 C** and **Table 3.2**). An authentic standard of 12-chloro-19,20-dihydroakuammicine **5a** co-eluted with this compound. The identities of the two smaller peaks at *m/z* 359 are not known. However, the two compounds also exhibit the characteristic isotopic pattern of chlorine ($^{35}Cl/^{37}Cl$ ratio of 3:1) and are likely isomers of **5a**. Natural products containing the akuammicine scaffold have a variety of pharmacological activities[24-26]. Although the parent compound, 19,20-dihydroakuammicine **5** has been isolated in good yields from other plants[27], it is not a major alkaloid in *C. roseus* hairy root culture. However, when wild-type *C. roseus* cell lines were incubated with 7-chlorotryptamine, 12-chloro-19,20-dihydroakuammicine was also the major chlorinated product (**Figure 3.11**). Therefore, the relatively high accumulation of 12-chloro-19,20-dihydroakuammicine **5a** in the RebH/RebF hairy root

line is likely due to substrate specificity of downstream enzymes for 7-chlorotryptamine **2a**. A hairy root line transformed with the 5-chlorotryptophan enzyme system, PyrH, RebF and STRvm, produced a variety of chlorinated alkaloids (**Figure 3.9 C-D** and **Table 3.3**). Two representative chlorinated alkaloids, 10-chloroajmalicine **6b** and 15-chlorotabersonine **7b**, were identified by co-elution with authentic standards[22]. Ajmalicine and tabersonine are two of the major alkaloids in *C. roseus* hairy root culture (**Appendix B**). As expected, the alkaloid profile of PyrH/RebF/STRvm hairy roots is similar to the alkaloid profile of STRvm hairy roots fed with 5-chlorotryptamine **2b** (**Chapter 2**).

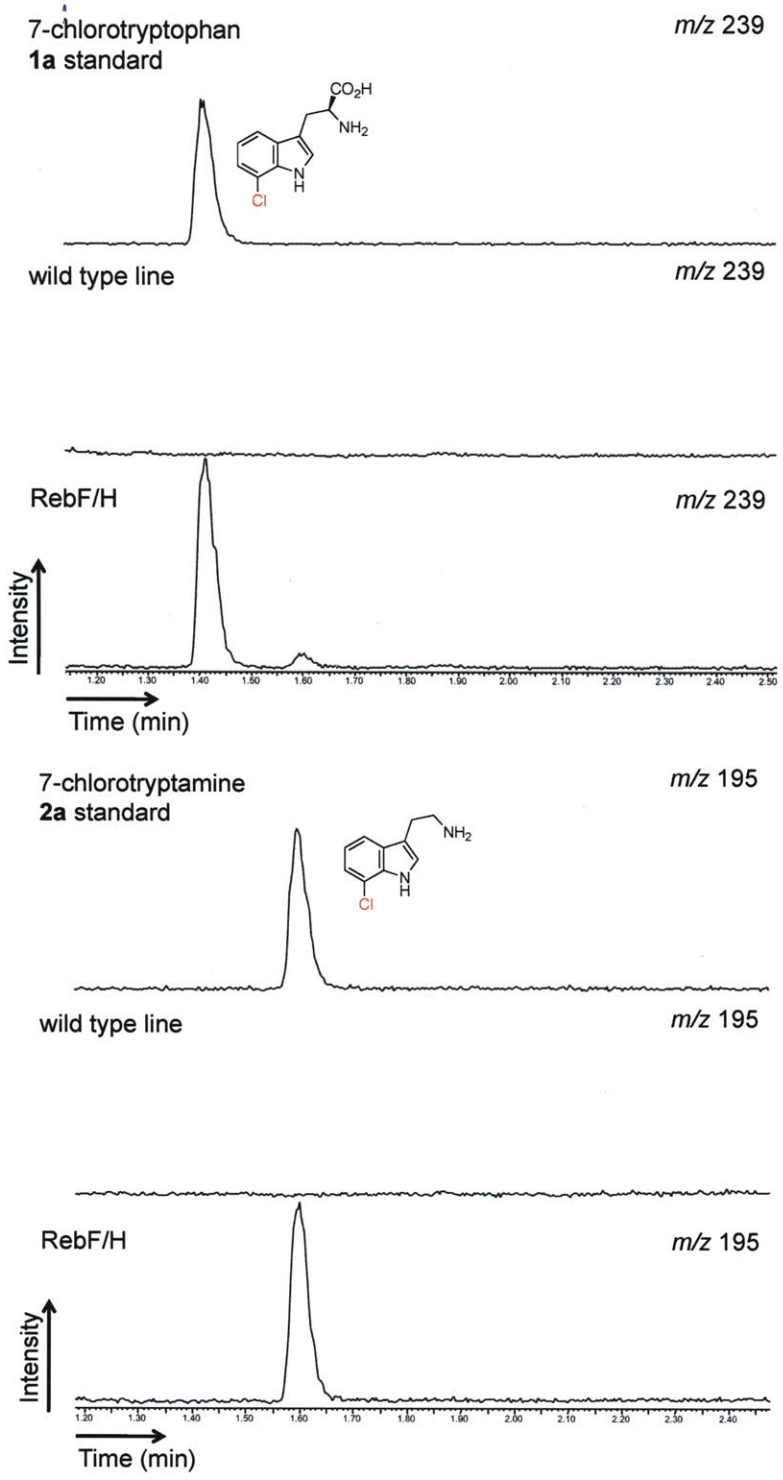

Figure 3.7 A (top) and B (bottom). Chlorinated alkaloids in *C. roseus* hairy root culture. Liquid chromatography-mass spectrometry (LC-MS) chromatograms showing 7-chlorotryptophan **1a** (**A,** *m/z* 239) and 7-chlorotryptamine **2a** (**B,** *m/z* 195) in RebF/H hairy roots, contrasted with control cultures transformed with no plasmid. Authentic standards of **1a** and **2a** validated the structural assignments.

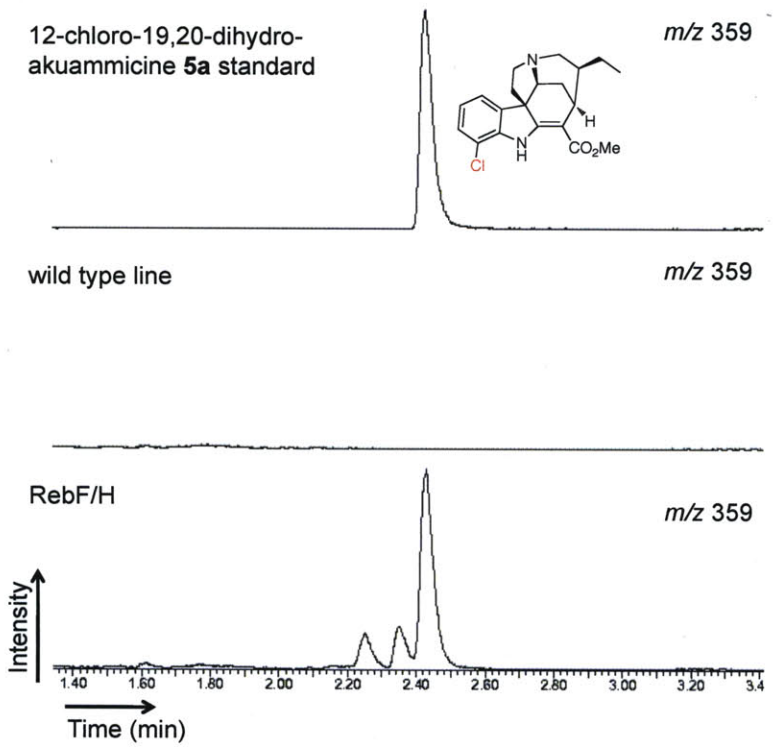

Figure 3.7 C. Chlorinated alkaloids in *C. roseus* hairy root culture. Liquid chromatography-mass spectrometry (LC-MS) chromatograms showing 12-chloro-19,20-dihydroakuammicine **5a** (*m/z* 359) in RebF/H hairy roots (red trace), contrasted with control cultures transformed with no plasmid (purple trace). An authentic standard of **5a** validated the structural assignment.

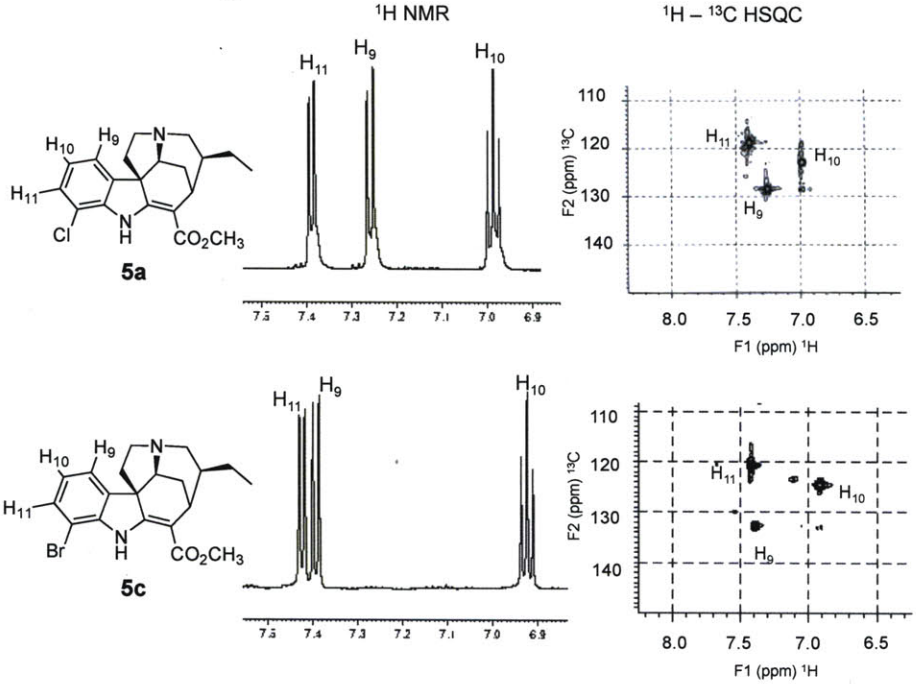

Figure 3.8. ^{1}H NMR and ^{1}H-^{13}C HSQC spectra of 12-chloro-19,20-dihydroakuammicine **5a** and 12-bromo-19,20-dihydroakuammicine **5c**.

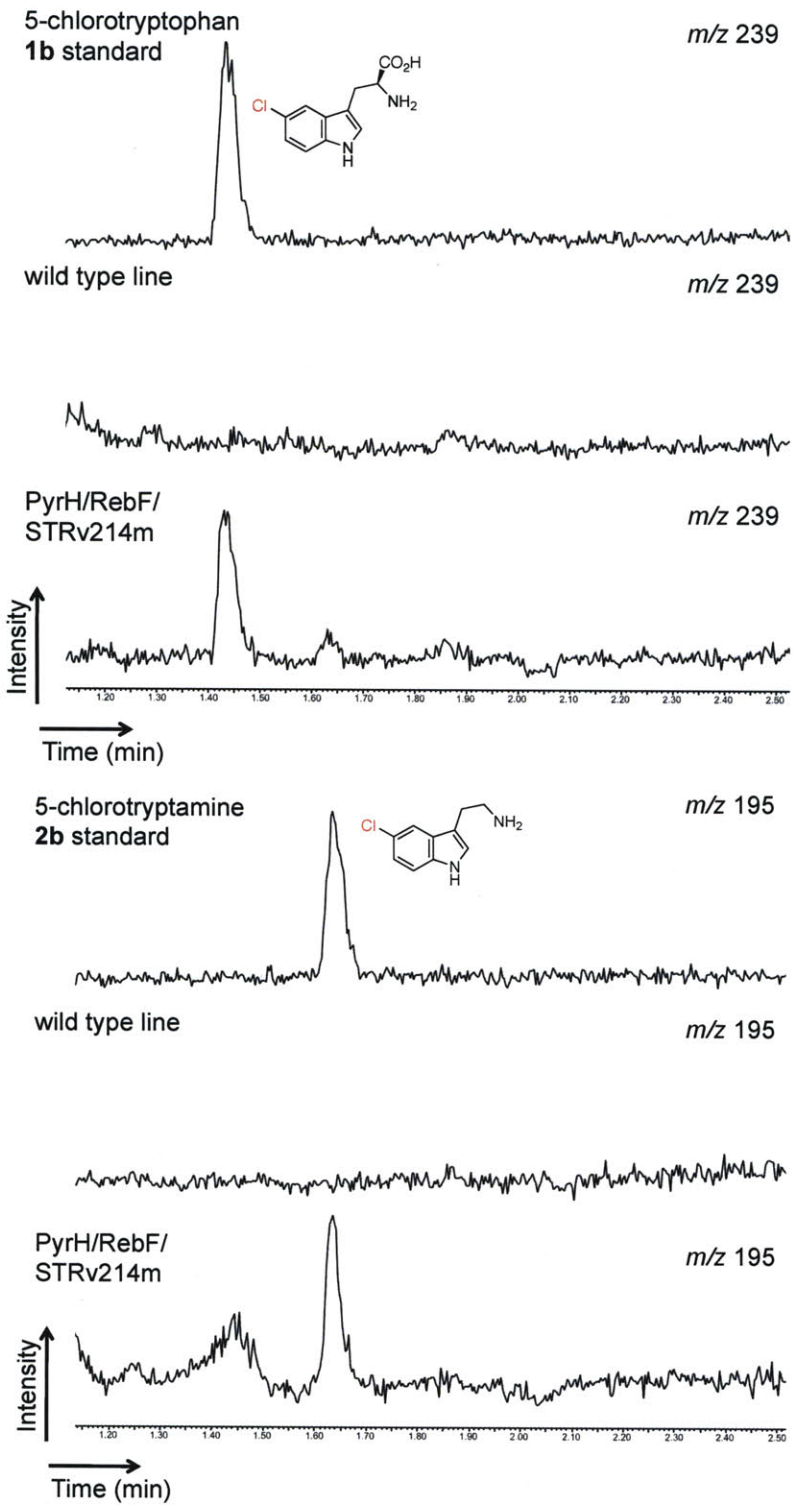

Figure 3.9 A (top) and B (bottom). Chlorinated alkaloids in *C. roseus* hairy root culture. Liquid chromatography-mass spectrometry (LC-MS) chromatograms showing 5-chlorotryptophan **1b** (**A**, *m/z* 239) and 5-chlorotryptamine **2b** (**B,** *m/z* 195) in PyrH/RebF/STRv214m hairy roots, contrasted with control cultures transformed with no plasmid. Authentic standards of **1b** and **2b** validated the structural assignments.

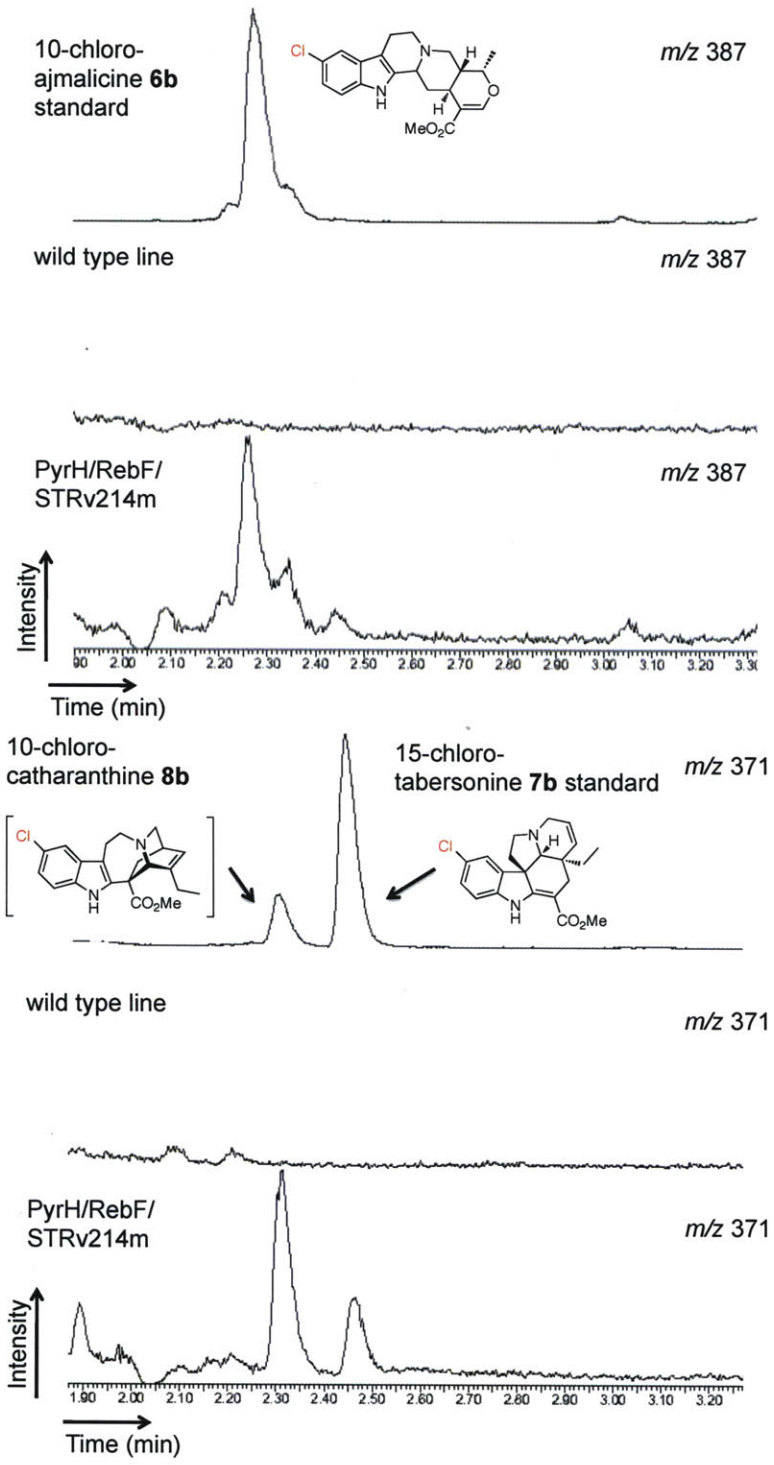

Figure 3.9 C (top) and D (bottom). Chlorinated alkaloids in *C. roseus* hairy root culture. Liquid chromatography-mass spectrometry (LC-MS) chromatograms showing 10-chloroajmalicine **6b** (**C**, *m/z* 387) and 15-chlorotabersonine **7b** (**D**, *m/z* 371) in PyrH/RebF/STRv214m hairy roots, contrasted with control cultures. Authentic standards of **6b** and **7b** are shown. The other major peak at *m/z* 371 had an exact mass and UV spectra consistent with a chlorinated catharanthine **8** analog.

Table 3.2. High-resolution MS data for alkaloids observed in RebF/H hairy root extracts.

	19,20-dihydro-akuammicine	**12-chloro (R = Cl)**	**12-bromo* (R = Br)**
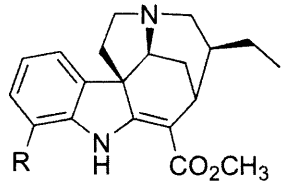	Expected [M+H]	359.1526	403.1021
	Observed [M+H]	359.1520	403.1011
	Accuracy (ppm)	-1.7	-2.5
	RT (min)	2.43	2.48

* This brominated alkaloid was observed in media supplemented with potassium bromide (see **section 3.4.8**).

Table 3.3. High-resolution MS data for alkaloids observed in PyrH/RebF/STRv214m hairy root extracts.

	ajmalicine 6	**10-chloro 6b (R = Cl)**
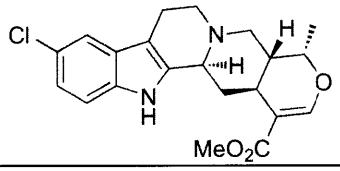	Expected [M+H]	387.1490
	Observed [M+H]	387.1483
	Accuracy (ppm)	2.1
	RT (min)	2.26
	tabersonine 7	**15-chloro 7b (R = Cl)**
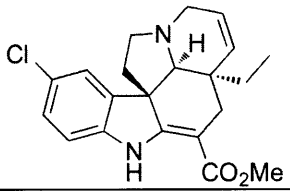	Expected [M+H]	371.1526
	Observed [M+H]	371.1528
	Accuracy (ppm)	0.5
	RT (min)	2.47
	catharanthine 8	**10-chloro 8b (R = Cl)**
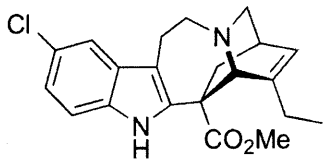	Expected [M+H]	371.1526
	Observed [M+H]	371.1531
	Accuracy (ppm)	1.3
	RT (min)	2.31

3.2.4 Quantification of Chlorinated Alkaloid Production in Transformed Hairy Roots

Chlorinated alkaloid production was stable over the course of at least six subcultures (**Figure 3.10**). The alkaloid 12-chloro-19,20-dihydroakuammicine **5a** was produced at 26 ± 4 μg per gram of fresh root weight of a representative cell line averaged over six subcultures. For comparison, wild-type cell lines produced ~25 μg per gram of fresh tissue weight of chlorinated alkaloids when the medium was supplemented with 200 mM 7-chlorotryptamine **2a** (**Figure 3.11**). Similarly, 10-chloroajmalicine and 15-chlorotabersonine **7b** were produced at 2.8 ± 0.9 and 4.0 ± 1.0 μg per gram of fresh root weight, respectively, for a representative cell line averaged over four subcultures (**Figure 3.12**). Additionally we determined whether the yields of chlorinated alkaloids could be improved by supplementing the hairy root media with chloride salts. Different concentrations of KCl (3 mM – 20 mM) were added to the media, but increasing amounts of exogenous chloride salt did not significantly affect the yields of chlorinated alkaloids (**Figure 3.13**).

Tryptophan **1** does not accumulate in either wild type or transformed hairy roots. However, accumulation of 7-chlorotryptophan **1a** (50 ± 12 μg per gram of fresh root weight for a representative RebH/RebF cell line; **Figure 3.10**) and 5-chlorotryptophan **1b** (8 ± 2 μg per gram of fresh root weight for a representative PyrH/RebF/STRvm cell line; **Figure 3.12**) was observed, suggesting that decarboxylation of chlorinated tryptophan is a bottleneck *in vivo*, a step that could potentially be subjected to future engineering efforts. This is consistent with the 30-fold-lower catalytic efficiency of the decarboxylase

enzyme for halogenated tryptophan *in vitro*. Interestingly, overexpression of tryptophan decarboxylase, in addition to RebH and RebF, in *C. roseus* hairy roots resulted in lower accumulation of 7-chlorotryptophan **1a,** but not higher accumulation of chlorinated alkaloids (Glenn and O'Connor, unpublished).

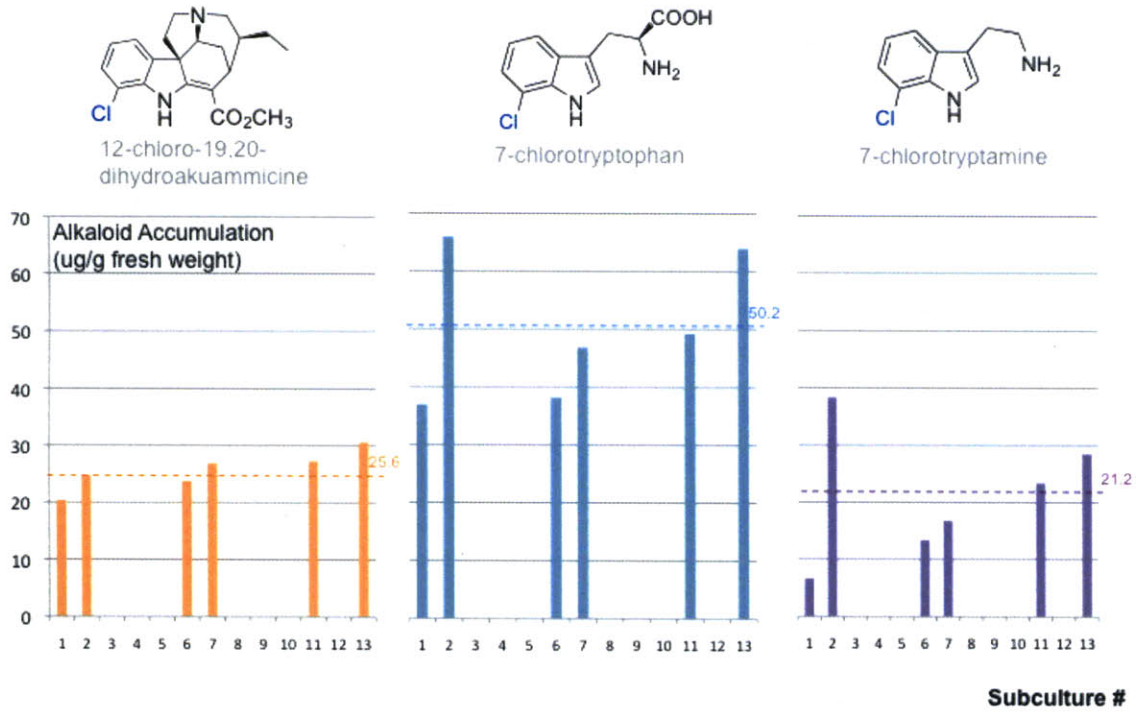

Figure 3.10. Tabulated amounts of chlorinated alkaloid production in RebF/H hairy roots after subsequent subcultures.

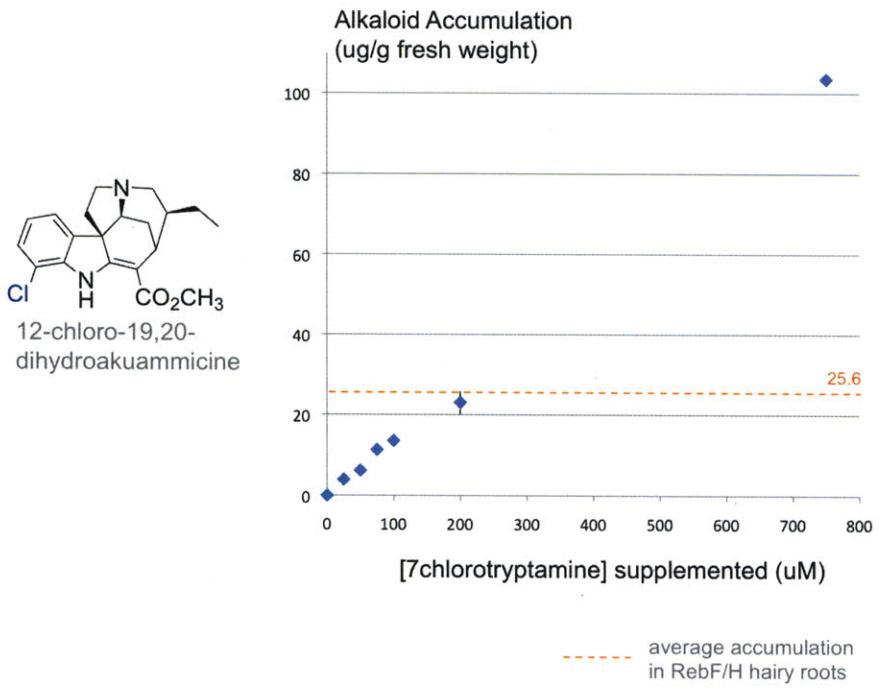

Figure 3.11. Chlorinated alkaloid production in wild type line incubated with 7-chlorotryptamine **1a**.

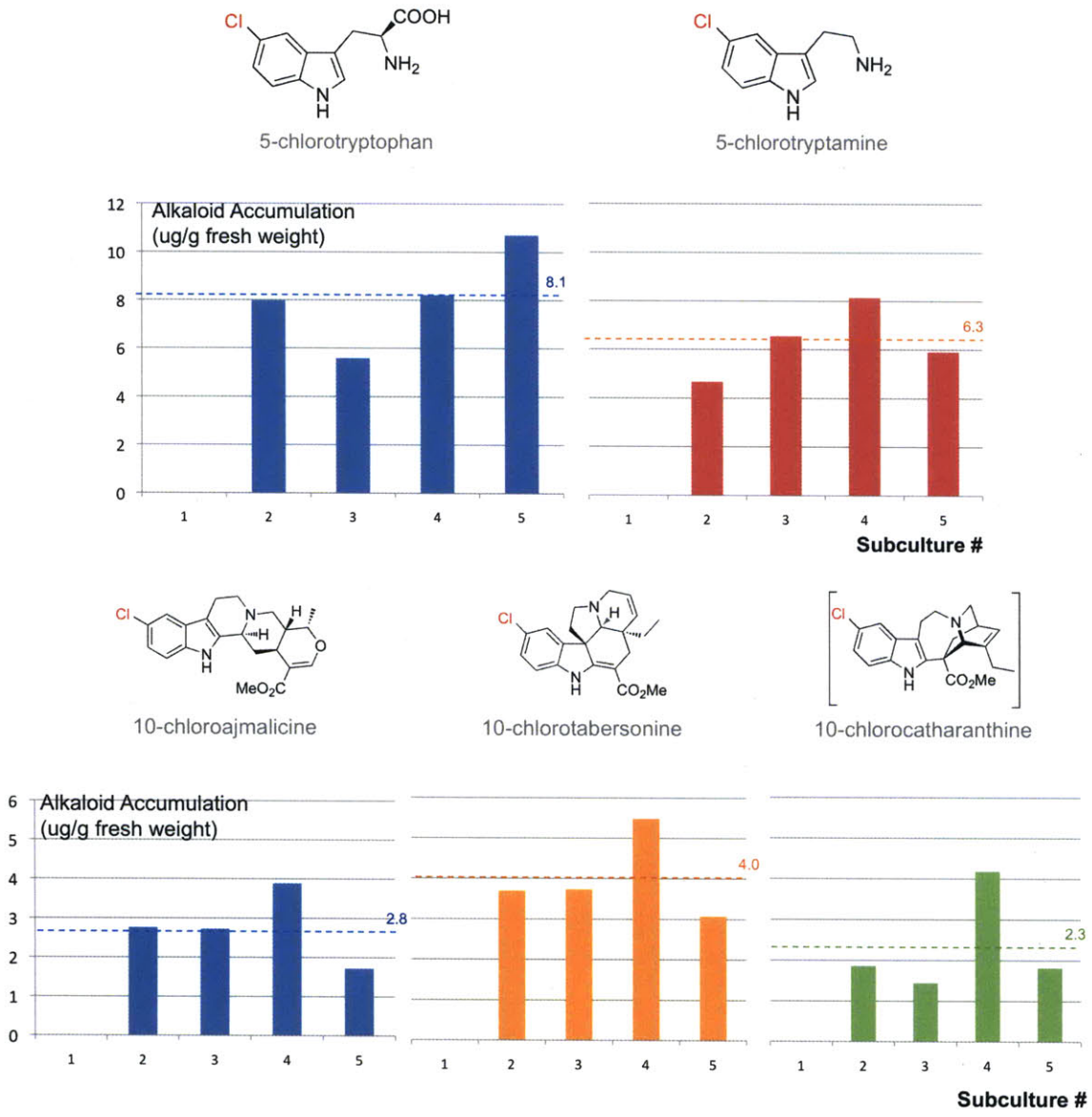

Figure 3.12. Tabulated amounts of chlorinated alkaloid production in PyrH/RebF/STRv214m hairy roots (line 1) after subsequent subcultures.

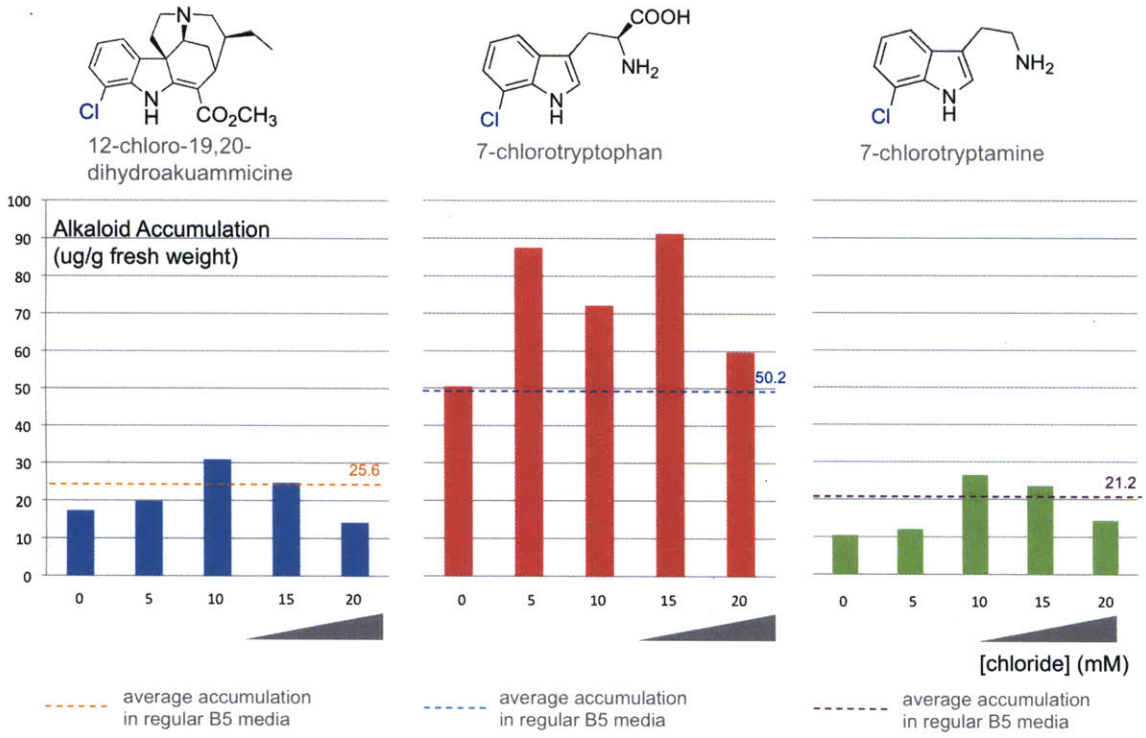

Figure 3.13. Tabulated amounts of chlorinated alkaloid **5a**, 7-chlorotryptophan **1a** and 7-chlorotryptamine **2a** in response to increasing KCl concentration.

Previous *in vitro* studies of RebH demonstrated that the enzyme can utilize bromide to yield brominated tryptophan **1c**[11]. To assess the capacity of RebH for bromination *in vivo*, we supplemented a low-chloride cell culture medium with KBr. The *in vitro* halide specificity of RebH correlated with the products generated *in vivo*, as we observed the formation of a compound that co-eluted with an authentic standard of 12-bromo-19,20-dihydroakuammicine **5c** (21 ± 8 and 49 ± 20 μg per gram of fresh root weight with 10 mM and 20 mM KBr supplementation, respectively; **Figure 3.14-3.15**). Production of brominated alkaloids did not seem to affect the yields of chlorinated alkaloids (**Figure 3.16**). We also assessed the capacity of RebH to iodinate *in vivo*. Supplementation of the media with KI (0-20 mM) failed to yield either iodinated tryptophan or iodinated alkaloids (**Figure 3.17**). These results correlated with *in vitro* studies demonstrating that RebH does not accept iodide as a substrate[11].

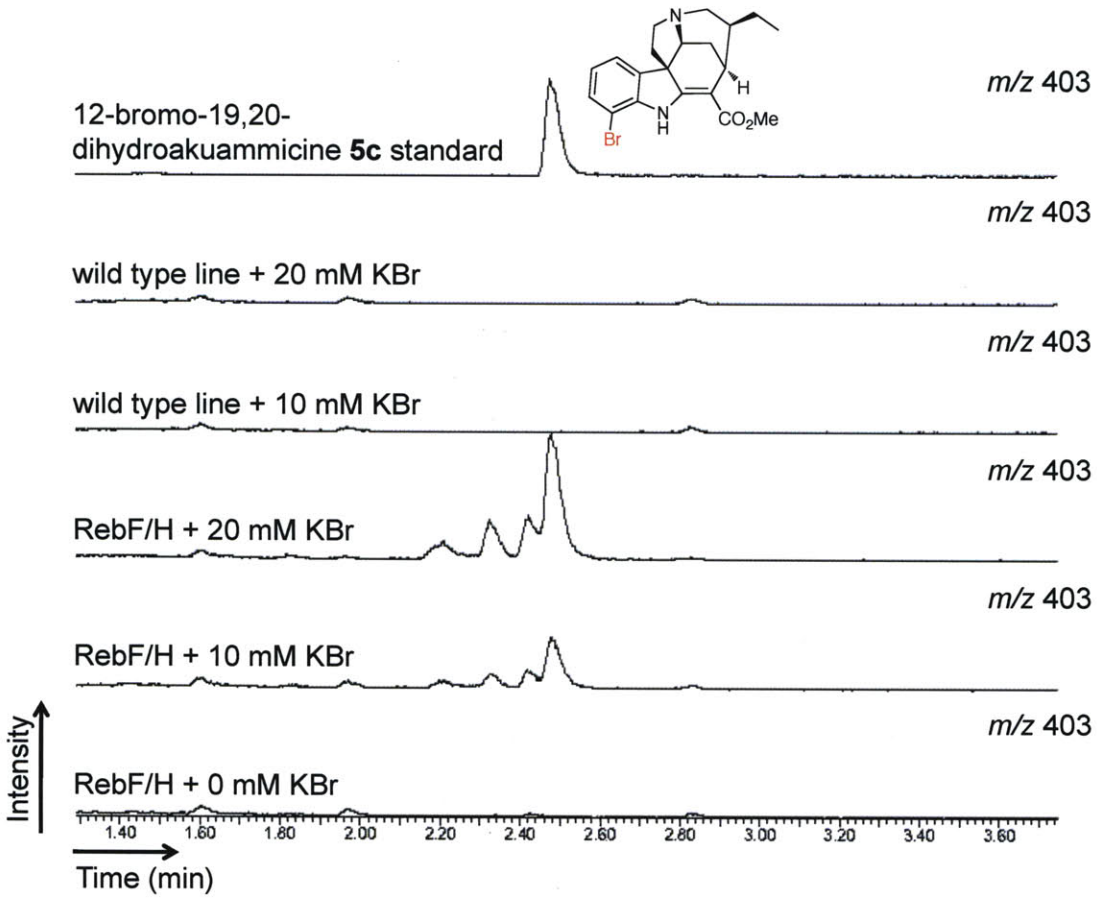

Figure 3.14. Extracted LC-MS chromatograms showing the presence of 12-bromo-19,20-dihydroakuammicine **5c** (*m/z* 403) in RebF/H hairy roots. Hairy roots are grown in media supplemented with KBr (0 – 20 mM final concentration) for two weeks prior to alkaloid extractions. 12-bromo-19,20-dihydroakuammicine **5c** is not observed in control cultures transformed with no plasmid after incubation in potassium bromide supplemented media. An authentic standard of 12-bromo-19,20-dihydroakuammicine **5c** is used to validate the structural assignment (**Appendix B**).

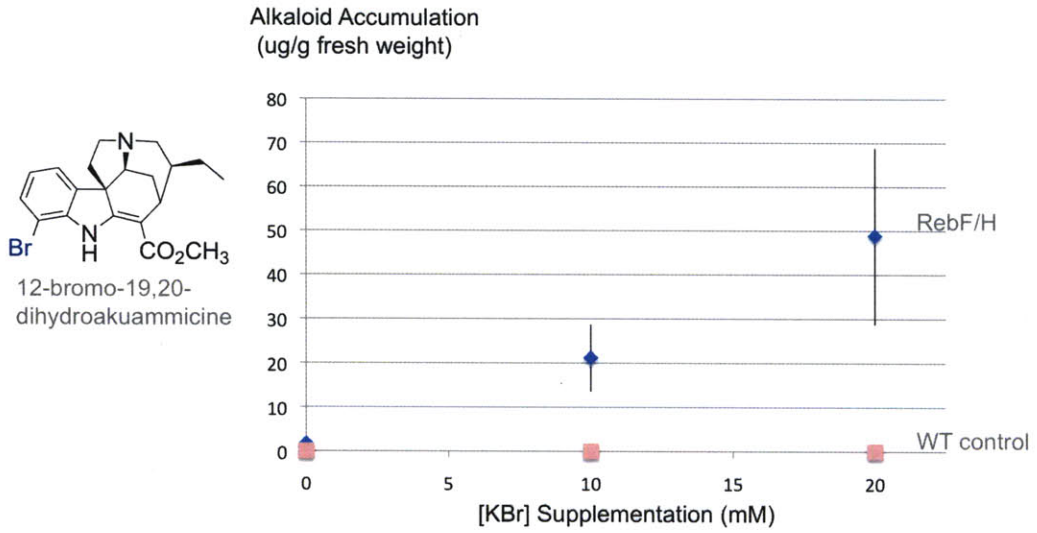

Figure 3.15. Brominated alkaloid production levels in selected RebF/H and wild type hairy roots growing on solid media that have been supplemented with KBr (0 – 20 mM).

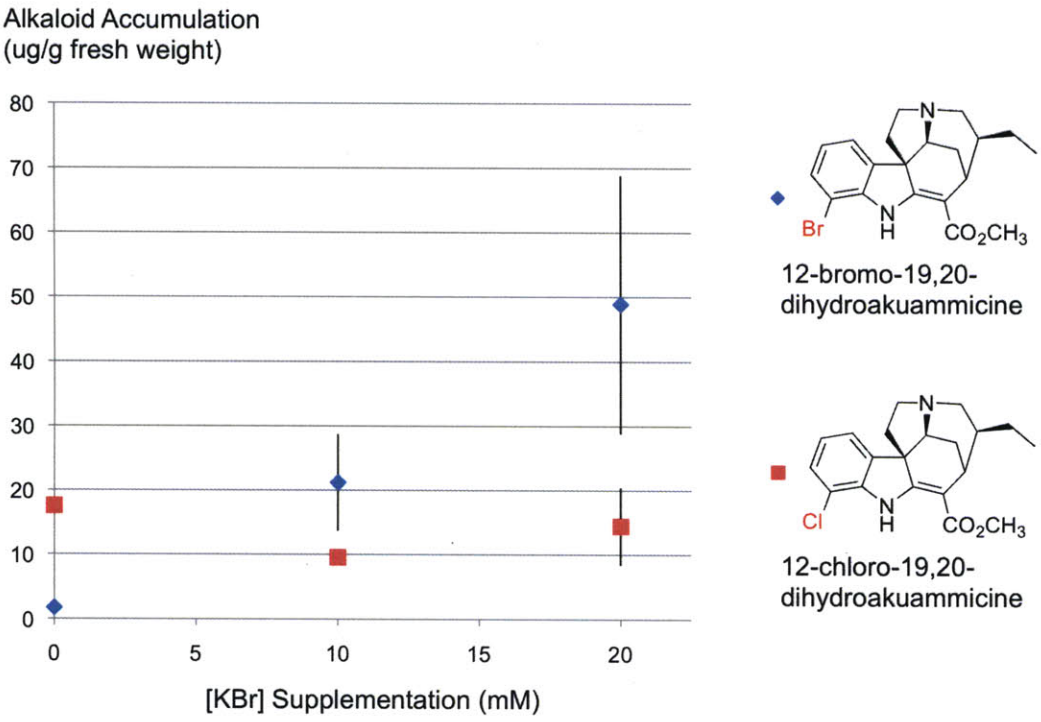

Figure 3.16. Brominated and chlorinated alkaloids production levels in selected RebF/H hairy roots growing on solid media that have been supplemented with KBr (0 – 20 mM).

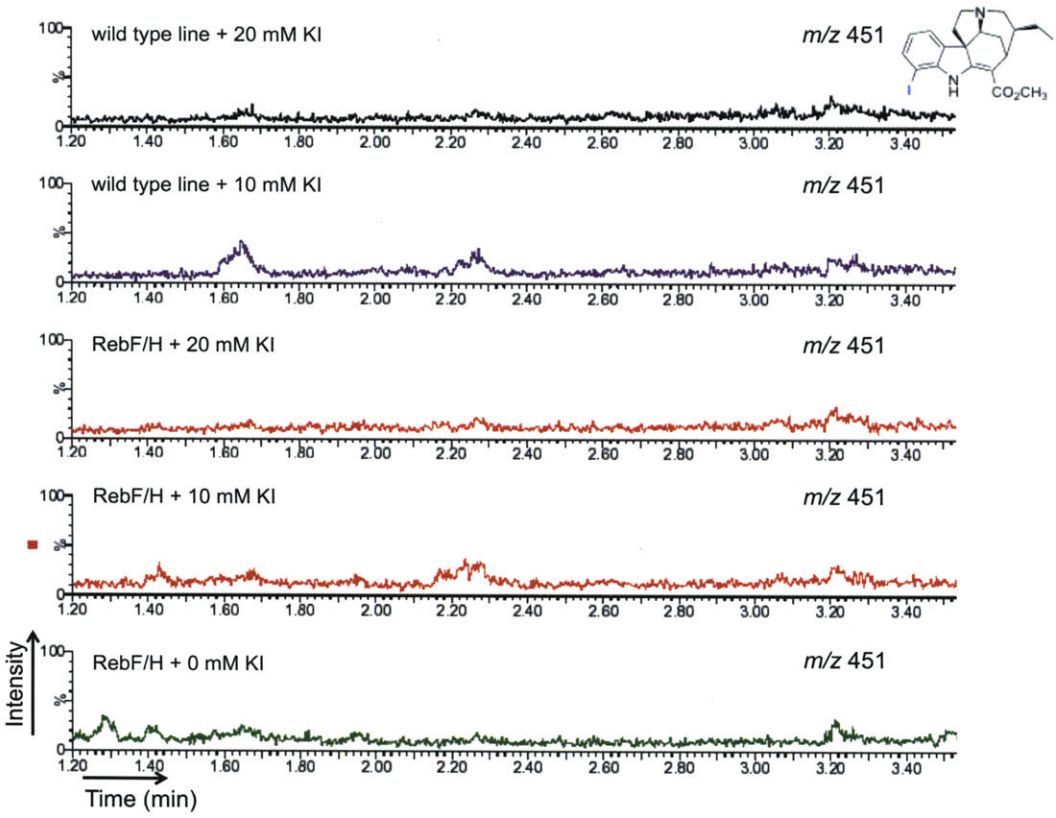

Figure 3.17. Extracted LC-MS traces showing the absence of iodinated alkaloids in selected RebF/H and wild type hairy roots growing on solid media that have been supplemented with KI (0 – 20 mM).

3.2.5 Verification of Expression of RebH, RebF and PyrH, STRvm Enzymes by Real Time RT-PCR

The transcript levels of the heterologous enzymes were measured by real-time PCR with reverse transcription (**Figure 3.18-3.19**). In RebH/RebF hairy roots, the production of halogenated compounds depended on the expression of both RebF and RebH. RebH/RebF cell line 5, which accumulates the highest levels of chlorinated alkaloids, has the highest expression levels of both RebF and RebH (**Figure 3.18**). In PyrH/RebF/STRvm hairy roots, the production of halogenated alkaloids depended not only on the expression of RebF and PyrH, but also on the expression of the strictosidine mutant STRvm. Notably, when STRvm was not expressed in the PyrH/RebF hairy root lines, we observed accumulation of 5-chlorotryptophan (representative cell line, 9 ± 1 μg per gram of fresh root weight) and 5-chlorotryptamine (representative cell line, 20 ± 9 μg per gram of fresh root weight), but did not observe downstream alkaloids (**Figure 3.19, Appendix B**).

A

HAIRY ROOT LINES	WT	RebF/H line 4	RebF/H line 5	RebF/H line 6	RebF/H line 10	RebF/H line 11
RELATIVE REBH EXPRESSION	0	6	100	13	27	4

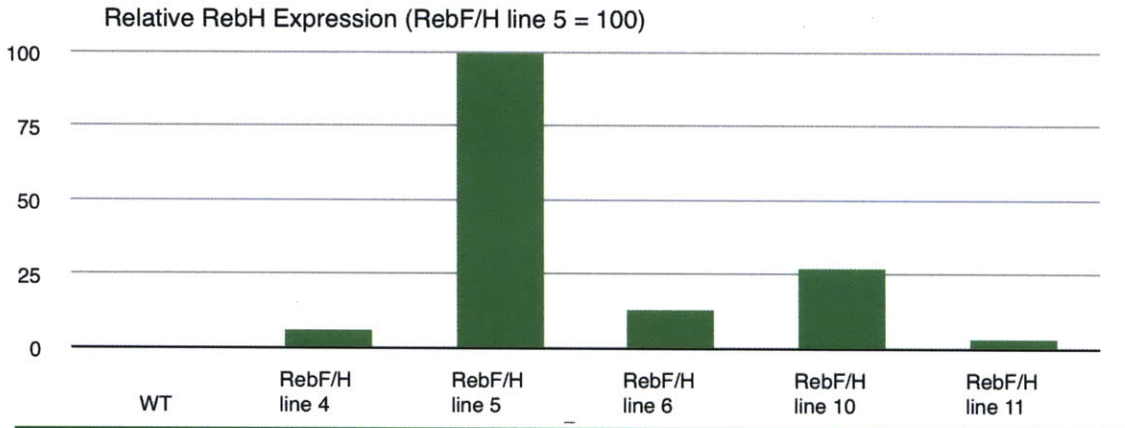

B

HAIRY ROOT LINES	WT	RebF/H line 4	RebF/H line 5	RebF/H line 6	RebF/H line 10	RebF/H line 11
RELATIVE REBF EXPRESSION	0	0	100	67	11	3

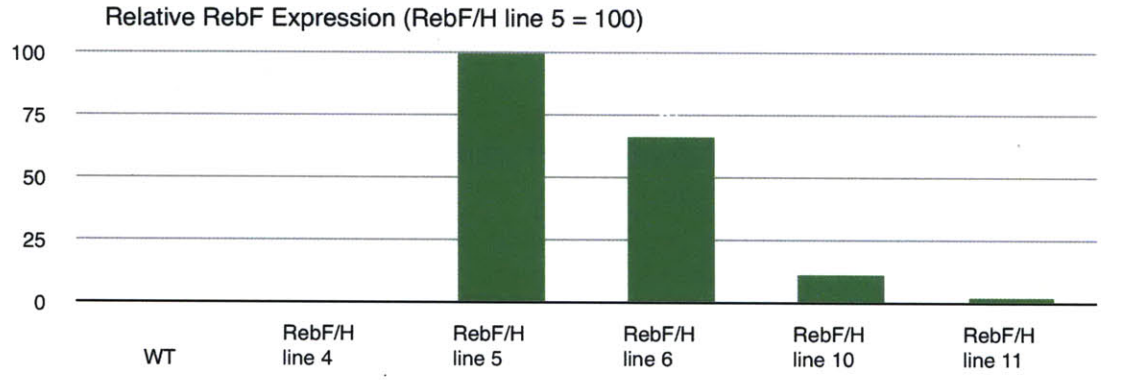

Figure 3.18 A (top) and B (bottom). Expression levels of RebH (**A**) and RebF (**B**) in 5 different RebF/H lines measured by RT-PCR. Expression levels of the transgenic lines are normalized to the expression levels in RebF/H hairy roots cell line 5.

A

HAIRY ROOT LINES	WT	PyrH/RebF/ STRvm line 1	PyrH/RebF/ STRvm line 3	PyrH/RebF/ STRvm line 6	PyrH/RebF/ STRvm line 7
RELATIVE PYRH EXPRESSION	0	100	2	0	97

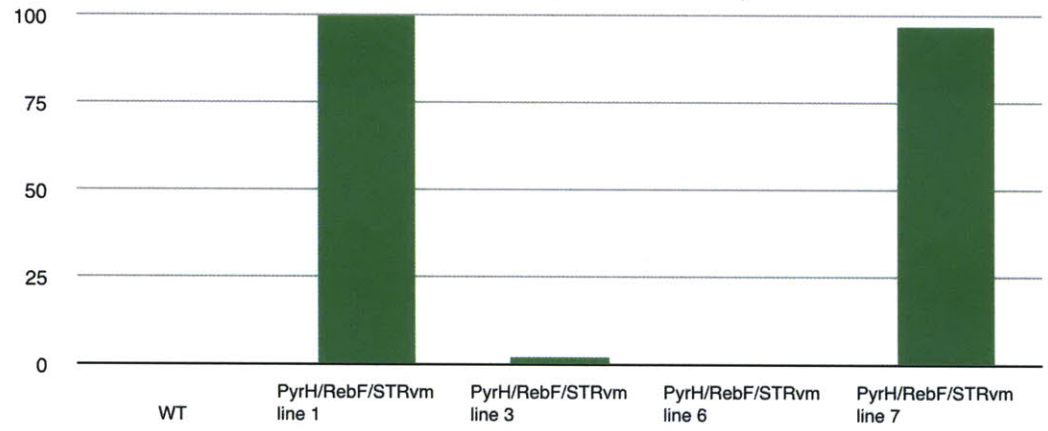

B

HAIRY ROOT LINES	WT	PyrH/RebF/ STRvm line 1	PyrH/RebF/ STRvm line 3	PyrH/RebF/ STRvm line 6	PyrH/RebF/ STRvm line 7
RELATIVE REBF EXPRESSION	0	100	2	1	35

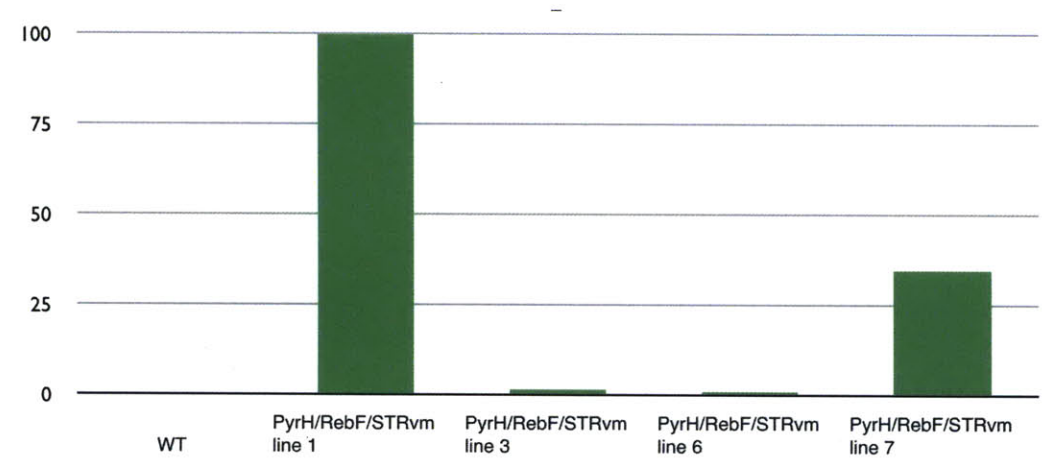

Figure 3.19 A (top) and B (bottom). Expression levels of PyrH (**A**) and RebF (**B**) in 4 different PyrH/RebF/STRv214m lines measured by RT-PCR. Expression levels of the transgenic lines are normalized to the expression levels in PyrH/RebF/STRvm hairy roots cell line 1.

C

HAIRY ROOT LINES	WT	PyrH/RebF/ STRvm line 1	PyrH/RebF/ STRvm line 3	PyrH/RebF/ STRvm line 6	PyrH/RebF/ STRvm line 7
RELATIVE STRvm EXPRESSION	0	100	49	94	0

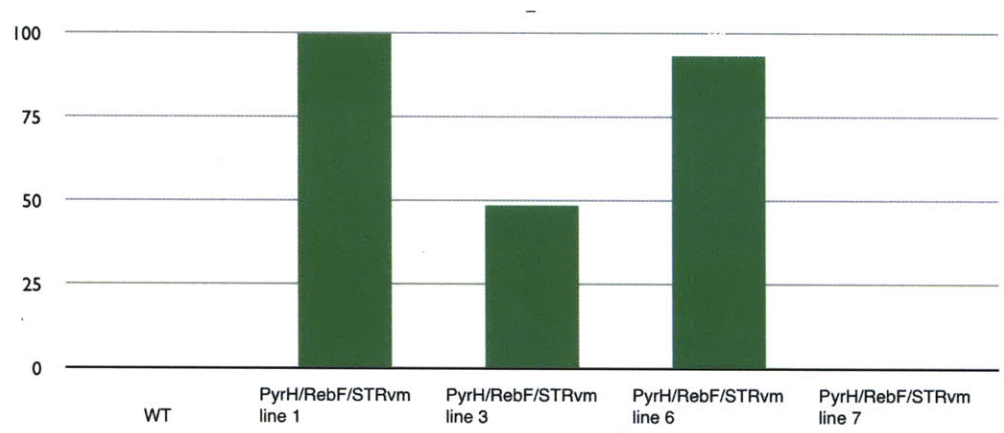

Figure 3.19 C. Expression levels of STRvm in 4 different pCAMPyrH/RebF/STRvm lines measured by RT-PCR. Expression levels of the transgenic lines are normalized to the expression levels in PyrH/RebF/STRvm hairy roots cell line 1.

3.2.6 Morphologies of Transgenic *C. roseus* Hairy Roots

The morphologies of the halogen producing lines were thicker and slower growing than those of wild type lines (**Figure 3.20**). Moreover, these lines did not seem to be adaptable to liquid media. We speculated that the accumulation of chlorinated tryptophan could unfavourably affect growth and morphology of transgenic hairy roots. Because tryptophan serves as the precursor for other small-molecule metabolites, chlorinated tryptophan may be diverted into other pathways such as auxins biosynthesis. Since auxins regulate plants growth and behavioural processes, altering this pathway is likely to affect hairy roots' morphology. Notably, 4-chloro indole acetic acid, which is found in several species of pea, has altered activity relative to the auxin indole acetic acid[28, 29]. Finally, despite numerous attempts, regeneration of *C. roseus* plants from RebH/RebF and PyrH/RebF/STRvm hairy roots did not yield viable whole plants.

3.3 Conclusions

While medicinal plants produce a wide range of complex natural products, only a few of these contain halogen atoms. Notably, chlorinated or brominated compounds are not found among the approximately 3,000 known monoterpene indole alkaloids produced by plants in the Apocynaceae, Rubiaceae and Loganiaceae families. Halogenation of natural products often plays a profound role in establishing the bioactivity of a compound, and can serve as a useful handle for further chemical derivatization[1, 30]. We have described in this chapter that, despite the metabolic and developmental complexity of plant tissue, transformation of prokaryotic halogenase genes into *C. roseus* led to the regioselective incorporation of halides into a range of alkaloid products. Remarkably, the yield of

RebF/H hairy roots (25 days old) in solid Gamborg's B5 media

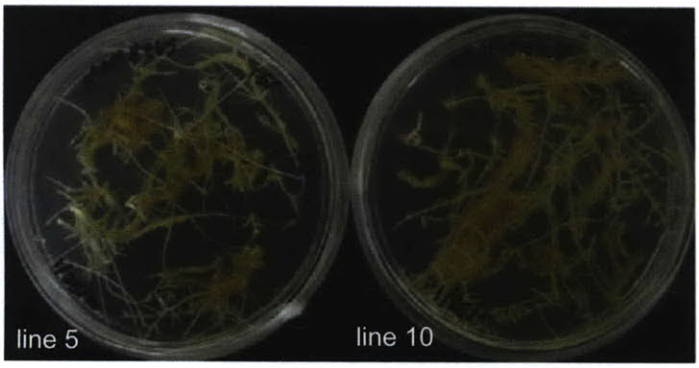

wild type line (16 days old) in solid Gamborg's B5 media

PyrH/RebF/STRvm hairy roots (25 days old) in solid Gamborg's B5 media

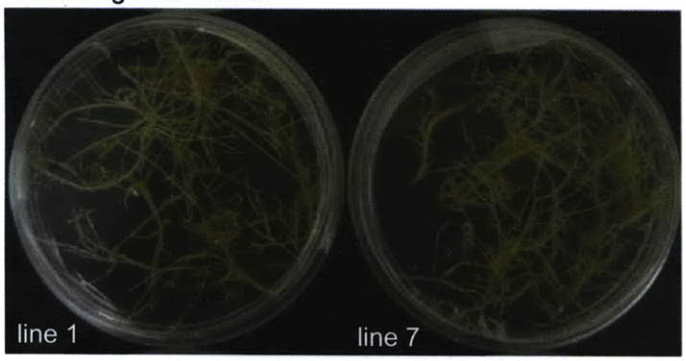

Figure 3.20. Morphology of RebF/H, PyrH/RebF/STRvm and wild type hairy roots. The halogen producing lines were thicker and slower growing than those of wild type lines.

chlorinated alkaloids in the most productive line (RebF/H hairy roots cell line 5, ~26 μg per gram of fresh weight of plant tissue) is only 15-fold lower than the yield of total natural alkaloids (compounds 19,20-dihydroakuammicine **5** + ajmalicine **6** + tabersonine **7** + catharanthine **8**) from wild-type tissue (~420 μg per gram of fresh weight of plant tissue) (**Appendix B**). Moreover, our yield compares favourably to the yields of reconstitution of other alkaloid pathways in microbial systems[16, 17]. We speculated that the yields of halogenated alkaloids could be improved further by re-engineering tryptophan decarboxylase to exhibit higher catalytic efficiency for chlorinated tryptophan substrates. Alternatively, since chlorinated tryptophan may potentially interfere with auxin biosynthesis, re-engineering RebH to preferentially chlorinate tryptamine instead of the natural substrate tryptophan could further improve the yield of chlorinated alkaloids while alleviating the slow growth of hairy roots. These engineering efforts are currently being investigated in our lab (Glenn and O'Connor). In summary, the ease with which we engineered the successful production of chlorinated alkaloids in *C. roseus*, a plant with limited genetic characterization, indicates that medicinal plants can provide a viable platform for synthetic biology.

3.4 Experimental Methods

3.4.1 Heterologous Expression and Purification of C. roseus Tryptophan Decarboxylase

The tryptophan decarboxylase (TDC) gene (accession number M25151.1) was obtained by reverse-transcription PCR amplification of mRNA isolated from *C. roseus* hairy root

culture (Invitrogen, Dynabeads® mRNA direct kit) with PCR primers that introduce sites for *Nde*I and *Xho*I (underlined):

5' AAAAAACATATGGGCAGCATTGATTCAACA 3' and

5' AAAAAACTCGAGTCAAGCTTCTTTGAGCAAATC 3'. The PCR fragment was subcloned into the pGEM-T Easy Vector (Promega), and then excised and ligated into the *Nde*I/*Xho*I site of the pET28-a plasmid (Novagen). The resulting pET28a-TDC construct was subsequently transformed into BL21 (DE3) pLysS electrocompetent *E. coli* (Promega). A single *E. coli* colony harboring pET28a-TDC was inoculated in 5 mL LB media supplemented with kanamycin (0.05 mg/L) and incubated overnight at 37 °C with shaking at 225 rpm. An aliquot of the overnight culture (1 mL) was then used to inoculate 100 mL LB media supplemented with kanamycin (0.05 mg/L) and incubated at 37 °C with shaking at 225 rpm until an OD_{600} of 0.6 was reached. Cells were induced for overexpression by the addition of isopropyl β-D-galactopyranoside (IPTG, final concentration 1 mM) and the culture was allowed to continue growth for 16 hrs at 18 °C. Cells were harvested by centrifugation and lysed by sonication. The hexa-histidine-tagged TDC was purified using Ni-NTA Spin Kit (Qiagen) using manufacturer's protocols. Eluted enzyme was subsequently buffer-exchanged into phosphate buffer (50 mM NaH_2PO_4, 100 mM NaCl, pH 8.0) and immediately assayed for activity. This enzyme was not stable upon extended storage.

3.4.2 Determining the Steady-State Kinetic Constants of TDC for Tryptophan Substrate Analogs, 5- and 7-chlorotryptophan 1a and 1b

Steady-state kinetic constants of TDC for 5- and 7-chlorotryptophan **1b** and **1a** (Amatek) were determined in phosphate buffer (0.1 M NaH_2PO_4, 3.5 mM β-mercaptoethanol, pH 8.5) containing 1 mM pyridoxal-5'-phosphate at 30 °C (0.3 mL reaction volume) with TDC concentrations appropriate for obtaining the initial rate of the reaction (0.6 – 0.9 μM). Aliquots (25 μL) were quenched in 1 mL methanol, containing yohimbine (500 nM) as an internal standard, at appropriate time points. The samples were centrifuged (13,000 rpm, 5 min) to remove particulates and then analyzed by LC-MS. Samples were ionized by ESI with a Micromass LCT Premier TOF Mass Spectrometer. The LC was performed on an Acquity Ultra Performance BEH C18, 1.7 μm, 2.1 x 100 mm column on a gradient of 10-90% acetonitrile/water (0.1% formic acid) over 5 minutes at a flow rate of 0.6 mL/min. The appearance of the corresponding tryptamine analogs (either 5-or 7-chlorotryptamine) was monitored by peak integration and normalized to the internal standard. 5-chlorotryptamine **2b** was obtained from a commercial source (Alfa Aesar). 7-chlorotryptamine **2a** was synthesized as previously reported[31]. Eight substrate concentrations (200 – 2500 μM) were tested for 7-chlorotryptophan **1a** substrate, while six substrate concentrations (200 – 1200 μM) were tested for 5-chlorotryptophan **1b** substrate. Each concentration was assayed three times and the averaged value is reported with standard deviations. The data were fitted using non-linear regression to the Michaelis-Menten equation using OriginPro 7 (OriginLab, Northhampton, MA). For reference, the kinetic constants for the natural substrate tryptophan **1** were also measured at concentrations ranging from 15 – 350 μM.

3.4.3 Construction of Halogenase Plant Expression Vectors pCAMPyrH/RebF/ STRvm and pCAMRebH/RebF

Construction of the plant expression vectors was designed and partly executed by Xudong Qu (**Figure 3.21**).

i. The CaMV35S:Gus:NosPolyA fragment was obtained by PCR amplification of pCAMBIA1305.1 (Cambia) with PCR primers CaMV35S-Nos polyA for and rev that introduce sites for *Xba*I and *Kpn*I at the 5' end, and *Pst*I and *Spe*I at the 3' end (underlined):

5' ACTTCTAGAGGTACCGGATCCTCTAGAGTCGACCTGCAG 3' and

5' ATTCTGCAGACTAGTCCCGATCTAGTAACATAGATGACACCG 3'

ii. The tryptophan 5-halogenase gene (PyrH, accession number AAU95674) was obtained by PCR amplification of genomic DNA isolated from *Streptomyces rugosporus* NRRL 21084 with PCR primers CrPyrH for and rev that introduce sites for *Xho*I and *Nco*I at the 5' end, and *Spe*I and *BstE*II at the 3' end (underlined):

5' ACTCTCGAGCCATGGATATCCGATCTGTGGTGATCG 3' and

5' ACTACTAGTGGTAACCTCATTGGATGCTGGCGAGGTA 3'

iii. The flavin reductase gene (RebF, accession number BAC15756) was obtained by PCR amplification of genomic DNA isolated from *Lechevalieria aerocolonigenese* ATCC 39243 with PCR primers CrRebF for and rev that introduce sites for *Xho*I and *Nco*I at the 5' end, and *Spe*I and *Pml*I at the 3' end (underlined):

5' ACTCTCGAGCCATGGATACGATCGAGTTCGACAGAC 3' and

5' ACTACTAGTCACGTGTCATCCCTCCGGTGTCCACAC 3'

iv. The tryptophan 7-halogenase gene (RebH, accession number BAC15758) was

obtained by PCR amplification of genomic DNA isolated from *Lechevalieria aerocolonigenese* ATCC 39243 with PCR primers CrRebH for and rev that introduce sites for *Spe*I and *Nco*I at the 5' end, and *Spe*I and *Pml*I at the 3' end (underlined):

5' AAGACTACTAGTCCATGGATTCCGGCAAGATTGAC 3' and

5' ACTACTAGTCACGTGTCAGCGGCCGTGCTGTTGCC 3'

CaMV35S:Gus:NosPolyA, PyrH, RebH and RebF PCR fragments were individually ligated into pGEM-Teasy vector (Promega) to yield pGEMCaMV35S, pGEMPyrH, pGEMRebH and pGEMRebF, respectively.

v. Codon-optimization for *Catharanthus roseus* was performed to ensure efficient expression of the prokaryotic halogenase and flavin reductase genes in plant cell culture. Using codon usage database software (http://www.kazusa.or.jp/codon/), the following codons were identified as occurring at low frequency (triplet, frequency per thousand): GCG, 4.8; CGG, 3.3; ACG, 4.0; TCG, 6.1; CCG, 6.0; and CCC, 6.7. Site-directed mutagenesis was performed using Stratagene QuikChange Site-Directed Mutagenesis kit to replace rare-codons with the most frequently occurring codons encoding the corresponding amino acids. Only codons that appeared within the first 300 nucleotides of the genes were subjected to mutagenesis.

The site-directed-mutagenesis primers are summarized below (the sites of mutation are underlined).

Primer Name	Primer Sequence ('5 → 3')
PyrH-SDM-for1	GTGGGTGGTGGCACTGCTGGCTGGATGACC
PyrH-SDM-rev1	GGTCATCCAGCCAGCAGTGCCACCACCCAC
PyrH-SDM-	GACATGCGGCCGTACACTACTGCTACCGCGATGAGCGCCGGC

for2	
PyrH-SDM-rev2	GCCGGCGCTCATCGCGGTAGCAGTAGTGTACGGCCGCATGTC
RebH-SDM-for	CCCCAATCTGCAGACTGCTTTCTTCGACTTCCTCGGA
RebH-SDM-rev	TCCGAGGAAGTCGAAGAAAGCAGTCTGCAGATTGGGG
RebF-SDM-for1	ACCGCGGCCGATCACAGGGCTCTGATGAGCCTGTTTCCC
RebF-SDM-rev1	GGGAAACAGGCTCATCAGAGCCCTGTGATCGGCCGCGGT
RebF-SDM-for2	CTCGTCTGCCTGAACAGGGCTAGCGGAACGTTGCAC
RebF-SDM-rev2	GTGCAACGTTCCGCTAGCCCTGTTCAGGCAGACGAG

vi. pGEMCaMV35S was digested and ligated into the *Kpn*I/*Eco*RI sites of pSP72 vector (Promega) to yield pSPCaMV35S.

vii. pGEMRebH and pGEMRebF were digested and ligated into the *Nco*I/*Pml*I sites of pSPCaMV35S to yield pSPRebH and pSPRebF, respectively. Similarly, pGEMPyrH was digested and ligated into the *Nco*I/*BstE*II sites of pSPCaMV35S to yield pSPPyrH. pSPRebF was then digested and ligated into the *Pst*I site of pSP72 to yield pSPRebF_2.

viii. pSPRebH and pSPPyrH were digested and ligated into the *Xba*I/*Eco*RI sites of pSPRebF_2 to yield pSPRebHRebF and pSPPyrHRebF, respectively. Finally, both pSPRebHRebF and pSPPyrHRebF were digested and ligated into the *Spe*I site of pCAMBIA1300A to yield pCAMRebHRebF and pCAMPyrHRebF. pCAMBIA1300A was constructed by introducing an SpeI restriction into pCAMBIA1300 (Cambia). The site-directed-mutagenesis primers are (*Spe*I site underlined):

5' CCCGCCTTCAGTTTAAACTAGTCAGTGTTTGACAGGAT 3'

5' ATCCTGTCAAACACTGACTAGTTTAAACTGAAGGCGGG 3'

pCAMSTRvm was constructed as previously described[22].

A

Primers: CaMV35S-Nos polyA for/rev
Template: pCAMBIA 1305.1
PCR product cloned into pGEM-T easy

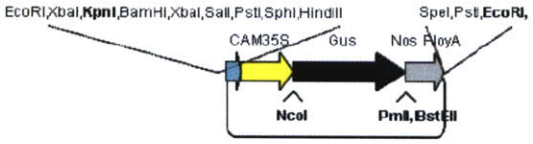

pGEMCaMV35S

KpnI/EcoRI fragment cloned into
KpnI/EcoRI sites of pSP72

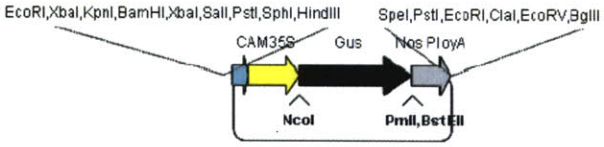

pSPCaMV35S

Primers: CrRebH for/rev, CrRebF for/rev, CrPyrH for/rev
Templates: *Lechevalieria aerocolonigenese* ATCC 39243 gDNA (for RebH and RebF) and *Streptomyces rugosporus* NRRL 21084 gDNA (for PyrH)
PCR product cloned into pGEM-T easy

pGEMRebH
pGEMRebF
pGEMPyrH

B

pGEMRebH. pGEMRebF NcoI/PmlI fragment cloned into NcoI/PmlI sites of pSPCaMV35S

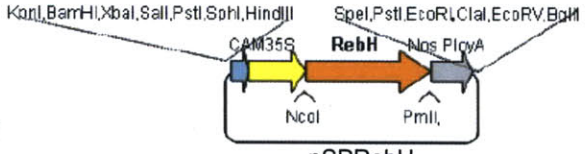

pSPRebH

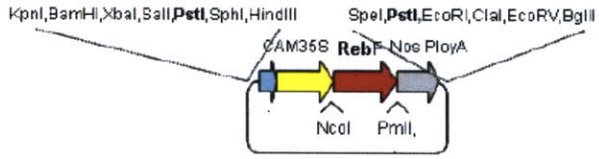

pSPRebF

pGEMPyrH NcoI/BstEII fragment cloned into NcoI/BstEII sites of pSPCaMV35S

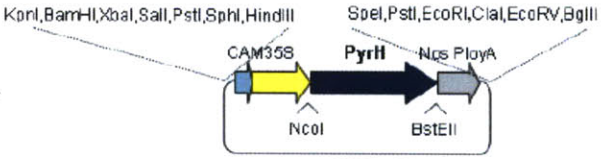

pSPPyrH

pSPRebF PstI fragment cloned into PstI site of pSP72

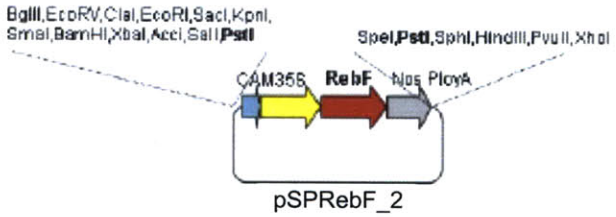

pSPRebF_2

C

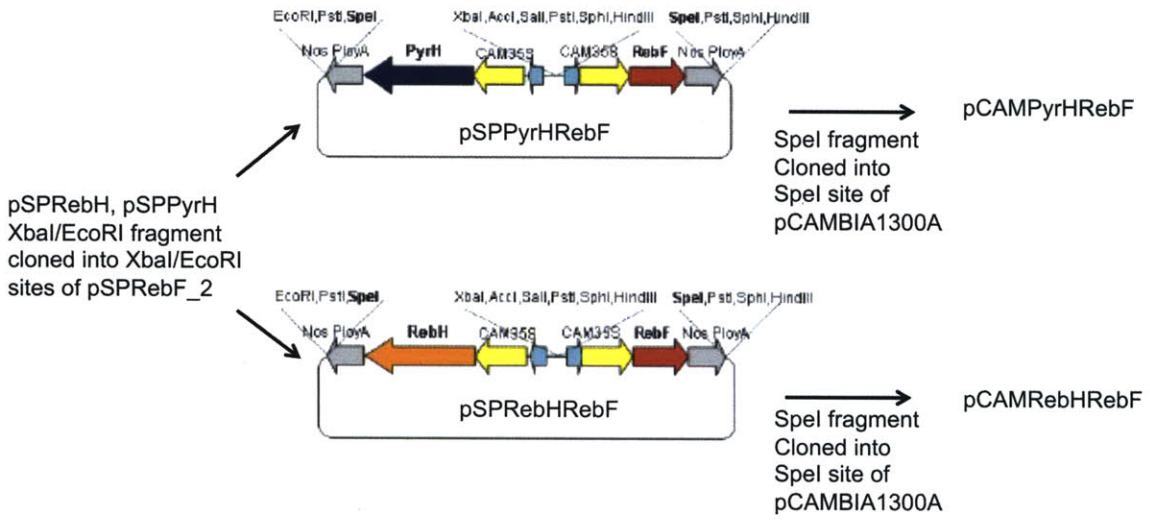

Figure 3.21. Construction of pCAMPyrHRebF and pCAMRebHRebF plasmids.

3.4.4 Generation of Transgenic *C. roseus* Hairy Root Cultures

The plant expression construct pCAMRebHRebF was transformed into *Agrobacterium rhizogenes* ATCC 15834 via electroporation (1mm cuvette, 1.25 kV). pCAMPyrHRebF and pCAMSTRvm were co-transformed into *Agrobacterium rhizogenes* ATCC 15834 via electroporation (1mm cuvette, 1.25 kV). Transformation of *C. roseus* seedlings with the generated *Agrobacterium* strains was performed as previously reported[21]. Briefly, 180 – 250 *C. roseus* seedlings (Vinca Little Bright Eyes, Nature Hills Nursery) were germinated aseptically on Gamborg's B5 media (full strength basal salts, full strength vitamins, 30 g/L sucrose, pH 5.7) and grown in a 16-hour light 8-hour dark cycle at 26 °C for three weeks. Seedlings were then wounded with extra-fine forceps at the stem tip, and 3-5 μL of *A. rhizogenes* from a freshly grown liquid culture were inoculated on the wound.

Hairy roots appeared at the wound site 2-3 weeks after infection for about 80% of the seedlings infected. After hairy roots reached 1-4 cm in length (usually about six weeks after infection), they were excised and transferred to Gamborg's B5 solid media (half strength basal salts, full strength vitamins, 30 g/L sucrose, 6 g/L agar, pH 5.7) containing hygromycin (0.03 mg/mL) for selection and the antibiotic cefotaxime (0.25 mg/mL) to remove remaining bacteria. The total chloride concentration in Gamborg's B5 formulation is 1 mM. All cultures were grown in the dark at 26°C. After the hygromycin selection process, hairy roots were maintained in solid media lacking both hygromycin and cefotaxime.

To adapt the line to liquid culture, approximately 200 mg of hairy roots (typically five 3-4 cm long stem tips) from each line that grew successfully on solid media were transferred to 50 mL of half-strength Gamborg's B5 liquid media. The cultures were grown at 26°C in the dark at 125 rpm. Hairy root growth in liquid media appeared to be slower than that in solid media. Hairy root transformants were screened for survival in solid media supplemented with hygromycin (**Table 3.4**). The number of transformants decreased significantly after solid media selection for each of the constructs transformed. Every line that grew in the selection media was analyzed for alkaloid production.

Table 3.4. Hairy root selection and adaptation processes.

Plasmid	# transformed hairy roots	# hairy roots after solid media selection
pCAMRebH/RebF	200	31
pCAMPyrH/RebF/STRvm	140	57

3.4.5 Verification of Transferred DNA (T-DNA) Integration by Genomic DNA Analysis

To verify the integration of transferred DNA (T-DNA) into the plant genome, the genomic DNA from transformed hairy roots was isolated (Qiagen DNeasy kit) and then subjected to PCR amplification using T-DNA specific primers with TDC primers serving as a positive control (see below). Specifically, for the pCAMRebHRebF hairy roots, primers for PCR amplification were designed to amplify the complete TDC gene (TDC_for and TDC_rev), a 660 bp region of the RebH gene (RebH_for and RebH_rev), a 680 bp region of the RebF gene (RebF_for and RebF_rev) and an 800 bp region of the selection marker HPT gene (HPT_for and HPT_rev) (see below).

PCR primers for verification of T-DNA integration of transformed hairy roots.

	Primer Name	Primer Sequence ('5 → 3')
1	TDC_for	AAAAAACATATGGGCAGCATTGATTCAACA
2	TDC_rev	AAAAAACTCGAGTCAAGCTTCTTTGAGCAAATC
3	RebH_for	GTCTTCGATGCCGACCTCTTC
4	RebH_rev	GTACATGTCGATCTTCTCCTGC
5	RebF_for	TAGAGGACCTAACAGAAC
6	RebF_rev	CGTGACACTGGTCAGGGA
7	HPT_for	GCCTGAACTCACCGCGACGTC
8	HPT_rev	CCTCCAGAAGAAGATGTTGGC

PCR amplification of genomic DNA from all of the selected transformed lines (pCAMRebH/RebF cell line 4: lanes 1-4, pCAMRebH/RebF cell line 5: lanes 5-8, pCAMRebH/RebF cell line 6: lanes 9-12, pCAMRebH/RebF cell line 10: lanes 13-16, and pCAMRebH/RebF cell line 11: lanes 17-20) was successful for all four sets of primers (**Figure 3.5**). PCR-amplification of hairy root transformed with *A. rhizogenes* lacking the pCAMBIA vector (provided by Professor Jacqueline Shanks (Iowa State) and

Professor Carolyn Lee-Parsons (Northeastern)) genomic DNA was successful only when TDC specific primers were used (lanes 21-24). These results indicated that RebH and RebF were successfully incorporated into the *C. roseus* genome in all chosen lines.

For the pCAMPyrH/RebF/STRvm hairy roots, primers for PCR amplification were designed to amplify the complete TDC gene (TDC_for and TDC_rev), the complete PyrH gene (PyrH_for and PyrH_rev), a 680 bp region of the RebF gene (RebF_for and RebF_rev), a 440 bp region of the STRvm gene, and an 800bp region of the selection marker HPT gene (HPT_for and HPT_rev) (see below) (**Figure 3.6**).

PCR primers for verification of T-DNA integration of transformed hairy roots.

	Primer Name	Primer Sequence ('5 → 3')
1	TDC_for	AAAAAACATATGGGCAGCATTGATTCAACA
2	TDC_rev	AAAAAACTCGAGTCAAGCTTCTTTGAGCAAATC
3	PyrH_for	ATGATCCGATCTGTGGTG
4	PyrH_rev	TCATTGGATGCTGGCGAG
5	RebF_for	TAGAGGACCTAACAGAAC
6	RebF_rev	CGTGACACTGGTCAGGGA
7	STRvm_for	CCTTATTATTGAAAGAGCTACATATG
8	STRvm_rev	GCTAGAAACATAAGAATTTCCCTTG
9	HPT_for	GCCTGAACTCACCGCGACGTC
10	HPT_rev	CCTCCAGAAGAAGATGTTGGC

PCR amplification of genomic DNA from three out of four of the selected transformed lines (pCAMPyrH/RebF/STRvm cell line 1: lanes 1-5, pCAMPyrH/RebF/STRvm cell line 3: lanes 6-10, pCAMPyrH/RebF/STRvm cell line 6: lanes 11-15) was successful for all five sets of primers (**Figure 3.6**). PCR amplification of genomic DNA from pCAMPyrH/RebF/STRvm cell line 7 (lanes 16-20) was successful when TDC, PyrH, RebF, HPT primers were used but not when STRvm primers were used. PCR-

amplification of hairy root transformed with *A. rhizogenes* lacking the pCAMBIA vector genomic DNA was successful only when TDC specific primers were used (lanes 21-25).

3.4.6 Evaluation of Alkaloid Production in Transgenic *C. roseus* Hairy Roots

Every transgenic hairy root line that survived hygromycin selection media was evaluated for alkaloid production. Transformed hairy roots were grown in Gamborg's B5 solid media (half strength basal salts, full strength vitamins, 30 g/L sucrose, 6 g/L agar, pH 5.7). The total chloride concentration in Gamborg's B5 formulation is ~ 1mM. Three-week-old hairy roots were ground with a mortar, pestle and 106 μm acid washed glass beads in methanol (10 mL/g of fresh weight hairy roots). The crude natural product mixtures were filtered through 0.2 μm cellulose acetate membrane (VWR) and subsequently subjected to LC-MS analysis. Additionally, hairy roots transformed with wild-type *A. rhizogenes* lacking the plasmid were also evaluated.

These crude alkaloid mixtures were diluted 30/830 with methanol for mass spectral analysis. Samples were ionized by ESI with a Micromass LCT Premier TOF Mass Spectrometer. The LC was performed on an Acquity Ultra Performance BEH C18, 1.7 μm, 2.1 x 100 mm column on a gradient of 10-90% acetonitrile/water (0.1% TFA) over 5 minutes at a flow rate of 0.6 mL/min. The capillary and sample cone voltages were 1300 and 60 V, respectively. The desolvation and source temperature were 300 and 100 °C. The cone and desolvation gas flow rates were 60 and 800 L/hour. Analysis was performed with MassLynx 4.1. Accurate mass measurements were obtained in W-mode. The spectra were processed using the Mass Lynx 4.1 mass measure, in which the mass

spectrum of peaks of interest was smoothed and centered with TOF mass correction, locking on the reference infusion of reserpine.

3.4.7 Feeding 7-chlorotryptamine 2a to Control *C. roseus* Hairy Root Cultures Transformed with No Plasmid

Alkaloid accumulation levels in hairy roots transformed with RebH and RebF were compared to alkaloid accumulation levels in control hairy root fed with 7-chlorotryptamine. The control hairy root line was grown for two weeks in half-strength Gamborg's B5 solid media. Hairy roots were then transferred to the same media supplemented with 7-chlorotryptamine **2a** (0, 25, 50, 100, 200 and 750 μM final concentration) and grown further for one week. Hairy roots were then processed and alkaloid production analyzed as described above in section **3.4.6.** Feeding studies were performed in duplicate.

3.4.8 Brominated Alkaloid Production in Transgenic C. roseus Hairy Roots

A selected transformed hairy root line was grown for two weeks in low chloride solid media (67 mg/L $(NH_4)_2SO_4$, 353 mg/L $Ca(NO_3)_2.4H_2O$, 61 mg/L $MgSO_4$, 1250 mg/L KNO_3, half strength Murashige and Skoog's micronutrient salts and full strength Murashige and Skoog's vitamins, 3 μM total chloride concentration). Hairy roots were transferred to the same media supplemented with either potassium bromide or potassium iodide (10 – 20 mM final concentration) and cultivated for an additional two weeks. Hairy roots were then processed and alkaloid production analyzed as described above in

section **3.4.6**. Hairy roots transformed with wild-type *A. rhizogenes* lacking the plasmid were also evaluated. Experiments were performed in duplicate.

3.4.9 Purification and Isolation of Alkaloids from Transformed TDC Suppressed Hairy Roots Supplemented with 7-chlorotryptamine and 7-bromotryptamine

To obtain chlorinated and brominated alkaloid standards, root tips (10-15) from TDC-suppressed hairy roots[32] were subcultured in six 50 mL Gamborg's B5 liquid media (half strength basal salts, full strength vitamins, 30 g/L sucrose, pH 5.7) and grown at 26°C in the dark at 125 rpm for three weeks prior to supplementing the media with either 7-chlorotryptamine **2a** or 7-bromotryptamine **2c** (750 μM final concentration). Both tryptamine analog substrates were synthesized as previously reported[31]. After two weeks of co-cultivation, hairy roots were extracted as described above in methanol (10 mL/g of fresh weight hairy roots). Alkaloid extracts were filtered, concentrated under vacuum and redissolved in 25% acetonitrile/water (0.1% TFA) (1 mL/g of fresh weight hairy roots).

For cultures supplemented with 7-chlorotryptamine **2a**, the redissolved mixture was purified on a 10 x 20 mm Vydec reverse phase column using a gradient of 25 – 52 % acetonitrile/water (0.1% TFA) over 24 minutes. Alkaloids were monitored at 228 nm and fractions containing the alkaloid analogs of interest, as determined by the characteristic isotopic distribution expected for chlorinated molecules ($^{35}Cl/^{37}Cl$) from LC-MS analysis, were combined and concentrated under vacuum (**Figure 3.22**).

For cultures supplemented with 7-bromotryptamine **2c**, similar procedures were performed to isolate alkaloids from transgenic hairy roots, except that the LC method was extended to 26 minutes. Alkaloids were monitored at 228 nm and fractions containing the alkaloid analogs of interest, as determined by LC-MS analysis, were combined and concentrated under vacuum (**Figure 3.23**).

Isolated alkaloids from both feedings were analyzed by LC-MS (same parameters as above), analytical HPLC, and where possible, high resolution LC-MS, UV-vis spectroscopy, tandem MS/MS and ^{1}H NMR, ^{13}C NMR, and ^{1}H-^{13}C HSQC using a Bruker AVANCE-600 NMR spectrometer equipped with a 5mm 1H{13C,31P} cryo-probe (**Appendix B**). Halogenated alkaloids generally displayed longer retention times than the natural alkaloids.

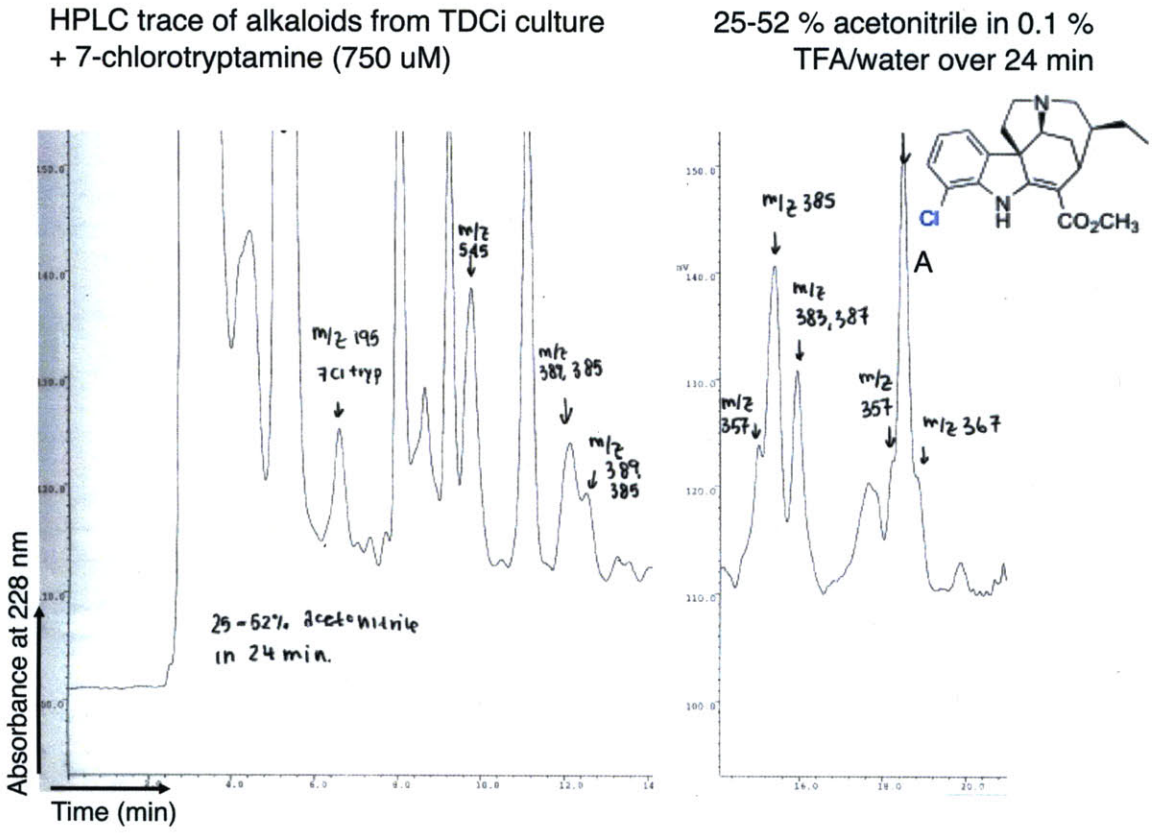

Figure 3.22. HPLC trace of alkaloids from TDCi hairy root fed with 7-chlorotryptamine **2a** (0.75 mM). Fraction A was collected and analyzed.

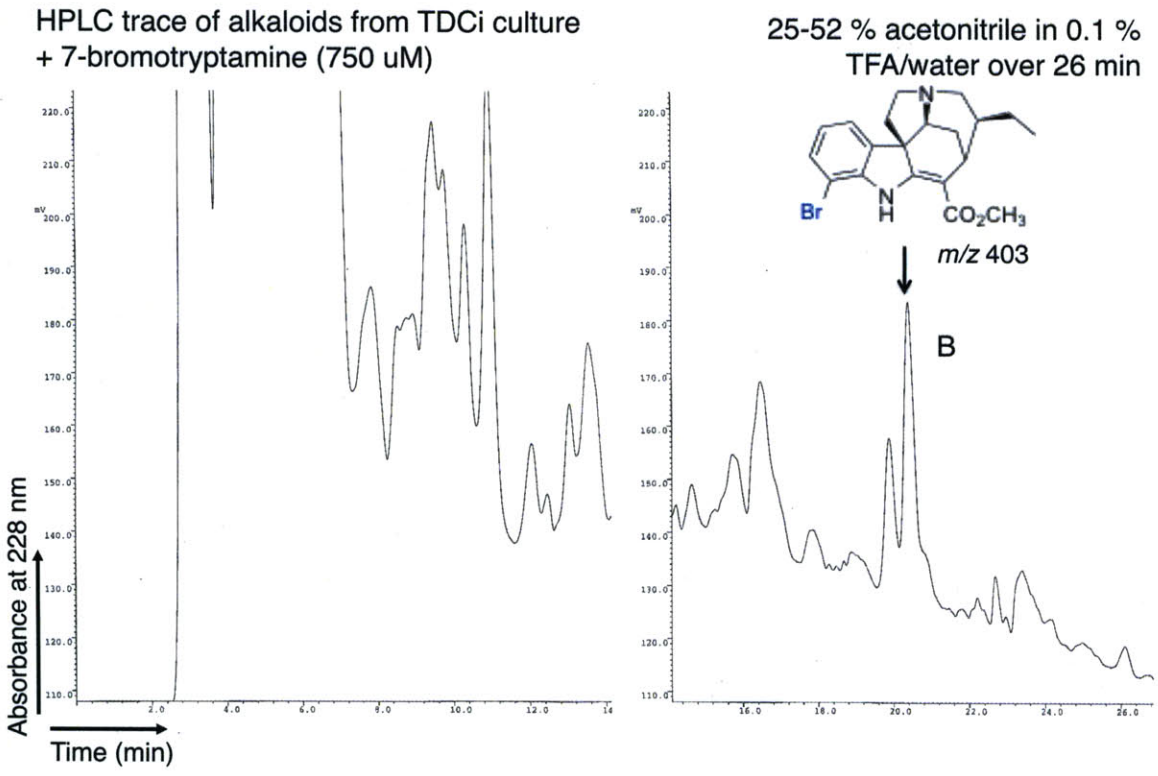

Figure 3.23. HPLC traces of alkaloids from TDCi hairy root fed with 7-bromotryptamine **2c** (0.75 mM). Fraction B was collected and analyzed.

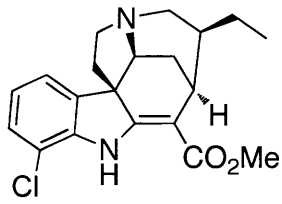

5a

Tabulated NMR data for 12-chloro-19,20-dihydroakuammicine **5a** (Fraction A in **Figure 3.22**).

^{1}H NMR (600 MHz, CD_3OD): δ 7.39 (d, J = 7.4 Hz, 1H), 7.26 (d, J = 8.2 Hz, 1H), 6.99 (t, J = 7.9 Hz, 1H), 4.66 (s, 1H), 3.82 (s, 3H), 3.70 (m, 1H), 3.56 (m, 1H), 3.40 (m, 1H), 3.30 (m, 1H), 3.16 (m, 1H), 3.05 (m, 1H), 2.18 (m, 1H), 2.12 (m, 1H), 2.04 (m, 2H), 0.95 (m, 2H), 0.78 (t, J = 7.3 Hz, 3H); ^{13}C NMR (500 MHz, CD_3OD): δ 128.80, 122.90, 118.80, 65.00, 52.10, 51.81, 51.06, 45.22, 40.04, 39.60, 29.60, 25.80, 22.30, 9.60 (note that quaternary carbon peaks are not observed in ^{1}H-^{13}C HSQC); ESI-MS (*m/z*): $[M]^+$ calcd. for $C_{20}H_{23}ClN_2O_2$, 359.1526; found, 359.1520.

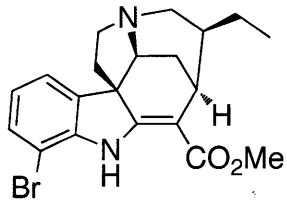

5c

Tabulated NMR data for 12-bromo-19,20-dihydroakuammicine **5c** (Fraction B in **Figure 3.23**)

^{1}H NMR (600 MHz, CD_3OD): δ 7.42 (d, J = 7.4 Hz, 1H), 7.39 (d, J = 7.8 Hz, 1H), 6.92 (t, J = 8.0 Hz, 1H), 4.66 (s, 1H), 3.82 (s, 3H), 3.70 (m, 1H), 3.57 (dt, J = 4.0, 13.5 Hz, 1H), 3.40 (m, 1H), 3.30 (m, 1H), 3.17 (m, 1H), 3.05 (m, 1H), 2.18 (dd, J = 7.7, 14.5 Hz, 1H), 2.12 (m, 1H), 2.04 (m, 2H), 0.95 (m, 2H), 0.78 (t, J = 7.3 Hz, 3H); ^{13}C NMR (500 MHz, CD_3OD): δ 168.84, 166.37, 143.79, 136.19, 132.55, 124.44, 120.52, 104.47, 99.21,

66.33, 54.17, 53.10, 52.24, 46.65, 41.41, 40.76, 30.46, 27.03, 24.01, 11.27; ESI-MS (*m/z*): $[M]^+$ calcd. for $C_{20}H_{23}BrN_2O_2$, 403.1021; found, 403.1011.

3.4.10 Quantification of Chlorinated Alkaloid Production in Transformed Hairy Roots

12-chloro-19,20-dihydroakuammicine **5a** and 12-bromo-19,20-dihydroakuammicine **5c** standard curves were constructed by quantifying the peak areas of several concentrations (20 – 1400 nM) of each alkaloid authentic standard using MassLynx 4.1. Similarly, 10-chloroajmalicine **6b**, 15-chlorotabersonine **7b** and 10-chlorocatharanthine **8b** standard curves were constructed by quantifying the peak areas of several concentrations (20 – 1400 nM) of each natural (i.e. non-chlorinated) alkaloid authentic standard using MassLynx 4.1.

3.4.11 Dependence of Chlorinated Alkaloid Production on Concentrations of Sodium Chloride

A selected transformed hairy root line was grown for two weeks in low chloride solid media (67 mg/L $(NH_4)_2SO_4$, 353 mg/L $Ca(NO_3)_2.4H_2O$, 61 mg/L $MgSO_4$, 1250 mg/L KNO_3, half strength Murashige and Skoog's micronutrient salts and full strength Murashige and Skoog's vitamins, 3 μM total chloride concentration). Hairy roots were transferred to the same media supplemented with potassium chloride (0 – 20 mM final concentration) and grown further for two weeks. Hairy roots were then processed and alkaloid production was analyzed as previously described.

3.4.12 Assessment of the Stability of Chlorinated Alkaloid Production in Subsequent Subcultures

Ten root tips from hairy roots transformed with pCAMRebH/RebF and pCAMPyrH/RebF/STRvm were subcultured every 3 weeks in Gamborg's B5 solid media (half strength basal salts, full strength vitamins, 30 g/L sucrose, 6 g/L agar, pH 5.7) and grown at 26°C in the dark. Alkaloids were isolated from twenty-one-day-old hairy roots and analyzed as described above.

3.4.13 Verification of Expression of RebH, RebF and PyrH, STRvm Enzymes by Real Time RT-PCR

Real time RT-PCR was used to assess the expression levels of RebH and RebF. Expression levels in hairy roots infected with *A. rhizogenes* lacking the pCAMRebH/RebF construct were compared to expression levels in hairy roots harboring pCAMRebH/RebF. mRNA from transformed hairy roots was isolated and purified from contaminant DNA using Qiagen RNeasy Plant Mini Kit and Rnase-free DnaseI, respectively. The resulting mRNA was then reverse-transcribed to cDNA using Qiagen QuantiTect Reverse transcription kit and then subjected to PCR with specific primers (see below), Qiagen SYBR Green PCR kit and a Biorad DNA Engine Opticon 2 system. The threshold-cycle (C_T) was determined as the cycle with a signal higher than that of the background plus 10 x standard deviation (SD). *C. roseus* 40S ribosomal protein S9 (Rps9), a house keeping gene, was used to adjust the amount of the total mRNA in all samples. Real time RT-PCR was performed in triplicate and the data are pictured as the

relative expression levels of RebH and RebF mRNA in transgenic hairy roots as well as hairy roots lacking the pCAMBIA plasmid.

PCR primers for real-time RT-PCR of pCAMRebH/RebF transformed hairy roots. Primers were designed using GenScript web tool (http://www.genscript.com/ssl-bin/app/primer)

Primer Name	Primer Sequence ('5 → 3')	Amplicon size
RebH_for	GACGGGCATCTACTTCGTCT	117
RebH_rev	TCGAACATCGTCTCGATCTC	
RebF_for	CTGATGAGCCTGTTTCCCA	99
RebF_rev	CGTGACACTGGTCAGGGA	
Rbps9_for	TTGAGCCGTATCAGAAATGC	122
Rbps9_rev	CCCTCATCAAGCAGACCATA	

Real time RT-PCR was used to assess the expression levels of PyrH, RebF, and STRvm. Expression levels in hairy roots infected with *A. rhizogenes* lacking the pCAMPyrH/RebF/STRvm construct were compared to expression levels in hairy roots harboring pCAMPyrH/RebF/STRvm.

PCR primers for real-time RT-PCR of pCAMPyrH/RebF/STRvm transformed hairy roots. Primers were designed using GenScript web tool (http://www.genscript.com/ssl-bin/app/primer)

Primer Name	Primer Sequence ('5 → 3')	Amplicon size
PyrH_for	GCCTGCTCATCAACCAGAC	137
PyrH_rev	CATCGCGGTAGCAGTAGTGT	
RebF_for	CTGATGAGCCTGTTTCCCA	99
RebF_rev	CGTGACACTGGTCAGGGA	
STRvm_for	TATTATTGAAAGAGCTACATATG	134
STRvm_rev	CTCTGCACTGCCTTTCTTG	
Rbps9_for	TTGAGCCGTATCAGAAATGC	122
Rbps9_rev	CCCTCATCAAGCAGACCATA	

3.4.14 Quantification of Natural Alkaloids in Wild Type Roots

The levels of natural alkaloids in wild type hairy roots were quantified as described in section **3.4.10**. The levels of the three most abundant alkaloids found in these hairy roots, ajmalicine **6**, tabersonine **7**, catharanthine **8**, as well as tryptophan **1** and tryptamine **2**, were measured (**Appendix B**).

3.5 Acknowledgements

We gratefully acknowledge financial support from the NIH (GM074820) and the American Cancer Society (RSG-07-025-01-CDD). Dr. Xudong Qu conceived the project and initiated its design. Dr. Xudong Qu also performed a portion of the steady-state kinetics studies. We thank Dr. Hyang-Yeol Lee and Dr. Meiliana Tjandra for assistance with NMR characterizations and Dr. Li Li for high-resolution mass spectroscopy analysis.

3.6 References

1. Neumann, C. S.; Fujimori, D. G.; Walsh, C. T., Halogenation strategies in natural product biosynthesis. *Chem Biol* **2008,** *15* (2), 99-109.
2. Gribble, G. W., The diversity of naturally produced organohalogens. *Chemosphere* **2003,** *52* (2), 289-97.
3. Blasiak, L. C.; Drennan, C. L., Structural perspective on enzymatic halogenation. *Acc Chem Res* **2009,** *42* (1), 147-55.
4. Vaillancourt, F. H.; Yeh, E.; Vosburg, D. A.; Garneau-Tsodikova, S.; Walsh, C. T., Nature's inventory of halogenation catalysts: oxidative strategies predominate. *Chem Rev* **2006,** *106* (8), 3364-78.
5. van Pee, K. H.; Dong, C.; Flecks, S.; Naismith, J.; Patallo, E. P.; Wage, T., Biological halogenation has moved far beyond haloperoxidases. *Adv Appl Microbiol* **2006,** *59*, 127-57.
6. Zehner, S.; Kotzsch, A.; Bister, B.; Sussmuth, R. D.; Mendez, C.; Salas, J. A.; van Pee, K. H., A regioselective tryptophan 5-halogenase is involved in pyrroindomycin biosynthesis in Streptomyces rugosporus LL-42D005. *Chem Biol* **2005,** *12* (4), 445-52.

7. Zhu, X.; De Laurentis, W.; Leang, K.; Herrmann, J.; Ihlefeld, K.; van Pee, K. H.; Naismith, J. H., Structural insights into regioselectivity in the enzymatic chlorination of tryptophan. *J Mol Biol* **2009,** *391* (1), 74-85.
8. Bitto, E.; Huang, Y.; Bingman, C. A.; Singh, S.; Thorson, J. S.; Phillips, G. N., Jr., The structure of flavin-dependent tryptophan 7-halogenase RebH. *Proteins* **2008,** *70* (1), 289-93.
9. Yeh, E.; Blasiak, L. C.; Koglin, A.; Drennan, C. L.; Walsh, C. T., Chlorination by a long-lived intermediate in the mechanism of flavin-dependent halogenases. *Biochemistry* **2007,** *46* (5), 1284-92.
10. Yeh, E.; Cole, L. J.; Barr, E. W.; Bollinger, J. M., Jr.; Ballou, D. P.; Walsh, C. T., Flavin redox chemistry precedes substrate chlorination during the reaction of the flavin-dependent halogenase RebH. *Biochemistry* **2006,** *45* (25), 7904-12.
11. Yeh, E.; Garneau, S.; Walsh, C. T., Robust in vitro activity of RebF and RebH, a two-component reductase/halogenase, generating 7-chlorotryptophan during rebeccamycin biosynthesis. *Proc Natl Acad Sci U S A* **2005,** *102* (11), 3960-5.
12. Sanchez, C.; Zhu, L.; Brana, A. F.; Salas, A. P.; Rohr, J.; Mendez, C.; Salas, J. A., Combinatorial biosynthesis of antitumor indolocarbazole compounds. *Proc Natl Acad Sci U S A* **2005,** *102* (2), 461-6.
13. Bernhardt, P.; McCoy, E.; O'Connor, S. E., Rapid identification of enzyme variants for reengineered alkaloid biosynthesis in periwinkle. *Chem Biol* **2007,** *14* (8), 888-97.
14. McCoy, E.; Galan, M. C.; O'Connor, S. E., Substrate specificity of strictosidine synthase. *Bioorg Med Chem Lett* **2006,** *16* (9), 2475-8.
15. McCoy, E.; O'Connor, S. E., Directed biosynthesis of alkaloid analogs in the medicinal plant Catharanthus roseus. *J Am Chem Soc* **2006,** *128* (44), 14276-7.
16. Hawkins, K. M.; Smolke, C. D., Production of benzylisoquinoline alkaloids in Saccharomyces cerevisiae. *Nat Chem Biol* **2008,** *4* (9), 564-73.
17. Minami, H.; Kim, J. S.; Ikezawa, N.; Takemura, T.; Katayama, T.; Kumagai, H.; Sato, F., Microbial production of plant benzylisoquinoline alkaloids. *Proc Natl Acad Sci U S A* **2008,** *105* (21), 7393-8.
18. O'Connor, S. E.; Maresh, J. J., Chemistry and biology of monoterpene indole alkaloid biosynthesis. *Nat Prod Rep* **2006,** *23* (4), 532-47.
19. Broothaerts, W.; Mitchell, H. J.; Weir, B.; Kaines, S.; Smith, L. M.; Yang, W.; Mayer, J. E.; Roa-Rodriguez, C.; Jefferson, R. A., Gene transfer to plants by diverse species of bacteria. *Nature* **2005,** *433* (7026), 629-33.
20. De Luca, V.; Cutler, A. J., Subcellular Localization of Enzymes Involved in Indole Alkaloid Biosynthesis in Catharanthus roseus. *Plant Physiol* **1987,** *85* (4), 1099-102.
21. Hughes, E. H.; Hong, S. B.; Shanks, J. V.; San, K. Y.; Gibson, S. I., Characterization of an inducible promoter system in Catharanthus roseus hairy roots. *Biotechnol Prog* **2002,** *18* (6), 1183-6.
22. Runguphan, W.; O'Connor, S. E., Metabolic reprogramming of periwinkle plant culture. *Nat Chem Biol* **2009,** *5* (3), 151-3.
23. Loris, E. A.; Panjikar, S.; Ruppert, M.; Barleben, L.; Unger, M.; Schubel, H.; Stockigt, J., Structure-based engineering of strictosidine synthase: auxiliary for alkaloid libraries. *Chem Biol* **2007,** *14* (9), 979-85.

24. Frederich, M.; Jacquier, M. J.; Thepenier, P.; De Mol, P.; Tits, M.; Philippe, G.; Delaude, C.; Angenot, L.; Zeches-Hanrot, M., Antiplasmodial activity of alkaloids from various strychnos species. *J Nat Prod* **2002,** *65* (10), 1381-6.
25. Menzies, J. R.; Paterson, S. J.; Duwiejua, M.; Corbett, A. D., Opioid activity of alkaloids extracted from Picralima nitida (fam. Apocynaceae). *Eur J Pharmacol* **1998,** *350* (1), 101-8.
26. Zhu, W.-M.; He, H.-P.; Fan, L.-M.; Shen, Y.-M.; Zhou, J.; Hao, X.-J., Components of stem barks of Winchia calophylla A. DC. and their bronchodilator activities. *J. Integ. Plant Biol.* **2005,** *47*, 892-896.
27. Amat, M.; Linares, A.; Bosch, J., A new synthetic entry to pentacyclic Strychnos alkaloids. Total synthesis of (±)-tubifolidine, (±)-tubifoline, and (±)-19,20-dihydroakuammicine. *J. Org. Chem.* **1990,** *55*, 6299-6312.
28. Gandar, J. C.; Nitsch, C., Isolement de l'ester methylique d'un acide chloro-3-indolylacetiqe a partir de graines immatures de pois Pisum sativum L. . *C.R. Acad. Sci. (Paris). Ser. D.* **1967,** *265*, 1795–1798.
29. Marumo, S.; Hattori, H.; Abe, H.; Munakata, K., Isolation of 4-chloroindolyl-3-acetic acid from immature seeds of Pisum sativum. *Nature* **1968,** *219*, 959-960.
30. Roy, A. D.; Grüschow, S.; Cairns, N.; Goss, R. J., Gene expression enabling synthetic diversification of natural products: chemogenetic generation of pacidamycin analogs. *J Am Chem Soc* **2010,** *132*, 12243-12245.
31. Schumacher, R. W.; Davidson, B. S., Synthesis of didemnolines A-D, N9-substituted β-carboline alkaloids from the marine ascidian *Didemnum* sp. *Tetrahedron* **1999,** *55* (4), 935-942.
32. Runguphan, W.; Maresh, J. J.; O'Connor, S. E., Silencing of tryptamine biosynthesis for production of nonnatural alkaloids in plant culture. *Proc Natl Acad Sci U S A* **2009,** *106* (33), 13673-8.

CHAPTER 4

SILENCING TRYPTAMINE BIOSYNTHESIS IN *C. ROSEUS* CELL CULTURE

Part of this chapter is published as an article in

PNAS **2009**, *106*, 13673-13678

4.1 Introduction

Functional group modification of a natural product often improves the biological activity of the compound[1]. However, despite the importance of plant derived natural products, metabolic engineering strategies to yield unnatural products from complex plant biosynthetic pathways have not been widely explored. In microbial systems, genetic engineering of natural product biosynthetic pathways has emerged as a powerful strategy to rapidly access complex novel molecules[2]. In one strategy, termed precursor-directed biosynthesis, the producer organism is supplemented with analogs of the naturally occurring starting materials where, ideally, these unnatural starting materials are converted by the enzymes of the biosynthetic pathway into the corresponding unnatural products[3]. The yields and purity of these unnatural products are typically improved if the biosynthesis of the natural starting material is genetically silenced, and the producing organism is forced to utilize exogenously supplied substrates for product biosynthesis. This approach, termed mutasynthesis, was first applied several decades ago to yield novel antibiotics in the soil bacterium *Streptomyces fradiae*[4]. While mutasynthesis has proven to be highly successful in microbial systems[5,6], the strategy has yet to be applied in more complex eukaryotes, notably plants.

Tryptamine **1** is the starting substrate for over one hundred monoterpene indole alkaloids produced by *C. roseus* (**Figure 4.1** and **Chapter 1**)[7,8]. This substrate is derived from decarboxylation of tryptophan **2** by tryptophan decarboxylase, an enzyme that serves as a key link between primary metabolism and natural product metabolism[9,10]. We envisioned that if tryptamine biosynthesis was silenced, alkaloid biosynthesis could be rescued by

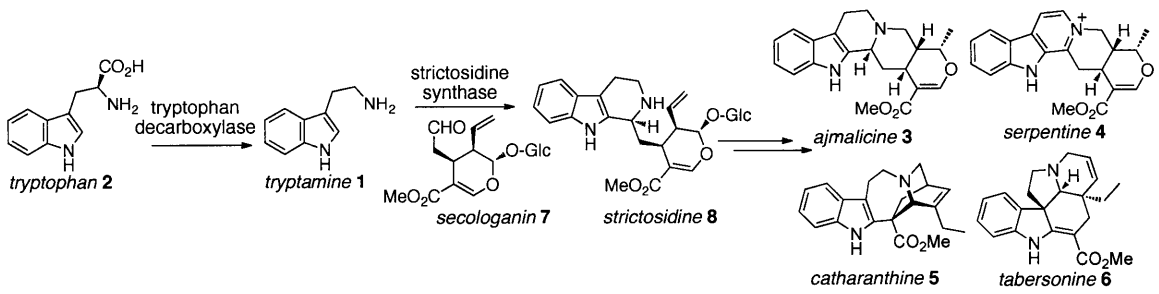

Figure 4.1 Monoterpene indole alkaloid biosynthesis in *C. roseus*. Tryptophan **2** is decarboxylated by tryptophan decarboxylase to yield tryptamine **1**, which reacts with secologanin **7** to form strictosidine **8**. After numerous rearrangements, strictosidine **8** is converted into over one hundred monoterpene indole alkaloids, such as ajmalicine **3**, serpentine **4**, catharanthine **5** and tabersonine **6**.

introducing exogenous tryptamine or tryptamine analogs to plant cell culture (**Figure 4.2**). Precursor-directed biosynthesis with wild type *C. roseus* plants and tissue culture has already demonstrated that tryptamine analogs can be taken up by the plant and incorporated into a wide variety of alkaloids[11-13]. However, if tryptamine **1** is required for plant growth or survival, silenced cell lines would not be viable. Studies of down-regulating or suppressing tryptamine biosynthesis in plants have not been reported, and little information is available in the literature to provide a definitive role for tryptamine, a metabolite that is found throughout the plant kingdom[14]. Overproduction of tryptamine has been shown to deter insect feeding[15], but this role is non-essential in the controlled environment of plant cell culture. Additionally, 5-hydroxytryptamine (serotonin), which may be produced by hydroxylation of tryptamine, has been implicated in certain physiological roles such as flower development[16]. Moreover, tryptamine, or its precursor tryptophan, may also be involved in auxin biosynthesis[17]. Again, these proposed roles are unlikely to be essential to plant tissue culture.

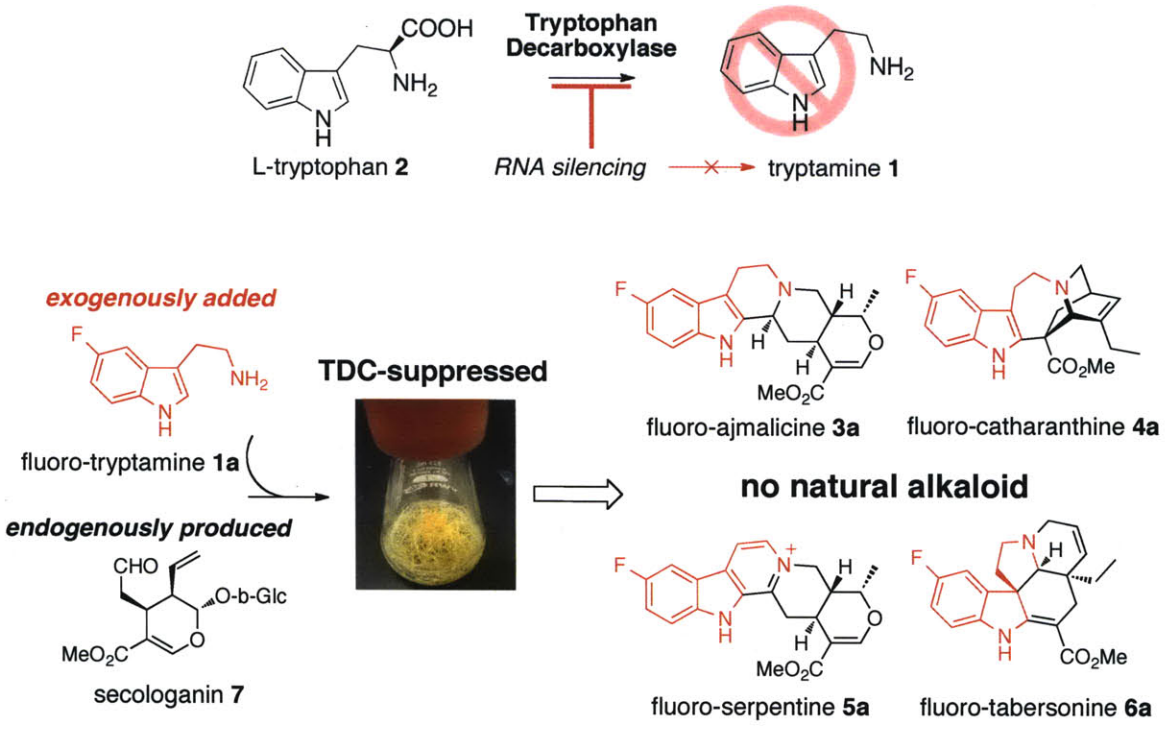

Figure 4.2. Silencing of tryptamine biosynthesis in *C. roseus*. Tryptamine **1** is produced by enzymatic decarboxylation of tryptophan **2**. Trypamine **1** reacts with secologanin **7** to yield a variety of monoterpene indole alkaloids. Ajmalicine **3**, serpentine **4**, catharanthine **5** and tabersonine **6** are produced in *Catharanthus roseus* hairy root culture.

Despite the uncertainty pertaining to the physiological role of tryptamine in plants, suppression of tryptophan decarboxylase nevertheless provided an attractive entry point for introduction of new substrate analogs. In prokaryotic pathways, the gene of interest is usually deleted or "knocked out" using homologous recombination-based strategies. However, although some success has been achieved with homologous recombination in higher plants[18], strategies to down-regulate or knockdown specific gene expression levels using RNA-mediated silencing are extremely well established for plants. Moreover, these transgenic lines can be constructed in a relatively short time (~ 6-9 months)[19-21].

This chapter describes mutasynthesis of the monoterpene indole alkaloids in the medicinal plant Madagascar periwinkle (*Catharanthus roseus*). Specifically, we used RNA-mediated silencing of tryptophan decarboxylase to suppress tryptamine biosynthesis in *C. roseus* culture. We show that alkaloid production almost completely disappeared in silenced cultures but could be rescued by the addition of exogenous tryptamine to the culture media. A representative unnatural tryptamine analog, 5-fluorotryptamine **1a**, was also incorporated into the pathway to yield several unnatural, fluorinated alkaloids. Silencing of this early biosynthetic enzyme did not impact the expression of known downstream alkaloid biosynthetic enzymes, indicating that changes can be made in the early part of this pathway without adversely affecting the alkaloid biosynthetic machinery. Notably, regenerated *C. roseus* plants from these transformed hairy roots exhibited severe growth retardation and were not viable. Together, these experiments demonstrate that while tryptamine and monoterpene indole alkaloids do not appear to play an essential role in growth or development in *C. roseus* hairy root culture, they may be vital for whole plant survival in a non-controlled environment.

4.2 Results and Discussion

4.2.1 Generation and Verification of Transgenic Hairy Root Cultures

Tryptophan decarboxylase, a pyridoxal phosphate dependent enzyme that produces tryptamine **1** from tryptophan **2**[9, 10], was targeted for gene silencing[19, 22-24] (**Figure 4.2**). The plasmid designed to suppress tryptophan decarboxylase (pTDCi, created by Justin Maresh based on pHELLSGATE vector[19]; **Figure 4.3**) was transformed into *Agrobacterium rhizogenes*, which was then used to infect *C. roseus* seedlings to generate

hairy root culture as previously described[25, 26]. PCR analysis of genomic DNA confirmed the incorporation of the tryptophan decarboxylase-silencing construct in two selected transgenic lines (**Figure 4.4**). Specifically, PCR amplification of genomic DNA from TDCi cell lines 3 and 15 was successful for all four sets of primers (strictosidine synthase (STR), Cauliflower Mosaic Virus 35S promoter (CaMV35S), kanamycin resistance gene (NPTII) and pyruvate dehydrogenase kinase (PDK) intron). PCR amplification of genomic DNA from hairy root transformed with *A. rhizogenes* lacking the pTDCi plasmid (designated "wild type line" and was provided by Professor Jacqueline Shanks (Iowa State) and Professor Carolyn Lee-Parsons (Northeastern)) was successful only when STR specific primers were used (lanes 1-4). These results indicated that the TDC silencing construct was successfully incorporated into the *C. roseus* genome in both chosen lines.

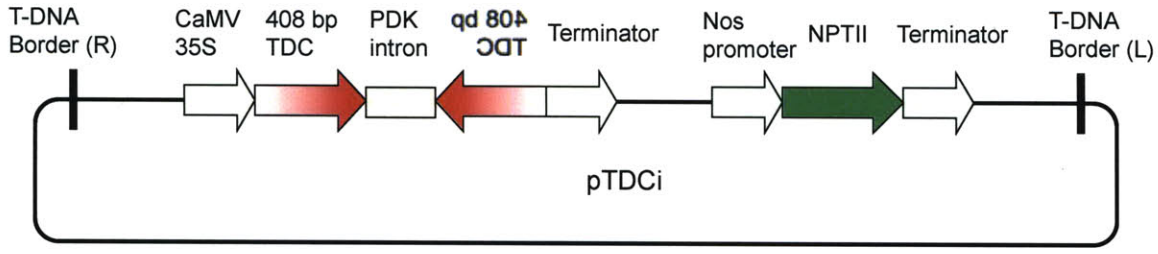

Figure 4.3. Schematic diagram of tryptophan decarboxylase silencing construct. CaMV35S: Cauliflower Mosaic Virus 35S promoter; 408bp TDC: a 408 bp fragment at the 5' end of tryptophan decarboxylase; PDK intron: the intron region of pyruvate dehydrogenase kinase; NPTII: kanamycin resistance gene.

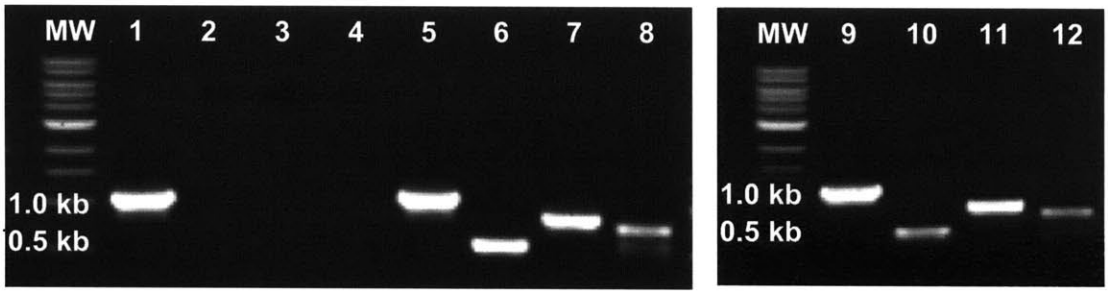

Figure 4.4. 1% agarose gel of PCR amplification of TDCi and wild-type hairy root genomic DNA.

Lane: template, primers.

1: wild type; STR.
2: wild type; CaMV35S.
3: wild type; NPTII.
4: wild type; PDK intron.
5: TDCi cell line 3; STR.
6: TDCi cell line 3; CaMV35S.
7: TDCi cell line 3; NPTII.
8: TDCi cell line 3; PDK intron.
9: TDCi cell line 15; STR.
10: TDCi cell line 15; CaMV35S.
11: TDCi cell line 15; NPTII.
12: TDCi cell line 15; PDK intron

4.2.2 Alkaloid Production in Tryptophan Decarboxylase Silenced Lines

Hairy root lines harboring the pTDCi silencing plasmid were cultured in liquid media, and alkaloids were extracted from the plant tissue according to standard protocols. Production of all major tryptamine derived alkaloids ajmalicine **3**, serpentine **4**, catharanthine **5** and tabersonine **6** was significantly decreased in the five silenced lines that were examined (**Figure 4.5 A-D**). We observed negligible changes in alkaloid production levels after at least seven subcultures suggesting that suppression of alkaloid production is stable (**Figure 4.6**).

A.

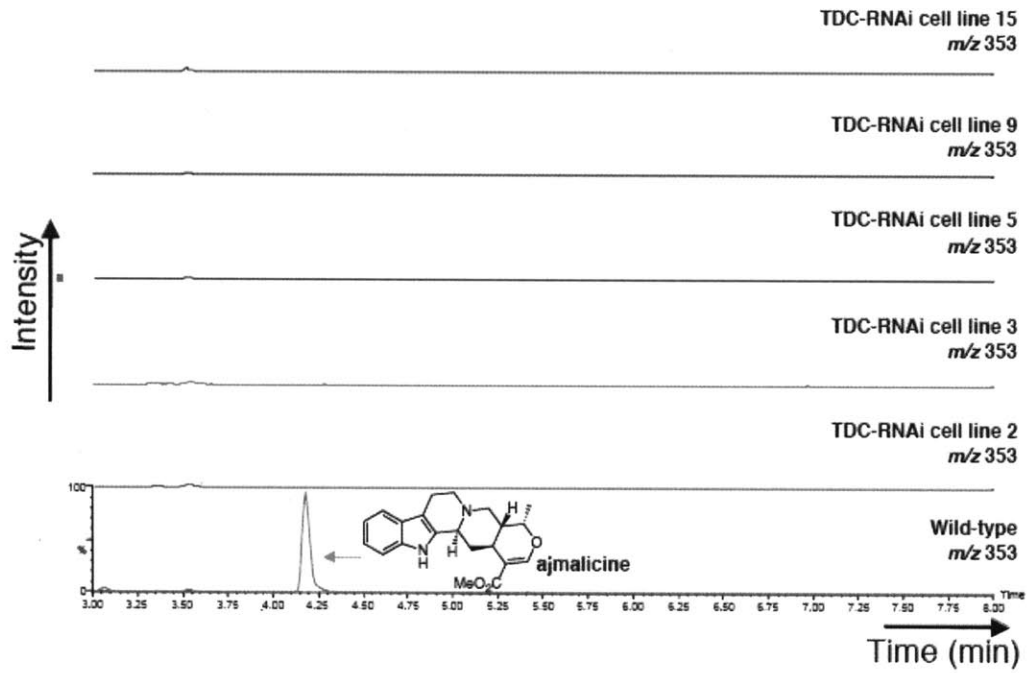

B.

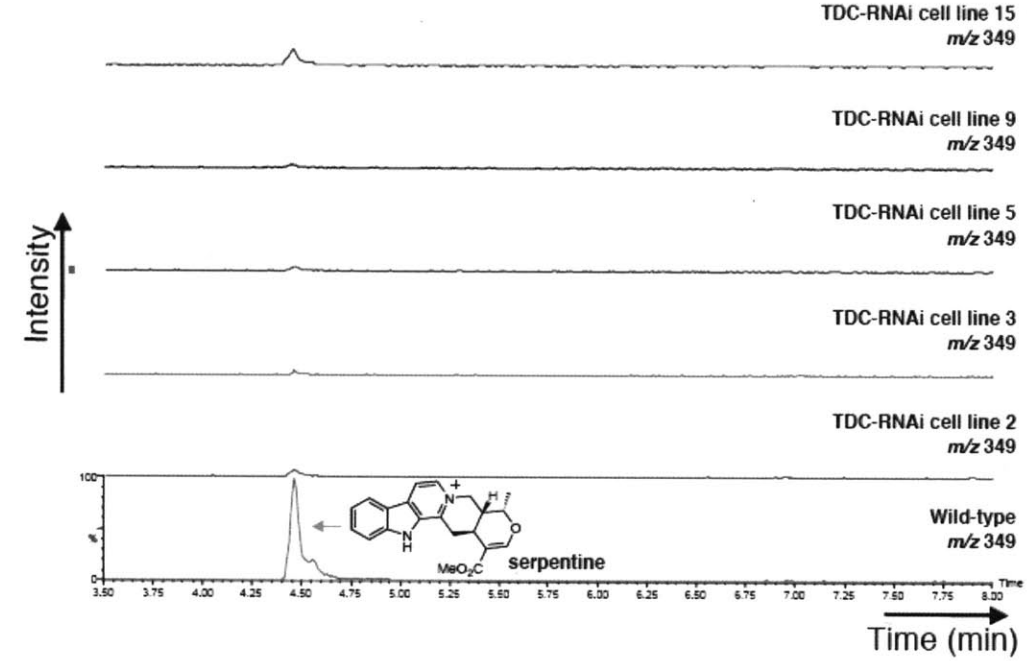

Figure 4.5 A (top) and B (bottom). Extracted LC-MS chromatograms showing the absence of **A.** ajmalicine and **B.** serpentine. Wild type lines are shown for comparison. LC-MS spectra are normalized to the same y-axis scale.

C.

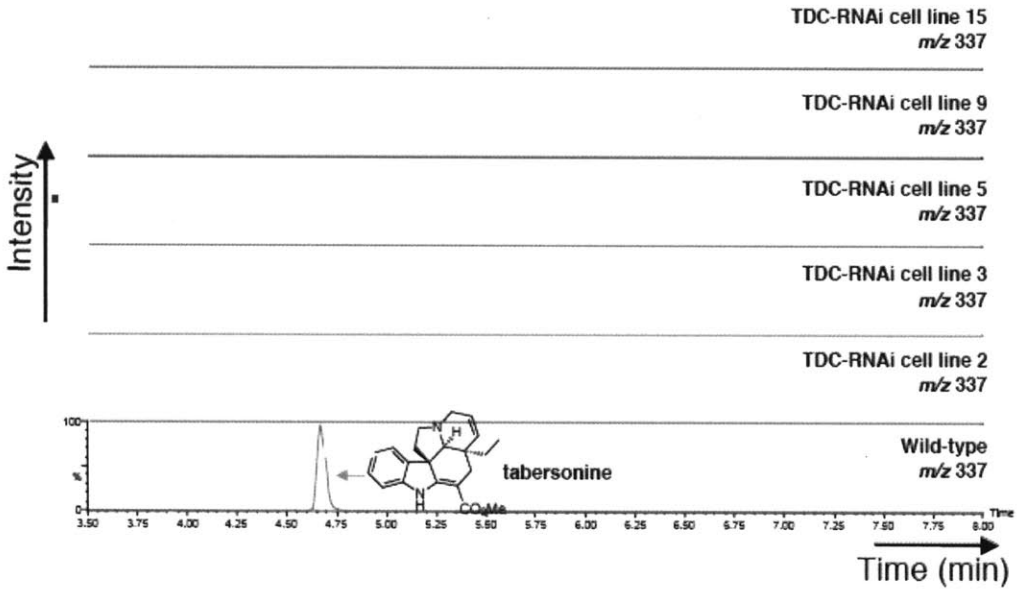

D.

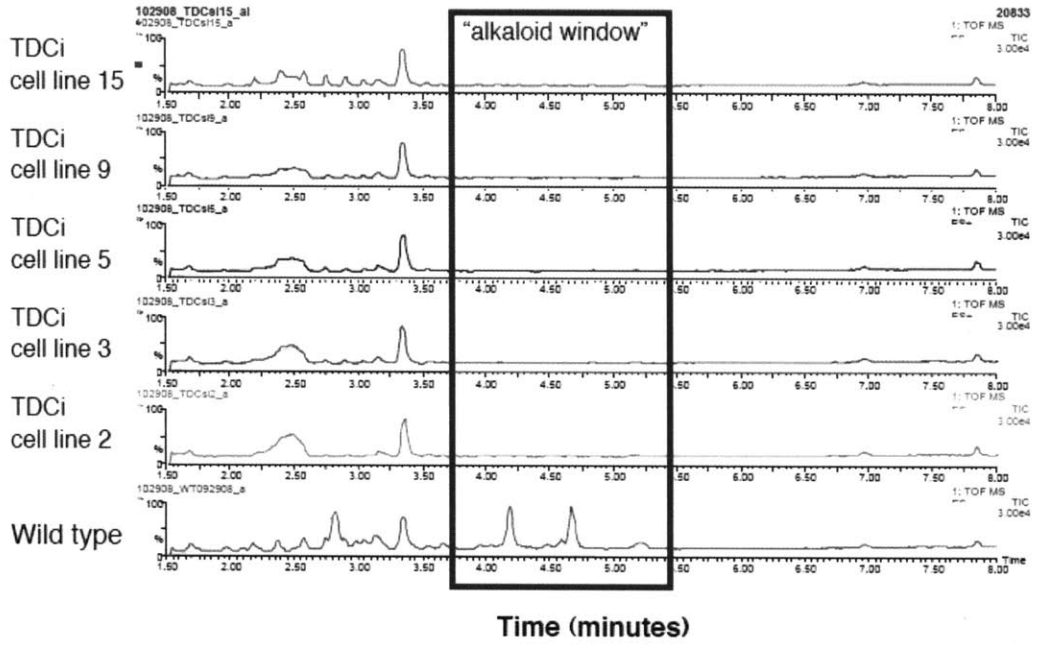

Figure 4.5 C (Top) and D (bottom). Extracted LC-MS chromatograms showing the absence of **C.** catharanthine and tabersonine in five silenced lines. Wild type lines are shown for comparison. Note that wild type lines do not produce catharanthine **5** at *m/z* 337; only tabersonine is observed in wild type lines at this mass. **D.** Total ion counts for five silenced lines. LC-MS spectra are normalized to the same y-axis scale.

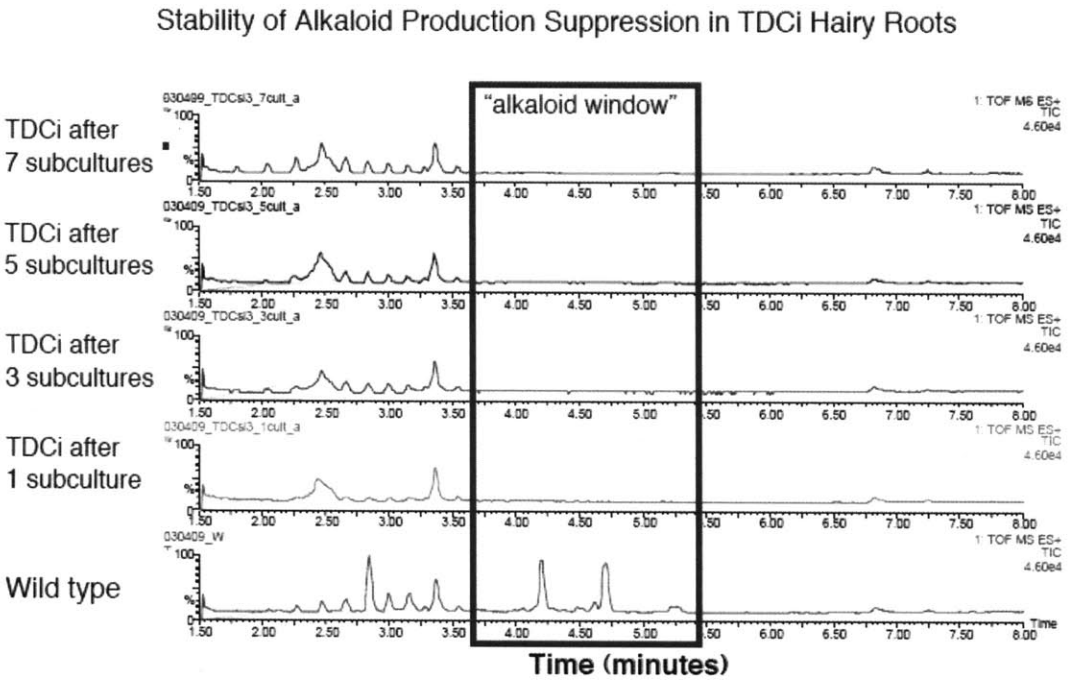

Figure 4.6. Metabolite production in TDCi hairy roots after 1, 3, 5 and 7 subcultures as evidenced by LC-MS analysis of *C. roseus* extracts. "Alkaloid window" represents the range of retention time that natural *C. roseus* alkaloids usually elute. LC-MS spectra are normalized to the same y-axis scale.

4.2.3 Gene Expression in Tryptophan Decarboxylase Silenced Lines

We quantified the levels of tryptophan decarboxylase mRNA in silenced lines. Real time reverse transcription PCR (RT-PCR) confirmed that the tryptophan decarboxylase gene was significantly down regulated at the mRNA level in two representative lines harboring the pTDCi silencing plasmid (**Figure 4.7**). Tryptophan decarboxylase is regulated by the transcription factor Orca3[27], which also controls a number of other alkaloid biosynthetic genes including strictosidine synthase (STR)[28] and strictosidine glucosidase (SGD)[29], enzymes that act immediately after tryptophan decarboxylase in the alkaloid biosynthetic pathway. To ensure that silencing of tryptophan decarboxylase did not affect the expression levels of these other genes in the alkaloid biosynthetic pathway, we quantified the expression levels of Orca3, STR and SGD. Gratifyingly, the mRNA levels of all three genes did not appear to be affected, indicating that the tryptophan decarboxylase gene could be silenced without perturbing the downstream pathway (**Figure 4.7**). In contrast, Allen and coworkers showed that down-regulation of a late stage morphine biosynthetic gene had an unpredictable effect on morphine biosynthesis, suggesting that suppression of a single metabolic enzyme can sometimes affect expression of other pathway enzymes[30]. Finally, the gene encoding the alpha subunit of anthranilate synthase[31], an enzyme involved in tryptophan **2** biosynthesis, showed modest decreases in expression levels in the silenced lines (**Figure 4.7**). This is consistent with a previous study which demonstrated that increased concentrations of tryptophan inhibit anthranilate synthase expression[32]. In the silenced lines, where tryptophan is no longer diverted to tryptamine biosynthesis, concentrations of tryptophan could increase, resulting in the decreased expression of anthranilate synthase. A full transcriptional analysis of the monoterpene

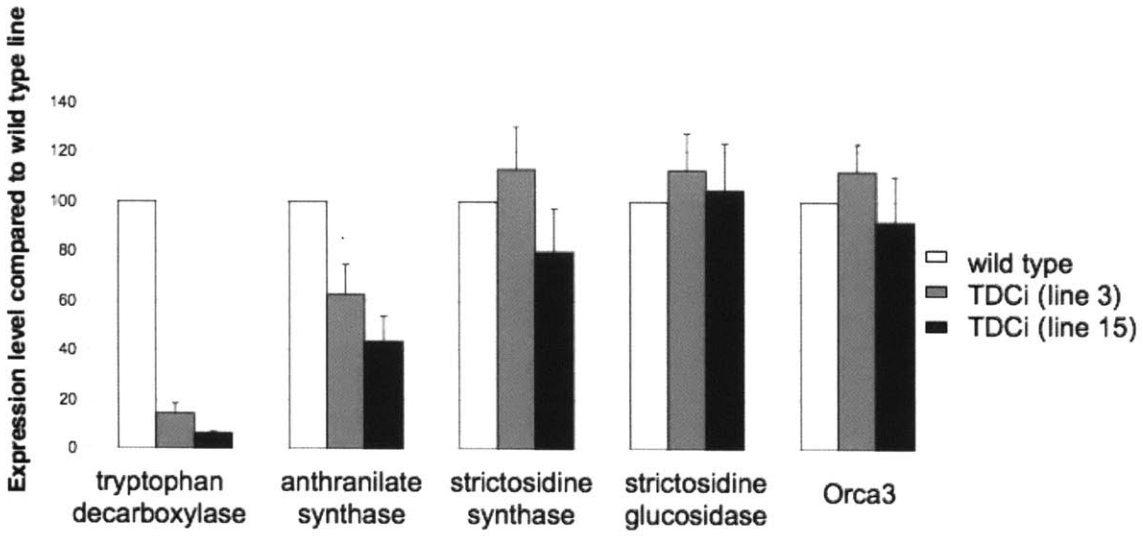

Figure 4.7. Real-time reverse transcriptase PCR (RT-PCR) of the mRNA encoding tryptophan decarboxylase, anthranilate synthase, strictosidine synthase, strictosidine glucosidase and Orca3. Levels of these genes are normalized to 100% in the wild type line. The gene expression levels of two representative silenced lines relative to the wild type levels are also shown. Levels represent the average of three trials, with error bars representing the standard deviation.

indole alkaloid pathway was not performed since the majority of the pathway enzymes have not been characterized at the genetic level.

4.2.4 Unnatural Alkaloid Production in Tryptophan Decarboxylase Silenced Lines

Alkaloid biosynthesis could be rescued by feeding tryptamine **1** or isotopically labeled d4-(deuterium) tryptamine to silenced cultures. We measured formation of the major alkaloids of hairy root culture, namely ajmalicine **3**, serpentine **4**, catharanthine **5** and tabersonine **6** (**Figure 4.1** and **Figure 4.8-4.10**). The identity of these alkaloids was assigned by exact mass and co-elution with authentic standards (**Table 4.1**). Isotopically labeled d5-L-tryptophan (500 μM) was also incubated with a wild type and a representative silenced line. As expected, the wild type culture could incorporate the exogenous isotopically labeled tryptophan into alkaloids while the suppressed line could not, clearly indicating that the required decarboxylation reaction did not occur when tryptophan decarboxylase was knocked down (**Figure 4.9 A-C**).

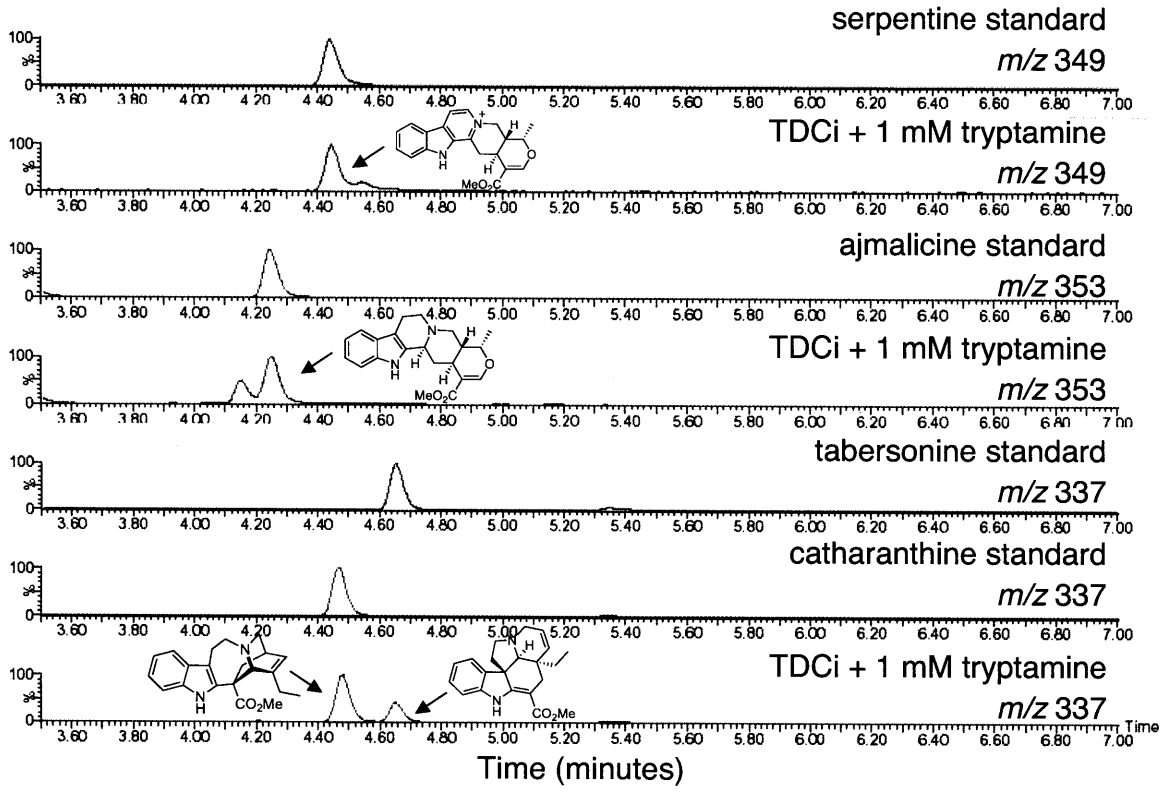

Figure 4.8. Extracted LC-MS chromatograms showing the presence of ajmalicine **3**, serpentine **4**, catharanthine **5** and tabersonine **6**. These compounds are only present when tryptamine **1** is added to the culture media. Results using a concentration of 1.0 mM tryptamine are shown. Authentic standards of ajmalicine **3**, serpentine **4**, catharanthine **5**, and tabersonine **6** are used to validate the structural assignments of these compounds

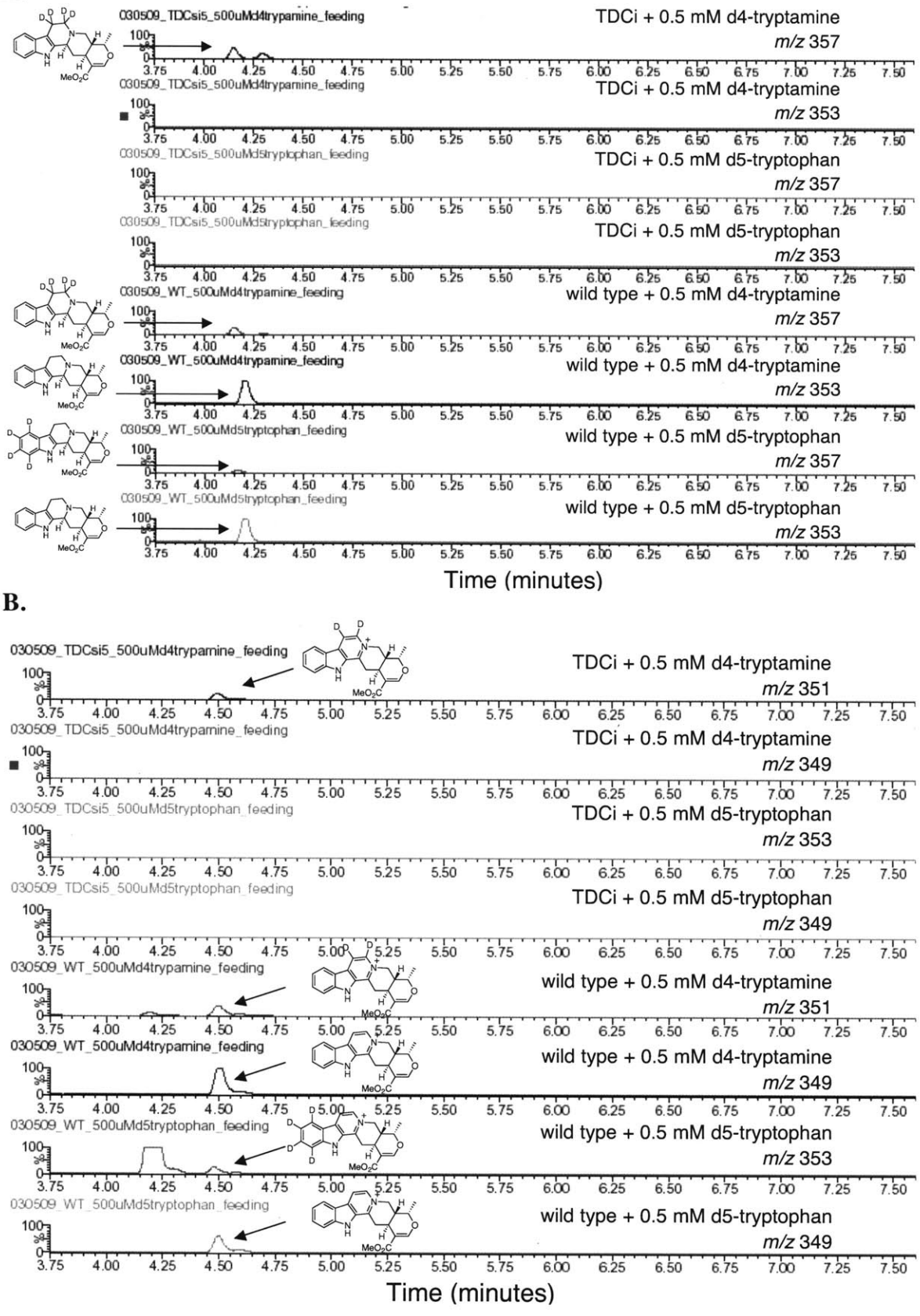
A.
030509_TDCsi5_500uMd4tryparnine_feeding
TDCi + 0.5 mM d4-tryptamine
m/z 357
030509_TDCsi5_500uMd4tryparnine_feeding
TDCi + 0.5 mM d4-tryptamine
m/z 353
030509_TDCsi5_500uMd5tryptophan_feeding
TDCi + 0.5 mM d5-tryptophan
m/z 357
030509_TDCsi5_500uMd5tryptophan_feeding
TDCi + 0.5 mM d5-tryptophan
m/z 353
030509_WT_500uMd4tryparnine_feeding
wild type + 0.5 mM d4-tryptamine
m/z 357
030509_WT_500uMd4tryparnine_feeding
wild type + 0.5 mM d4-tryptamine
m/z 353
030509_WT_500uMd5tryptophan_feeding
wild type + 0.5 mM d5-tryptophan
m/z 357
030509_WT_500uMd5tryptophan_feeding
wild type + 0.5 mM d5-tryptophan
m/z 353
3.75 4.00 4.25 4.50 4.75 5.00 5.25 5.50 5.75 6.00 6.25 6.50 6.75 7.00 7.25 7.50
Time (minutes)
B.
030509_TDCsi5_500uMd4tryparnine_feeding
TDCi + 0.5 mM d4-tryptamine
m/z 351
030509_TDCsi5_500uMd4tryparnine_feeding
TDCi + 0.5 mM d4-tryptamine
m/z 349
030509_TDCsi5_500uMd5tryptophan_feeding
TDCi + 0.5 mM d5-tryptophan
m/z 353
030509_TDCsi5_500uMd5tryptophan_feeding
TDCi + 0.5 mM d5-tryptophan
m/z 349
030509_WT_500uMd4tryparnine_feeding
wild type + 0.5 mM d4-tryptamine
m/z 351
030509_WT_500uMd4tryparnine_feeding
wild type + 0.5 mM d4-tryptamine
m/z 349
030509_WT_500uMd5tryptophan_feeding
wild type + 0.5 mM d5-tryptophan
m/z 353
030509_WT_500uMd5tryptophan_feeding
wild type + 0.5 mM d5-tryptophan
m/z 349
3.75 4.00 4.25 4.50 4.75 5.00 5.25 5.50 5.75 6.00 6.25 6.50 6.75 7.00 7.25 7.50
Time (minutes)

C.

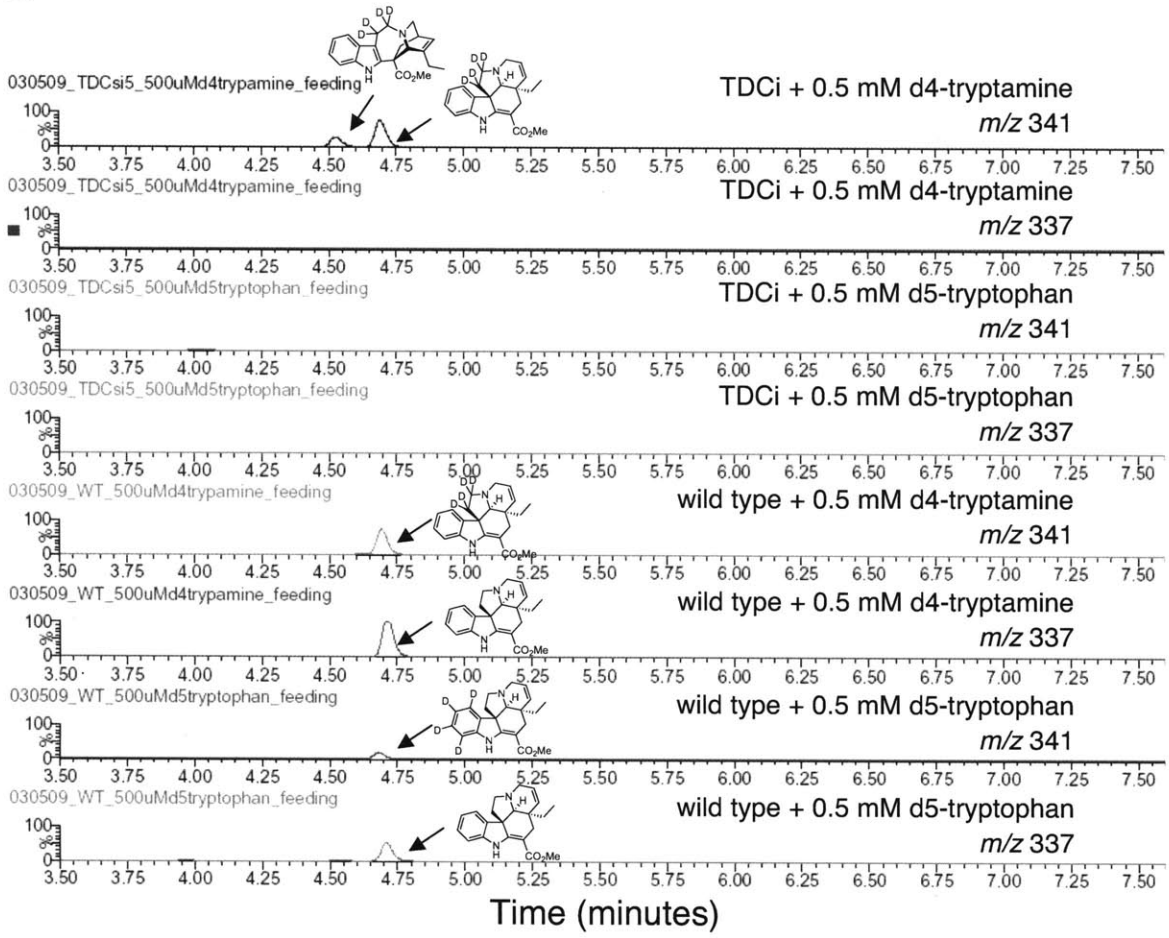

Figure 4.9 A-C. Extracted LC-MS chromatograms showing the presence of deuterated **A.** ajmalicine **3**, **B.** serpentine **4**, **C.** catharanthine **5** and tabersonine **6**. In the tryptophan decarboxylase suppressed line, these compounds are only present when a,a,b,b-d4-tryptamine (CDN Isotopes) is added to the culture media. In the wild type line, deuterated alkaloids are present when either a,a,b,b-d4-tryptamine (CDN Isotopes) or 2',4',5',6',7'-d5-tryptophan (CDN isotope) is added to the culture media. Results using a concentration of 0.5 mM d4-tryptamine or 0.5 mM d5-tryptophan are shown. LC-MS spectra are normalized to the same y-axis scale.

Table 4.1. High-resolution MS data for alkaloids observed in hairy root extracts.

		R = H	R = F
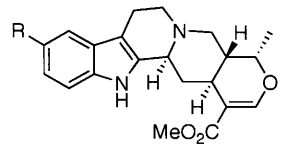	**Ajmalicine**	**3**	**3a**
	Expected [M+H]	353.1865	371.1765
	Observed [M+H]	353.1856	371.1760
	Accuracy (ppm)	-2.5	-3.0
	RT (min)	4.25	4.66
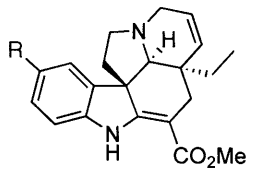	**Tabersonine**	**6**	**6a**
	Expected [M+H]	337.1916	355.1816
	Observed [M+H]	337.1922	355.1811
	Accuracy (ppm)	1.8	-3.1
	RT (min)	4.65	5.20
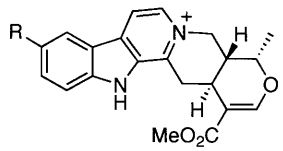	**Serpentine**	**4**	**4a**
	Expected [M+H]	349.1552	367.1452
	Observed [M+H]	349.1548	367.1453
	Accuracy (ppm)	-1.1	-1.4
	RT (min)	4.45	4.72
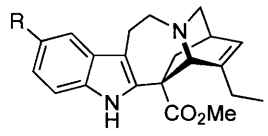	**Catharanthine**	**5**	**5a**
	Expected [M+H]	337.1916	355.1816
	Observed [M+H]	337.1916	355.1818
	Accuracy (ppm)	0.0	-1.1
	RT (min)	4.48	4.88

RT = retention time, LC gradient 10-60% acetonitrile/water (0.1% TFA) in 13 minutes

A hairy root line that showed maximal suppression of alkaloid production (cell line 3) was incubated with varying concentrations of tryptamine **1** (62.5 - 2500 μM) in the cell culture media. The production of ajmalicine **3**, serpentine **4**, catharanthine **5**, and tabersonine **6** were monitored by mass spectrometry in tandem with high performance liquid chromatography (**Figure 4.8, 4.10**). The production levels increased as more tryptamine **1** was added to the media, though catharanthine **5** and tabersonine **6** production was highest at 1000 μM tryptamine **1**. Notably, growth inhibition and browning of wild type hairy roots was typically observed when exogenous tryptamine was added to the media of wild type cultures at concentrations of 1000 μM or greater. However, this was not observed in the silenced lines where the natural tryptamine production was suppressed.

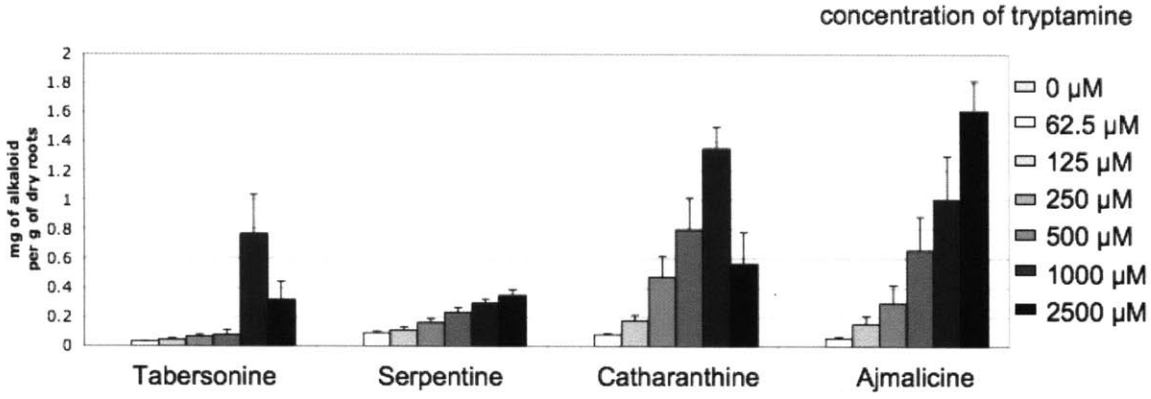

Figure 4.10. Levels of ajmalicine **3**, serpentine **4**, catharanthine **5** and tabersonine **6** production in a representative silenced line supplemented with tryptamine **1** (0, 62.5, 125, 250, 500, 1000, 2500 μM) in the culture media. Levels were estimated in *C. roseus* extracts by LC-MS and represent the average of three trials, with error bars representing the standard deviation.

The suppression of natural alkaloid biosynthesis in these transformed lines provided the first opportunity to explore the prospects of mutasynthesis– replacement of natural alkaloids with unnatural products– in plant culture. A representative tryptamine analog, 5-fluorotryptamine **1a** (**Figure 4.2**), was chosen to illustrate the potential of mutasynthesis for the monoterpene indole class of alkaloids. Previous precursor-directed feeding studies have shown that 5-fluorotryptamine substrate **1a** could be turned over by downstream biosynthetic enzymes to yield a variety of fluorinated monoterpene indole alkaloid analogs[13]. A representative silenced line (cell line 3) was incubated with varying concentrations (250 – 2500 μM) of 5-fluorotryptamine **1a** (**Figure 4.11**). Two representative fluorinated alkaloids, fluoro-ajmalicine **3a**, and fluoro-serpentine **4a** were identified by exact mass (**Table 4.1**), UV spectrum (**Figure 4.12**) and by co-elution with authentic standards that were previously characterized by NMR[13] (**Figure 4.11**). When supplemented with natural tryptamine **1**, silenced hairy root cultures produced catharanthine **5** and tabersonine **6** as the only observable compounds with *m/z* 337. When supplemented with 5-fluorotryptamine **1a**, silenced lines yielded two compounds at *m/z* (337 + 18), the expected molecular weight of fluoro-catharanthine **5a** (expected, 355.1816; observed, 355.1818) and fluoro-tabersonine **6a** (expected, 355.1816; observed, 355.1811). Additionally, UV spectra (**Figure 4.12**) and tandem MS/MS (**Figure 4.13**) of these two compounds matched authentic standards of catharanthine **5** and tabersonine **6,** suggesting a structural assignment of **5a** and **6a**.

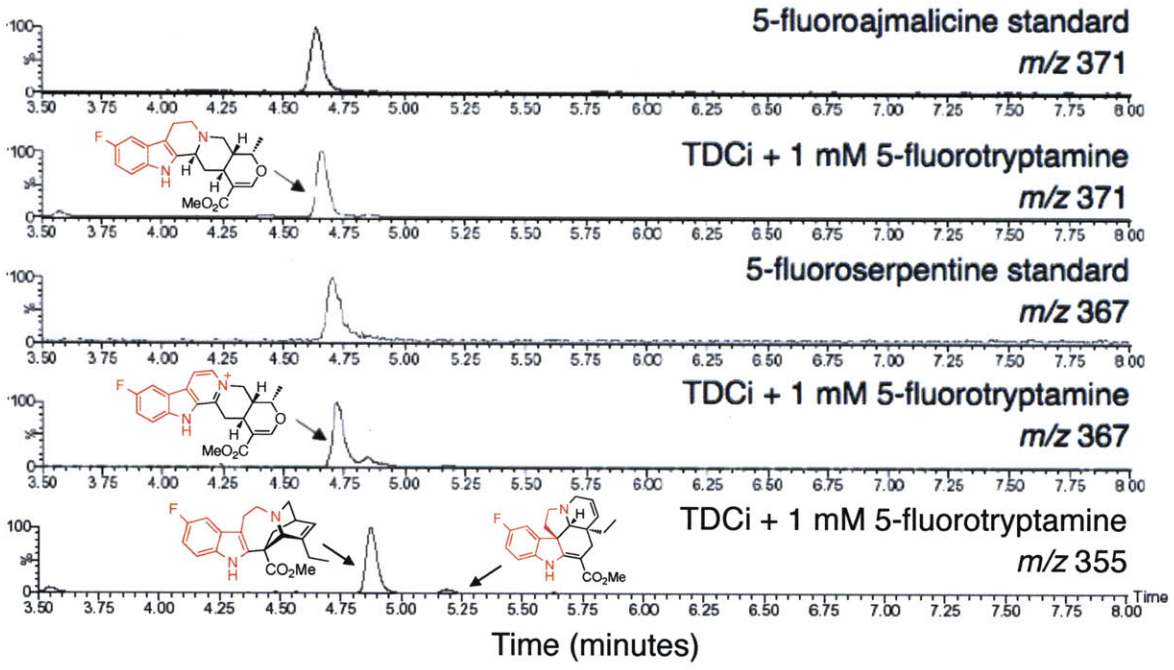

Figure 4.11. Extracted LC-MS chromatograms showing the presence of fluorinated ajmalicine **3a**, serpentine **4a**, catharanthine **5a** and tabersonine **6a**. These compounds are only present when 5-flourotryptamine **1a** is added to the culture media. Results using a concentration of 1.0 mM 5-fluorotryptamine are shown. Authentic standards of fluorinated ajmalicine are serpentine are also shown.

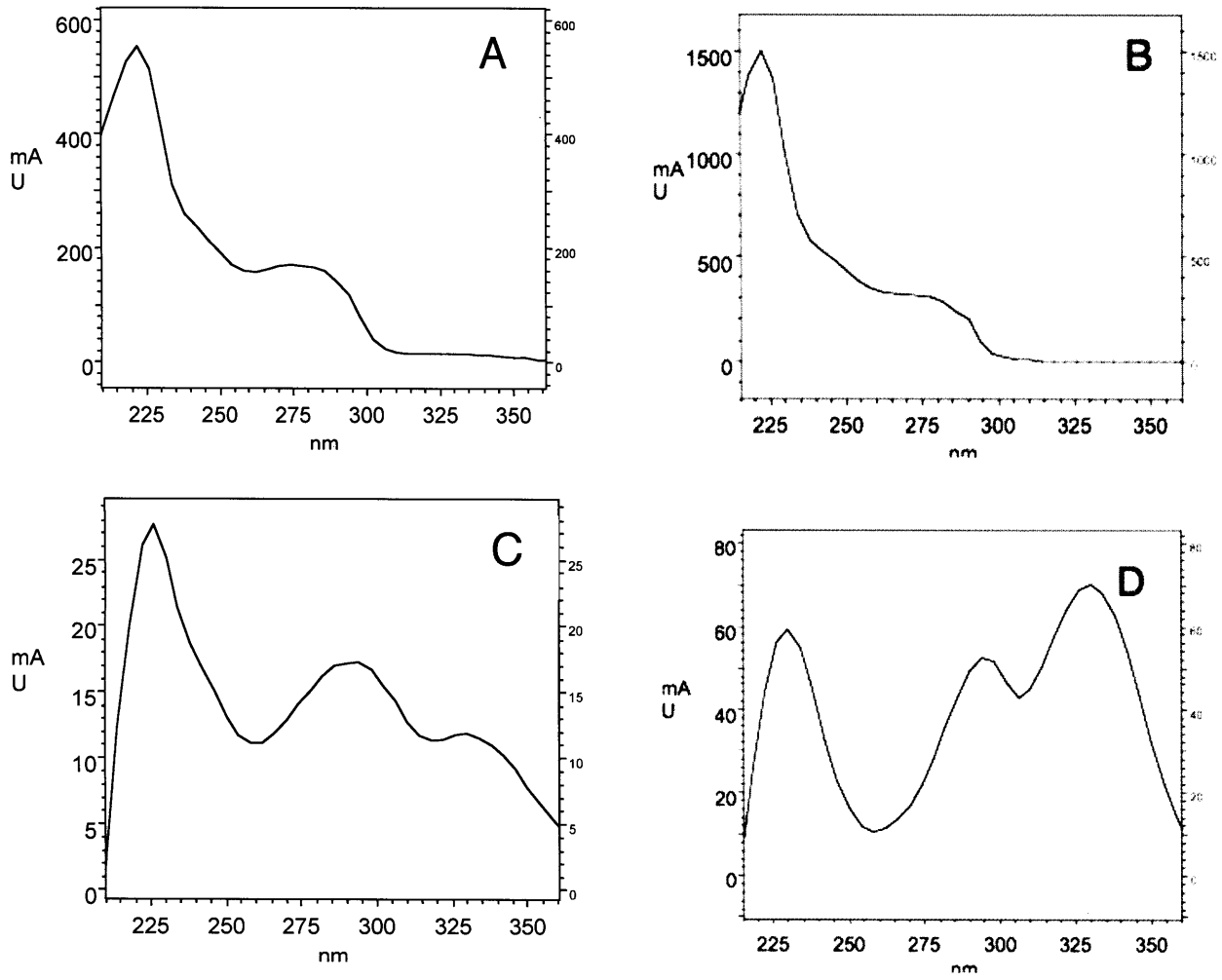

Figure 4.12 A-D. UV spectra of alkaloid standards and selected unnatural alkaloids from TDCi hairy root fed with 5-fluorotryptamine **1a** (0.5 mM). **A.** 5-fluoroajmalicine **3a**. **B.** ajmalicine **3** standard. **C.** 5-fluorotabersonine **6a**. **D.** tabersonine **6** standard.

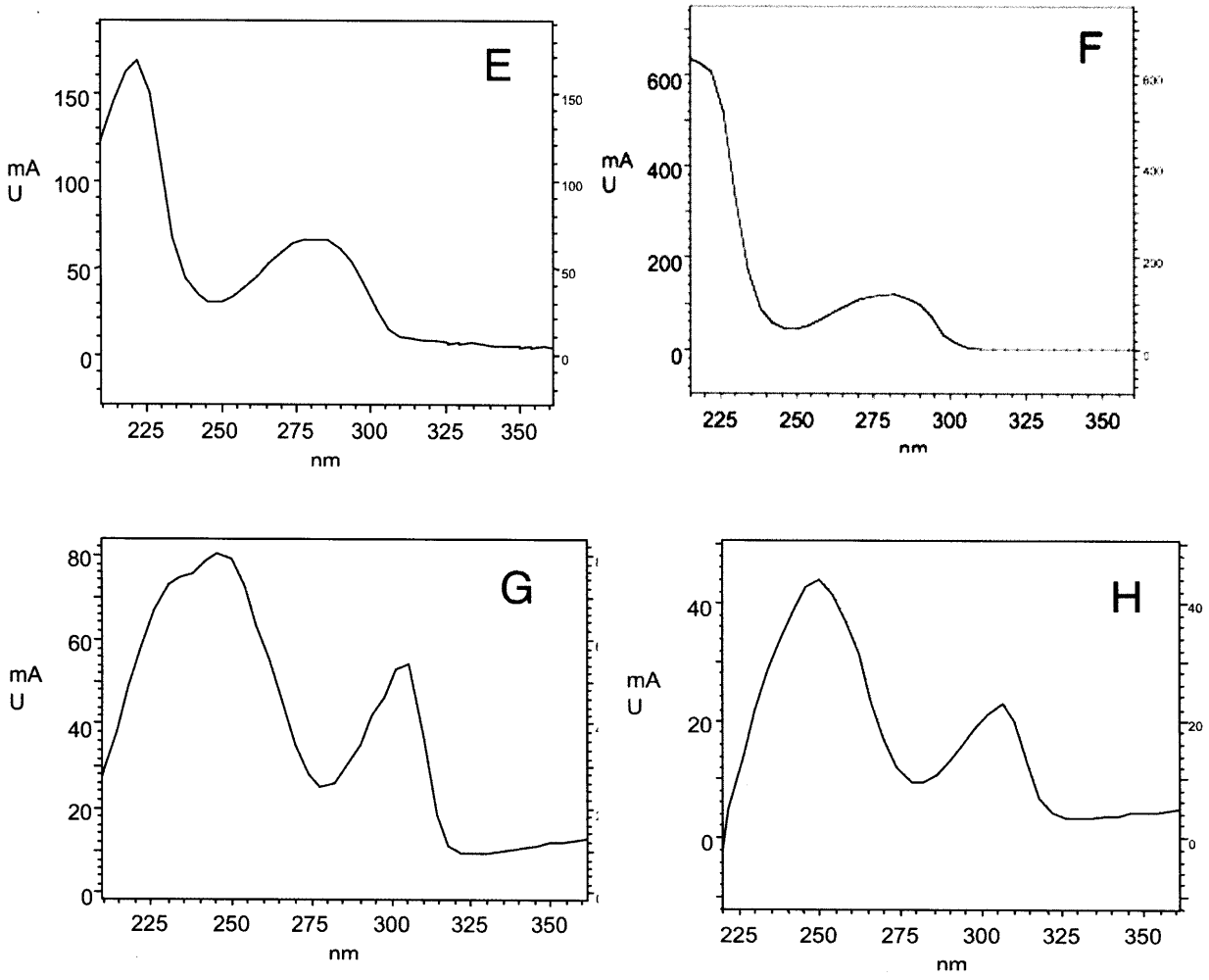

Figure 4.12 E-H. UV spectra of alkaloid standards and selected unnatural alkaloids from TDCi hairy root fed with 5-fluorotryptamine **1a** (0.5 mM). **E.** 5-fluorocatharanthine **5a**. **F.** catharanthine **5** standard. **G.** 5-fluoroserpentine **4a**. **H.** serpentine **4**standard.

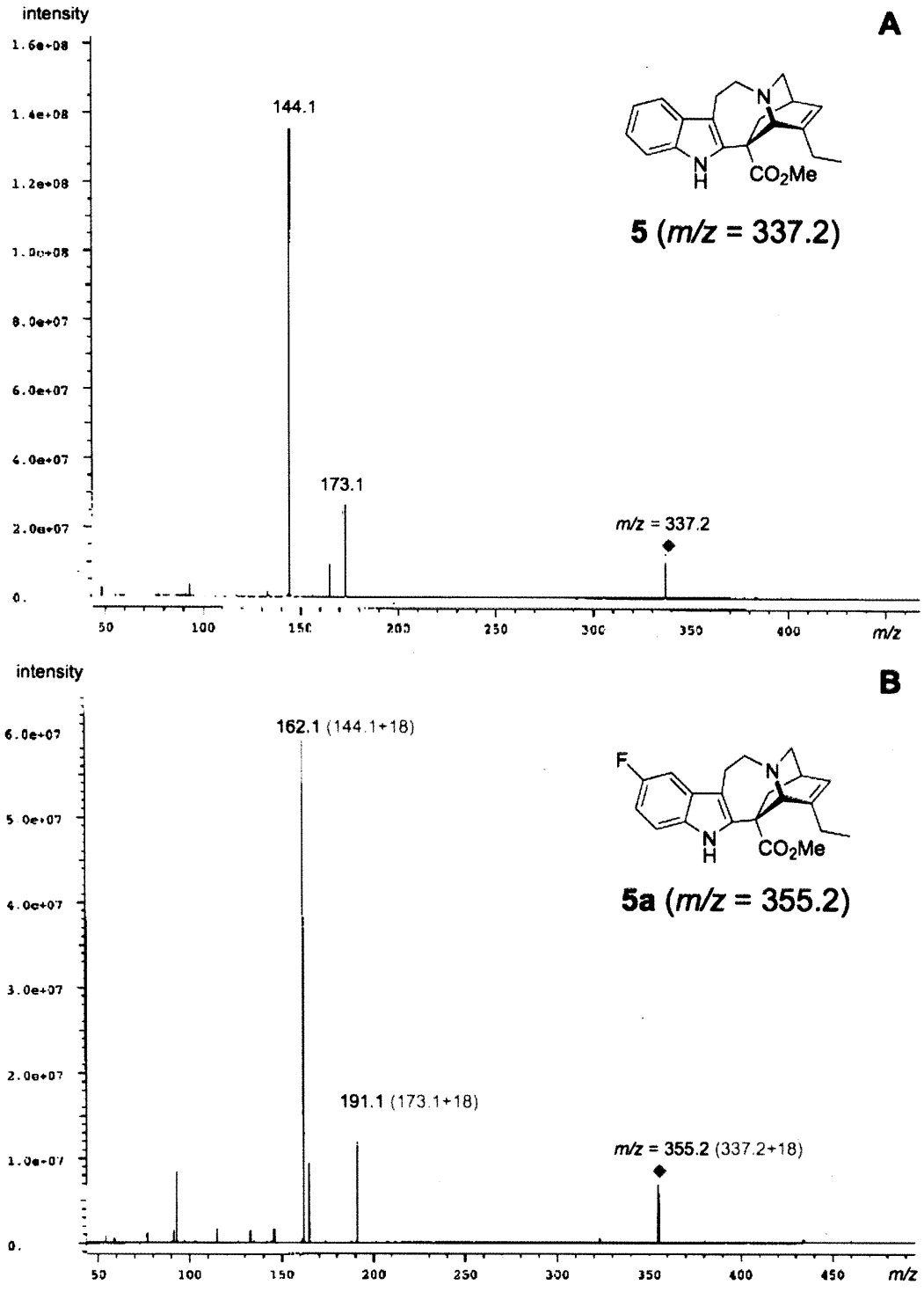

Figure 4.13 A (top) and B (bottom). MS/MS analysis for **(A)** catharanthine **5** standard and **(B)** fluorinated catharanthine **5a**. **(A)** Catharanthine is identified as the *m/z* = 337.2 ion showing the fragments *m/z* = 173.1 and 144.1. **(B)** Fluorinated catharanthine is identified as the *m/z* = 355.2 (337.2 + 18) ion showing the fragments *m/z* = 191.1 (173.1 + 18) and 162.1 (144.1 + 18).

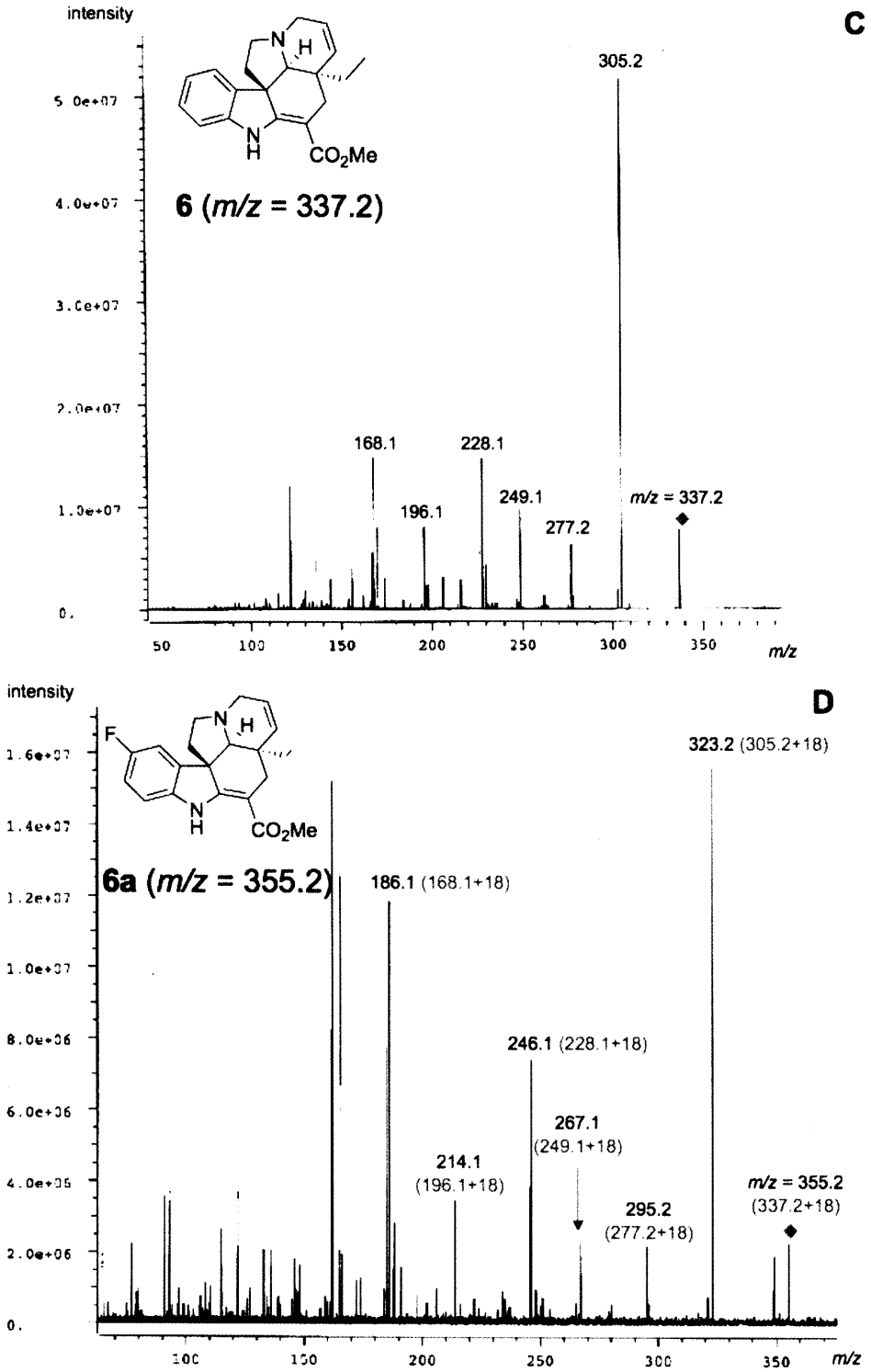

Figure 4.13 C (top) and D (bottom). MS/MS analysis for **(C)** tabersonine **6** standard and **(D)** fluorinated tabersonine. **(C)** Tabersonine is identified as the m/z = 337.2 ion showing the fragments m/z = 305.2, 277.2, 249.1, 228.1, 196.1 and 168.1. **(D)** Fluorinated tabersonine is identified as the m/z = 355.2 (337.2 + 18) ion showing the fragments m/z = 323.2 (305.2 + 18), 295.2 (277.2 + 18), 267.1 (249.1 + 18), 246.1 (228.1 + 18), 214.1 (196.1 + 18), and 186.1 (168.1 + 18).

Mutasynthesis often leads to higher yields and purity of unnatural products over precursor-directed feeding since the biosynthesis of the natural starting material is genetically silenced, and the producing organism is forced to utilize exogenously supplied substrates for product biosynthesis. This proved to be the case for TDC silenced lines; the complex mixture of alkaloid products was greatly simplified, since no natural alkaloids derived from endogenous tryptamine **1** were present (**Figure 4.14**). We also compared the yields of fluorinated alkaloids in both wild type and a representative silenced line fed with 5-fluorotryptamine using mass spectrometry in tandem with high performance liquid chromatography (**Figure 4.15**). The levels of fluorinated ajmalicine **3a** and the compound assigned as catharanthine **5a** were greater in the representative silenced line, suggesting that some pathway branches could support increased production levels of the desired nonnatural compounds when not challenged with competing natural substrate. Yields of fluorinated serpentine **4a** remained approximately the same in silenced and wild type cultures, suggesting that serpentine biosynthesis may be tightly regulated. Surprisingly, the yield of the compound assigned as fluorinated tabersonine **6a** was approximately two-fold higher in the wild type line compared to the silenced line, suggesting that tabersonine biosynthesis was somewhat adversely affected by suppression of tryptophan decarboxylase or the transformation process (**Figure 4.15**). The proportions of the fluorinated alkaloids produced in the silenced cultures are different from the proportions of fluorinated alkaloids produced with the wild lines. As the genes involved in the biosynthesis of ajmalicine **3**, serpentine **4**, catharanthine **5** and tabersonine **6** are identified, it will become possible to understand the underlying mechanism for the different alkaloid accumulation levels between wild type and silenced lines.

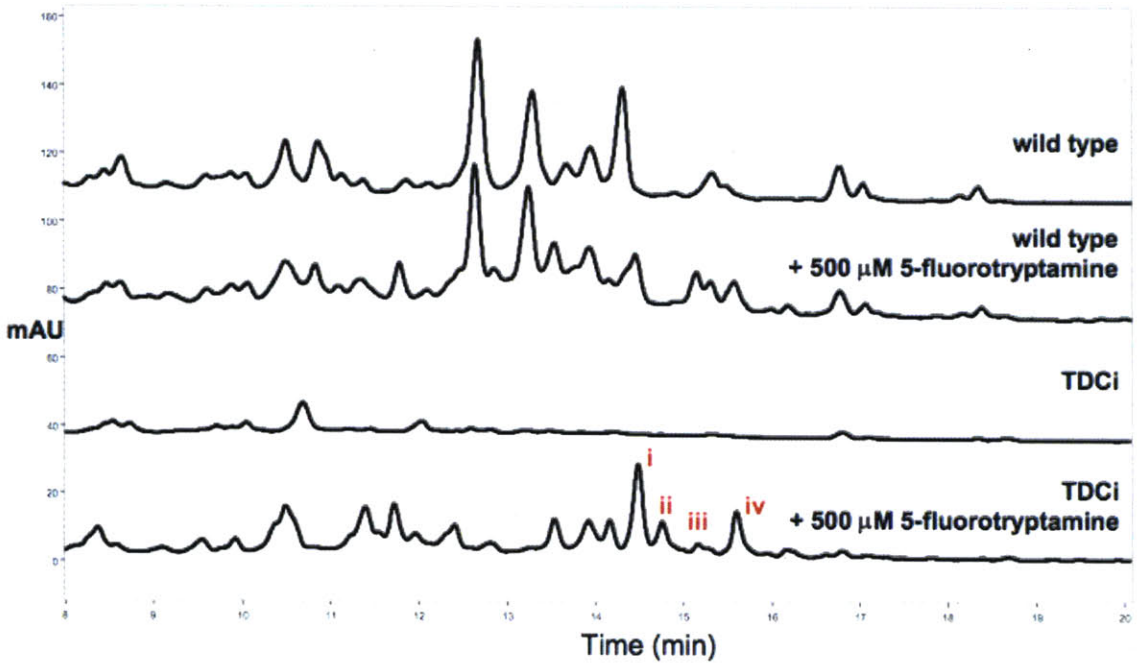

Figure 4.14. Metabolite production in wild type and TDCi line as evidenced by high performance liquid chromatography analysis of *C. roseus* hairy root extracts. The alkaloid extracts were run on a Hibar RT 250-4 prepacked reverse phase column using a gradient of 10-60% acetonitrile/water (0.1% TFA) over 25 minutes at 1 mL/min. Alkaloids were monitored at 280 nm. i, fluoro-ajmalicine **3a**; ii, fluoro-catharanthine **5a**; iii, fluoro-tabersonine **6a**; and iv, fluoro-serpentine **4a**.

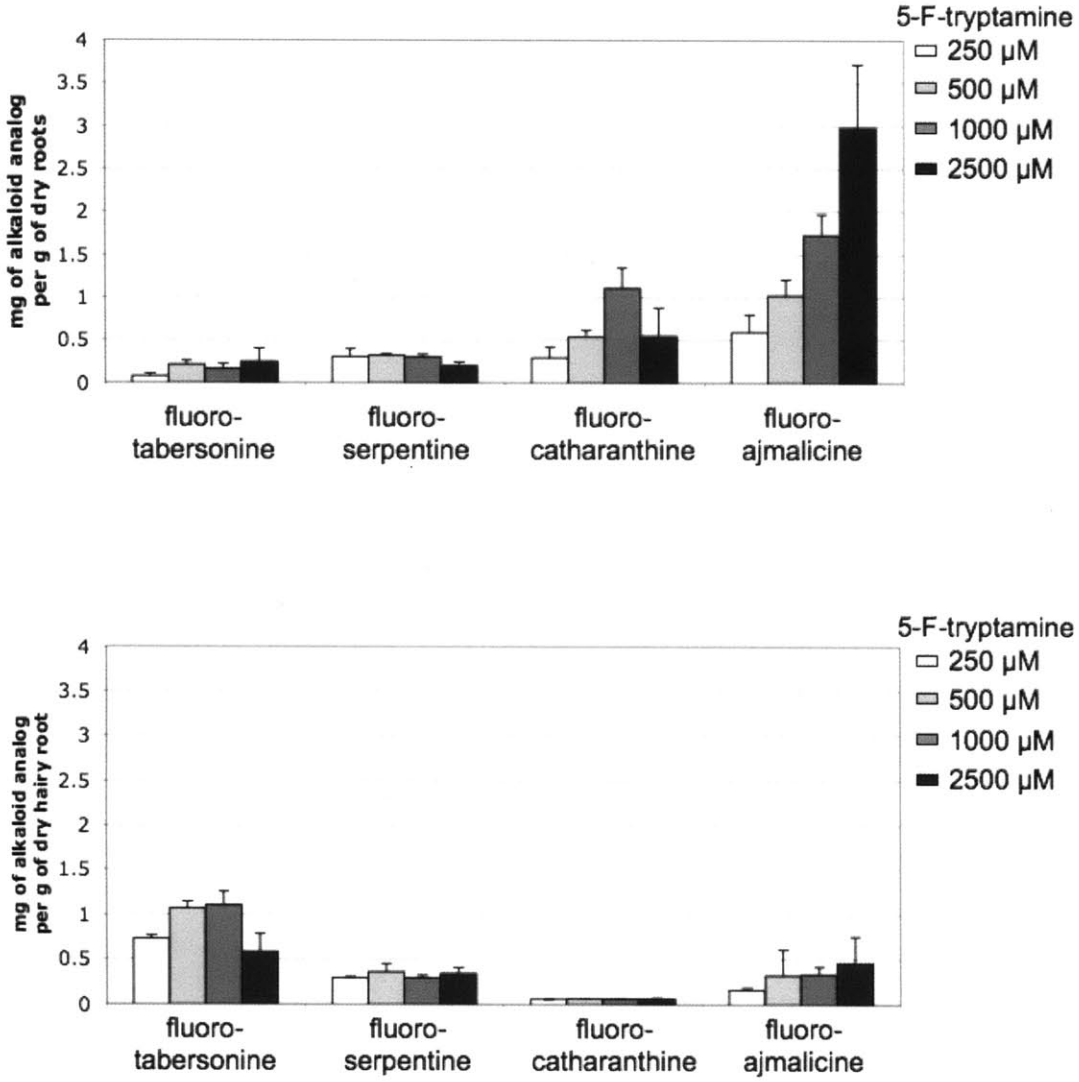

Figure 4.15. Quantification of unnatural alkaloid production in a suppressed and wild type line fed with 5-fluorotryptamine **1a** (500 μM, 1000 μM and 2500 μM). Production levels were evaluated in *C. roseus* extracts by mass spectrometry and represent the average of three measurements. **Top.** Levels of fluorinated alkaloids produced in a representative silenced line incubated with 5-fluorotryptamine **1a**. **Bottom.** Levels of fluorinated alkaloids produced in a wild type line incubated with 5-fluorotryptamine **1a**.

The levels of natural (non-fluorinated) ajmalicine **3**, serpentine **4**, catharanthine **5** and tabersonine **6** alkaloids were also quantified in wild type cultures fed with 5-fluorotryptamine **1a** (**Figure 4.16**). In the wild type line, natural ajmalicine **3** levels were significantly greater than fluorinated ajmalicine **3a**, while catharanthine **5** or **5a** was not observed at all in the wild type hairy root line for reasons that are not clear[26]. Natural serpentine **4** was produced at approximately the same level as fluorinated serpentine **4a** in the wild type line. At high concentrations of 5-fluorotryptamine **1a**, levels of natural tabersonine **6** and the compound assigned as fluorinated tabersonine **6a** were similar. We speculated that the flux of the unnatural substrate through some branches of the pathway increased when the natural, endogenous substrate was unavailable.

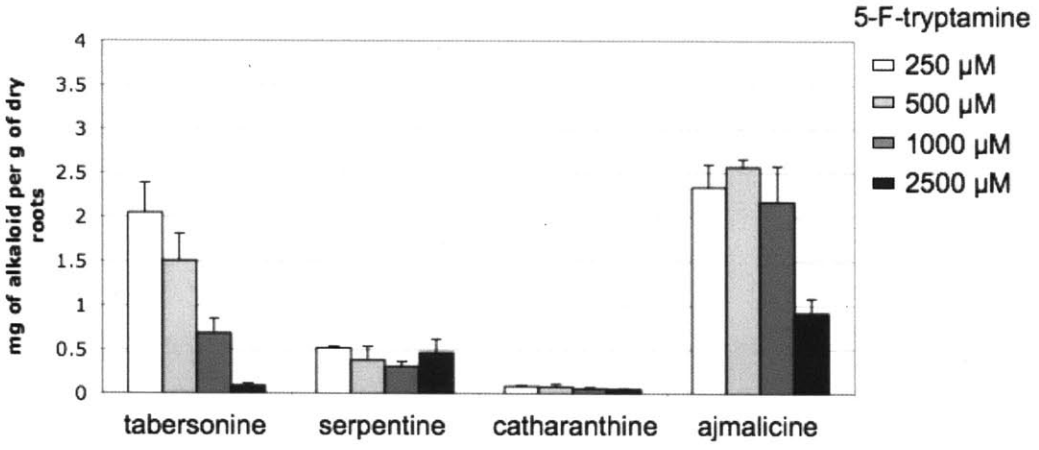

Figure 4.16. Quantification of unnatural alkaloid production in wild type line fed with 5-fluorotryptamine **1a** (500 μM, 1000 μM and 2500 μM). Production levels were evaluated in *C. roseus* extracts by mass spectrometry and represent the average of three measurements. **c.** Levels of natural, non-fluorinated alkaloids produced in a wild type line incubated with 5-fluorotryptamine **1a**.

4.2.5 Accumulation of Secologanin in Tryptophan Decarboxylase Silenced Lines

In *C. roseus*, tryptamine **1** reacts with the iridoid terpene secologanin **7** to form strictosidine **8** (**Figure 4.1**). The absence of tryptamine should therefore lead to increased accumulation of secologanin. Yields of secologanin **7** were estimated by mass spectrometry analysis of crude *C. roseus* extracts. While secologanin **7** is not normally found in large quantities in wild type *C. roseus* plants or tissue, silenced lines showed a dramatic increase in **7** (**Figure 4.17**). Approximately 0.15 g of secologanin per g dry weight in a representative silenced culture was observed, indicating that silencing of tryptophan decarboxylase led to dramatically increased secologanin **7** levels. When tryptamine **1** or a tryptamine analog was added to this silenced culture, the levels of secologanin decreased as this iridoid terpene was converted into alkaloids. Nevertheless, 0.11 g secologanin **7** per g culture dry weight remained even when 500 μM tryptamine **1** was incubated with this silenced culture for 7 days. The levels of secologanin **7** in these silenced lines appeared to far exceed the capacity for downstream alkaloid biosynthesis (approximately 5 mg monoterpene indole alkaloid per gram of dry culture weight) (**Figure 4.10, 4.15-4.16**).

Although most of the genes involved in secologanin biosynthesis remain uncharacterized, real time reverse transcription PCR indicated that one or both of the two best characterized secologanin biosynthetic genes, secologanin synthase (SLS)[33,34] and geraniol-10-hydroxylase (G10H)[35], were upregulated in seven silenced lines (**Figure 4.18**). As stated above, high concentrations of secologanin (0.11 g/ g dry weight) were observed even after tryptamine was added to silenced lines, indicating that tryptamine

does not repress secologanin production. Therefore, while the exact mechanism of how secologanin is upregulated remains unclear, silencing of tryptophan decarboxylase clearly affects the expression of upstream biosynthetic enzymes. Further work to explore the regulatory network of alkaloid biosynthetic genes in *C. roseus* is imperative.

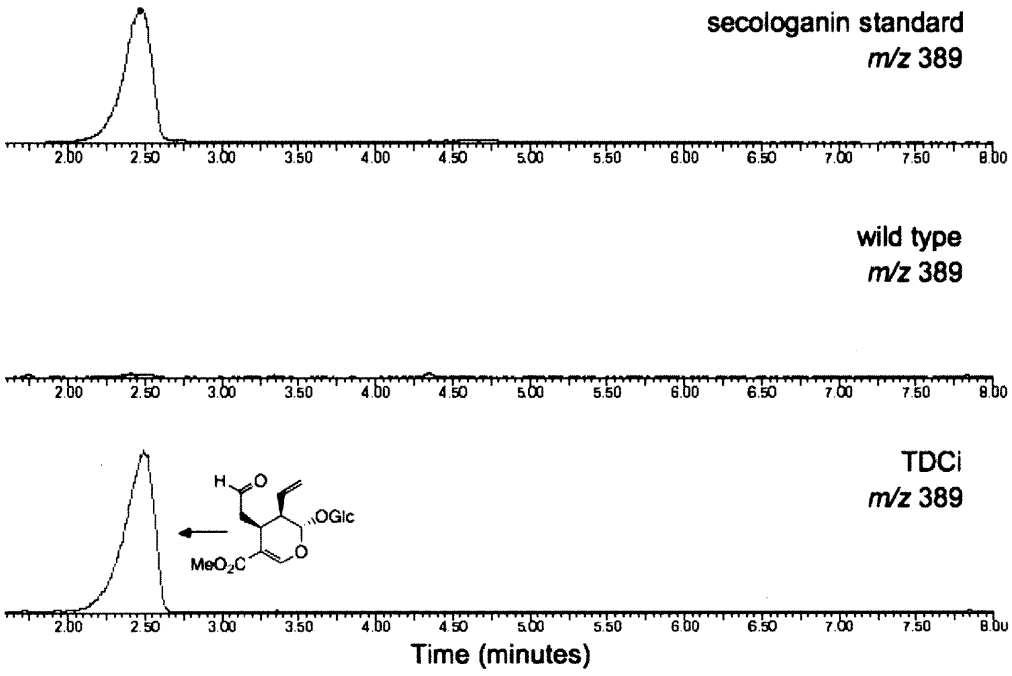

Figure 4.17. Secologanin **7** production in wild type and tryptophan decarboxylase suppressed lines as evidenced by LC-MS analysis of *C. roseus* extracts. An authentic standard of secologanin **7** is also shown.

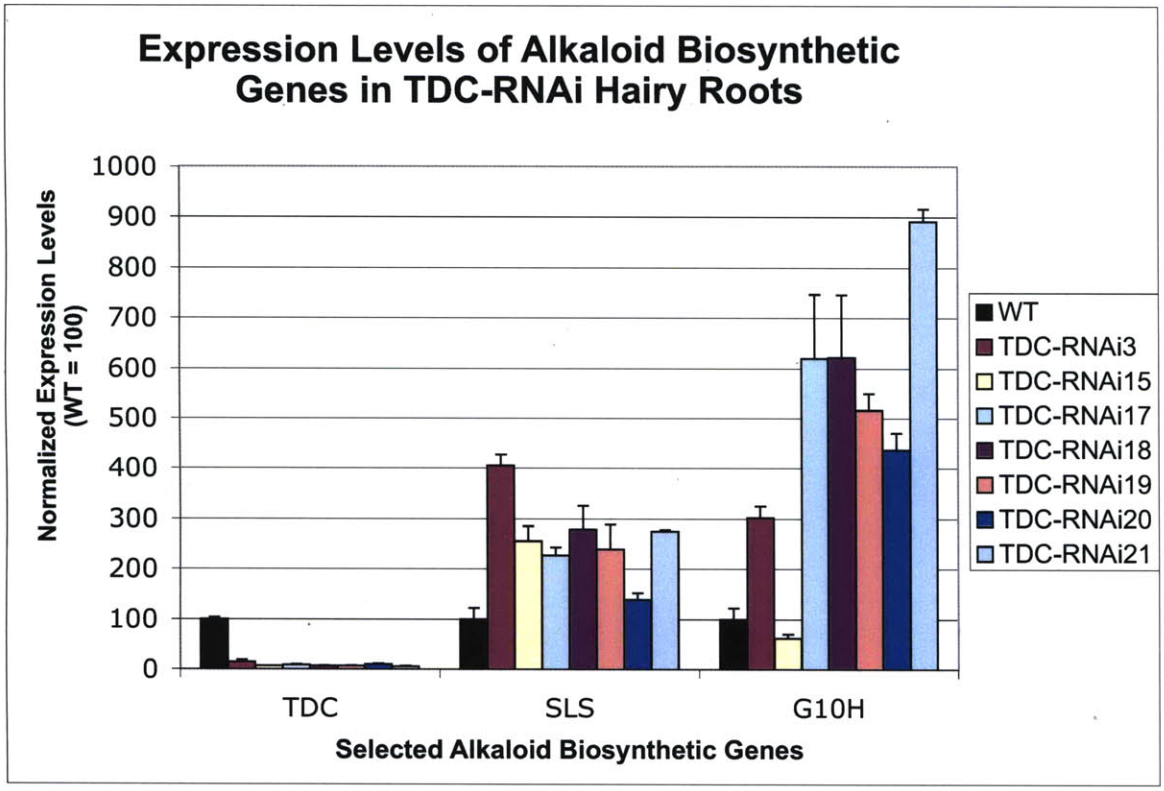

Figure 4.18. Expression levels of SLS and G10H in 7 different TDC-suppressed lines measured by RT-PCR. Expression levels of the silenced lines are normalized to the expression levels in the wild type hairy root line. TDC (tryptophan decarboxylase) expression levels are shown for comparison. SLS (secologanin synthase), G10H (geraniol-10-hydroxylase).

4.2.6 Regeneration of *C. roseus* Plants from Tryptophan Decarboxylase Silenced Lines

The lack of tryptamine **1** and downstream alkaloids, along with secologanin **7** accumulation, did not appear to affect the growth or morphology of the silenced cultures, indicating that tryptamine and downstream alkaloids do not play an essential role in *C. roseus* hairy root culture development (**Figure 4.19**). While the endogeneous role of alkaloids in plants has not been fully elucidated, current evidence suggests that alkaloids are generally involved in plant defense against pathogens, insects, and herbivores due to their potent toxicity[36]. We envisioned that the regeneration of alkaloid deficient *C. roseus* plants from TDCi hairy roots would give further insight into this long-standing assumption. A regeneration process of *C. roseus plants* from hair root culture has previously been reported [37]. We applied this strategy using the TDCi hairy roots to yield whole plants (**Figure 4.20**). Interestingly, the regenerated plants exhibited significant growth retardation and died several days after they were transferred to Miracle Gro soil. Together, these experiments suggest that while tryptamine and monoterpene indole alkaloids do not appear to play an essential role in growth or development in *C. roseus* hairy root culture, they may be vital for whole plant survival in a non-controlled environment.

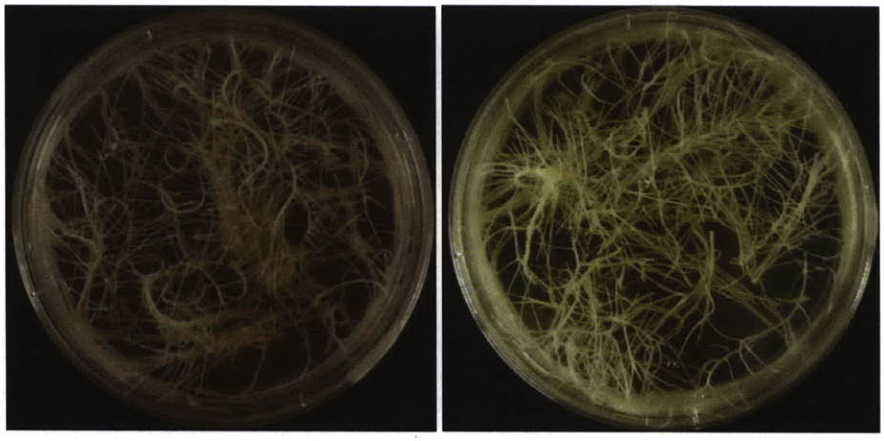

Figure 4.19. Two-week-old wild-type (left) and TDCi (right) hairy roots in solid Gamborg's B5 media.

Figure 4.20. Regeneration of alkaloid deficient *C. roseus* plants from TDCi root culture.

4.3 Conclusions

Fermentation is an attractive and powerful strategy for large-scale production of natural product analogs. Replacement of an endogenous starting material with an unnatural compound, a strategy that has been broadly applied in prokaryotic biosynthetic pathways, has now been successfully used in a plant alkaloid pathway to yield exclusively unnatural alkaloid products. Downregulation of tryptophan decarboxylase in *C. roseus* hairy root culture allowed the strategic incorporation of exogenously supplied tryptamine substrate **1** into the monoterpene indole alkaloid pathway. Using this strategy, natural alkaloid production was suppressed, and only unnatural alkaloids were produced when a fluorinated tryptamine analog **1a** was introduced to the culture media. Silencing tryptophan decarboxylase did not impact the expression levels of either the key transcription factor Orca3 or the known downstream biosynthetic enzymes, strictosidine synthase and strictosidine glucosidase. We envision that RNA silencing methods can also be used with other known downstream biosynthetic enzymes—or even unknown ones as they become identified—to more effectively engineer the production of the desired unnatural alkaloid in plants and plant culture. In conclusion, our strategy allows for practical and efficient production of novel monoterpene indole alkaloids that are not synthetically accessible.

4.4 Experimental Methods

4.4.1 Construction of pTDCi Vector

The construction of pTDCi vector was designed and executed by Justin Maresh. A 408 base pair fragment at the 5' end of the tryptophan decarboxylase open reading frame,

which did not show significant homology to any known *C. roseus* genes, flanked by *att*B1 (forward) and *att*B2 (reverse) was obtained by reverse-transcription PCR amplification from *C. roseus* seedling mRNA (forward primer: CACCGCAGCATTGATTCAACAAATGTAG; reverse primer: AGCTATCGATGGTACCTCATTTCTAATTCGGTGGCGGCTG). The resulting PCR product was then inserted into pENTR-TOPO (Invitrogen) vector via BP clonase mediated recombination using the manufacturer's protocol. The gene fragment from the intermediate clone was subsequently inserted into pHELLSGATE12 using LR clonase mediated recombination. The final pTDCi construct was verified by sequencing to ensure plasmid integrity.

4.4.2 Generation of pTDCi Hairy Roots

The pTDCi vector was transformed into *A. rhizogenes* ATCC 15834 via electroporation (1mm cuvette, 1.25 kV). Transformation of *C. roseus* seedlings with the generated *Agrobacterium* strain was performed as previously reported[25]. Briefly, 250-300 *C. roseus* seeds (Vinca Little Bright Eyes, Nature Hills Nursery) were germinated aseptically and grown in a 16-hour light/dark cycle for 2-3 weeks on standard Gamborg's B5 media (full strength basal salts, full strength vitamins, 30 g/L sucrose, pH 5.7). Seedlings were wounded with a scalpel at the stem tip, and transformed *A. rhizogenes* from a freshly grown liquid culture was inoculated on the wound. Hairy roots appeared at the wound site 2-3 weeks after infection. Root tips longer than 5 mm were excised after 6 weeks and transferred to Gamborg's B5 solid media (half strength basal salts, full strength vitamins, 30 g/L sucrose, 6 g/L agar, pH 5.7) containing kanamycin (0.1 mg/mL) for selection, and

cefotaxime (0.25 mg/mL) for removal of the remaining bacteria. Lines were cultured on media with and without tryptamine (50 μM), in case tryptamine proved to be essential for cell survival. Since tryptamine did not appear to be required for survival of these lines, all subsequent culture media used for second and third rounds of subculturing was not supplemented with tryptamine. All cultures were grown in the dark at 26°C. After the selection process, hairy roots were subcultured at least once on solid media lacking both kanamycin and cefotaxime prior to adaptation to liquid culture.

To adapt hairy roots to liquid media, approximately 200 mg of hairy roots (typically five 3-4 cm long stem tips) from each line that grew successfully on solid media were transferred to 50 mL of half-strength Gamborg's B5 liquid media (half strength basal salts, full strength vitamins, 30 g/L sucrose, pH 5.7). The cultures were grown at 26°C in the dark at 125 rpm. All lines were maintained on a 14-21 day subculture cycle depending on the growth rate of each line.

4.4.3 Verification of Transferred DNA (T-DNA) Integration by Genomic DNA Analysis

The genomic DNA from transformed hairy roots was isolated (Qiagen DNeasy kit) and subjected to PCR amplification using T-DNA specific primers with STR primers serving as a positive control. Specifically, primers for PCR amplification were designed to amplify the complete STR gene, a region of the CaMV 35S promoter, the antibiotic resistance NPTII gene and the PDK intron.

4.4.4 Quantification of mRNA Production of Biosynthetic Genes by Real Time RT-PCR

mRNA from transformed hairy roots was isolated and purified from genomic DNA using Qiagen RNeasy Plant Mini Kit and RNase-free DNaseI, respectively. The resulting mRNA was then reverse-transcribed to cDNA using Qiagen QuantiTect Reverse transcription kit and subjected to PCR analysis with Qiagen SYBR Green PCR kit and a Biorad DNA Engine Opticon 2 system. The threshold-cycle (C_T) was determined as the cycle with a signal higher than that of the background plus 10 x standard deviation (SD). *C. roseus* 40S ribosomal protein S9 (Rps9), a house keeping gene, was used to normalize the amount of the total mRNA in all samples.

4.4.5 Assessment of Alkaloid Production Rescue by Addition of Tryptamine

Ten root tips from hairy roots transformed with pTDCi were subcultured in 50 mL Gamborg's B5 liquid media and grown at 26°C in the dark at 125 rpm for eighteen days prior to supplementing the media with tryptamine **1** (Alfa Aesar) at 0, 62.5, 125, 250, 500, 1000 and 2500 μM. After one week of co-cultivation with the substrate, hairy roots were ground with a mortar, pestle and 100 μm glass beads in methanol (10 mL/g of fresh weight hairy roots) from the harvested tissue. The crude natural product mixtures were subjected to LC-MS analysis (Micromass LCT Premier TOF Mass Spectrometer). Peak integration and analysis was performed with MassLynx 4.1. To convert peak area to milligrams, standard curves of the natural alkaloids ajmalicine **3**, serpentine **4**, catharanthine **5** and tabersonine **6** were constructed. The levels shown in **Figures 4.10, 4.15** and **4.16** represent the average of three feeding experiments, with the with error bars representing the standard deviation.

4.4.6 Assessment of Alkaloid Mutasynthesis

Ten root tips from hairy roots transformed with pTDCi were subcultured in 50 mL Gamborg's B5 liquid media and grown at 26°C in the dark at 125 rpm for eighteen days prior to supplementing the media with either d4-tryptamine (500 μM) (Aldrich), d5-L-tryptophan (500 μM) (Aldrich), or 5-fluorotrytamine **1a** (250, 500, 1000, 2500 μM) (MP Biomedicals). After one week of co-cultivation with the substrates, hairy roots were processed as described above. Authentic standards of fluorinated ajmalicine **3a** and fluorinated serpentine **4a** were previously isolated and characterized[13].

4.4.7 Expression Levels of Secologanin Biosynthetic Genes SLS and G10H

Primers for real-time RT-PCR of transformed hairy roots for secologanin synthase (SLS) (SLS_for: GGATTGGGCATGGTTTACTC and SLS_rev: CCATGGGTTTAGACAAGGCT, amplicon size 140 bp) and geraniol-10-hydroxylase (G10H) (G10H_for: TGCTTGGACCTGTTTGTAGC and G10H_rev: TCCTCTGCCGATTACTTGTG amplicon size 132 bp).

4.4.8 Regeneration of C. roseus Plants from Transformed Hairy Roots Expressing STR Mutant

Regeneration of transformed hairy roots expressing STR mutant to whole plants was performed as previously reported[37]. Briefly, one-centimeter-long root tips of two-week-old transformed hairy roots were excised and transferred to shoot regeneration media (full strength Murashige and Skoog basal salts and vitamins, 31 μM 6-benzyladenine, 5.4 μM α-naphthaleneacetic acid, 30 g/L sucrose, pH 5.7). After nine weeks on this media,

explants were transferred to root regeneration media (half strength Murashige and Skoog basal, full strength Murashige and Skoog vitamins, 30 g/L sucrose, pH 5.7). After four weeks on this media, regenerated plants were transferred to full strength Gamborg's B5 media (full strength basal salts, full strength vitamins, 30 g/L sucrose, pH 5.7). After three weeks of acclimation, regenerated plants were transferred to Miracle gro soil and maintained in a culture room.

4.5 Acknowledgements

We gratefully acknowledge financial support from the NIH (GM074820), the National Science Foundation and the American Cancer Society (RSG-07-025-01-CDD). We thank Dr. Li Li for obtaining mass spectrometric data at the MIT Department of Chemistry Instrumentation Facility. I thank Dr. Justin J. Maresh for designing and constructing pTDCi vector.

4.6 References

1. Ganesan, A., The impact of natural products upon modern drug discovery. *Curr Opin Chem Biol* **2008,** *12* (3), 306-17.
2. Khosla, C.; Keasling, J. D., Metabolic engineering for drug discovery and development. *Nat. Rev. Drug Disc.* **2003,** *2* (1019-1025).
3. Birch, A. J., The biosynthesis of antibiotics. . *Pure Appl. Chem.* **1963,** *7*, 527-537.
4. Shier, W. T.; Rinehart, K. L.; Gottlieb, D., Preparation of four new antibiotics from a mutant of Streptomyces fradiae. . *Proc. Natl. Acad. Sci. USA* **1969,** *63*, 198-204.
5. Weissman, K., Mutasynthesis- uniting chemistry and genetics for drug discovery. *Trends Biotechnol.* **2007,** *25*, 139-142.
6. Weist, S.; Sussmuth, R. D., Mutational biosynthesis—a tool for the generation of structural diversity in the biosynthesis of antibiotics. *Appl. Microbiol. Biotechnol.* **2005,** *68*, 141-150.
7. O'Connor, S. E.; Maresh, J., Chemistry and biology of monoterpene indole alkaloid biosynthesis. *Nat. Prod. Rep.* **2006,** *23*, 532-547.

8. Van der Heijden, R.; Jacobs, D. I.; Snoeijer, W.; Hallard, D. V., R., The Catharanthus alkaloids: pharmacognosy and biotechnology. *Curr. Med. Chem.* **2004,** *11*, 607-628.
9. de Luca, V.; Marineau, C.; Brisson, N., Molecular cloning and analysis of a cDNA encoding a plant tryptophan decarboxylase. *Proc. Natl. Acad. Sci. USA* **1989,** *86*, 2582-2586.
10. Facchini, P. J.; Huber-Allanach, K. L.; Tari, L. W., Plant aromatic L-amino acid decarboxylases: evolution, biochemistry, regulation, and metabolic engineering applications. *Phytochemistry* **2000,** *54*, 121-138.
11. Bernhardt, P.; McCoy, E.; O'Connor, S. E., Rapid identification of enzyme variants for reengineered alkaloid biosynthesis in periwinkle. *Chem. Biol.* **2007,** *14*, 888-897.
12. McCoy, E.; Galan, M. C.; O'Connor, S. E., Substrate specificity of strictosidine synthase. *Bioorg. Med. Chem. Lett.* **2006,** *16*, 2475-2478.
13. McCoy, E.; O'Connor, S. E., Directed biosynthesis of alkaloid analogues in the medicinal plant periwinkle. *J. Am. Chem. Soc.* **2006,** *128*, 14276-14277.
14. Smith, T. A., Tryptamine and related compounds in plants. *Phytochemistry* **1977,** *16*, 171-177.
15. Gill, R. I. S.; Ellis, B. E.; Isman, M. B., Tryptamine induced resistance in tryptophan decarboxylase transgenic poplar and tobacco plants against their specific herbivores. *J. Chem. Ecol.* **2003,** *29*, 779-793.
16. Kang, S.; Kang, K.; Lee, K.; Back, K., Characterization of tryptamine 5-hydroxylase and serotonin
synthesis in rice plants. *Plant Cell Rep.* **2007,** *26*, 2009-2015.
17. Zhao, Y.; Christensen, S. K.; Fankhauser, C.; Cashman, J. R.; Cohen, J. D.; Weigel, D.; Chory, J., A role for flavin monooxygenase-like enzymes in auxin biosynthesis. *Science* **2001,** *291*, 306-309.
18. Kempin, S. H.; Liljegren, S. J.; Block, L. M.; Rounsley, S. D.; Yanofsky, M. F., Targeted disruption in Arabidopsis. *Nature* **1997,** *389*, 802-803.
19. Helliwell, C. A.; Waterhouse, P. M., RNA-mediated gene silencing in plants. *Meth. Enzymol.* **2005,** *392*, 24-35.
20. Voinnet, O.; Vain, P.; Angell, S.; Baulcombe, D. C., Systemic spread of sequence-specific transgene RNA degradation in plants is initiated by localized introduction of ectopic promoterless DNA. *Cell* **1998,** *95*, 177-187.
21. Waterhouse, P. M.; Graham, M. W.; Wang, M.-B., Virus resistance and gene silencing in plants can be induced by simultaneous expression of sense and antisense RNA. *Proc. Natl. Acad. Sci. USA* **1998,** *95*, 13959–13964.
22. Courdavault, V.; Thiersault, M.; Courtois, M.; Gantet, P.; Oudin, A.; Doireau, P.; St-Pierre, B.; Giglioli-Guivarc'h, N., CaaX-prenyltransferases are essential for expression of genes involved in the early stages of monoterpenoid biosynthetic pathway in Catharanthus roseus cells. *Plant Mol. Biol.* **2005,** *57*, 855-870.
23. Papona, N.; Vansiria, A.; Ganteta, P.; Chenieux, J. C.; Rideaub, M.; Creche, J., Histidine-containing phosphotransfer domain extinction by RNA interference turns o¡ a cytokinin signalling circuitry in Catharanthus roseus suspension cells. *FEBS Lett.* **2004,** *558*, 85-88.

24. Wesley, S. V.; Helliwell, C. A.; Smith, N. A.; Wang, M.; Rouse, D. T.; Liu, Q.; Gooding, P. S.; Singh, S. P.; Abbott, D.; Stoutjesdijk, P. A.; Robinson, S. P.; Gleave, A. P.; Green, A. G.; Waterhouse, P. M., Construct design for efficient, effective and high-throughput gene silencing in plants. . *Plant J.* **2001,** *27*, 581-590.
25. Hughes, E. H. H., Seung-Beom; Shanks, Jacqueline V.; San, Ka-Yiu; Gibson, Susan I., Characterization of an inducible promoter system in Catharanthus roseus hairy roots. *Biotechnology Progress* **2002,** *18*, 1183-1186.
26. Runguphan, W.; O'Connor, S. E., Metabolic reprogramming of plant cell culture. *Nat. Chem. Biol.* **2009,** *5*, 151-153.
27. van der Fits, L.; Memelink, J., ORCA3, a Jasmonate-responsive transcriptional regulator of plant primary and secondary metabolism. *Science* **2000,** *289*, 295-297.
28. McKnight, T. D.; Roessner, C. A.; Devagupta, R.; Scott, A. I.; Nessler, C., Nucleotide sequence of a cDNA encoding the vacuolar protein strictosidine synthase from Catharanthus roseus. *Nuc. Acids Res.* **1990,** *18*, 4939.
29. Geerlings, A.; Ibanez, M. M.-L.; Memelink, J.; Van der Heijden, R.; Verpoorte, R., Molecular cloning and analysis of strictosidine b-D-glucosidase, an enzyme in terpenoid indole alkaloid biosynthesis in Catharanthus roseus. *J. Biol. Chem.* **2000,** *275*, 3051-3056.
30. Allen, R. S.; Millgate, A. G.; Chitty, J. A.; Thisleton, J.; Miller, J. A. C.; Fist, A. J.; Gerlach, W. L.; Larkin, P. J., RNAi-mediated replacement of morphine with the nonnarcotic alkaloid reticuline in opium poppy. *Nat. Biotechnol.* **2004,** *22*, 1559-1566.
31. Romero, R. M.; Roberts, M. F.; Phillipson, J. D., Anthranilate synthase in microorganisms and plants. *Phytochemistry* **1995,** *39*, 263-276.
32. Miozzari, G.; Niederberger, P.; Hütter, R., Tryptophan biosynthesis in Saccharomyces cerevisiae: control of the flux through the pathway. *J. Bacteriol.* **1978,** *134*, 48-59.
33. Irmler, S.; Schroder, G.; St-Pierre, B.; Crouch, N. P.; Hotze, M.; Schmidt, J.; Strack, D.; Matern, U.; Schroder, J., Indole alkaloid biosynthesis in Catharanthus roseus: new enzyme activities and identification of cytochrome P450 CYP72A1 as secologanin synthase. *Plant J.* **2000,** *24*, 797-804.
34. Yamamoto, H.; Katano, N.; Ooi, A.; Inoue, K., Secologanin synthase which catalyzes the oxidative cleavage of loganin into secologanin is a cytochrome P450. *Phytochemistry* **2000,** *53*, 7-12.
35. Collu, G.; Unver, N.; Peltenburg-Looman, A. M. G.; van der Heijden, R.; Verpoorte, R.; Memelink, J., Geraniol 10-hydroxylase, a cytochrome P450 enzyme involved in terpenoid indole alkaloid biosynthesis. *FEBS Lett.* **2001,** *508*, 215-220.
36. Hartmann, T., Plant-derived secondary metabolites as defensive chemicals in herbivorous insects: a case study in chemical ecology. *Planta* **2004,** *219* (1), 1-4.
37. Choi, P. S.; Kim, Y. D.; Choi, K. M.; Chung, H. J.; Choi, D. W.; Liu, J. R., Plant regeneration from hairy root cultures transformed by infection with Agrobacterium rhizogenes. *Plant Cell Rep.* **2004,** *22*, 828-831.

CHAPTER 5

CHEMOGENETIC APPROACHES TO

FURTHER DERIVATIZE HALOGENATED ALKALOIDS

5.1 Introduction

Modification of natural products can yield analogs of natural products, or "unnatural products", with improved or novel medicinal properties[1]. Traditional approaches to generate analogs include total and semi-syntheses, precursor-directed biosynthesis, mutasynthesis and combinatorial biosynthesis[2-7]. More recently, Goss and coworkers have utilized a new approach that involves the introduction of a gene to complement a native biosynthetic pathway followed by postbiosynthetic chemical derivatization[8]. Using this "chemogenetic" approach, the team successfully generated analogs of the uridyl peptide antibiotic pacidamycin.

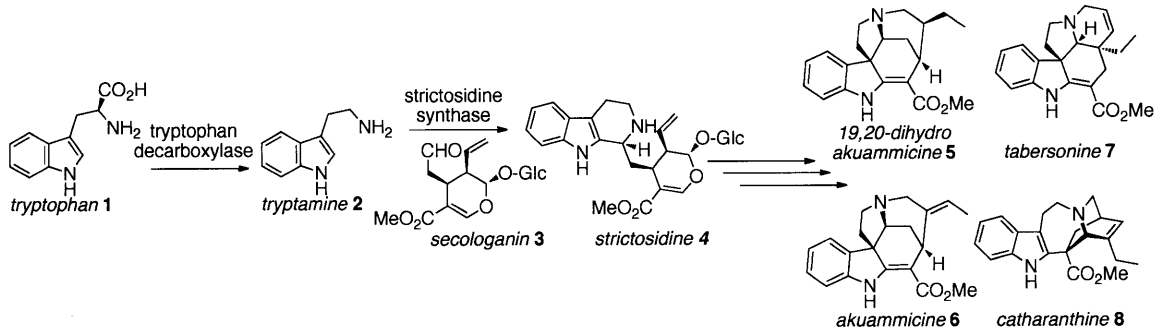

Figure 5.1 Biosynthesis of monoterpene indole alkaloids in *C. roseus*.

The biosynthesis of monoterpene indole alkaloid (MIA) in *C. roseus* is exceptionally complicated and only partially characterized[9]. This pathway produces a variety of alkaloids with diverse biological activities and complex molecular architecture from the iridoid terpene secologanin **3** and tryptamine **2** (**Figure 5.1** and **Chapter 1**). Until now, only traditional approaches have been applied to generate analogs of MIAs[2, 10-15]. New approaches are required to broaden the scope of alkaloid analogs to contain other

pharmacologically important functional groups, such as the aryl and heteroaryl groups, that might alter drug potency and specificity while reducing undesirable side effects.

Over the past decade, the O'Connor group and others have utilized several strategies to generate halogenated analogs of structurally diverse classes of MIAs at all four possible positions of the indole ring (**Figure 5.2** and **Chapter 2-4**)[2, 10-15]. For example, precursor-directed biosynthesis in *C. roseus* has led to the production of chlorinated and brominated analogs at the 4- and 7- positions of the indole ring[12]. Similarly, RNAi-silencing of endogenous tryptamine biosynthesis followed by halogenated precursors feeding afforded chlorinated and brominated analogs at the 4- and 7- positions of the indole ring (**Chapter 4**)[13]. This strategy, termed mutasynthesis, simplified the alkaloid profile since no natural, non-halogenated alkaloids derived from endogenous tryptamine **2** were present.

Analogs at the 5- and 6- positions cannot be obtained via precursor-directed biosynthesis or mutasynthesis due to the stringent substrate specificity of strictosidine synthase (STR), the enzyme that catalyzes formation of strictosidine **4**[10, 12]. To overcome this problem, we applied a combinatorial biosynthetic approach by introducing a re-engineered STR gene with a broadened substrate scope (V214M mutant)[10] into *C. roseus* cell culture (**Figure 5.2** and **Chapter 2**)[14]. The resulting transgenic cell culture produced chlorinated and brominated analogs at the remaining 5- and 6- positions when co-cultured with the corresponding tryptamine **2** analogs. Finally, we introduced prokaryotic halogenases that chlorinate tryptophan **1**, the immediate precursor of tryptamine **2**, into *C. roseus* cell culture (**Chapter 3**)[15]. These halogenases, RebF with either PyrH or RebF, function

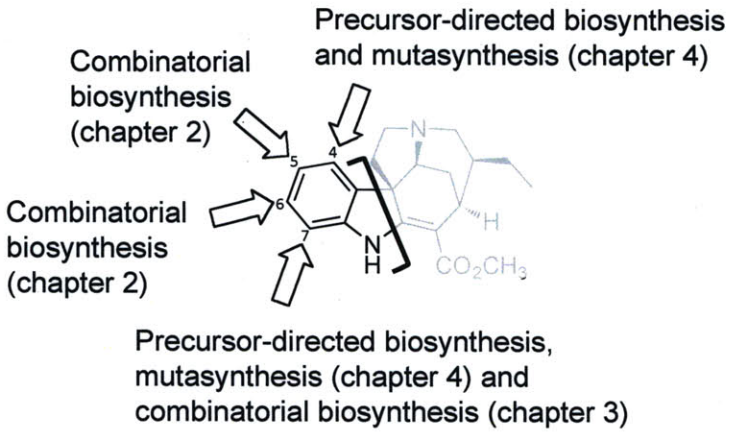

Figure 5.2 Approaches to generate halogenated MIA analogs at the 4 possible positions of the indole ring[12-15].

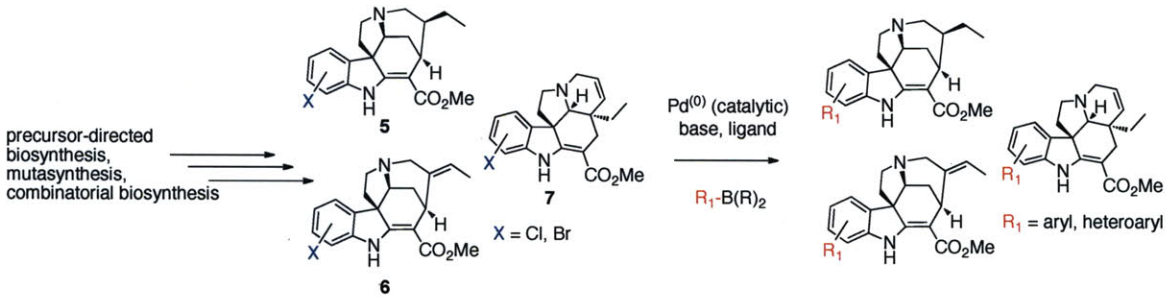

Figure 5.3 Strategy for synthetic diversification of monoterpene indole alkaloids using palladium-catalyzed Suzuki-Miyaura coupling reaction. Halogenated alkaloids are obtained via genetic engineering of *C. roseus* either with or without precursor-feeding. These analogs are further modified synthetically via suitable cross-coupling reactions.

within the context of the plant cell to generate chlorinated tryptophan at 5- and 7-position, respectively, which is then incorporated into monoterpene indole alkaloid metabolism to yield chlorinated alkaloids. Thus, these hairy roots autonomously produce halogenated alkaloids without the need for precursor-feeding.

While halogenation, in and of itself, often has profound effects on the bioactivity of natural products[16], we envisioned that halides could also serve as a useful handle for further chemical derivatization[8]. Using metal-catalyzed cross-coupling reactions, these halogenated analogs can be derivatized with functional groups that could further improve the bioactivity and bioavailability of the compounds. Achieving this goal requires two steps: (1) obtain halogenated analogs by genetic engineering of *C. roseus* either with or without precursor-feeding and (2) modify these halogenated analogs synthetically via suitable cross-coupling reactions. This chapter demonstrates that the introduction of a chemical handle—the organohalogens—into the indole moiety of the alkaloids, followed by postbiosynthetic chemical derivatizations using palladium-catalyzed Suzuki-Miyaura cross-coupling reactions robustly afforded aryl and heteroaryl analogs of MIAs (**Figure 5.3**).

5.2 Results and Discussion

5.2.1 Generations of Halogenated Alkaloids

To achieve our first goal, we considered several options for obtaining halogenated analogs. Since wild type STR accepts 7-chlorotryptamine **2a** and 7-bromotryptamines **2b**[12], we decided to use the TDC-suppressed hairy root lines[13] to obtain halogenated analogs. The yields and purity of halogenated products are higher in TDC-suppressed lines fed with halogenated tryptamine substrates compared to feeding of the wild type line (**Figure 5.6**). Specifically, we obtained alkaloid analogs with chlorine and bromine at the 7-position of the indole ring by culturing TDC-suppressed hairy root lines in liquid Gamborg's B5 media in the presence of either 0.6 mM 7-chlorotryptamine **2a** or 7-bromotryptamine **2b** (**Figure 5.4**). After one week of culture, the plant material was lysed and alkaloids were extracted into an organic solvent. Liquid chromatography mass spectral (LC-MS) analysis of these extracts indicated accumulation of one major product, 12-chloro-19,20-dihydroakuammicine **5a** (for 7-chlorotryptamine **2a** feeding) or 12-bromo-19,20-dihydroakuammicine **5b** (for 7-bromotryptamine **2b** feeding) (**Figure 5.7**). Alternatively, 12-chloro-19,20-dihydroakuammicine **5a** can also be obtained from transgenic hairy roots that express prokaryotic halogenases, RebF and RebH (**Figure 5.5**)[15].

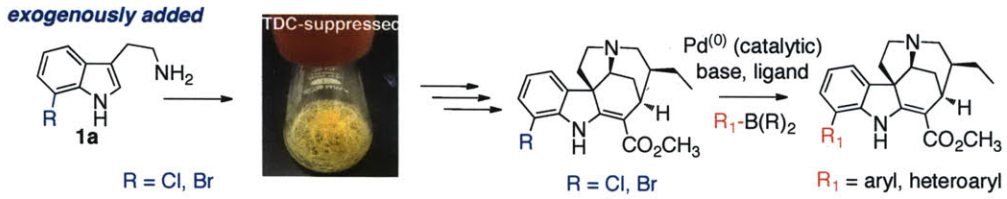

Figure 5.4 Strategy for synthetic diversification of monoterpene indole alkaloids at the 7-position of the indole ring using palladium-catalyzed Suzuki-Miyaura coupling reaction (I). Feeding of either 7-chlorotryptamine **2a** or 7-bromotryptamine **2b** to TDC-suppressed hairy root cultures (chapter 4) will produce 12-chloro-19,20-dihydroakuammicine **5a** and 12-bromo-19,20-dihydroakuammicine **5b**, respectively. These halogenated alkaloids can undergo the Suzuki-Miyaura coupling reactions with aryl and heteroaryl boronic acid substrates to form the corresponding alkaloid analogs.

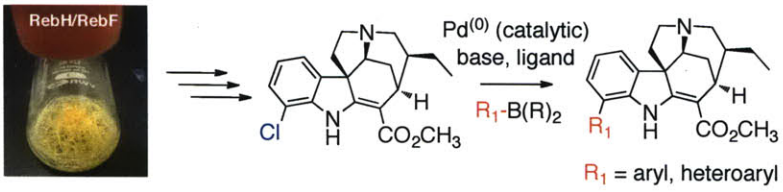

Figure 5.5 Strategy for synthetic diversification of monoterpene indole alkaloids at the 7-position of the indole ring using palladium-catalyzed Suzuki-Miyaura coupling reaction (II). RebH/RebF hairy root cultures produce 12-chloro-19,20-dihydroakuammicine **5a** (*m/z* 359) (chapter 3), which can undergo the Suzuki-Miyaura coupling reactions with aryl and heteroaryl boronic acid substrates to form the corresponding alkaloid analogs.

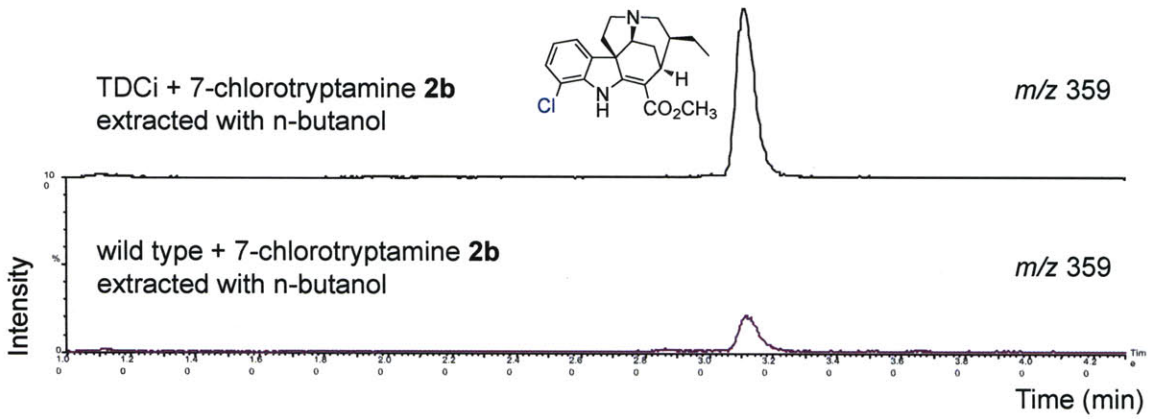

Figure 5.6 Extracted LC-MS chromatograms showing 12-chloro-19,20-dihydroakuammicine **5a** (*m/z* 359) production in crude extracts from TDC-suppressed (top) and wild type (bottom) hairy root cultures fed with 0.6 mM 7-chlorotryptamine **2a**. LC-MS spectra are normalized to the same y-axis scale.

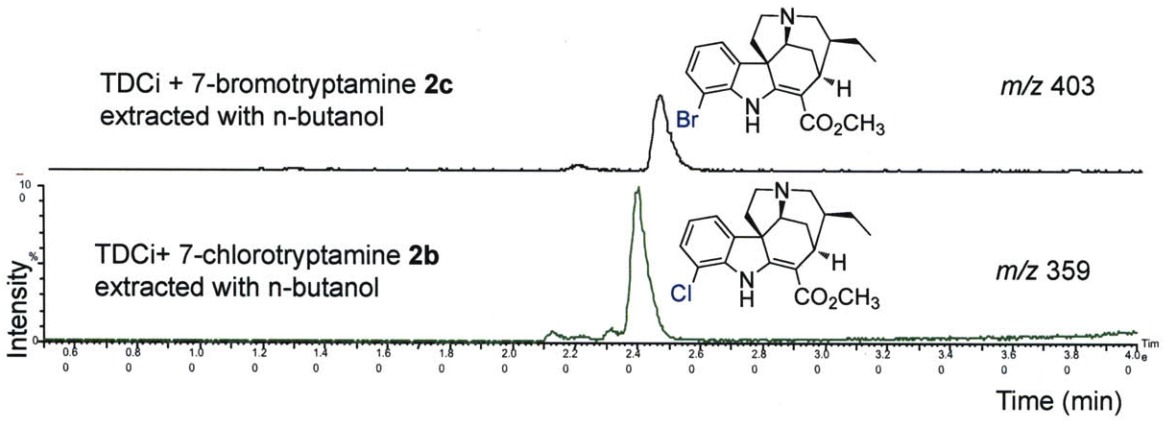

Figure 5.7 Extracted LC-MS chromatogram showing 12-chloro-19,20-dihydroakuammicine **5a** (*m/z* 359, top) and 12-bromo-19,20-dihydroakuammicine **5b** (*m/z* 403, bottom) production in crude extracts from TDC-suppressed hairy root culture fed with 7-chlorotrypamine **2a** and 7-bromotryptamine **2b**, respectively. LC-MS spectra are normalized to the same y-axis scale.

Tryptamine analogs with substituents at the 6-position are not accepted by wild type STR[12]. Therefore, to obtain analogs of alkaloids with chlorine at the 6-position of the indole ring, we cultured transgenic hairy root lines that express V214M mutant STR enzyme (STRvm)[14] in liquid Gamborg's B5 media in the presence of 0.6 mM 6-chlorotryptamine **2c** (**Figure 5.8**). After one week of culture, the plant material was processed as described above. LC-MS analysis of these extracts indicated accumulations of three major analogs: 11-chloro-19,20-dihydroakuammicine **5c,** 11-chloroakuammicine **6c** and 11-chlorotabersonine **7c** (**Figure 5.9**).

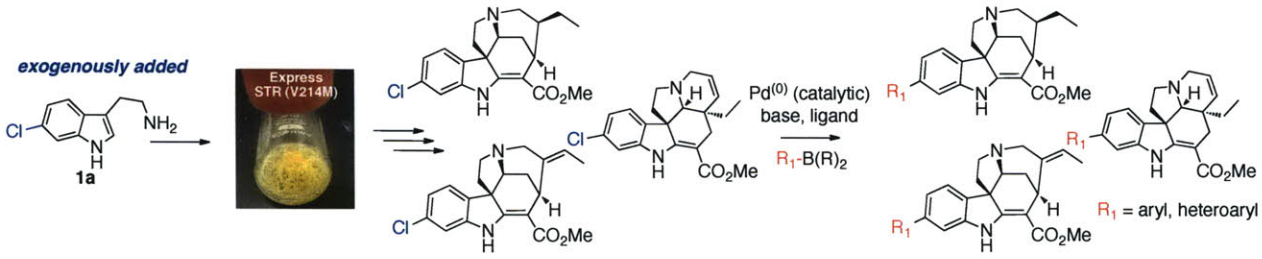

Figure 5.8 Strategy for synthetic diversification of monoterpene indole alkaloids at the 6-position of the indole ring using palladium-catalyzed Suzuki-Miyaura coupling reaction. Feeding of 6-chlorotryptamine to STRvm hairy root cultures (chapter 3) will produce 11-chloro-19,20-dihydroakuammicine **5c**, 11-chloroakuammicine **6c** and 11-chlorotabersonine **7c**. These halogenated alkaloids can undergo the Suzuki-Miyaura coupling reactions with aryl and heteroaryl boronic acid substrates to form the corresponding alkaloid analogs.

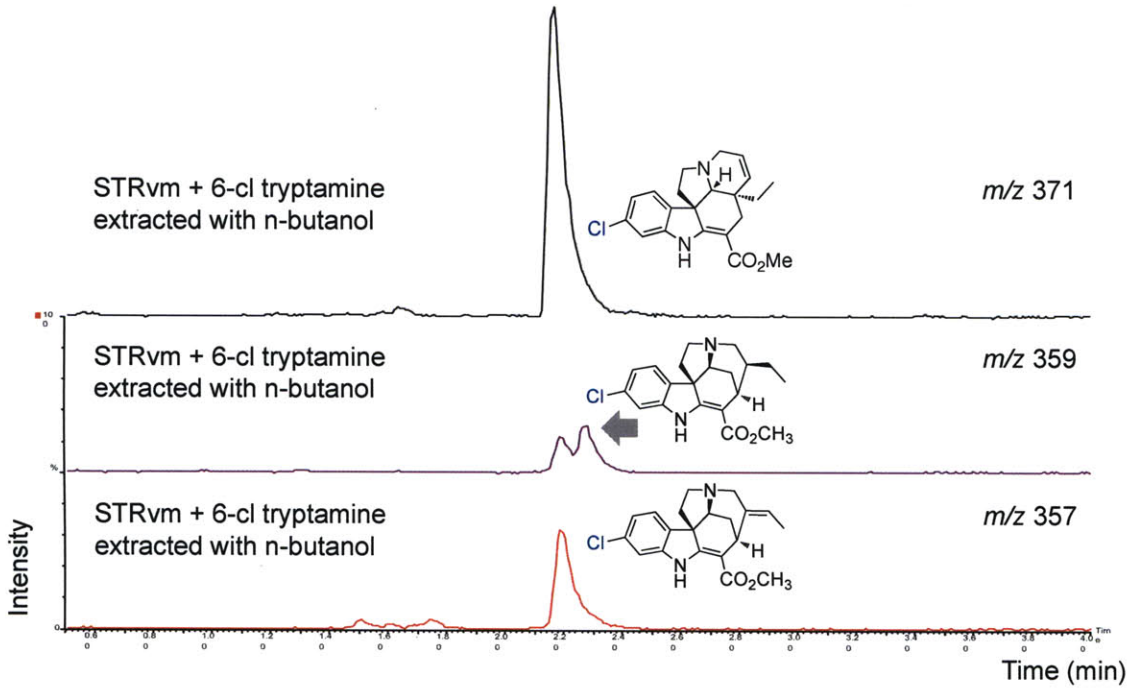

Figure 5.9 Extracted LC-MS chromatograms showing 11-chloroakuammicine **6c** (*m/z* 357, bottom), 11-chloro-19,20-dihydroakuammicine **5c** (*m/z* 359, middle) and 11-chlorotabersonine **7c** (*m/z* 371, top) production in crude extracts from STRvm hairy root culture fed with 6-chlorotrypamine **2c**. LC-MS spectra are normalized to the same y-axis scale.

5.2.2. Suzuki-Miyaura Coupling of Halogenated Alkaloids with Aryl and Heteroaryl Boronic Acids

With halogenated analogs readily available as a component of crude plant extracts, we then set out to achieve our second goal by exploring chemical functionalization reactions that will derivatize halogenated analogs under sufficiently mild reaction conditions. Voss and coworkers demonstrated the utilization of iodinated analogs of several alkaloids, which were obtained through semisynthesis, in several cross-coupling reaction conditions that are unlikely to be applicable to chlorinated analogs, which are less reactive[2]. Prompted by the work of Goss and coworkers[8], we turned our attention to the palladium-catalyzed Suzuki-Miyaura cross-coupling reactions. While crossing-coupling reactions of aryl iodides and bromides with arylboronic acids are well precedented, reactions involving aryl chlorides require the use of more recently developed catalyst systems, which employ highly active and sterically demanding ligands, such as Sphos[17]. Since non-halogenated metabolites present in crude extracts are unlikely to interfere with the progression of the cross-coupling reactions, as demonstrated by the work of Goss and coworkers[8], crude extracts containing chlorinated and brominated alkaloids were used directly in the cross-coupling reactions without any purification. In our experience, preparative high-performance liquid chromatography (HPLC) using a reverse phase column can sufficiently purify alkaloid analogs from other metabolites for structural characterization[14, 15]. Therefore, we envisioned using preparative HPLC to purify the resulting aryl and heteroaryl analogs from crude reaction mixtures.

We performed the Suzuki-Miyaura cross-coupling reactions of 12-chloro-19,20-

dihydroakuammicine **5a** and 12-bromo-19,20-dihydroakuammicine **5b** using six aryl and heteroaryl boronic acid substrates (**Figure 5.4** and **Table 5.1**). Gratifyingly, small-scale coupling reactions of crude extracts containing either 12-chloro-19,20-dihydroakuammicine **5a** or 12-chloro-19,20-dihydroakuammicine **5b** from 100 mg of fresh hairy roots with every boronic acids tested went to completion as observed by LC-MS in under one hour at 100 °C. LC-MS chromatograms showing the progression of the cross-coupling reactions at 0 and 10 min time points are shown in **Figure 5.10-5.13**. Crude extracts from transgenic hairy roots that express prokaryotic halogenases (RebF and RebH) (**Chapter 3**) were also used as substrates for the Suzuki-Miyaura cross-coupling reactions with three representative boronic acids, phenylboronic acid **9d**, 4-methylphenylboronic acid **9g** and 4-methoxyphenylboronic acid **9f.** LC-MS analysis of crude reaction mixtures demonstrated that the reactions were completed in ten minutes (**Figure 5.14**).

Encouraged by these results, we performed large-scale cross-coupling reactions using crude extracts from 14-23 grams of hairy roots with three different boronic acids, phenylboronic acid **9d**, 4-fluorophenylboronic acid **9e** and furanylboronic acid **9i**. Standard work-up followed by reverse-phase preparative HPLC purification of the reaction mixture afforded milligram quantities of these analogs (**Table 5.1**). ^{1}H and ^{13}C NMR spectroscopy, high-resolution mass spectrometry, tandem MS/MS and UV absorption spectra confirmed their identities (**Table 5.2**, **Figure 5.15-5.16** and **Appendix C**). High-resolution mass spectrometry and tandem MS/MS were used to confirm the identities of the three remaining analogs **5f**, **5g** and **5h** (**Table 5.2** and **Figure 5.15**).

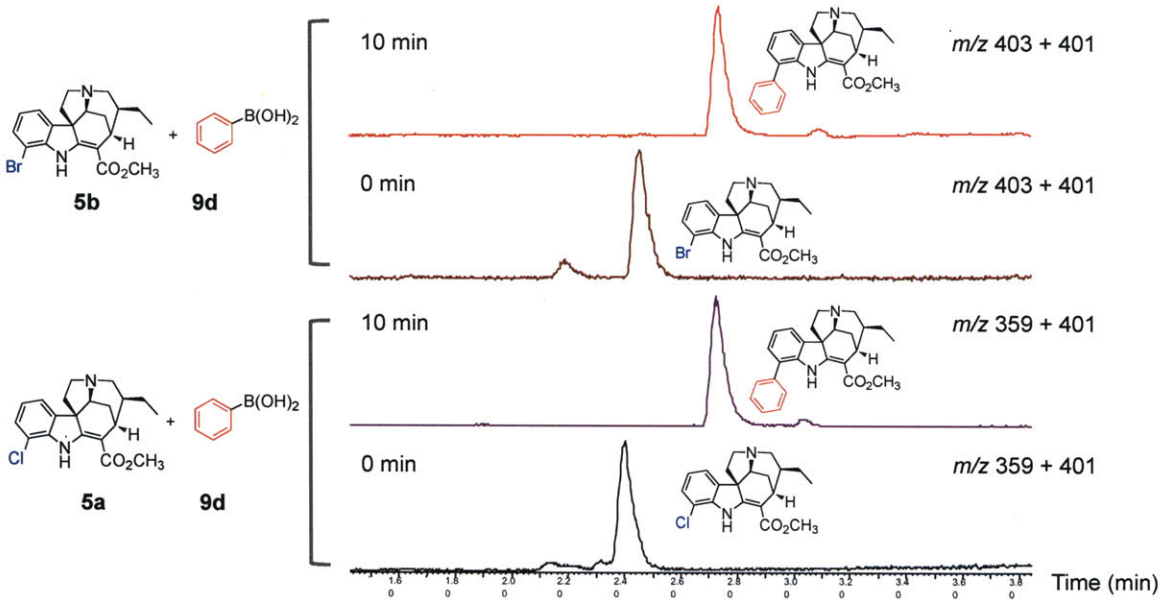

Figure 5.10 LC-MS traces showing the progression of Suzuki-Miyaura cross-coupling reactions of TDC-suppressed hairy root extracts containing 12-chloro-19,20-dihydroakuammicine **5a** (*m/z* 359, bottom) and 12-chloro-19,20-dihydroakuammicine **5b** (*m/z* 403, top) with phenylboronic acid **9d** to form 12-phenyl-19,20-dihydroakuammicine **5d** (*m/z* 401).

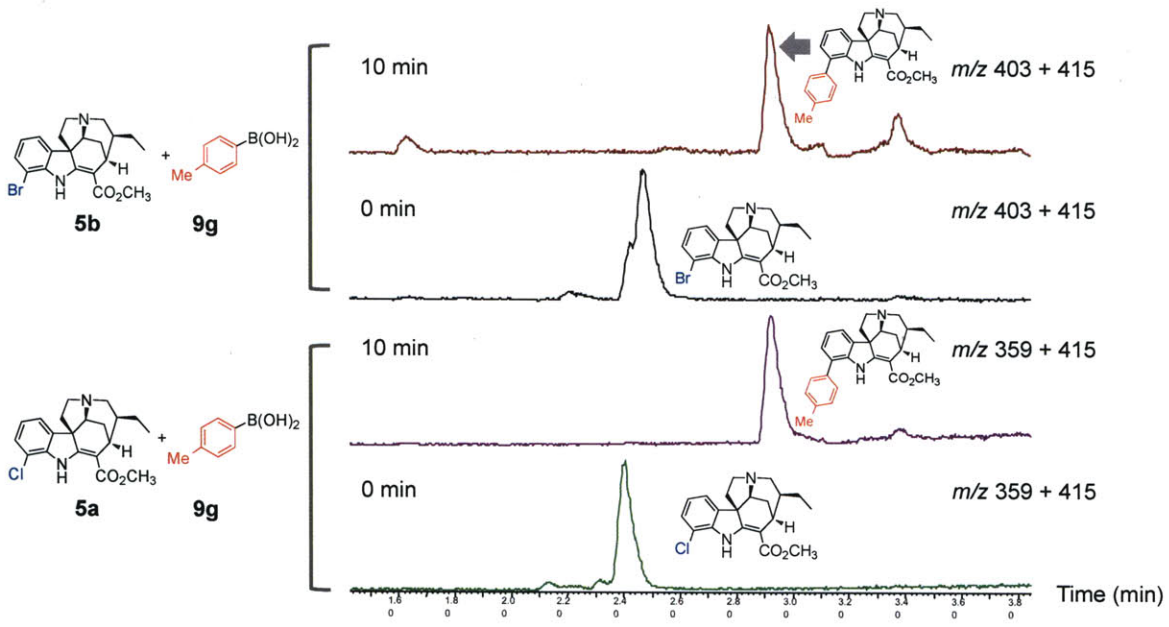

Figure 5.11 LC-MS traces showing the progression of Suzuki-Miyaura cross-coupling reactions of TDC-suppressed hairy root extracts containing 12-chloro-19,20-dihydroakuammicine **5a** (*m/z* 359, bottom) and 12-chloro-19,20-dihydroakuammicine **5b** (*m/z* 403, top) with 4-methylphenylboronic acid **9g** to form 12-(4-methylphenyl)-19,20-dihydroakuammicine **5g** (*m/z* 415).

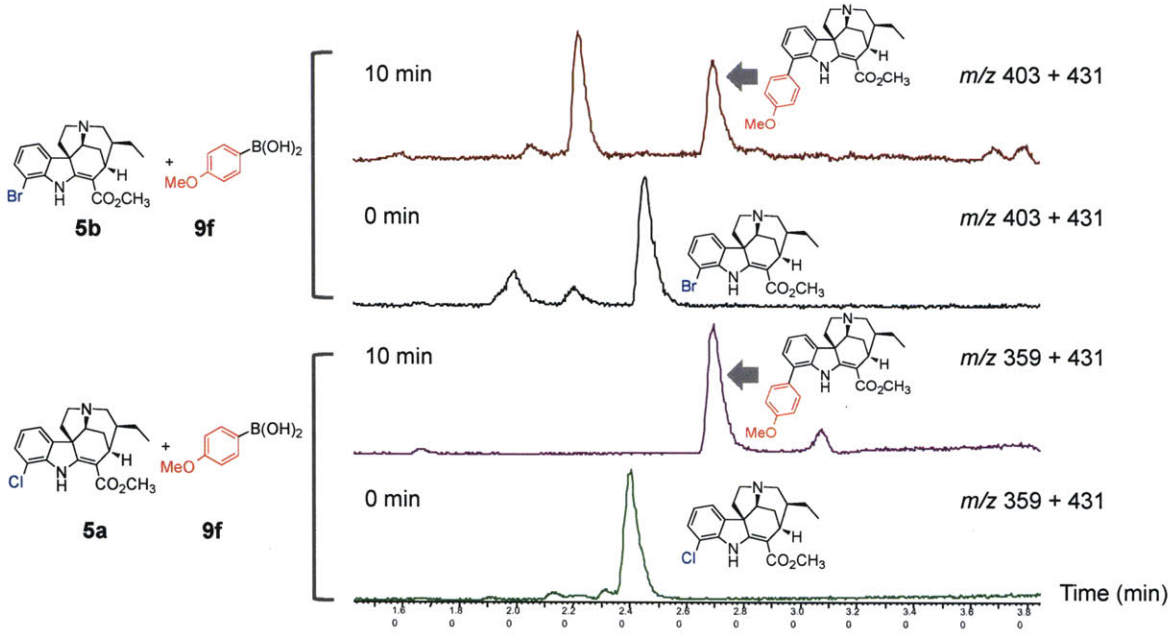

Figure 5.12 LC-MS traces showing the progression of Suzuki-Miyaura cross-coupling reactions of TDC-suppressed hairy root extracts containing 12-chloro-19,20-dihydroakuammicine **5a** (*m/z* 359, bottom) and 12-chloro-19,20-dihydroakuammicine **5b** (*m/z* 403, top) with 4-methoxyphenylboronic acid **9f** to form 12-(4-methoxyphenyl)-19,20-dihydroakuammicine **5f** (*m/z* 431).

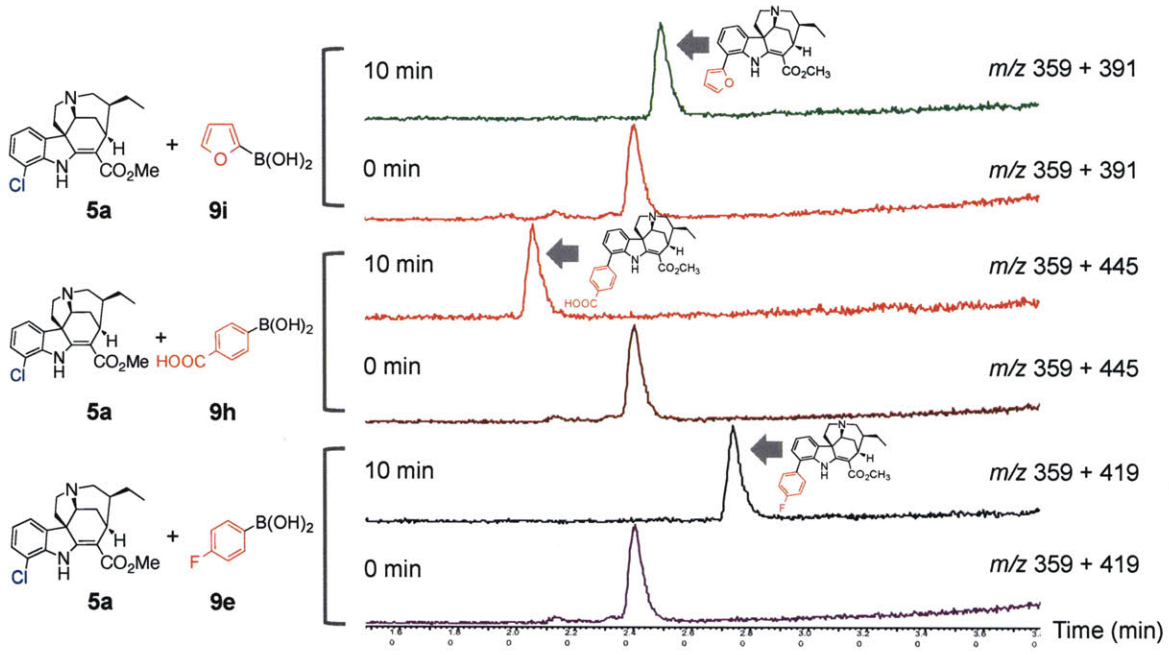

Figure 5.13 LC-MS traces showing the progression of Suzuki-Miyaura cross-coupling reactions of TDC-suppressed hairy root extracts containing 12-chloro-19,20-dihydroakuammicine **5a** (*m/z* 359) with 4-fluorophenylboronic acid **9e** (bottom), 4-carboxyphenylboronic acid **9h** (middle) and furanylboronic acid **9i** (top). Expected products were 12-(4-fluorophenyl)- 19,20-dihydroakuammicine **5e** (*m/z* 419), 12-(4-carboxyphenyl)- 19,20-dihydroakuammicine **5h** (*m/z* 445) and 12-furanyl-19,20-dihydroakuammicine **5i** (*m/z* 391).

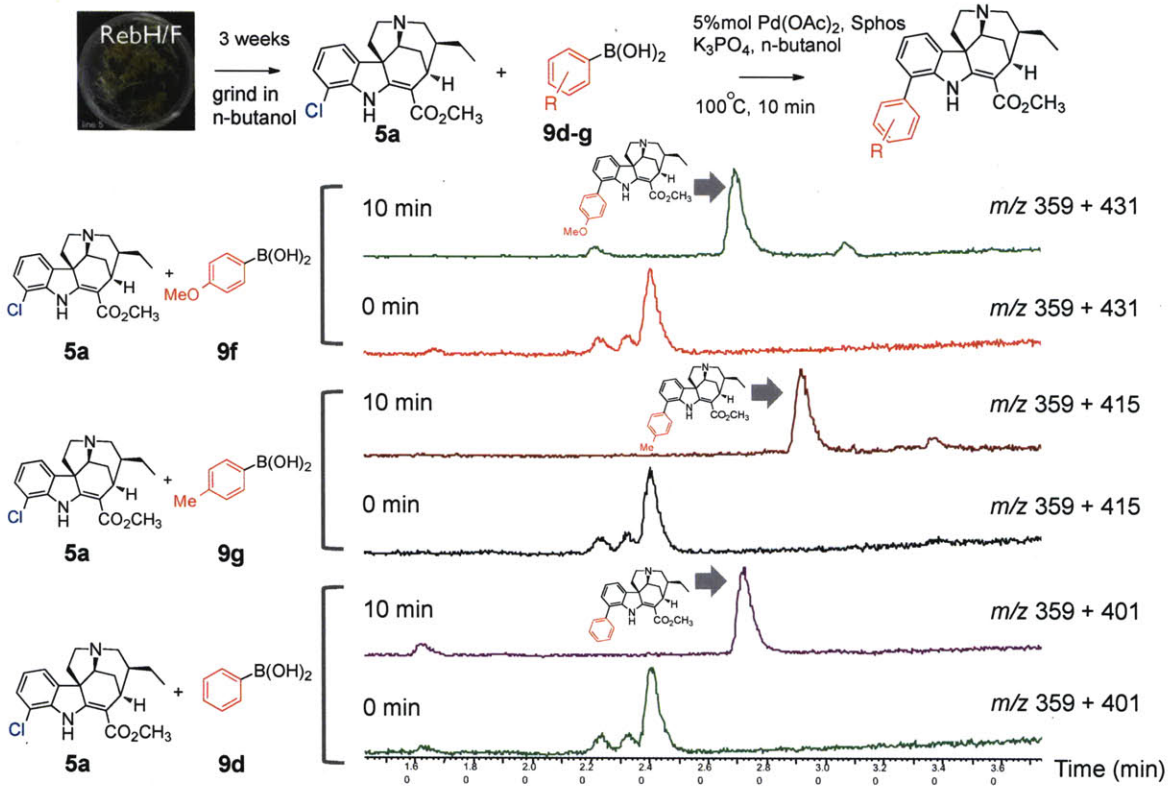

Figure 5.14 LC-MS traces showing the progression of Suzuki-Miyaura cross-coupling reactions of RebH/F hairy root extracts containing 12-chloro-19,20-dihydroakuammicine **5a** (*m/z* 359) with phenylboronic acid **9d** (bottom), 4-methylphenylboronic acid **9g** (middle) and 4-methoxyphenylboronic acid **9f** (top). Expected products were 12-phenyl-19,20-dihydroakuammicine **5d** (*m/z* 401), 12-(4-methylphenyl)-19,20-dihydroakuammicine **5g** (*m/z* 415) and 12-(4-methoxyphenyl)-19,20-dihydroakuammicine **5f** (*m/z* 431).

Table 5.1. Suzuki-Miyaura cross-coupling reactions of 12-chloro-19,20-dihydroakuammicine **5a** with aryl and heteroaryl boronic acids **9d-i**.

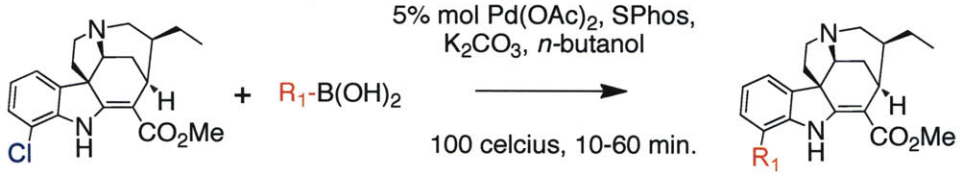

boronic acid substrates	products	isolated yield (%)*
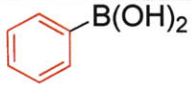 **9d**	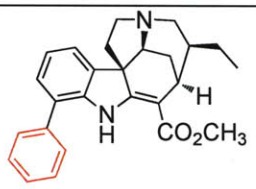 **5d**	50
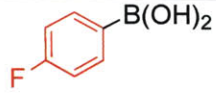 **9e**	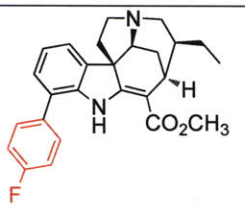 **5e**	51
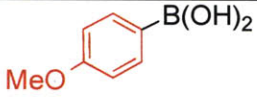 **9f**	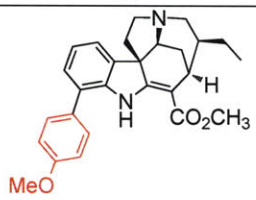 **5f**	Small-scale reaction Product not isolated
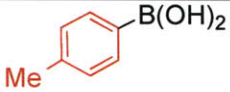 **9g**	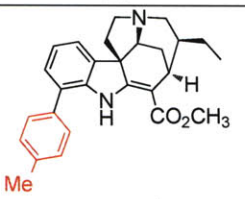 **5g**	Small-scale reaction Product not isolated
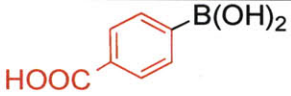 **9h**	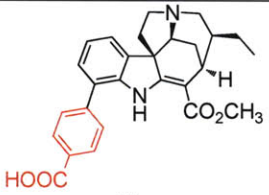 **5h**	Small-scale reaction Product not isolated
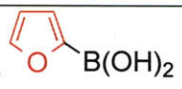 **9i**	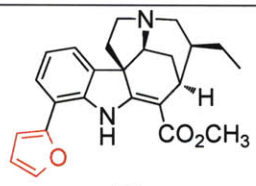 **5i**	25

* compounds were purified using reverse-phase preparative HPLC

Table 5.2. High-resolution MS data for 19,20-dihydroakuammicine analogs **5a-i** (analogs with substituent at the 7-position of the indole ring).

19,20-dihydro-akuammicine **5**	**R = Cl** 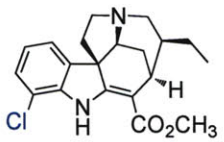 **5a**	**R = Br** 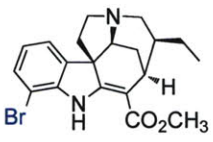 **5b**	**R = phenyl** 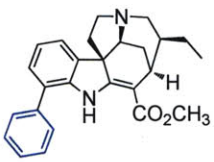 **5d**	**R = 4-Fphenyl** 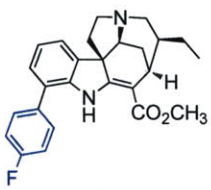 **5e**
Expected [M+H]	359.1526	403.1021	401.2224	419.2129
Observed [M+H]	359.1520	403.1011	401.2228	419.2133
Accuracy (ppm)	-1.7	-2.5	+1.0	+1.0
MS/MS fragments	359.2, 327.1	403.1, 371.1	401.2, 369.2	419.2, 387.2
RT (min)	2.40	2.46	2.73	2.74
19,20-dihydro-akuammicine **5**	**R = 4-methoxy phenyl** 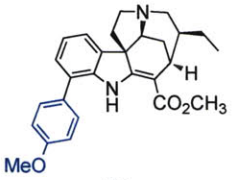 **5f**	**R = 4-methyl phenyl** 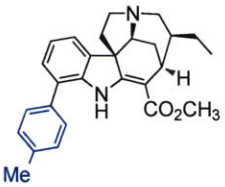 **5g**	**R = 4-carboxy phenyl** 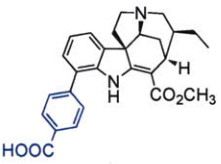 **5h**	**R = furanyl** 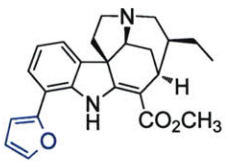 **5i**
Expected [M+H]	431.2329	415.2380	445.2121	391.2016
Observed [M+H]	431.2330	415.2376	445.2123	391.2015
Accuracy (ppm)	+0.2	-1.0	+0.4	-0.3
MS/MS fragments	431.2, 399.2	415.2, 383.2	445.2, 413.2	391.2, 359.2
RT (min)	2.70	2.92	2.06	2.50

RT = retention time, LC gradient 10-90% acetonitrile/water (0.1% TFA) in 5 minutes

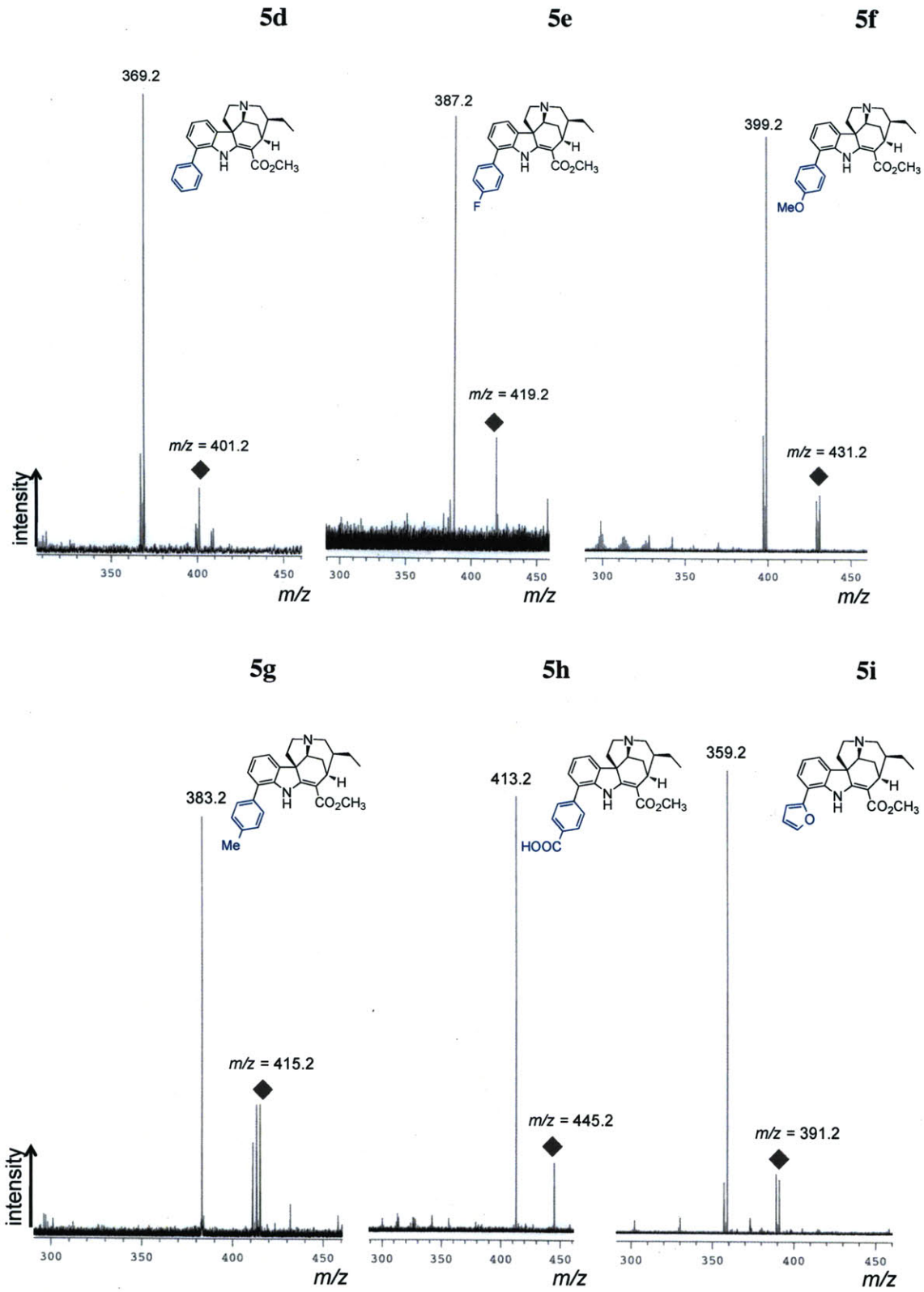

Figure 5.15 MS/MS analysis for 19,20-dihydroakuammicine analogs **5d-i** (analogs with substituent at the 7-position of the indole ring)

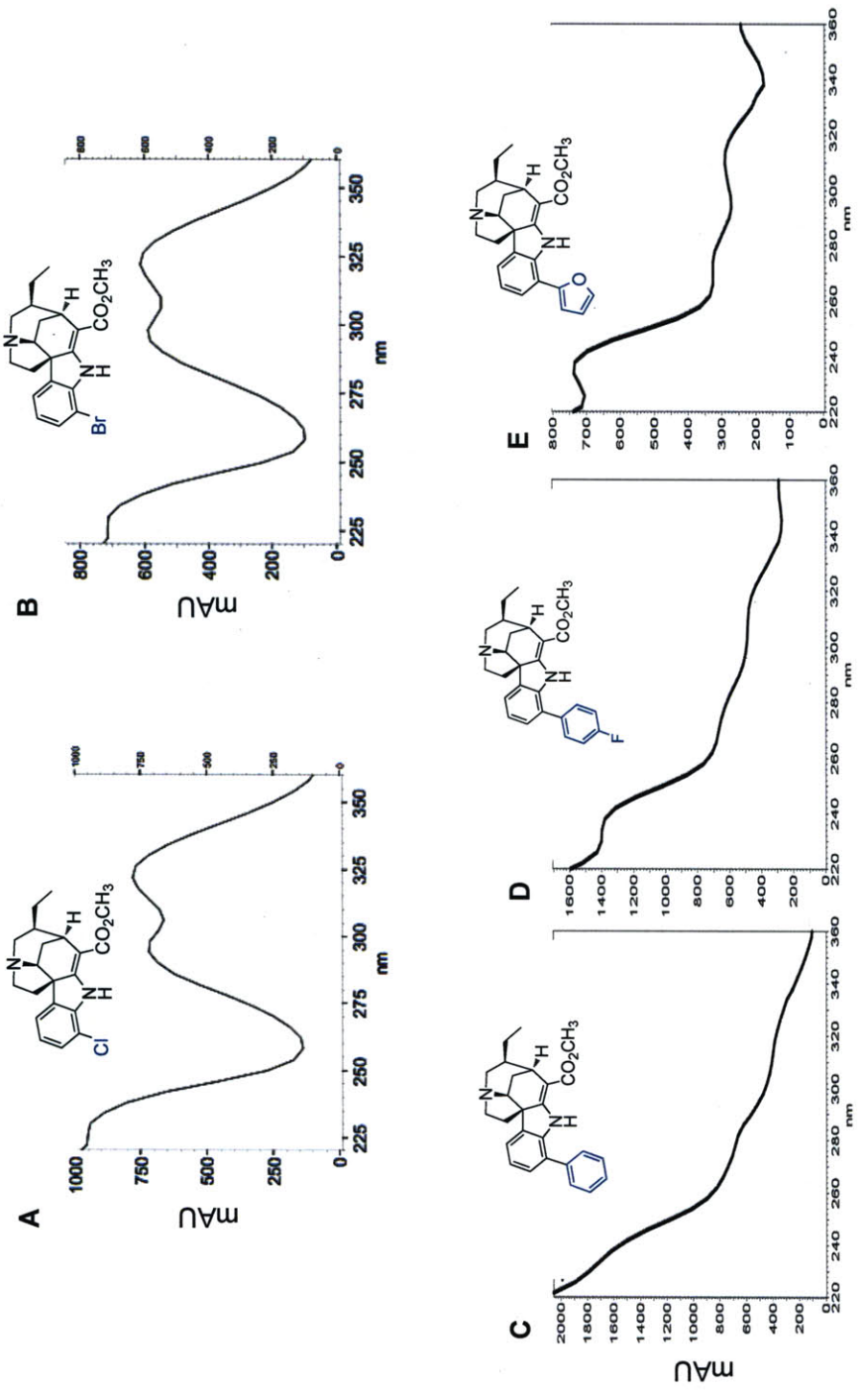

Figure 5.16 UV spectra of 19,20-dihydroakuammicine analogs **5a-e** and **5i**. **A.** 12-chloro-19,20-dihydroakuammicine **5a. B.** 12-bromo-19,20-dihydroakuammicine **5b**. **C.** 12-phenyl-19,20-dihydroakuammicine **5d. D.** 12-(4-fluorophenyl)-19,20-dihydroakuammicine **5e**. **E.** 12-furanyl-19,20-dihydroakuammicine **5i**.

We next focused our attention on the chemical derivatization of alkaloid analogs with a chlorine at the 6-position of the indole ring (**Figure 5.8**). Crude extracts containing 11-chloro-19,20-dihydroakuammicine **5c**, 11-chloroakuammicine **6c** and 11-chlorotabersonine **7c** appeared to be good substrates for the Suzuki-Miyaura cross-coupling reactions using aryl and heteroaryl boronic acid substrates (**Figure 5.17-5.22**). Of the six aryl and heteroaryl boronic acids (**9d-i**) tested, only the electron-deficient 4-carboxyphenylboronic acid **9h** did not yield the desired analogs (**Figure 5.18**, **5.20** and **5.22**). High-resolution mass spectrometry and tandem MS/MS were used to confirm the identities of all alkaloid analogs (**Table 5.3-5.5** and **Figure 5.23-5.25**).

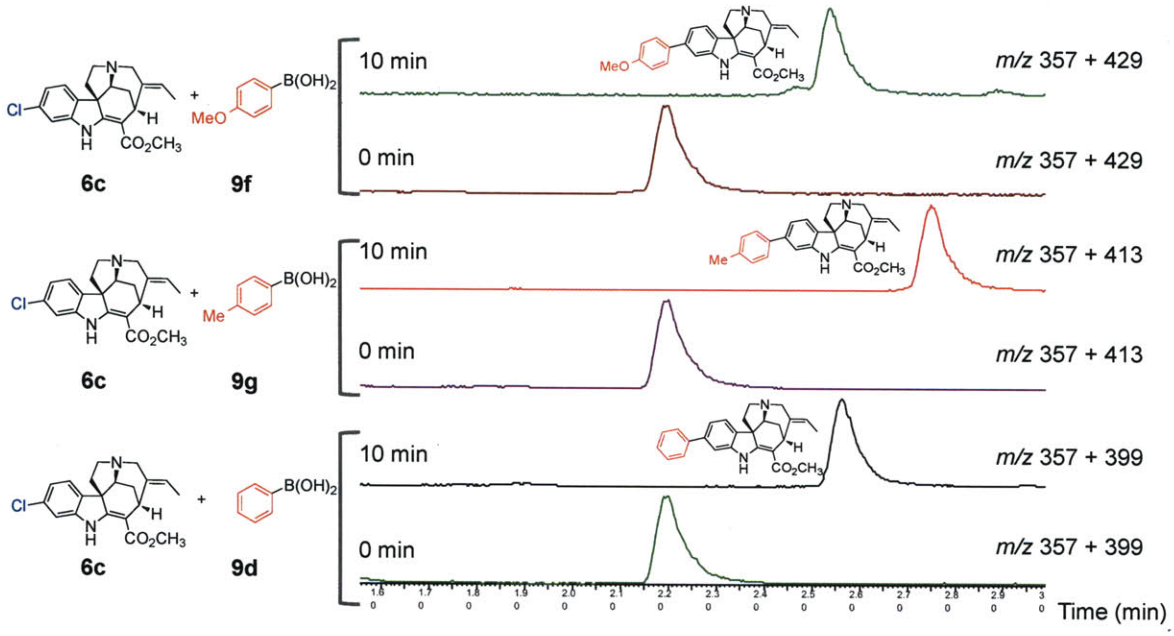

Figure 5.17 LC-MS traces showing the progression of Suzuki-Miyaura cross-coupling reactions of 11-chloroakuammicine **6c** (*m/z* 357) with phenylboronic acid **9d** (bottom), 4-methylphenylboronic acid **9g** (middle) and 4-methoxyphenylboronic acid **9f** (top). Expected products were 11-phenylakuammicine **6d** (*m/z* 399), 11-(4-methylphenyl)-akuammicine **6g** (*m/z* 413) and 11-(4-methoxyphenyl)-akuammicine **6f** (*m/z* 429).

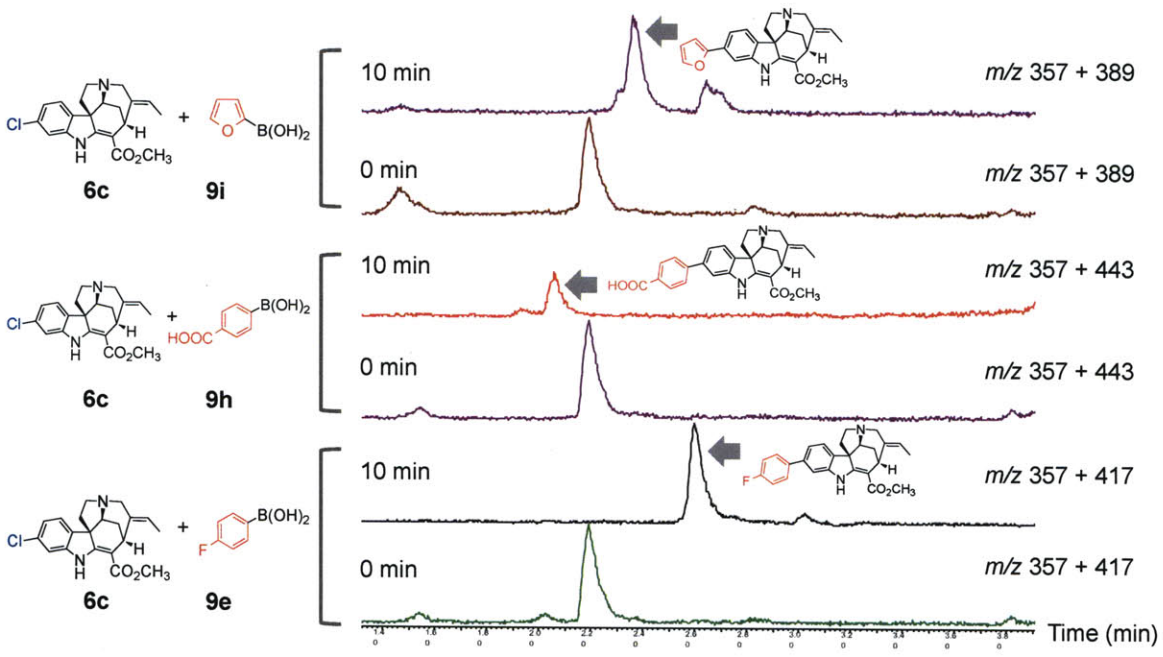

Figure 5.18 LC-MS traces showing the progression of Suzuki-Miyaura cross-coupling reactions of 11-chloroakuammicine **6c** (*m/z* 357) with 4-fluorophenylboronic acid **9e** (bottom), 4-carboxyphenylboronic acid **9h** (middle) and furanylboronic acid **9i** (top). Expected products were 11-(4-fluorophenyl)-akuammicine **6e** (*m/z* 417), 11-(4-carboxyphenyl)-akuammicine **6h** (*m/z* 443) and 11-furanyl-akuammicine **6i** (*m/z* 389).

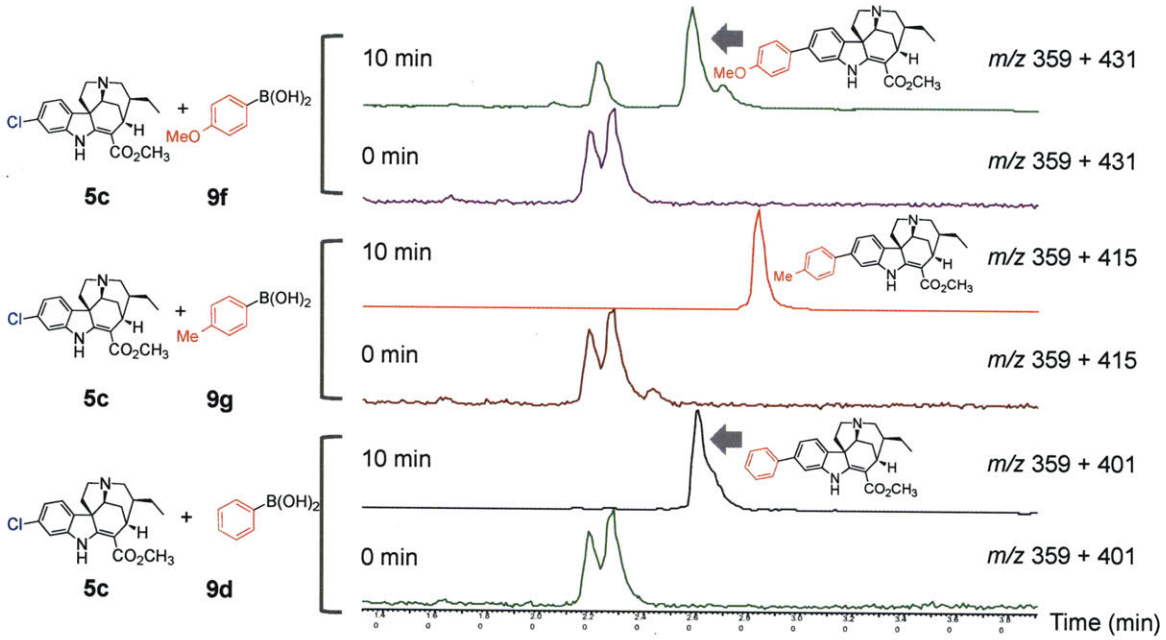

Figure 5.19 LC-MS traces showing the progression of Suzuki-Miyaura cross-coupling reactions of 11-chloro-19,20-dihydroakuammicine **5c** (*m/z* 359) with phenylboronic acid **9d** (bottom), 4-methylphenylboronic acid **9g** (middle) and 4-methoxyphenylboronic acid **9f** (top). Expected products were 11-phenyl-19,20-dihydroakuammicine **5d'** (*m/z* 401), 11-(4-methylphenyl)-19,20-dihydroakuammicine **5g'** (*m/z* 415) and 11-(4-methoxyphenyl)-19,20-dihydroakuammicine **5f'** (*m/z* 431).

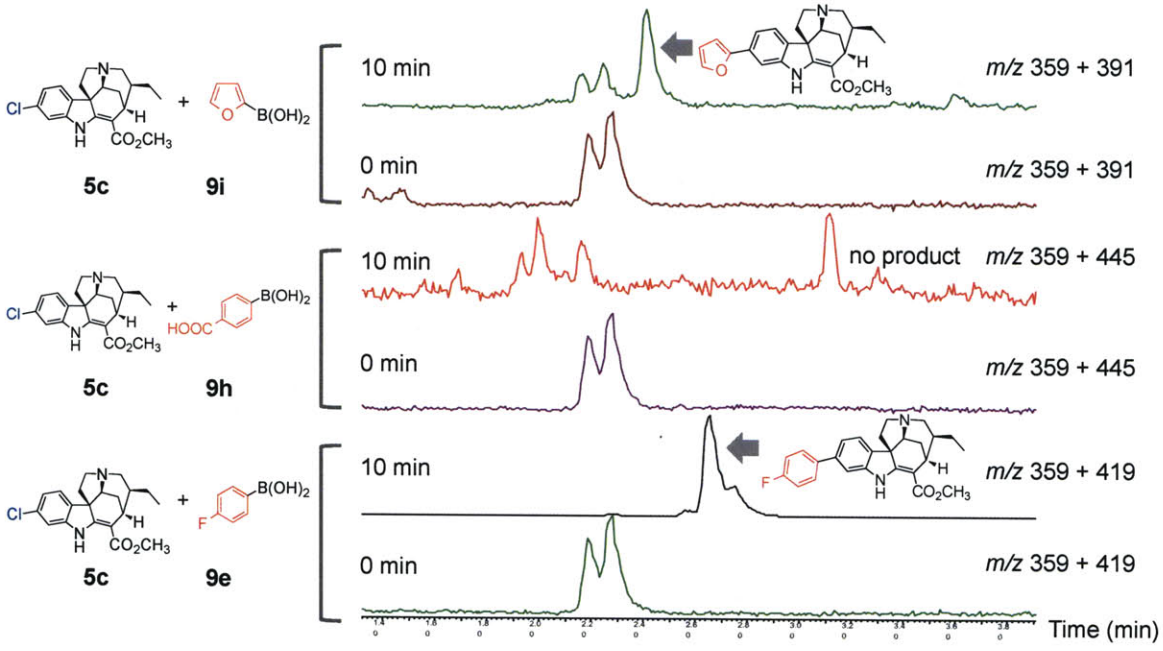

Figure 5.20 LC-MS traces showing the progression of Suzuki-Miyaura cross-coupling reactions of 11-chloro-19,20-dihydroakuammicine **5c** (*m/z* 359) with 4-fluorophenylboronic acid **9e** (bottom), 4-carboxyphenylboronic acid **9h** (middle) and furanylboronic acid **9i** (top). Expected products were 11-(4-fluorophenyl)-19,20-dihydroakuammicine **5e'** (*m/z* 419), 11-(4-carboxyphenyl)-19,20-dihydroakuammicine **5h'** (*m/z* 445) and 11-furanyl-19,20-dihydroakuammicine **5i'** (*m/z* 391).

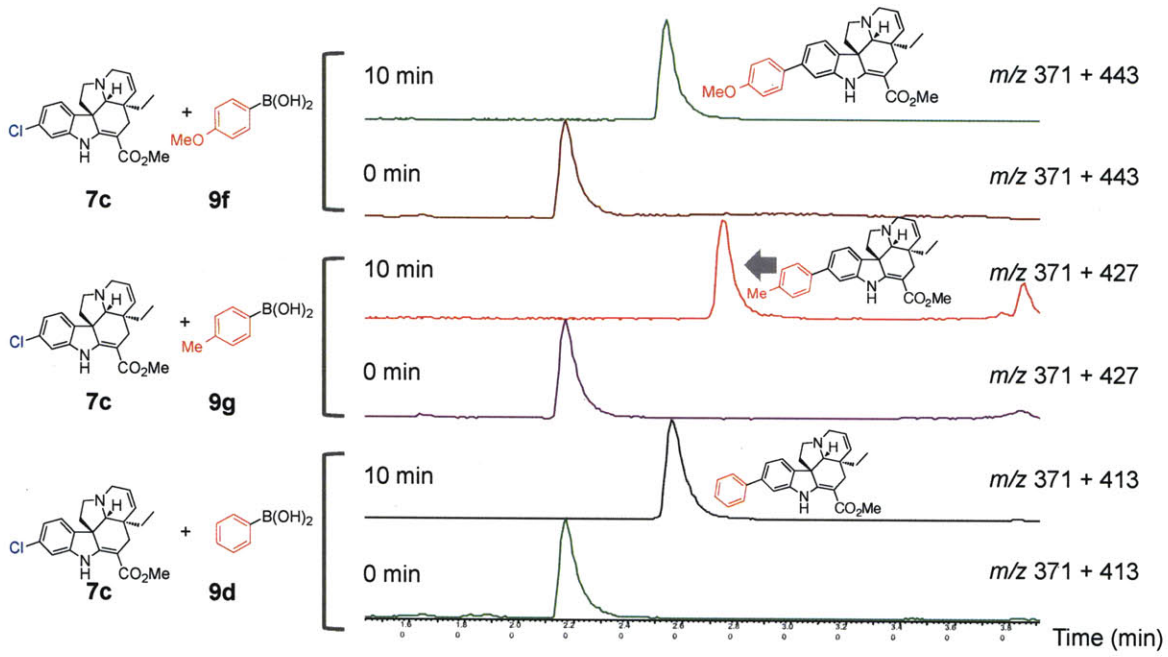

Figure 5.21 LC-MS traces showing the progression of Suzuki-Miyaura cross-coupling reactions of 11-chlorotabersonine **7c** (*m/z* 371) with phenylboronic acid **9d** (bottom), 4-methylphenylboronic acid **9g** (middle) and 4-methoxyphenylboronic acid **9f** (top). Expected products were 11-phenyltabersonine **7d** (*m/z* 413), 11-(4-methylphenyl)-tabersonine **7g** (*m/z* 427) and 11-(4-methoxyphenyl)-tabersonine **7f** (*m/z* 443).

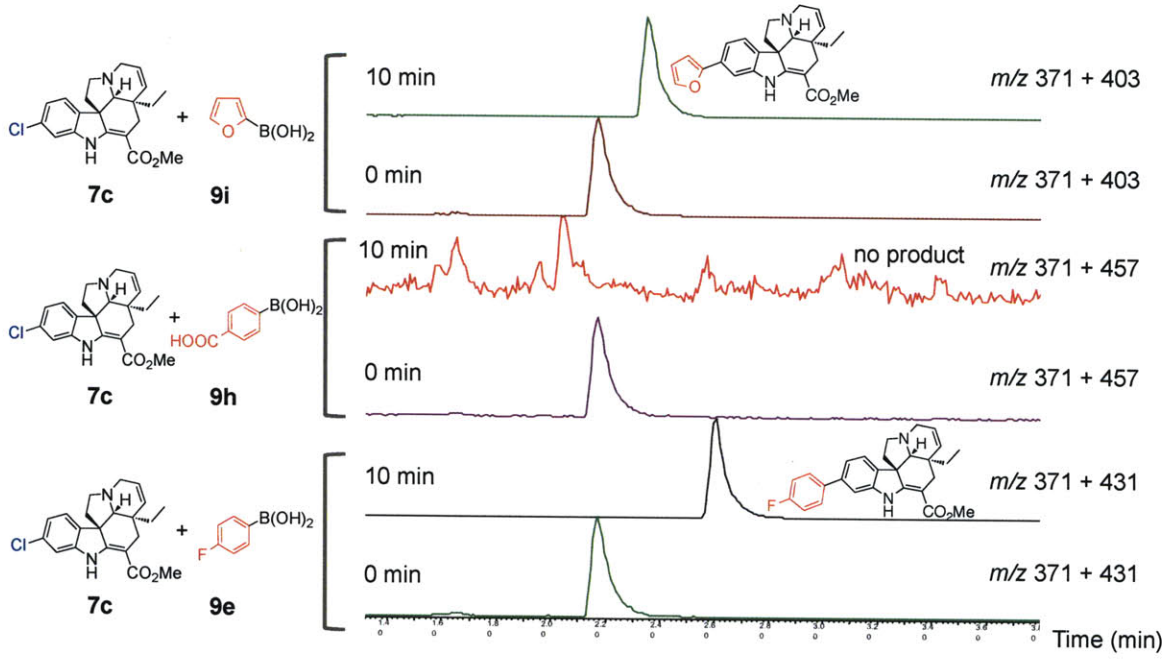

Figure 5.22 LC-MS traces showing the progression of Suzuki-Miyaura cross-coupling reactions of 11-chlorotabersonine **7c** (*m/z* 371) with 4-fluorophenylboronic acid **9e** (bottom), 4-carboxyphenylboronic acid **9h** (middle) and furanylboronic acid **9i** (top). Expected products were 11-(4-fluorophenyl)-tabersonine **7e** (*m/z* 431), 11-(4-carboxyphenyl)-tabersonine **7h** (*m/z* 457) and 11-furanyl-tabersonine **7i** (*m/z* 403).

Table 5.3. High-resolution MS data for akuammicine analogs **6c-i** (analogs with substituent at the 6-position of the indole ring).

Akuammicine **6**	**R = Cl** 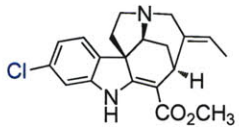 **6c**	**R = phenyl** 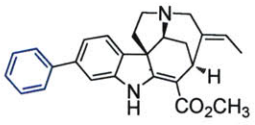 **6d**	**R = 4-Fphenyl** 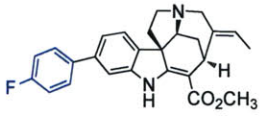 **6e**
Expected [M+H]	357.1364	399.2067	417.1955
Observed [M+H]	357.1355	399.2062	417.1955
Accuracy (ppm)	-2.5	-1.3	0.0
MS/MS fragments	357.1, 325.1	n/a*	417.2, 385.1
RT (min)	2.19	2.61	2.57

Akuammicine **6**	**R = 4-methoxy phenyl** 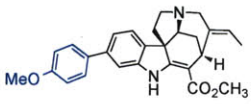 **6f**	**R = 4-methylphenyl** 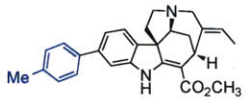 **6g**	**R = furanyl** 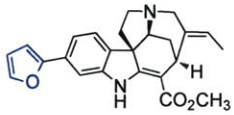 **6i**
Expected [M+H]	429.2173	413.2224	389.1860
Observed [M+H]	429.2191	413.2219	389.1867
Accuracy (ppm)	+4.3	-1.2	+1.8
MS/MS fragments	n/a*	413.2, 381.2	389.2, 357.2
RT (min)	2.55	2.79	2.37

RT = retention time, LC gradient 10-90% acetonitrile/water (0.1% TFA) in 5 minutes
* Tandem MS/MS are not available because these analogs cannot be separated from 19,20-dihydroakuammicine analogs. Since the masses of akuammicine analogs and the corresponding 19,20-dihydroakuammicine analogs only differ by 2 units, the ions are too close to isolate prior to fragmentation.

Table 5.4. High-resolution MS data for 19,20-dihydroakuammicine analogs **5c, 5d'-i'** (analogs substituent at the 6-position of the indole ring).

19,20-dihydro-akuammicine **5**	**R = Cl** 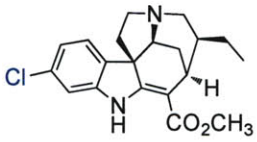 **5c**	**R = phenyl** 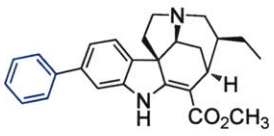 **5d'**	**R = 4-Fphenyl** 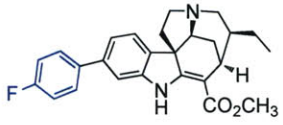 **5e'**
Expected [M+H]	359.1521	401.2224	419.2129
Observed [M+H]	359.1526	401.2216	419.2138
Accuracy (ppm)	+1.4	-2.0	+1.9
MS/MS fragments	359.2, 327.1	n/a*	419.2, 387.2
RT (min)	2.28	2.65	2.65

19,20-dihydro-akuammicine **5**	**R = 4-methoxy phenyl** 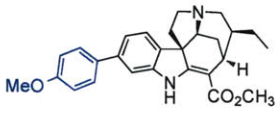 **5f'**	**R = 4-methylphenyl** 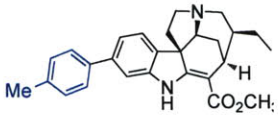 **5g'**	**R = furanyl** 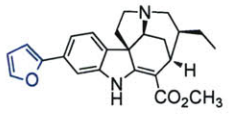 **5i'**
Expected [M+H]	431.2329	415.2380	391.2016
Observed [M+H]	431.2347	415.2395	391.2053
Accuracy (ppm)	+4.2	+3.6	+9.4
MS/MS fragments	n/a*	415.2, 383.2	n/a*
RT (min)	2.58	2.84	2.41

RT = retention time, LC gradient 10-90% acetonitrile/water (0.1% TFA) in 5 minutes
* Tandem MS/MS are not available because these analogs cannot be separated from akuammicine analogs. Since the masses of akuammicine analogs and the corresponding 19,20-dihydroakuammicine analogs only differ by 2 units, the ions are too close to isolate prior to fragmentation.

Table 5.5. High-resolution MS data for tabersonine analogs **7c-i** (analogs with substituent at the 6-position of the indole ring).

Tabersonine **7**	**R = Cl** 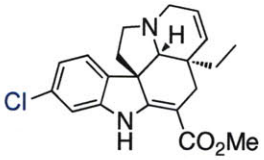 **7c**	**R = phenyl** 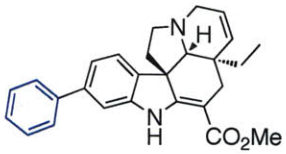 **7d**	**R = 4-Fphenyl** 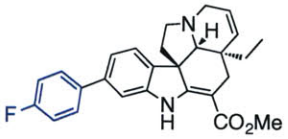 **7e**
Expected [M+H]	371.1521	413.2224	431.2129
Observed [M+H]	371.1514	413.2233	431.2136
Accuracy (ppm)	-1.8	+2.2	+1.6
MS/MS fragments	371.1, 339.1	413.2, 381.2	431.2, 399.2
RT (min)	2.17	2.61	2.61

Tabersonine **7**	**R = 4-methoxy phenyl** 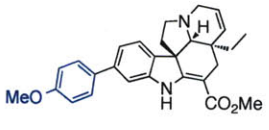 **7f**	**R = 4-methyl phenyl** 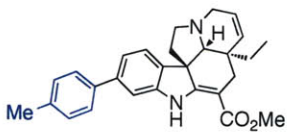 **7g**	**R = furanyl** 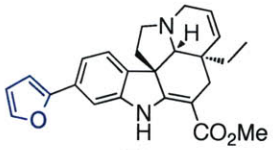 **7i**
Expected [M+H]	443.2329	427.2380	403.2016
Observed [M+H]	443.2331	427.2376	403.2019
Accuracy (ppm)	+0.5	-0.9	+0.7
MS/MS fragments	443.2, 411.2	427.2, 395.2	403.2, 371.2
RT (min)	2.55	2.79	2.36

RT = retention time, LC gradient 10-90% acetonitrile/water (0.1% TFA) in 5 minutes

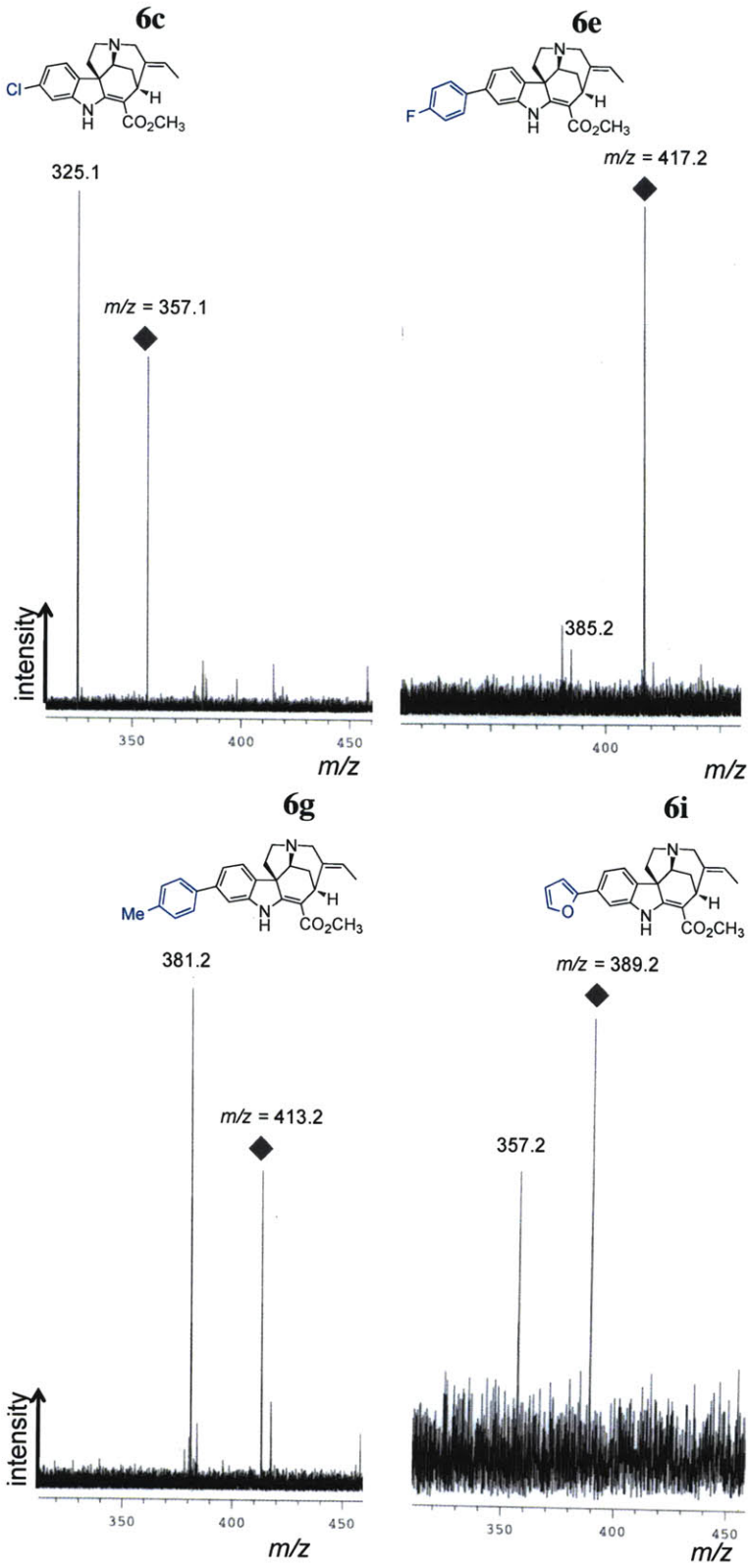

Figure 5.23 MS/MS analysis for akuammicine analogs **6c, 6e, 6g and 6i** (analogs with substituent at the 6-position of the indole ring).

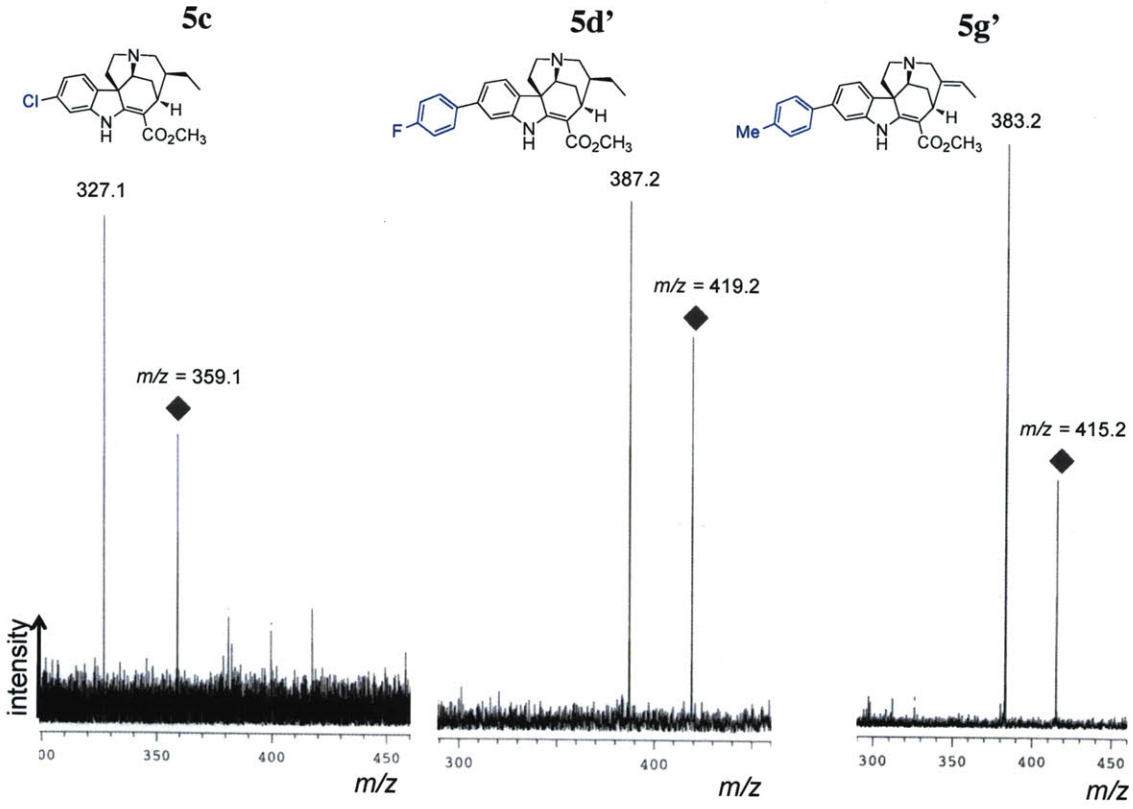

Figure 5.24 MS/MS analysis for 19,20-dihydroakuammicine analogs **5c**, **5d'** and **5g'** (analogs with substituent at the 6-position of the indole ring).

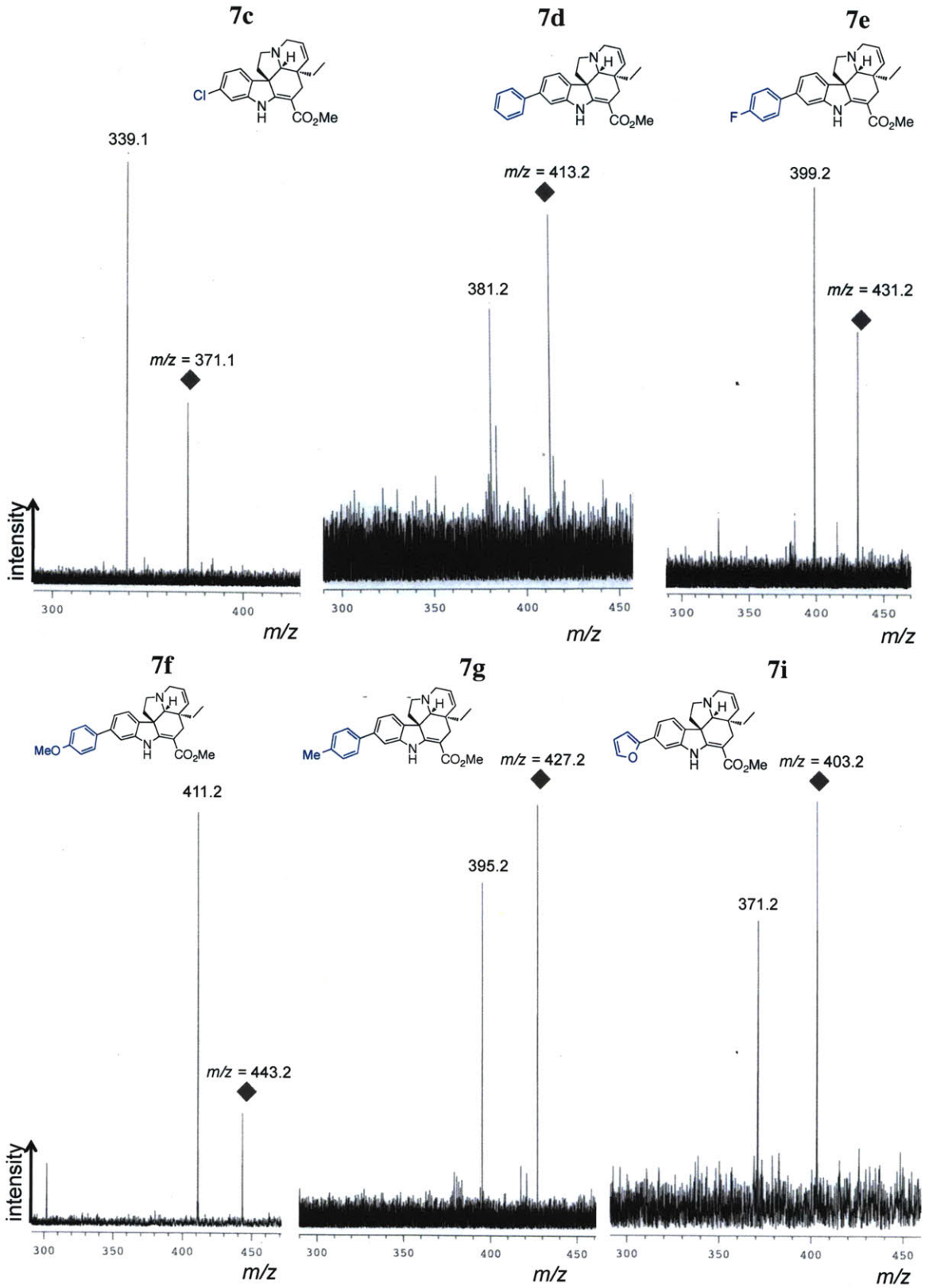

Figure 5.25 MS/MS analysis for tabersonine analogs **7c-i** (analogs with substituent at the 6-position of the indole ring).

5.3 Conclusions

Analogs of natural products, or "unnatural products", sometimes exhibit improved or altered biological activities[1]. Efficient access to these analogs will greatly facilitate drug discovery screening efforts. Efforts to modify *C. roseus* natural products described in previous chapters have enabled regioselective installation of a chemical handle—the organohalogens—into the indole moiety of monoterpene indole alkaloids. Using mild cross-coupling reactions, these halogenated analogs were successfully derivatized with several aryl and heteroaryl functional groups, which could further improve the bioactivity of the compounds. In short, we have applied a chemogenetic approach—installation of a chemical handle into the alkaloids, followed by postbiosynthetic chemical derivatizations—to produce analogs of *C. roseus* MIAs. Efforts to screen these new analogs for biological activies are underway. The effectiveness of this approach should facilitate rational modification of other classes of natural products for biological activity screening and drug development.

5.4 Experimental Methods

5.4.1 Extraction of Alkaloids from Transformed TDC-Suppressed Hairy Roots Fed with Tryptamine Analog Subtrates

To obtain chlorinated and brominated alkaloids, root tips (10-15) from TDC-suppressed[13] (for 7-chlorotryptamine **2a** and 7-bromotryptamine **2b**) and STRvm[14] (for 6-chlorotryptamine **2c**) hairy roots were subcultured in 50 mL Gamborg's B5 liquid media (half strength basal salts, full strength vitamins, 30 g/L sucrose, pH 5.7) and grown at 26°C in the dark at 125 rpm for three weeks prior to supplementing the media with

tryptamine analogs **2a-c** (600 μM final concentration). All tryptamine analog substrates were synthesized as previously reported[18]. After two weeks of co-cultivation, hairy roots were ground with a mortar, pestle and 106 μm acid washed glass beads in *n*-butanol (10 mL/g of fresh weight hairy roots). The crude natural product mixtures were filtered through 0.2 μm cellulose acetate membrane (VWR) and subsequently subjected to LC-MS analysis.

These crude alkaloid mixtures were diluted 1/100 with methanol for mass spectral analysis. Samples were ionized by ESI with a Micromass LCT Premier TOF Mass Spectrometer. The LC was performed on Acquity Ultra Performance BEH C18, 1.7 μm, 2.1 x 100 mm column on a gradient of 10-90% acetonitrile/water (0.1% TFA) over 5 minutes at a flow rate of 0.6 mL/min. The capillary and sample cone voltages were 1300 and 60 V, respectively. The desolvation and source temperature were 300 and 100 °C. The cone and desolvation gas flow rates were 60 and 800 L/hour. Analysis was performed with MassLynx 4.1.

LC-MS analysis of these extracts indicated accumulation of 12-chloro-19,20-dihydroakuammicine **5a** when 7-chlorotryptamine **2a** was supplemented to the media (**Figure 5.6**); 12-bromo-19,20-dihydroakuammicine **5b** when 7-bromotryptamine **2b** was added to the media (**Figure 5.7**); and 11-chloro-19,20-dihydroakuammicine **5c,** 11-chloroakuammicine **6c** and 11-chlorotabersonine **7c** when 6-chlorotryptamine **2c** was supplemented to the media (**Figure 5.9**).

5.4.2 General Procedure for the Small-Scale Synthesis of Aryl Alkaloid Analogs

Crude extract mixtures containing chlorinated or brominated alkaloids were obtained through extraction as described above from 100 mg of fresh hairy roots. The solvent was removed from the mixtures under reduced pressure and the resulting crude solid was placed under vacuum overnight. The crude solid was redissolved in 0.7 mL degassed anhydrous *n*-butanol and to this mixture was added arylboronic acid (3.0 equiv.), $Pd(OAc)_2$ (0.05 equiv.), SPhos (0.13 equiv.) and K_3PO_4 (5.0 equiv.). The mixture was purged with argon and then stirred at 100 °C for 10 minutes until all of the chlorinated alkaloid starting material has been consumed as observed by LC-MS.

The reaction mixture was allowed to cool to room temperature and then diluted with *n*-butanol (4 mL). The mixture was filtered through 0.2 μm cellulose acetate membrane (VWR) and concentrated under vacuum. This oil was then sonicated for 30 minutes in 0.1 % TFA/water (5 mL). The acidified solution was washed with hexanes (3 X 5 mL) to remove hydrophobic compounds. A solution of NH_4OH was then used to adjust the pH of the solution to 9. The basic aqueous solution was then extracted with ethyl acetate (3 X 5 mL). The organic fractions were combined and the solvent was concentrated under vacuum to yield brown oil. This oil was redissolved in 25% acetonitrile/water (0.1% water) and was purified on a 10 x 20 mm Vydec reverse phase column using a gradient of 25 – 60 % acetonitrile/water (0.1% TFA) over 30 minutes. Alkaloids were monitored at 228 nm and fractions containing the alkaloid analogs of interest were combined and concentrated under vacuum. Isolated alkaloids were analyzed by LC-MS (same parameters as above), analytical HPLC, high resolution LC-MS and tandem MS/MS.

5.4.2 General Procedure for the Large-Scale Synthesis of Aryl Alkaloid Analogs

Crude extract mixtures containing chlorinated were obtained through extraction as described in section **5.4.1** from 14-23g of fresh hairy roots. To quantify the amounts of 12-chloro-19,20-dihydroakuammicine **5a** in the extracts, a standard curve was constructed by quantifying the peak areas of several concentrations (20 – 1400 nM) of 12-chloro-19,20-dihydroakuammicine **5a** authentic standard using MassLynx 4.1.

The solvent was removed from the mixtures under reduced pressure and the resulting crude solid was placed under vacuum overnight. The crude solid was redissolved in 30-50 mL degassed anhydrous *n*-butanol and to this mixture was added arylboronic acid (3.0 equiv.), $Pd(OAc)_2$ (0.05 equiv.), SPhos (0.13 equiv.) and K_3PO_4 (5.0 equiv.). The mixture was purged with argon and then stirred at 100 °C for 60 minutes until all of the chlorinated alkaloid starting material has been consumed as observed by LC-MS.

The reaction mixture was allowed to cool to room temperature and then filtered through 0.2 μm cellulose acetate membrane (VWR) and concentrated under vacuum. This oil was then sonicated for 30 minutes in 0.1 % TFA/water (25 mL). The acidified solution was washed with hexanes (3 X 25 mL) to remove hydrophobic compounds. A solution of NH_4OH was then used to adjust the pH of the solution to 9. The basic aqueous solution was then extracted with ethyl acetate (3 X 25 mL). The organic fractions were combined and the solvent was concentrated under vacuum to yield brown oil. This oil was redissolved in 25% acetonitrile/water (0.1% water) and was purified on a 10 x 20 mm Vydec reverse phase column using a gradient of 25 – 60 % acetonitrile/water (0.1% TFA)

over 30 minutes. Alkaloids were monitored at 228 nm and fractions containing the alkaloid analogs of interest were combined and concentrated under vacuum.

Isolated alkaloids were analyzed by LC-MS (same parameters as above), analytical HPLC, high resolution LC-MS, tandem MS/MS, UV-vis spectroscopy, ^{1}H NMR and ^{13}C NMR using a Bruker AVANCE-600 NMR spectrometer equipped with a 5mm 1H{13C,31P} cryo-probe.

12-phenyl-19,20-dihydroakuammicine 5d

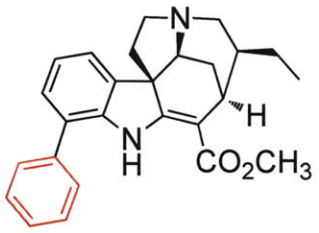

^{1}H NMR (600 MHz, CD_3OD): δ 7.55 (m, 4H), 7.43 (m, 2H), 7.31 (d, J = 7.2 Hz, 1H), 7.10 (t, J = 7.8 Hz, 1H), 4.68 (s, 1H), 3.77 (m, 1H), 3.73 (s, 3H), 3.58 (m, 1H), 3.42 (m, 1H), 3.35 (m, 1H), 3.21 (m, 1H), 3.09 (m, 1H), 2.28 (dd, J = 7.8, 13.8 Hz, 1H), 2.12 (m, 1H), 2.03 (m, 2H), 0.97 (m, 2H), 0.79 (t, J = 7.8 Hz, 3H); ^{13}C NMR (126 MHz, CD_3OD): δ 169.06, 168.33, 141.86, 138.84, 135.41, 130.39 (2×), 129.99, 129.02, 128.78 (2×), 123.67, 120.35, 101.22, 97.43, 66.40, 53.51, 53.18, 52.05, 46.75, 41.64, 40.99, 30.51, 27.25, 24.06, 11.33; ESI-MS (*m/z*): $[M]^+$ calcd. for $C_{26}H_{28}N_2O_2$, 401.2224; found, 401.2228.

12-(4-fluorophenyl)-19,20-dihydroakuammicine 5e

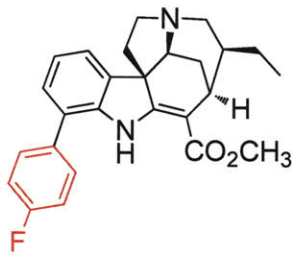

^{1}H NMR (600 MHz, CD_3OD): δ 7.59 (m, 2H), 7.43 (d, J = 7.2 Hz, 1H), 7.29 (m, 3H), 7.10 (t, J = 7.2 Hz, 1H), 4.68 (s, 1H), 3.74 (s, 3H), 3.72 (m, 1H), 3.56 (m, 1H), 3.42 (m, 1H), 3.35 (m, 1H), 3.19 (m, 1H), 3.09 (m, 1H), 2.27 (dd, J = 7.8, 14.4 Hz, 1H), 2.12 (m, 1H), 2.03 (m, 2H), 0.96 (m, 2H), 0.78 (t, J = 7.8 Hz, 3H); ^{13}C NMR (126 MHz, CD_3OD): δ 169.07, 168.28, 135.47, 130.83, 130.76, 129.98, 124.98, 123.71, 120.47, 117.25, 117.08, 97.64, 66.38, 53.48, 53.16, 52.08, 46.73, 41.60, 40.98, 30.49, 27.22, 24.04, 11.32 (note that quaternary carbon peaks are not observed in ^{13}C NMR); ^{19}F NMR (376 MHz, CD_3OD): δ 116.41; ESI-MS (*m/z*): $[M]^+$ calcd. for $C_{26}H_{27}N_2O_2F$, 419.2129; found, 419.2133.

12-furanyl-19,20-dihydroakuammicine 5i

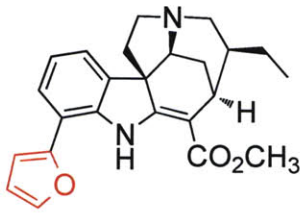

^{1}H NMR (600 MHz, CD_3OD): δ 7.73 (s, 1H), 7.53 (d, J = 7.8 Hz, 1H), 7.37 (d, J = 7.2 Hz, 1H), 7.04 (t, J = 7.2 Hz, 1H), 6.83 (d, J = 3.6 Hz, 1H), 6.62 (t, J = 1.2 Hz, 1H), 4.67 (s, 1H), 3.84 (s, 3H), 3.72 (m, 1H), 3.58 (m, 1H), 3.41 (m, 1H), 3.20 (m, 2H), 3.06 (m, 1H), 2.21 (dd, J = 7.8, 14.4 Hz, 1H), 2.13 (m, 1H), 2.06 (m, 2H), 0.97 (m, 2H), 0.78 (t, J

= 7.2 Hz, 3H); ^{13}C NMR (126 MHz, CD_3OD): δ 143.75, 125.78, 123.23, 120.19, 112.88, 107.42, 97.50, 66.36, 53.21, 53.02, 52.14, 46.78, 41.78, 40.96, 30.52, 27.23, 24.05, 11.29 (note that quaternary carbon peaks are not observed in ^{13}C NMR); ESI-MS (*m/z*): $[M]^+$ calcd. for $C_{24}H_{26}N_2O_3$, 391.2016; found, 391.2015.

5.5 Acknowledgements

We gratefully acknowledge financial support from the NIH (GM074820), the National Science Foundation and the American Cancer Society (RSG-07-025-01-CDD). We thank Dr. Li Li for obtaining mass spectrometric data at the MIT Department of Chemistry Instrumentation Facility.

5.6 References

1. Ganesan, A., The impact of natural products upon modern drug discovery. *Curr Opin Chem Biol* **2008,** *12* (3), 306-17.
2. Voss, M. E.; Ralph, J. M.; Xie, D.; Manning, D. D.; Chen, X.; Frank, A. J.; Leyhane, A. J.; Liu, L.; Stevens, J. M.; Budde, C.; Surman, M. D.; Friedrich, T.; Peace, D.; Scott, I. L.; Wolf, M.; Johnson, R., Synthesis and SAR of vinca alkaloid analogues. *Bioorg Med Chem Lett* **2009,** *19* (4), 1245-9.
3. Birch, A. J., The biosynthesis of antibiotics. . *Pure Appl. Chem.* **1963,** *7*, 527-537.
4. Khosla, C.; Keasling, J. D., Metabolic engineering for drug discovery and development. *Nat. Rev. Drug Disc.* **2003,** *2* (1019-1025).
5. McCoy, E.; O'Connor, S. E., Directed biosynthesis of alkaloid analogues in the medicinal plant periwinkle. *J. Am. Chem. Soc.* **2006,** *128*, 14276-14277.
6. Weissman, K., Mutasynthesis- uniting chemistry and genetics for drug discovery. *Trends Biotechnol.* **2007,** *25*, 139-142.
7. Weist, S.; Sussmuth, R. D., Mutational biosynthesis—a tool for the generation of structural diversity in the biosynthesis of antibiotics. *Appl. Microbiol. Biotechnol.* **2005,** *68*, 141-150.

8. Roy, A. D.; Grüschow, S.; Cairns, N.; Goss, R. J., Gene expression enabling synthetic diversification of natural products: chemogenetic generation of pacidamycin analogs. *J Am Chem Soc* **2010,** *132*, 12243-12245.
9. O'Connor, S. E.; Maresh, J. J., Chemistry and biology of monoterpene indole alkaloid biosynthesis. *Nat Prod Rep* **2006,** *23* (4), 532-47.
10. Bernhardt, P.; McCoy, E.; O'Connor, S. E., Rapid identification of enzyme variants for reengineered alkaloid biosynthesis in periwinkle. *Chem Biol* **2007,** *14* (8), 888-97.
11. McCoy, E.; Galan, M. C.; O'Connor, S. E., Substrate specificity of strictosidine synthase. *Bioorg Med Chem Lett* **2006,** *16* (9), 2475-8.
12. McCoy, E.; O'Connor, S. E., Directed biosynthesis of alkaloid analogs in the medicinal plant Catharanthus roseus. *J Am Chem Soc* **2006,** *128* (44), 14276-7.
13. Runguphan, W.; Maresh, J. J.; O'Connor, S. E., Silencing of tryptamine biosynthesis for production of nonnatural alkaloids in plant culture. *Proc Natl Acad Sci U S A* **2009,** *106* (33), 13673-8.
14. Runguphan, W.; O'Connor, S. E., Metabolic reprogramming of periwinkle plant culture. *Nat Chem Biol* **2009,** *5* (3), 151-3.
15. Runguphan, W.; Qu, X.; O'Connor, S. E., Integrating carbon-halogen bond formation into medicinal plant metabolism. *Nature* **2010,** *468* (7322), 461-4.
16. Neumann, C. S.; Fujimori, D. G.; Walsh, C. T., Halogenation strategies in natural product biosynthesis. *Chem Biol* **2008,** *15* (2), 99-109.
17. Barder, T. E.; Walker, S. D.; Martinelli, J. R.; Buchwald, S. L., Catalysts for Suzuki-Miyaura coupling processes: scope and studies of the effect of ligand structure. *J Am Chem Soc* **2005,** *127* (13), 4685-96.
18. Schumacher, R. W.; Davidson, B. S., Synthesis of didemnolines A-D, N9-substituted β-carboline alkaloids from the marine ascidian *Didemnum* sp. *Tetrahedron* **1999,** *55* (4), 935-942.

CHAPTER 6

CONCLUSIONS AND FUTURE DIRECTIONS

6.1 Conclusions

Medicinal plants produce an array of clinically useful compounds that have continued to be an inspiration for synthetic chemists[1]. The work discussed in the preceding chapters demonstrates that, despite their genetic and developmental complexity, medicinal plants are also a viable platform for synthetic biology efforts. Chapter 2 describes the successful introduction of a biosynthetic enzyme with redesigned substrate specificity into periwinkle, a medicinal plant that produces monoterpene indole alkaloids including the anticancer agents, vinblastine and vincristine (**Figure 6.1**)[2]. We show that the resulting transgenic plant cell culture produced a variety of unnatural alkaloid compounds when co-cultured with simple, achiral, commercially available precursors that the re-engineered enzyme was designed to accept. Regenerated *C. roseus* plants from transformed hairy roots have an apparent morphology and alkaloid profiles similar to that of wild-type plants. To the best of our knowledge, this is the first time that this type of metabolic engineering has been accomplished in plant culture.

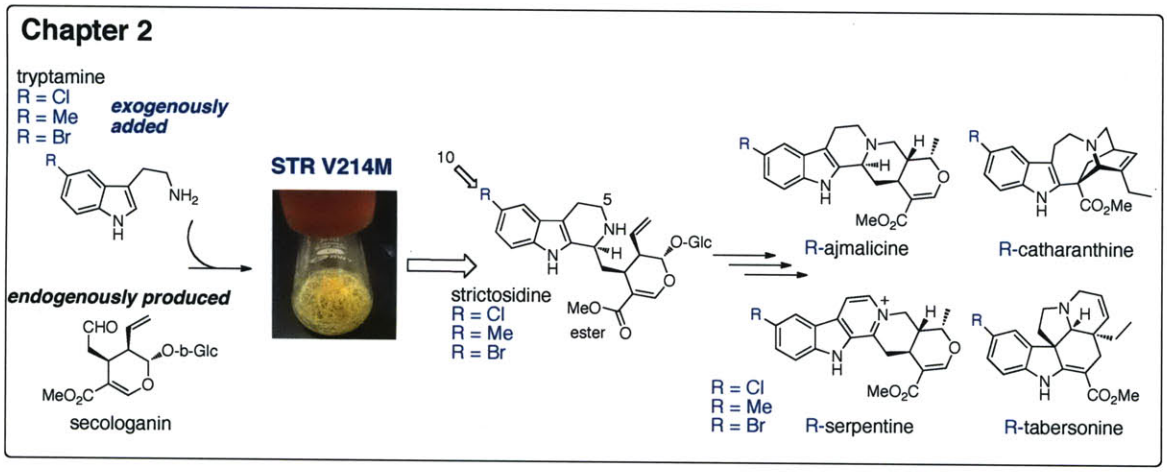

Figure 6.1. Overexpression of an engineered gene in *C. roseus* cell culture. STR: strictosidine synthase.

Chapter 3 describes the introduction of a new functional group– the organohalide– into periwinkle alkaloid biosynthesis (**Figure 6.2**)[3]. We transformed prokaryotic halogenase enzymes into the genome of periwinkle, which lacks the biosynthetic ability to produce halogenated compounds. These prokaryotic halogenases function in the plant cell to generate halogenated tryptophan, which is then shuttled into alkaloid metabolism yielding halogenated monoterpene indole alkaloids. A new functional group– an organohalide– is thereby introduced into the complex metabolism of *C. roseus*, and is incorporated in a predictable and regioselective manner onto the plant alkaloid products.

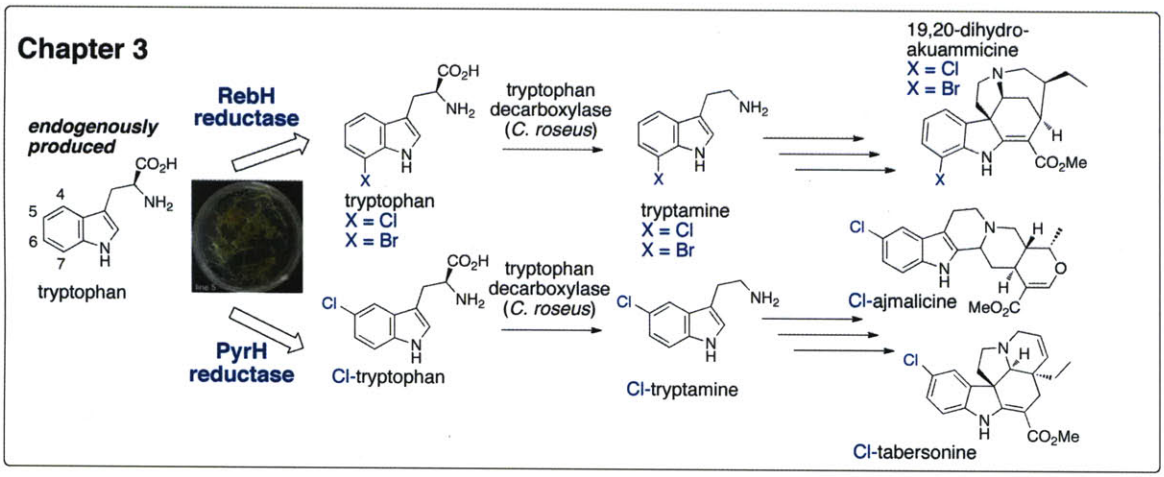

Figure 6.2. Introduction of prokaryotic halogenases into *C. roseus* cell culture.

Chapter 4 describes mutasynthesis of tryptamine-derived alkaloids in periwinkle cell culture (**Figure 6.3**)[4]. We used RNA-mediated silencing of tryptophan decarboxylase to suppress the biosynthesis of the endogenous tryptamine substrate. Monoterpene indole alkaloid production almost completely disappeared in transformed hairy roots. Monoterpene indole alkaloid biosynthesis could be rescued by the addition of tryptamine

or a number of analogs to the culture medium. Notably, the yields of a number of unnatural alkaloids derived from an exogenous unnatural tryptamine substrate were improved because the natural alkaloids were no longer present. To the best of our knowledge, this is the first example of mutasynthesis in a plant system.

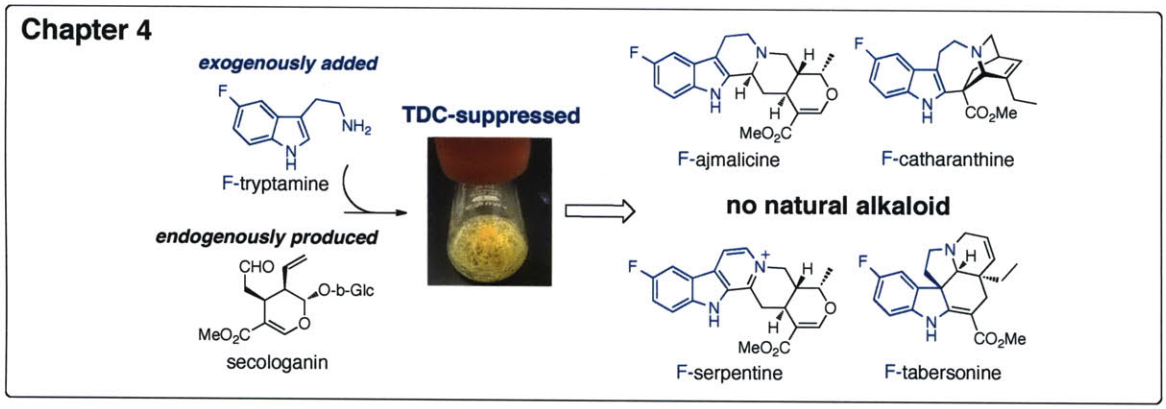

Figure 6.3. Mutasynthesis of tryptamine-derived alkaloids in *C. roseus* cell culture. TDC: tryptophan decaboxylase.

Chapter 5 describes post-biosynthetic diversification of monoterpene indole alkaloids (**Figure 6.4**). We utilized halogenated alkaloids that have been generated via strategies described in Chapter 2-4 in palladium-catalyzed Suzuki-Miyaura cross-coupling reactions. Several aryl and heteroaryl analogs of monoterpene indole alkaloids were synthesized and purified in milligram quantities. The effectiveness of this approach will facilitate rational modification of other classes of natural products for biological activity screening and drug development.

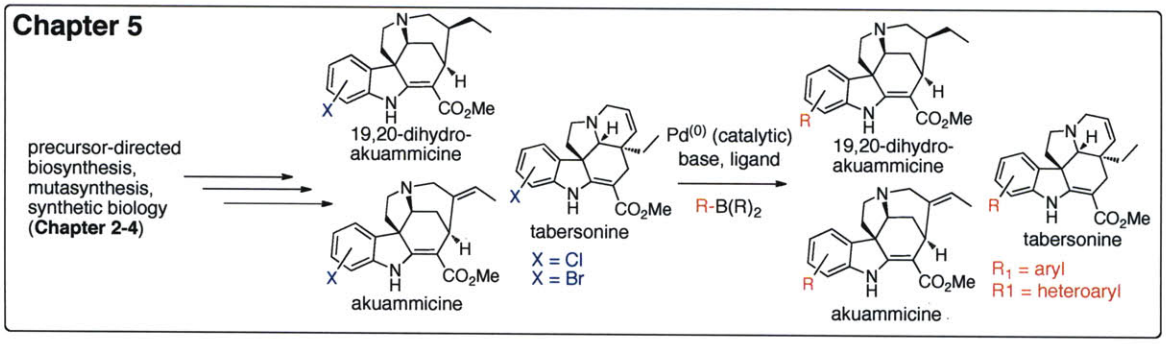

Figure 6.4. Chemogenetic approaches to derivatize halogenated alkaloids.

Appendix D describes the re-engineering of *Papaver somniferum* codeine O-demethylase (*Ps*CODM), a 2-oxoglutarate/Fe(II)-dependent dioxygenase in morphine biosynthesis, to exhibit higher substrate specificity towards codeine (**Figure 6.5**). Wild type *Ps*CODM can catalyze the O-demethylation of both codeine and thebaine[5]. Homology model of *Ps*CODM based on the crystal structure of *Arabidopsis thaliana* anthocyanidine synthase (*At*ANS) was created, and *Ps*CODM's substrate binding site, based on this protein model, was identified. Rational site-directed mutagenesis of the residues that form the substrate-binding pocket yielded a mutant that maintains its demethylase activity towards codeine but not thebaine. We envision that this *Ps*CODM mutant will be of great use in microbial production of morphine. Specifically, reconstitution of morphine biosynthetic pathway in yeast using this mutant instead of the wild type enzyme will prevent accumulation of an off-pathway intermediate oripavine, thereby increasing the yield of morphine.

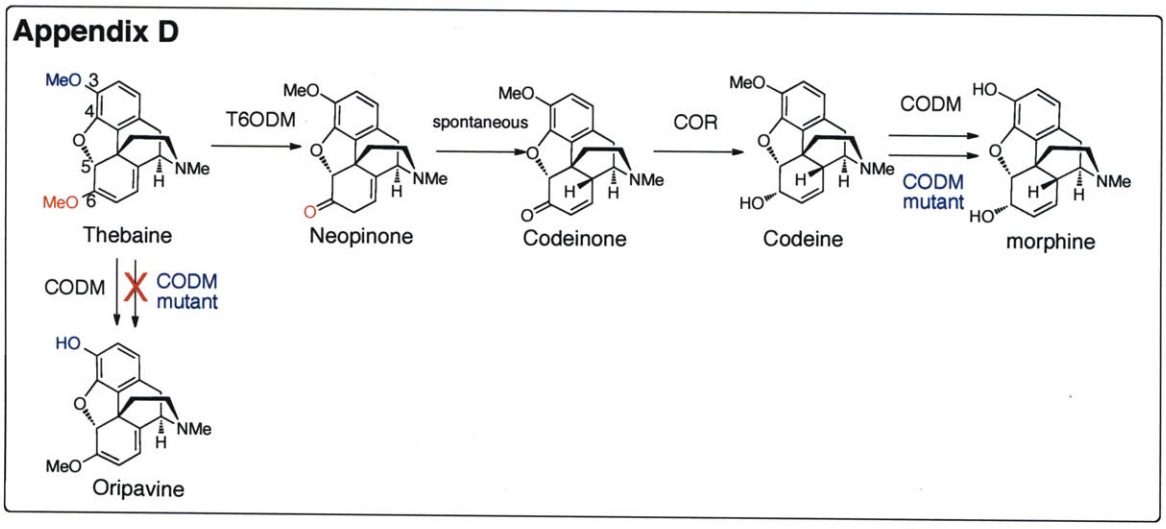

Figure 6.5. Re-engineering of *Papaver somniferum* codeine O-demethylase (*Ps*CODM) in morphinan alkaloid biosynthetic pathway. T6ODM: thebaine 6-O-demethylase; COR: codeinone reductase; CODM: codeine O-demethylase.

6.2 Future Directions

6.2.1 Overcoming the Bottleneck in Halogenated Alkaloid Biosynthesis in RebH/F Hairy Root Cultures

Chapter 3 describes the successful engineering of plant cell culture to produce halogenated alkaloids autonomously[3]. We introduced halogenase enzymes into periwinkle hairy root culture, which lacks the biosynthetic ability to produce halogenated compounds natively. These prokaryotic halogenases function in the plant cell to generate halogenated tryptophan, which is then incorporated into alkaloid metabolism yielding halogenated monoterpene indole alkaloids. Normally, tryptophan does not accumulate in either wild type or transformed hairy roots. However, we observed chlorinated tryptophan accumulation in transformed hairy roots, suggesting that decarboxylation of chlorinated tryptophan is a bottleneck *in vivo*. This is consistent with the 30-fold-lower

catalytic efficiency of the decarboxylase enzyme (TDC) for chlorinated tryptophan *in vitro*. Accumulation of chlorinated tryptophan is not only "wasteful", but may cause the apparent slow growth morphology in the hairy roots. Thus, we are presented with a unique metabolic engineering problem to aleviate this bottleneck in halogenated alkaloid production. Possible solutions are illustrated in **Figure 6.6**. i) Overexpress *C. roseus* TDC along with RebH and RebF in *C. roseus* hairy root cultures. Both the constitutive and inducible promoters should be explored to yield hairy root cultures with optimal halogenated alkaloid production capacity and with no apparent growth abnormalities. ii) Re-engineer *C. roseus* TDC to have greater substrate promiscuity. Specifically, identify a TDC mutant that can decarboxylate halogenated tryptophan analogs with higher catalytic efficiency compared to that of the wild type enzyme. Introduction of this re-engineered enzyme into *C. roseus* should yield transformed hairy root cultures that accumulate lower levels of chlorinated tryptophan and higher levels of chlorinated alkaloids. iii) Re-engineer halogenases to chlorinate tryptamine preferentially over native substrate tryptophan.

i. Overexpress C. roseus TDC along with RebH and RebF in C. roseus hairy root cultures

In the first engineering effort to overcome this bottleneck, Weslee Glenn constitutively overexpressed TDC, in addition to RebH and RebF, in *C. roseus* hairy roots (**i, Figure 6.6**). Transformed lines accumulated lower levels of 7-chlorotryptophan, suggesting that higher expression of TDC led to the expected greater clearance of the compound (Glenn and O'Connor, unpublished). However, for reasons that remain unclear, lower levels of chlorinated alkaloids were observed in these transgenic lines compared to lines that had

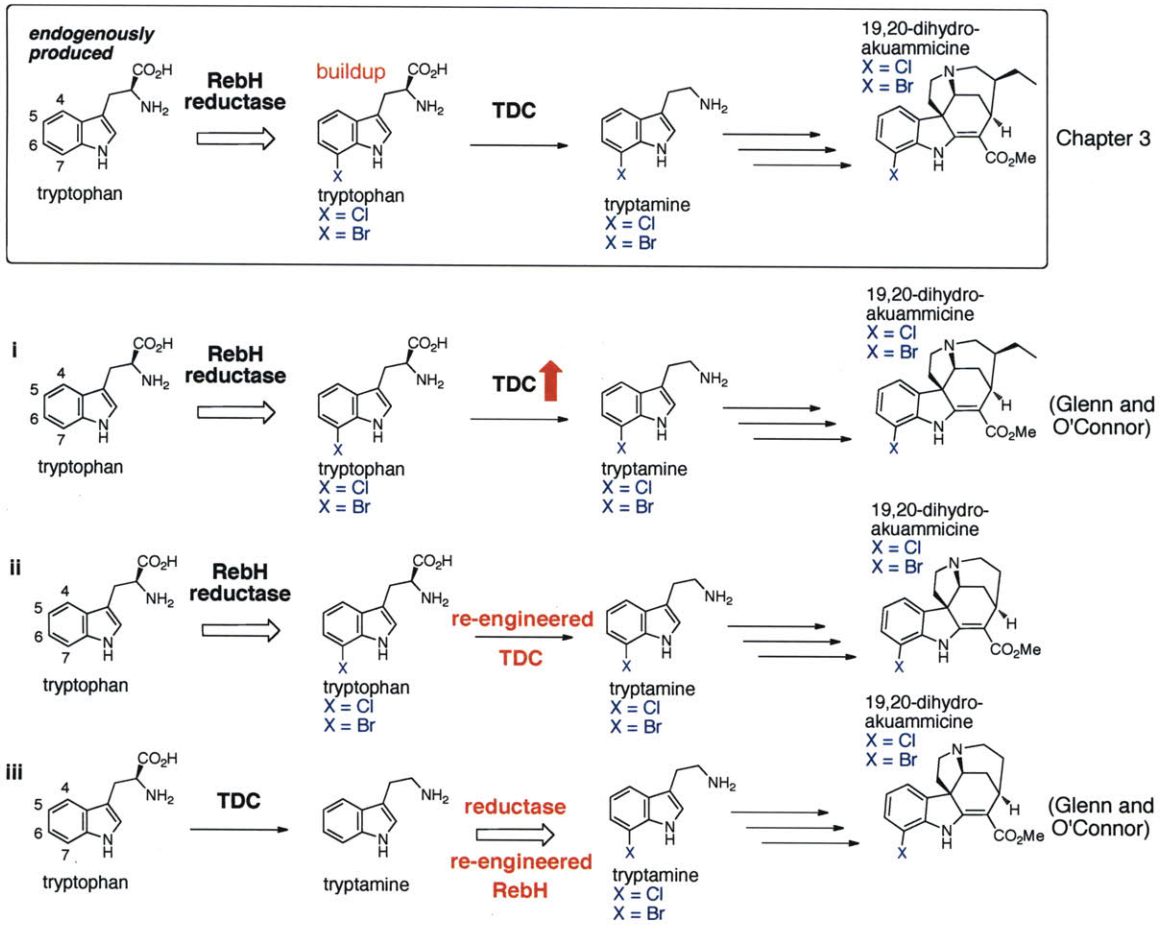

Figure 6.6. Strategies to overcome the bottleneck in halogenated alkaloid biosynthesis in RebH/F hairy root cultures. TDC: tryptophan decarboxylase.

been transformed with only RebH and RebF. Moreover, TDC/RebF/H transformed lines grew significantly slower than RebF/H lines and stopped growing altogether after several subcultures. Glenn and O'Connor's findings are consistent with previous studies that observed similar growth retardation and low alkaloid levels in *C. roseus* cell cultures that constitutively overexpress TDC. Therefore, instead of using constitutive promoters to drive the expression of TDC, future engineering efforts should utilize inducible promoters, such as the glucocorticoid- and ethanol-inducible promoters[6,7]. In addition to enabling temporal control of gene expression, these promoters have been shown to be dose dependent; expression level correlates with the concentration of the inducer (i.e. glucocortisone or ethanol) in the culture media. We envision that having the ability to control both when and how much to overexpress TDC will allow us to prevent the wasteful buildup of chlorinated tryptophan while minimizing the detrimental effects of TDC constitutive overexpression.

ii. Re-engineer C. roseus TDC to have greater substrate promiscuity

Another strategy to prevent the accumulation of chlorinated tryptophan is to improve the rate of the decarboxylation step. Specifically, TDC should be re-engineered to carry out the decarboxylation of chlorinated and brominated tryptophan with higher catalytic efficiency (**ii, Figure 6.6**). While the crystal structure of *C. roseus* TDC has not been determined at this time, the structures of several mammalian aromatic amino acid decarboxylases are available. Of these, *C. roseus* TDC shows the highest sequence identity (42%) to the pig kidney L-DOPA decarboxylase, which converts L-dihydroxyphenylalanine (L-DOPA) to dopamine[8]. Homology models of *C. roseus* TDC

based on the structure of the pig kidney L-DOPA decarboxylase will provide structural insights into the enzyme's substrate binding pocket. Rational re-design of TDC should be done to yield mutants with enhanced catalytic efficiency towards chlorinated and brominated tryptophan analogs. Introduction of this re-engineered enzyme along with RebH and its reductase partner into *C. roseus* should yield transformed hairy root cultures that accumulate lower levels of chlorinated tryptophan and higher levels of chlorinated alkaloids.

iii. Re-engineer halogenases to chlorinate tryptamine preferentially over native substrate tryptophan

Plant primary metabolism is an essential part of plant survival, whereas secondary metabolites (sometimes referred to as 'specialized metabolites'), while not fully elucidated, are implicated to be involved in plant defense[9]. The modification—integration of a halogen moiety—that we have introduced into *C. roseus* occurs immediately after the proposed final step of primary metabolism. Engineering at this step may affect plant development more strongly than modifications done later in secondary metabolism. Ideally, we should introduce halogenase enzymes that modify tryptamine, the substrate proposed to be at the beginning of secondary metabolism. Engineering at this step may prevent any undesirable, detrimental effects on plant growth (**iii**, **Figure 6.6**). Therefore, RebH should be re-engineered to chlorinate tryptamine preferentially over native substrate tryptophan. An ongoing effort by Weslee Glenn has identified a RebH mutant that prefers tryptamine over tryptophan at physiological concentrations of both substrates

(Glenn and O'Connor). The re-engineered mutant should be introduced to *C. roseus* hairy root culture for *in vivo* production of halogenated MIAs.

6.2.2 Generation of Transgenic Plant Culture Expressing 6- and 4-halogenases

The experiments described in chapter 3 demonstrate that a new functional group– an organohalide– can be introduced into the complex metabolism of *C. roseus* (**Figure 6.7**)[3]. At present, we have successfully incorporated halides in a regioselective manner onto the plant alkaloid products at two different positions (5- and 7-positions) on the indole ring. A halogenase enzyme that chlorinates tryptophan at the 6-position has been identified[10]. Like RebH and PyrH, the 6-halogenase enzyme, called Thal, is flavin-dependent and requires a partner reductase to maintain flavin at the functional oxidation state. *In vitro* studies demonstrate that Thal can also use bromide to yield 6-bromotryptophan[10]. Future efforts should focus on the introduction of Thal, along with flavin reductase RebF and the strictosidine synthase mutant STRvm into *C. roseus* to generate transformed plant culture capable of producing chlorinated and brominated alkaloids.

Though there is speculation of their existence, at present halogenases that chlorinate tryptophan at the 4-position have not yet been identified. Several proposed auxin biosynthetic pathways use tryptophan as the precursor[11]. In one proposed pathway, tryptophan is converted to tryptamine before being further metabolized in several steps to the auxin indole-3-acetic acid (IAA). It is mechanistically plausible that another auxin, 4-chloroindole-3-acetic acid (the 4-chloro analog of IAA), is derived from either 4-chlorotryptophan or 4-chlorotryptamine, suggesting that plant 4-halogenase enzymes may

exist. Once such a halogenase is identified, it should be introduced into *C. roseus* to generate transformed plant culture capable of producing chlorinated alkaloids.

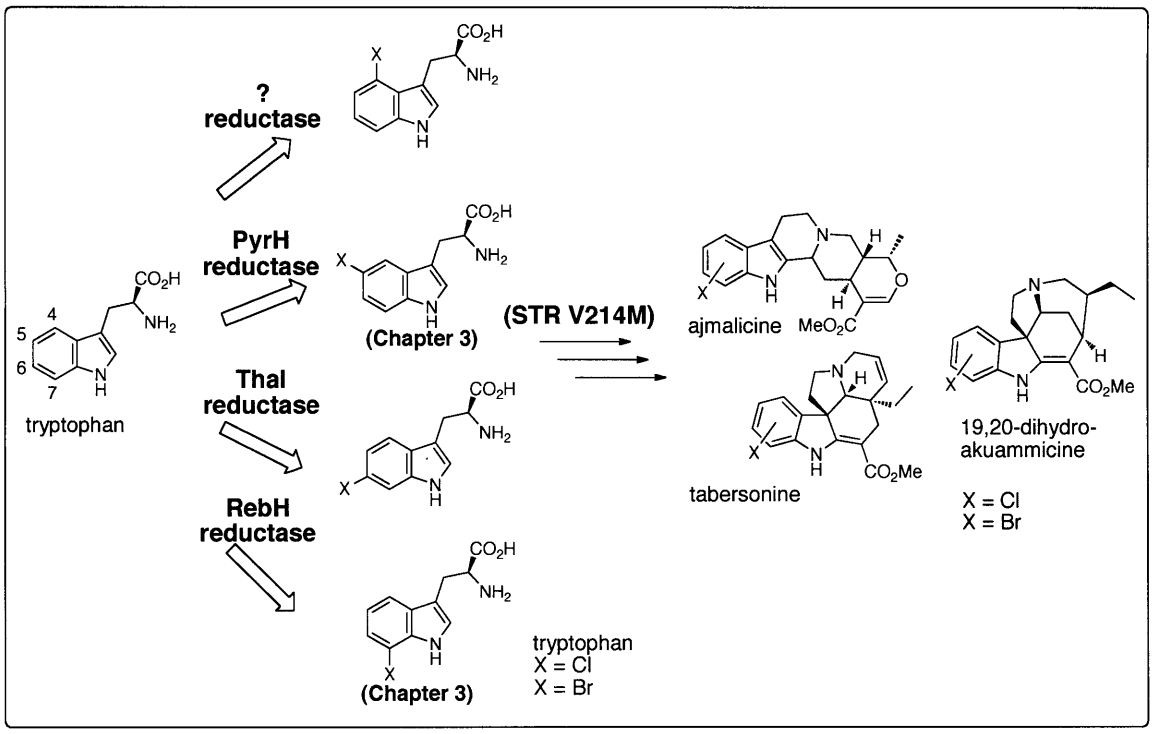

Figure 6.7. Generation of transgenic plant cultures capable of producing chlorinated and brominated alkaloids.

6.2.3 Applying Combinatorial Biosynthesis to Other Monoterpene Indole Alkaloid Pathways

Plants in the Apocynaceae, Loganiaceae, Rubiaceae and Nyssaceae families all produce monoterpene indole alkaloids with dramatically diverse structures[12]. The studies described in the preceding chapters focused primarily on *C. roseus* for various practical reasons: *C. roseus* seedlings grow relatively quickly (1 week germination time); are amenable to genetic transformation and hairy root-to-plant regeneration; and the

biosynthetic pathway has been partially elucidated. From medicinal chemistry standpoint, however, other MIA-producing plants are equally important and similarly deserving of metabolic reprogramming/synthetic biology efforts (**Figure 6.8**). *Camptotheca acuminata* and *Ophiorrhiza pumila* both produce the antitumor agent camptothecin; *Rauwolfia serpentina* produces the antiarrhythmic agent ajmaline; and *strychnos nux-vomica* produces the convulsant strychnine. The success of these engineering efforts depends on how substrate specific these other MIA biosynthetic pathways are. We envision that the introduction of re-engineered STR or prokaryotic halogenases into other MIA producing plants will lead to production of unnatural alkaloids.

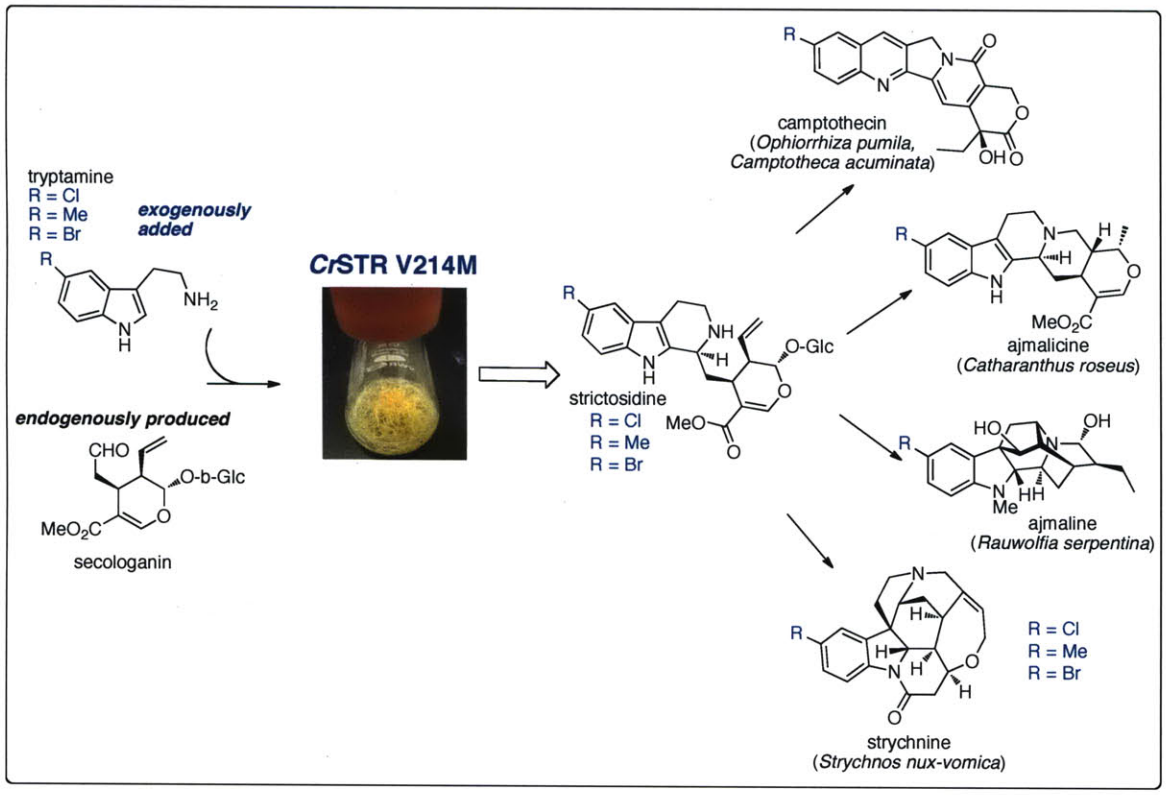

Figure 6.8. Metabolic reprogramming of alkaloid biosynthesis in MIA-producing plant cell cultures.

6.2.4 Cloning of MIA Biosynthetic Genes and Elucidation of MIA Biosynthetic Pathway

Advances in plant metabolism research have not been as dramatic as those in prokaryotic and fungal systems. Recent decades have witnessed successful engineering of microbial systems to produce high-value natural and unnatural compounds at industrial scale (**Chapter 1**)[13-17]. The primary reason for the lag in plant metabolism research is the complexity associated with cloning plant biosynthetic genes in plants. Genes of plant biosynthetic pathways are normally unclustered, and many biosynthetic enzymes are labile or expressed in low abundance. Therefore, the identification of enzymes is typically more arduous in plant metabolism research. While traditional purification strategies remain an effective strategy for identifying certain plant enzymes, modern approaches are clearly needed to fully elucidate the monoterpene indole alkaloid pathway—along with many other plant pathways—in a rapid timeframe. A collaborative research endeavor among the O'Connor group and several other groups is focused on obtaining the transcriptomic and metabolomic data for *C. roseus* and 13 other medicinal plants. By correlating the transcript levels and metabolite profiles for each tissue types (e.g. root, stem, shoot, flowers, leaves), gene-metabolite maps can be created to facilitate the identification of genes involved in the biosynthesis of a specific metabolite. These gene discovery efforts will enable heterologous production of natural and unnatural alkaloids in microbial systems.

6.2.5 Biological Activity Screening of MIA Analogs

The experiments described in the preceding chapters produced a variety of analogs of ajmalicine, tabersonine, catharanthine, serpentine, akuammicine and dihydroakuammicine. Many of these natural alkaloids have known biological activities. Ajmalicine is an adrenergic receptor antagonist and is used clinically to treat high blood pressure[18, 19]. Serpentine is a topoisomerase II inhibitor[20] and several serpentine analogs have been shown to exhibit superior inhibitory activity to the natural serpentine (McCoy, Usera and O'Connor, unpublished). Akuammicine is an opioid receptor agonist[21]. Tabersonine derivatives, Jerantinines A–G, exhibit cytotoxic activity against human KB cells[22]. It is imperative to screen MIA analogs for biological activity. We have submitted several of these compounds for biological activity screening at Vanderbilt University. Future experiments should aim to assay the remaining analogs for a broad range of biological assays.

6.2.6 Coupling Reactions *In Planta*

Chapter 5 describes chemical derivatization of chlorinated and brominated alkaloids with a variety of aryl and heteroaryl boronic acids via the palladium-catalyzed Suzuki-Miyaura coupling reactions. Our current approach involves two separate steps: 1) obtain halogenated analogs by genetic engineering of *C. roseus* either with or without precursor-feeding and (2) modify these halogenated analogs synthetically via the Suzuki-Miyaura coupling reactions. After one week of culture in the presence of halogenated tryptamine substrates, the plant material is lysed and alkaloids are extracted into an organic solvent. The crude alkaloid extracts are then used in the chemical derivatization reaction. We

envision that the efficiency of the process will be improved if the coupling reactions can be performed inside the plant cells.

In a recent work, Bradley and coworkers have extended the versatility of the Suzuki-Miyaura coupling reactions by performing the reaction inside living cells[23]. Palladium is normally toxic to cells, rendering previous attempts at *in vivo* coupling reactions unsuccessful. To overcome this problem, the team trapped palladium nanoparticles within polystyrene microspheres, thereby preventing the metal catalyst from killing the cells. The polystyrene microspheres with immobilized palladium can enter eukaryotic cells and mediate the Suzuki–Miyaura cross-coupling reactions. Applying this strategy to plant cell and tissue cultures will provide a direct one-step access to MIA analogs. Brominated analogs are sufficiently activated to undergo the coupling reactions at 26°C, the temperature at which hairy roots are normally maintained. Specifically, one week after supplementing the culture with brominated tryptamine substrates, the polystyrene microspheres with immobilized palladium nanoparticles will be supplemented into the hairy root media along with the other coupling reagents. Portions of hairy roots will be taken out from the culture at different time intervals for alkaloid assessment. The success of this strategy depends on, among other factors, whether or not the palladium catalyst and the other coupling reagents will be accessible to brominated alkaloids. Will polystyrene microspheres and other coupling reagents be able to enter plant cells? If so, will they all be localized in the organelle(s) where brominated alkaloids are accumulated? These are not easy questions to answer, and the underlying challenges are by no means

straightforward to overcome. Nevertheless, we envision that the success of this strategy will find broad applications in *in planta* labeling and alkaloid localization studies.

6.2.7. Elucidating the Physiological Role of MIAs

Extensive efforts have led to the elucidation of physiological functions of a number of plant-derived alkaloids, such as the pyrrolizidine and tropane alkaloids[24]. For example, transgenic tobacco plants in which the nicotine biosynthetic pathway is genetically silenced have been used to demonstrate the defensive role of nicotine[25]. In contrast, while medicinal properties of MIAs are well documented, their physiological roles remain largely unknown. In *C. roseus,* MIA biosynthesis can be elicited by fungal extracts[26], suggesting that MIA biosynthesis appears to be a plant response to fungal attack. Moreover deglycosylated strictosidine has been shown to exhibit weak anti-microbial activity[27], suggesting that the compound may deter pathogens. However, aside from these examples, the roles MIAs play in *C. roseus* are not known. Specifically, what advantage do these compounds confer to the producing organism?

Chapter 4 describes suppression of tryptamine biosynthesis in *C. roseus* hairy root cultures[4]. Alkaloid production almost completely disappeared in transformed hairy roots. The lack of tryptamine and downstream alkaloids did not appear to affect the growth or morphology of the silenced cultures, indicating that tryptamine and downstream alkaloids do not play an essential role in the controlled environment of plant cell culture. We attempted to regenerate *C. roseus* plants from these transformed hairy roots. These tryptamine-deficient plantlets appeared to be regenerating normally in plant media under

sterile environment. However, once the plantlets were transferred to soil (Miracle gro), they exhibited severe growth retardation and were unviable. Together, these experiments suggest that while tryptamine and MIAs do not appear to play an essential role in growth or development in *C. roseus* hairy root culture, they may be vital for whole plant survival in a non-controlled environment.

Tryptamine and its precursor tryptophan may be involved in the biosynthesis of auxins, which play an essential role in plant development[11]. Therefore, the primary reason that tryptamine-deficient plants are not viable in a non-controlled environment may not be directly related to the absence of MIAs but rather the detrimental perturbation of auxin biosynthesis associated with TDC silencing. To determine the ecological roles of MIAs, another precursor should be targeted for suppression. Previous attempts to suppress secologanin biosynthesis in *C. roseus* hairy root cultures using the chemical inhibitor fosmidomycin had no apparent adverse effects on root growth[28]. Moreover, secologanin is produced in only a few plant species, suggesting that it does not have a general function in plant metabolism. Simply put, suppression of secologanin biosynthesis provides a more unambiguous route to elucidate the physiological roles of MIAs. To accomplish this, at least one of the three known biosynthetic enzymes in secologanin pathway (i.e. geraniol 10-hydroxylase (G10H), loganic acid methyl transferase (LOMT) and secologanin synthase (SLS)) will be silenced (**Chapter 1**). Suppression of the more upstream enzyme—G10H, in this case—is ideal because it will not lead to any wasteful buildup of pathway intermediates. We envision that silencing of G10H, just as in the case of silencing of TDC, will completely obliterate alkaloid biosynthesis. By using the same

procedure described in Chapter 4, G10H-suppressed hairy roots will be generated. Mass spectrometry and reverse transcription PCR analyses will be used to ensure suppression of alkaloid biosynthesis. Transformed hairy roots will be used to regenerate the corresponding transgenic plants. As a control, all regenerated plants will be compared to a control plant that has been regenerated from wild type hairy root culture that lacks any silencing plasmid. If G10H-suppressed plants appear to be viable on soil, we will assess the alkaloid content in the leaves, stems and the root tissue of these regenerated plants. Finally, a more thorough study detailing how 'alkaloid-free' C. roseus plants interact with pathogens from the environment will provide some of the very first data regarding the ecological roles of MIAs.

6.3 References

1. Ganesan, A., The impact of natural products upon modern drug discovery. *Curr Opin Chem Biol* **2008,** *12* (3), 306-17.
2. Runguphan, W.; O'Connor, S. E., Metabolic reprogramming of periwinkle plant culture. *Nat Chem Biol* **2009,** *5* (3), 151-3.
3. Runguphan, W.; Qu, X.; O'Connor, S. E., Integrating carbon-halogen bond formation into medicinal plant metabolism. *Nature* **2010,** *468* (7322), 461-4.
4. Runguphan, W.; Maresh, J. J.; O'Connor, S. E., Silencing of tryptamine biosynthesis for production of nonnatural alkaloids in plant culture. *Proc Natl Acad Sci U S A* **2009,** *106* (33), 13673-8.
5. Hagel, J. M.; Facchini, P. J., Dioxygenases catalyze the O-demethylation steps of morphine biosynthesis in opium poppy. *Nat Chem Biol* **2010,** *6* (4), 273-5.
6. Hughes, E. H.; Hong, S. B.; Shanks, J. V.; San, K. Y.; Gibson, S. I., Characterization of an inducible promoter system in Catharanthus roseus hairy roots. *Biotechnol Prog* **2002,** *18* (6), 1183-6.
7. Peebles, C. A.; Gibson, S. I.; Shanks, J. V.; San, K. Y., Characterization of an ethanol-inducible promoter system in Catharanthus roseus hairy roots. *Biotechnol Prog* **2007,** *23* (5), 1258-60.

8. Burkhard, P.; Dominici, P.; Borri-Voltattorni, C.; Jansonius, J. N.; Malashkevich, V. N., Structural insight into Parkinson's disease treatment from drug-inhibited DOPA decarboxylase. *Nat Struct Biol* **2001,** *8* (11), 963-7.
9. Hartmann, T., Plant-derived secondary metabolites as defensive chemicals in herbivorous insects: a case study in chemical ecology. *Planta* **2004,** *219* (1), 1-4.
10. Seibold, C.; Schnerr, H.; Rumpf, J.; Kunzendorf, A.; Hatscher, C.; Wage, T.; Ernyei, A. J.; Dong, C.; Naismith, J. H.; Van Pee, K.-H., A flavin-dependent tryptophan 6-halogenase and its use in modification of pyrrolnitrin biosynthesis. *Biocatalysis and Biotransformation* **2006,** *24* (6), 401-408.
11. Zhao, Y.; Christensen, S. K.; Fankhauser, C.; Cashman, J. R.; Cohen, J. D.; Weigel, D.; Chory, J., A role for flavin monooxygenase-like enzymes in auxin biosynthesis. *Science* **2001,** *291*, 306-309.
12. O'Connor, S. E.; Maresh, J., Chemistry and biology of monoterpene indole alkaloid biosynthesis. *Nat. Prod. Rep.* **2006,** *23*, 532-547.
13. Ajikumar, P. K.; Xiao, W. H.; Tyo, K. E.; Wang, Y.; Simeon, F.; Leonard, E.; Mucha, O.; Phon, T. H.; Pfeifer, B.; Stephanopoulos, G., Isoprenoid pathway optimization for Taxol precursor overproduction in Escherichia coli. *Science* **2010,** *330* (6000), 70-4.
14. Hawkins, K. M.; Smolke, C. D., Production of benzylisoquinoline alkaloids in Saccharomyces cerevisiae. *Nat. Chem. Biol.* **2008,** *4*, 564-573.
15. Khosla, C.; Keasling, J. D., Metabolic engineering for drug discovery and development. *Nat. Rev. Drug Disc.* **2003,** *2* (1019-1025).
16. Leonard, E.; Ajikumar, P. K.; Thayer, K.; Xiao, W. H.; Mo, J. D.; Tidor, B.; Stephanopoulos, G.; Prather, K. L., Combining metabolic and protein engineering of a terpenoid biosynthetic pathway for overproduction and selectivity control. *Proc Natl Acad Sci U S A* **2010,** *107* (31), 13654-9.
17. Minami, H.; Kim, J.-S.; Ikezawa, N.; Takemura, T.; Katayama, T.; Kumagai, H.; Sato, F., Microbial production of plant benzylisoquinoline alkaloids. *Proc. Natl. Acad. Sci. USA* **2008,** *105*, 7393-7398.
18. Roquebert, J.; Demichel, P., Inhibition of the alpha 1 and alpha 2-adrenoceptor-mediated pressor response in pithed rats by raubasine, tetrahydroalstonine and akuammigine. *Eur J Pharmacol* **1984,** *106* (1), 203-5.
19. Li, S.; Long, J.; Ma, Z.; Xu, Z.; Li, J.; Zhang, Z., Assessment of the therapeutic activity of a combination of almitrine and raubasine on functional rehabilitation following ischaemic stroke. *Curr Med Res Opin* **2004,** *20* (3), 409-15.
20. Dassonneville, L.; Bailly, C., Stimulation of topoisomerase II-mediated DNA cleavage by an indazole analogue of lucanthone. *Biochem Pharmacol* **1999,** *58* (8), 1307-12.
21. Menzies, J. R.; Paterson, S. J.; Duwiejua, M.; Corbett, A. D., Opioid activity of alkaloids extracted from Picralima nitida (fam. Apocynaceae). *Eur J Pharmacol* **1998,** *350* (1), 101-8.
22. Lim, K.-H.; Hiraku, O.; Komiyama, K.; Kam, T.-S., Jerantinines A-G, Cytotoxic *Aspidosperma* Alkaloids from *Tabernaemontana corymbosa*. *Journal of Natural Products* **2008,** *71* (9), 1591-1594.
23. Yusop, R. M.; Unciti-Broceta, A.; Johansson, E. M.; Sanchez-Martin, R. M.; Bradley, M., Palladium-mediated intracellular chemistry. *Nat Chem* **2011,** *3* (3), 241-5.

24. Hartmann, T., Plant-derived secondary metabolites as defensive chemicals in herbivorous insects: a case study in chemical ecology. *Planta* **2004,** *219*, 1-4.
25. Voelckel, C.; Krügel, T.; Gase, K.; Heidrich, N.; Dam, N. M. v.; Winz, R.; Baldwin, I. T., Anti-sense expression of putrescine N-methyltransferase confirms defensive role of nicotine in Nicotiana sylvestris against Manduca sexta. *Chemoecology* **2001,** *11* (3), 121-126-126.
26. Zhao, J.; Zhu, W.-H.; Hu, Q., Selection of fungal elicitors to increase indole alkaloid accumulation in catharanthus roseus suspension cell culture. *Enzyme and Microbial Technology* **2001,** *28* (7-8), 666-672.
27. Luijendijk, T. J. C.; van der Meijden, E.; Verpoorte, R., Involvement of strictosidine as a defensive chemical in Catharanthus roseus. *J. Chem. Ecol.* **1996,** *22*, 1355-1366.
28. Zeidler, J.; Schwender, J.; Mueller, C.; Wiesner, J.; Weidemeyer, C.; Beck, E.; Jomaa, H.; Lichtenthaler, H. K., Inhibition of the non-mevalonate 1-deoxy-D-xylulose-5-phosphate pathway of plant isoprenoid biosynthesis by fosmidomycin. *Zeitschrift fuer Naturforschung, C: Biosciences* **1998,** *53*, 980-986.

CHAPTER 2 - APPENDIX A

LC-MS TRACES AND NMR SPECTRA:

EVALUATION OF ALKALOID

PRODUCTION IN ENGINEERED *C. ROSEUS*

Part of this appendix is published as a brief communication in

Nature Chemical Biology **2009**, *5*, 151-153

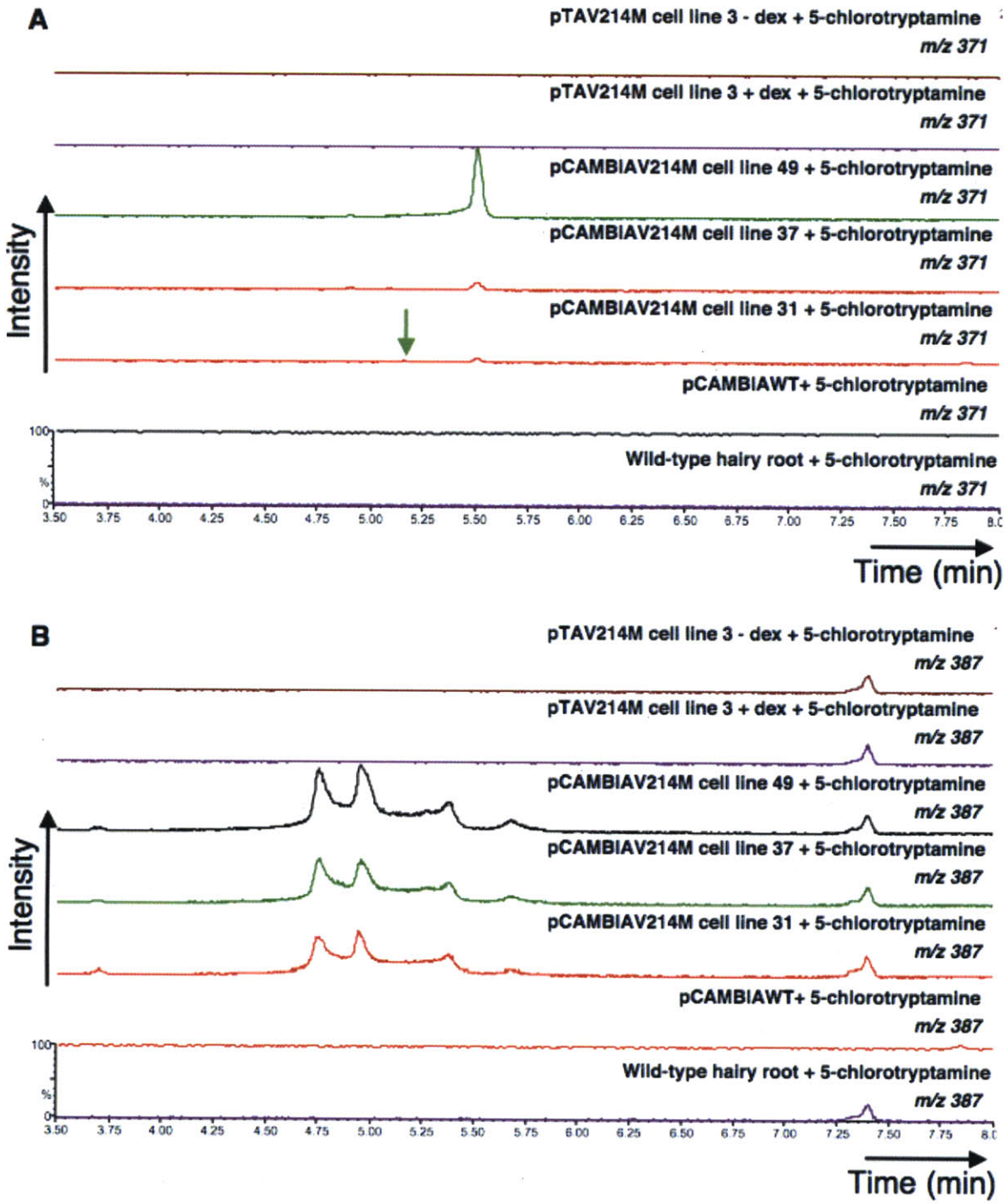

Figure 2A.1, A-B Chapter 2. LC-MS traces of selected alkaloid analogs formed by feeding 5-chlorotryptamine **2a** to 2-week-old pCAMV214M hairy roots (cell lines 31, 37 and 49). Formation of chlorinated analogs (**A,** *m/z* 371, 337+34; and **B**, *m/z* 387, 353+34) upon feeding of 5-chlorotryptamine **2a** to hairy roots. These analogs (*m/z* M+34) are absent in pTAV214M cultures (cell lines 3) fed with 5-chlorotryptamine **2a** either with or without the glucocorticoid inducer, dexamethasone, as well as in wild-type and pCAMWT cultures fed with 5-chlorotryptamine **2a**.

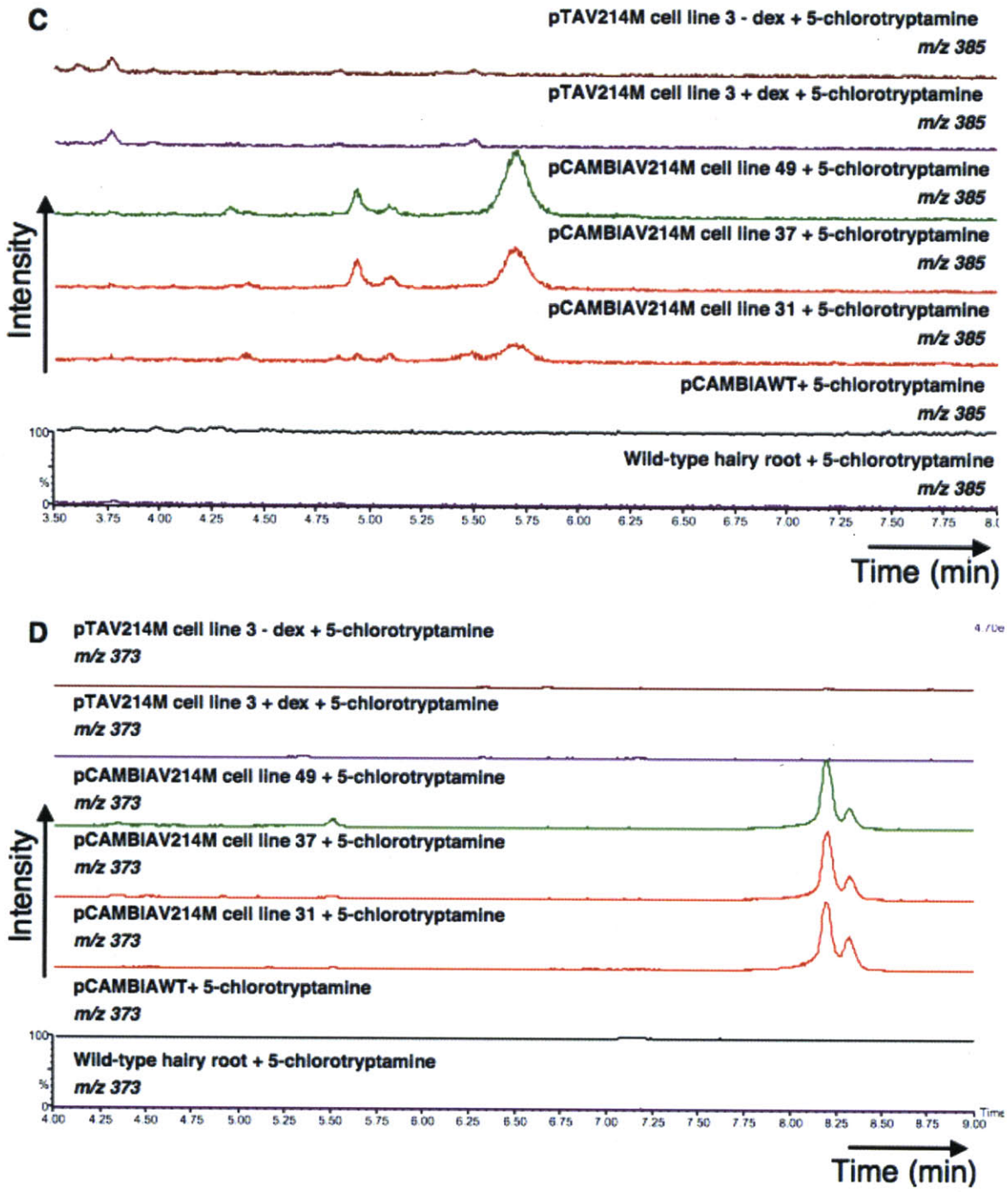

Figure 2A.1, C-D Chapter 2. LC-MS traces of selected alkaloid analogs formed by feeding 5-chlorotryptamine **2a** to 2-week-old pCAMV214M hairy roots (cell lines 31, 37 and 49). Formation of chlorinated analogs (**C**, *m/z* 385, 351+34; and **D**, *m/z* 373, 339+34) upon feeding of 5-chlorotryptamine **2a** to hairy roots. These analogs (*m/z* M+34) are absent in pTAV214M cultures (cell lines 3) fed with 5-chlorotryptamine **2a** either with or without the glucocorticoid inducer, dexamethasone, as well as in wild-type and pCAMWT cultures fed with 5-chlorotryptamine **2a**.

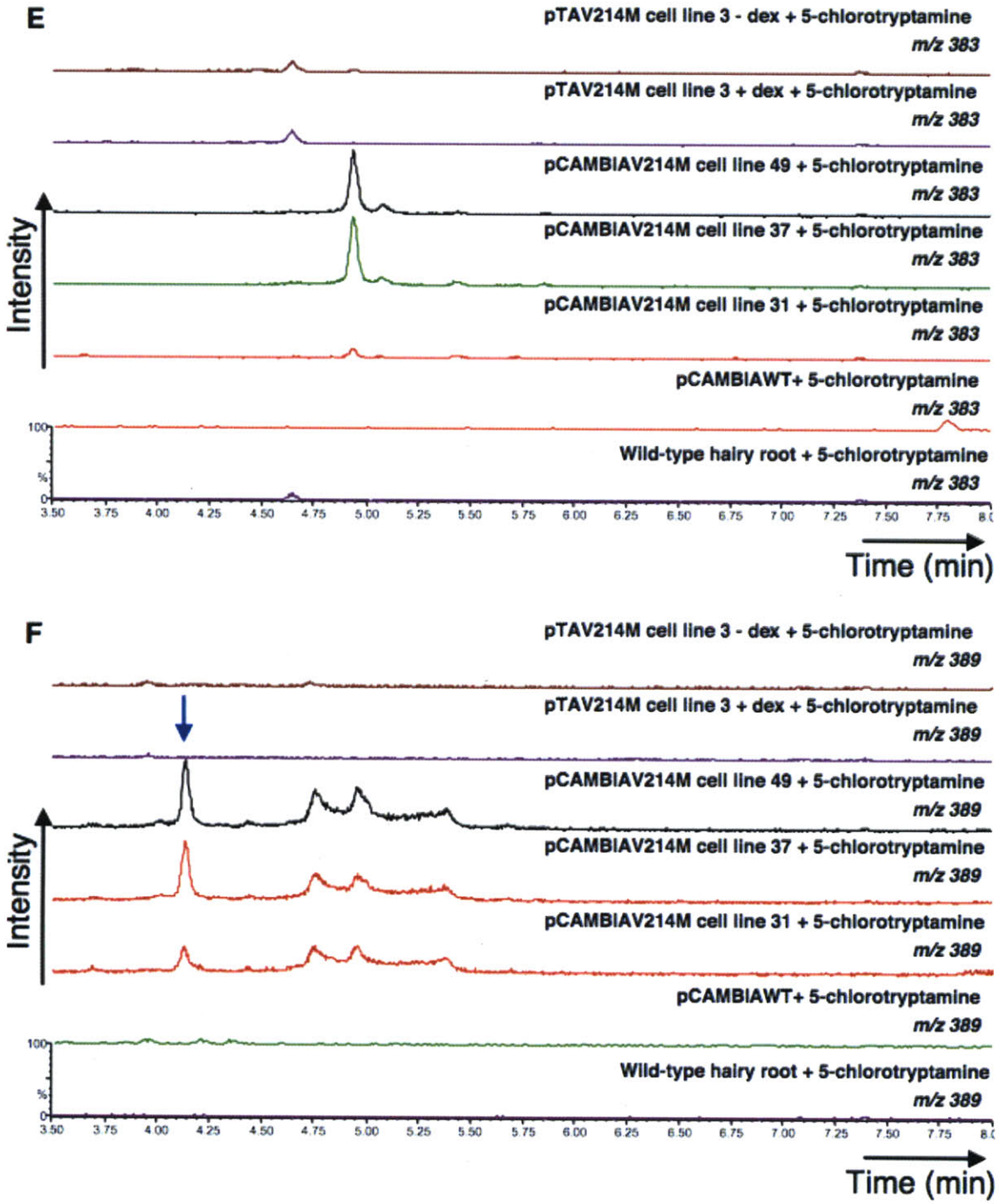

Figure 2A.1, E-F Chapter 2. LC-MS traces of selected alkaloid analogs formed by feeding 5-chlorotryptamine **2a** to 2-week-old pCAMV214M hairy roots (cell lines 31, 37 and 49). Formation of chlorinated analogs (**E**, *m/z* 383, 349+34; and **F**, *m/z* 389, 355+34) upon feeding of 5-chlorotryptamine **2a** to hairy roots. These analogs (*m/z* M+34) are absent in pTAV214M cultures (cell lines 3) fed with 5-chlorotryptamine **2a** either with or without the glucocorticoid inducer, dexamethasone, as well as in wild-type and pCAMWT cultures fed with 5-chlorotryptamine **2a**.

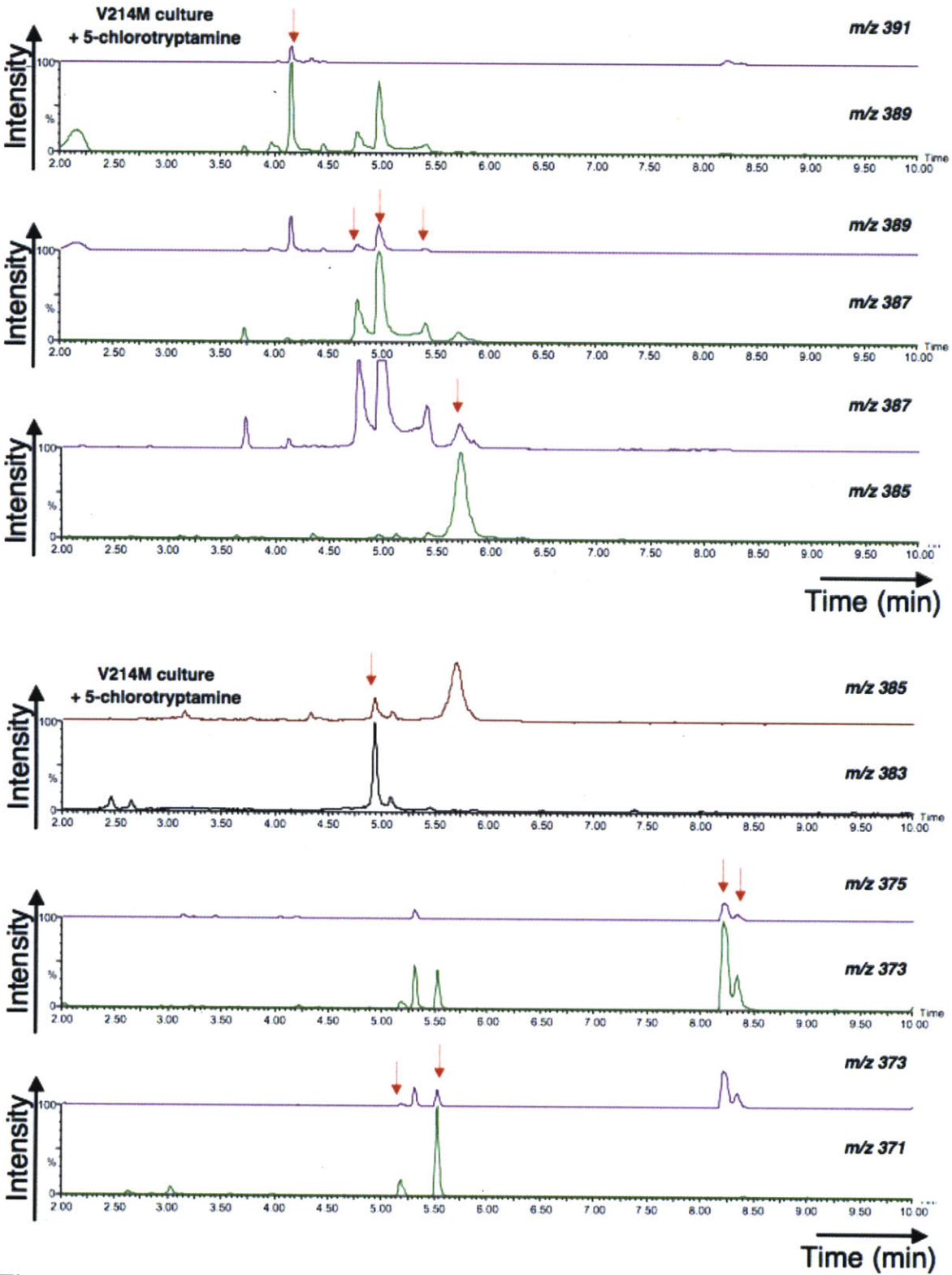

Figure 2A.2 Chapter 2. LC-MS traces of selected alkaloid analogs formed by feeding 5-chlorotryptamine **2a** to 2-week-old pCAMV214M hairy roots showing characteristic isotopic signature of chlorine. Intensities are normalized pairwise.

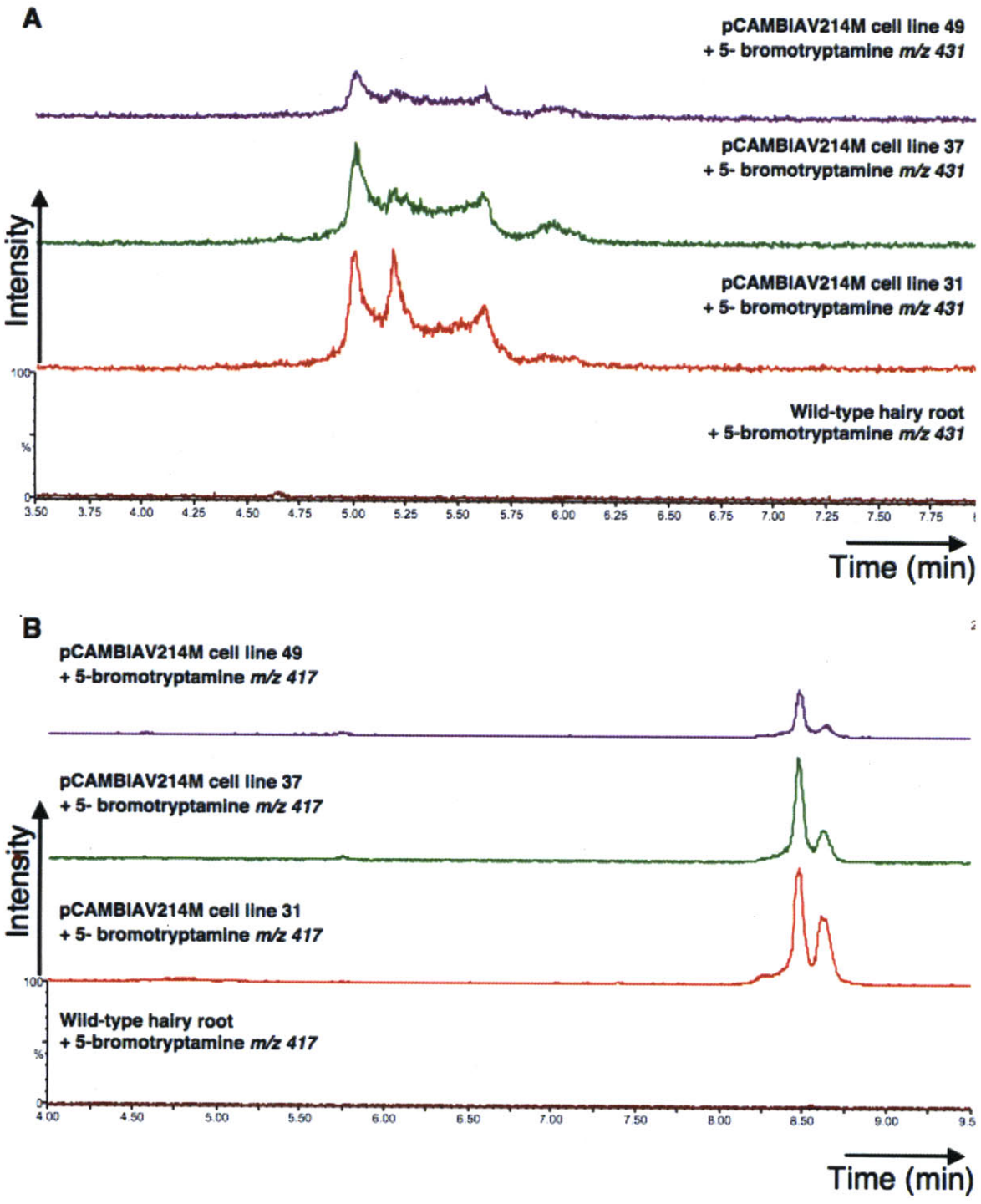

Figure 2A.3, A-B Chapter 2. LC-MS traces of selected alkaloid analogs formed by feeding 5-bromotryptamine **2c** to 2-week-old pCAMV214M hairy roots (cell lines 31, 37 and 49). Formation of brominated analogs (**A,** *m/z* 431, 353+78; and **B,** *m/z* 417, 339+78) upon feeding of 5-bromotryptamine **2c** to hairy roots. These analogs (*m/z* M+78) are absent in wild-type culture fed with 5-bromotryptamine **2c**.

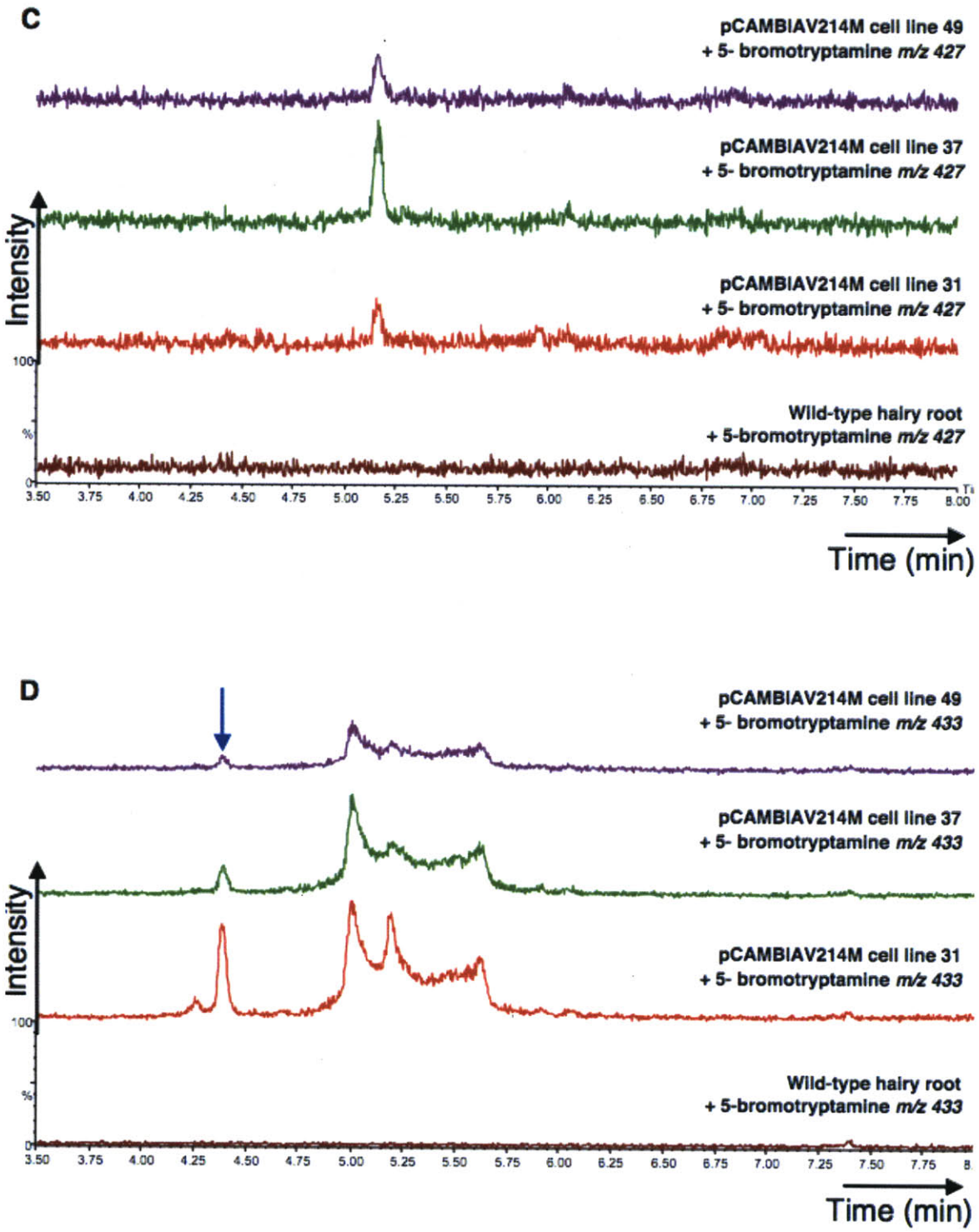

Figure 2A.3, C-D Chapter 2. LC-MS traces of selected alkaloid analogs formed by feeding 5-bromotryptamine **2c** to 2-week-old pCAMV214M hairy roots (cell lines 31, 37 and 49). Formation of brominated analogs (**C,** *m/z* 427, 349+78; and **D,** *m/z* 433, 355+78) upon feeding of 5-bromotryptamine **2c** to hairy roots. These analogs (*m/z* M+78) are absent in wild-type culture fed with 5-bromotryptamine **2c**.

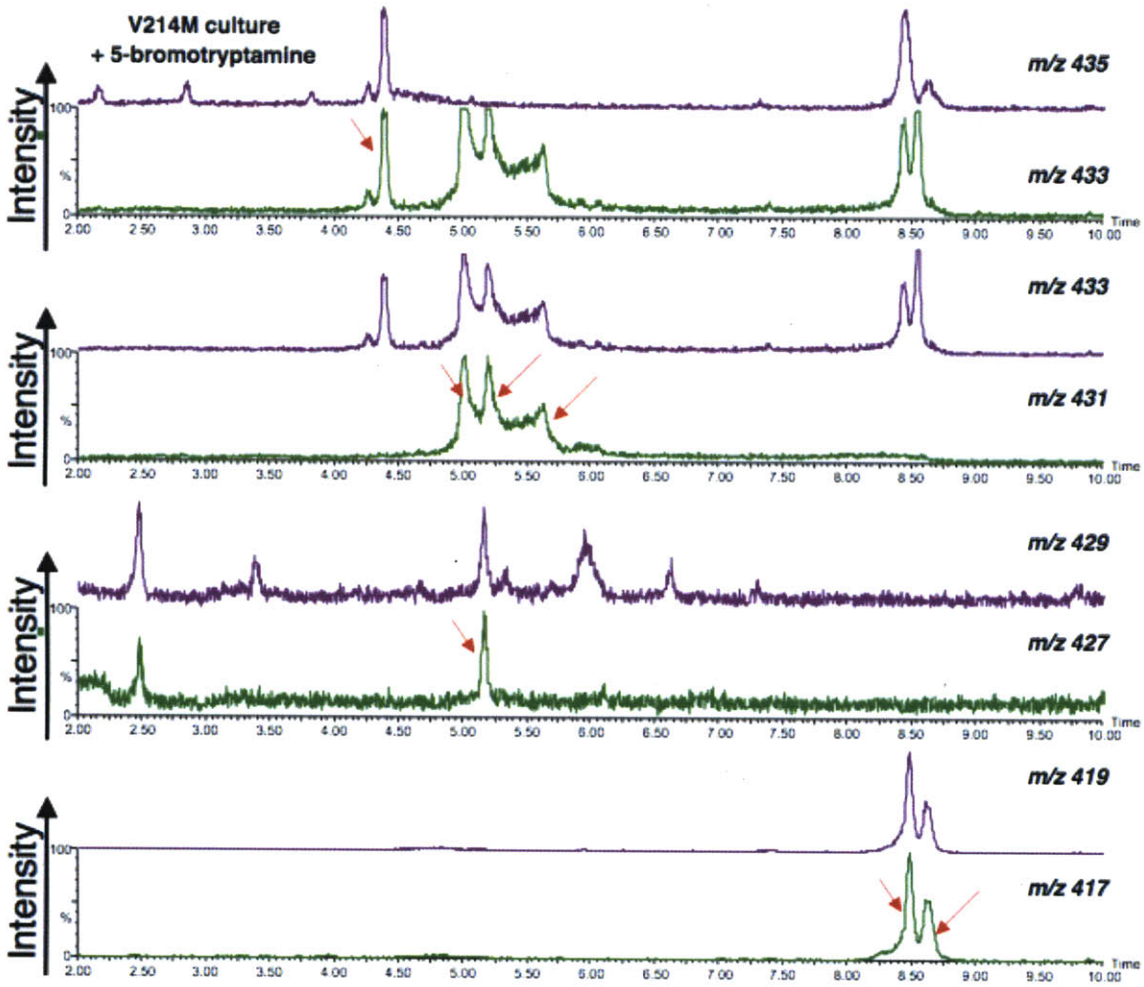

Figure 2A.4 Chapter 2. LC-MS traces of selected alkaloid analogs formed by feeding 5-bromotryptamine **2c** to 2-week-old pCAMV214M hairy roots showing characteristic isotopic signature of bromine. Intensities are normalized pairwise.

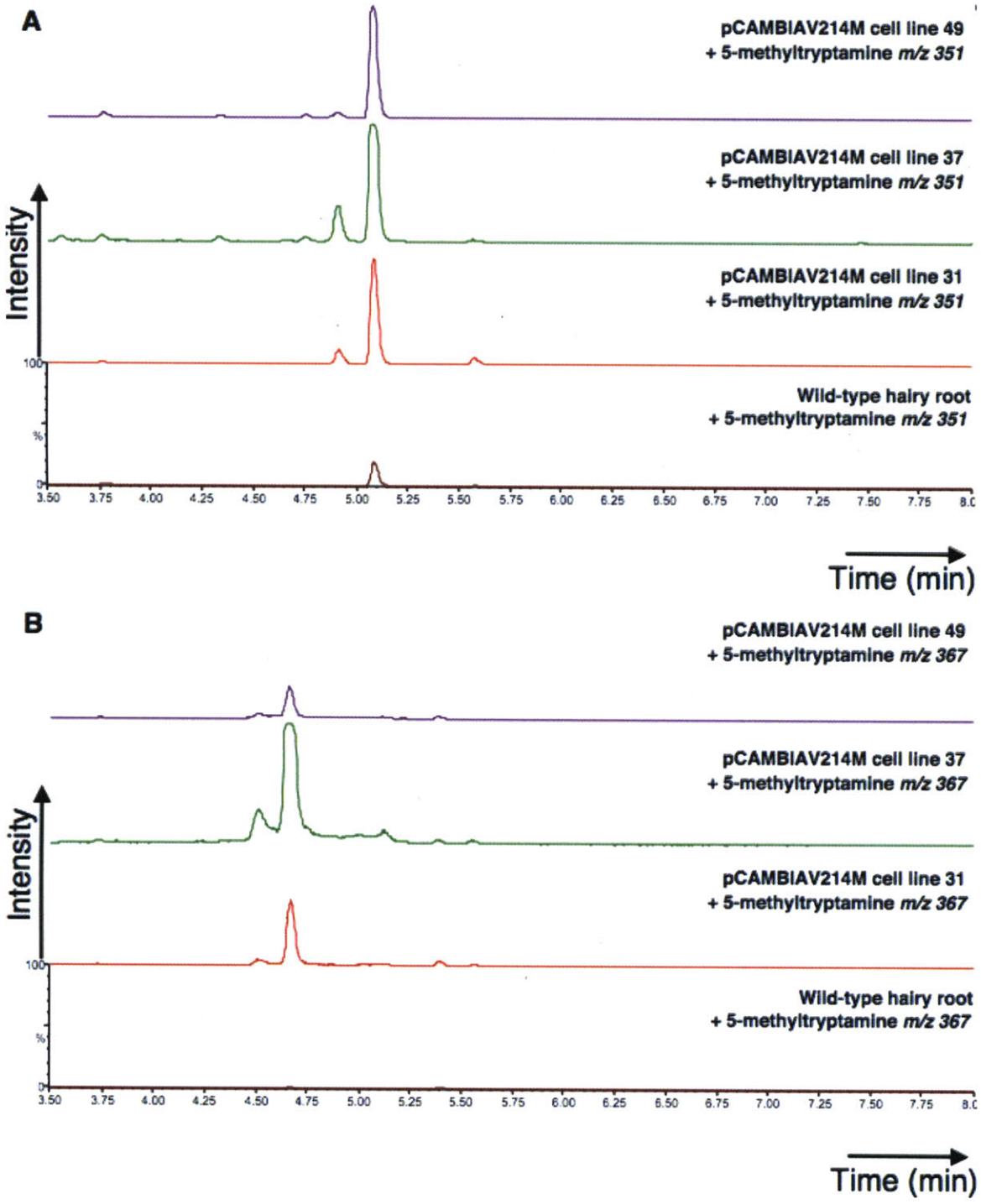

Figure 2A.5, A-B Chapter 2. LC-MS traces of selected alkaloid analogs formed by feeding 5-methyltryptamine **2b** to 2-week-old pCAMV214M hairy roots (cell lines 31, 37 and 49). Formation of methylated analogs (**A,** *m/z* 351, 337+14; and **B**, *m/z* 367, 353+14) upon feeding of 5-methyltryptamine **2b** to hairy roots. Note that some of these analogs (*m/z* M+14) are still present, though in significantly lower quantities, in wild-type culture fed with 5-methyltryptamine **2b**. Definitive assignment of the structure of these compounds as originating from **2b** depends on more detailed structural characterization.

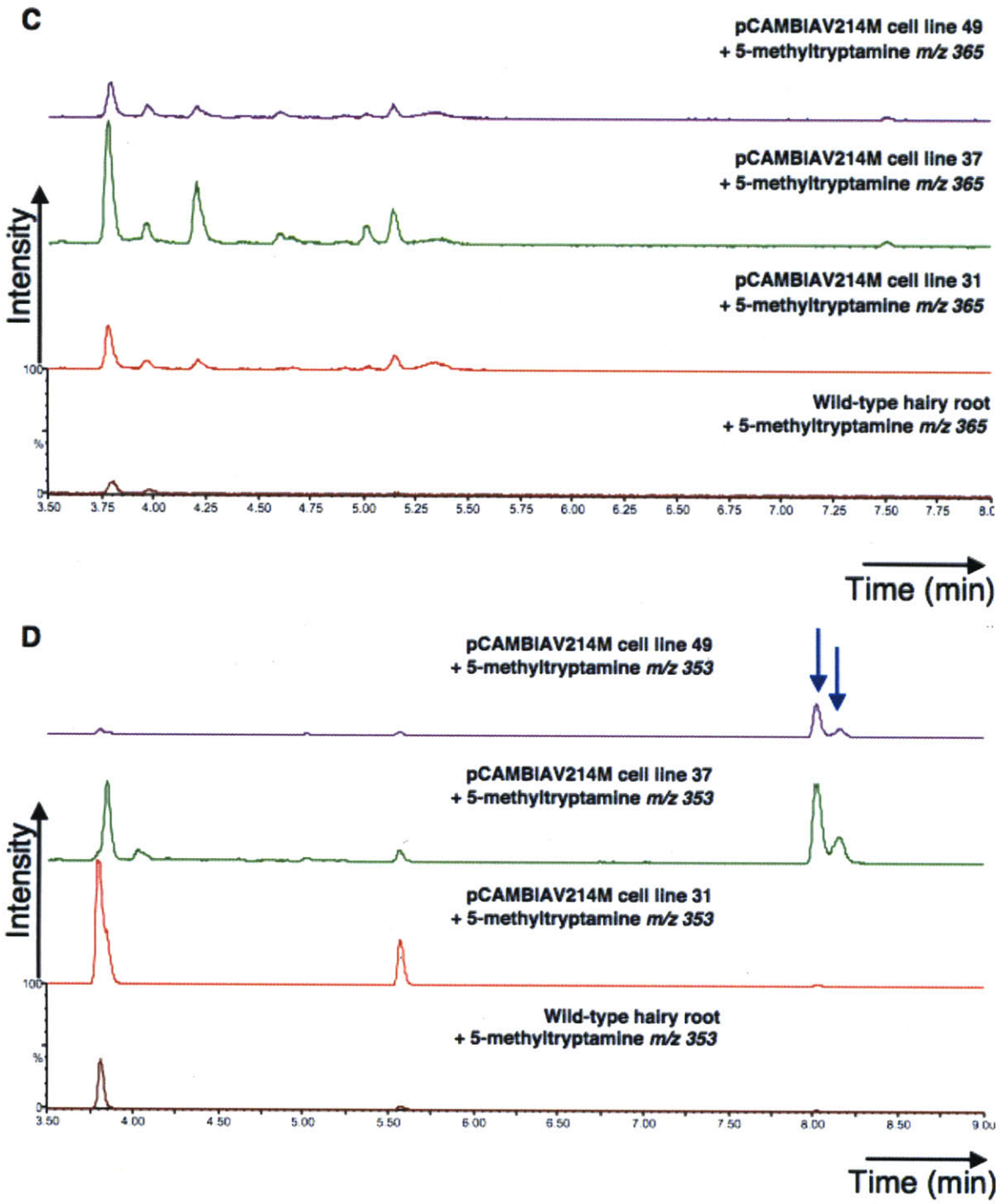

Figure 2A.5, C-D Chapter 2. LC-MS traces of selected alkaloid analogs formed by feeding 5-methyltryptamine to 2-week-old pCAMV214M hairy roots (cell lines 31, 37 and 49). Formation of methylated analogs (**C**, *m/z* 365, 351+14; and **D**, *m/z* 353, 339+14) upon feeding of 5-methyltryptamine **2b** to hairy roots. Note that some of these analogs (*m/z* M+14) are still present, though in significantly lower quantities, in wild-type culture fed with 5-methyltryptamine **2b**. Definitive assignment of the structure of these compounds as originating from **2b** depends on more detailed structural characterization.

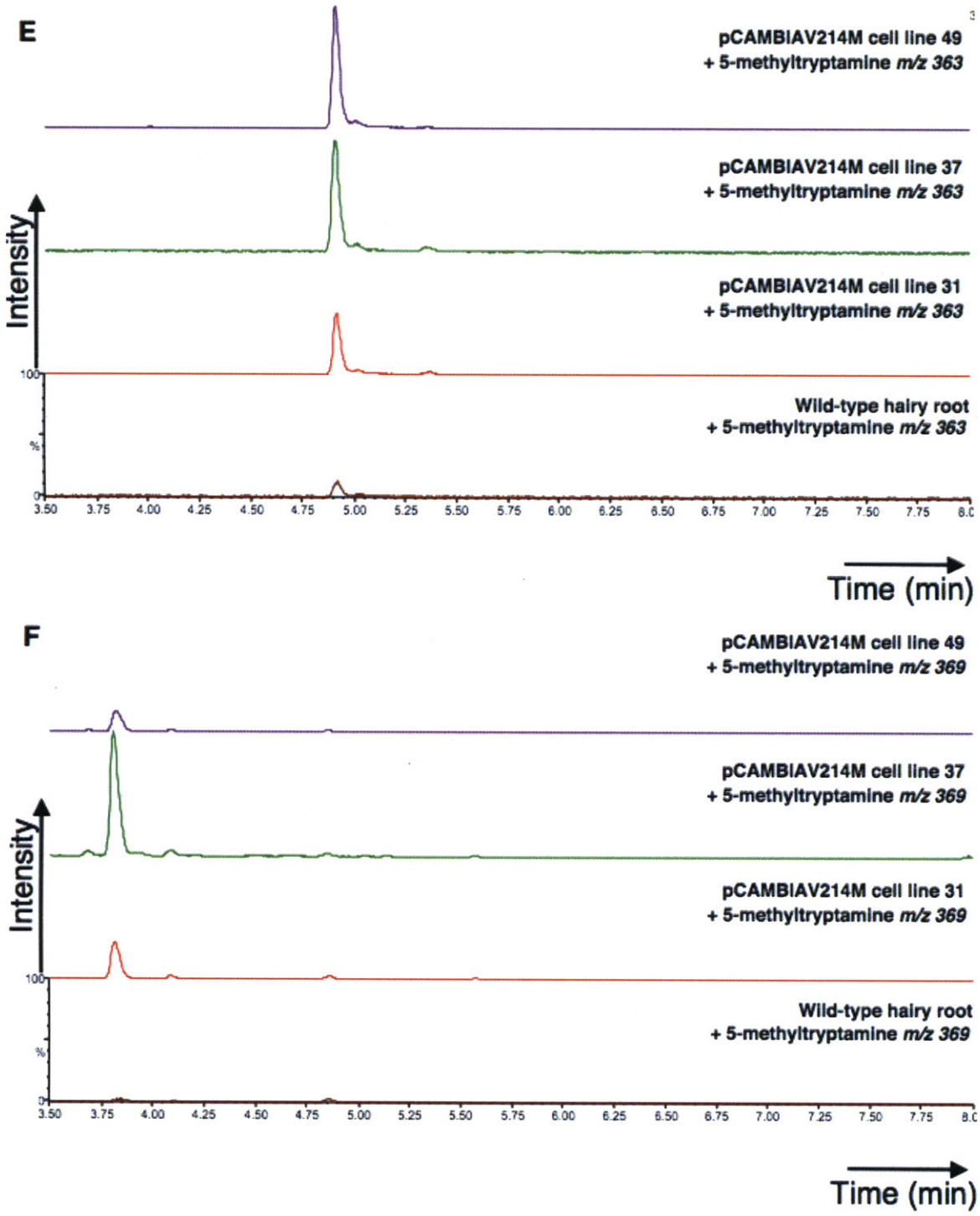

Figure 2A.5, E-F Chapter 2. LC-MS traces of selected alkaloid analogs formed by feeding 5-methyltryptamine to 2-week-old pCAMV214M hairy roots (cell lines 31, 37 and 49). Formation of methylated analogs (**E**, *m/z* 363, 349+14; and **F**, *m/z* 369, 355+14) upon feeding of 5-methyltryptamine **2b** to hairy roots. Note that some of these analogs (*m/z* M+14) are still present, though in significantly lower quantities, in wild-type culture fed with 5-methyltryptamine **2b**. Definitive assignment of the structure of these compounds as originating from **2b** depends on more detailed structural characterization.

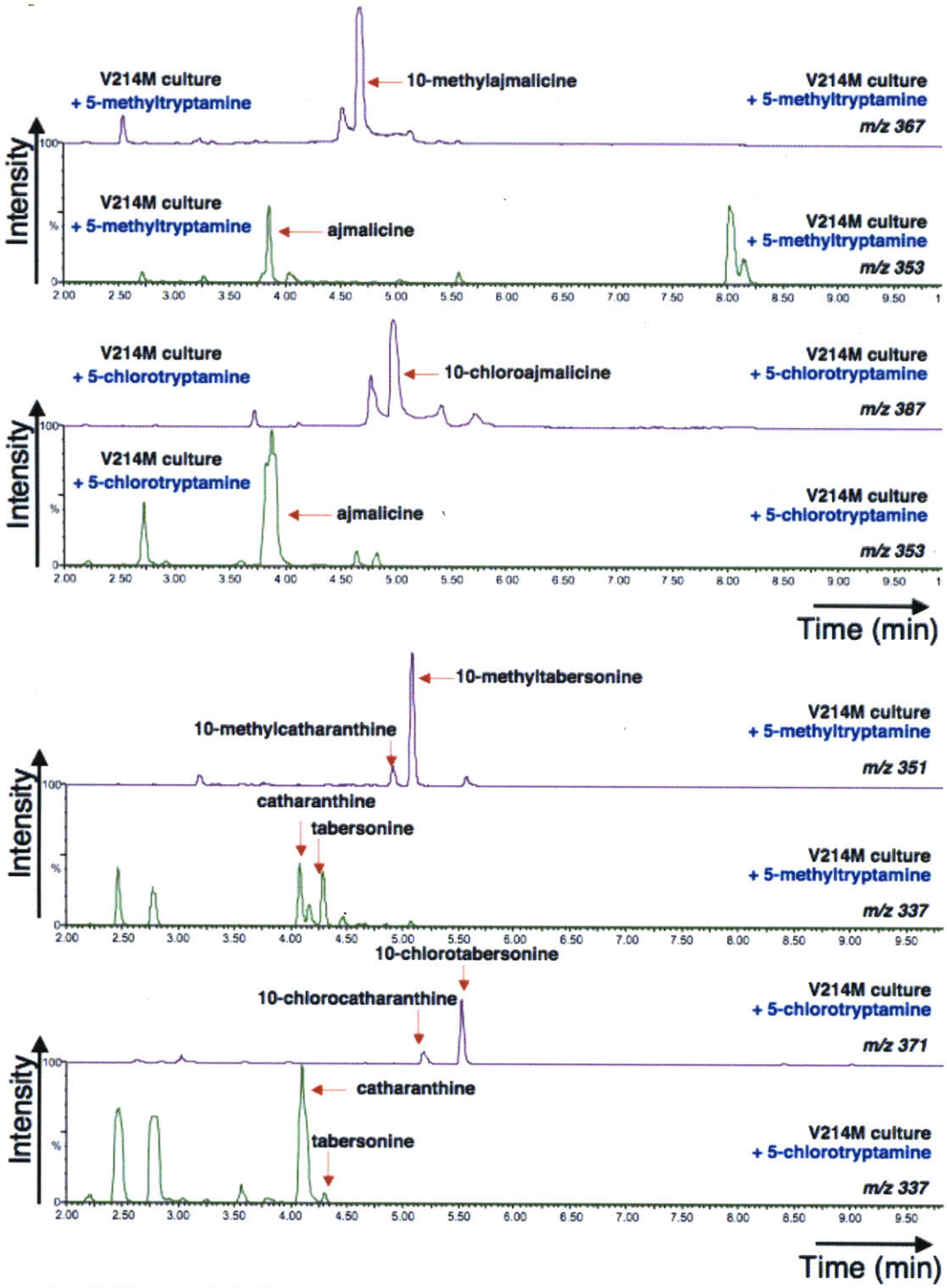

Figure 2A.6 Chapter 2. LC-MS traces of selected alkaloid analogs formed by feeding either 5-chlorotryptamine or 5-methyltryptamine to 2-week-old pCAMV214M hairy roots showing relative production levels of natural alkaloids (ajmalicine **4** and tabersonine **5**) compared to unnatural chlorinated/methylated alkaloids. Intensities are normalized pairwise. The ratio of natural catharanthine to natural tabersonine (green traces) changes depending on whether **2a** or **2b** is fed to the cultures.

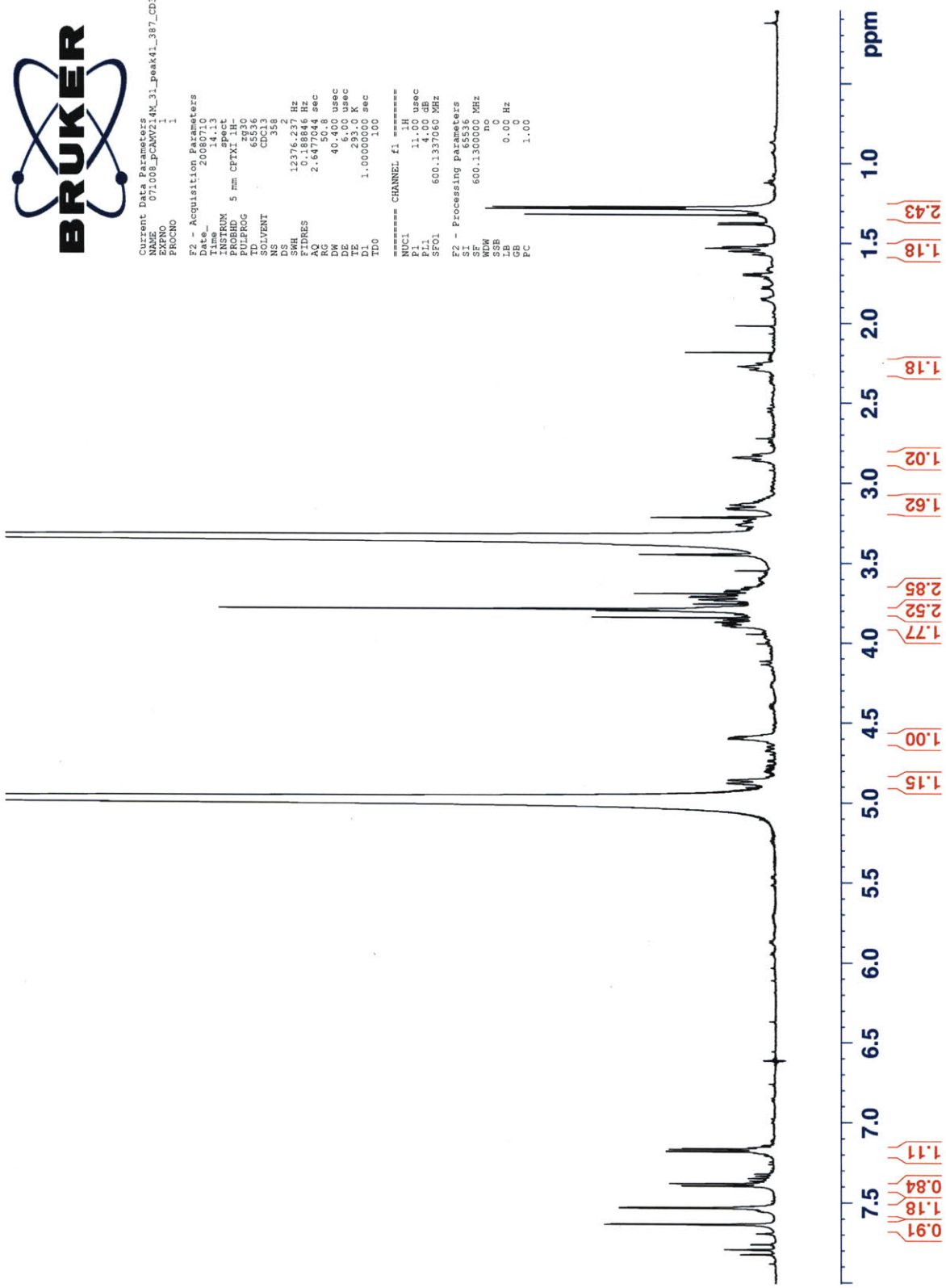

Figure 2A.7 Chapter 2. ^{1}H NMR spectrum of 10-chloroajmalicine **4a**. All alkaloids were isolated from pCAMV214M hairy root (cell line 31) fed with 5-chlorotryptamine **2a** (0.5 mM).

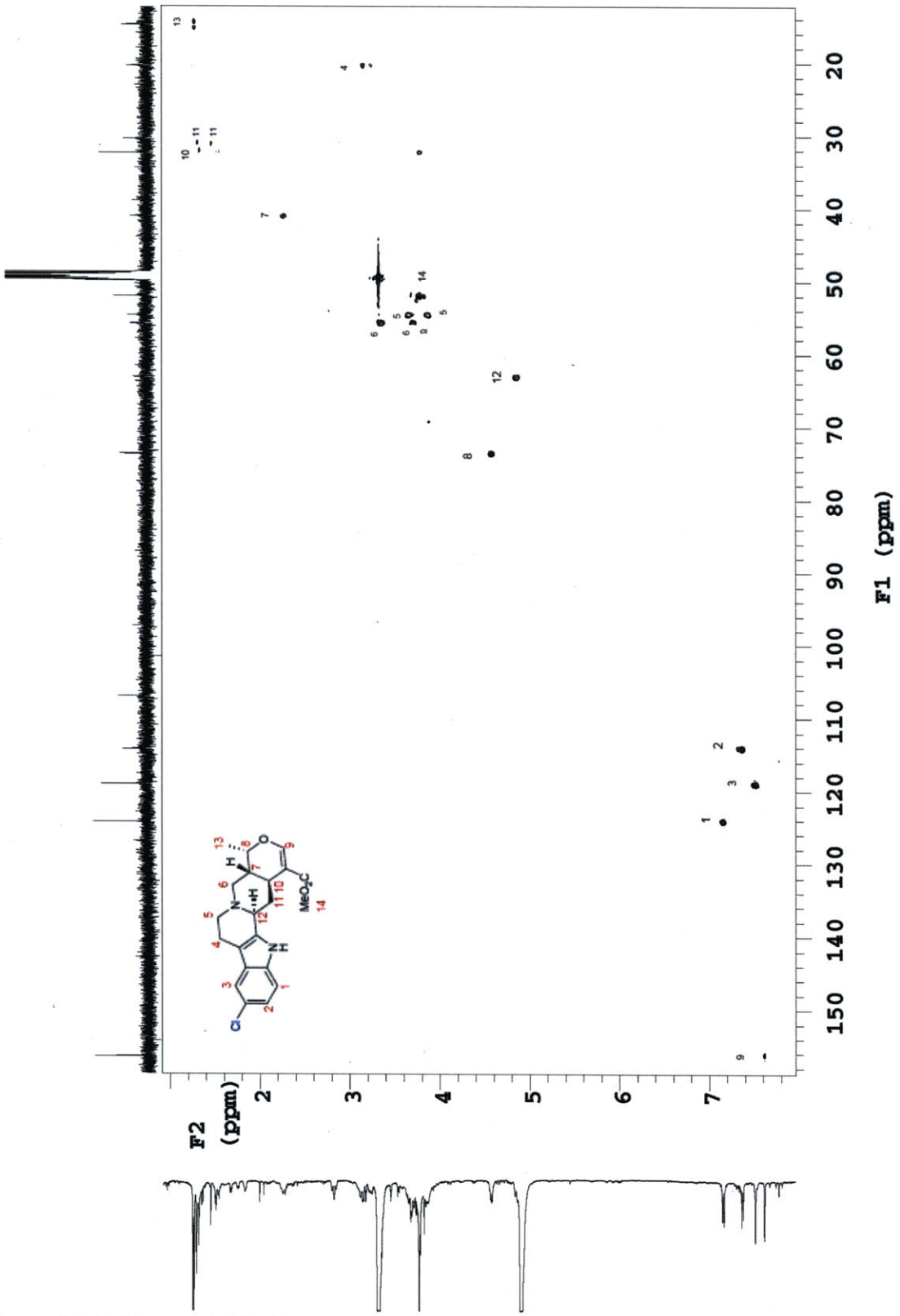

Figure 2A.8 Chapter 2. ^{13}C-^{1}H HSQC spectrum of 10-chloroajmalicine **4a**. All alkaloids were isolated from pCAMV214M hairy root (cell line 31) fed with 5-chlorotryptamine **2a** (0.5 mM).

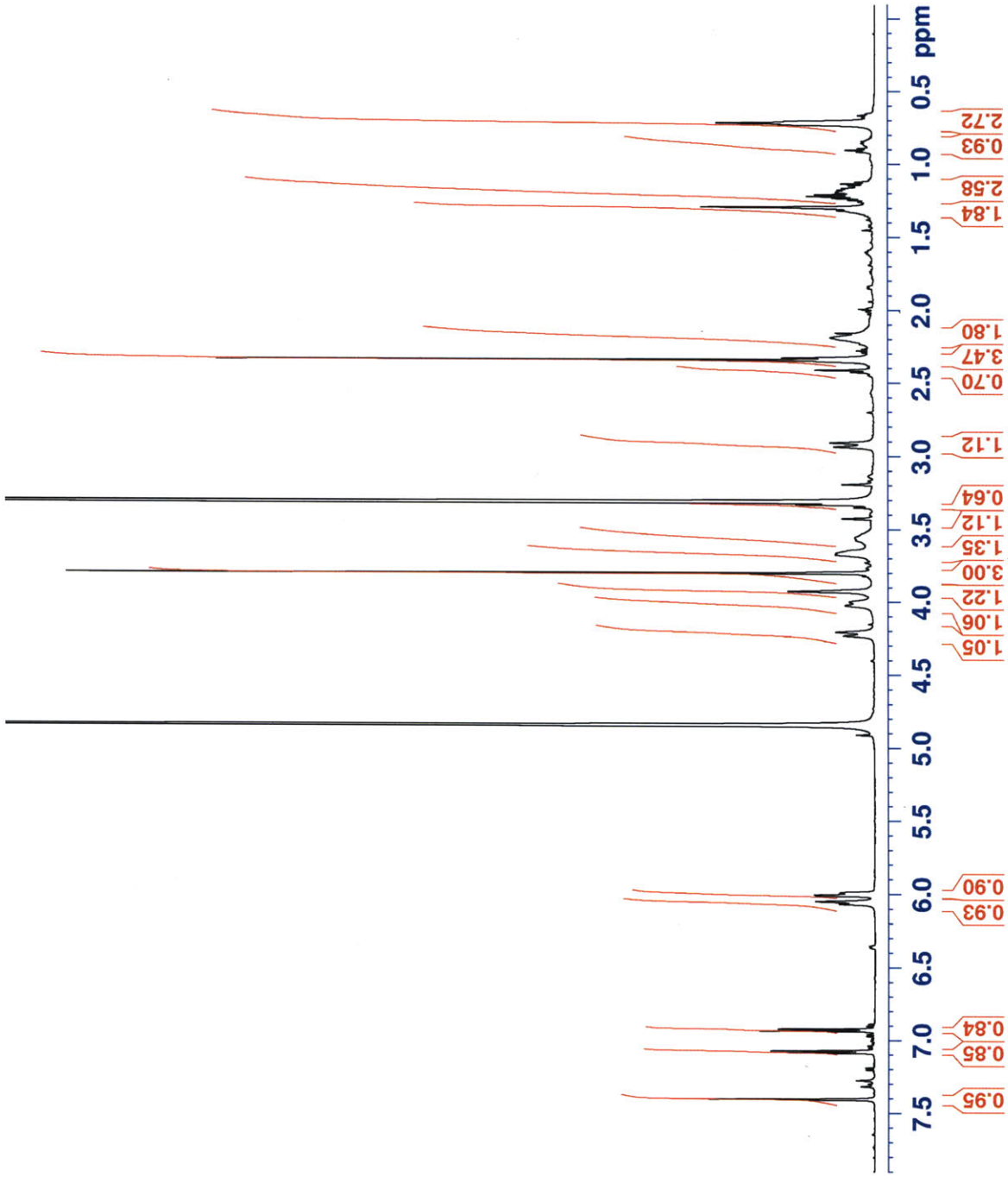

Figure 2A.9 Chapter 2. ^{1}H NMR spectrum of 10-methyltabersonine **5b.** The alkaloid was isolated from pCAMV214M hairy root (cell line 31) fed with 5-methyltryptamine **2b** (0.5 mM).

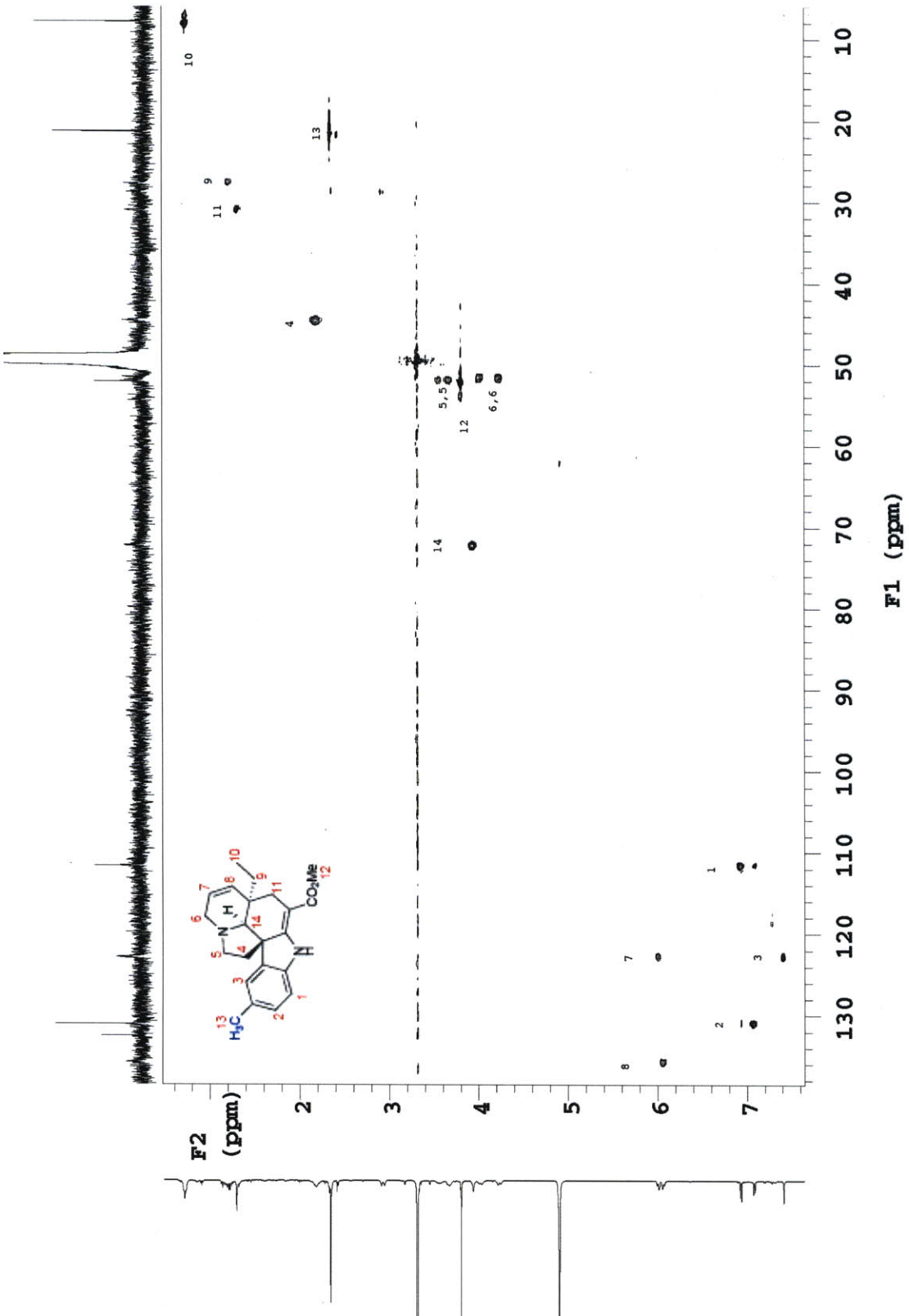

Figure 2A.10 Chapter 2. ^{13}C-^{1}H HSQC spectrum of 10-methyltabersonine **5b.** The alkaloid was isolated from pCAMV214M hairy root (cell line 31) fed with 5-methyltryptamine **2b** (0.5 mM).

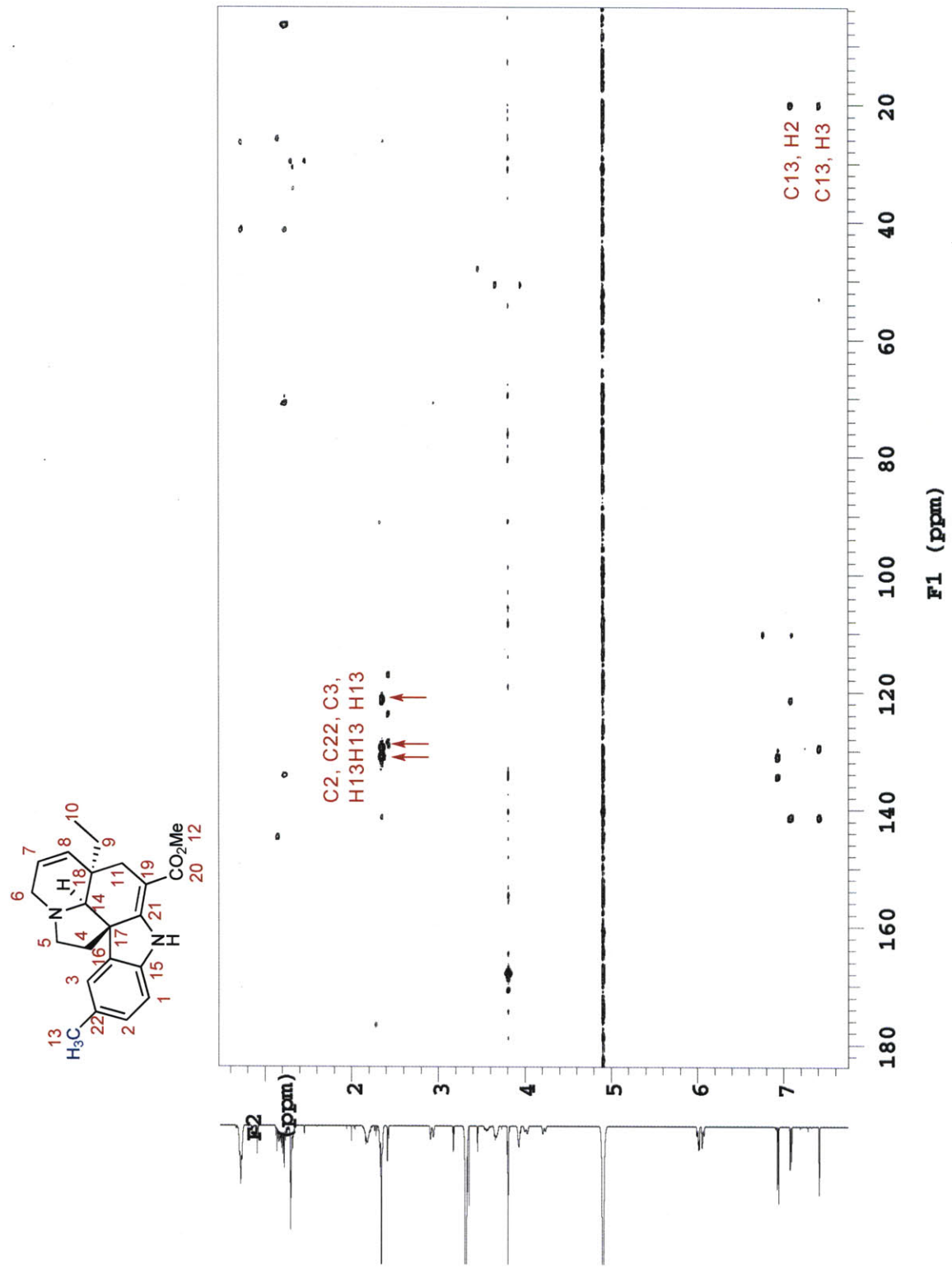

Figure 2A.11 Chapter 2. ^{13}C-^{1}H HMBC spectrum of 10-methyltabersonine **5b.** The alkaloid was isolated from pCAMV214M hairy root (cell line 31) fed with 5-methyltryptamine **2b** (0.5 mM).

CHAPTER 3 - APPENDIX B

LC-MS TRACES, NMR SPECTRA, UV SPECTRA AND MS/MS ANALYSIS:

EVALUATION OF ALKALOID PRODUCTION IN ENGINEERED *C. ROSEUS*

Part of this appendix is published as a letter in

Nature **2010**, *468*, 461-464

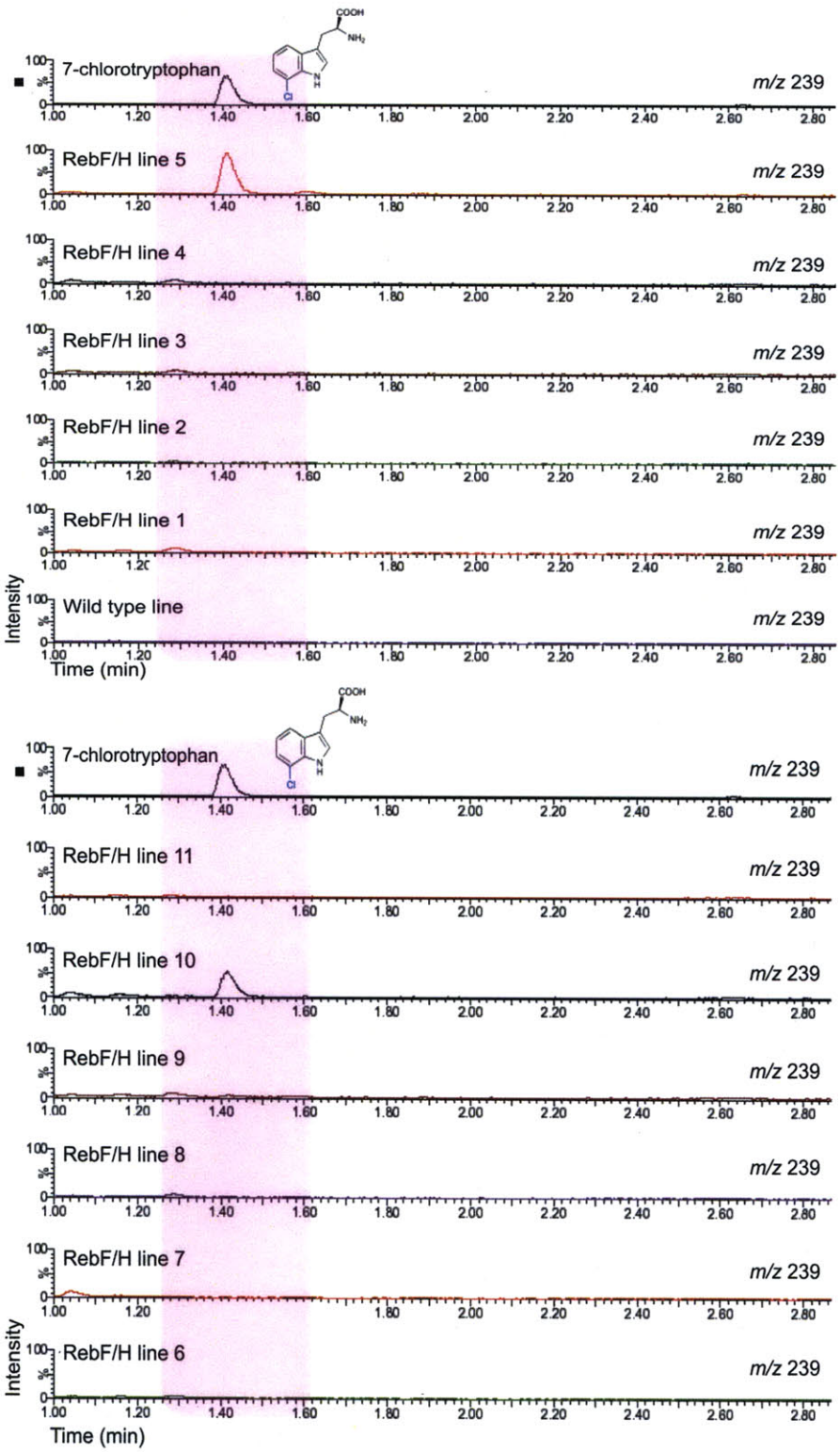

Figure 3B.1, A-B Chapter 3. Extracted LC-MS chromatograms showing the presence of 7-chlorotryptophan **1a** (*m/z* 239) in several RebF/H hairy roots. This compound, which is not observed in control cultures transformed with no plasmid, co-elutes with an authentic standard of 7-chlorotryptophan **1a**.

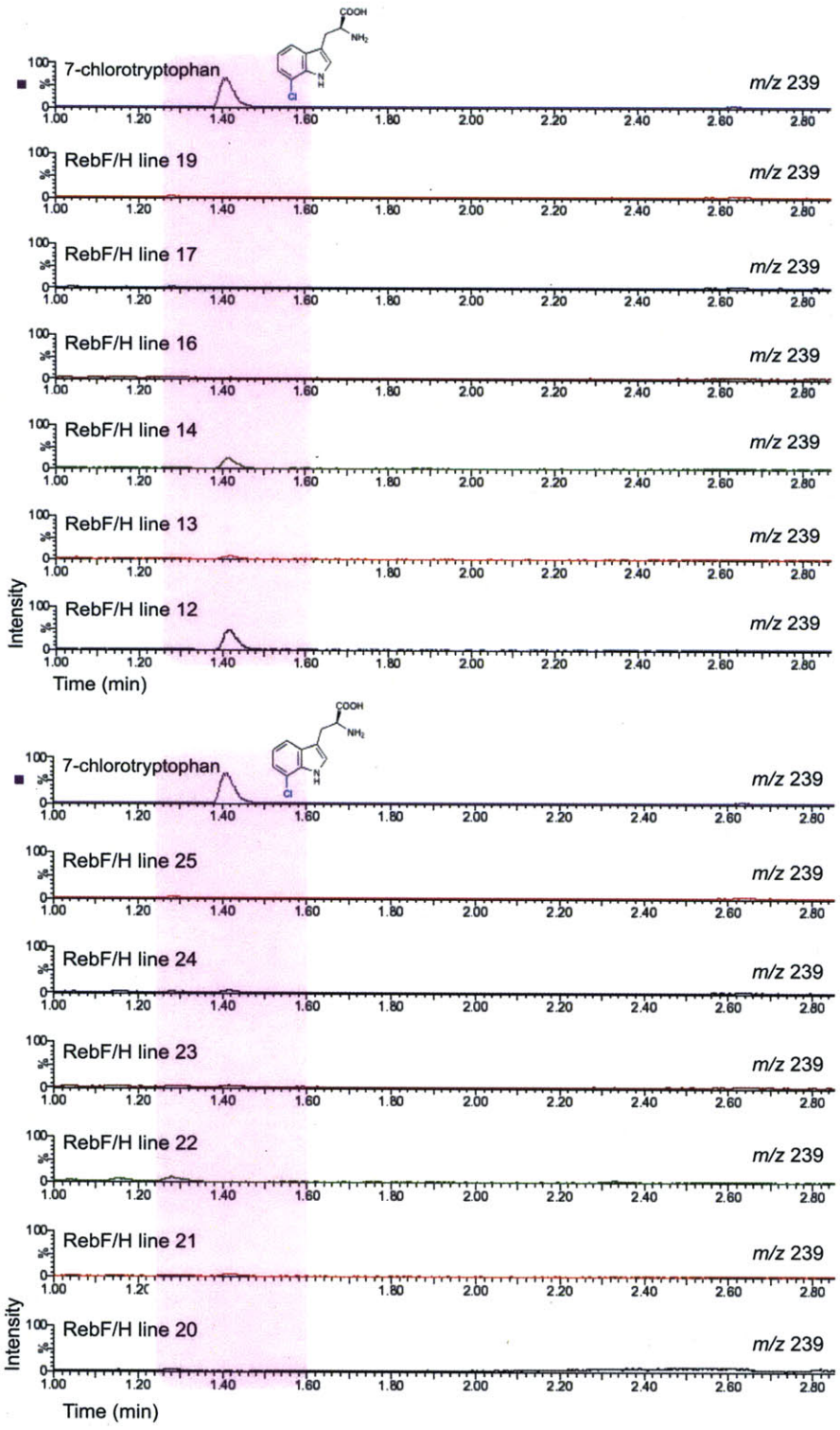

Figure 3B.1, C-D Chapter 3. Extracted LC-MS chromatograms showing the presence of 7-chlorotryptophan **1a** (*m/z* 239) in several RebF/H hairy roots. This compound, which is not observed in control cultures transformed with no plasmid, co-elutes with an authentic standard of 7-chlorotryptophan **1a**.

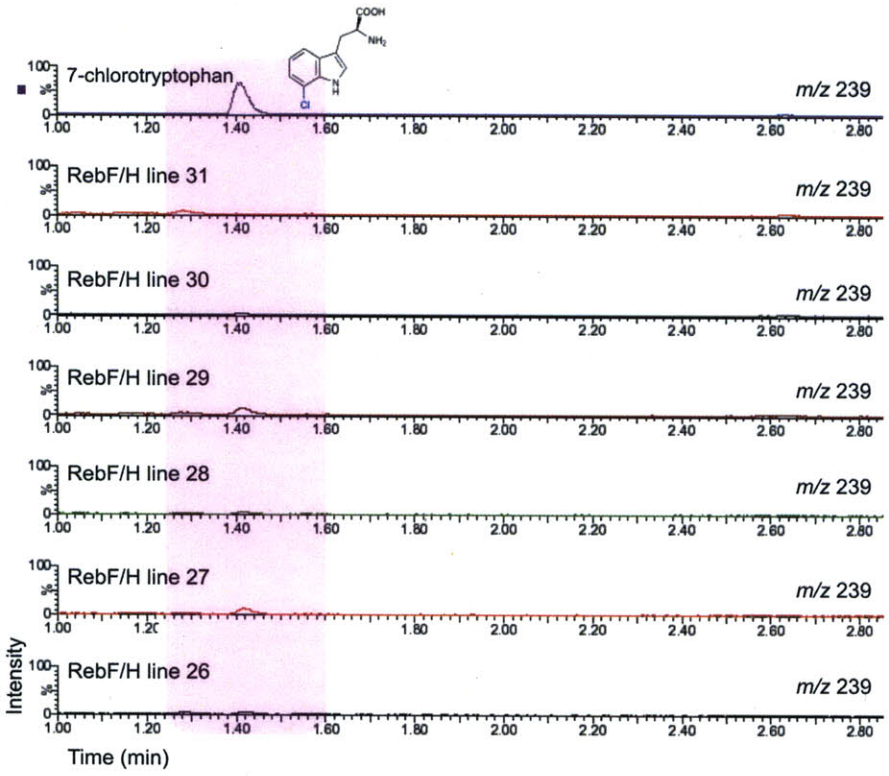

Figure 3B.1, E Chapter 3. Extracted LC-MS chromatograms showing the presence of 7-chlorotryptophan **1a** (*m/z* 239) in several RebF/H hairy roots. This compound, which is not observed in control cultures transformed with no plasmid, co-elutes with an authentic standard of 7-chlorotryptophan **1a**.

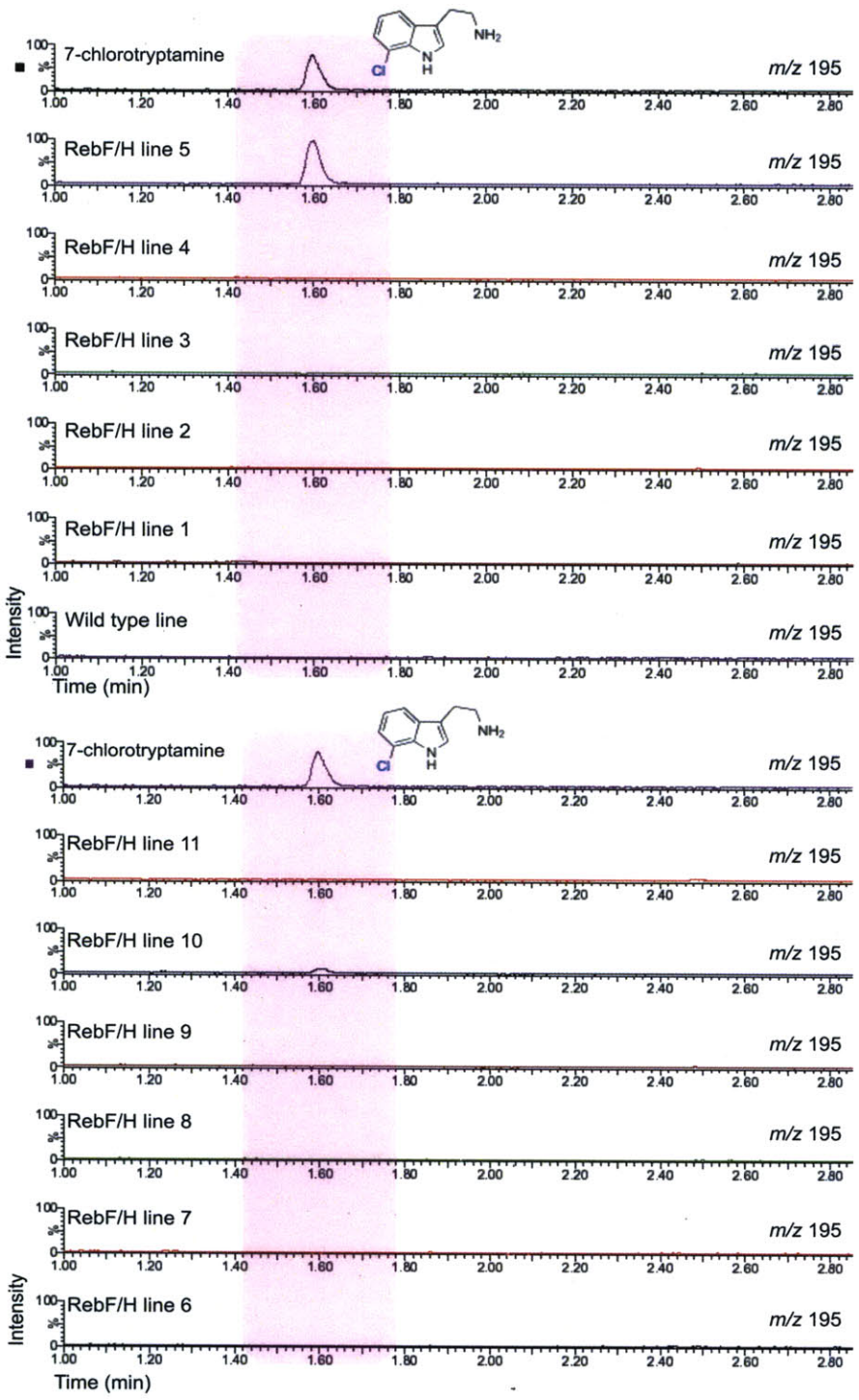

Figure 3B.2, A-B Chapter 3. Extracted LC-MS chromatograms showing the presence of 7-chlorotryptamine **2a** (*m/z* 195) in several RebF/H hairy roots. This compound, which is not observed in control cultures transformed with no plasmid, co-elutes with an authentic standard of 7-chlorotryptamine **2a**.

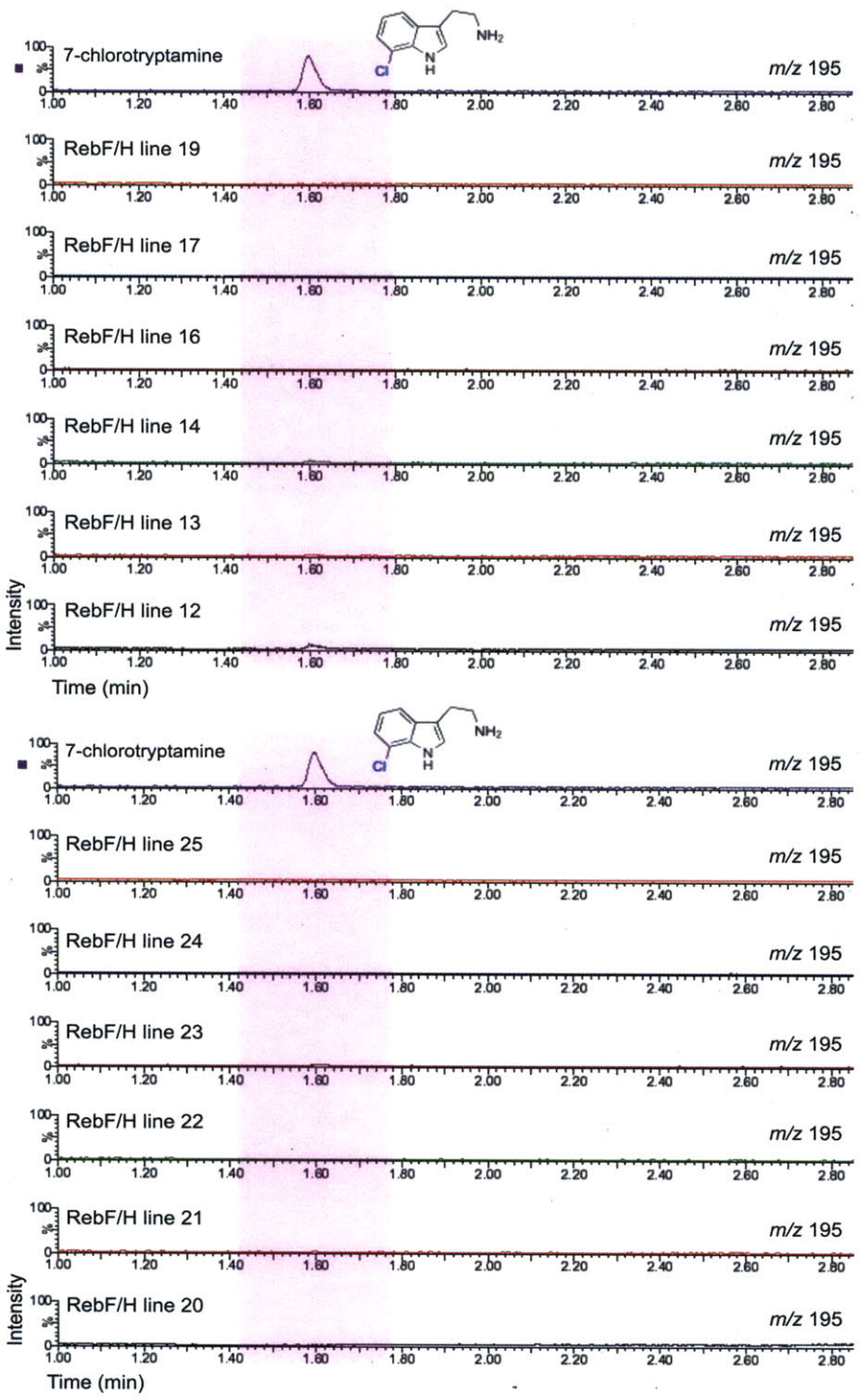

Figure 3B.2, C-D Chapter 3. Extracted LC-MS chromatograms showing the presence of 7-chlorotryptamine **2a** (*m/z* 195) in several RebF/H hairy roots. This compound, which is not observed in control cultures transformed with no plasmid, co-elutes with an authentic standard of 7-chlorotryptamine **2a**.

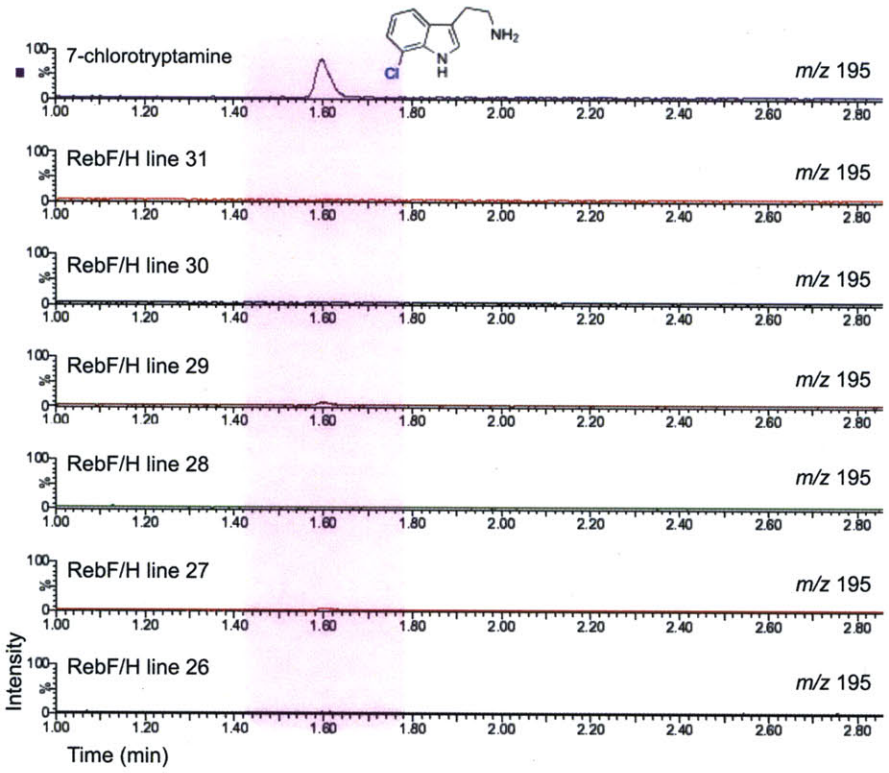

Figure 3B.2, E Chapter 3. Extracted LC-MS chromatograms showing the presence of 7-chlorotryptamine **2a** (*m/z* 195) in several RebF/H hairy roots. This compound, which is not observed in control cultures transformed with no plasmid, co-elutes with an authentic standard of 7-chlorotryptamine **2a**.

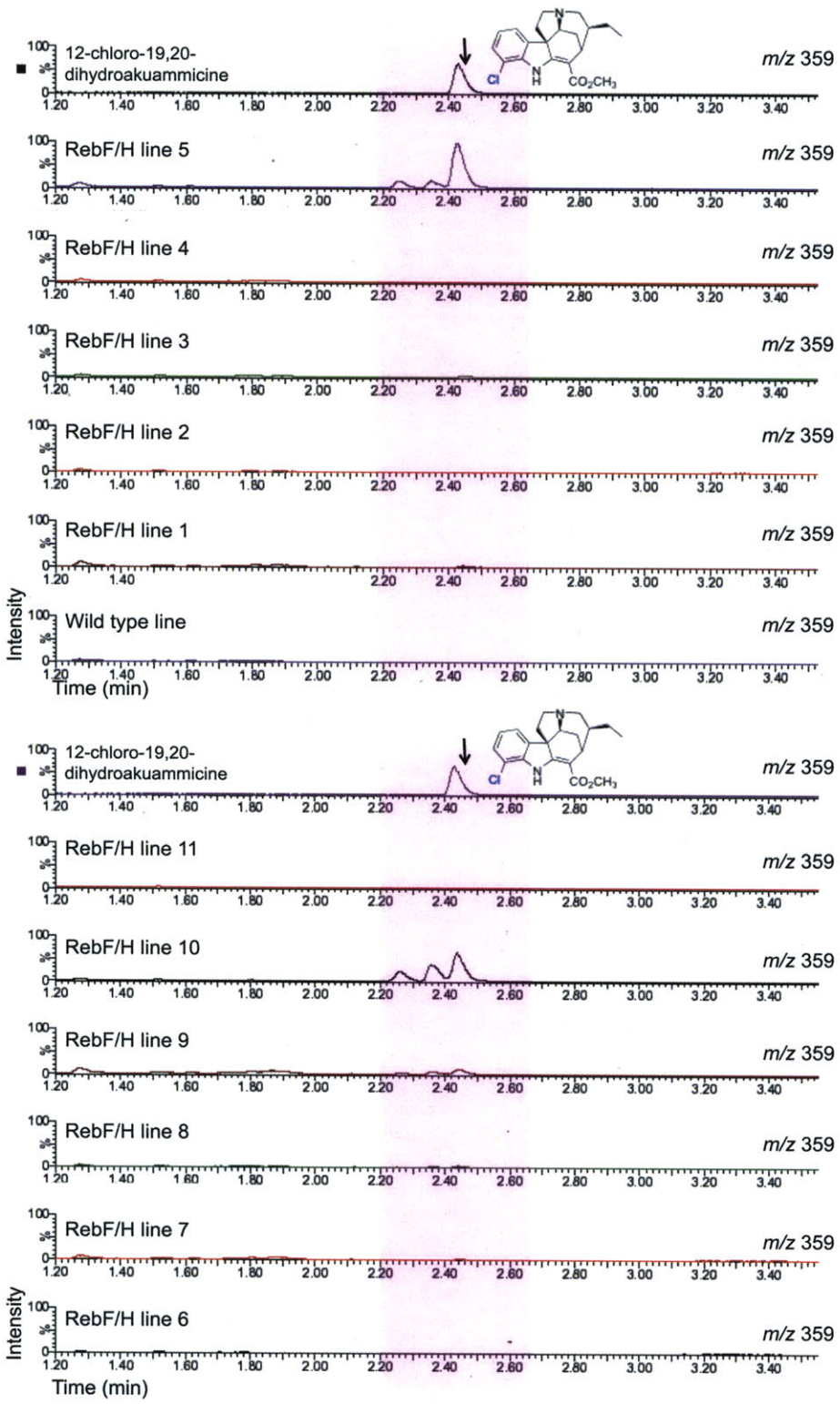

Figure 3B.3, A-B Chapter 3. Extracted LC-MS chromatograms showing the presence of 12-chloro-19,20-dihydroakuammicine **5a** (*m/z* 359) in selected RebF/H hairy roots. This compound, which is not observed in control cultures transformed with no plasmid, co-elutes with an authentic standard of 12-chloro-19,20-dihydroakuammicine **5a**.

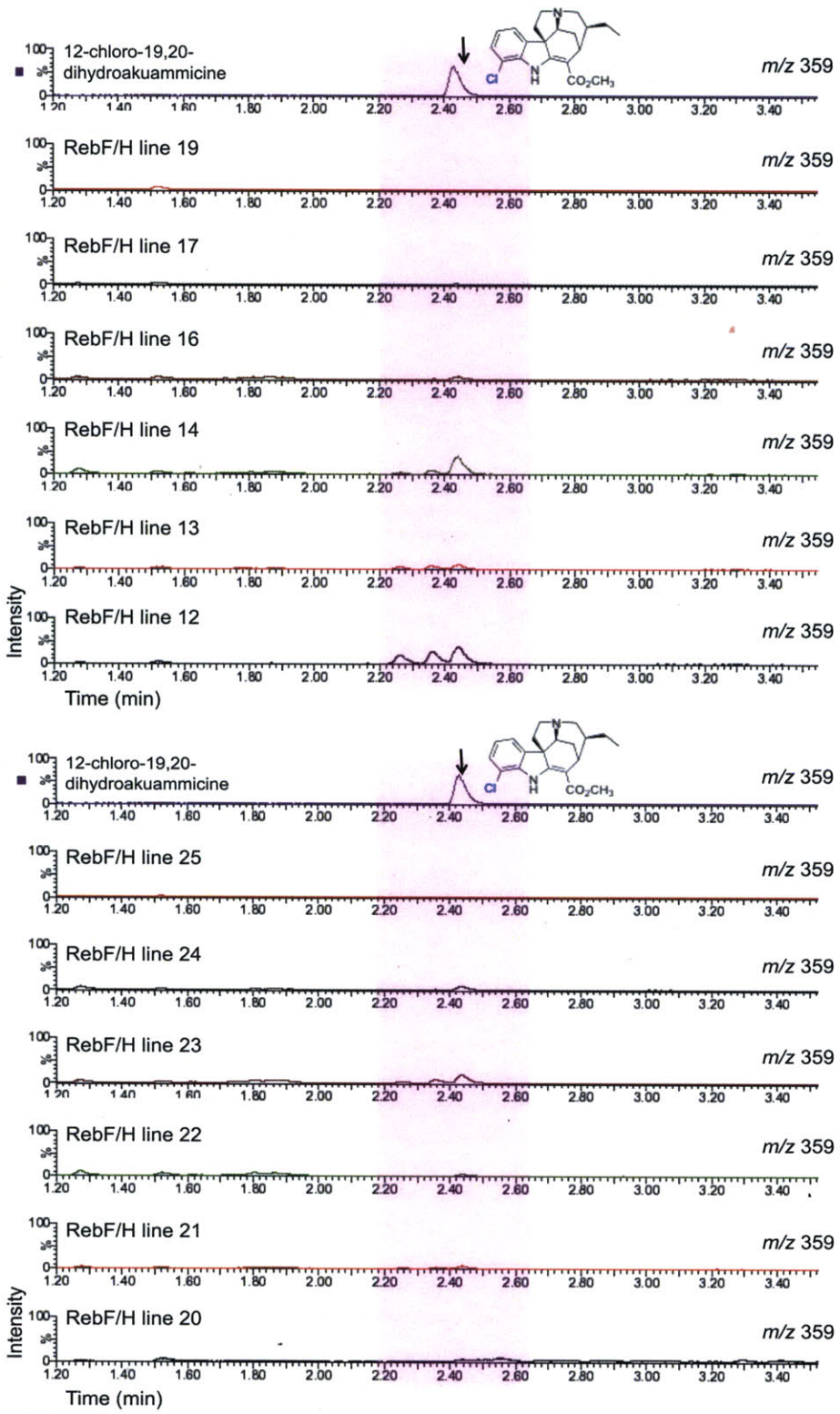

Figure 3B.3, C-D Chapter 3. Extracted LC-MS chromatograms showing the presence of 12-chloro-19,20-dihydroakuammicine **5a** (*m/z* 359) in selected RebF/H hairy roots. This compound, which is not observed in control cultures transformed with no plasmid, co-elutes with an authentic standard of 12-chloro-19,20-dihydroakuammicine **5a**.

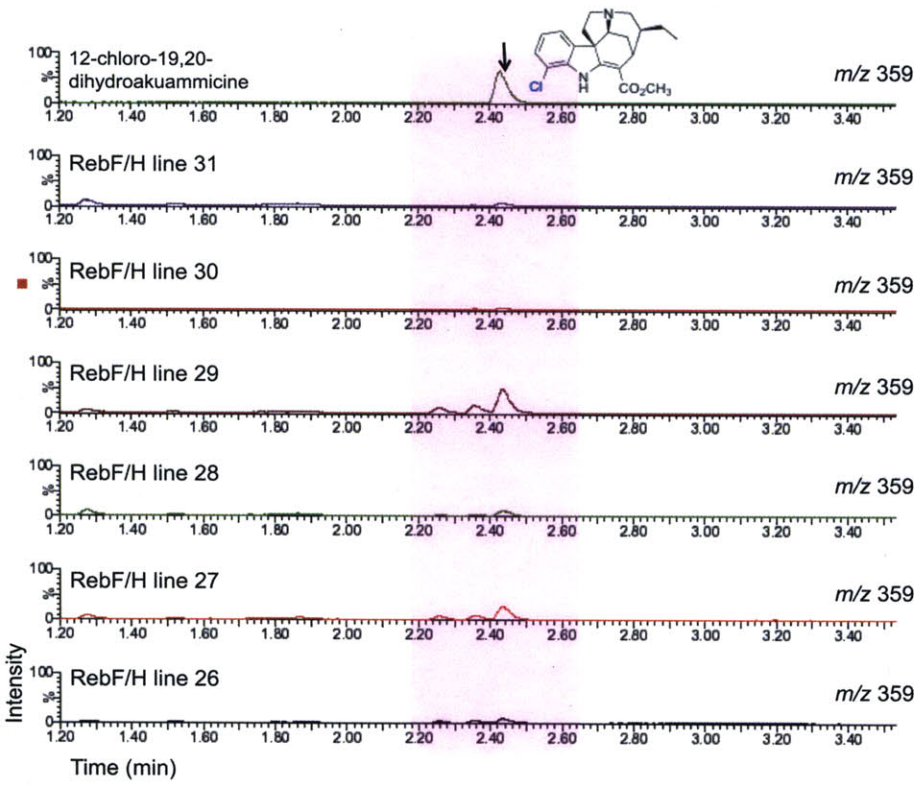

Figure 3B.3, E Chapter 3. Extracted LC-MS chromatograms showing the presence of 12-chloro-19,20-dihydroakuammicine **5a** (*m/z* 359) in selected RebF/H hairy roots. This compound, which is not observed in control cultures transformed with no plasmid, co-elutes with an authentic standard of 12-chloro-19,20-dihydroakuammicine **5a**.

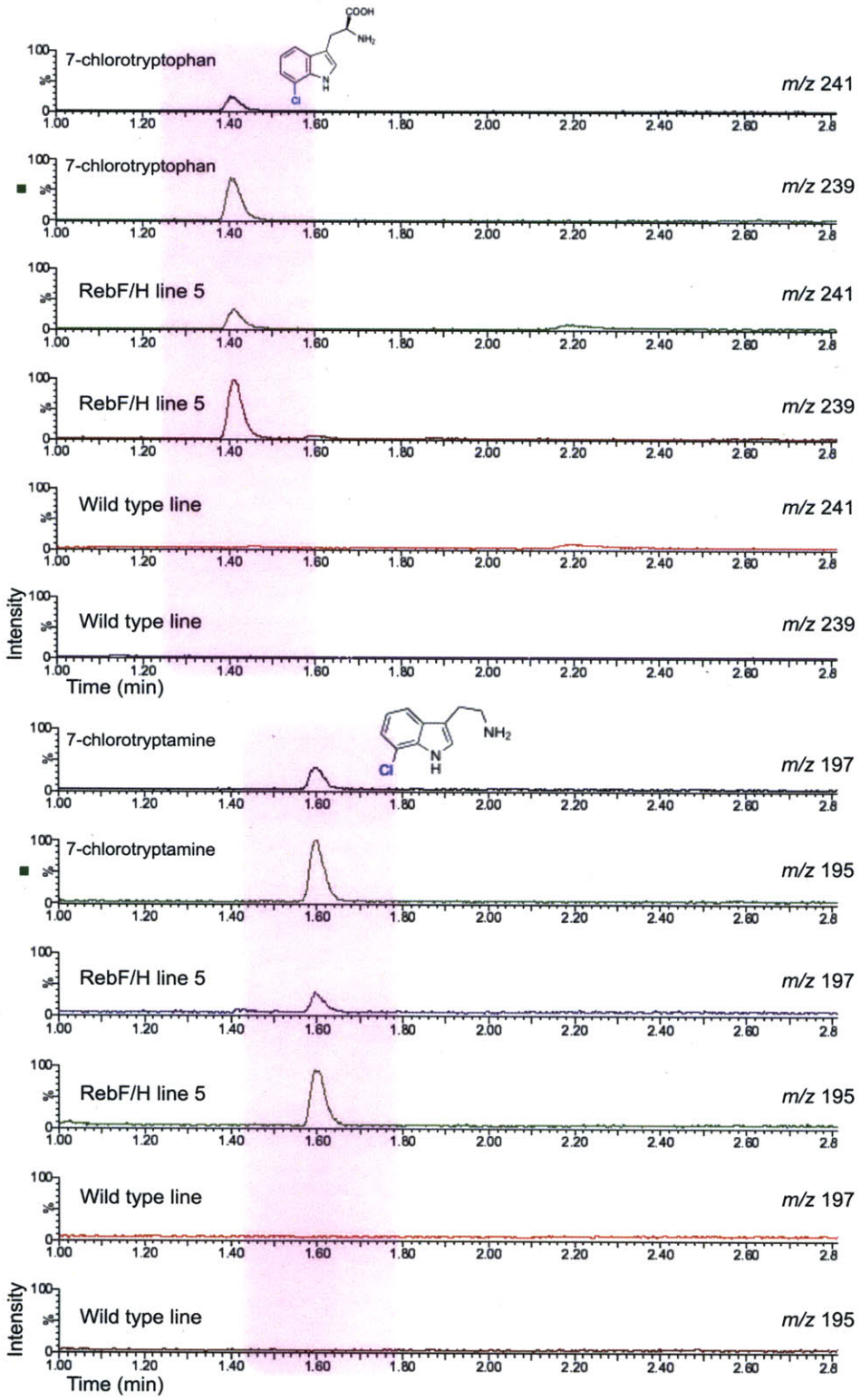

Figure 3B.4, A-B Chapter 3. Extracted LC-MS traces showing the isotopic distribution expected for a chlorinated compound.

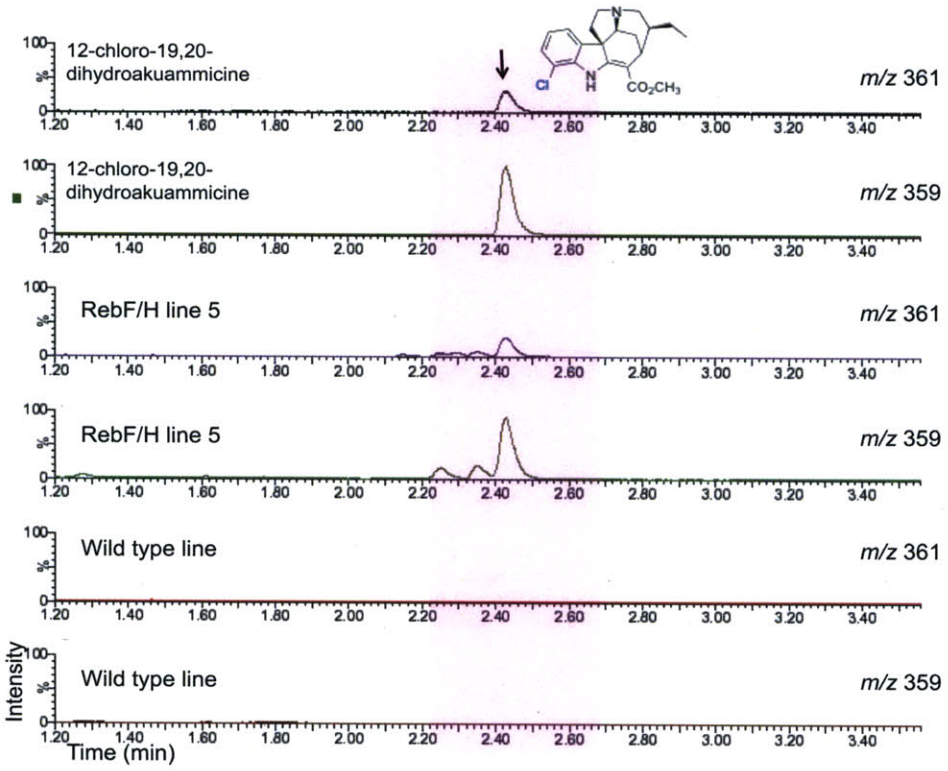

Figure 3B.4, C Chapter 3. Extracted LC-MS traces showing the isotopic distribution expected for a chlorinated compound.

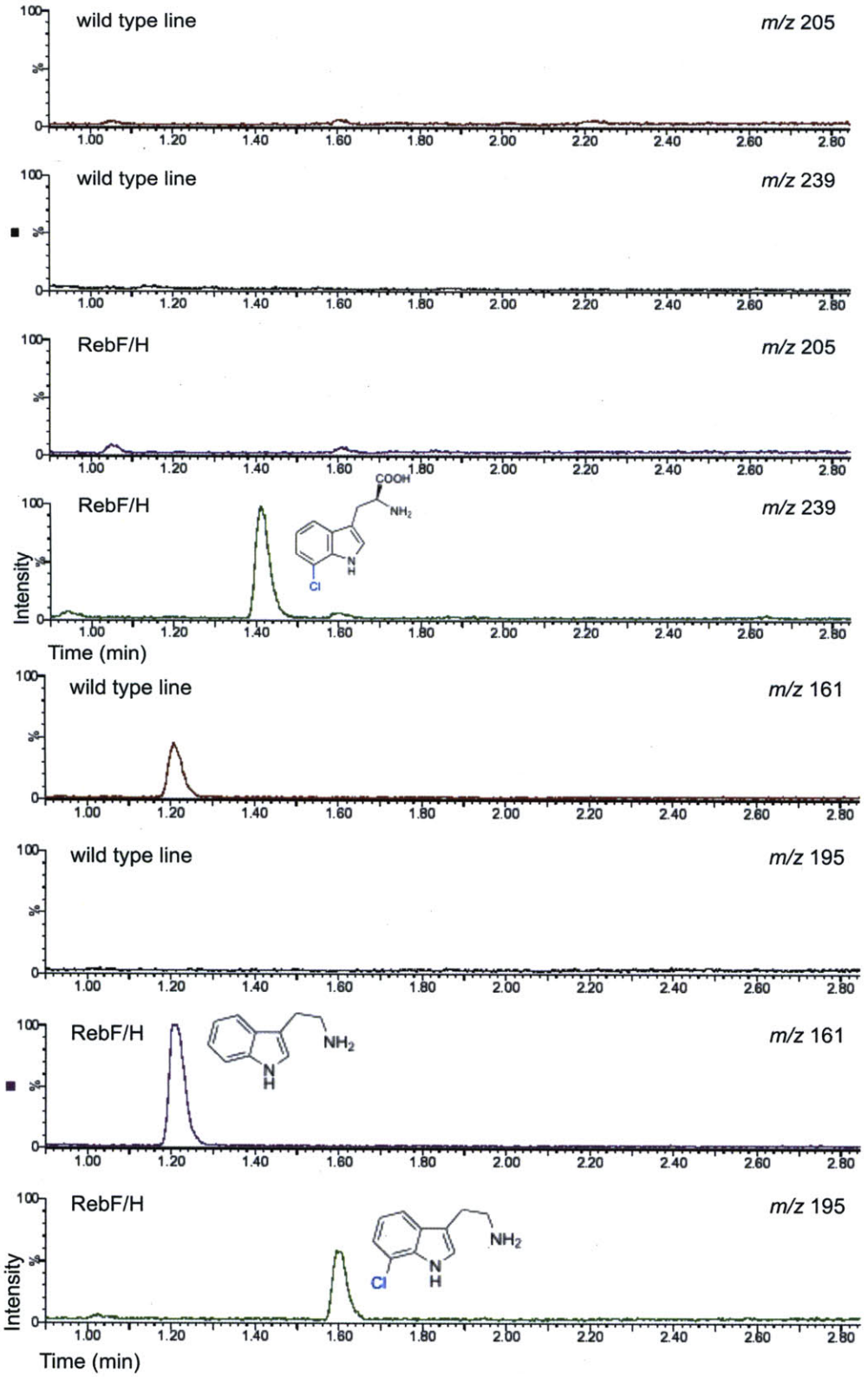

Figure 3B.5, A-B Chapter 3. Extracted LC-MS traces showing the production of chlorinated alkaloids along with the traces showing production of the parent natural alkaloids from the same cultures.

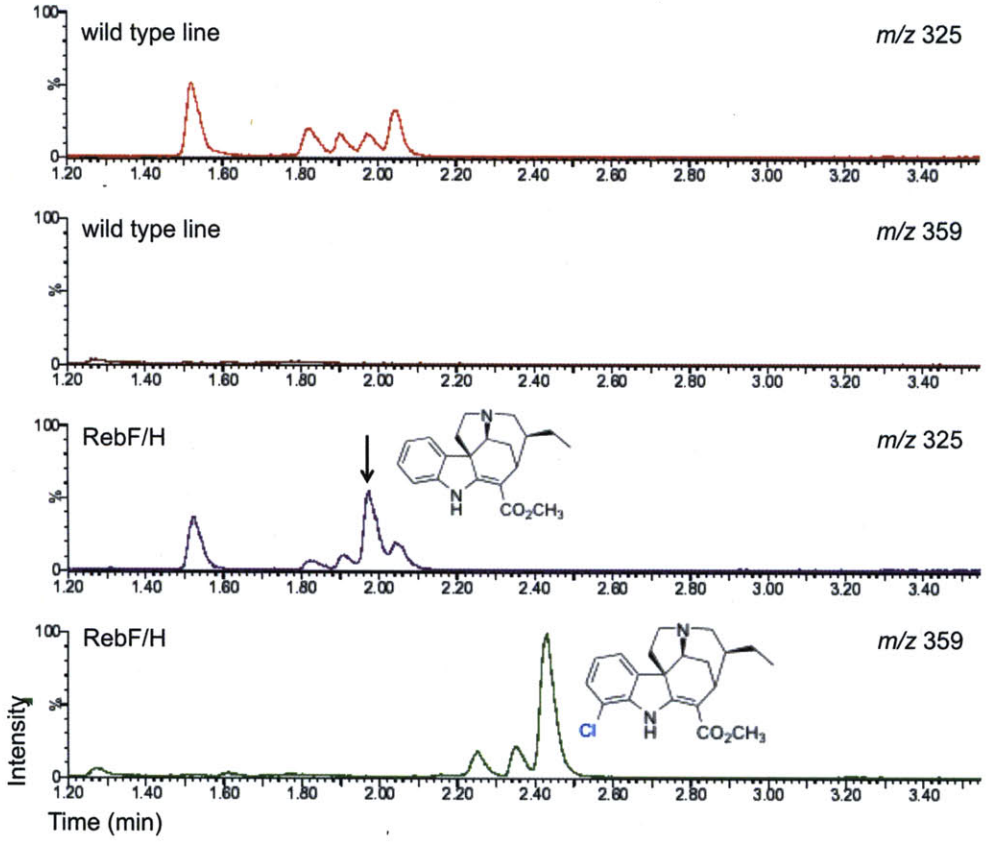

Figure 3B.5, C Chapter 3. Extracted LC-MS traces showing the production of chlorinated alkaloids along with the traces showing production of the parent natural alkaloids from the same cultures.

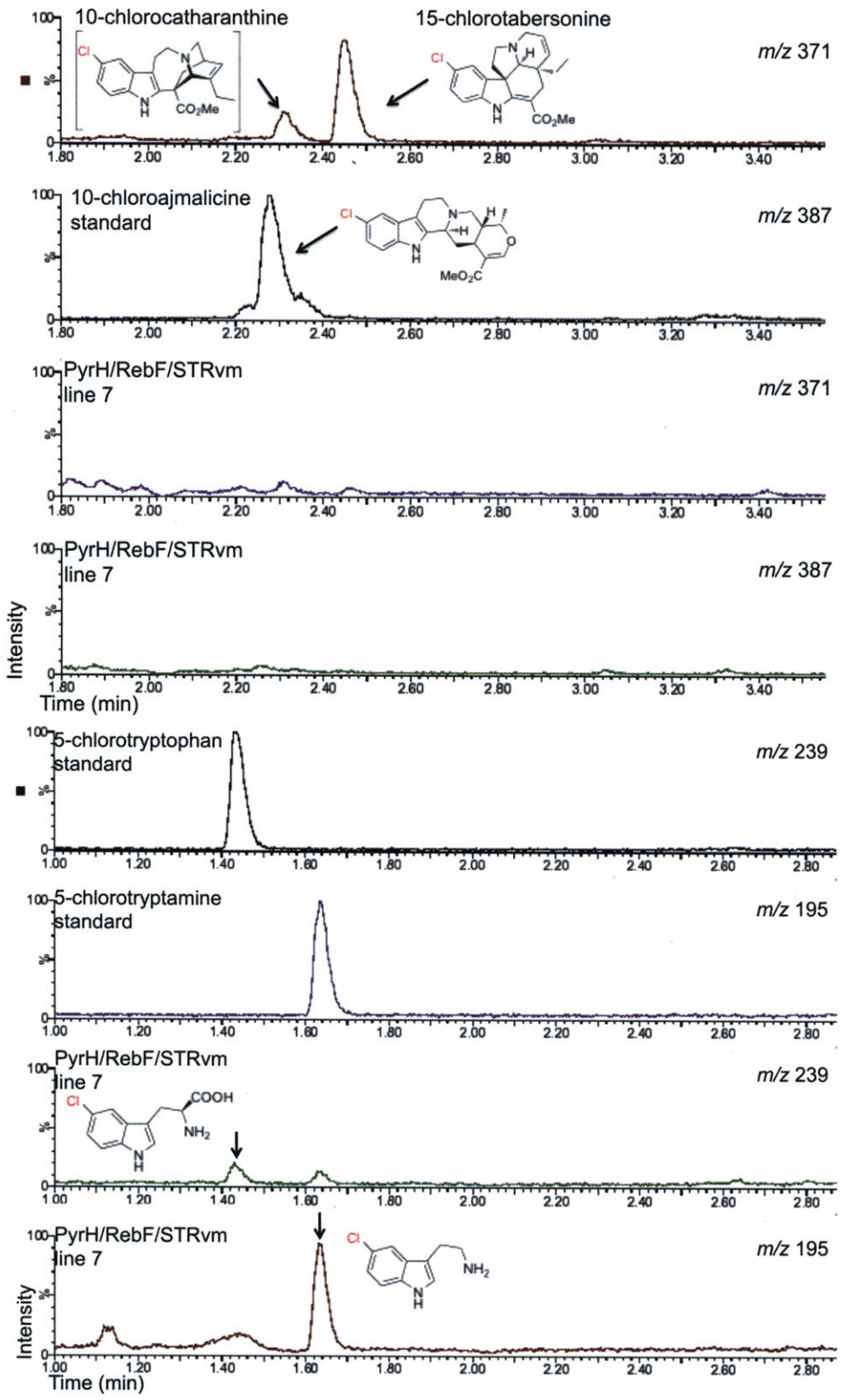

Figure 3B.6, A-B Chapter 3. Chlorinated alkaloid production in PyrH/RebF/STRvm hairy roots (line 7) as evidenced by LC-MS analysis of *C. roseus* extracts. The mutant strictosidine synthase enzyme, STRvm, is not expressed in this line as evidenced by real time PCR.

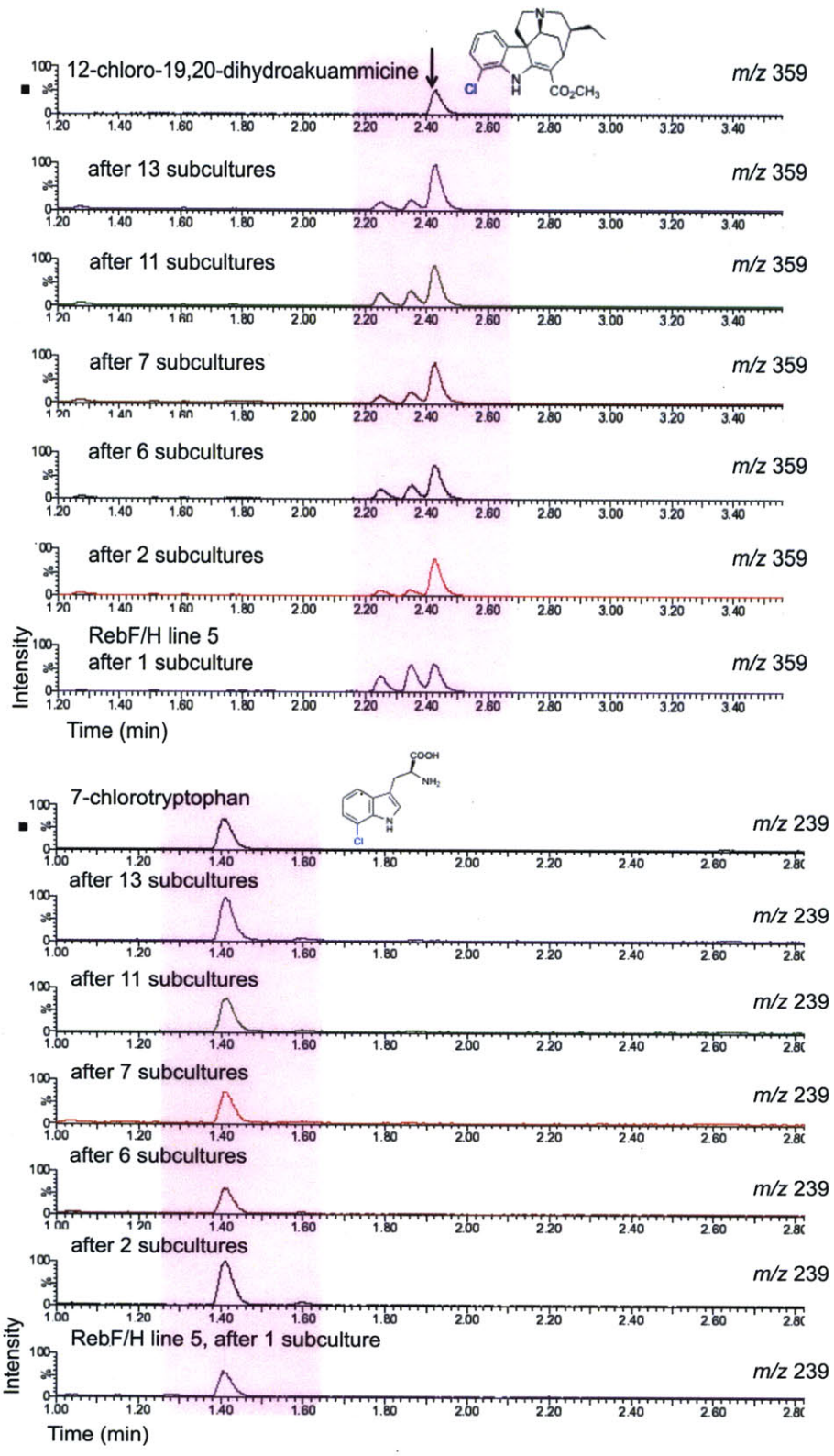

Figure 3B.7, A-B Chapter 3. Chlorinated alkaloid production in RebF/H hairy roots after 1, 2, 6, 7, 11 and 13 subcultures as evidenced by LC-MS analysis of *C. roseus* extracts.

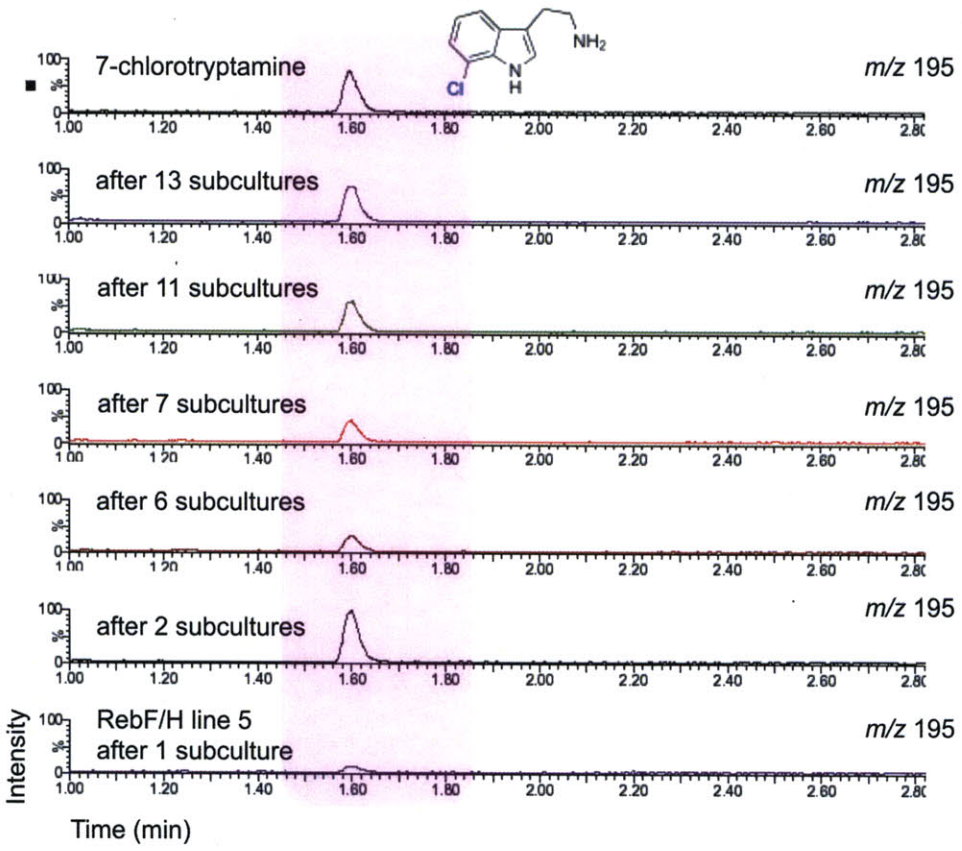

Figure 3B.7, C Chapter 3. Chlorinated alkaloid production in RebF/H hairy roots after 1, 2, 6, 7, 11 and 13 subcultures as evidenced by LC-MS analysis of *C. roseus* extracts.

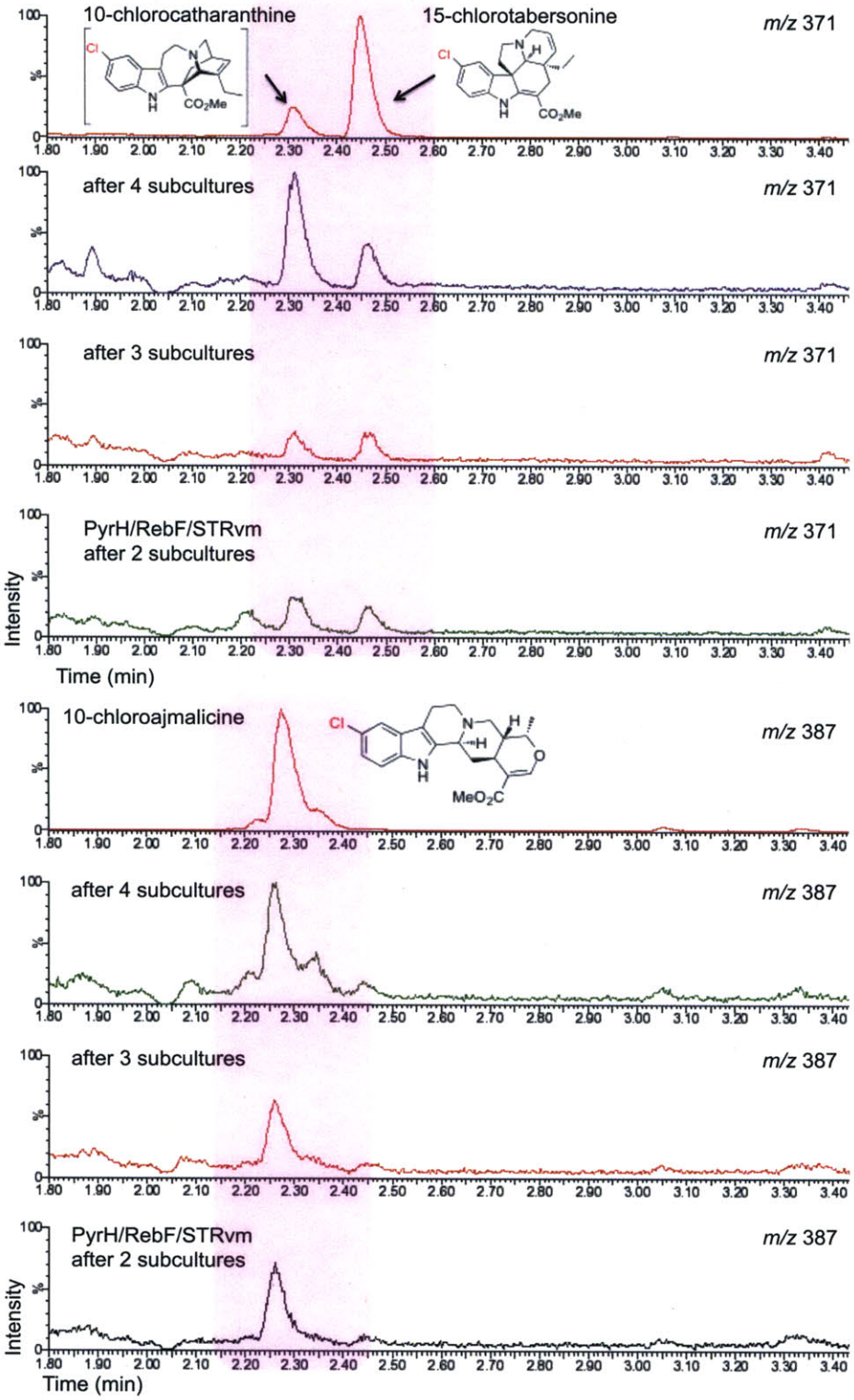

Figure 3B.8, A-B Chapter 3. Chlorinated alkaloid production in PyrH/RebF/STRvm hairy roots (line 1) after 2, 3 and 4 subcultures as evidenced by LC-MS analysis of *C. roseus* extracts.

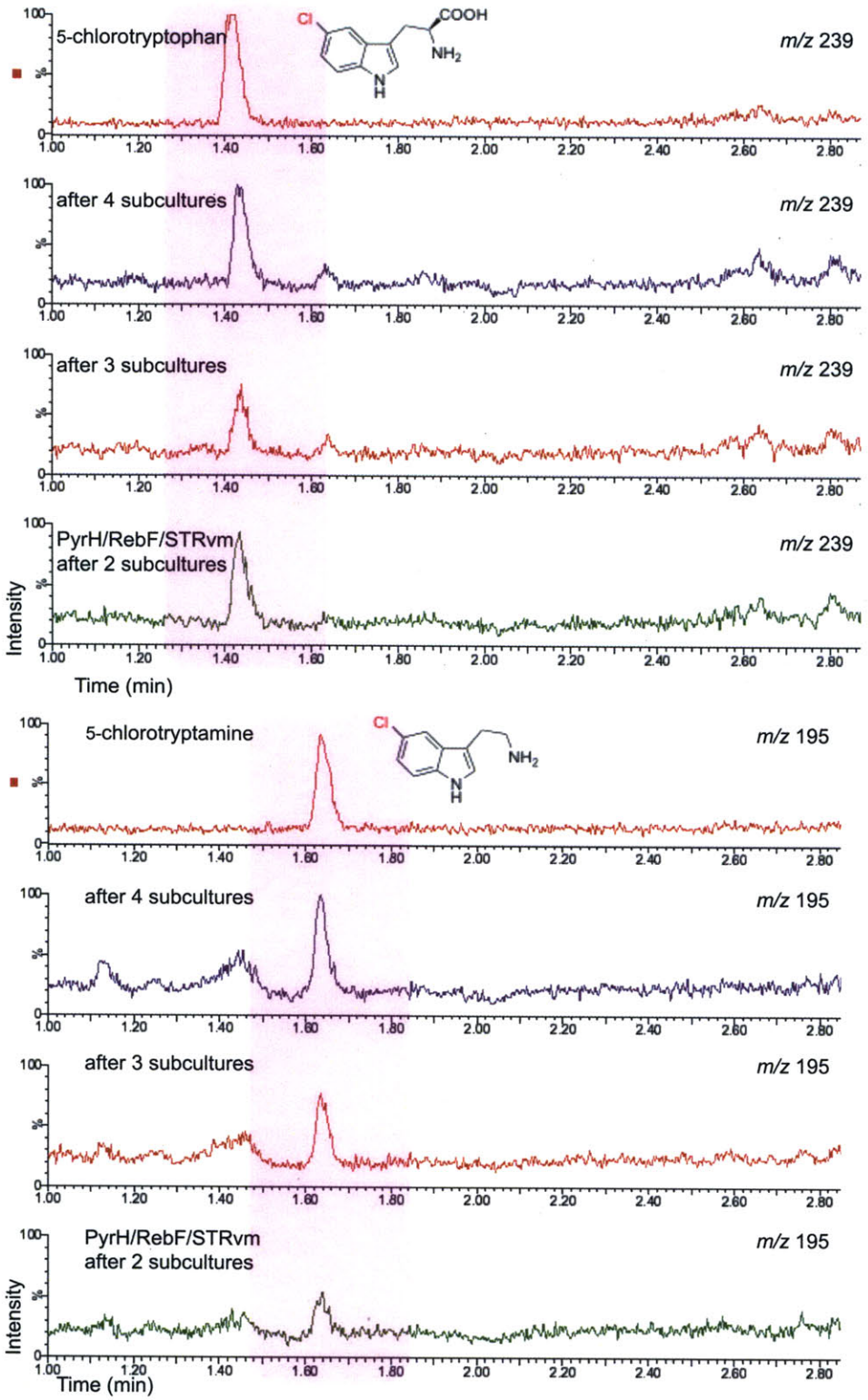

Figure 3B.8, C-D Chapter 3. Chlorinated alkaloid production in PyrH/RebF/STRvm hairy roots (line 1) after 2, 3 and 4 subcultures as evidenced by LC-MS analysis of *C. roseus* extracts.

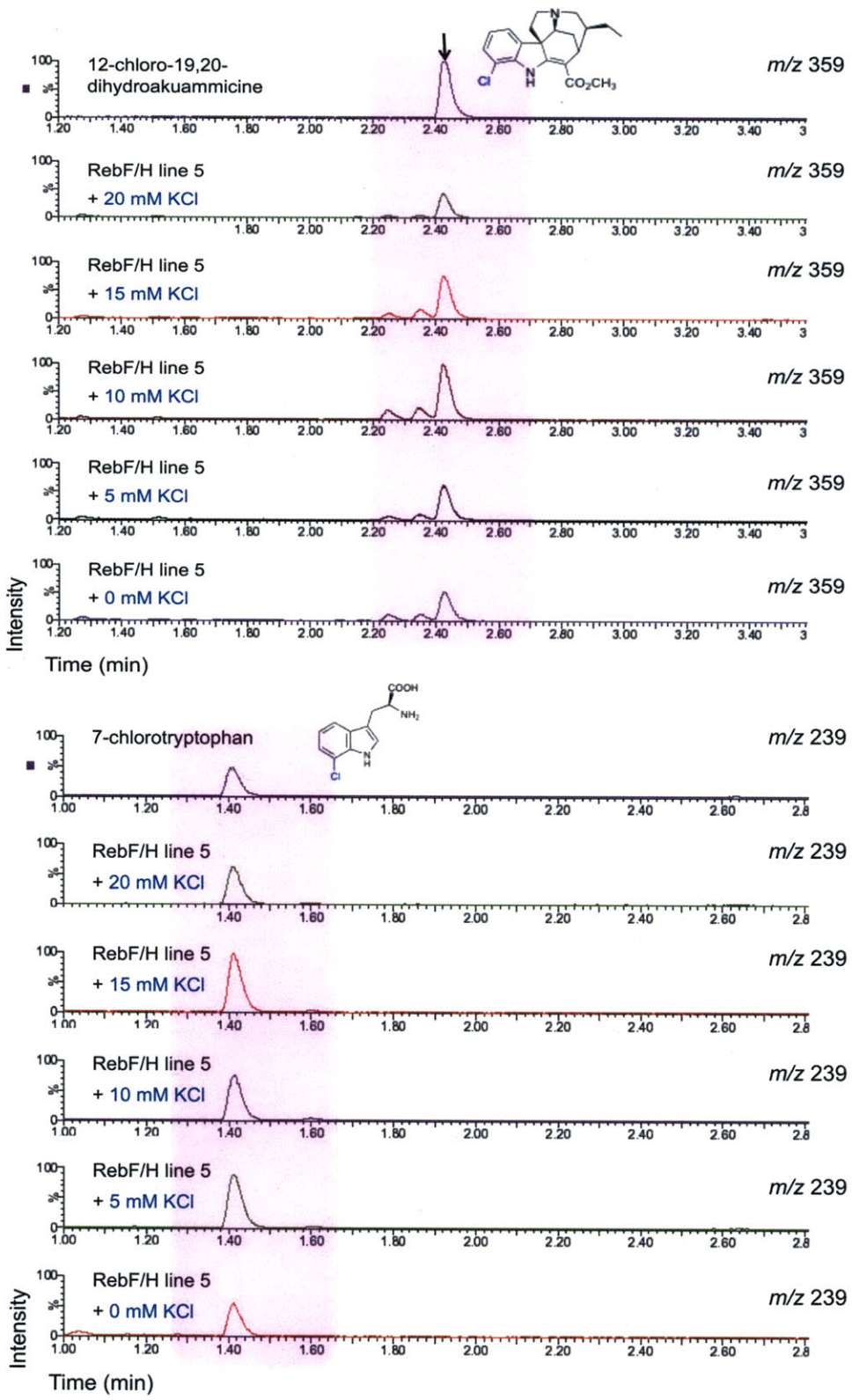

Figure 3B.9, A-B Chapter 3. Levels of chlorinated alkaloid **5a** and 7-chlorotryptophan **1a** in response to increasing KCl concentration.

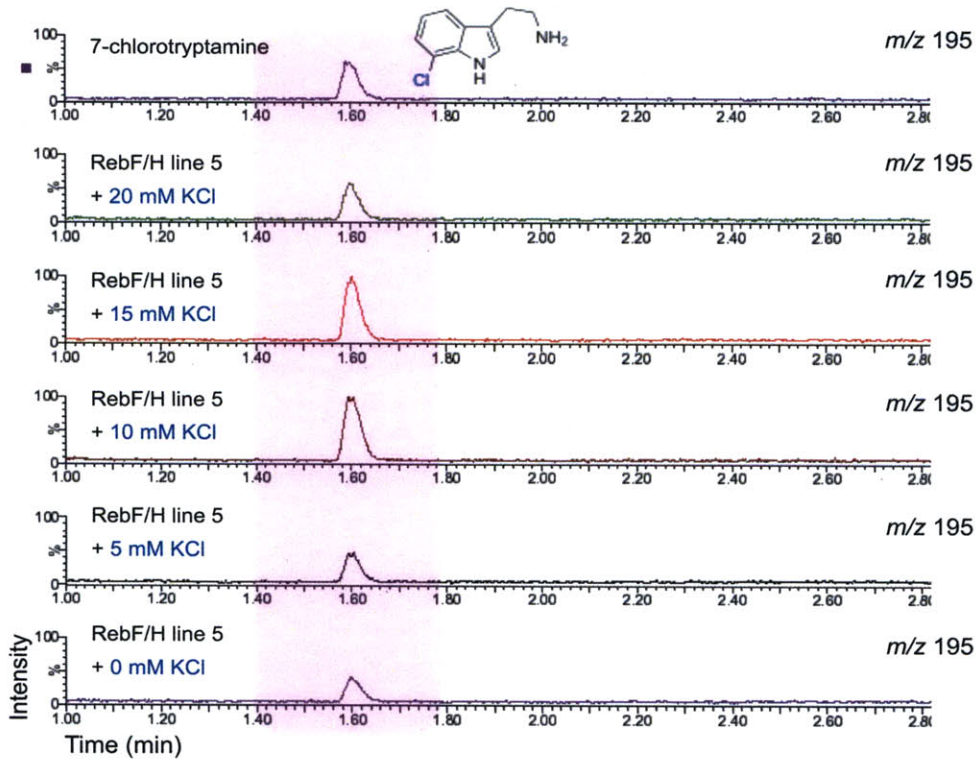

Figure 3B.9, C Chapter 3. Levels of 7-chlorotryptamine **2a** in response to increasing KCl concentration.

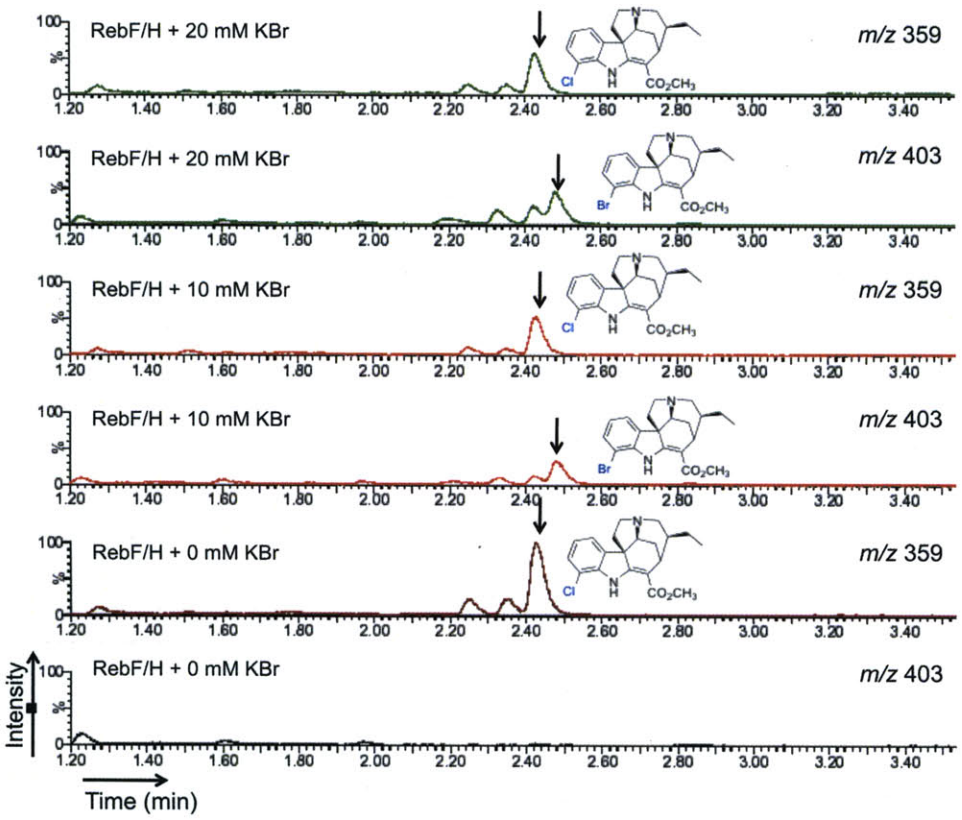

Figure 3B.10 Chapter 3. Extracted LC-MS traces comparing the production of chlorinated and brominated alkaloids in selected RebF/H hairy roots growing on solid media that have been supplemented with KBr (0 – 20 mM).

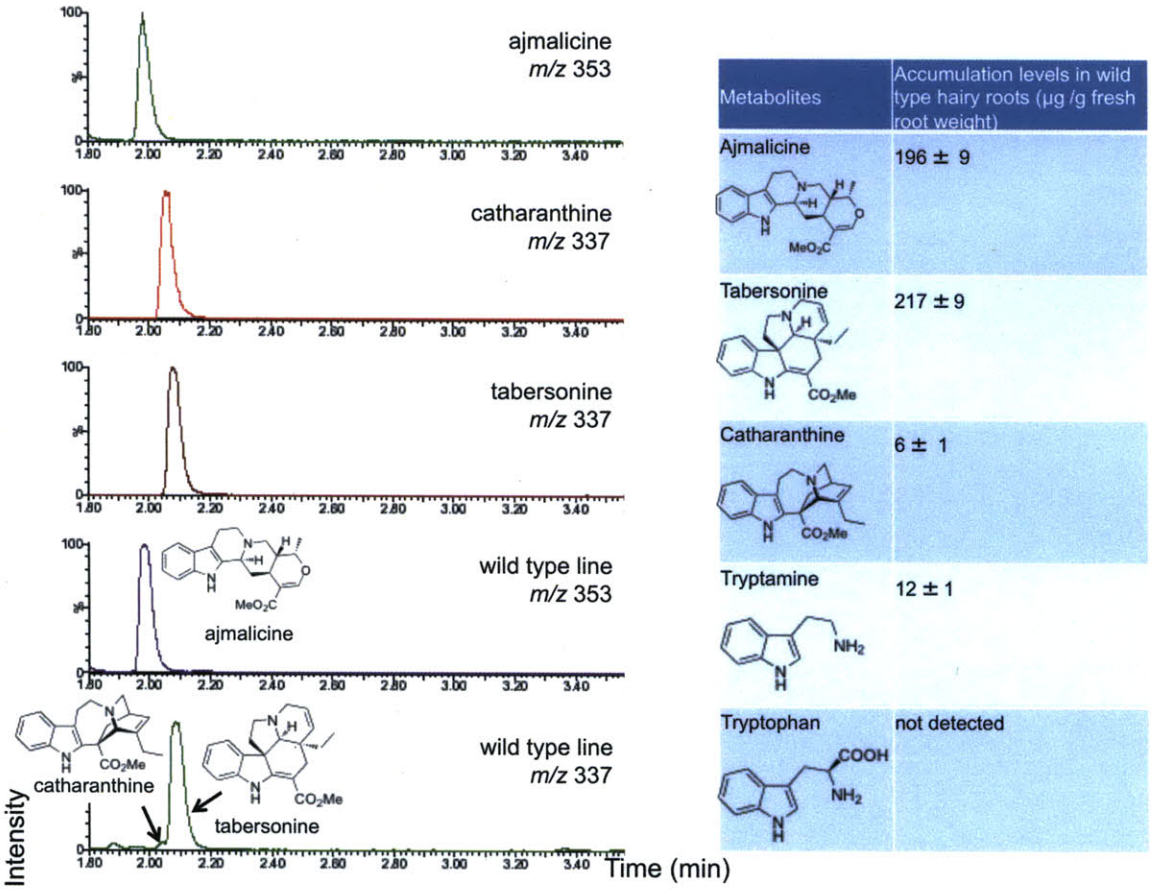

Metabolites	Accumulation levels in wild type hairy roots (µg /g fresh root weight)
Ajmalicine	196 ± 9
Tabersonine	217 ± 9
Catharanthine	6 ± 1
Tryptamine	12 ± 1
Tryptophan	not detected

Figure 3B.11 Chapter 3. Accumulation of the major natural alkaloids (tabersonine **7**, catharanthine **8** and ajmalicine **6**) that are produced in wild type hairy roots.

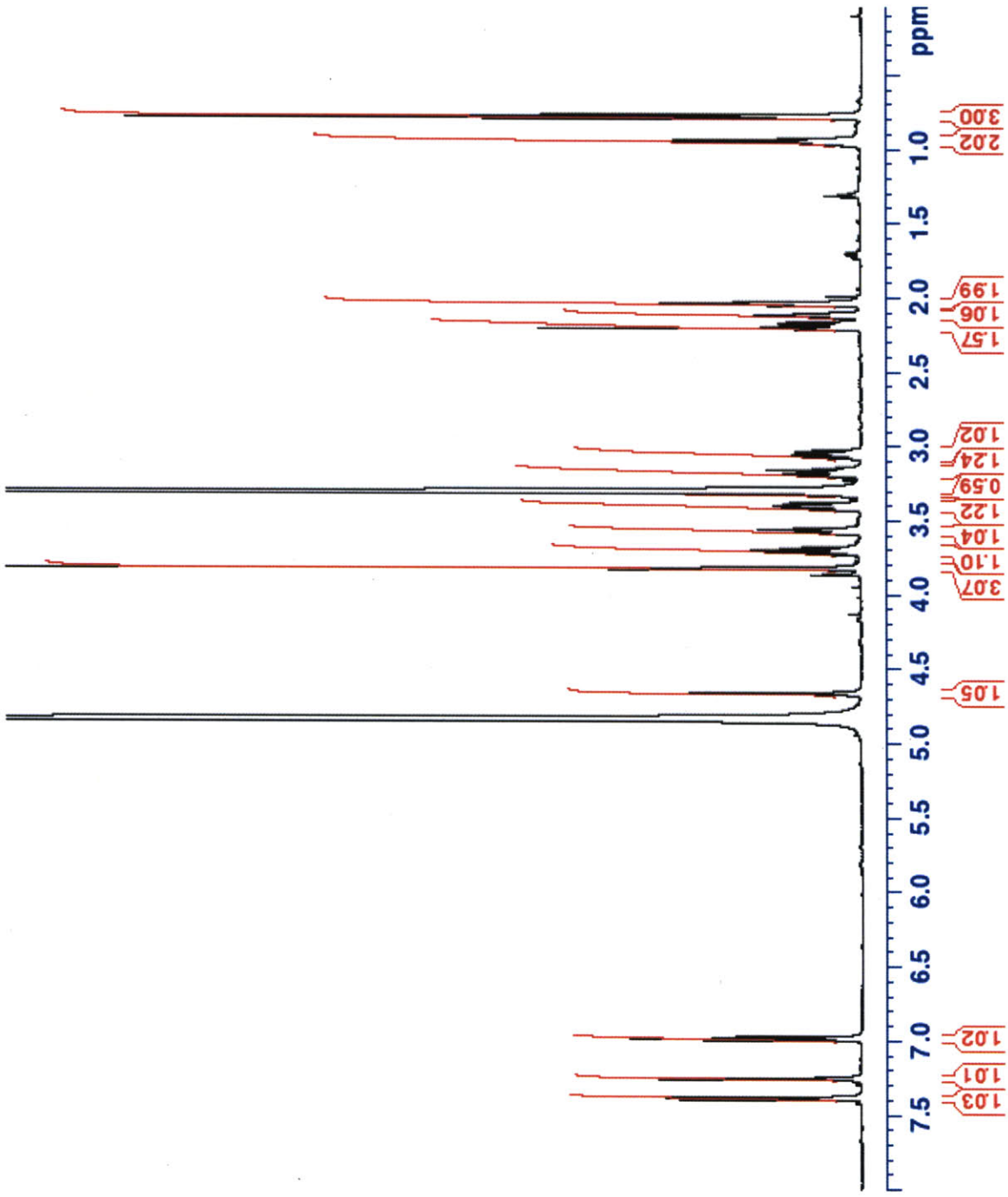

Figure 3B.12 Chapter 3. ^{1}H NMR spectrum of 12-chloro-19,20-dihydroakuammicine **5a**.

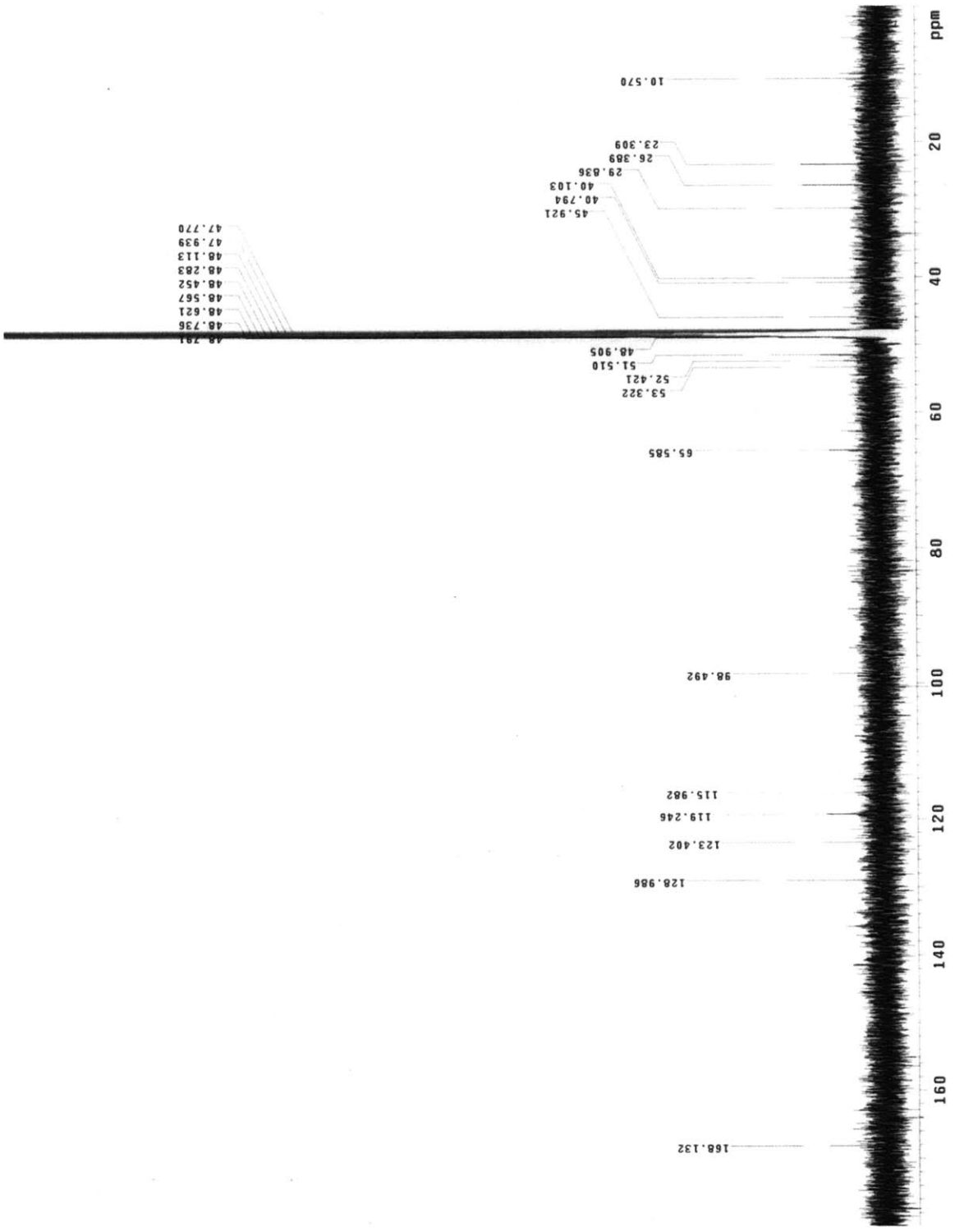

Figure 3B.13 Chapter 3. ^{13}C NMR spectrum of 12-chloro-19,20-dihydroakuammicine **5a**. Note that quaternary carbon peaks are not observed in ^{13}C NMR.

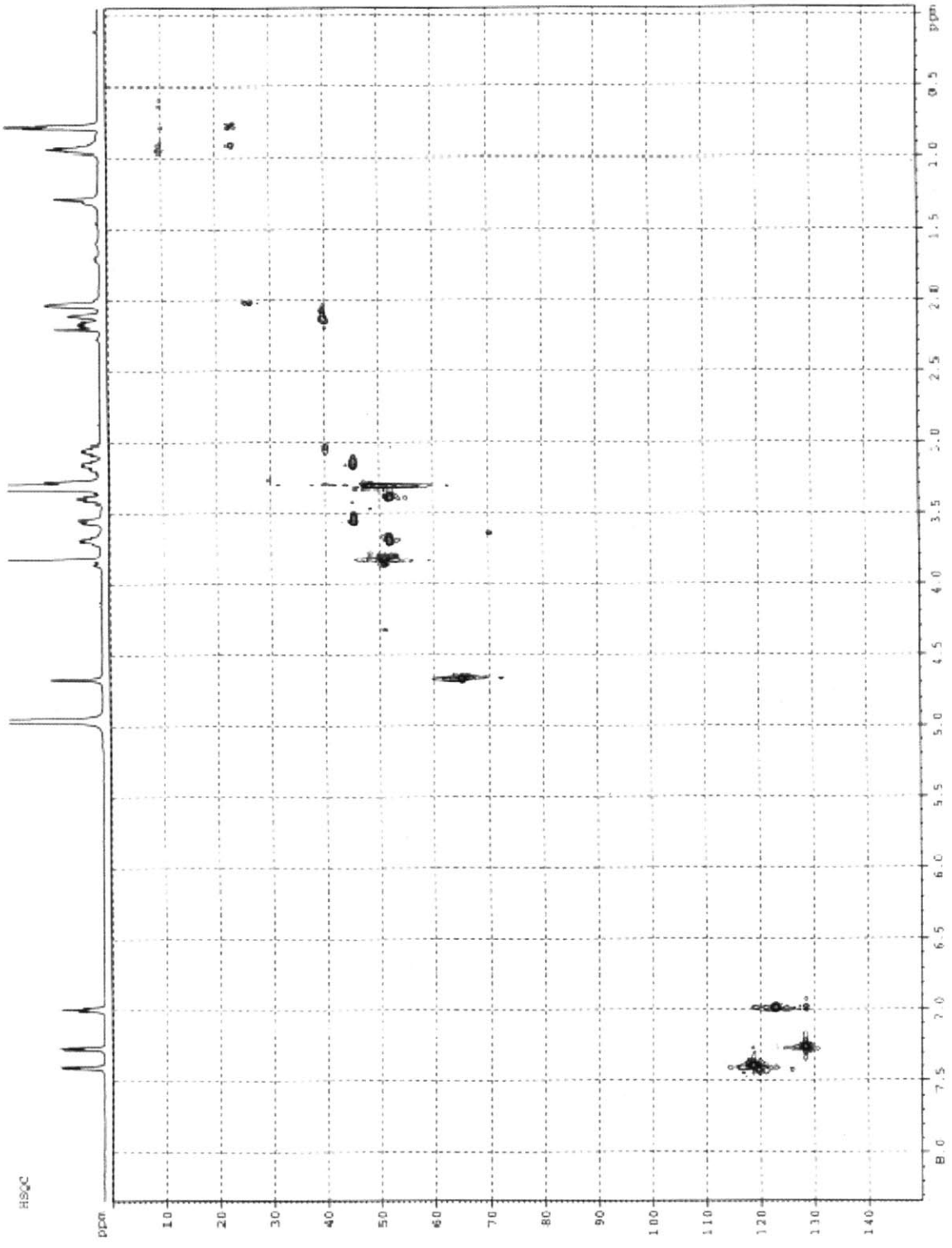

Figure 3B.14 Chapter 3. ^{13}C-^{1}H HSQC spectra of 12-chloro-19,20-dihydroakuammicine **5a**.

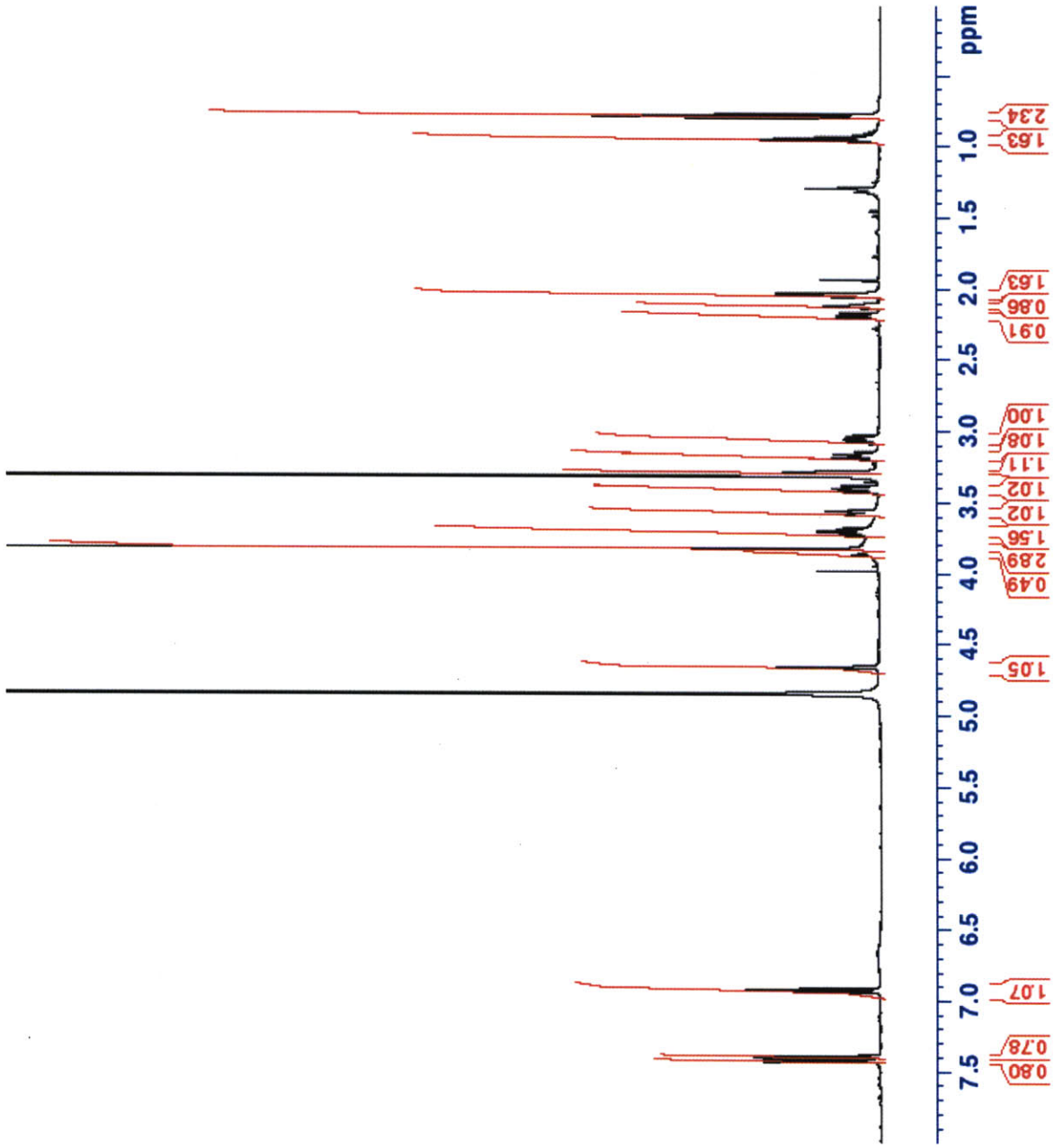

Figure 3B.15 Chapter 3. ^{1}H NMR spectrum of 12-bromo-19,20-dihydroakuammicine **5c.**

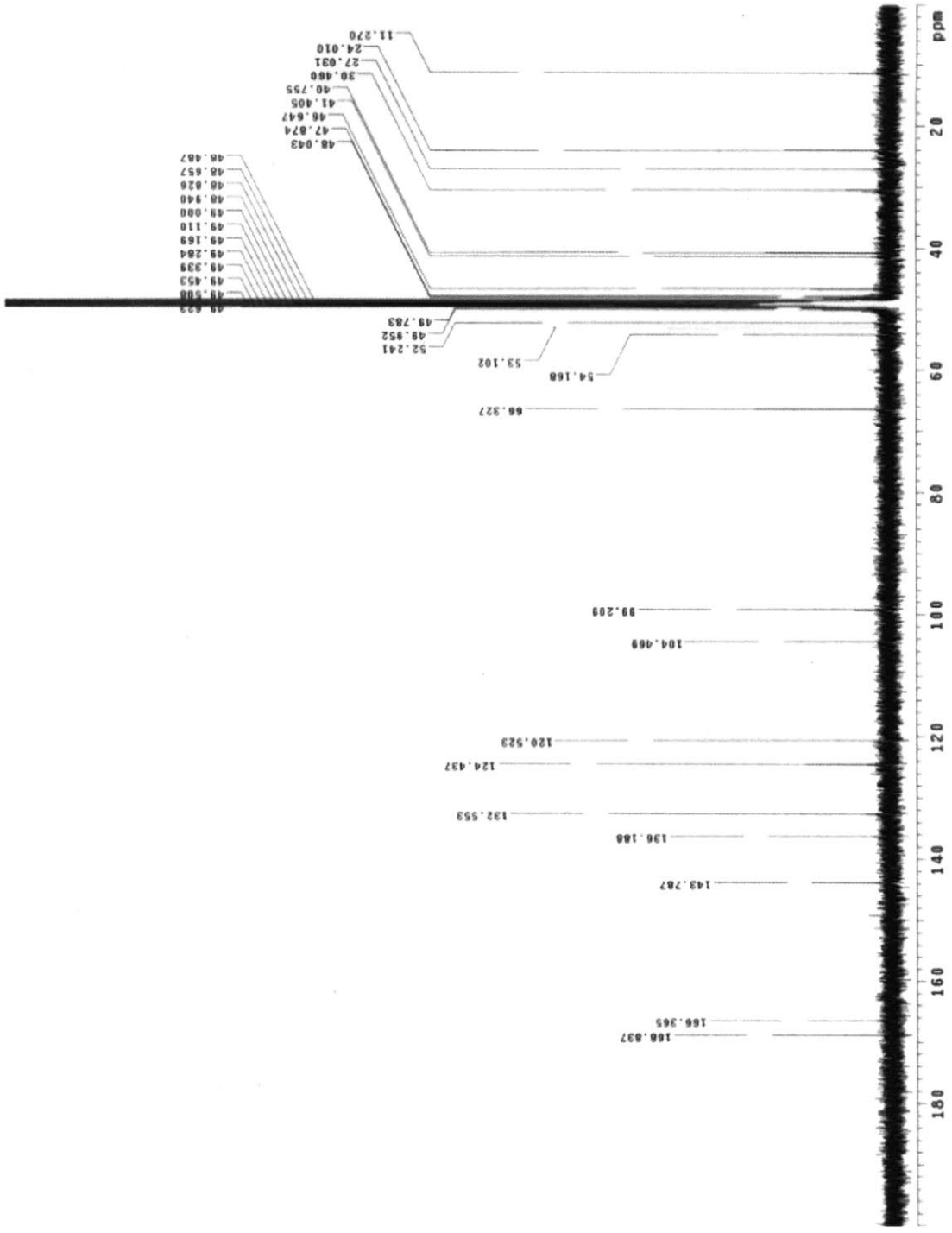

Figure 3B.16 Chapter 3. ^{13}C NMR spectrum of 12-bromo-19,20-dihydroakuammicine **5c.**

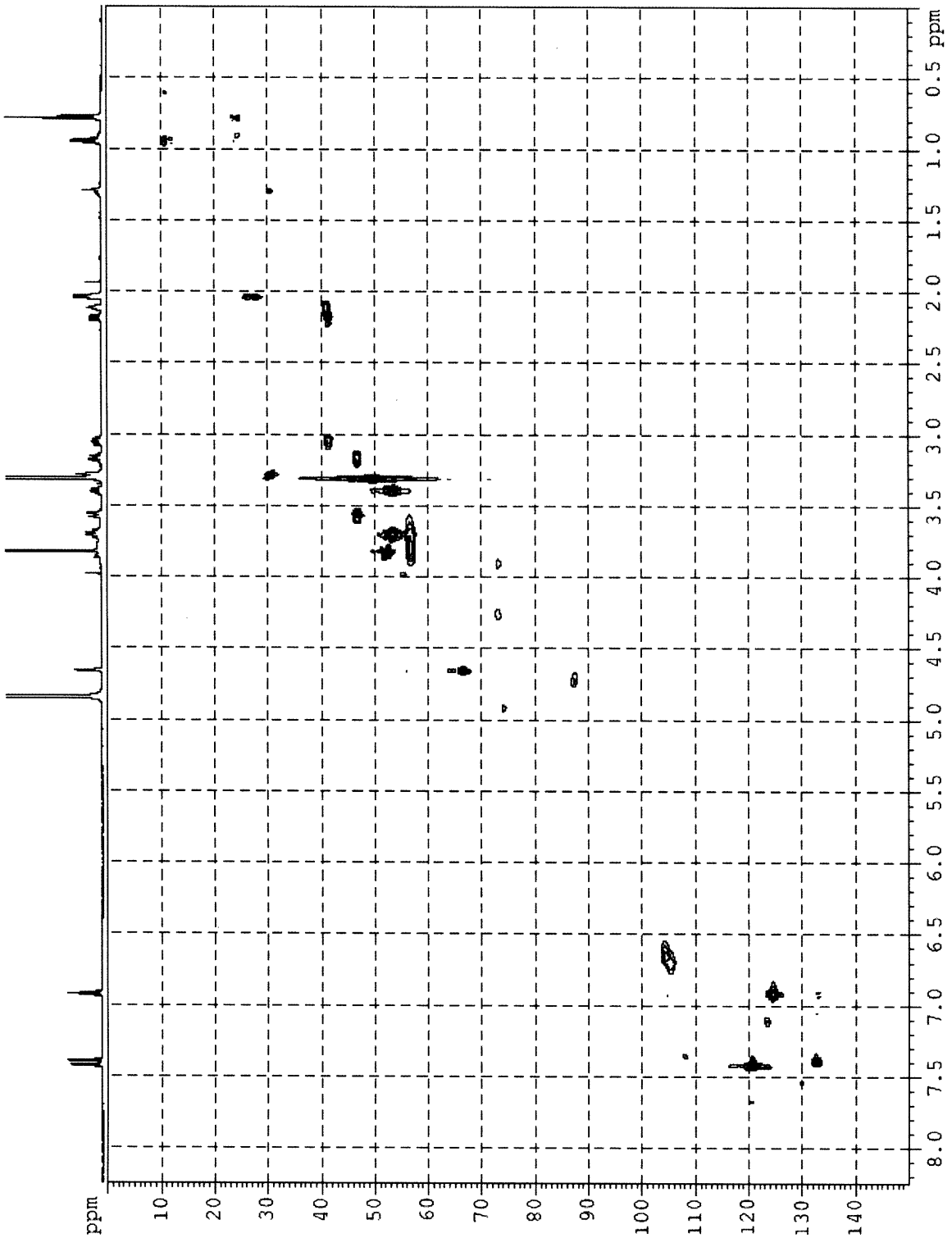

Figure 3B.17 Chapter 3. ^{13}C-^{1}H HSQC spectrum of 12-bromo-19,20-dihydroakuammicine **5c.**

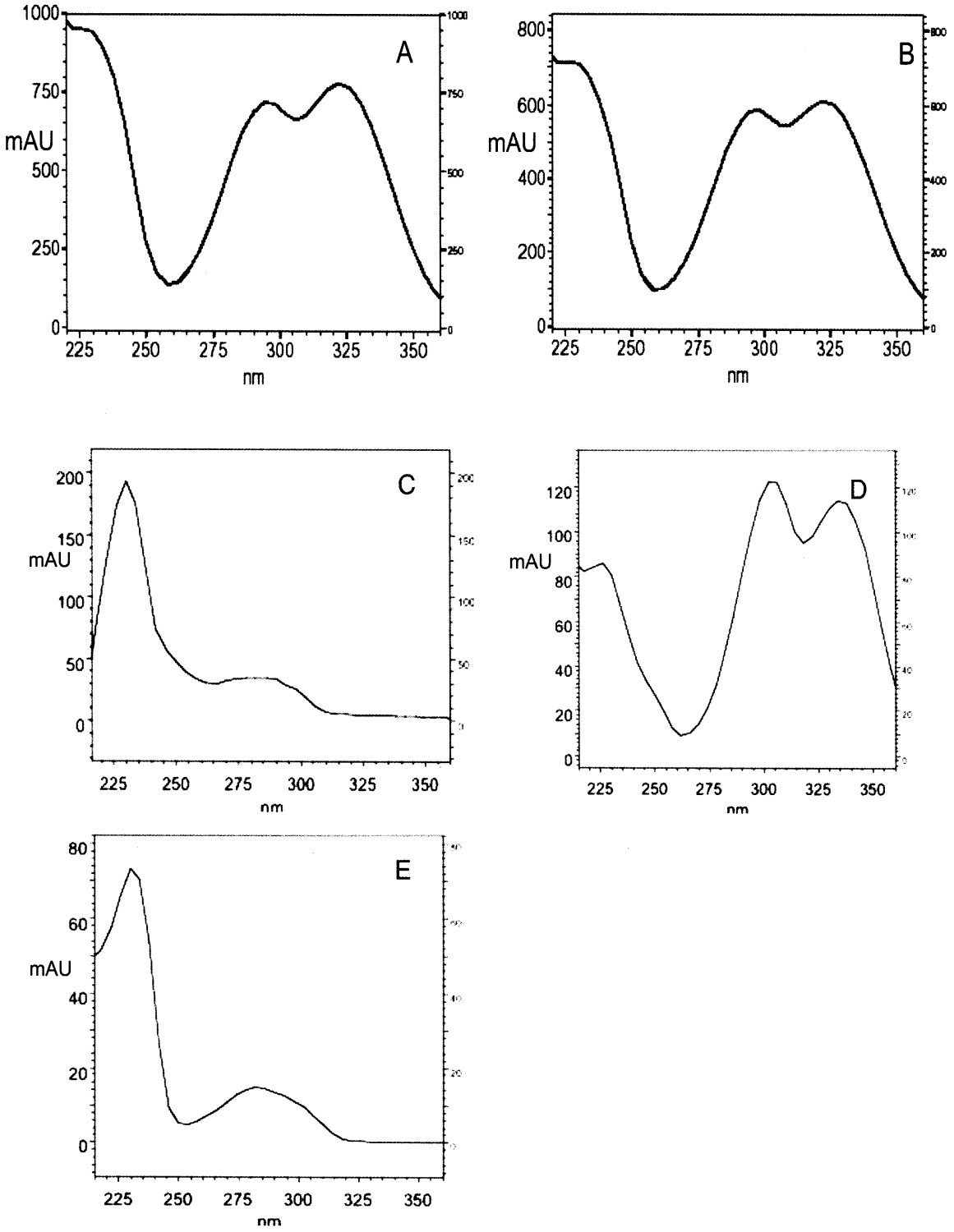

Figure 3B.18 Chapter 3. UV spectra of chlorinated and brominated alkaloids. **A.** 12-chloro-19,20-dihydroakuammicine **5a**. **B.** 12-bromo-19,20-dihydroakuammicine **5c.** **C.**10-chloroajmalicine **6b**. **D.** 15-chlorotabersonine **7b**. **E.** 10-cholorocatharanthine **8b**.

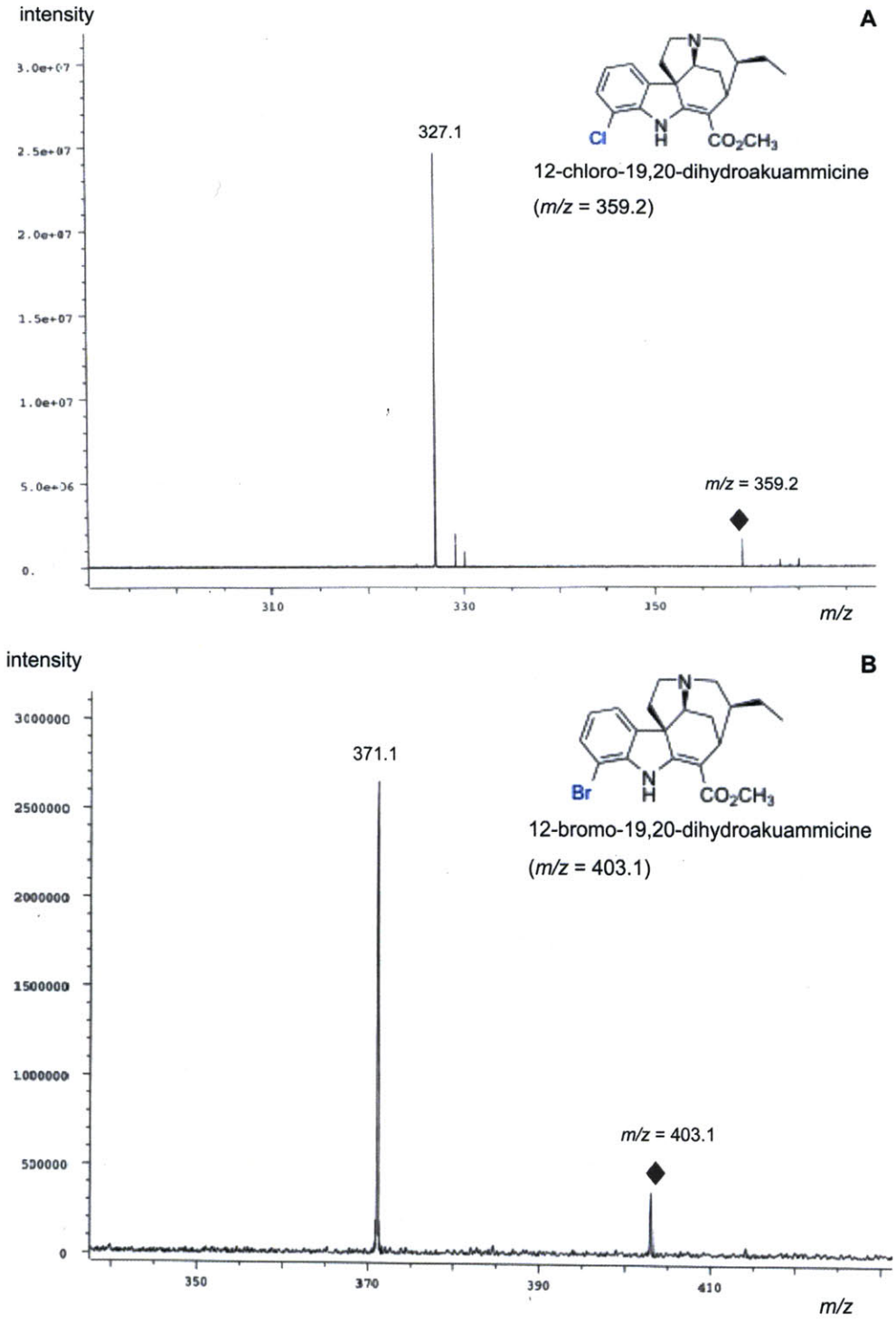

Figure 3B.19 Chapter 3. MS/MS analysis for **(A)** 12-chloro-19,20-dihydroakuammicine **5a** and **(B)** 12-bromo-19,20-dihydroakuammicine **5c**. **(A)** 12-chloro-19,20-dihydroakuammicine **5a** is identified as the $m/z = 359.2$ ion showing the fragment $m/z = 327.1$. **(B)** 12-bromo-19,20-dihydroakuammicine **5c** is identified as the $m/z = 403.1$ ion showing the fragment $m/z = 371.1$.

CHAPTER 5 - APPENDIX C

NMR SPECTRA:

CHEMOGENETIC APPROACHES TO

FURTHER DERIVATIZE HALOGENATED ALKALOIDS

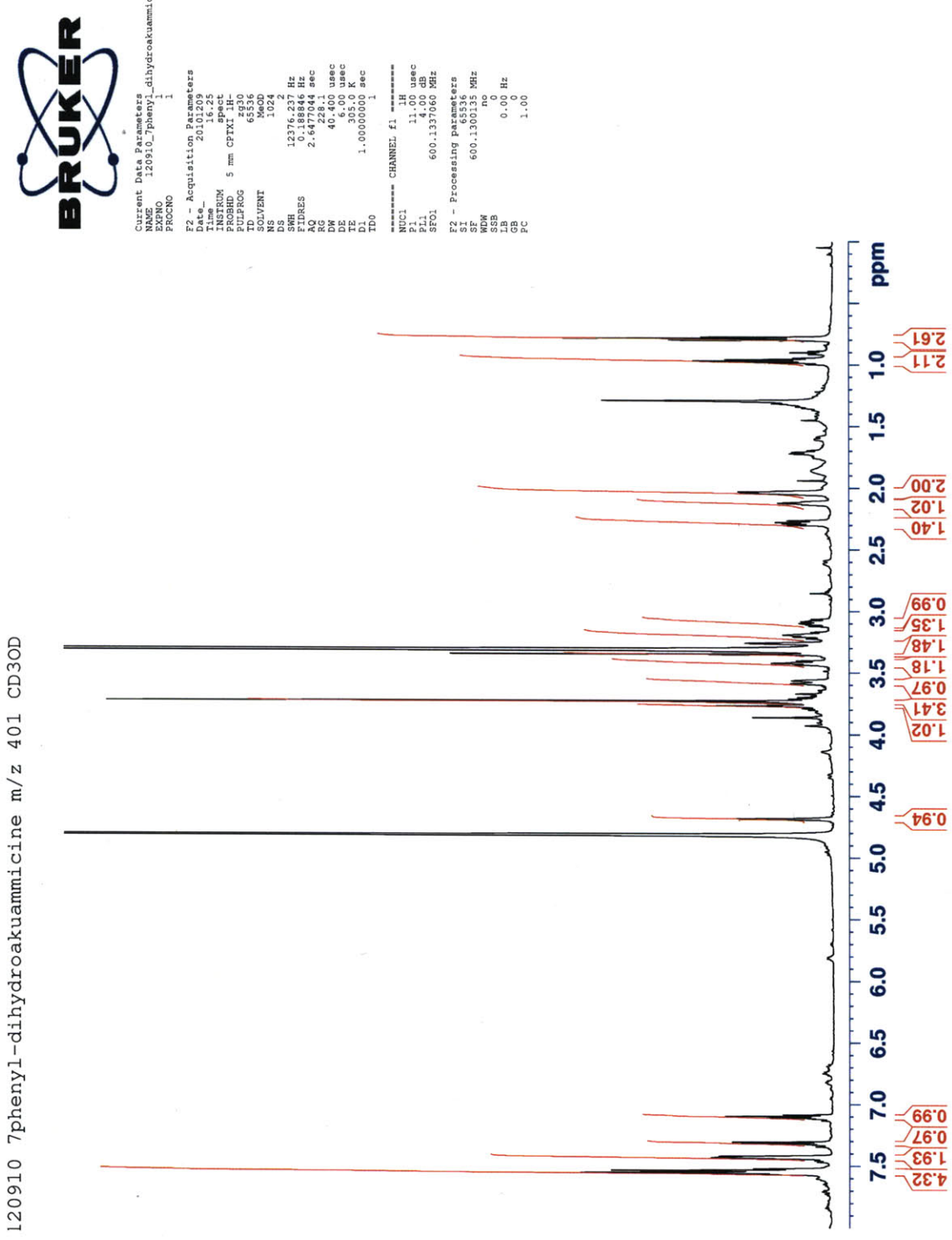

Figure 5C.1 Chapter 5. ^{1}H NMR spectrum of 12-phenyl-19,20-dihydroakuammicine **5d**

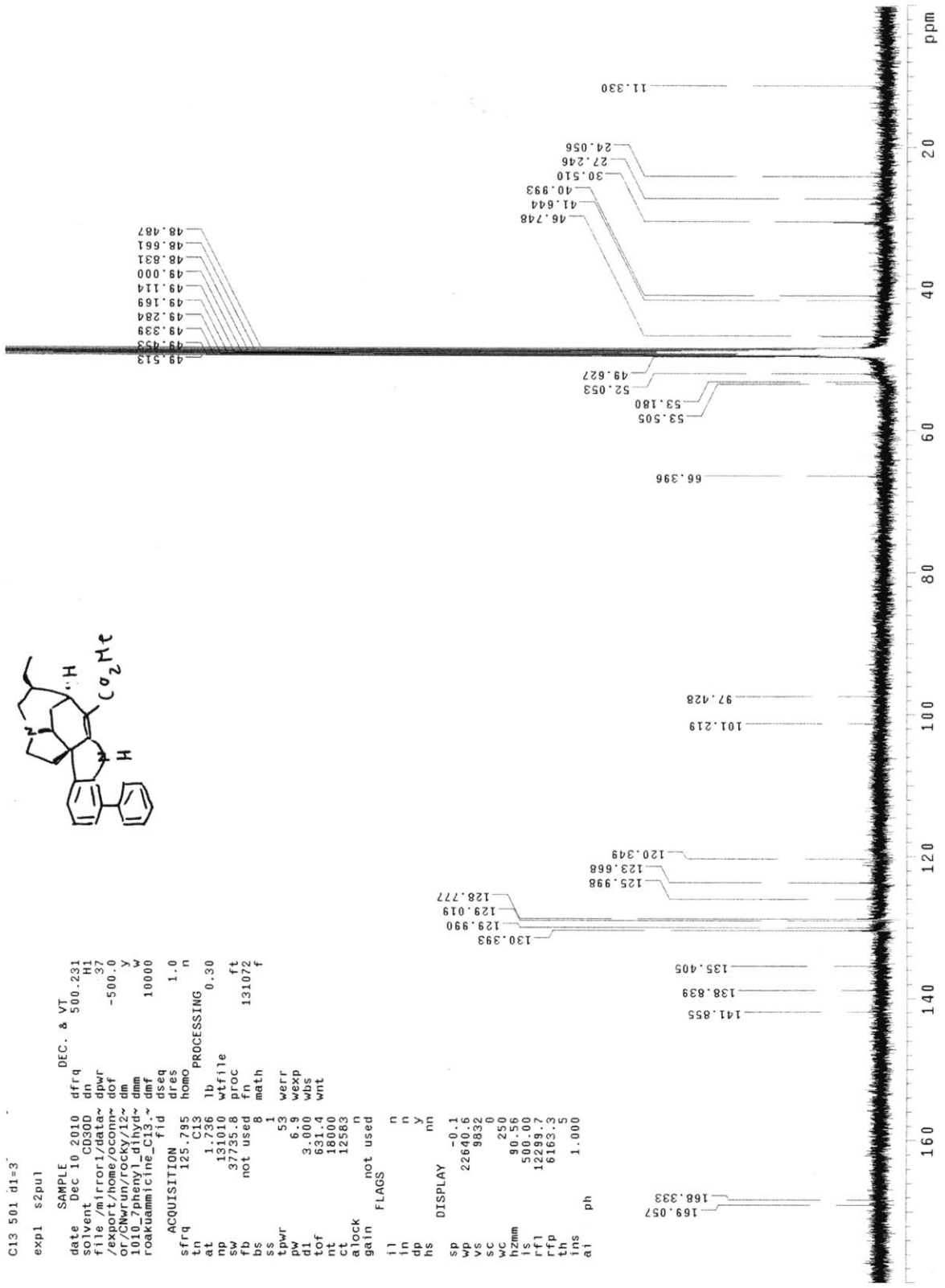

Figure 5C.2 Chapter 5. ^{13}C NMR spectrum of 12-phenyl-19,20-dihydroakuammicine **5d**

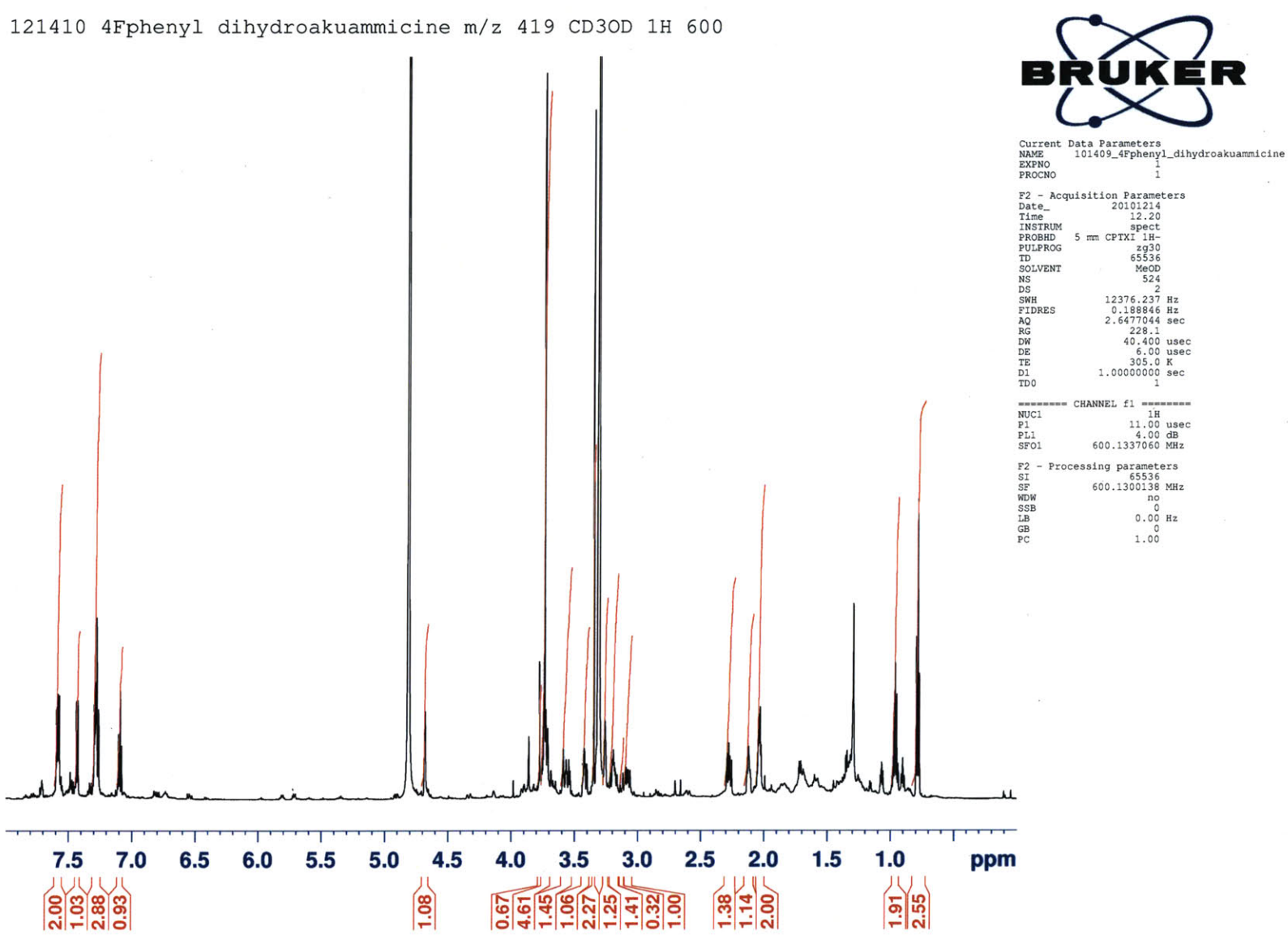

Figure 5C.3 Chapter 5. ^{1}H NMR spectrum of 12-(4-fluorophenyl)-19,20-dihydroakuammicine **5e**

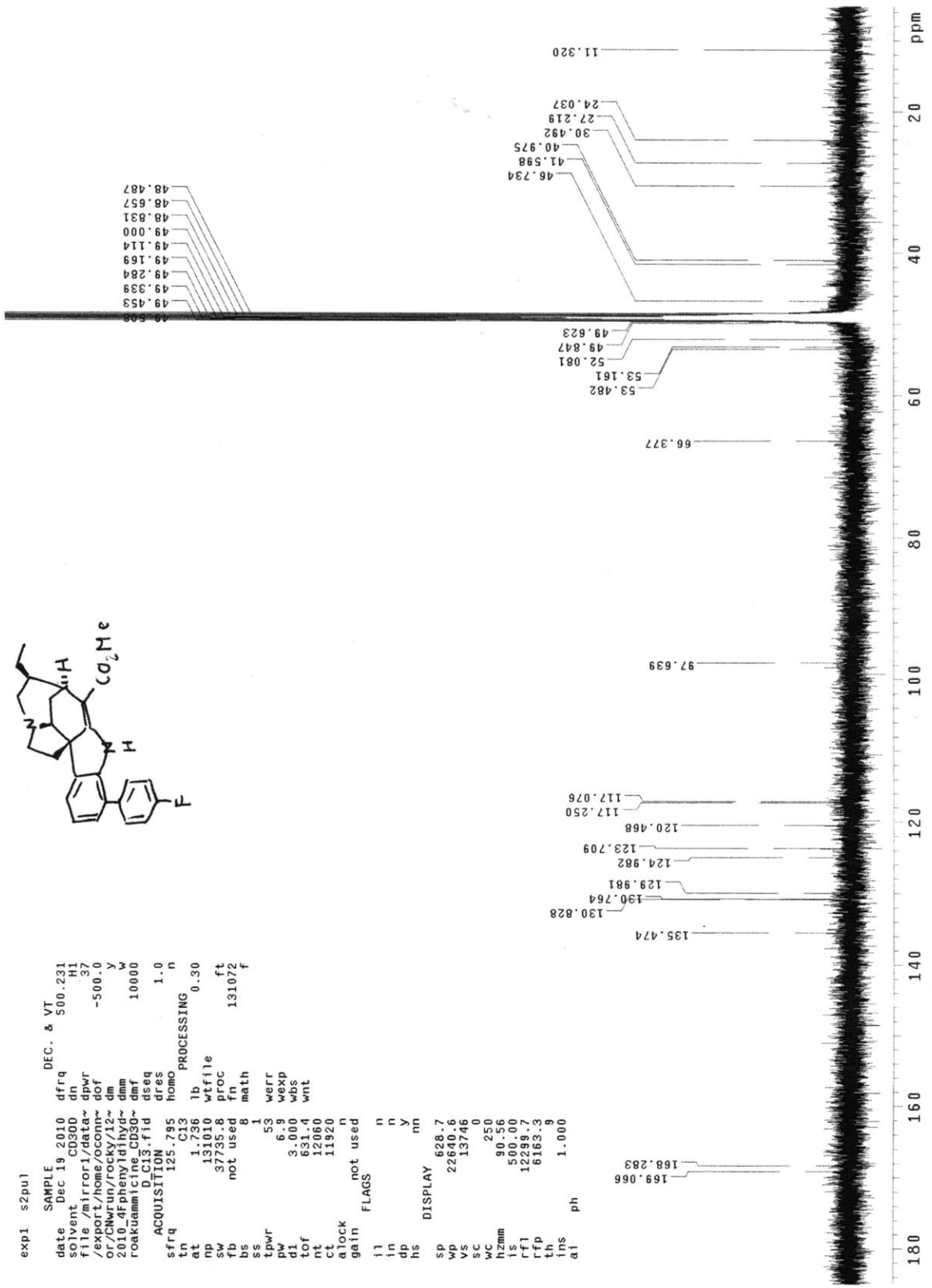

Figure 5C.4 Chapter 5. ^{13}C NMR spectrum of 12-(4-fluorophenyl)-19,20-dihydroakuammicine **5e**

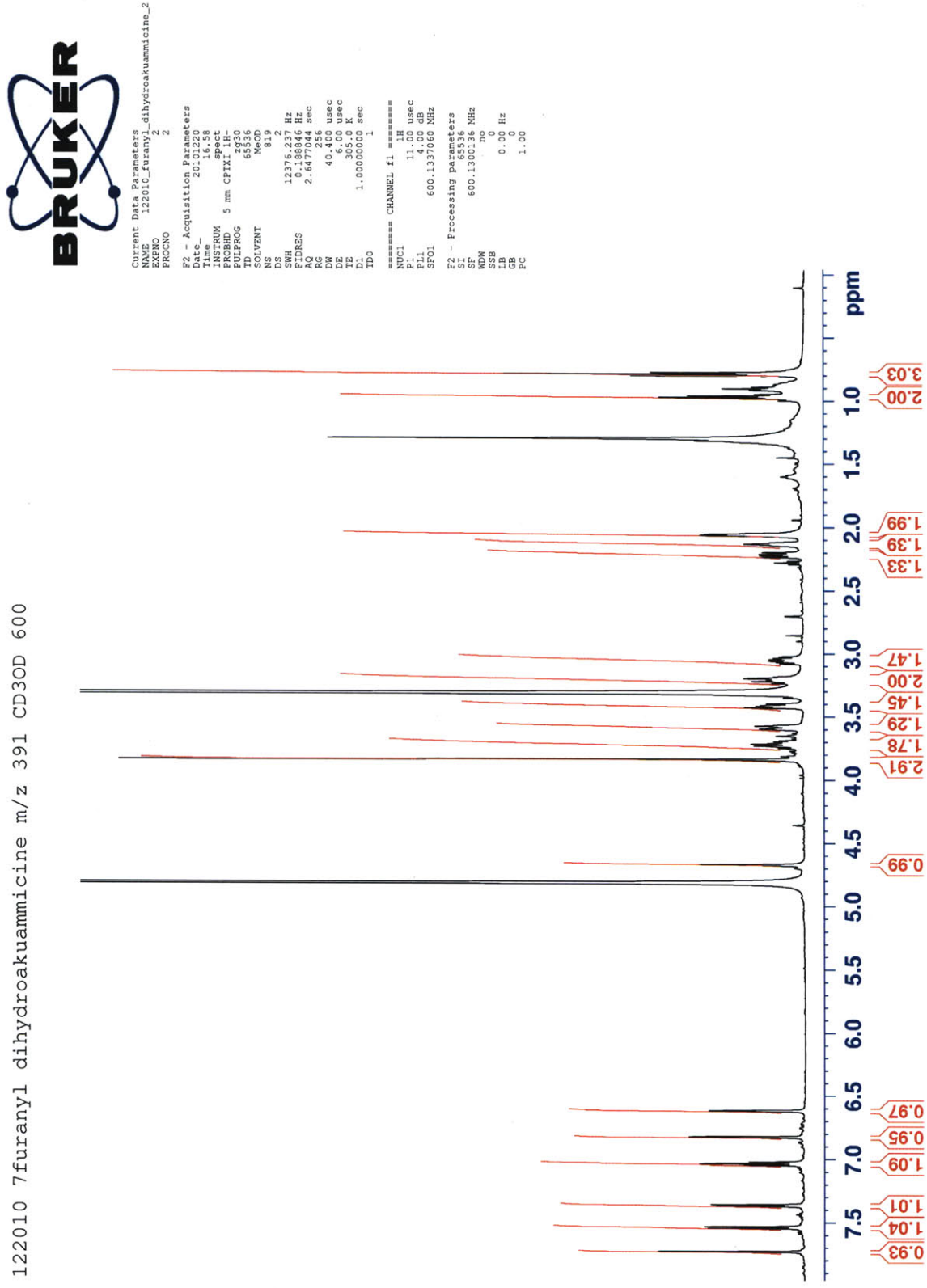

Figure 5C.5 Chapter 5. ^{1}H NMR spectrum of 12-furanyl-19,20-dihydroakuammicine **5i**

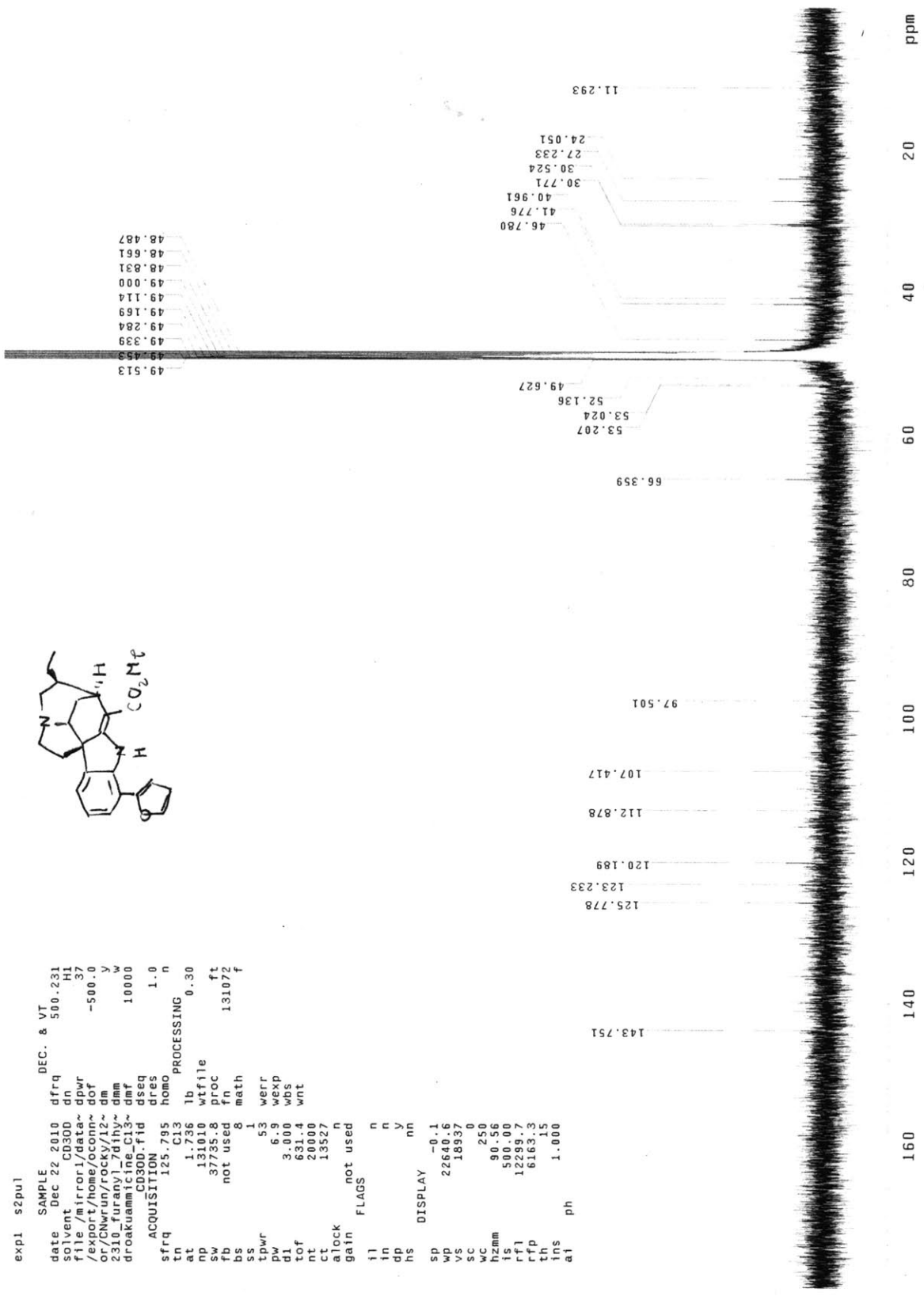

Figure 5C.6 Chapter 5. ^{13}C NMR spectrum of 12-furanyl-19,20-dihydroakuammicine **5i**

APPENDIX D

RE-ENGINEERING DIOXYGENASES IN MORPHINE BIOSYNTHETIC PATHWAY

D.1 Introduction

The opium poppy (*Papaver somniferum)* produces an array of medicinally important benzylisoquinoline alkaloids (BIAs) such as the analgesics codeine **10** and morphine **11** (**Figure D.1**)[1,2]. The biosynthesis of these alkaloids begins with the condensation of dopamine **1** and 4-hydroxyphenylacetaldehyde (4HPAA) **2** to form *(S)*-norcoclaurine **3**. Through a series of methylation and hydroxylation steps, *(S)*-norcoclaurine **3** is converted into *(S)*-reticuline **4**, the pivotal intermediate of many BIAs in the downstream pathways. *(S)*-reticuline **4** is further converted in six enzymatic steps to thebaine **5**, the alkaloid intermediate at the entry point of the morphinan alkaloid pathway.

Two biosynthetic routes have been proposed for the conversion of thebaine **5** to morphine **11** (**Figure D.1**)[3]. In the first route (**route A, Figure D.1**), thebaine **5** is demethylated at the 6 position by thebaine 6-O-demethylase (T6ODM) to form β,χ-unsaturated ketone neopinone **7**, which spontaneously isomerizes to form the more stable α,β-unsaturated ketone codeinone **8**. Reduction of the carbonyl in **8** by codeinone reductase (COR) yields codeine **10**. Finally, demethylation of **10** at the 3 position by codeine O-demethylase (CODM) leads to morphine **11**. Alternatively, in the second route (**route B, Figure D.1**), thebaine **5** is demethylated at the 3 position by CODM to form oripavine **6**. Second demethylation—this time at the 6 position—of **6** by T6ODM leads to morphinone **9**, which is subsequently reduced by COR to form morphine **11**. Morphinan alkaloids thebaine **5**, oripavine **6**, codeine **10** and morphine **11** accumulate in *P. somniferum* suggesting that both routes are operative *in vivo*[1,2].

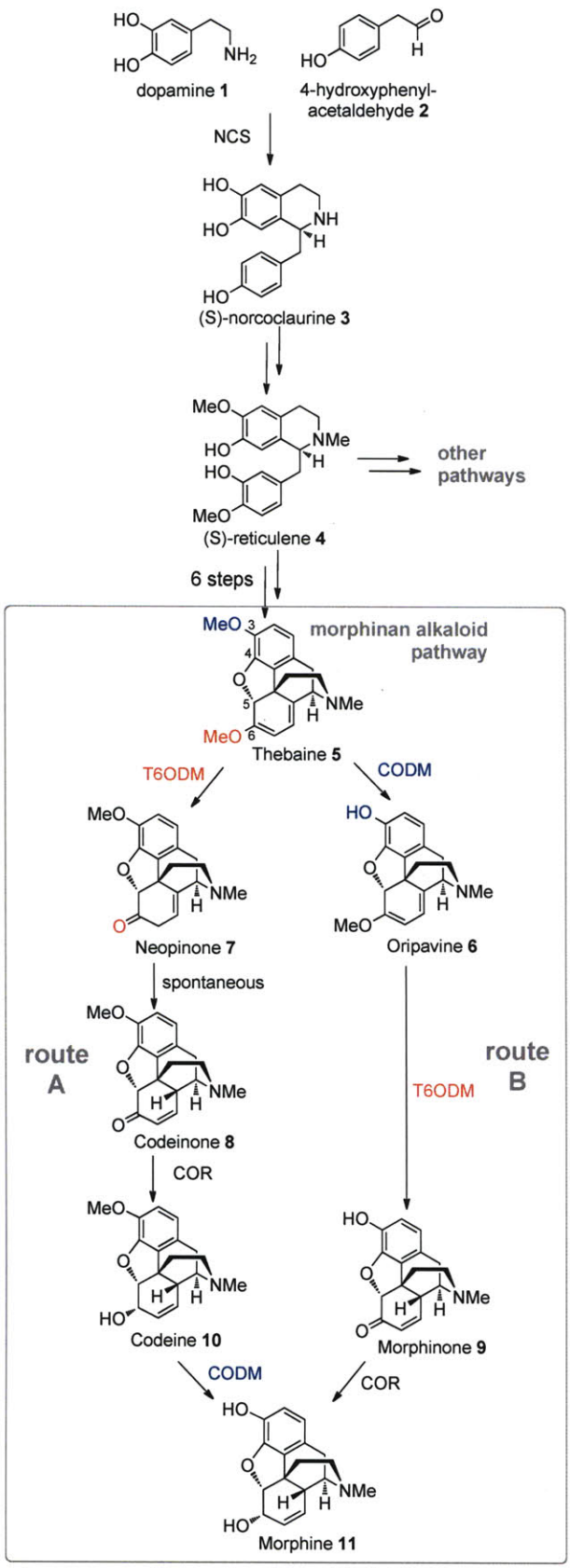

Figure D.1 Biosynthesis of benzylisoquinoline alkaloids in *Papaver somniferum*.

The entire morphinan alkaloid pathway in *P. somniferum* has been fully elucidated at the genetic level[1,2]. Genes encoding thebaine 6-O-demethylase (*Ps*T6ODM) and codeine O-demethylase (*Ps*CODM) have recently been cloned[3]. Surprisingly, they both encode for 2-oxoglutarate/Fe(II)-dependent dioxygenases. While this family of enzymes has previously been shown to catalyze N-demethylation[4], this is the first report of 2-oxoglutarate/Fe(II)-dependent dioxygenases catalyzing O-demethylation. Remarkably, *Ps*T6ODM and *Ps*CODM exhibit high sequence similarity (73% identity at the amino acid level) and yet they are able to carry out O-demethylation regioselectively; T6ODM, which accepts both thebaine (k_{cat}/K_m = 837 $s^{-1}M^{-1}$, K_m = 20 ± 7 uM) and oripavine (k_{cat}/K_m = 1242.6 $s^{-1}M^{-1}$, K_m = 15 ± 3 μM) as substrates, catalyzes O-demethylation at position 6, while CODM, which accepts both codeine (k_{cat}/K_m = 785 $s^{-1}M^{-1}$, K_m = 21 ± 8 uM) and thebaine (k_{cat}/K_m = 235 $s^{-1}M^{-1}$, K_m = 42 ± 8 uM), catalyzes O-demethylation at position 3 (**Figure D.1**)[3]. From a structural standpoint, it is interesting to understand how these two highly similar enzymes are able to carry out O-demethylation regioselectively. Furthermore, such an understanding will help rationalize the seemingly redundant way in which nature synthesizes morphine **11**.

This appendix describes rational re-design of *Papaver somniferum* CODM (*Ps*CODM) to exhibit higher substrate specificity towards codeine **10**. Homology structural model of *Ps*CODM based on the crystal structure of *Arabidopsis thaliana* anthocyanidine synthase (*At*ANS) was created, and *Ps*CODM's substrate binding site based on this protein model was identified. Rational redesign of the substrate-binding pocket yielded a mutant that maintains its demethylase activity towards codeine **10** but not thebaine **5**. We envision

that this *Ps*CODM mutant will be of great use in microbial production of morphine **11**. Specifically, reconstitution of morphine biosynthetic pathway in yeast using this mutant instead of the wild type enzyme will prevent accumulation of an off-pathway intermediate oripavine **6**, thereby improving the yield of morphine. Moreover, introduction of the re-engineered enzyme into *Papaver somniferum* could yield plant varieties with altered alkaloid profiles.

D.2 Results and Discussion

D.2.1 Construction of CODM Mutant Expression Plasmids

E. coli expression plasmids pQEDIOX1 and pQEDIOX3, which contain the open reading frames of *Papaver somniferum* T6ODM and CODM, respectively, were provided by Dr. Jillian Hagel and Professor Peter Facchini (University of Calgary). Initial protein expression screening revealed that *Ps*T6ODM mutants are expressed at very low levels. Therefore, we chose to focus our initial re-engineering efforts on *Ps*CODM. Since the crystal structure of *Ps*CODM is not available at present, we decided to build homology models[5] of *Ps*CODM based on the crystal structure of an enzyme that has the highest amino acid sequence similarity to *Ps*CODM. Blast search revealed that *Ps*CODM shows moderate sequence similarity (32% identity at the amino acid level) to *Arabidopsis thaliana* anthocyanidin synthase (*At*ANS), which is also a 2-oxoglutarate/Fe(II)-dependent dioxygenase[6]. To obtain homology models of *Ps*CODM based on the crystal structure of *At*ANS, we used automated protein-homology-modeling server SWISS-MODEL (**Figure D.2**)[5]. From this model, the substrate and co-factor binding site was identified. Key residues that are important for Fe(II)/2-oxoglutarate binding are

highlighted in **Figure D.3.** Clustal alignment of *Ps*CODM, *Ps*T6ODM and *Ps*DIOX2 (another *Papaver somniferum* 2-oxoglutarate/Fe(II)-dependent dioxygenase whose native substrate has not yet been identified) revealed three specific regions within the substrate binding pockets where *Ps*CODM and *Ps*T6ODM differ significantly at the amino acid level: region A_1-A_2, region B and region C_1-C_2 (**Figure D.2 - D.3**). We decided to convert *Ps*CODM to *Ps*T6ODM at these three regions using sequential site-directed mutagenesis. In total, 16 CODM mutants were constructed (**Table D.1**)

Table D.1 *Ps*CODM mutants that were constructed in this study. * indicates that the residues in that region were mutated to those of *Ps*T6ODM

	A_1	A_2	B	C_1	C_2	(wild type *Ps*CODM)
1)	A_1*	A_2*	B	C_1*	C_2*	
2)	A_1*	A_2	B	C_1*	C_2*	
3)	A_1*	A_2*	B	C_1	C_2*	
4)	A_1*	A_2*	B	C_1*	C_2	
5)	A_1*	A_2*	B	C_1	C_2	
6)	A_1*	A_2	B	C_1	C_2*	
7)	A_1*	A_2	B	C_1*	C_2	
8)	A_1*	A_2	B	C_1	C_2	
9)	A_1	A_2*	B	C_1*	C_2*	
10)	A_1	A_2	B	C_1*	C_2*	
11)	A_1	A_2*	B	C_1	C_2*	
12)	A_1	A_2*	B	C_1*	C_2	
13)	A_1	A_2*	B	C_1	C_2	
14)	A_1	A_2	B	C_1	C_2*	
15)	A_1	A_2	B	C_1*	C_2	
16)	A_1	A_2	B*	C_1	C_2	

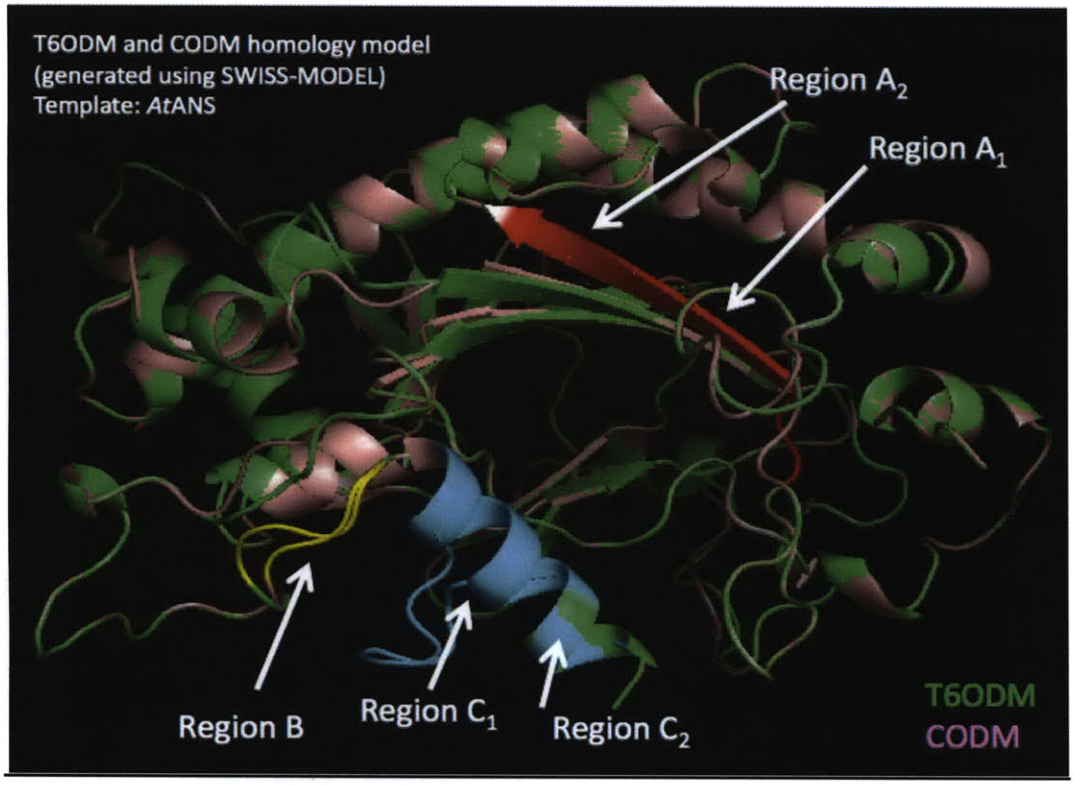

Figure D.2. Homology models of *Ps*T6ODM (green) and *Ps*CODM (pink) based on the crystal structure of *At*ANS. The models were created using SWISS-MODEL.

Figure D.3. Sequence alignment of *Ps*DIOX1 (*Ps*T6ODM), *Ps*DIOX2 and *Ps*DIOX3 (*Ps*CODM). ♦ indicates residues that have been proposed to be important in 2-oxoglutarate binding. ♠ indicates residues that have been proposed to be important in coordinating Fe(II).

D.2.2 Heterologous Expression of *Ps*CODM Mutants and *In vitro* Activity Assay of *Ps*CODM Mutants

Heterologous expression of *Ps*CODM wild type and mutant enzymes in *E. coli* were adapted from a previously reported protocol[3]. Robust protein expression was observed in most of the mutants (**Figure D.4**). The only mutant that had low expression level was the A_1A_2*BC_1C_2 mutant. Mutant *Ps*CODM enzymes were screened with substrates thebaine **10** and codeine **5** under assay conditions containing saturating concentrations of the alkaloids (0.25 mM). Briefly, the assay was performed using a 100 μL reaction mixture of 100 mM Tris-HCl (pH 7.4), 10% (v/v) glycerol, 14 mM 2-mercaptoethanol, 0.25 mM alkaloid, 10 mM 2-oxoglutarate, 10 mM sodium ascorbate, 0.5 mM $FeSO_4$, and 1 μM purified enzyme. The assays were incubated at 30°C and were quenched after 4 hours.

Product formation was observed using liquid chromatography-mass spectrometry (LC-MS). LC-MS traces of representative *in vitro* enzymatic assays of wild type and mutant *Ps*CODM enzymes are shown in **Figure D.5 – D.6.** Endpoint assays indicated that the majority of the mutants lost their O-demethylase activity towards both thebaine **5** and codeine **10**. Out of the total of sixteen mutants, only two ($A_1A_2B\,C_1$* C_2 and A_1A_2B* C_1 C_2 mutants) maintained O-demethylase activity towards codeine **10** (**Figure D.5**). Interestingly, while the A_1A_2B* C_1 C_2 mutant also maintained O-demethylase activity towards thebaine **5**, the $A_1A_2B\,C_1$* C_2 mutant can no longer O-demethylate thebaine **5** (**Figure D.6**).

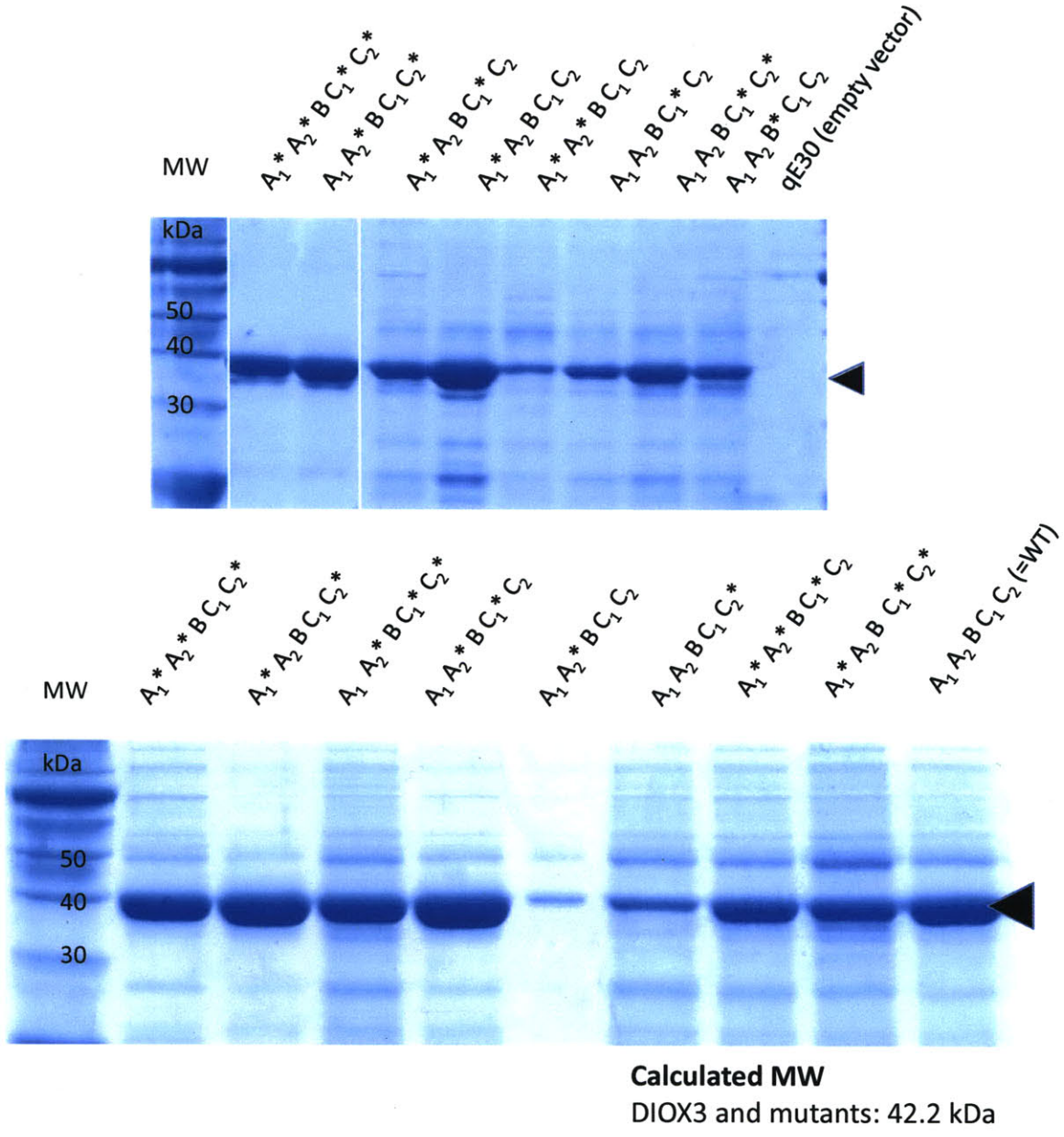

Figure D.4. SDS-PAGE of purified wild type and mutant *Ps*CODM enzymes from Talon colbalt affinity column (Clontech).

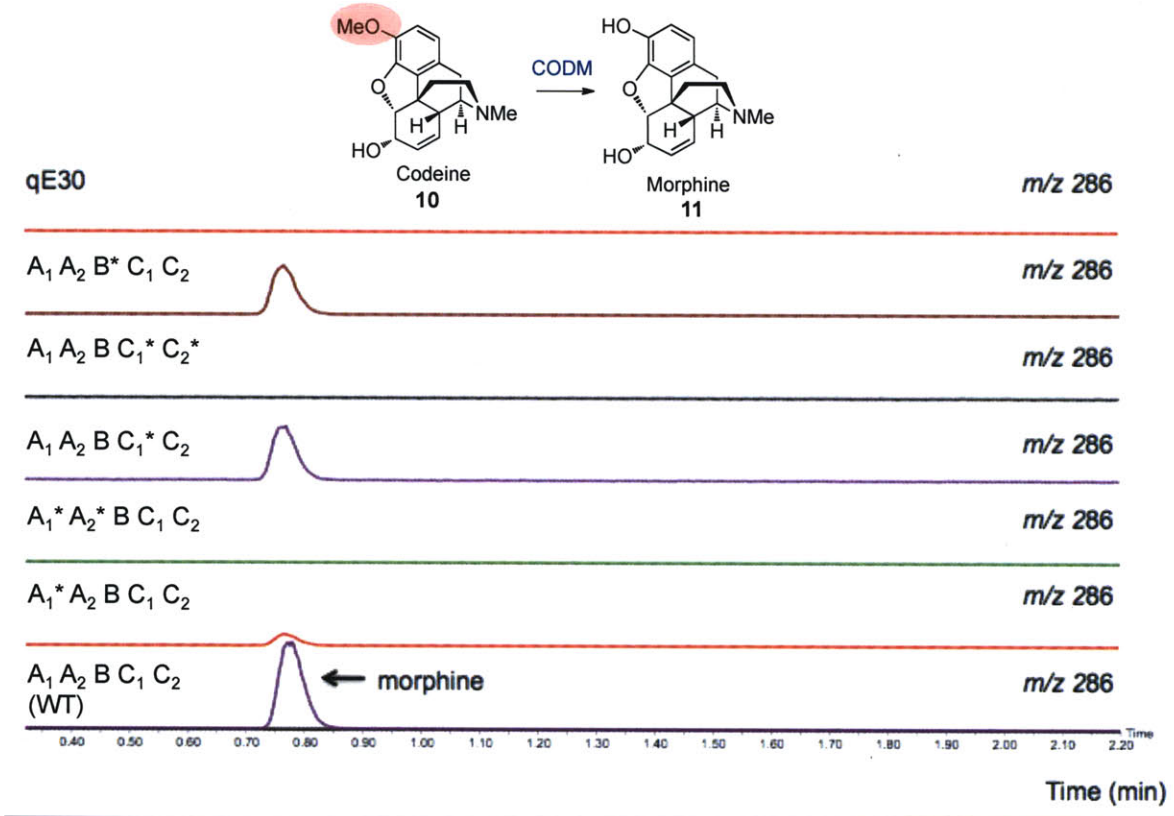

Figure D.5. LC-MS traces of an *in vitro* enzymatic assay of wild type and mutant *Ps*CODM enzymes (1 μM final enzyme concentration) with 0.25 mM codeine **10** in Tris buffer (100 mM Tris-HCl, 10% (v/v) glycerol, 14 mM 2-mercaptoethanol, pH 7.4) containing 10 mM 2-oxoglutarate, 10 mM sodium ascorbate and 0.5 mM $FeSO_4$. Reactions were performed at 30°C for 4 hours. *m/z* 286 corresponds to morphine **11**. LC-MS spectra are normalized to the same y-axis scale.

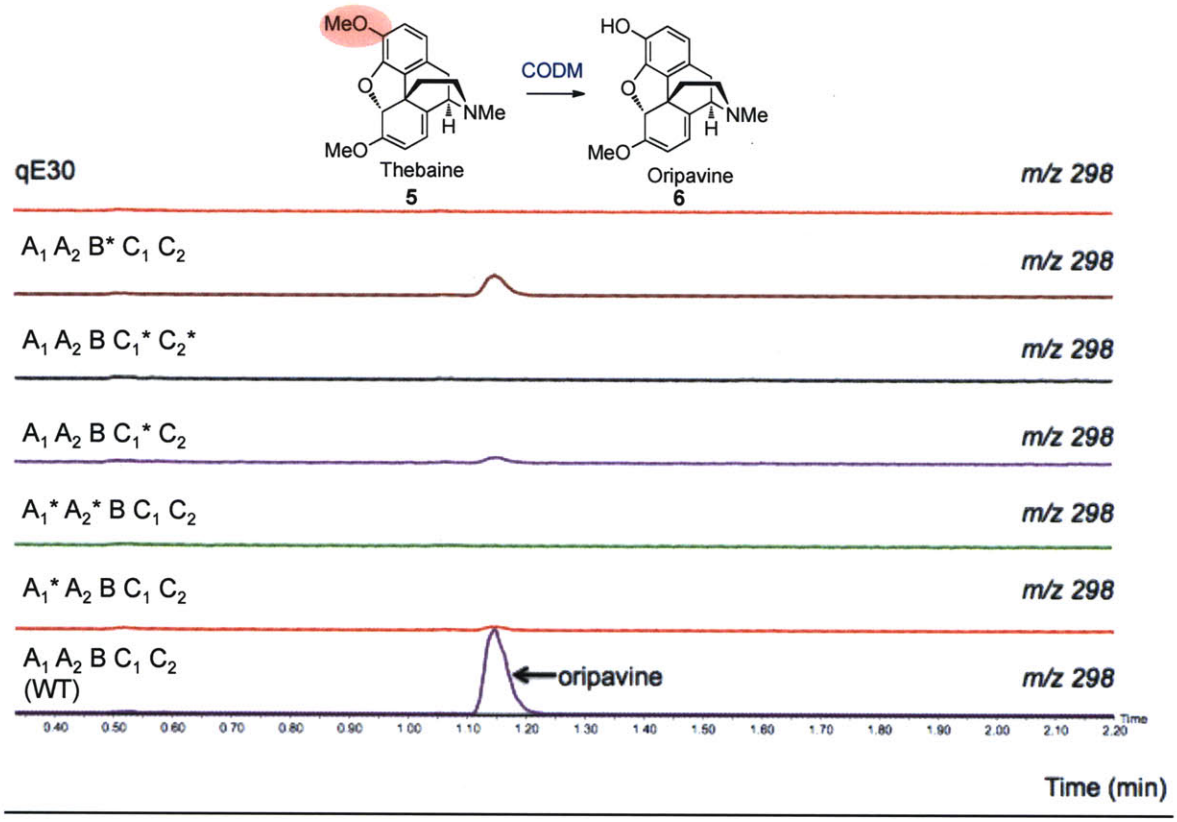

Figure D.6. LC-MS traces of an *in vitro* enzymatic assay of wild type and mutant *Ps*CODM enzymes (1 μM final enzyme concentration) with 0.25 mM thebaine **5** in Tris buffer (100 mM Tris-HCl, 10% (v/v) glycerol, 14 mM 2-mercaptoethanol, pH 7.4) containing 10 mM 2-oxoglutarate, 10 mM sodium ascorbate and 0.5 mM $FeSO_4$. Reactions were performed at 30°C for 4 hours. *m/z* 298 corresponds to oripavine **6**. LC-MS spectra are normalized to the same y-axis scale.

Competitive assay conditions with saturating concentration (0.25 mM) of both thebaine **5** and codeine **10** were also used to screen *Ps*CODM mutants (**Figure D.7**). Formation of morphine **11** and oripavine **6** at 4:1 ratio was observed when wild type *Ps*CODM was used. Similarly, the $A_1 A_2 B^* C_1 C_2$ mutant yielded both morphine **11** and oripavine **6** at approximately 4:1 ratio, though at lower concentrations compared to the wild type enzyme. Finally, the $A_1 A_2 B C_1^* C_2$ mutant produced only morphine **11,** indicating that it is selective towards codeine **10**.

In addition to screening with natural alkaloid substrates thebaine **5** and codeine **10**, we also screened *Ps*CODM mutants with the synthetic morphinan alkaloid analog hydrocodone (dihydrocodeinone) **12** (**Figure D.8**). Hydrocodone **12** can be derived from codeine **10** by oxidizing the hydroxyl group at the 6-position and reducing the adjacent alkene. Not surprisingly, at saturating concentration (0.25 mM) of **12**, *Ps*CODM mutants exhibited similar O-demethylase activity between hydrocodone **12** and codeine **10**. Out of the total of sixteen mutants, only two ($A_1 A_2 B C_1^* C_2$ and $A_1 A_2 B^* C_1 C_2$ mutants) formed the product hydromorphone (dihydromorphinone) **13**.

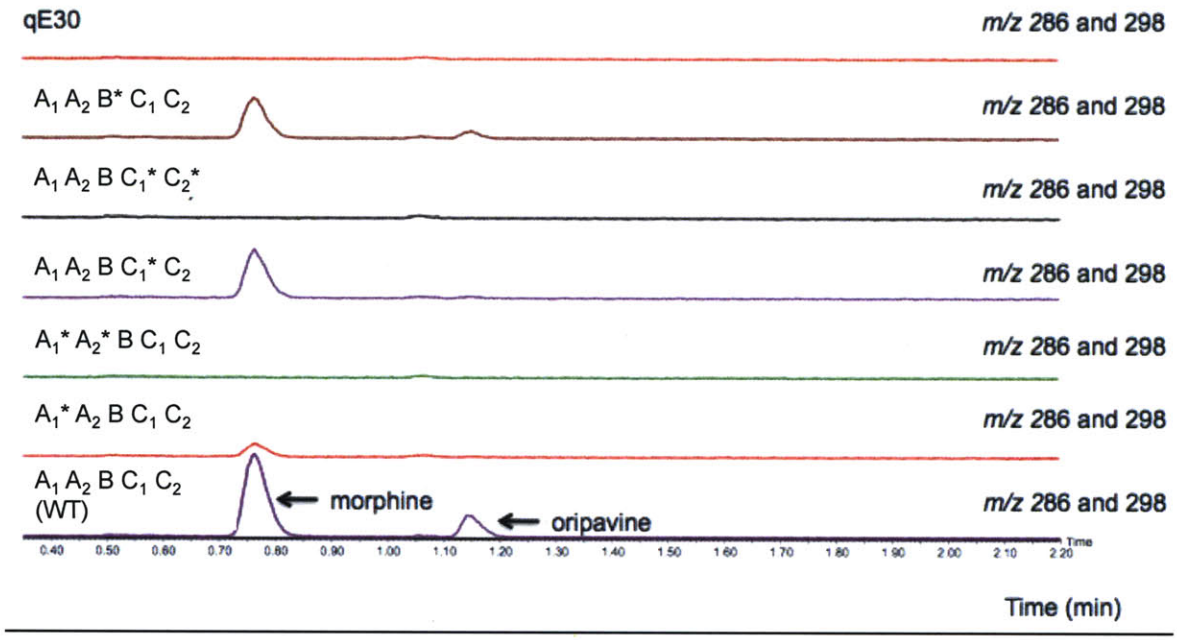

Figure D.7. LC-MS traces of an *in vitro* enzymatic assay of wild type and mutant *Ps*CODM enzymes (1 μM final enzyme concentration) with 0.25 mM thebaine **5** and 0.25 mM codeine **10** in Tris buffer (100 mM Tris-HCl, 10% (v/v) glycerol, 14 mM 2-mercaptoethanol, pH 7.4) containing 10 mM 2-oxoglutarate, 10 mM sodium ascorbate and 0.5 mM $FeSO_4$. Reactions were performed at 30°C for 4 hours. *m/z* 286 corresponds to morphine **11**; *m/z* 298 corresponds to oripavine **6**. LC-MS spectra are normalized to the same y-axis scale.

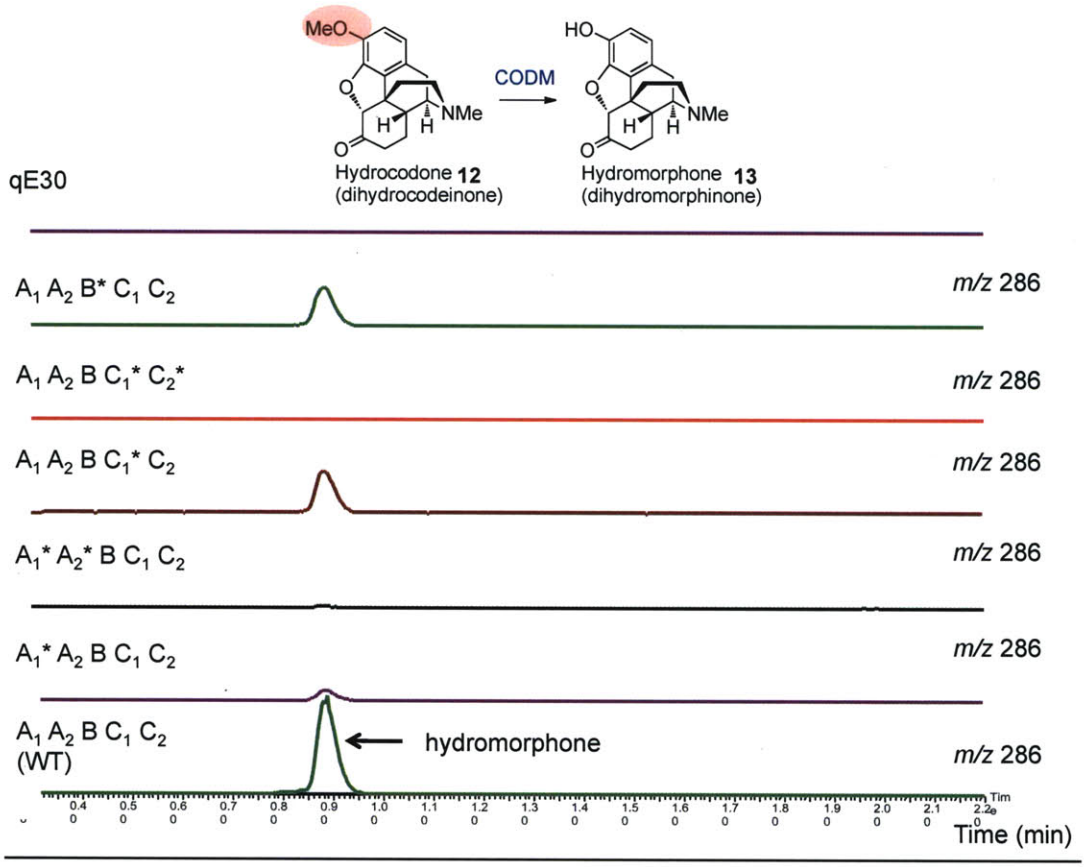

Figure D.8. LC-MS traces of an *in vitro* enzymatic assay of wild type and mutant *Ps*CODM enzymes (1 μM final enzyme concentration) with 0.25 mM hydrocodone **12** in Tris buffer (100 mM Tris-HCl, 10% (v/v) glycerol, 14 mM 2-mercaptoethanol, pH 7.4) containing 10 mM 2-oxoglutarate, 10 mM sodium ascorbate and 0.5 mM $FeSO_4$. Reactions were performed at 30°C for 4 hours. *m/z* 286 corresponds to hydromorphone **13**. LC-MS spectra are normalized to the same y-axis scale.

D.3 Conclusions

Papaver somniferum codeine O-demethylase (*Ps*CODM), a 2-oxoglutarate/Fe(II)-dependent dioxygenase in morphine biosynthesis, was re-engineered to exhibit higher substrate specificity towards codeine **10**. Rational site-directed mutagenesis of the residues that form the substrate-binding pocket, as determined by a homology structural model, yielded a mutant ($A_1 A_2 B C_1^* C_2$) that maintained its demethylase activity towards codeine **10** but not thebaine **5**. Reconstitution of morphine biosynthetic pathway in yeast using this *Ps*CODM mutant instead of the wild type enzyme will improve the yield of morphine by preventing the accumulation of an off-pathway intermediate oripavine **6**. Moreover, we envision that the simultaneous suppression of wild type *Ps*CODM and overexpression of this mutant enzyme in *P. somniferum* will yield plant varieties with improved morphine production.

D.4 Experimental Methods

D.4.1 Construction of CODM Mutant Expression Plasmids

pQEDIOX1 (pQET6ODM) and pQEDIOX3 (pQECODM), which contain the open reading frames of *Ps*T6ODM and *Ps*CODM, respectively, were provided by Professor Peter Facchini and Dr. Jillian Hagel (University of Calgary). To obtain the sixteen CODM mutants (**Table D.1**), site-directed mutagenesis (SDM) was performed using Stratagene QuikChange Site-Directed Mutagenesis kit. SDM primers are summarized in **Table D.2.** The *Ps*CODM mutant constructs were sequenced to verify their identities and were subsequently transformed into *E. coli* strain SG13009 (Qiagen) via electroporation using standard protocols.

Table D.2. Primers and templates for site-directed mutagenesis

Plasmid	Template used in SDM	Primers used in SDM
pQECODM A_1* A_2 B C_1 C_2	pQECODM A_1 A_2 B C_1 C_2	**Forward**: 5'-ggaccaaagacttgattgggctgatgtgtttagcatgttaagtc-3' **Reverse**: 5'-gacttaacatgctaaacacatcagcccaatcaagtctttggtcc-3' Then perform the second round of SDM with the following primers **Forward**: 5'-ccaaagacttgattgggctgatatatttagcatgttaagtcttcctc-3' **Reverse**: 5'-gaggaagacttaacatgctaaatatatcagcccaatcaagtctttgg-3'
pQECODM A_1* A_2* B C_1 C_2	pQECODM A_1* A_2 B C_1 C_2	**Forward**: 5'-aaagacttgattgggctgatatatttatgatgttaagtcttcctctccatt-3' **Reverse**: 5'-aatggagaggaagacttaacatcataaatatatcagcccaatcaagtcttt-3' Then perform the second round of SDM with the following primers **Forward**: 5'-cttgattgggctgatatatttatgatgttcactcttcctctccatttaagga-3' **Reverse**: 5'-tccttaaatggagaggaagagtgaacatcataaatatatcagcccaatcaag-3'
pQECODM A_1 A_2* B C_1 C_2	pQECODM A_1 A_2 B C_1 C_2	**Forward:** 5'-caaagacttgattggactgaagtgtttatgatgttcactcttcctctccatttaaggaagcc-3' **Reverse:** 5'-ggcttccttaaatggagaggaagagtgaacatcataaacacttcagtccaatcaagtctttg-3'
pQECODM A_1 A_2 B* C_1 C_2	pQECODM A_1 A_2 B C_1 C_2	**Forward:** 5'-gacacctgctttgttcaaaagtggatctacatatgaggatattttgaagg-3' **Reverse:** 5'-ccttcaaaatatcctcatatgtagatccacttttgaacaaagcaggtgtc-3'
pQECODM A_1 A_2 B C_1* C_2	pQECODM A_1 A_2 B C_1 C_2	**Forward**: 5'-tttgttcaaaagaggtaggtatggggatcttttgaaggaaaatctttcaagg-3' **Reverse**: 5'-ccttgaaagattttccttcaaaagatccccatacctacctcttttgaacaaa-3' Then perform the second round of SDM with the following primers **Forward**: 5'-caaaagaggtaggtatggggatcttgtggaggaaaatctttcaagga-3' **Reverse**: 5'-tccttgaaagattttcctccacaagatccccatacctacctctttg-3'
pQECODM A_1 A_2 B C_1* C_2*	pQECODM A_1 A_2 B C_1* C_2	**Forward**: 5'-gtatggggatcttgtggaggaatgtctttcaaggaagcttga-3' **Reverse**: 5'-tcaagcttccttgaaagacattcctccacaagatccccatac-3' Then perform the second round of SDM with the following primers **Forward**: 5'-agaggtaggtatggggatcttgtggaggaatgtaagacgaggaagcttgatggaaa-3' **Reverse**: 5'-tttccatcaagcttcctcgtcttacattcctccacaagatccccatacctacctct-3'
pQECODM A_1 A_2 B C_1 C_2*	pQECODM A_1 A_2 B C_1 C_2	**Forward**: 5'-gacacctgctttgttcaaaagaggtaggtatgaggatattttgaa ggaatgtaagacgaggaagcttgatggaaaatcatttct-3' **Reverse**: 5'-agaaatgattttccatcaagcttcctcgtcttacattccttcaa aatatcctcatacctacctcttttgaacaaagcaggtgtc-3'
pQECODM A_1* A_2 BC_1* C_2*	pQECODM A_1 A_2 B C_1* C_2*	**Forward**: 5'-ggaccaaagacttgattgggctgatgtgtttagcatgttaagtc-3' **Reverse**: 5'-gacttaacatgctaaacacatcagcccaatcaagtctttggtcc-3' Then perform the second round of SDM with the following primers **Forward**: 5'-ccaaagacttgattgggctgatatatttagcatgttaagtcttcctc-3' **Reverse**: 5'-gaggaagacttaacatgctaaatatatcagcccaatcaagtctttgg-3'

Table D.2 (continued) Primers and templates for site-directed mutagenesis.

Plasmid	Template used in SDM	Primers used in SDM
pQECODM A_1*A_2* BC_1*C_2*	pQECODM A_1* A_2 BC_1* C_2*	**Forward**: 5'-aaagacttgattgggctgatatatttatgatgttaagtcttcctctccatt-3' **Reverse**: 5'-aatggagaggaagacttaacatcataaatatatcagcccaatcaagtcttt-3' Then perform the second round of SDM with the following primers **Forward**: 5'-cttgattgggctgatatatttatgatgttcactcttcctctccatttaagga-3' **Reverse**: 5'-tccttaaatggagaggaagagtgaacatcataaatatatcagcccaatcaag-3'
pQECODM A_1 A_2* B C_1* C_2	pQECODM A_1 A_2 B C_1* C_2	**Forward:** 5'-caaagacttgattggactgaagtgtttatgatgttcactcttcctctccatttaaggaagcc-3' **Reverse:** 5'-ggcttccttaaatggagaggaagagtgaacatcataaacacttcagtccaatcaagtctttg-3'
pQECODM A_1* A_2 B C_1 C_2*	pQECODM A_1* A_2 B C_1 C_2	**Forward**: 5'-gacacctgctttgttcaaaagaggtaggtatgaggatattttgaa ggaatgtaagacgaggaagcttgatggaaaatcatttct-3' **Reverse**: 5'-agaaatgattttccatcaagcttcctcgtcttacattccttcaa aatatcctcatacctacctcttttgaacaaagcaggtgtc-3'
pQECODM A_1 A_2* B C_1 C_2*	pQECODM A_1 A_2* B C_1 C_2	**Forward**: 5'-gacacctgctttgttcaaaagaggtaggtatgaggatattttgaa ggaatgtaagacgaggaagcttgatggaaaatcatttct-3' **Reverse**: 5'-agaaatgattttccatcaagcttcctcgtcttacattccttcaa aatatcctcatacctacctcttttgaacaaagcaggtgtc-3'
pQECODM A_1* A_2* BC_1 C_2*	pQECODM A_1* A_2* B C_1 C_2	**Forward**: 5'-gacacctgctttgttcaaaagaggtaggtatgaggatattttgaa ggaatgtaagacgaggaagcttgatggaaaatcatttct-3' **Reverse**: 5'-agaaatgattttccatcaagcttcctcgtcttacattccttcaa aatatcctcatacctacctcttttgaacaaagcaggtgtc-3'
pQECODM A_1 A_2* B C_1*C_2*	pQECODM A_1 A_2 B C_1* C_2*	**Forward:** 5'-caaagacttgattggactgaagtgtttatgatgttcactcttcctctccatttaaggaagcc-3' **Reverse:** 5'-ggcttccttaaatggagaggaagagtgaacatcataaacacttcagtccaatcaagtctttg-3'
pQECODM A_1* A_2* BC_1* C_2	pQECODM A_1* A_2* B C_1 C_2	**Forward**: 5'-tttgttcaaaagaggtaggtatggggatcttttgaaggaaaatctttcaagg-3' **Reverse**: 5'-ccttgaaagattttccttcaaaagatccccatacctacctcttttgaacaaa-3' Then perform the second round of SDM with the following primers **Forward**: 5'-caaaagaggtaggtatggggatcttgtggaggaaaatctttcaagga-3' **Reverse**: 5'-tccttgaaagattttcctccacaagatccccatacctacctcttttg-3'
pQECODM A_1* A_2 B C_1* C_2	pQECODM A_1* A_2 B C_1 C_2	**Forward**: 5'-tttgttcaaaagaggtaggtatggggatcttttgaaggaaaatctttcaagg-3' **Reverse**: 5'-ccttgaaagattttccttcaaaagatccccatacctacctcttttgaacaaa-3' Then perform the second round of SDM with the following primers **Forward**: 5'-caaaagaggtaggtatggggatcttgtggaggaaaatctttcaagga-3' **Reverse**: 5'-tccttgaaagattttcctccacaagatccccatacctacctcttttg-3'

D.4.2 Heterologous Expression of *Ps*CODM Mutants

A single transformed *E. coli* colony was inoculated in 10 mL LB media supplemented with kanamycin (0.05 g/L) and ampicillin (0.1 g/L) and incubated overnight at 37 °C with shaking at 225 rpm. An aliquot of the overnight culture (8 mL) was then used to inoculate 800 mL LB media supplemented with kanamycin (0.05 g/L) and ampicillin (0.1 g/L) and incubated at 37 °C with shaking at 225 rpm until an OD_{600} of 0.6 was reached. Cells were induced for overexpression by the addition of isopropyl β-D-galactopyranoside (IPTG, final concentration 0.3 mM) and the culture was allowed to continue growth for 24 hrs at 6 °C. Cells were harvested by centrifugation and lysed by sonication. The hexa-histidine-tagged CODM mutants were purified using Talon colbalt affinity column (Clontech) using manufacturer's protocols. Eluted enzyme was subsequently buffer-exchanged into Tris buffer (100 mM Tris-HCl pH 7.4, 10% (v/v) glycerol and 14 mM 2-mercaptoethanol) and immediately assayed for activity. This enzyme was not stable upon extended storage.

D.4.3 *In Vitro* Activity Assay of *Ps*CODM Mutants

The conditions for the *in vitro* activity assay were adapted from a previously reported protocol[3]. Briefly, the assay for 2-oxoglutarate/Fe(II)-dependent dioxygenase activity was performed using a 100 μL reaction mixture of 100 mM Tris-HCl (pH 7.4), 10% (v/v) glycerol, 14 mM 2-mercaptoethanol, 0.25 mM alkaloid(s), 10 mM 2-oxoglutarate, 10 mM sodium ascorbate, 0.5 mM $FeSO_4$, and 1 μM purified enzyme. Assays were carried out for 4 hours at 30°C. Aliquots (25 μL) were quenched in 1 mL methanol, containing yohimbine (500 nM) as an internal standard. The samples were centrifuged in a

microcentrifuge (13,000 rpm, 5 min) to remove particulates and then analyzed by LC-MS. Samples were ionized by ESI with a Micromass LCT Premier TOF Mass Spectrometer. The LC was performed on an Acquity Ultra Performance BEH C18, 1.7 μm, 2.1 x 100 mm column on a gradient of 10-90% acetonitrile/water (0.1% formic acid) over 5 minutes at a flow rate of 0.6 mL/min. The appearance of morphine **11**, oripavine **6** and hydromorphone **13** was monitored by peak integration and normalized to the internal standard. All chemicals were obtained from a commercial source (Sigma Aldrich).

D.5 References

1. Facchini, P. J., Alkaloid biosynthesis in plants: Biochemistry, cell biology, molecular regulation and metabolic engineering applications. *Annu. Rev. Plant Physiol. Plant Mol. Biol.* **2001,** *52*, 29-66.
2. Facchini, P. J.; Bird, D. A.; Bourgault, R.; Hagel, J. M.; Liscombe, D. K.; MacLeod, B. P.; Zulak, K. G., Opium poppy: a model system to investigate alkaloid biosynthesis in plants. *Can. J. Bot.* **2005,** *83*, 1189-1206.
3. Hagel, J. M.; Facchini, P. J., Dioxygenases catalyze the O-demethylation steps of morphine biosynthesis in opium poppy. *Nat Chem Biol* **2010,** *6* (4), 273-5.
4. Loenarz, C.; Schofield, C. J., Expanding chemical biology of 2-oxoglutarate oxygenases. *Nat. Chem. Biol.* **2008,** *4*, 152-156.
5. Schwede, T.; Kopp, J.; Guex, N.; Peitsch, M. C., SWISS-MODEL: An automated protein homology-modeling server. *Nucleic Acids Res* **2003,** *31* (13), 3381-5.
6. Wilmouth, R. C.; Turnbull, J. J.; Welford, R. W.; Clifton, I. J.; Prescott, A. G.; Schofield, C. J., Structure and mechanism of anthocyanidin synthase from Arabidopsis thaliana. *Structure* **2002,** *10* (1), 93-103.

Weerawat Runguphan

Massachusetts Institute of Technology
77 Massachusetts Avenue, 18-125
Cambridge, MA 02139
weerawat@mit.edu
Voice, (617) 253-1832; FAX, (617) 324-0550

EDUCATION

2006-2011 ***Massachusetts Institute of Technology***
Degree of Doctor of Philosophy in Chemistry

2002-2006 ***Harvard University***
Bachelor of Arts in Chemistry and Physics
Magna Cum Laude with Highest Honors
Foreign Language Citation in Chinese

RESEARCH EXPERIENCE

2006-present **Graduate Research Assistant**
Massachusetts Institute of Technology, Cambridge, MA
Mentor: Professor Sarah E. O'Connor
♦*Reprogramming alkaloid biosynthesis: synthetic biology in plants*
-Overexpression of an engineered gene in planta to produce halogenated and methylated terpene indole alkaloids
-Reprogramming precursor biosynthesis via overexpression of prokaryotic halogenases in planta to produce halogenated terpene indole alkaloids
-Silencing of tryptamine biosynthesis to produce unnatural alkaloids
♦*Re-engineering substrate regioselectivity of enzymes involved in morphine and codeine biosynthesis*
♦*Identifying genes involved in secologanin biosynthesis*

2006 **Laboratory Research Assistant**
National Center for Engineering and Biotechnology, Pathumthani, Thailand
Mentor: Dr. Sumalee Kamchonwongpaisan
♦*Protein-ligand engineering of* Trypanosoma brucei *dihydrofolate reductase*

2004-2006 **Independent Organic Chemistry Research**
Harvard University, Cambridge, MA
Mentor: Professor Stuart L. Schreiber
♦*Combinatorial synthesis of novel epoxide inhibitors of hepatitis C virus*

TEACHING EXPERIENCE

2006 **Graduate Teaching Assistant**
Massachusetts Institute of Technology, Cambridge, MA
Laboratory Chemistry
Instructor: Dr. Janet Schrenk

SKILLS (instruments and chromatography)

SDS-PAGE and agarose gel electrophoresis, Bruker and Varian NMRs (600, 500, 400, 300 MHz, ^{1}H, ^{13}C, ^{19}F, ^{1}H-^{13}C HSQC, ^{1}H-^{13}C HMBC), UPLC-MS, HPLC, FTIR, UV, CD, flash chromatography.

PROFESSIONAL AND ACADEMIC AWARDS

2011	**Morse Travel Award** Massachusetts Institute of Technology, Cambridge, MA ♦*Awarded to present at 241st ACS national meeting, Anaheim, CA*
2011	**Graduate Student Council Travel Award** Massachusetts Institute of Technology, Cambridge, MA ♦*Awarded to present at 241st ACS national meeting, Anaheim, CA*
2010	**Poster Presentation Award** Banff Conference on Plant Metabolism, Banff, Canada ♦*Awarded for best poster presentation*
2010	**Banff Conference on Plant Metabolism Travel Award** Samuel Roberts Noble Foundation, Ardmore, OK ♦*Awarded to present at Banff Conference on Plant Metabolism, Banff, Canada*
2010	**Morse Travel Award** Massachusetts Institute of Technology, Cambridge, MA ♦*Awarded to present at Banff Conference on Plant Metabolism, Banff, Canada*
2006-2007	**Massachusetts Institute of Technology/DuPont Presidential Fellowship Award** Massachusetts Institute of Technology, Cambridge, MA ♦*Awarded to outstanding incoming graduate students*
2004	**Harvard University Herschel Smith Fellowship Award** Harvard University, Cambridge, MA ♦*Awarded to conduct research at the Office of Atoms for Peace, Bangkok, Thailand*
2003	**Kennedy School of Government Human Rights Internship Award** Harvard University, Cambridge, MA ♦*Awarded to conduct research at Duang Prateep Foundation, Bangkok, Thailand*
2002-2003	**Philips Exeter Academy George Sutro Loewenstein Scholarship** Philips Exeter Academy, Exeter, NH ♦*Awarded to a graduating senior for academic excellence*
2001	**Silver Medal, Thailand National Chemistry Olympiad** Bangkok, Thailand

PUBLICATIONS

1. **Runguphan, W.**, and O'Connor, S.E. Chemogenetic Generation of Monoterpene Indole Alkaloid Analogs. Manuscript in preparation.

2. **Runguphan, W.**, and O'Connor, S.E. Re-engineering of 2-oxoglutarate/Fe(II)-dependent Dioxygenases in Codeine and Morphine Biosynthesis. Manuscript in preparation.

3. **Runguphan, W.***, Qu, X.*, and O'Connor, S.E. Integrating Carbon-Halogen Bond Formation into Medicinal Plant Metabolism. *Nature* **2010**, 468, 461 – 461. * denotes equal contributions. Featured in *Nature* **2010**, 468, 380 – 381; *Chemical and Engineering News* **2010**, 88, 13; and *ACS Chemical Biology* **2010**, 5, 1093.

4. **Runguphan, W.**, Maresh, J., and O'Connor, S.E. Silencing of Tryptamine Biosynthesis for Production of Unnatural Alkaloids in Plant Culture. *Proceedings of the National Academy of Sciences* **2009**, 106, 13673 – 13678.

5. Effendi, L.*, **Runguphan, W.***, O'Connor, S.E., and Prather, K.J. Opportunities in Metabolic Engineering to Enable Scalable Alkaloid Production. *Nature Chemical Biology* **2009**, 5, 292 – 300. * denotes equal contributions.

6. **Runguphan, W.**, and O'Connor, S.E. Metabolic Reprogramming of Periwinkle Plant Culture. *Nature Chemical Biology* **2009**, 5, 151 – 153.
Featured in *Nature Chemical Biology* **2009**, 5, 140 – 141, and *Chemical and Engineering News* **2009**, 87, 31. Highlighted as the "Greenest Chemistry" in *Nature Chemical Biology* **2010**, 6, 387 (the fifth anniversary issue).

7. Peng, L.F., Kim, S.S., Matchacheep, S., Lei, X., Su, S., Lin, W., **Runguphan, W.**, Choe, W., Sakamoto, N., Ikeda, M., Kato, N., Beeler, A.B., Porco, J.A., Schreiber, S.L., and Chung, R.T. Identification of Novel Epoxide Inhibitors of HCV Replication Using a High-Throughput Screen. *Antimicrobial Agents and Chemotherapy* **2007**, 51, 3756 – 3759.

8. Taweechai, S., **Runguphan, W.**, Sukplang, P., Janyapoon, K., Yuthavong, Y., and Kamchonwongpaisan, S. Engineering *Trypanosoma brucei rhodesiense* dihydrofolate reductase mutants. *Proceeding for the 1st Biochemistry and Molecular Biology (BMB) Conference, Chulalongkorn University, Thailand.* **2007**.

SELECTED PRESENTATIONS

1. Integrating carbon–halogen bond formation into medicinal plant metabolism. **Runguphan, W.**, Qu, X., and O'Connor, S.E. 241st American Chemical Society National Meeting. Anaheim, CA **2011**.

2. Reprogramming Alkaloid Biosynthesis: Synthetic Biology in Plants**. Runguphan, W.**, Qu, X., Maresh, J., and O'Connor, S.E. Banff Conference on Plant Metabolism. Banff, Canada **2010**.

3. Engineering *Catharanthus roseus* Cell Cultures to Produce Unnatural Products. **Runguphan, W.**, and O'Connor, S.E. MIT Interdepartmental Supergroup Meeting. MIT, Cambridge, MA **2008**.